UNIVERSIDADE DE LISBOA
INSTITUTO SUPERIOR TÉCNICO

Extracellular vesicles: agents of gut communication in prediabetes scenario

Inês Raquel Antunes Ferreira

Supervisor: Doctor Maria Paula Borges de Lemos Macedo
Co-supervisors: Doctor Bruno Costa da Silva
Doctor Cláudia Alexandra Martins Lobato da Silva

Thesis approved in public session to obtain the PhD Degree in
Bioengineering

Jury final classification: Pass with Distinction

2021

Obra entregue para apreciação da prova de Doutoramento em Bioengenharia para obtenção do grau de Doutor concedido pela Universidade de Lisboa, no Instituto Superior Técnico, ao abrigo do D.L. 74/2006/, de 24 de março.

Lisboa, 1 de março de 2021

O presidente do júri
Homologo

Assinado por : **JOAQUIM MANUEL SAMPAIO CABRAL**
Num. de Identificação: BI057972524
Data: 2021.03.01 20:36:33 +0000

CARTÃO DE CIDADÃO

TÉCNICO LISBOA

UNIVERSIDADE DE LISBOA
INSTITUTO SUPERIOR TÉCNICO

Extracellular vesicles: agents of gut communication in prediabetes scenario

Inês Raquel Antunes Ferreira

Supervisor: Doctor Maria Paula Borges de Lemos Macedo

Co-supervisors: Doctor Bruno Costa da Silva

Doctor Cláudia Alexandra Martins Lobato da Silva

Thesis approved in public session to obtain the PhD Degree in
Bioengineering

Jury final classification: Pass with Distinction

Jury

Chairperson:

Doctor Joaquim Manuel Sampaio Cabral, Instituto Superior Técnico, Universidade de Lisboa

Members of the Committee:

Doctor Joaquim Manuel Sampaio Cabral, Instituto Superior Técnico, Universidade de Lisboa

Doctor Maria Paula Borges de Lemos Macedo, Faculdade de Ciências Médicas da Universidade Nova de Lisboa

Doctor Gabriel António Amaro Monteiro, Instituto Superior Técnico, Universidade de Lisboa

Doctor John Griffith Jones, Centro de Neurociências e Biologia Celular da Universidade de Coimbra

Doctor Rune Matthiesen, Faculdade de Ciências Médicas da Universidade Nova de Lisboa

Doctor Fábio Monteiro Fernandes, Instituto Superior Técnico, Universidade de Lisboa

FUNDING INSTITUTIONS
Fundação para a Ciência e Tecnologia
Sociedade Portuguesa de Diabetologia

2021

The research described in this dissertation was financially supported by:

Fundação para a Ciência e Tecnologia (FCT – Portugal)

PhD Fellowship: PD/BD/114044/2015

PTDC/MEC-MET/29314/2017

Table of Contents

List of Figures

Figures Pages

Tables

Pages

Supplementary Data

Pages

Appendix Document

Pages

List of Abbreviations

α-KC	Alpha-ketoglutarate
Acaa2	Acetyl-CoA acyltransferase 2
Acadl	Acyl-CoA dehydrogenase long chain
Acadvl	Acyl-CoA dehydrogenase very long chain
Acat1	Acetyl-CoA acetyltransferase 1
Acat2	Acetyl-CoA acetyltransferase 2
ACC	Acetyl-CoA carboxylase
Acetyl-CoA	Acetyl coenzyme A
ACK	Ammonium chloride-potassium buffer
ACLY	ATP-citrate lyase
Acot 3	Acyl-CoA thioesterase 3
Acot 5	Acyl-CoA thioesterase 5
Acot1	Acyl-CoA thioesterase 1
Acot2	Acyl-CoA thioesterase 2
Acot6	Acyl-CoA thioesterase 6
Acox1	Acyl-CoA oxidase 1
Acss2	Acyl-CoA synthetase short chain family member 2
Acta1	Actin alpha 1, skeletal muscle
Acta2	Actin alpha 2, smooth muscle, aorta
Actb	Actin beta
Actc1	Actin alpha, cardiac muscle 1
Actg1	Actin gamma 1
Actg2	Actin gamma 2, smooth muscle, enteric
Acyl-CoA	Acyl-coenzime A
ALD	Alcoholic liver disease
Aldh1b1	Aldehyde dehydrogenase 1 family member B1
Aldh2	Aldehyde dehydrogenase 2 family (mitochondrial)
Aldh5a1	Aldehyde dehydrogenase 5 family member A1
Aldh9a1	Aldehyde dehydrogenase 9 family member A1
Aldoa	Aldolase, fructose-bisphosphate A
Aldob	Aldolase, fructose-bisphosphate B
AMPK	Adenosine monophosphate-activated kinase
ANOVA	Analyses of variance
Ap2b1	Adaptor related protein complex 2 beta 1 subunit
ApoB	Apolipoprotein B

Arg2	Arginase 2
ATP	Adenosine triphosphate
Atp5i	ATP synthase inhibitory factor subunit 1
AUC	Area under the curve
BCA	Bicinchoninic acid assay
BCAA	Branched-chain amino acids
Bdh2	3-hydroxybutyrate dehydrogenase 2
C57Bl/6J	C57 black 6
Cavin1	Caveolae associated protein 1
CCL2	Monocyte chemoattractant protein 2
CCL5	Monocyte chemoattractant protein 5
CD11b	Cluster of differentiantion 11b
CD36	Cluster of differentiation 36
CD45	Cluster of differentiation 45
CD63	Cluster of differentiation 63
CD81	Cluster of differentiation 81
CD9	Cluster of differentiation 9
Cdh17	Cadherin 17
ChREBP	Carbohydrate response element binding protein
CoA	Coenzime A
Coro1c	Coronin 1C
COVID-19	Coronavirus Disease 2019
Cpa1	Carboxypeptidase A1
DAPI	2-(4-Amidinophenyl)-6-indolecarbamidine dihydrochloride
DG	Diacylglicerol
DGAT1	Diacylglycerol acyltransferase 1
DGAT2	Diacylglycerol acyltransferase 2
Dlst	Dihydrolipoamide S-succinyltransferase.
DNA	Deoxyribonucleic acid
DNL	*De novo* lipogenesis
Dnpep	Aspartyl aminopeptidase
DPP-4	Dipeptidyl peptidase-4
Ech1	Enoyl-CoA hydratase 1
Echs1	Enoyl-CoA hydratase, short chain 1
Eno1	Enolase 1
ER	Endoplasmic reticulum
ESCRT	Endosomal sorting complexes required for transport
Etfa	Electron transfer flavoprotein alpha subunit

Etfb	Electron transfer flavoprotein beta subunit
EV	Extracellular vesicle
FA	Fatty acid
FAS	FA synthase
FBS	Fetal Bovine Serum
FCS	Fetal Calf Serum
FFA	Free Fatty Acids
Flna	Filamin A
FSC	Forward side scatter
Fth1	Ferritin heavy chain 1
G3P	Glycerol-3-phosphate
G6P	Glucose-6-phosphate
GCK	Glucokinase
GDE	Gut-derived extracelular vesicle
GIP	Glucose-dependent insulinotropic peptide
GK	Glucokinase
GLP-1	Glucagon-like peptide 1
GLUT-2	Glucose-transporter 2
GO	Gene Ontology
Gsta1	Glutathione S-transferase alpha 1
Gsta2	Glutathione S-transferase alpha 2
Gsta4	Glutathione S-transferase alpha 4
Gstm2	Glutathione S-transferase mu 2
GTT	Glucose tolerance test
GWA	Genome-wide association
Hadha	Hydroxyacyl-CoA dehydrogenase trifunctional multienzyme complex subunit alfa
HbA1c	Glycosylated Hemoglobin
HCl	Hydrochloric acid
HDL	High-density lipoproteins
HFD	High fat diet
HFD-GDE	Gut-derived extracellular vesicle from high fat diet-fed mice
HHEX/IDE	Hematopoietically exxpressed homeobox gene
Hist1h2bf	Histone cluster 1 H2B family member f
Hist1h4a	Histone cluster 1 H4 family member a
Hist2h2be	Histone cluster 2 H2B family member 3
Hist3h2ba	Histone cluster 3 H2B family member a
Hist3h2bb	Histone cluster 3 H2B family member b
HPLC	High performance liquid chromatography

HSP	Heat shock proteins
IDF	International Diabetes Federation
Idh1	Isocitrate dehydrogenase (NADP(+)) 1, cytosolic
IDL	Intermediate-density lipoprotein
IFG	Impaired Fasting Glucose
IFN-γ	Interferon gama
IGF2BP2	Insulin Like Growth Factor 2 MRNA Binding Protein 2 gene
IGF-R	Insulin-like growth factor 1
IGT	Impaired Glucose Tolerance
IL-1β	Interleukin-1 beta
IL-13	Interleukin-13
IL-4	Interleukin-4
Ilk	Integrin linked kinase
ILV	Intraluminal vesicle
IR	Insulin resistance
ITT	Insulin tolerance test
KC	Kupffer cell
KEGG	Kyoto Encyclopedia for Genes and Genomes
Krt5	Keratin 5
Krt6a	Keratin 6a
Krt75	Keratin 75
LB	Luria-Bertani
LC-MS-MS	Liquid chromatography with tandem mass spectrometry
LD	Lipid droplets
LDL	Low-density lipoproteins
Lgals3bp	Galectin 3 binding protein
LPS	lipopolysaccharide
LXR	Liver X receptor
Mac-1	Macrophage 1
MG	Monoacylglycerol
MHC	Major histocompatibility complex
Mif	Macrophage migration inhibitory factor
miRNA	Micro ribonucleic acid
mRNA	Messenger ribonucleic acid
MS	Mass spectometry
MS/MS	Tandem mass spectrometry
MTBE	Methyl-tert-butyl ether
MTTP	Microsomal triglyceride transfer protein

MVB	Multivesicular bodies
Myl6	Myosin light chain 6
Myl6b	Myosin light chain 6B
Na3VO4	Sodium orthovanadate
Na4P2O7	Sodium pyrophosphate decahydrate
NaF	Sodium fluoride
NAFLD	Non-alcoholic fatty liver disease
NCD	Normal chow diet
NCD-GDE	Gut-derived extracellular vesicle from normal chow diet-fed mice
Ndufv1	NADH:ubiquinone oxidoreductase core subunit V1
nIR	Near infra-red
NO	Nitric oxide
NPC	Non-parenchymal cell
NTA	Nanoparticle tracking analysis
OCT	Optimal Cutting Temperature compound
PBS	Phosphate buffered saline
PBS-T	Phosphate Buffered Saline with Tween-20
Pdha1	Pyruvate dehydrogenase E1 alpha 1 subunit
PFA	Paraformaldehyde
Pfkl	Phosphofructokinase, liver type
Pgam2	Phosphoglycerate mutase 2
Pgm5	Phosphoglucomutase 5
PI3K	Phosphoinositide-3 kinase
PKA	Protein kinase A
PKB	Protein kinase B
Pnlip	Pancreatic lípase
PPAR α	Proliferator-activated receptor alpha
Prdx6	Peroxiredoxin 6
Psbm1	Proteasome subunit beta 1
Psma1	Proteasome subunit alpha 1
Psma2	Proteasome subunit alpha 2
Psma3	Proteasome subunit alpha 3
Psma4	Proteasome subunit alpha 4
Psma5	Proteasome subunit alpha 5
Psma6	Proteasome subunit alpha 6
Psma7	Proteasome subunit alpha 7
Psmb10	Proteasome subunit beta 10
Psmb2	Proteasome subunit beta 2

Psmb3	Proteasome subunit beta 3
Psmb8	Proteasome subunit beta 8
PVDF	Polyvinylidene fluoride
PYY	Peptide YY
RHM	Recruited hepatic macrophages
RNA	Ribonucleic acid
ROS	Reactive oxygen species
RT	Room temperature
SCFA	Short-chain fatty acid
SDS-PAGE	Sodium dodecyl sulfate-polyacrylamide gel electrophoresis
SEM	Standard error of mean
Serpina1a	Serpin family A member 1, alpha-1-antitrypisn1-1
Serpina1c	Serpin family A member 1, alpha-1-antitrypsin1-3
SGLT2	Sodium-glucose transporter 2
SGLT3	Sodium-glucose transporter 3
Slc25a5	Solute carrier family 25 member 5
SLC30A8	Solute Carrier Family 30 Member 8 gene
SREBP1c	Sterol regulatory element-binding protein 1c
SSC	Side scatter
Suclg2	Succinate-CoA ligase GDP-forming beta subunit
Suox	Sulfite oxidase
T1D	Type 1 diabetes
T2D	Type 2 diabetes
TBS-T	Tris-buffered saline with 0,1% Tween
TCA	Tricarboxylic acid cycle
TG	Triglyceride
TLR4	Toll-like receptor 4
TNF- α	Tumor necrosis factor alpha
Txn	Thioredoxin
VAT	Visceral-adipose tissue
Vcp	Valosin containing protein
VLDL	Very-low density lipoproteins
WHO	World Health Organization
WT	Wild-type
Xdh	Xanthine dehydrogenase

Acknowledgements

Quatro anos que terminam e que contam uma viagem. Chegar ao fim desta caminhada em plena pandemia, num cenário que eu, e ninguém, jamais imaginaria, posso dizer que, no mínimo...faz todo o sentido.

Parece que tudo se resume a este "livro", que materializa todas as ferramentas que vim conquistando. Contudo, umas das componentes mais importantes que levo são as pessoas e tudo o que aprendi com elas. Esse valor é inqualificável.

Antes demais quero fazer o meu agradecimento formal às instituições que me permitiram desenvolver o meu doutoramento, o Instituto Superior Técnico, o CEDOC/Nova Medical School e a Fundação Champalimaud.

Começo também pelos principais responsáveis do meu sucesso, os meus orientadores. Quero agradecer, profundamente, à Maria Paula Macedo e ao Bruno Costa-Silva, que confiaram em mim para dar corpo a este projeto. Não só confiaram, como orientaram, no verdadeiro sentido da palavra orientar, profissionalmente e emocionalmente. Obrigada. Espero não vos ter deixado ficar mal. Tenho por vocês o maior respeito e admiração.

Logo de seguida, uma pessoa que contribuiu extraordinariamente para este projeto, e para o meu progresso. Muito obrigada Rita Oliveira. A euforia com que viveste cada êxito, a desilusão com cada insucesso, deu-me animo e força. Reconheço e valorizo muito todo o apoio que me deste, até ao último dia, sem teres qualquer tipo de responsabilidade de o fazer. És uma cientista de corpo e alma e coração.

I want to leave a very special acknowledgment to Rune Matthiesen. Thank you so much Rune for spending all that time with me, teaching me about proteomics. You not only gave me a new skill but also a new set of batteries for keep going. In the end, I really enjoyed.

Foi um privilégio ter tido a oportunidade de trabalhar em dois grupos, dois laboratórios, duas instituições.

Quero agradecer ao meu grupo no CEDOC. Ao qual ainda incluo a Margarida, que me fazia sempre sentir muito bem-vinda, e a Bárbara, que me deu umas boas lições de motivação. O Diego, que vi crescer e ficar gigante, gosto muito de ti, ajudaste-me imenso. À Maria João, que está sempre disponível, e deixa-me de boca aberta com todas as competências que tem. À Rita Patarrão, que é mega multi-tasking, e trata das contas como se fossem dela. À Ana Pina, que me deu sempre imenso apoio com o entusiasmo e interesse que demonstra no meu trabalho. Akiko you arrived more recently, but I already have a lot to thank you about, you never let me down; thank you for all the support.

Agradeço também ao Pedro que me ajudou em tantas crises de géis. Quero deixar um agradecimento especial à Inês Coelho, que é só a melhor pessoa para dar continuidade a este projeto; obrigada Inês por toda a tua ajuda, foste incansável, admiro imenso a seriedade com que encaras cada tarefa. E outro à Inês Lima, não só pela preciosa ajuda que me deu no final da linha, mas também por me ter acompanhado desde o primeiríssimo dia, sempre com algo de valor a acrescentar. Obrigada Inês, foste incrível.

Quero agradecer ao meu grupo na Fundação Champalimaud, que me adotou e fez-me sempre sentir em casa. Quero agradecer à Bruna que me disse sempre a coisa certa, na hora certa. À minha querida Joana, que é uma máquina, com uma maturidade científica fora do normal. À Sílvia, que é a minha referência de cientista, pensa e faz as coisas com uma clareza espantosa. À Ana que é outra fora de série, e se acreditar mais nela, chega onde quiser. I want to thank Julia, for the good vibes, for the color she brings, for sharing the frustrations of being a PhD student, and actually, of life in general! We complain but we always end laughing. Quero agradecer ao Cristian, por tratar sempre de tudo com uma facilidade impressionante. Ao Nuno, pela boa disposição e por adoçar o laboratório com os mimos que os doentes lhe trazem. Quero agradecer à Carol por sempre, desde o início, me fazer sentir bem e transmitir tanta calma e tranquilidade.

Quero também agradecer à Ana Vieira, que eu admiro e gosto muito, não só pelo backup na citometria de fluxo, mas pela amizade e pelas palavras sensatas.

Gostava ainda de agradecer a um grupo de pessoas que foi muito importante na minha vida e nesta tomada de decisão.

Quero agradecer à Cláudia Lobato, ao João Lacerda, à Maria Soares e à minha querida Rita Azevedo por me terem impulsionado a fazer a candidatura a doutoramento. Trabalhar com eles foi um privilégio.

Minha querida Rita, a ti deixo uma palavra especial porque foste, és, muito importante para mim. Trago um bocadinho de Rita comigo, e isso não é para todos.

E como o ser humano é todo um universo, cheio de estrelas que trocam energias, eu tive algumas que tiveram mais influencia sobre mim neste período.

Quero agradecer ao Jorge, que é o meu maior exemplo de disciplina, determinação e força. Às minhas miguxas, Diana e Márcia, que este doutoramento me trouxe; o orgulho que eu tenho delas. À Diana São Miguel e à Joana Bianchi, que foram minhas confidentes, e são duas referências para mim. À minha Cristininha e ao meu Ricardinho, que conhecê-los trouxe ainda mais cor à minha vida, vocês são o combo perfeito de diversão e trabalho. Ao André, que é o homem prodígio, com um talento gigante, que eu tive a fortuna de conhecer. Às minhas queridas hommies, Inês, Teresa e Ana, nas quais eu não podia ter tido mais sorte – viver convosco foi sagrado. Inês obrigada pela tua paz. Teresa obrigada pela tua potência. Ana obrigada pela tua perícia. Obrigada também à minha querida Mari, artista da cabeça aos pés, que me ajudou a pôr esta tese bonita e que me compreende como mais ninguém. Ainda, obrigada à minha Sara, que decidiu ter uma maluca como madrinha - mas não é por isso que eu te vou agradecer agora. Obrigada pela tua preciosa ajuda, e expertise!

Termino com o centro do meu universo. Obrigada aos melhores do mundo, os meus pais. Obrigada por me darem confiança e a certeza que, aconteça o que acontecer, no final vai mesmo correr tudo bem. Vocês iluminam o meu caminho. Obrigada à minha soul-mate, a minha irmã, que em qualquer parte do mundo que ela esteja, está comigo, e está em mim.

E vou deixar um agradecimento especial às minhas três avós guerreiras, que quanto mais velha eu fico, mais as admiro. É surreal já se ter vivido tanta coisa.

Abstract

Western-style diet is a leading cause of metabolic diseases, specifically type 2 diabetes (T2D). T2D is a systemic disease that cannot be seen from the perspective of one only single organ affected. While the liver is a fundamental player in global glucose and lipid metabolism; experimental evidences show that rearrangements of gastro-intestinal anatomy can directly affect glucose homeostasis, and not only through weight loss. In particular, metabolic surgery, initially designed to promote weight loss, can significantly improve glucose homeostasis more effectively than any known pharmaceutical or behavioural methodology, causing total remission of T2D. Therefore, understanding the importance of the intestine as a metabolically active organ is crucial for the development of novel therapies to improve metabolic health. A wide variety of circulating factors, including hormones, cytokines and chemokines work together to orchestrate the systemic response of metabolic organs to diet composition. In the last few years, a new organismal communication mode has emerged. This novel type of systemic communication is mediated by extracellular vesicles (EVs) produced via the multivesicular endosomal pathway and released by every cell. EVs are of great interest because they have the capacity to carry genetic and protein cargoes inside its membranes, along the organism. The high level of technological advance we have nowadays, both in equipment and methods of analysis, enables the detailed characterization of every protein in the cell and in the EVs. The gut plays a poorly explored role in metabolism, partially uncovered by the ameliorations of T2D after metabolic surgery and prior to weigh loss. Moreover, EVs participate in the pathophysiology of diabetes. Based on that, we hypothesize that gut derived EVs (GDE) carry a diabetogenic message from the gut to the liver, in response to high fat and sucrose diet, mimicking the western diet.

For this study we used two groups of C57Bl/6J mice fed with normal chow diet (NCD) or high fat diet (HFD). We observed that GDE from HFD-fed mice (HFD-GDE) carry more protein inside compared with GDE from NCD-fed mice (NCD-GDE). Interestingly, by proteomics we revealed that GDE protein cargo are highly affected by diet. Carbohydrates, amino acids and lipids metabolism-related proteins are noticeable affected in HFD-GDE, being the latter ones particularly up-regulated, in opposition to the ones involved in glycolysis. Additionally, proteins involved in fatty acid metabolism, as well as oxidative stress are up-regulated, both are critical pathways underlying prediabetes development. That might also explain why proteins related with the oxidative milieu appear up-regulated in the HFD-GDE. On the other hand, proteasome-related proteins, that are responsible for the degradation of polyubiquitinated composites are extremely down-regulated in HFD-GDE, revealing a typical pathological profile; this will eventually lead to the accumulation of misfolded, damaged and unnecessary proteins causing a disruption in normal cellular function and can even cause cell death. Importantly, decrease proteasome function has been reported in a broad array of chronic diseases.

In a second stage, chronic exposure of healthy mice to HFD-GDE revealed that GDE have affinity to the liver and are preferentially up-taken by the resident macrophages of this tissue, the Kupffer cells (KC), that are described to trigger an inflammatory response under metabolic stress. Moreover, we observed that HFD-GDE mice livers manifested increased levels of triglycerides. Collectively, these evidences further strength that the altered protein content in HFD-GDE are translated into hepatic biological alternation, revealed by the upregulation of lipid metabolism related proteins in HFD-GDE and the concomitant augment in triglycerides hepatic content.

In summary, we demonstrated that GDE are vehicles of communication in the entero-hepatic axis, and disclosed lipids as their relevant cargos. Thus, corroborating our hypothesis that GDE content is altered by different dietetic scenarios and their cargos reflect the environment of the producer cell,

which in turn signals to the gut. The proficiency of HFD to alter the proteome of GDE and, these ones to increase the hepatic lipid content indicates that GDE carry lipids from the gut to the liver. Our findings suggest that GDE translate diet alteration into a prediabetic hepatic dyslipidaemia signature.

Key-words: prediabetes, extracellular vesicles, gut, liver, lipids

Resumo

As dietas hipercalóricas, características da sociedade ocidental, estão diretamente associadas ao desenvolvimento de doenças metabólicas como é o caso da diabetes tipo 2 (DT2). Esta é considerada uma epidemia mundial, atingindo números alarmantes e despesas colossais. No sentido de prevenir a DT2 é crucial a deteção e intervenção precoce, nomeadamente na prediabetes, identificada como um estado inicial da doença, no qual ainda é possível reverter o quadro clínico através de alterações do estilo de vida. Apesar do papel fundamental do fígado no metabolismo de glucose e lípidos, um dos órgãos que se tem mostrado particularmente relevante no controlo da doença é o intestino. A cirurgia metabólica, inicialmente desenvolvida para o tratamento da obesidade mórbida, mostrou ter elevadas taxas de êxito na remissão da DT2. De salientar, que esta remissão ocorre antes da acentuada perda de peso, indicando que o intestino por si desempenha uma função primordial no controlo da DT2; contudo o mecanismo molecular subjacente a este controlo ainda não está clarificado. Desta forma o intestino ganha um papel de relevo como órgão metabolicamente ativo e potencial alvo no diagnóstico precoce e intervenção terapêutica na DT2. A homeostasia metabólica é atingida através de uma intrincada comunicação entre os diversos órgãos. Variados mediadores circulatórios, como é o caso de hormonas e citocinas participam na resposta sistémica dos diferentes órgãos metabólicos às alterações externas, nomeadamente à dieta. Nos últimos anos, foi descrito uma nova forma de comunicação no organismo denominadas de vesículas extracelulares (VE). As VEs são produzidas a partir de corpos multivesiculares formados pela via endossomal e posteriormente libertados para o meio extracelular. As VEs transportam, dentro da sua dupla membrana, material genético e proteico, assim como lípidos, de uma célula para outra vizinha, ou distante. Sabendo que os enterócitos libertam VE, neste trabalho avaliamos a hipótese de que o "millieu" intestinal, no contexto da dieta hipercalórica no modelo de prediabetes, é modificado originando alterações do conteúdo proteico das VEs derivadas do intestino (VE-intestinais) que, por sua vez, têm um efeito diabetogénico ao comunicar com o fígado, nomeadamente com as células de kupffer, responsáveis por ativar o processo inflamatório característico da T2D.

Neste contexto, murganhos C57/Bl6J foram expostos a dieta normal e dieta hipercalórica durante 12 semanas, em dois grupos. As VE foram isoladas diretamente do intestino limpo, garantindo que não há contaminação de microbiota, a partir de um processo de separação por gradiente de tamanho, e adicionalmente, de densidade. Estas VE-intestinais foram analisadas pelo seu tamanho e quantidade a partir de um equipamento de rastreio de nanopartículas. Uma caraterização detalhada ao conteúdo proteico das VE-intestinais, foi efetuado por espectrometria de massa e consequente análise proteómica com ferramentas bioinformáticas.

É de evidenciar que o perfil proteico das VE-intestinais de animais submetidos a uma dieta hipercalórica é amplamente alterado, concluindo que há uma clara influência da dieta no conteúdo proteico das VE-intestinais. As VE-intestinais de animais submetidos a uma dieta hipercalórica, para além do número de proteínas ser maior, também o seu perfil proteico está significativamente alterado, quando comparadas com VE-intestinais de animais saudáveis.

Observámos que proteínas específicas envolvidas em vias metabólicas de hidratos de carbono, aminoácidos e lípidos estão significativamente afetadas. Nomeadamente uma diminuição de proteínas associadas à via de degradação de glucose.

No entanto, as vias utilizadas por ácidos gordos encontram-se aumentadas, tanto no que toca ao catabolismo de ácidos gordos para produção de energia como de armazenamento na forma de triglicéridos.

Analogamente às vias associadas ao metabolismo proteico, observamos que vias associadas a amino ácidos essenciais aparecem bastante alteradas. As vias de síntese de aminoácidos de cadeia curta, que são produzidos a partir da atividade microbiana também se encontram aumentadas. É interessante observar que, embora as VE sejam exclusivamente de origem celular intestinal, refletem efeitos da relação simbiótica que a flora intestinal tem com o intestino, evidenciada aqui em consequência do regime nutricional.

Nas VE-intestinais também se observa um aumento, tanto em número como em expressão, de proteínas com função protetora contra o stress oxidativo. Stress oxidativo este muito característico de ambientes hipercalóricos onde as vias lipídicas e mitocondriais estão sobre ativadas. O que está em conformidade com o cenário fisiopatológico em estudo.

Neste seguimento, vemos também, e de uma forma muito clara, que as proteínas do proteossoma, se encontram expressivamente diminuídas nas VE-intestinais de animais submetidos a dieta hipercalórica. Este resultado sugere a função celular estar comprometida, consequente da diminuição da principal via de degradação proteica.

Estabelecido que as VE-intestinais se encontram alteradas pela dieta fizemos, seguidamente, o estudo do seu efeito no organismo. Para avaliação do tropismo das VE-intestinais e do seu potencial efeito fisiopatológico na disseminação da prediabetes, injetámos VE-intestinais, marcadas com fluorescência, em animais wild-type.

Após injeção retro-orbital de VE-intestinais previamente marcadas em animais wild-type, observámos que estas vão preferencialmente para o fígado, em específico para as células de Kupffer, que são os macrófagos residentes deste tecido, com grande capacidade fagocítica, o que facilita a captação preferencial. O papel das células de Kupffer no metabolismo hepático tem sido recentemente evidenciado como principal ativador de inflamação.

Com o objetivo de analisar o papel das VE-intestinais no fenótipo prediabético, injetámos três vezes por semana, durante seis semanas, VE-intestinais de animais submetidos a dieta hipercalórica e VE-intestinais de animais submetidos a dieta normal, e analisámos alguns parâmetros metabólicos. Deste modo, e sabendo que as VE-intestinais vão maioritariamente para o fígado, observámos que, após as seis semanas, os animais não manifestam alterações estatisticamente significativas na tolerância à glucose e na resistência à insulina. Por outro lado, os fígados destes animais apresentam níveis de triglicéridos alterados, com um perfil gradual, ou seja, aqueles que apresentam valores mais elevados de triglicéridos são os animais injetados com VE-intestinais de animais submetidos a dieta hipercalórica.

Estes resultados evidenciam uma relação muito interessante com a análise proteómica feita previamente. Sobressai que VE-intestinais de animais submetidos a dieta hipercalórica contêm um aumento de proteínas envolvidas no metabolismo lipídico. Em concordância, também identificámos uma família de enzimas, as ACOT, que está extremamente aumentada, e participam no direcionamento de ácidos gordos para a síntese de triglicéridos.

Em suma, relativamente à nossa hipótese , observamos que as células intestinais são produtoras de VEs, e que as VE do intestino sofrem alterações em contexto de prediabetes. O intestino como órgão primordial na digestão e absorção dos nutrientes, obriga às células intestinais ajustarem o seu mecanismo face à dieta. As VE-intestinais vão conter mensagens que refletem estas alterações transportando-as para o fígado onde o seu conteúdo vai ser depositado. Visto haver grande acumulação de triglicéridos no fígado dos animais injetados, uma hipótese é que as VE-intestinais estejam a transportar lípidos, provenientes da dieta, do intestino para o fígado. Contudo, precisamos de mais dados para poder tirar essas conclusões.

Finalmente, com este trabalho destacamos o impacto da dieta nas VE-intestinais e no papel que estas pequenas vesiculas podem ter como portadores de conteúdos funcionais, dos quais destacamos os lípidos, tanto em contexto de doença como de saúde.

Palavras-chave: Prediabetes, vesículas extracelulares, intestino, fígado, lípidos

Chapter 1

Introduction

1. Prevalence of diabetes and economic impact

Diabetes is a chronic metabolic disease, of multiple etiology, characterized by hyperglycemia as a result of insulin deficiency and/or decreased insulin action. The prevalence of diabetes worldwide is exponentially increasing because of a combined interplay of factors such as socioeconomic, demographic, environmental and genetic. Despite all the diabetes awareness campaigns run by multiple international organizations aiming at informing the public of the causes, symptoms, complications and treatments associated with the condition, western societies are still not totally convinced that lifestyle has a huge impact on health. This is clearly demonstrated by the positive correlation between diabetes incidence and obesity, frequently associated with sedentarism and an unhealthy diet. A poor diet , rich in fat and sugar, with large intake of finely processed grains and starchy carbohydrates have been shown to be directly associated with this disease (Hamdy et al. 2018).

The International Diabetes Federation (IDF) in 2000 estimated 150 M adult people worldwide had diabetes. Shockingly, this number triplicated in 2019 and today there are almost 500 M people with diabetes and the projections for the future clearly indicate that the global impact of this disease will continue to increase substantially (Fig. 1), 11% of global deaths are related with diabetes (IDF 2019). In Portugal, in 2015, The Portuguese National Observatory of Diabetes assessed that 13% of the adult population had diabetes and, approximately, half of those were not diagnosed (Observatório Nacional da Diabetes 2016).

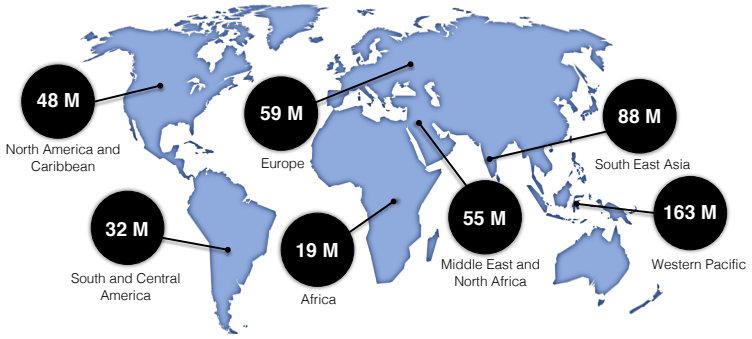

Figure 1. Prevalence of diabetes worldwide in 2019 in adults (aged between 20-79 years). Representation of the number of people living with diabetes around the world, by IDF region, accounting that ~90% of the cases are of type 2 diabetes (T2D) (adapted from IDF, 2019).

An important matter of remark is the health costs due to diabetes. The expenditure has been rising considerably over the years. IDF estimated, in 2019, that total diabetes-related health spending reached 680 billion euros. The economic impact of diabetes is expected to grow year by year (IDF 2019). In Portugal, the last studies in 2015, diabetes predicted costs were near 1100 million euros, that represents 12% of the expenses in health (Observatório Nacional da Diabetes 2016). Clearly by preventing the growth of the disease, by performing high quality fundamental research, we will positively impact not only on global well-being but also on decreasing the public and out-pocket-spending on health; and importantly this may grant access to quality health care systems to underprivileged groups.

2. *Diabetes mellitus*, the disease

Diabetes mellitus, or diabetes, is a condition characterized by high levels of glucose in peripheral blood due to an impairment in the production of the hormone insulin or in the inability to use it effectively.

Insulin is a hormone produced in the pancreatic β-cells that allows glucose from the bloodstream to enter the body's cells where it is converted into energy. The deficiency or the incapacity of cells to respond to insulin gives rise to high levels of blood glucose – hyperglycemia – which is a clinical indicator of diabetes.

There are two main forms of diabetes, type 1 (T1D) and type 2 (T2D), with the second one accounting for the vast majority (~90-95%) of total prevalence.

Type 1 diabetes (T1D) is an autoimmune disease in which the immune system attacks insulin-producing β-cells of the pancreas. Therefore, these cells produce very few or no insulin at all. The causes are not fully understood but one liable explanation is the combination of genetic susceptibility and an environmental trigger, such as viral infection. There are also evidences of toxins or some dietary products to be implicated (Barnett 2018). This condition can appear at any age, although in children and young people occurs more frequently.

2.1. Type 2 Diabetes

Type 2 Diabetes (T2D) is characterized by hyperglycemia and insulin resistance (IR). One leads to the other in a relation cause-consequence but it is still not clear which one happens first. This state is characterized by an initial intensification of insulin production known as hyperinsulinemia. At this point the disease enters in a stage called intermediate glycemia or prediabetes, that will be discussed in more detail later on. Consequently, in order to keep up with the demand, pancreatic β-cells may start to fail resulting in inadequate production of insulin. At the same time, another factor contributing for hyperinsulinemia is the decreasing rates of insulin clearance over time. Insulin clearance determines the availability of insulin in the systemic circulation. Insulin is produced in the pancreas but 50-80% is degraded, in great extent by the liver, working as a buffer of accessible insulin (Henry 1998; Najjar and Perdomo 2019) (Fig. 2). Frank diabetes occurs when the glucose levels surpass either in fast or postprandially states of homeostasis.

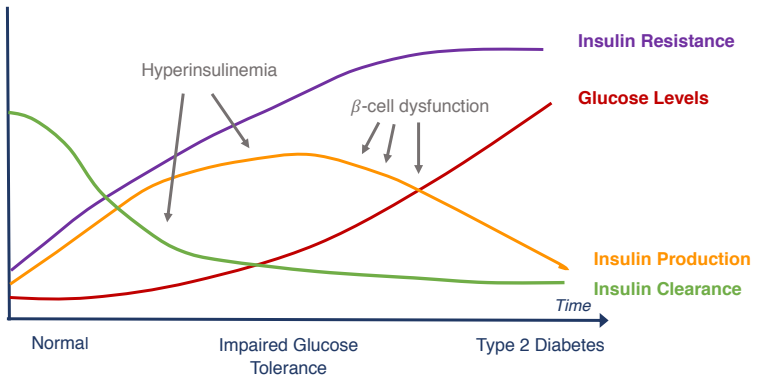

Figure 2. Time-course evolution curves from healthy stage to T2D stage. Curve in purple shows the progress of insulin resistance over time; curve in yellow is about insulin production development along time; curve in green is insulin clearance decreasing; the inter-play of this three determines the curve in red that represents glucose levels growth. The x-axis denotes the advancement with time from normoglycemia to intermediate hyperglycemia and hyperglycemia in T2D (adapted from Henry, 1998).

Frequently, the manifestation of T2D is not noticeable and the condition may be symptomless. Also, the exact time of the onset of T2D is usually impossible to precisely determine. As an effect, there is a long pre-diagnostic period and is estimated that 50-80% of people with T2D in the population may

be undiagnosed. That is why, by the time of the diagnosis, typically there are already more than one associated comorbidity. More importantly, in the prediabetic state some of these comorbidities are already installed (Tabák et al. 2012). The causes of T2D are not entirely understood but it is known that it is triggered by a combination of genetic predisposition and environmental factors.

T2D has a heritability range of 20%-80% and that evidence comes from a variety of population, family and twin-bases studies. Certain mutations in genes are associated with glucose levels control, insulin production and regulation and how it is sensed in the body. The advent of genome-wide association (GWA) studies led to identification of some genes, namely *IGF2BP2, HHEX/IDE* and *SLC30A8*, with a role in T2D development (Hansen 2002; Saxena et al. 2007; Zeggini et al. 2007).

Environmental factors known to impact the development of T2D include stress, sedentary lifestyle, obesity and diet, that is already naturally related with obesity. Adoption of western diet patterns, characterized by a high consumption of meats as well as refined foods, sugary beverages and fast-food has shown to be related with increased numbers of T2D in developing countries (Qi et al. 2009).

2.2. Diabetes associated comorbidities

There are several comorbidities associated with T2D explaining its tremendous social and economic impact (Fig.3).

The most common cause of both morbidity and mortality associated are cardiovascular diseases. The risk of coronary vascular disease is extremely increased by insulin resistance, as inflammation, endothelial dysfunction, and glucose has many toxic effects on microvasculature (Gerstein 2015; Paneni et al. 2013). Other diabetes complication is diabetic eye disease, specifically diabetic retinopathy, that is one of the leading causes of blindness worldwide (Bunce and Wormald 2006; World Health Organization 2015). Also, chronic kidney disease is often associated to diabetic patients with hypertension (Coresh et al. 2003; Steinke 2009). Noticeably, one major cause of lower limb amputation is the diabetic foot, that is a consequence of peripheral neuropathy affecting the distal nerves of the limbs, predominantly those of the feet (Moxey et al. 2011; Davies et al. 2006). High blood glucose is also associated to increased blood pressure and high triglycerides (TG) and cholesterol, named dyslipidemia. The combination of these factors is generally called metabolic syndrome, leading to other pathologies like non-alcoholic fatty liver disease (NAFLD), which initial phase is accumulation of fat in the liver known as liver steatosis (Perry et al. 2014) and compromised gut permeability associated with general inflammatory over-state (Gurung et al. 2020). NAFLD includes a spectrum of liver diseases initiated by liver lipid accumulation and progression up to cirrhosis and, in more severe cases, hepato-carcinoma. NAFLD seems to be a risk factor for diabetes and vice-versa: in Europe, the latest numbers estimated that 70% of T2D patients also have NAFLD. Indication of NAFLD increases the occurrence of T2D and rushes the development of its complications. Intrahepatic fat accumulation activates liver inflammation that additionally aggravates dyslipidemia and hypertension. On the other hand, T2D and systemic IR cause increase of free fatty acid (FFA) influx from peripheral organs to the liver, leading to NAFLD progression (Xia, Bian, and Gao 2019).

The gut is directly affected by T2D, specially driven by diet, since the microbiota composition changes. By interacting with dietary constituents, microbiota modulates inflammation and affects gut barrier, causing metabolic endotoxemia, allowing the passage of lipopolysaccharides (LPS) derived from intestinal bacteria to the bloodstream (Gurung et al. 2020). Alterations in intestinal barrier integrity will have consequences on glucose and lipid metabolism, insulin sensitivity and overall energy homeostasis (Chelakkot et al. 2018).

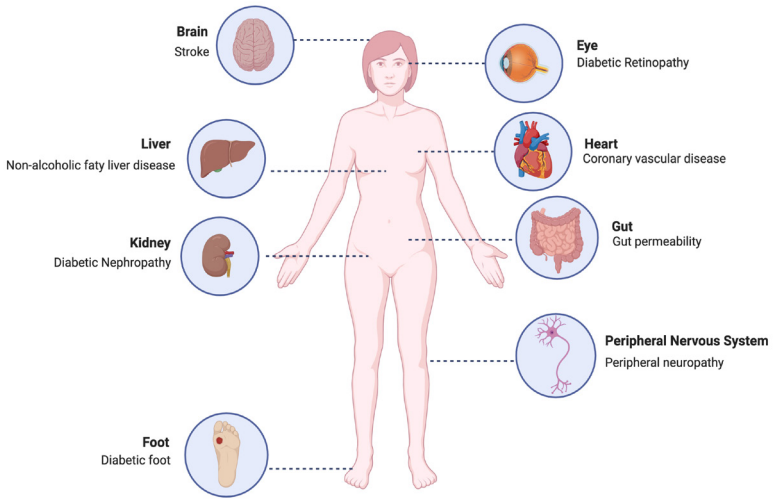

Figure 3. Comorbidities associated with diabetes. Diabetes is manifested by high blood glucose that has a deleterious impact upon the whole organism. The most common complications associated are stroke, in the brain; diabetic retinopathy, in the eye; coronary vascular disease linked to high blood pressure, in the heart; non-alcoholic fatty liver disease, in the liver; diabetic nephropathy, in the kidney; permeability impairment in the gut; peripheral neuropathy, that affects the peripheral nervous system; and finally diabetic foot.

Other critical diseases like cancer are also at greater threat in T2D patients. Mortality rates are increased in these individuals, making T2D a cause of concern in relation to global cancer impact (Tsilidis et al. 2015; Pearson-Stuttard et al. 2018).

Generally, diabetes patients are at major risk of several complications specially because the fluctuations in blood glucose levels compromises the immune system. It is also unclear whether T2D is a predisposing factor to emerging diseases, such as COVID-19 (Fang, Karakiulakis, and Roth 2020).

It is not new that diabetes itself is an epidemy, it has been for years the spotlight of medical sciences, pharmaceuticals, public health, and many others areas of research, however it is not solved and we believe the sooner it is detected, the better it can be fixed or even, avoided.

3. Prediabetes: the opportunity for intervention

The diagnosis of diabetes is based on blood glucose concentration. The amount of glucose in circulation results from the balance of its usage and storage that is, fundamentally, the glucose metabolism. Nevertheless, there is a period termed prediabetes or intermediate hyperglycemia that is an early stage of T2D, characterized by blood glucose levels above the normal range, but still below the recommended diabetes diagnostic (Fig. 4). Nevertheless, the levels of systemic glucose are directly related with insulin activity, since it is the responsible for facilitating cellular glucose uptake (Fargion et al. 2005).

The identification of prediabetes is not straight forward, as glucose concentrations increase not only in the fasting state but also can be increased postprandially, which is not usually evaluated in the clinical setting. Figure 5 represents the threshold values used to categorize from prediabetes to diabetes. Prediabetes can be characterized by impaired glucose tolerance (IGT), or impaired fasting glucose (IFG) or both, at a smaller scale. The table is in accordance with the parameters followed by World Health Organization (WHO). American Diabetes Association (AAA) also includes glycated hemoglobin (HbA1c) as a parameter, if people present 5.7% to 6.4%, of IFG.

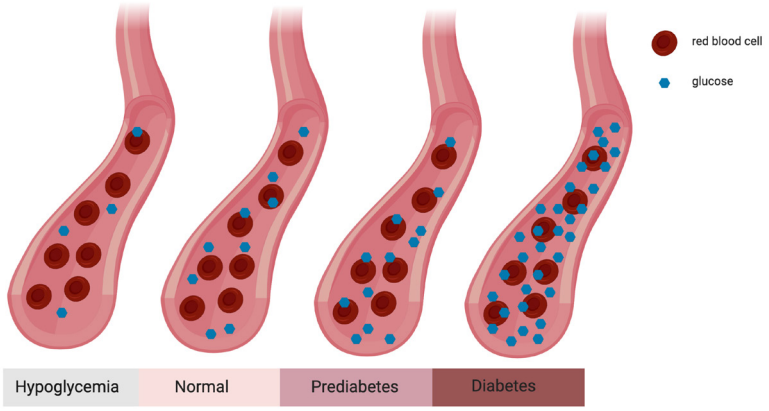

Figure 4. Schematic representation of glycemic profiles in peripheral blood circulation. From left to right it is illustrated the four different scenarios of blood glycemia; hypoglycemia, levels of glucose (in blue) under the necessary; normoglycemia, with balanced ration between red blood cells (in red) and glucose; prediabetic stage, with glucose levels above the expected already evidencing hyperglycemia; and diabetic stage with glucose levels excessively increased (adapted from Observatório Nacional da Diabetes 2016).

Recognition of IGT and IFG is extremely relevant, as they not only represent high risk to develop T2D, but also opens the opportunity for intervention and prophylaxis. Progression from IGT and IFG to T2D depend on the extent of hyperglycemia but it is known that other factors matter, like age, weight, sex and ethnicity (Tabák et al. 2012). The incidence of T2D five years after diagnosis for IGT and IFG are of 26% and 50%, respectively (IDF 2019). There is a big lack of information on the prevalence of prediabetes worldwide, but if we use Portugal as reference, the last studies in 2016, point out for ~30% of the population to have prediabetes (Observatório Nacional da Diabetes 2016). Extrapolating for the globe, this represents more than one third of the people, which, on top of that, are not aware of their condition which may be silently aggravating over time.

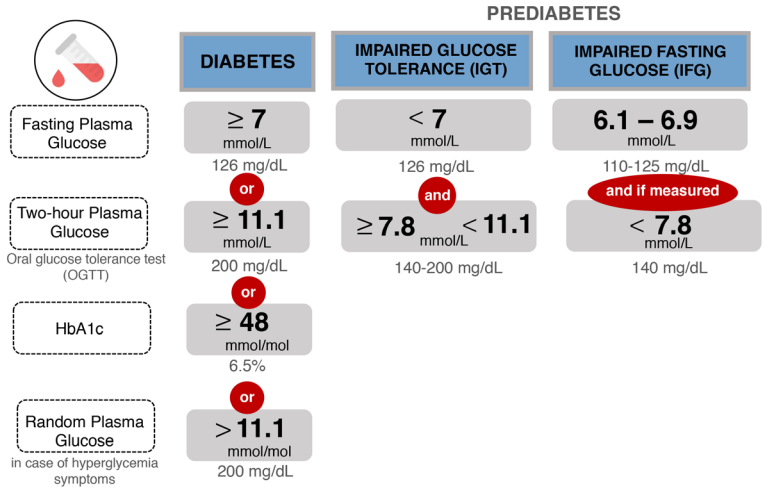

Figure 5. Parameters of diagnostic criteria for diabetes and prediabetes. Diabetes and Prediabetes can be due to impaired glucose tolerance (IGT) or impaired fasting glucose (IFG), or both. It can be diagnosed by one of the four blood glucose measure methods: fasting plasma glucose; two-hour plasma glucose; glycosylated hemoglobin (HbA1c) random plasma glucose. In the grey boxes are the threshold values for each parameter. Fasting is defined as no caloric intake for at least 8 hours and the 2-hour postprandial glucose test should be performed using a glucose load containing the equivalent of 75g anhydrous glucose dissolved in water (adapted from IDF, 2019).

3.1. In health: glucose homeostasis in fasting and fed state

Before understanding the pathological state of diabetes, preceded by prediabetes, when glucose homeostasis is impaired, it is necessary to clarify the physiological mechanism. In order to always have energy available for our basic functional needs, and because humans feed intermittently, our organism built a dynamic network of permanent supply of metabolic fuels – carbohydrates, lipids and proteins – to the tissues. Carbohydrates are broken down into monosaccharides, such as glucose and fructose. Lipids are commonly addressed as fat and are turned into fatty acids (FA). Proteins are degraded into amino acids. Noteworthy, glucose is the main source of energy used by our organs, the brain in particular uses it exclusively. Glucose results from the digestion of carbohydrates, is absorbed in the gut, and it is consequently stored in the form of glycogen in other tissues. Basically, our body has a storage of energy that can be mobilized efficiently to the tissues when in need.

In the fasting state, after an overnight fast, the liver is the responsible for providing glucose, either by breaking down its own stores of glycogen via glycogenolysis or by synthesizing glucose from gluconeogenic precursors via gluconeogenesis. The regulation of hepatic glucose production is largely done by the action of insulin. During prolonged fasting periods, the scenario is different – ketone bodies are used as major fuel. They are formed in the liver from the oxidation of FFA. During fasting, the basal rate of tissue glucose uptake is correspondent to the rate of glucose output by the liver (DeFronzo and Ferrannini 2015).

In response to an increase in blood glucose and amino acids levels after a meal, in the fed state, that fine balance between hepatic glucose production and tissue glucose utilization is disrupted. Maintenance of normal glucose homeostasis is dependent on insulin secretion that is stimulated in response to tissue glucose uptake that suppresses hepatic glucose production. In the presence of insulin, the liver inhibits glucose production and shift its functions to glucose storage (glycogenesis) and usage as energy (glycolysis). The liver, together with the pancreas, regulates the levels of plasma insulin. While these two organs are key regulators of organismal insulin levels the gut also plays a fundamental role in insulin homeostasis. In that context, the gut secretes hormones, addressed as incretins, that will positively increment insulin. The two incretins responsible for that is glucagon-like peptide 1 (GLP-1) and glucose-dependent insulinotropic peptide (GIP) that potentiate insulin secretion and hepatic glucose uptake. In the muscle, insulin will promote glucose and FA uptake (Kelley 2005). In the adipose tissue, insulin will inhibit lipolysis and promote glucose uptake to be converted into lipids (adipogenesis), also it will stimulate the uptake of TG and protein synthesis (DeFronzo and Ferrannini 2015). Glucose will also be transported to the β-cells in the pancreas, intensifying insulin production, meaning that insulin has a positive feedback on its own metabolism.

Counteracting insulin action, there is glucagon, another hormone produced in the pancreas, in the α-cells. Glucagon has the opposite effect of insulin, showing up with a central role during the fasting state where it is responsible for keeping the concentration of glucose and FAs in the bloodstream balanced and high enough for our body's need.

Figure 6 summarizes, in a simplified manner the complex regulation of glucose homeostasis by these two hormones: during the fed state – insulin – and when in the fasting state – glucagon (Bedinger and Adams 2015).

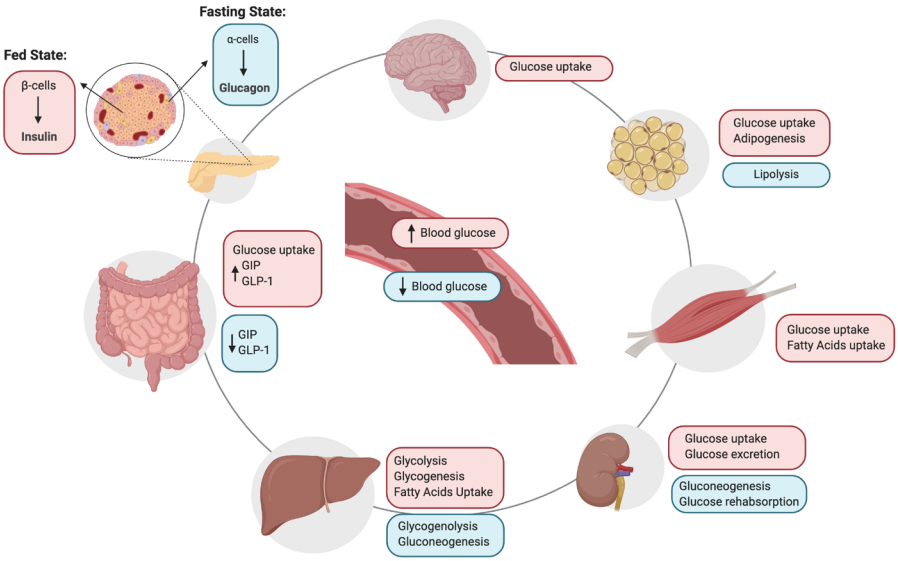

Figure 6. Summary of glucose homeostasis in post-prandial and fasting state. After a meal, glucose reaches the blood mainly through the gut where it is absorbed and incretins are released (GIP and GLP-1). They act in pancreas stimulating the secretion of insulin triggered as soon as glucose reaches the blood. Insulin promotes the uptake of glucose by the peripheral organs, especially muscle and adipose tissue. The kidney, the last line of selectivity, plays an important role regulating glucose levels, when in fasting instead of excretion it reabsorbs glucose to the blood. The liver, in fasting conditions is the main source of glucose, through glycogenolysis and gluconeogenesis, allowing the brain to always have glucose available; in the post-prandial, inhibits glucose production and stores it. At this point the adipocytes start to produce energy by lipolysis. In fasting state, the hormone in charge is the glucagon, that has the opposite effect of insulin. GIP: Glucose-dependent insulinotropic peptide peptide; GLP-1:Glucagon-like peptide 1

3.2. In disease: insulin resistance effect

Now, talking about the disease state, one of the features of T2D is IR, but it is established that IR starts very early in time, even before the disease, and can be an indicator of prediabetes. While it is still a matter of discussion what happens first, IR, hyperglycemia and β-cell dysfunction, are undoubtedly in the core of prediabetes (Kahn 2003). IR by definition is the inability of the body to respond appropriately to circulating insulin, therefore euglycemia is lost.

Again, the usage of glucose depends on the balance between insulin and glucagon production by the pancreas and degradation, done majorly by the liver. This asks for a close inter-organ crosstalk to keep up with the organisms' requirements (Petersen and Shulman 2018) (Fig. 7).

IR in the pancreas leads to a dysregulation of hormone's secretion both by β and α-cells. The latter ones become less responsive to insulin inhibitory effects (Ferrannini, Gastaldelli, and Iozzo 2011) and the β-cells, for being under extreme demand of insulin secretion, start to fail leading to the other major feature of prediabetes – β-cells dysfunction (Defronzo 2009).

After a meal, proteins, lipids and glucose are absorbed by the gut. The gut is responsible for the secretion of a class of hormones, called incretins that play a primary role in the regulation of the amount of insulin that is secreted by the pancreas. The two incretins that share common actions in the pancreas are GLP-1 and GIP (Kim and Egan 2008). Upon a pathologic scenario, there are abnormalities in this incretin axis. In prediabetes it is observed deficiency of GLP-1 and resistance to the stimulatory effect of GIP on insulin secretion (Defronzo 2009) contributing for the general state of hyperglycemia.

In the post-prandial state, FFA uptake by the liver is increased and consequently FFA hepatic oxidation happens. This oxidation stimulates the activity of key gluconeogenic enzymes and provides

energy (Ferrannini et al. 2004). IFG, one of the phenotypes of prediabetes, characterized by high levels of glucose in the fasting state, is characterized by accelerated rate of hepatic glucose production that is directly related with hepatic IR (Campbell et al. 2020).

Moreover the kidney contributes for this imbalance by increasing glucose absorption back to the blood flow instead of excrete it, therefore further contributing for the aggravation of the hyperglycemia as the glucose transporters SGLT2 in the proximal tubules are overexpressed (Ferrannini, Gastaldelli, and Iozzo 2011; Defronzo 2009).

Adipose tissue IR leads to the continuously FFA stratification, giving rise to an excessive FFA release into the bloodstream. As consequence, FFA start to be preferentially uptaken, instead of glucose, from insulin target tissues. In fact, studies have demonstrated that lipid oxidation rates increase in negative correlation with glucose oxidation, causing a phenomenon named metabolic inflexibility (Kelley 2005).

Skeletal muscle IR causes impaired glucose uptake after a meal and contributes to post-prandial hyperglycemia (Defronzo 2009). IGT, which is described by high glucose levels in the postprandial state, even though its etiology is complex, appears to be characterized by high muscular IR (Campbell et al. 2020).

In conclusion, our organism functions as a whole system very well organized and regulated. When it comes to its metabolism there are main players with very specific roles. Figure 7 (Alfa et al.2015) summarizes the participants, and the need of a close communication among each other by using a common route, the blood flow. Dysregulation of any organ will consequently affect the others and a general defective state is created, like the prediabetic state. This leads to a succession of negative feedbacks, accumulating dysfunctional responses and along the time it culminates in an endpoint of disease.

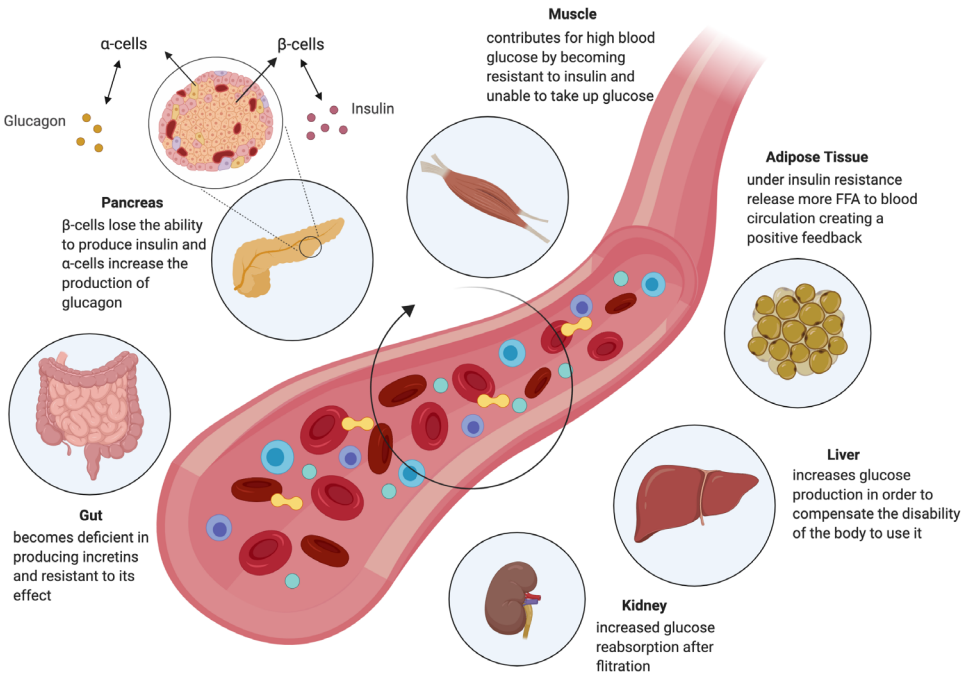

Figure 7. Metabolic organs cross-talk among each other and blood circulation. Representation of the main tissues with metabolic function and the effect of insulin resistance in each one of them. Muscle is the tissue with higher demand of glucose, especially during exercise, adipose tissue is the major store of energy, liver has the ability to produce glucose in fasting, kidney filtrates the glucose from blood, gut is the first tissue absorbing glucose after a meal, and pancreas is where insulin and glucagon are constructed (adapted from www.cisbio.com/diabetes-and-metabolic-disorders) (Ii, n.d.).

3.3. Clinical approaches

The best way to prevent prediabetes, and avoid T2D, is focus on lifestyle, especially diet and exercise. When it is no longer possible, or hard to keep it for a long-term, the approach needs to be more complex by combining changes in routine with pharmacological interventions. Drug therapy needs to be precise to each case individually and consists, generally, in an initial phase of hypoglycemic agents and, later on, intensification strategies to maintain glycemic control. Invariably the sooner the intervention, the better the outcomes (Marín-Peñalver et al. 2016). This is why early diagnosis of prediabetes is so important – it is the only way of effectively counteract T2D. Several therapeutic approaches have been done for T2D, from oral, to injectable agents, to surgical procedures. The most common ones are the insulin sensitizers, such metformin and thiazolidinediones, that have some evidences of effectiveness. Metformin for example inhibits gluconeogenesis in the liver and improves both hepatic and peripheral IR; thiazolidinediones acts on muscle, adipose tissue and liver to increase glucose utilization, decrease its productions, improving IR (Xia, Bian, and Gao 2019). Injection of insulin analogues with short and long-actions is used in a later stage as treatment for T2D. However, the only procedure able to completely revert T2D is metabolic surgery (Rubino 2008).

3.3.1. Metabolic surgery: the only efficient practice

Given the global social-economic impact of T2D, the pharmaceutical industry has been working for many years on tackling it from all possible ways. Curiously, the only procedure that demonstrated to be capable of T2D remission is metabolic surgery (Pareek et al. 2018; Kashyap et al. 2010; Buchwald et al. 2009; Singh, Singh, and Kota 2015). Surgical operations with intestinal diversion and mainly duodenal-jejunal exclusion, have reliably shown positive effects on glucose homeostasis (Aguilar-Olivos et al. 2016). Essentially, metabolic surgery consists on ways of manipulating gastrointestinal tract (Koliaki et al. 2017).

Bariatric surgery, initially called like that, started to be done to treat obesity (generally characterized by body mass index ≥ 30 kg/m2) (Pareek et al. 2018) but it showed to be effective in inducing remission of T2D before any significant weight reduction (Mingrone and Castagneto-Gissey 2014). Inclusively, the name metabolic surgery comes from the metabolic implications that the surgery revealed to have (Pareek et al. 2018; Batterham and Cummings 2016).

After metabolic surgery, diabetes starts to improve within days to weeks, while weight loss occurs more slowly and later in time. This suggests that the mechanisms of metabolic benefit extends beyond of weight loss by itself (Pareek et al. 2018; Singh, Singh, and Kota 2015). Figure 8 represents a very simplified model of the potential effect of metabolic surgery on glucose metabolism (Pareek et al. 2018). Despite the pathophysiology being not well understood, clearly the gut is a major player in glucose homeostasis.

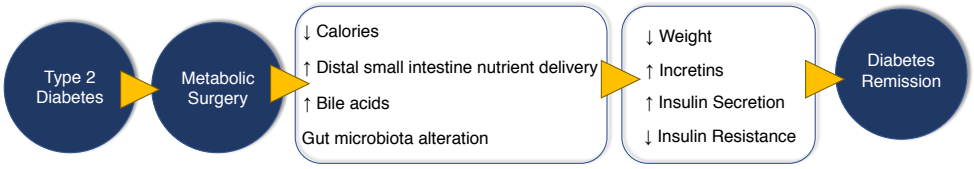

Figure 8. Potential effects of metabolic surgery in glucose metabolism. Several physiological alterations observed after metabolic surgery contribute to its metabolic benefits. Caloric restriction; increased nutrient delivery to the distal part of the small intestine; increased bile acid concentrations; and changes in the gut microbiome contribute to weight loss and favorable hormonal changes that will stop insulin resistance and consequently revert diabetes, eliminating comorbidities associated. Arrow down: decrease; arrow up: increase (adapted from Pareek et al. 2018).

4. The Gut

Many therapies for T2D target several organs, namely the pancreas, adipose tissue, muscle, kidney and liver; curiously, the most effective strategy involves the gut. Gut, or intestine, consist of two very different parts, small intestine and large intestine. We will focus on small intestine, which is responsible for nutrient absorption and metabolism.

4.1. Small intestine anatomic structure and cellular organization

In order to digest and absorb the nutrients the gut has to keep the integrity of its anatomical structure. The small intestine is around 6 meters long and has 2.5 cm of diameter and is composed by three distinct zones. The first 25 cm is the duodenum, curving downwards after leaving the stomach and until the middle of the abdomen; the jejunum accounts for the 2 meters followed and finally the ileum is about 2.5-3 meters long (Fig. 9).

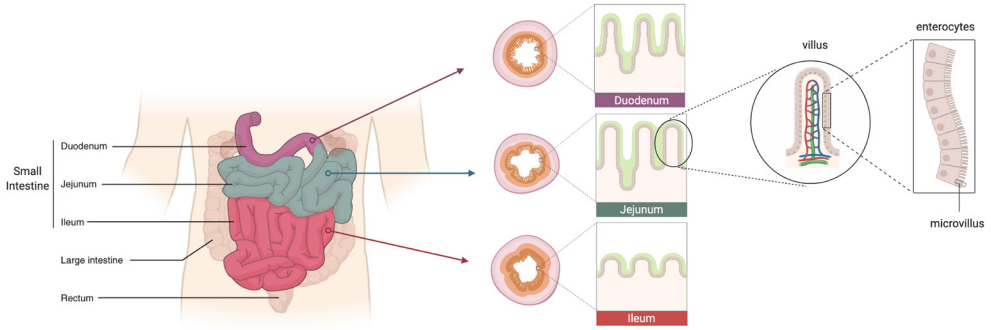

Figure 9. Anatomic representation of the small intestine. The intestine is divided in two parts with some differences in anatomy and behavior – the small intestine and the large intestine. The small intestine comprises three areas: duodenum, jejunum and ileum. The intestine is covered by smooth muscle in the outside. The inside is covered by a mucous (green layer) around each villus. The villi are constituted by enterocytes that also have small villi themselves, the microvilli (adapted from https://courses.lumenlearning.com/suny-ap2/chapter/the-small-and-large-intestines/).

The intestine is formed by a single layer of tall columnar cells that are epithelial cells of different types: i) enterocytes, the primary and more predominant; ii) paneth cells that secrete antimicrobial substances; iii) goblet cells which produce mucins, responsible for the mucus layer above; iv) enteroendocrine cells, that secrete hormones; v) tuft cells that have immune function, ready for immunity responses; and vi) stem cells, that are proliferative cells and live in the invaginations what allows the renewal of the epithelial layer by a cycle of migration to the top, maturing along the way (Yang and Liao 2019). They are all connected by transmembrane proteins, known as intercellular junctions, that regulate the transport among them and are composed by gap junctions, tight junctions, adherens junctions and desmosomes (Khan and Asif 2015; Odenwald and Turner 2017). These cells are structurally arranged as finger-like projections called villi separated by invaginations called crypts. The surface of each epithelial cell on the villi has also projections called microvilli. The brush border is composed by all the microvilli together which accounts for a huge surface of contact between the cells and the extracellular environment, allowing nutrient digestion and absorption. Also, these microvilli keep in its plasma membrane digestive enzymes for that process. The stem cells are located in the crypts, intercalated with the endothelial cells, allowing for a continuous replacement of the cells in the villi in a process designated epithelium turnover (Yang and Liao 2019). Above the epithelial layer is a mucus layer that consists of a viscous secretion of goblet cells. Importantly, these two layers together are the first line of defense against the outside aggressions. Under the epithelial layer is the lamina propria with dense network of capillaries

surrounding a channel that is a branch of the lymphatic system. The lamina propria is densely filled with immune cells, making the intestine one of the largest immunological organs in the body, hosting more than 70% of all the immune cells (Kagnoff 1993). Overall, the epithelial cells layer with the mucus layer on top and the lamina propria underneath, provide an ideal microenvironment for chemical digestion, selective permeability and battle against endotoxins and pathogens (Fig. 10). The intestinal mucosa promotes nutrient and water transport and serve as a protective barrier at the same time. The intestine is protected in the outside by layers of smooth muscle around its circumference. The direct interaction with the liver is provided by the venous blood vessels that merge and form the hepatic portal vein (Frayn, 2010).

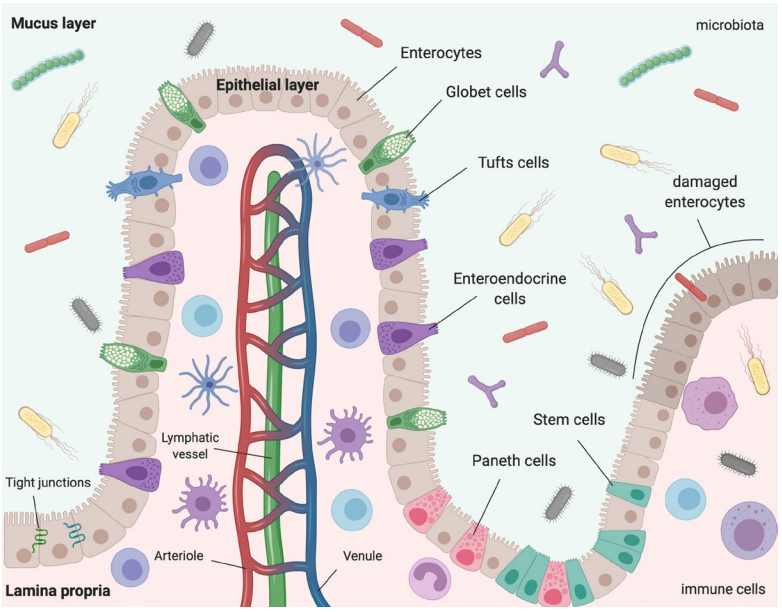

Figure 10. Intestinal villi and surrounding environment. The villi are finger-shaped projections formed by one layer of multiple cell types. These cells vary in shape and function, and are connected by tight junctions. The most abundant cells in the villi are the enterocytes (brown), which primary function is to absorb nutrients; the goblet cells (green) produce mucins that create a mucus layer on top, offering protection and a good habitat for microbiota; tuft cells (blue) have immunity function; the enteroendocrine cells (purple) secrete hormones; paneth cells (pink) produce anti-microbial peptides; and stem cells that reside normally in the crypts are responsible for the constant renewal of the epithelial layer. The three structural layers of intestine in charge of protection and stability are: the epithelial layer that is covered by a mucus layer and sits over the lamina propria. The superior zone is filled with bacteria and other microorganisms. The lamina propria is the interface for blood and lymph exchanges and is the microenvironment of a huge population of immune cells. On the right part of the image the dark brown cells represent damaged enterocytes, in those conditions, the permeability of the gut is compromised and the lamina propria is invaded by foreign bodies, activating and increasing the immune response.

4.2. Gut: the major host of microbiota in our body

Besides its anatomical structure there is other vital element in gut health and function – its microbiota. The immense microbial community that lives in the gastrointestinal tract is a particular feature of this tissue. It is extremely diverse, consisting of a mixture of bacteria, yeasts, protozoa and virus. It is generally agreed that the biggest part of these microorganisms are beneficial to the host, although some of them can be harmful or opportunistically harmful (Aron-Wisnewsky et al. 2020). Naturally, microbiota and the host have a symbiotic relationship extremely diverse, it degrades indigestible components of our diet, harvest energy and nutrients, shape host immune system and maintains the integrity of gut mucosal

barrier as well as xenobiotic metabolism (Narita 2020).

Microbiota population is determined by some individual factors. In adulthood, some factors can alter the microbiome, like changes in diet (David et al. 2014), the use of several types of medication, such as antibiotics (Falony et al. 2016) and metformin (Wu et al. 2017) and some other interventions like metabolic surgery (Zhang et al. 2009; Ramírez-Pérez et al. 2017).

Low diversity in the gut microbiome is associated with obesity and higher prevalence of IR, NAFLD and low-grade inflammation. This pro-inflammatory properties increase mucin-degrading bacteria that leads to gut integrity impairment potentiating inflammation though endotoxemia that is related with IR and T2D (Le Chatelier et al. 2013).

It is not yet well clear but amazingly gut microbiota and the host immune system have co-evolved so closely that they influence each other (Lee and Mazmanian 2010). One evidence of that is observed in germ-free mice experiments, where absence of microbiota leads to defects in the development and function of the immune system (Macpherson and Harris 2004). Also, the dynamic characteristic of gut microbe revels host susceptibility to infection, inflammatory diseases, and autoimmunity (Narita 2020).

Gut microbiota itself produces small molecules according to diet. From the various substrates (amino acids, lipids, carbohydrates, iron) presented to the intestinal lumen, gut microbes produce specific metabolites. Carbohydrates that are not digestible are fermented by the microbial community to produce short-chain FA (SCFA), of which acetate, propionate, lactate, and butyrate are the most important (Stephens, Arhire, and Covasa 2018; Roy et al. 2006). These metabolites are important factors, influencing host physiology. In the case of bile acids, those are first synthesized from cholesterol in the liver and later metabolized by gut microbiota into secondary bile acids, that are responsible for diverse metabolic pathways in the host, regulating as well gut microbiota composition (Ramírez-Pérez et al. 2017).

Also, the gut-brain axis has been widely explored as a fundamental pathway that connects gut microbiota and its metabolites with central regulation of metabolism, namely appetite and nutrient sensing (Narita 2020). Several evidences have demonstrated the importance of microbiota, such as each individual have his own microbiota signature and that can tell a lot about overall health state.

4.3. Gut: a metabolic organ

The gut performs numerous functions, such as mixing and impulsion of luminal content, absorption and secretion of ions, water, and nutrients, pathogens defense, and waste products elimination (Horváth et al. 2015). Inclusively, gut plays a major role in the regulation of post-prandial glucose state. Digestion and absorption of nutrients consist on a complex set of processes along the digestive tract, where intestine has a central role (Holst et al. 2016).

4.3.1. Gastric emptying

Before absorption into the bloodstream, nutrients are retained for some time in the stomach. The rate of gastric emptying is directly related with the composition and macronutrients of the meal. More recently was found that the rate of gastric emptying is a major factor of overall post-prandial glucose excursion in healthy and T2D individuals, where it shows to be delayed (Phillips et al. 2015). In the stomach, the emptying of nutrients is adjusted in order to have a relatively constant entry rate of the meal into the gut. Generally, the dominant mechanisms that regulate gastric emptying result from the interaction of nutrients with the intestine. Small intestinal feedback is mediated by the digestion

products and is regulated by the area of the tissue that is exposed to nutrients. Gastric emptying is also influenced by GLP-1 and Peptide YY (PYY), that inhibits gastric motility and suppress pancreatic hormone secretion (Little et al. 2006).

Naturally, these mechanisms are all connected and any intervention on those, will affect the rate of nutrient absorption from the gut and, consequently, alter glucose and other nutrients concentrations in the blood.

4.3.2. Incretins

Intestine is responsible for releasing a group of hormones that regulates the release of insulin, causing downregulation of hepatic glucose production and enabling the delivery of glucose in insulin-sensitive tissues. These hormones are called incretins, GLP-1 and GIP. Those are secreted in response to glucose ingestion, amplifying its effect on pancreatic β-cells. The insulin secretory response to incretins is known as the incretin effect; and it accounts for 50% of total insulin secreted after glucose ingestion (Kim and Egan 2008). This response is quite fast, incretins plasma levels start to increase as soon as nutrient intakes. Simultaneously to insulin secretion increasing, GLP-1 and GIP modulate the release of other pancreatic islet hormones, namely glucagon; while GIP enhances glucagon release, GLP-1 suppresses it (Holst et al. 2016). The main nutrients that stimulate incretins secretion are glucose and other carbohydrates; proteins have a weaker effect. Both GIP and GLP-1 are substrates of dipeptidyl peptidase-4 (DPP-4) that degrade and inactivates them (Nauck and Meier 2018).

4.3.3. Intestinal gluconeogenesis

Together with liver and kidney, the gut is one of the few organs where gluconeogenesis can happen (Penhoat et al. 2014). Besides, it was recently described that intestinal gluconeogenesis (IGN) is extremely important maintaining glucose homeostasis in the post-prandial state, with great anti-diabetes and anti-obesity activity (Vily-Petit et al. 2020). Due to its connection to the liver, glucose derived from gut is detected in the portal vein by a glucose receptor in the neural system (sodium glucose co-transporter 3, SGLT3) transmitting that signal to the hypothalamus. IGN is able through the gut-brain-liver axis to minors body weight gain, reduces hepatic glucose production and improves insulin sensitivity (Mithieux 2009). Additionally, IGN has an impact on regulating appetite where gut hormones also interfere, such as GLP-1 and PYY, with an inhibitory action of that feeling. The existence of intestinal sensory nerves sent to the hypothalamus (Grill and Hayes 2012) is another feature of gut explaining the excitatory impulses generated by food presentation and eating experience on that tissue (Alfa et al. 2015). Also, by controlling appetite and energy intake, gut hormones influence the size of adipose stores, which are a major determinant of peripheral insulin sensitivity (Schroeder and Bäckhed 2016).

Some of the effects of metabolic surgery are precisely eliminating or impairing some of these above mentioned mechanisms, namely, gastric emptying, incretin activity and IGN (Holst et al. 2016).

4.3.4. Lipid absorption: chylomicrons

The digestion of lipids begins in the oral cavity, continuing in the stomach where dietary fat and fat-soluble vitamins are emulsified. In the duodenum, bile and pancreatic juice provide pancreatic lipase, bile salts, and colipase that together contribute for the digestion and absorption of lipids (Iqbal and Hussain 2009).

The degradation of fats results in FA and monoacylglycerols that are absorbed in the intestine and synthetized into TG by enterocytes. Most TG biosynthesis within the enterocyte happens alongside with monoacylglycerol (MG) pathway, in which MG and fatty acyl-CoA join to form diacylglycerol (DG). DG acylation leads to the formation of TG, by diacylglycerol acyltransferases (DGAT1 and DGAT2), that are particularly relevant for TG synthesis. During absorption of dietary lipids, FA and MG are released in the lumen and enter in the enterocyte from the apical side. Those originate TGs that are synthetized in the endoplasmic reticulum (ER). TGs are transported from ER in a specialized vesicle, the prechylomicron transport vesicle that is sent to the trans-Golgi network for additional processing. The mature chylomicron fully packaged into another vesicle is directed to the basolateral membrane and is exocytosed, entering the lymphatic vessels located within intestinal villi (Cifarelli and Abumrad 2018).

Intestine produces two types of lipoproteins: chylomicrons and very low-density lipoproteins (VLDL). Chylomicrons transport all the dietary lipids, the VLDL transport the endogenous lipids. Lipoproteins allows lipids to be in suspension and interact with enzymes and receptors on surface of cells. They are composed by an internal hydrophobic core and a peripheral layer composed by amphipathic molecules, such as proteins, phospholipids, and non-esterified cholesterol (Sirwi and Mahmood Hussain 2018).

The absorption of lipids from the intestinal lumen into the enterocytes and their consequent discharge to lymph is a complex process. CD36 has been identified as particularly important mediating FA transport for uptake, and regulating the packaging of lipids into lipoproteins (Drover et al. 2005). There are two mandatory requisites in the assembly of lipoproteins: Apolipoprotein B (ApoB) and microsomal triglyceride transfer protein (MTTP). ApoB is the essential surface structural protein that enables the construction of lipoproteins within the ER. MTTP fosters lipoprotein biogenesis by shuttling neutral lipid from within the bilayer of the ER to an acceptor ApoB molecule (Abumrad and Davidson 2012).

TG is the dominant fat derived from diet synthetized in the gut but other lipids may be metabolized there, namely phospholipids, sterols, such as cholesterol, and others such as fat-soluble vitamins.

Cholesterol of exogenous source, meaning dietary source is absorbed in the intestine and only in its non-esterified form, incorporated into bile acid can be absorbed by enterocytes (Cohen and Fisher 2013).

4.4. Large intestine

This work focuses on small intestine, but the large intestine is essential to optimize small intestine work. Large intestine is about 1.5 meters long and extents from the end of the ileum to the rectum. It contains water, bacteria, residual food particles, sheded epithelial cells, and mucus. Its main functions are absorption of water and there is a considerable bacterial activity for the products that escaped small intestine digestion. Usually the energy we excrete in feces represents only 5% of the energy we ingest and much of its weight consists of bacteria from this part of the gut and materials that are unable to be digested.

While the intestine is the main gate of food we ingest, it has a very close relationship with the liver. In fact, the intestinal tract is supplied along his tunnel with innumerous blood channels that send the blood to the portal vein towards the liver.

5. The Liver

The liver is the largest organ in the body and has a leader metabolic role regulating whole-body homeostasis and energy management. It has a central privileged position in the blood circulatory

system being supplied with two major vessels from below: the hepatic artery and the hepatic portal vein, or simply portal vein. The blood in the portal vein comes directly from the system of blood vessels around the intestine. Thus, the nutrients derived from the diet are directed to the liver, before reaching the general circulation. The pancreatic veins are another important group that join the portal vein in the entrance to the liver and carry blood from the pancreas transporting insulin and glucagon. In the way-out, the blood goes through the hepatic veins which enter the inferior cava vein and points towards the heart (Frayn, 2010).

5.1. The structural heterogeneity of the liver

What allows the liver to be a multi-tasking organ is its heterogeneity in cell composition. Several types of cells can be found in the liver. The most abundant ones are the parenchymal cell: hepatocytes, accounting for approximately 60% of liver cells. The non-parenchymal cells comprise the 40% hepatic cells left, and correspond to the sinusoidal endothelial cells (~20%), the Kupffer Cells (KC) (~15%) and stellate cells (~5%). In a much smaller percentage other types of cells reside in the liver, like fibroblasts, smooth muscle cells, lymphocytes and progenitor cells. Sinusoidal endothelial cells are the interface between blood and hepatocytes, acting as a buffer. KC, that will be explored in more detail later on, are derived from circulating monocytes and have the ability to proliferate locally, to phagocyte and produce cytokines to mediate the inflammatory response. Hepatic stellate cells have the particularity of storing 50-80% of all vitamin A in the body as retinyl ester into lipid droplets (LDs), that in pathological circumstance, such as liver fibrosis, the vitamin A is lost to synthesize components of the extracellular matrix such as collagen, proteoglycan, glycosaminoglycan and adhesive glycoproteins, altering considerably the morphology of these cells (Senoo 2017; Malarkey et al. 2005; Seo and Jeong 2016).

Hepatocytes contain all the necessary machinery for liver metabolic functions. With age the numbers of hepatocytes tend to decrease. Hepatocytes have a very particular organization, which appears in a cross-section as hexagonal units and at each corner of the hexagon are formed by three vessels: small arms of the portal vein, hepatic artery and bile duct. The function of periportal hepatocytes modulates the microenvironment sensed by pericentral hepatocytes and to that is called liver zonation. The hepatocytes on the periphery of each lobule (periportal hepatocytes) are exposed to blood arriving from the portal vein and hepatic artery, meaning these hepatocytes in particular are well oxygenated and well supplied with nutrients, and that is mainly where the oxidative metabolism happens. Thus, gluconeogenesis, the synthesis of glucose, takes place mostly in the aforenoted region, whereas glycolysis occurs in the central part of the lobule (pericentral hepatocytes) (Ben-Moshe and Itzkovitz 2019; MacParland et al. 2018) (Fig. 11).

5.2. Metabolism of the liver

As all the blood leaving the intestine goes into the hepatic portal vein, the liver has the essential role of metabolizing and sorting dietary-derived carbohydrates, lipids and proteins (Sadri et al. 2006). Simultaneously, the liver is responsible for maintaining glucose homeostasis, managing energy storage and supply (Macedo et al. 2014). Moreover, liver also converts lipids into FAs that are stored as TG or synthetized as cholesterol or phospholipids (Maxson & Mitchell 2016). Some of those are packed into lipoproteins and made available for the other tissues. Also, liver metabolizes amino acids or turn them into FAs so it can be used as source of energy. There is a close interaction among the different macronutrient metabolic pathways in order to guarantee well balanced glucose levels and steady supply of energy for cellular demands.

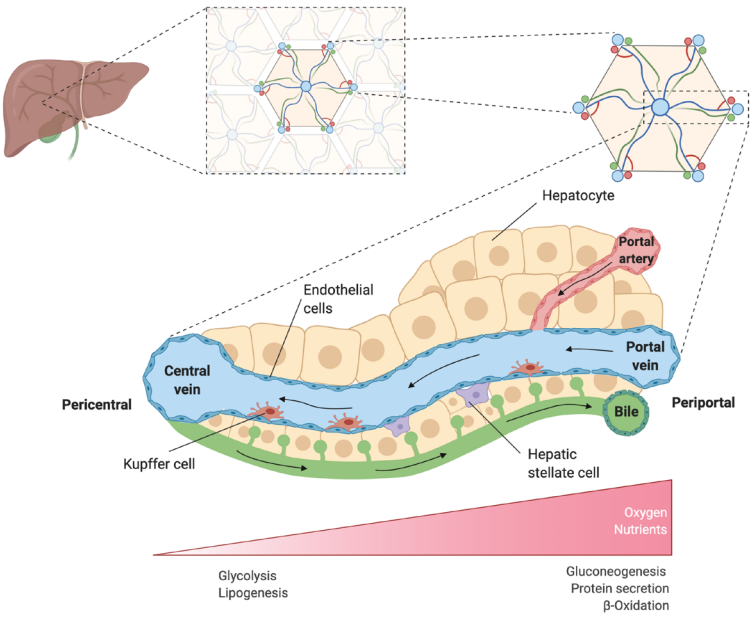

Figure 11. Schematic representation of a cross-section of the liver. The liver structure is made of hexagonal lobules. In each corner of the lobule are located a hepatic portal artery (red), a portal vein (blue) and a bile duct (green). Blood enters the lobules from the corners and flows inwards towards the central vein through blood vessels that are sustained by liver endothelial cells (cells in blue) and might intercalate with Kupffer cells (KC) (cells in red). The mode hepatocytes (cells in yellow) are arranged, confer the structure of the lobule and have some hepatic stellate cells as neighbors (cells in purple). Bile canal transport bile acids secreted by the hepatocytes in the opposite direction to blood flow into the bile duct to be sent to intestine. The blood arriving to liver comes well supplied of oxygen and nutrients, along the way to the central vein, the concentration decreases gradually so that will determine the functions of hepatocytes according to their localization. Process like gluconeogenesis, protein secretion and β-oxidation will occur in the periportal area and glycolysis and lipogenesis will be localized to the pericentral area. The specialization of the liver different zones in distinct metabolic reactions is called liver zonation (adapted from Ben-Moshe and Itzkovitz 2019; MacParland et al. 2018).

5.2.1. Carbohydrate metabolism in the liver

In the fed condition, glucose is absorbed from the intestine into the portal vein sending it immediately to the liver and exposing the hepatocytes to high concentrations of glucose. The uptake of glucose by this organ is insulin independent and it is mediated by the glucose-transporter 2 (GLUT-2). Inside the hepatocyte, glucose is phosphorylated by glucokinase enzyme (GCK) to form glucose-6-phosphate (G6P) which is the first step of both glycogenesis (glycogen synthesis) and glycolysis (glucose degradation), therefore being the major regulatory step in glucose uptake. Both, the insulin arriving from the pancreas, and the glucose coming from the gut, promotes glucose storage as glycogen, by stimulating glycogenesis and inhibiting glycogenolysis (glycogen breakdown). In the fed state, G6P can also be metabolized to pyruvate via glycolysis. What happens in glycolysis is that pyruvate can be either oxidized in the tricarboxylic acid cycle (TCA) or converted into lactate to be released. Glycolysis pathway is activated under fed state, but when in fasting state gluconeogenesis is favored. Gluconeogenesis convert non-carbohydrate molecules into glucose. They catalyze opposite functions and the first is stimulated by insulin, while the other by glucagon.

Under fasting conditions, when there is no income of glucose from the ingestion of food, glucose concentration in the blood falls, and liver needs to release it to maintain tight glycemic values

preventing hypoglycemia. First, glycogen is broken down, controlled, simultaneously, by the activation of glycogen phosphorylase and inhibition of glycogen synthase. This is mainly regulated by glucagon. Gluconeogenesis can also use amino acid substrates to synthesize glucose, depending on the supply of nutrients and its rate (Lisa C. Hudgins et al. 2000).

Liver works as a sensor of glucose though the activity of insulin. The insulin secreted by the pancreas, in response to higher levels of glucose in the blood, travels directly to the liver through the portal vein. This means that liver is exposed to much higher insulin levels than the systemic circulation. In this first passage, the liver immediately removes 50 to 70% of secreted insulin from circulation through receptor-mediated endocytosis, a process known as insulin clearance that have been evidenced to be impaired in T2D (Bedinger and Adams 2015). This way, the liver determines the insulin available for the peripheral organs.

Abundancy of carbohydrates, such as glucose and fructose, makes the liver converts glucose into FA, in a process called *de novo* lipogenesis (DNL) (Lisa Cooper Hudgins et al. 1996). DNL starts with the conversion by the ATP-citrate lyase (ACLY) of citrate to acetyl-CoA, that is later carboxylated to malonyl-CoA by acetyl-CoA carboxylase (ACC). FA synthase (FAS) intermediates the conversion of malonyl-CoA and NADH into palmitate that can generate different FA, predominantly TG. These TG can later provide energy via β-oxidation. DNL is regulated by two transcriptional factors, sterol regulatory element binding protein 1c (SREBP1c) and carbohydrate response element binding protein (ChREBP), that are activated by increasing insulin signaling and increased glucose concentrations, respectively, both stimulated by feeding (Sanders and Griffin 2016). The activation of SREBP1 happens via two main pathways downstream of insulin receptor, one causing the phosphorylation of the SREBP1c itself and the other activating the liver X receptor (LXR), both comprising the phosphoinositide-3 kinase (PI3K)/protein kinase B (PKB) (Horton, Goldstein, and Brown 2002). ChREBP is activated by the delivery of glucose into hepatocytes. ChREBP, by its turn, is regulated by dephosphorylation of Ser196 and other protein kinase A (PKA) or adenosine monophosphate-activated kinase (AMPK) phosphorylation sites (Silva et al. 2019; Ortega-Prieto and Postic 2019). SREBP1c and ChREBP act synergistically mediating the response to dietary carbohydrates.

5.2.2. Fat metabolism in the liver

In a healthy scenario, the liver metabolizes great quantities of FA, but stores much lesser amounts.

FA in the liver derives from exogenous or endogenous sources. The exogenous or dietary source, corresponds to the chylomicron TG produced in the intestine that are taken up mainly by muscle and adipose tissue. The remaining are delivered back to the liver where chylomicrons are received by receptor mediated endocytosis, releasing the FA during lysosomal processing (Cohen and Fisher 2013). The endogenous source can be DNL, that happens when carbohydrates are abundant, and the liver converts glucose into FA or direct uptake from plasma, when in fasting.

In fasting periods, when insulin concentrations are low, white adipose tissue enters in lipolysis, increasing the plasma FA pool sending it to the liver (Cohen and Fisher 2013). In the liver, specifically in the hepatocytes, FA are esterified to glycerol-3-phosphate (G3P) and to cholesterol in order to generate TG or cholesteryl esters, respectively. These lipids can be either accumulated in cytoplasmic LDs, or released to the bloodstream in VLDL.

The liver is able to synthetize TG, incorporating it to lipoproteins different of chylomicrons, named VLDL, which are responsible for carrying endogenous lipids in blood. In normal conditions, the liver

stores few amounts of TG but sends considerable FA in the form of VLDL to muscle and adipose tissue (Kawano and Cohen 2013). Also, in the liver, FA may originate other complex lipids, like phospholipids. In fasting periods, FA can be used as local energy suppliers or substrate for ketone bodies (Gray, Tompkins, and Taylor 2014).

Considering cholesterol, a lipid also prevenient from both dietary or endogenous source, is an essential constituent of cell membranes and a precursor of steroidal hormones and bile acids. Cholesterol can either be stored in LD or packaged into lipoproteins, that can vary in density. Based on density there are five categories of lipoproteins, ordered from lower to higher density: chylomicrons, VLDLs, intermediate-density lipoproteins (IDLs), low-density lipoproteins (LDLs) and high-density lipoproteins (HDLs). TGs are packed into chylomicrons, VLDL and IDL, while cholesterol are present in all (Cohen and Fisher 2013).

However, the primary pathways for cholesterol catalysis is bile-acid synthesis. They are produced in the liver from cholesterol and secreted by hepatocytes into the bile ducts and subsequently stored in the gall bladder. Upon ingestion of food, bile flows into the duodenum, where it participates in the digestion of lipid-soluble nutrients. Bile acids are afterwards absorbed by passive diffusion and active transport from the terminal ileum to the liver via portal vein (Thomas et al. 2008).

LDs are dynamic cellular structures that transitorily stock lipids. After white adipose tissue, the liver is the second greatest organ with capacity to store TG in LDs. An overnight fasting is enough to originate these LDs accommodating FA derived from adipose tissue lipolysis (Jr. 2012).

There are multiple ways for FA oxidation derived from hydrolysis of hepatic TG stores, circulating lipids or DNL. The primary route in hepatocytes is mitochondrial β-oxidation,when it comes to short-, medium-, and long-chain FA.Secondarily, β-oxidation of very long and branched-chain FA starts in the peroxisomes. Additionally, α-oxidation and ω-oxidation within the endoplasmic reticulum, mediated by cytochrome P450, are alternative pathways for FA oxidation (Lavoie and Gauthier 2006). The expression of genes involved in mitochondrial and extramitochondrial FA oxidation is regulated by peroxisome proliferator-activated receptor α (PPARα) activity (Ortega-Prieto and Postic 2019).

5.2.3. Amino acids metabolism in the liver

Before being taken up by the liver, dietary proteins are broken down into their component amino acid in the gut. Contrasting with glucose and FA, amino acids cannot be stored in the liver, thus they are metabolized through deamination to provide energy or to be used for synthesis of nonessential amino acids, FA or glucose, by gluconeogenesis. The liver plays a catabolic role in terms of excess of amino acids coming from the diet. The resulting toxic metabolite, ammonia, can be transformed to less toxic urea, and be excreted in urine as a waste product of digestion, by the kidney. On the fed state the supply is done by the nutrients intake, and in the fasting state depends on the net rate body protein breakdown. It is proved that glucose together with amino acids are required to trigger insulin sensitization in the gut, in the fed state, independently of insulin secretion (Afonso et al. 2016).

The word “central” used often to characterize the role the liver plays in metabolism is not euphemistic. Liver is localized in the center of our body and is the first passage of many components that enter in our system, giving to the liver the responsibility of maintaining physiological homeostasis. Therefore, despite the ability to metabolize all the nutrients coming from gut, it also complies with detoxification processes, forming the first line of defense against pathogens and xenobiotics, that were able to cross the intestinal barrier. The population of KC in the liver are the ones in charge of this protection.

5.3. The role of Kupffer cells on metabolism

Macrophages are the effector cells of the innate immunity with major role in inflammation and host defense. Some of the particular features of cells from the monocyte-macrophage lineage are the diversity and the plasticity. In reaction to environmental signals macrophages present great extent in phenotype and function. They have two ways of activation: M1, the classical one, and M2, the alternative one. M1 activation occurs in response to toll-like receptors ligands LPS and interferon-γ(IFN-γ), resulting in the secretion of pro-inflammatory cytokines, reactive oxygen species (ROS) and nitric oxide (NO). The M2 activation happens after stimulation with interleukin-4/interleukin-13 (IL-4/IL-13), promoting tissue renovation and other immune regulatory functions by producing polyamines (Luo et al. 2017).

KC are the hepatic resident macrophages of the liver, comprising the largest tissue with specific population of macrophages in the body (80-90% of tissue macrophages). They can be activated by several endogenous and exogenous stimuli, regulating the phenotype and function of neighboring parenchymal and non-parenchymal cells. The localization of KC in the hepatic sinusoid allows them to efficiently phagocytize antigens coming from the portal vein or arterial circulation. Absence or decreased functional activity of KC may lead to pathogens invasion and systemic inflammation. In the other hand, over-activation of KC, in NAFLD cases, results in uncontrolled inflammatory stated of the liver (Dixon et al. 2016). Changes in the functional activity of KC are associated to the wide variety of disease states in the liver.

NAFLD and alcoholic liver disease (ALD) progression is strongly associated with KC activity. This progression is marked by the manifestation of fatty liver, hepatocyte necrosis and apoptosis, inflammation, nodules regeneration, fibrosis and cirrhosis. Hepatic fibrosis results from dysregulated inflammatory processes in consequence of hepatocellular damage (Dixon et al. 2016; Luo et al. 2017).

In addition to immune function, KC are very important to iron and lipid metabolism. They can uptake lipids and digest them in the lysosome, generating cholesterol and FA. Also, there are evidences that high fat diet (HFD) induces hepatic steatosis and significantly increase hepatic expression of pro-inflammatory cytokines and disturbances of phagocytic functions (Ferrere et al. 2016; Luo et al. 2017). Another fact is that diet composition alters microbiota and that alteration has effects on the inflammatory pattern of the liver double-stating the close communication between gut and liver (Ferrere et al. 2016). KC also appear to have a role on insulin resistance in cases of obesity since its associated with chronic inflammation and altered lipid metabolism (Clementi et al. 2009). There are data inclusively showing that depletion of KC protects against diet-induced steatosis and IR demonstrating an active role they have in mediation factors from diet (Huang et al. 2010).

The direct communication between gut and liver is quite relevant on their individual functions. Thus, there is an inherent need to look at them, especially in the pathologic scenario, in the perspective of interaction and communication. Actually, communication, has been the topic between the lines. T2D is fundamentally a systemic disease, extremely complex, resulting from the dysfunction of many tissues, or a dysfunction that is communicated and translocated from tissue to tissue.

6. Tissue communication

We cannot talk about tissue communication without first mention cell communication. Along evolution cells developed strategies of communication among them through signaling pathways. Small unicellular creatures evolved to big and complex multicellular organisms, and with that, new strategies came along. To successful survive in changing environments, organism had to develop

sensing mechanisms to external conditions and adapt to maintain homeostasis, so the tissues of multicellular organisms had to communicate with each other via many signals. Intercellular signaling can be autocrine, paracrine or endocrine. Autocrine signaling means that a cell secretes a signaling molecule that will bind to receptors and perform its action in the same cell. Paracrine signaling means that molecules will bind to receptors in the nearby cells. Endocrine signaling is when a cell releases a signaling molecule, classically known as hormone, into the bloodstream and binds to receptors in distant cells, exerting their action there. These molecules are soluble factors, with bioactive function, and include hormones, growth factors and cytokines, the latest ones are commonly used by immune cells. We will not look into that, but in the matter of tissue communication, nervous system has a spotlight. Inclusively, metabolic homeostasis results from the interaction between the central nervous system and the peripheral organs, requiring a coordinated release of multiple hormones and signaling molecules. The nervous system combines a vast network of innervation where neurotransmitters and neuropeptides transfer the information in the form of electrochemical messages (Castillo-Armengol, Fajas, and Lopez-Mejia 2019).

Inter-organ communication has always been a topic of great curiosity from the perspective of several diseases, but metabolism, in particular, is a very suitable field to approach that. From peptide hormones to lipids, several molecules coordinate the responses of the tissues to the fluctuating nutritional states. Besides cell-to-cell contact and transfer of secreted molecules, a third mechanism of intercellular communication has recently captured our attention: the extracellular vesicles (EVs).

EVs were discovered long ago, by the middle of the last century. In the late 1980's the term exosome was used for the first time to coin these vesicles but, by then, they were seen as a waste removal mechanism, or a vehicle to excrete unwanted and unnecessary cellular components (Johnstone et al. 1987). Only in 2001 it was demonstrated these EVs have functional activity and after that, many studies about their function, especially in the cancer field, have been published (Maia et al. 2018; Raposo et al. 1996; Janowska-Wieczorek et al. 2001).

Essentially, EVs are double phospholipid bilayer membrane vesicles, whose origin can be from endosomes or plasma membrane, that contain cytosolic and cell-surface proteins, DNA, RNA, lipids and metabolites (Raposo and Stoorvogel 2013; Are 2016). Although the classification of EVs is quite polemic, to some extent a consensus was found by characterize them according to size and cellular origin – endosomal or plasma membrane (Théry et al. 2018). The larger EVs (100-1000 nm in diameter) that are formed and released directly from the plasma membrane of both living or dying cells are generally known as microvesicles or ectosomes. In this class of EV can be also included the apoptotic bodies whose size can go until 5000 nm. The EVs displaying a smaller size (40-160 nm) with multivesicular endosomal origin, that are generated inside multivesicular bodies (MVBs), and are secreted upon its fusion with the plasma membrane are called exosomes (Théry et al. 2018; Are 2016; Maia et al. 2018). EVs are a recent field and the detailed nomenclature is a matter of active discussion. The lack of well-established markers and the heterogeneity of isolation protocols generates a technical issue of debate.

Figure 12 characterizes the different types of EVs and also compare its size and density with other non-EV structures that circulate in the body (Mathieu et al. 2019).

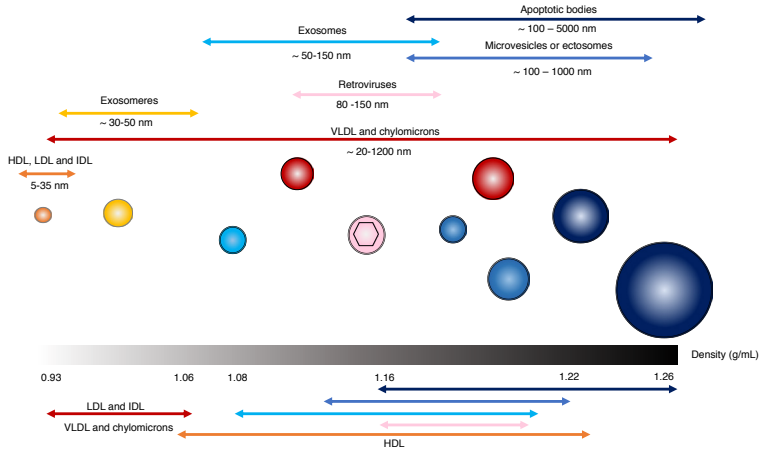

Figure 12. EV subtypes in perspective with other non-EV structures, that can be co-isolated, in terms of size and density. The three groups of EVs according size. Unlike ectosomes and exosomes, the apoptotic bodies are bigger and undergo apoptosis soon after secretion. EVs are being compared with other non-EV structures, present in the organism, that can have similar sizes. Density is a characteristic that should be considered to correctly separate the population of interest. HDL, high-density lipoprotein; IDL, intermediate-density lipoprotein; LDL, low-density lipoprotein; VLDL, very-low-density lipoprotein (adapted from Mathieu et al. 2019).

6.1. Extracellular vesicles: biogenesis

EVs are membrane-derived vesicles, being microvesicles and exosomes the most prevalent. Exosomes are formed through the invagination of the plasma membrane that engulfs cell-surface proteins and soluble proteins of the extracellular environment. This results in the formation of early-sorting endosomes, that in some cases can fuse with pre-existing ones. At this point, trans-Golgi network, ER and mitochondrion may contribute to the content that is being encapsulated through close interactions (Van Niel, D'Angelo, and Raposo 2018; Mathieu et al. 2019). The early-sorting endosomes mature to late-sorting endosomes and finally to MVBs, that can be also called multivesicular endosomes. Fundamentally this MVBs are inward invaginations of the endosomal membrane, that were already originated by invagination of the plasma membrane, meaning a double invagination happens. This process originates MVBs with intraluminal vesicles (ILV) inside. This MVBs have normally two potential directions: they can fuse with lysosomes or autophagosomes for degradation or, in the other hand, fuse with plasma membrane to release the ILVs as exosomes (Van Niel, D'Angelo, and Raposo 2018) (Fig. 13). The sequential invaginations, the interactions with other cellular compartments, and the formation of exosomes contributes for the EVs great heterogeneity. They can carry a vast range of cargoes offering a unique package to transport information by providing a safe and protective environment to travel (Yáñez-Mó et al. 2015).

One feature that contributes to EV biogenesis is its membrane curvature. The residents of the membrane are, some way, flexible and move along the membrane, so some molecules will accumulate in certain regions that are energetically favorable, determining its shape and influencing its physiological role, non-specific mechanism manner (Kralj-Iglic 2012; Yáñez-Mó et al. 2015).

It is important to have in mind that EVs are produced both in pathological and healthy conditions, and its biogenesis, degradation or secretion are part of the natural mechanism of a cell.

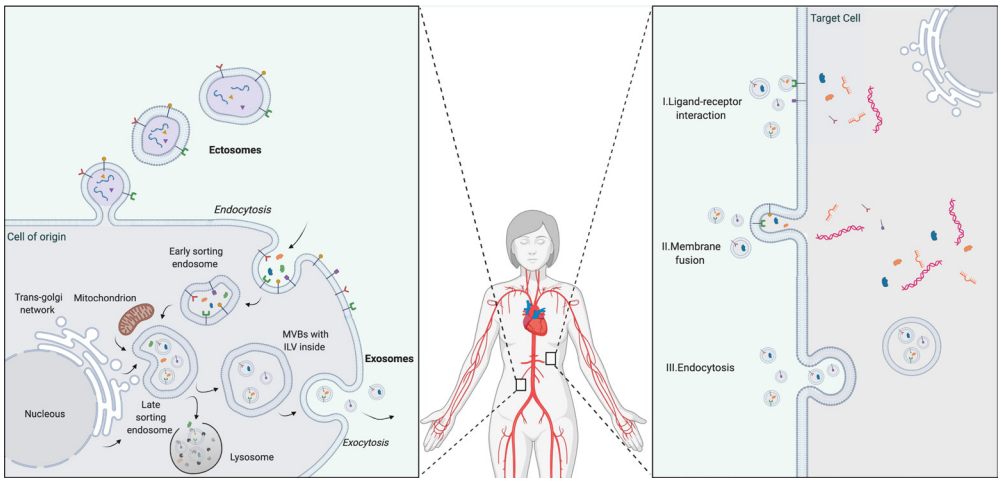

Figure 13. How EVs are produced and secreted (left) and how EVs are received by the target cells (right). (Left) Large extracellular vesicles (EVs) are formed by budding of plasma membrane and are called ectosomes or microvesicles. Exosomes are smaller EVs that result from the invagination of plasma membrane, collecting extracellular components, forming in a first stage, an early sorting endosome, that may fuse with other endosomal compartments and inclusively interact with endoplasmic reticulum (ER), trans-Golgi network and mitochondria, developing to late sorting endosomes; a second invagination happens at this stage generating intraluminal vesicles (ILVs); the volume and dimension of these invaginations will determine the future exosomes cargos; late sorting endosomes will give rise to multivesicular bodies (MVBs), that can either fuse with autophagossomes and ultimately be degraded by lysosomes, or they can follow the pathway of exocytosis, through the cytoskeletal and microtubule network; exocytosis will result in the release of exosomes. The EVs may be delivered in a proximal cell or in the blood flow to reach a distant target cell. (Right) At the target cell, EVs can deliver its cargoes by three general mechanisms: I. Direct interaction ligand-receptor between EV membrane and cell membrane, activating the correspondent signaling pathways; II. Membrane fusion, when fluidity level of both membranes allows it; III. Endocytosis such as phagocytosis, micropinocytosis or receptor-mediated endocytosis. (adapted from Maia et al. 2018; Van Niel, D'Angelo, and Raposo 2018; Kalluri and LeBleu 2020).

6.2. Extracellular vesicles: delivery

According with their composition and surface protein profile, EVs can be delivered to a proximal cell or, on the other hand, to a very distal cell. Thus, protein content and especially membrane composition are responsible for biodistribution.

The way EVs are up taken appears to depend, at least in part, on the target cell. Upon arrival, EVs trigger three major deliver routes; the first is through the direct interaction between surface receptor or ligands of target cells, activating intracellular signaling. The second, is by membrane fusion. The third is by endocytosis, that can happen in three different ways, by phagocytosis, by micropinocytosis or by receptor-mediated endocytosis (Maia et al. 2018; Kalluri and LeBleu 2020) (Fig. 13). There is an interesting point regarding membrane fusion – both membranes need to display similar fluidity and that only is possible at a pH~5, limiting this mechanism to acidic environments, that are characteristic of tumor cells. This also calls the attention for the electrostatic behavior of EVs that may be critical determining its physiological role. A certain molecule carried in the EV may be more active in the membrane rather than its soluble form, or vice-versa (Yáñez-Mó et al. 2015).

The basal level of EVs in circulation results from the balance between their production and clearance. This requires a tight regulation of EV biogenesis by the parent cell and availability of target cells to internalize them. It is still not well understood how this organization is achieved but there are some cargoes in the vesicles that participate in this process.

Importantly, besides delivering biomolecules, EVs can also act as decoys sequestering circulation factors and targeting them for degradation. In particular, EVs can scavenge multiple toxins, acting as a defense mechanism (Keller et al. 2020). It is still unclear, however, whether the decoy effect of EVs play a role in the progression of metabolic diseases.

6.3. Extracellular vesicles: heterogeneity

EVs are quite heterogeneous. They can vary in origin, size and importantly in cargoes. On top of that, they differ on the functional impact on the recipient cells. Nevertheless, extensive literature exists about the effect of some specific components they transport in a variety of pathological contexts. Namely, in cancer (Costa-Silva et al. 2015), neurodegeneration (Jan et al. 2017), and interestingly to us, also in metabolic disorders (Chelakkot et al. 2018).

The microenvironment of cells determines the content of EVs and their surface markers. Noteworthy, the extracellular environment is an important determinant factor in this equation, the composition of EVs reflects their interaction with the extracellular milieu and not merely their intracellular biogenesis, which will ultimately influence their fate. EVs contain membrane proteins, cytosolic and nuclear proteins, extracellular matrix proteins, metabolites and nucleic acids, namely mRNA, noncoding RNA, and DNA. Figure 14 represents a classic view of an EV (Kalluri and LeBleu 2020; Colombo, Raposo, and Théry 2014).

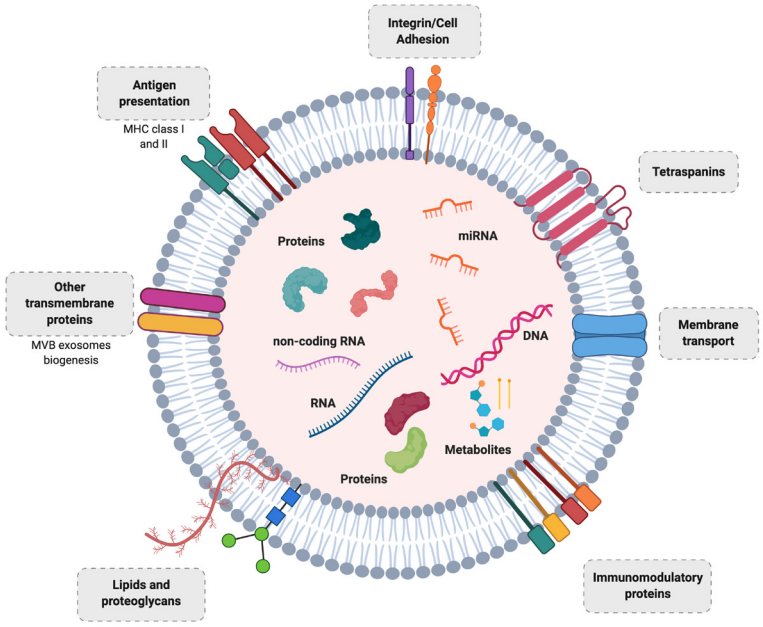

Figure 14. Schematic representation of an EV in terms of composition and membrane orientation. Common membrane proteins in EVs are tetraspanins; antigen presenting factors; cell adhesion-related proteins; immunomodulatory components; lipids and other proteins related with biogenesis. Inside, cargoes can go from proteins, to lipids, to metabolites, and to nucleic acids (DNA to RNA) (adapted from Kalluri and LeBleu 2020; Colombo, Raposo, and Théry 2014).

The most common luminal proteins among EVs are cytoskeletal, cytosolic, heat shock and plasma membrane proteins, likewise trafficking proteins. One category of proteins that are less abundant are the intercellular organelle ones. Characterization of EVs protein have been done by proteomics, immunoblotting, immune gold labelling combined with electron microscopy and antibody-coupled

bead flow cytometry. Proteins identified to be enriched in exosome-EVs are used as markers; and we can divide them in two groups: the ones present in the membrane and the luminal ones. Concerning the first ones, we have the tetraspanins (CD9, CD63 and CD81), integrins and major compatibility complex (MHC) molecules. Regarding the cytosolic proteins, stress proteins (heat shock proteins (HSPs)), tumor susceptibility gene 101 (Tsg101), and the endosomal sorting complex required for transport (ESCRT-3) binding protein ALIX (Yáñez-Mó et al. 2015; Kalluri and LeBleu 2020; Van Niel, D'Angelo, and Raposo 2018; Hoshino et al. 2015). Also, several glycan-binding proteins are present in exosome-EV and they appear to be fundamental for the targeting of these vesicles. Likewise, active lipolytic moieties, such as phospholipases, that lead to the formation of lipid mediators, like the case of FAs and prostaglandins, that have the ability to interact with peripheral G-proteins coupled to receptors on the cell membrane, are also present in these vesicles (Yáñez-Mó et al. 2015; Van Niel, D'Angelo, and Raposo 2018). Cytokines are another category of bioactive proteins found in EVs, that are normally produced as intermediaries of an immunological response (Maia et al. 2018).

Extracellular RNA is a curious occurrence, it can exist bound to a protein complex, freely in circulation or well protected inside EVs. Inclusively, there are evidence that certain populations of RNA are enriched in EVs compared with the parental cells where they were formed (Nolte'T Hoen et al. 2012). Even in the case that this enrichment happens because of size restriction, there is a specific repertoire of miRNAs selectively exported to EVs, while other miRNAs are excluded, indicating the presence of an active sorting mechanism (Mittelbrunn et al. 2011). It is documented functional mRNA in EVs that are internalized and translated by the target cells, however it is still challenging to understand the extent of the effect of each individual mRNA that is carried (Koppers-Lalic et al. 2014).

When protected in EVs miRNAs can avoid degradation during circulation in blood. While we know that the miRNAs carried inside EVs play an important role in intercellular communication, the amount of miRNA required to elicit a paracrine or endocrine effect is an open question (Squadrito et al. 2014). DNA was also found in EVs, but less explored. Nevertheless there are studies evidencing the presence of mitochondrial DNA, single-stranded DNA, double-stranded DNA and also oncogene amplifications (Lázaro-Ibáñez et al. 2014).

Another component identified, through metabolomic analyses in EVs, are the lipids; these are key players in their physiological role, not only in its formation, but also in its function. Compared with the parent cells, EVs seem to be enriched in sphingomyelin, cholesterol, polysaccharides and glycosphingolipids. These are particularly important in the membrane to confer stability in different environments. Also, it was observed that, similarly to other EVs components, they are not randomly included in the vesicles (Choi et al. 2013; Record et al. 2014).

EVs, due to their advantage of having a lipid membrane encapsulating the cargoes and protecting its content of degradation, carry information from one organ to another using majorly the blood flow, importantly EVs are present in every fluid of the body: urine, saliva, synovial fluid, bile, cerebrospinal fluid, bronchoalveolar fluid, nasal fluids, uterine fluid, amniotic fluid, breast milk, seminal plasma and also feces (Yáñez-Mó et al. 2015).

6.4. Extracellular vesicles: isolation

In the last decade the number of papers studying EVs rose exponentially, consequently the debate regarding isolation methods gained particular attention. Isolation methods are quite diverse, thus substantially affecting yield, purity and quality. The most commonly used methods for EV isolation are: differential ultra-centrifugation; size-exclusion chromatography; and commercially available

kits (polymer-based precipitation or immunocapture by antibody-coated beads). Additionally to ultracentrifugation, in order to acquire a more enriched exosomal sample, by separating membrane-enclosed vesicles from proteins aggregates, a sucrose gradient can be added – as protein aggregates deposit in the sucrose layer, whereas lipid-containing vesicles float on top of an equilibrated gradient, allowing to filtrate better the vesicles population (Colombo, Raposo, and Théry 2014).

In total, given the diversity of isolation methods, when comparing EVs findings across the literature, we should be cautious and play particular attention to EV characterization. When looking at EVs as potential disease biomarkers, we have to keep in mind that methods developed for research purposes are time-consuming and labor intensive and are not yet adequate to be used in clinical laboratories.

6.5. Extracellular vesicles in metabolic disorders

With the ubiquitous nature of EV secretion by most cells in the human body, and their role in cell-to-cell communication, it is expectable to also have EVs participation in regulating the complex multiorgan interaction with insulin function and glucose homeostasis. Numerous studies have explored the involvement of EVs in metabolism, especially in the context of metabolic disorders such as T2D. Accumulative evidence shows that EV levels are higher in those conditions and with effects on pathophysiology, including vascular complications and inflammation (Lakhter and Sims 2015).

Several papers have reported EVs being released by the insulin-producing pancreatic β-cell. One interesting study demonstrated that increased β-cell EV secretion was stimulated by glucose or calcium treatment (Hyo, Jeong, and Lee 2009). Also β-cell EV secretion and cargo seems to be modified by contact with inflammatory cytokines (Hospital and Diseases 1990). Furthermore, proteomic studies revealed significant disparities among EV contents of cytokine-stimulated and non-stimulated rat β-cells. The first ones presented increased protein levels from tumor necrosis factor-α (TNF-α) signaling pathways, suggesting EVs with a role in inflammatory response (Palmisano et al. 2012).

Adipose tissue has also been greatly explored from EV perspective studies, since it revealed to be involved in glucose homeostasis. Adiponectin, an adipokine associated to IR, was described in circulating EVs, and EV adiponectin content is reduced in HFD-fed mice compared with control (Palmisano et al. 2012). Additionally, visceral-adipose tissue (VAT)-derived EVs confirmed to have the capacity to trigger systemic inflammation and IR; after VAT-EVs intravenous injection into wild-type (WT) mice, serum IL-6 and TNFα levels were increased and glucose intolerance was induced, the same way as IR (Deng et al. 2009). Adipose tissue EVs inclusively showed to have influence on other metabolic syndrome-related tissues; in obese patients, adipose tissue-EVs were able to modulate insulin responses in hepatocytes and muscle cells (Kranendonk et al. 2014).

Effect of skeletal muscle-derived EVs in obesity and IR has also been explored. Data showed EVs derived from lipotoxic skeletal muscle with ability to transfer lipids and impact gene regulation of recipient muscle cells, not directly inducing IR (Aswad et al. 2014).

Other tissue focus of great attention on this field was the liver, where the role of EVs have been explored over the years. EV release from hepatocytes have demonstrated to activate inflammation through the induction of pro-inflammatory cytokines and macrophage activation (Lakhani 2019). Also, liver-EVs are quite relevant in liver diseases, such as NAFLD and metabolic syndrome, since they are able to modulate and regulate drug resistance and even hepatocellular carcinoma (Chen et al. 2018).

In the case of the gut, curiously, the study on EVs was done mostly on microbiota EVs that showed to be quite relevant in scenarios of disease. Exosomes released into the mucosa demonstrated

to participate on local innate responses to invading bacteria through microbicidal activity (Hu et al. 2013) and also to mediate gut permeability though the regulation of tight junctions (Chelakkot et al. 2018). EVs definitely play an important role in the interaction of the microbiota with intestinal cells and even more distant cells in the body (Chang et al. 2020; Smythies and Smythies 2014).

Plasma EVs lipid content such as FAs, prostaglandins and cholesterol, also demonstrated to affect endogenous cell lipid metabolism and trafficking, having this a great relevance on T2D field (Record et al. 2014).

Chapter II

Aims and Hypothesis

Aims and Hypothesis

Maintenance of metabolic homeostasis in response to nutritional cues requires the coordinated action of multiple organs. Therefore, higher organisms developed diverse communication systems through which one organ can affect metabolic pathways in distant ones. Impairment of systemic communication contributes to human pathologies, namely obesity and diabetes. Recently, EVs emerged as an important mean of organismal communication and were implicated in the pathophysiology of diabetes. Furthermore, technical advances such as proteomics and associated data-driven bioinformatics help us to a better understand of the complex metabolic crosstalk going on in the organism. The complex and vast network of tissues involved in the pathophysiology of prediabetes led us to look for an intermediary of such demanding communication, the EVs, small vesicles capable of transporting specific cargo and inducing functional changes in recipient cells. From the impressive outcomes of metabolic surgery, the gut holds the key for the treatment of metabolic disorders, such as prediabetes and T2D. Importantly, epithelial cells in the gut secrete EVs. Thus, focusing our attention on that tissue, we aimed at studying gut derived EVs (GDE) in the context of prediabetes.

In the present thesis, we explored the hypothesis that prediabetes has a gut specific trigger, which in turn communicates with the liver, by secreting GDE, which are capable of imprinting a hepatic dysmetabolic phenotype.

The main objectives of this thesis are:

AIM 1. To characterize the impact of prediabetes in the protein cargo of GDE.

AIM 2. To elucidate the gut communication with other organs mediated by GDE; by identify the target organ(s) and cell type of GDE action.

AIM3. To shed light into the pathophysiological role of GDE in modulating metabolism.

Our approach to study GDE in prediabetes is schematized in Figure 15. To achieve the proposed goals, we used the routinely used in the field diet (high fat and sugar) induced mouse model of prediabetes. First, GDEs were isolated from prediabetic mice, then analyzed and characterized. Consequently, GDE were administered in lean healthy mice so that we could understand their biodistribution and metabolic function in the organism.

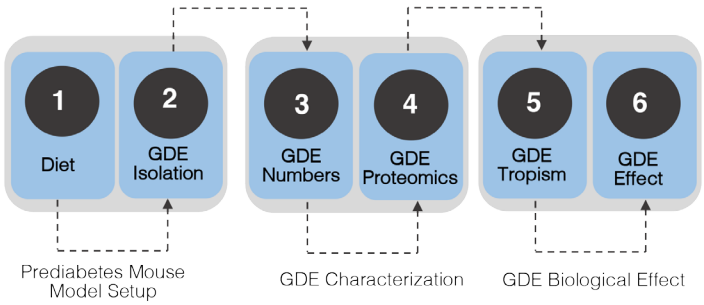

Figure 15. Schematic representation of the experimental design in chronologic order. This project consisted in the following phases. 1)Prediabetic mouse model: mice fed with high fat and normal chow diet for 12 weeks; 2) Gut-derived EV (GDE) isolation by sequential ultracentrifugation and sucrose gradient; 3) GDE numbers – EVs isolated from both groups were quantified in terms of size, concentration and total protein; 4) GDE proteomics – EVs protein cargo was analyzed by mass spectrometry; 5) GDE tropism – GDE were injected in healthy mice and traced; 6) GDE effect – GDE were injected in healthy mice for several weeks to evaluate its pathophysiological effect. Two first points compose the first task of obtaining GDEs (prepare and extract the material), the following two were the second task of GDE characterization (in terms of amount and content), the last two were GDE application to analyze the behavior in the organism (evaluation of tropism and metabolic impact).

Chapter III

General Methodology

General Methodology

Animal studies

1. Animals producers of extracellular vesicles

1.1. Diet-induced prediabetic model

Male C57Bl/6J mice were housed in a temperature controlled room, in a 12-hour light/dark cycle. For induction of prediabetic phenotype, C57BL/6J mice started on a high-fat diet at 6 weeks of age, with free access to food and water, for 12 weeks. High-fat diet (HFD) (OpenSource Diet, D12331) composition is 16.5% protein, 25.5% carbohydrate, and 58% fat with 700 kcal of sucrose. The control normal chow diet (NCD) (Special Diets Services, RM3) composition is 26.51% proteins, 62.14% carbohydrates and 11.35% fat. All studies were performed in male mice. All animals were treated according with National (Portaria 1005/92) and European Union Directive for Protection of Vertebrates.

1.2. Glucose tolerance test (GTT)

At week 11 of diet GTT was performed. Mice were fasted overnight and weighed in the morning. Mice were then given an intra-peritoneal injection of a glucose solution (20% m/v – Sigma Aldrich) at 2g/kg body weight. Serum blood glucose levels were measured at 15, 30, 60, 90 and 120 min after injection. Blood glucose levels we measured using OneTouch Ultra glucose meter (LifeScan Inc.).

1.3. Anesthesia and sacrifice

At week 12 of diet mice were sacrificed. Mice were anesthetized using isoflurane 1.5-3%. Mice were scarified under 12 hours of fasting, with a previous feeding period of 2 hours, with the previous 8 hours of fasting. Blood, liver and gut were collected from prediabetic mice and respective controls.

1.4. Tissue preparation in OCT for histology

After sacrifice, the small intestine and the liver were well-washed and fixated for histology. A small portion of the tissues were processed in the following manner: gut was placed in 2% Paraformaldehyde (PFA) with 20% Sucrose, overnight at 4^{o}C; washed three times in Phosphate Buffered Saline (PBS) , 10 min each; transferred to 30% sucrose for 2 hours at 4^{o}C; left overnight at 4^{o}C in Optimal Cutting Temperature compound (OCT) with 30% Sucrose (1:1). In the following day, tissues were embbeded in molds in 20% Sucrose (dilution of 1:4) + (OCT) (dilution of 3:4) in a box with dry ice and immediately stored -80^{o}C. Consequently, tissues were sliced into 6 µm thin sections in the cryostat and stored at -80^{o}C for following applications. Gut samples were used for CD81 staining and liver samples for Hematoxylin-Eosin staining.

1.4.1. Immunohistochemistry

Gut coverslips were fixed with 4% PFA for 10 min. In a covered dark humidified chamber, the slides with the cells were incubated for 20 min with Phosphate Buffered Saline with Tween-20 (PBS-T) and after with 5%Goat Serum in PBS-T for 1 hour. Cells were washed and then incubated with primary antibody CD81 (Santa Cruz) diluted in 1%Bovine Serum Albumin (BSA)/PBS-T overnight, at 4^{o}C. In the following day, slides are washed with PBS-T, three times, 10 min, and incubated with the secondary antibody anti-mouse Alexa-Fluor 488-conjugated, at 1:500 (Invitrogen). Coverslips were mounted in mounting media

Pro-Long Gold Antifade Mountant with DAPI (ThermoFisher) to visualize the nuclei.

Fluorescence was observed using a Zeiss Axiolmager M2 motorized upright widefield fluorescence microscope. Images were taken adjusting the levels of fluorescence of each channel up to a maximum threshold defined by the absence of signal in the negative control and processed using ImageJ software.

1.4.2. Hematoxylin-eosin staining

Histological analysis of liver sections were performed in the Histopathology Unit of Instituto Gulbenkian de Ciência. Liver cells were stained wih hematoxylin-eosin and examined under light microscope (Leica DM LB2, Leica Microsystems).

2. Animals receptors of extracellular vesicles

2.1. Biodistribution experiments

Mice were anesthetized using isoflurane 1.5-3% for few seconds, then injected retro-orbitally, specifically in the orbital sinus of the mice, with 5µg of near infra-red (nIR)-labelled GDE derived from mice fed with HFD and NCD, and PBS as control, in a total volume of 100 µl. 24 hours post-injection mice were sacrificed and the following tissues were collected: brain, gut, liver, fat, muscle, kidney and lung. Tissues were washed in PBS and signal emission was recorded in Odyssey imagem system (LI-COR Biosciences). Settings of acquisition and analysis used were in accordance to manufacture's instructions.

2.2. Education experiments

Male C57Bl/6J mice at 8 weeks of age were injected with gut EV, in different experiments, that were optimized along time. To the method of prolongued injections of gut EV we called education, this concept is further explored in the second part of Chapter IV.

5, 10 and 20 µg of gut EV protein was injected directly into the blood flow, through the orbital sinus in a volume of 100 µl PBS. Mice were injected every other day, 3 times a week. 5 µg dosage was injected for 3 weeks. 10 µg and 20 µg for 6 weeks. Retro-orbital injection of PBS was used as control. Mice were fed with NCD with unlimited access to water and food, with the exception of mice of education 5 that were fed with HFD. Animals were injected under anesthesia using isoflurane 1.5-3% for few seconds until no sensory perception.

ITT was performed to mice of education 5 two weeks before sacrifice and GTT performed one week before sacrifice (according to previous section 1.2).

2.3. Insulin tolerance test (ITT)

ITT performed on educated mice two weeks prior to sacrificate. Mice were fasted for 4 hours and weighed. Mice were then given an intra-peritoneal injection of human insulin at 0.75U/kg body weight (Humulin, Eli, Lilly). Serum blood glucose levels were measured at 15, 30, 60, 90 and 120 min after injection. Blood glucose levels were measured using OneTouch Ultra glucose meter (LifeScan Inc.).

2.4. Tissue harvesting

At the end of each education and prior to sacrifice, mice were weighed. Blood was collected through orbital sinus under anesthesia through a heparinized capillary. The liver was divided in two parts, one

part was snap frozen in liquid nitrogen and the other one fixed for histology. The small intestine was carefully removed, washed with PBS with a syringe and a needle.

2.5. Liver lipid assay

Hepatic lipids were extracted as previously described (Matyash et al. 2008). Briefly, approximately 250 mg of frozen tissue was rapidly mixed with high performance liquid chromatography (HPLC)-grade methanol (4.6 mL/g) followed by methyl-tert-butyl ether (MTBE) (15.4 mL/g). The mixture was placed in a shaker for 4 h and then centrifuged at 13.000g for 10 min. The liquid fraction was collected, and phase separation was induced by adding 1 mL of distilled water and letting it rest at RT for 10 min. The liquid was then centrifuged for 10 min at 1000g. The organic phase, which contained the lipids, was separated and dried under nitrogen gas in a glass vial protected from light. It was then dissolved in butanol/(Triton X-100:methanol [2:1]).

2.6. Liver cell suspension non-parenchymal cells purification

Non-parenchymal cells (NPC) were isolated from liver lobes by perfusion with Collagenase H (Sigma) and density centrifugation as described by (Duarte et al. 2018). To enrich for KCs, NPC were placed on top of 4 layers of a Percoll (GE Healthcare) gradient of 80%, 60%, 40% and 20% Percoll and centrifuged for 20min at 400g. The interface between the 60% and 40% Percoll layer containing the KCs was collected. To sort purify KCs, the enriched fraction was re-suspended in PBS with 2%Fetal Calf Serum (FCS) (Life Technologies).

2.7. Flow cytometry analysis

2.7.1 Liver

For the biodistribution experiments, after one single-injection of labelled-EV, the liver was collected and placed in media 2% Fetal Bovine Serum (FBS) in PBS, followingly is smashed against a 70 µm cell strainer with the help of a syringe. Cells were centifuged at 500g for 5 min. Red blood cells were depleted from the pellet by incubation with ammonium chloride-potassium buffer (ACK) for 3 min at RT and add 10 ml of 2% FBS. Cells were centrifuged at 500g for 5 min, supernatant is discharged ans cells were resuspended in PBS. The whole liver cells are next blocked for flow cytometry staining.

Livers of educated mice were treated as described in the previous point 2.6.

2.7.2. Bone marrow

In educated mice, femurs were cutted at both ends and with a needle and syringe filled with ice-cold 0.5%BSA+2mM EDTA PBS bone marrow was flashed, cell suspension was collected. Cell suspension is filtered in a 70µm cell strainer and washed with same media. Cells were centrifuged at 500g for 10 min at 4°C, and pellet was collected. Pellet was ressuspended with ACK (Life Technologies) and incubated for 5 min at RT. Cells were centrifugated at 4°C, supernatant was discharged and pellet resuspended in PBS.

After blocking with Fc Receptor Blocking Solution (anti-CD16/CD32 antibodies) (BioLegend) (dilution 1:50), cells were stained with specific antibodies CD45 APC-Cy7 (BD, Biosciences) (dilution 1:100); F4/80 PE (BioLegend) (dilution 1:200); CD11b PE-Cy7 (BioLegend) (dilution 1:400); Ly6c BV421 (BioLegend) (dilution 1:200). Flow cytometry analysis was carried out on LSR Fortessa X20 (BD, Beckma n Coulter). All data were acquired with DIVA software (BD) and analyzed by FlowJo software (TreeStar).

Extracellular vesicles studies

1. Extracellular vesicles isolation

1.1. Extracellular vesicles isolation from blood

Blood (600-1000 µL from each animal) was collected with a heparinized capillary from anesthetized mice to a 1,5 mL tube with 100 µL of heparin. Blood was centrifuged at 500g for 10 min; supernatant was collected and centrifuged at 3000g for 20 min; in order to obtain plasma. Plasma was stored at -80^{o}C for future EV isolation or continue to ultracentrigulation (section 1.3).

1.2. Extracellular vesicles isolation from small intestine

After sacrifice the small intestine was removed, washed with PBS and cultured overnight in RPMI medium (Sigma) supplemented with 1% PenStrep and 10% Fetal Bovine Serum EV-free, to avoid contaminations from serum EVs. In the following day medium was collected and centrifuged at 500g for 10 min; supernatant was collected and centrifuged at 3.000g for 20 min. Supernatant was stored at -80^{o}C for later EV isolation or continue to ultracentrifugation (next section 1.3).

1.3. Ultracentrifugation

The supernatant stored at -80^{o}C was transferred to ultracentrifuges tubes and centrifuged at 12.000g for 20 min at 10^{o}C; supernatant was collected and another ultracentrifugation was done at 100.000g, for 140 min at 10^{o}C;at this step, the supernatant was discharded and the pellet was collected.

At this step EV can be labelled how it is described in the next section and continue to sucrose cushion; or continue immediately for sucrose cushion.

Sucrose Cushion: The pellet was ressuspended in 1 mL of filtered PBS and transferred to a new tube and it was added filtered PBS until a total volume of 16 ml. Next, sucrose solution was prepared with 30g of protease-free sucrose (Sigma), 2.4g of Tris-base (Sigma) and 50 ml of heavy water (Sigma) to a total volume of 200 ml, and pH was adjusted to 7.4 with HCl; solution was then filtered with 0.22 µm filter vacuum inside the laminar flow. In a medium ultracentrifuge tube it was transfered 4 mL of the sucrose solution and, on top of that, the 16 ml of sample was added in a very carefull way. The sucrose cushion and the EV pellet were centrifuged at 100.000g, for 70 min at 10^{o}C. The fraction of interest (which is the sucrose cushion with the EV) was collected and added to a new tube with 16 mL of PBS that was centrifuged at 100.000g overnight. The next day the pellet was collected and resuspended in 200 µl of PBS.

Isolation of EV was done by ultracentrifugation (Beckman Ti70, rotor 70Ti).

2. Extracellular vesicles labelling

2.1. Extracellular vesicles labelling for odyssey image system

At the step that was mentioned in the previous section, after the first three ultracentrifugations, to the pellet that was collected was added 1 mL of diluent C from the CellVue NIR815 Kit for Membrane Labeling (Polysciences, Inc.) into a new tube. To that mixture of EV and diluente C it was added 4 µL Cell Vue NIR815 dye (Polysciences, Inc.) (excitation of 786 nm and emission of 814 nm).Then 2 mL 0.5% BSA

was added and labeled EV were washed at 100.000g for 70 min.

Labbelling of EV is normally done during the isolation but can also be done afterwards, with the drawback of losing some EVs during the extra ultra centrifugation that need to be done if the labelling is post-isolation.

In that case, to the EV sample it was added 20 ml of filtered PBS and ultracentrifuged at 100.000g overnight. In the next day, the pellet is collected and the procedure is the same of the one just mentioned.

2.2. Extracellular vesicles labelling for fluorescence

For fluorescence microscopy and flow cytometry analysis, purified EV were fluorescently labelled using PKH67 Fluorescent Cell Linker Kit with excitation (490 nm) and emission (504 nm) similar to fluorescein (Sigma). The protocol is exactly the same of the previous section.

3. Nanoparticle tracking analysis (Nanosight)

The concentration and size of EVs were analyzed in NanoSight NS300 (NS3000) system equipped with a blue laser (405 nm), according to the manufacturer's instructions. EVs were diluted 1:1000 in filtered sterile PBS. 1 mL of sample is collected with a 1 mL syringe that was inserted in the equipment flow system. Each sample analysis was conducted for 90 seconds and measured 5 times using Nanosight automatic analysis settings. The software calculated the size distribution in nanometers and the concentration in number of particles per mL.

4. Protein extracts, SDS-PAGE and western blot

Protein extracts for western blot analysis were obtained using cold lysis buffer (20 mM Tris- HCl pH 7.4, 5 mM EDTA pH 8.0, 1% Triton-X 100, 2 mM Na3VO4, 100 mM NaF, 10 mM Na4P2O7) in the presence of protease inhibitors (completeTM, Mini, EDTA-free Protein inhibitor cocktail tablets, Roche, Sigma). Gut tissue and gut EVs were homogenized in the lysis buffer and sonicated three time for 30 seconds each at 10 µm amplitude with 1 minute incubation on ice between each sonication step. Lysates were centrifuged at 18.000 g for 10 min at 4°C. Soluble fraction was collected and protein concentration was determined using the PierceTM BCA Protein Assay kit (Thermo Fisher). For protein expression analysis, equal amounts of total protein (15 – 20 µg) were mixed with sample buffer (250 mM Tris-HCl pH 6.8, 8% SDS, 40% glycerol, 8% β-mercaptoethanol, bromophenol), before being denaturated at 95°C for 10 min. Samples were then resolved by an 8% sodium dodecyl sulfate-polyacrylamide gel electrophoresis (SDS-PAGE). Proteins were subsequently electrotransferred to a polyvinylidene fluoride (PVDF) membrane (Immobilon-P Membrane, PVDF, Millipore) for 22 min at 25 mA and 2,5 mV in a Trans-Blot Turbo TM Transfer System (BioRad). Membranes were blocked for 1 hour at RT with 5% non-fat milk (Molico, Nestlé) in tris-buffered saline with 0,1% Tween (TBS-T) (blocking solution). Membranes were incubated overnight at 4°C, with CD63 antibody (Santa Cruz Biotechnology) prepared in 3% BSA in TBS-T, diluted 1:1000. Membranes were washed three times with TBS-T and incubated for 1 hour at RT with the secondary antibody anti-rabbit antibody diluted 1:5000 (Santa Cruz Biotechnology). Blots were developed with ECL (ECL Prime, GE Healthcare, Enzymatic), according to the manufacturer's instructions, and a Chemidoc touch equipment (Bio-Rad) was used to detect chemiluminescence. Band intensities were quantified using ImageLab software and normalized using ß-actin as loading control.

5. Proteomic analysis of extracellular vesicles

Mass spectometry of gut EV were performed by Rune Mathiessen, Principal Investigator of Computational and Experimental Biology in CEDOC, Lisbon.

5.1. Nano-LC-MSMS analysis

Peptide samples were analysed by nano-LC-MSMS (Dionex RSLCnano 3000) coupled to a Q-Exactive Orbitrap mass spectrometer (Thermo Scientific). Briefly, 5 µL of sample was loaded onto a custom made fused capillary pre-column (2 cm length, 360 µm OD, 75 µm ID) with a flow of 5 µL per min for 7 min. Trapped peptides were separated on a custom made fused capillary column (20 cm length, 360 µm outer diameter, 75 µm inner diameter) packed with ReproSil Pur C18 3-µm resin (Dr. Maish, Ammerbuch-Entringen, Germany) with a flow of 300 nL per minute using a linear gradient from 92 % A (0.1% formic acid) to 28 % B (0,1% formic acid in 100 acetonitrile) over 93 min followed by a linear gradient from 28 % B to 35 % B over 20 min at a flowrate of 300 nl per minute. Mass spectra were acquired in positive ion mode applying automatic data-dependent switch between one Orbitrap survey MS scan in the mass range of 400 to 1200 m/z followed by HCD fragmentation and Orbitrap detection of the 15 most intense ions observed in the MS scan. Target value in the Orbitrap for MS scan was 1,000,000 ions at a resolution of 70,000 at m/z 200. Fragmentation in the HCD cell was performed at normalized collision energy of 31 eV. Ion selection threshold was set to 25,000 counts and maximum injection time was 100 ms for MS scans and 300 and 500 ms for MSMS scans. Selected sequenced ions were dynamically excluded for 45 seconds.

5.2. MSMS analysis

Mass accuracy was set to 5 ppm on the peptide level and 10 Da on the fragment ions. A maximum of four missed cleavages was used. Carbamidomethyl was set as a fixed modification. M oxidation, N-terminal protein Acetyl, Q Deamidation and N Deamidation were set as variable modifications. The MSMS data was searched against all reviewed mouse proteins from UniProt with concatenation of all the sequences in reverse maintaining only lysine and arginine in place. The data was searched and quantified with both MaxQuant and VEMS.

6. Statistical Analysis

Data are presented as means ± SEM. GTT curves, bar plots, volcano plots, heatmap and linear regression analyses were done using GraphPad Prism 8 (GraphPad Software). Differences significance was calculated through unpaired student's t tests with Welch's correction; one-way ANOVA followed by Tukey-Kramer multiple comparison tests. Differences were accepted as statistically significant at $p<0.05$.

Chapter IV

Results

1. Extracellular vesicles in prediabetes: a proteomic characterization

1.1. Messages from the intestine carried by extracellular vesicles

The escalating incidence of T2D as a consequence of sedentary lifestyle and caloric-unbalanced diets, imposes a substantial burden to the health care systems explaining why it is considered a major public concern. Prediabetes or intermediate hyperglycemia is a high-risk state for diabetes and is defined by glycemic levels higher than normal, but lower than diabetes limits. Furthermore, IR at the level of the liver and peripheral tissues is observed. Metaphorical, this stage can be seen as a fork in the road, when left untreated, the likelihood to progress to diabetes is high. Additionally, when timely diagnosed and with patients compliance to lifestyle intervention, this condition is reversible to normoglycemia (Tabák et al. 2012). Over the past, scientists studied each organ as an individual part of a complex metabolic network. However, recent data suggest that inter-organ communication is crucial, and it can be mediated by EV. These small vesicles are important vehicles of systemic communication in multiple physiologic and pathologic contexts. They are able to transfer proteins and nucleic acids from a releasing cell to a distant target cell, thus modulating gene and protein expression and leading to functional changes (Zhang et al. 2015; Théry, Zitvogel, and Amigorena 2002). Epithelial cells in the gut secrete EVs and their content may reflect the cell environment (Mallegol, Van Niel, and Heyman 2005). In fact, metabolic surgery is the only known intervention that leads to diabetes remission (Evers, Sandoval, and Seeley 2017). Interestingly, gut dysbiosis recently emerged as a possible player in the development of T2D. (David et al. 2014). Despite the abundant literature on the impact of microbiota in T2D onset and development, the role of the intestine independent of its biota is still elusive. While gut-derived EV (GDE) are considered to play an important role in intestinal diseases (Burcelin et al. 2011) it is not known whether GDE protein content is modulated in prediabetes. Therefore, the present chapter aims at characterizing GDE proteome.

Since we wanted to study prediabetes, we used a mouse model that recapitulates many features of prediabetes (Kowalski and Bruce 2014). High fat and sugar feeding can lead to obesity, hyperinsulinemia and altered glucose homeostasis. So, we used HFD which composition is 58%fat and sucrose, in contrast with normal-chow diet (NCD) that is 11%fat. Since obesity is induced by environmental manipulation rather than genes, it is considered the best model to mimic the human condition. By administration of diet for 12 weeks, HFD mice demonstrated significantly increased body weight (Fig.16B) and liver steatosis (Fig.16C). They also developed glucose intolerance that was evaluated by a glucose tolerance test (GTT) in the previous week of sacrifice and correspondent area under the curve (AUC) for each group (Fig.16D; E).

After 12 weeks of diet, with confirmed glucose intolerance, mice were sacrificed, and gut was removed. Small intestine was washed with saline solution and placed in culture media, EV-free, at 37^{o}C overnight. Post-incubation EVs were isolated according to well established protocol, consisting on a sequence of high-speed centrifugations, where fraction by fraction, the particles were separated by size and an intermediate step of sucrose gradient was added in order to exclude free lipid compounds, which were separated based on density. In the last step of the isolation, EVs were labelled with a dye that intercalates with the lipids present on their membranes. Note that from now on the tissue will always be referred as gut or intestine, but specifically, EVs were isolated from small intestine.

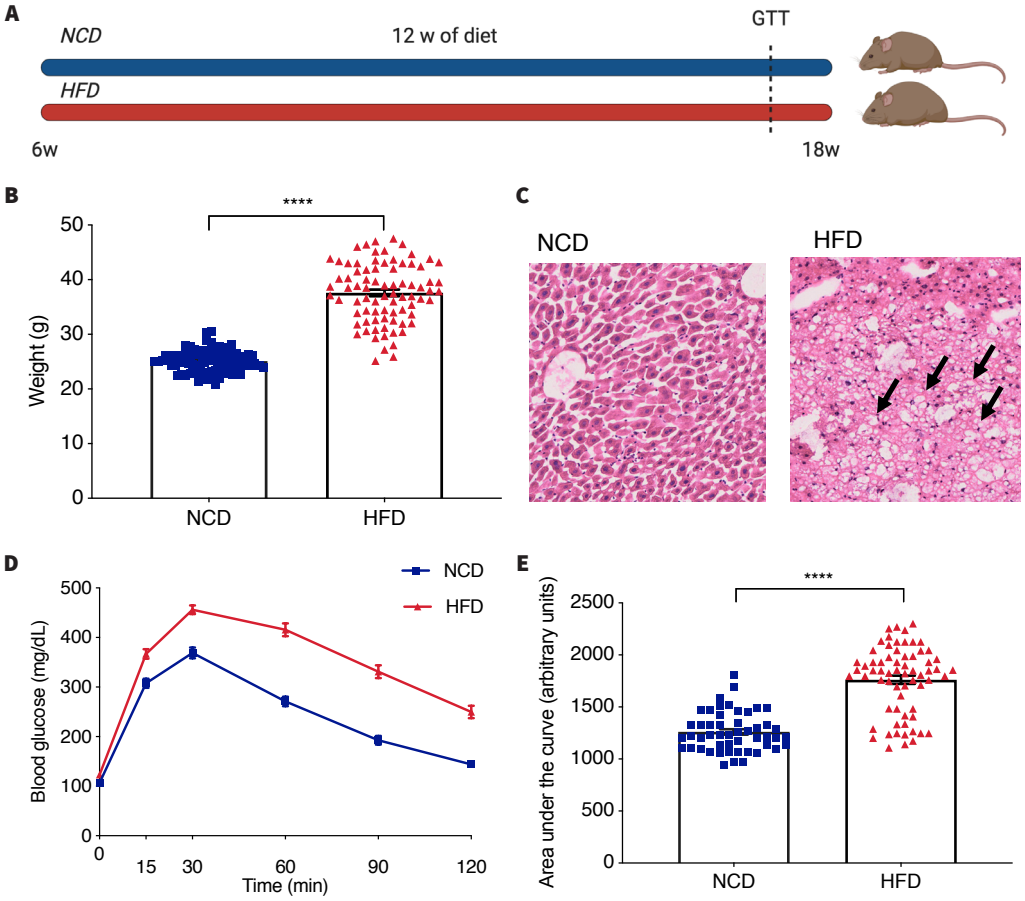

Figure 16. High fat diet is an efficient model for prediabetes. Metabolic characterization of prediabetic mice. A. Diet plan schematic representation. **B.** Statistical analysis of mice body weight. **C.** Hematoxylin-Eosin staining in liver, histological sections of NCD and HFD mice. White circles (black arrows) are lipid droplets, revealing steatosis in the liver of mice subjected to HFD. **D.** Glucose tolerance test (GTT) at different time points after glucose bolus (0, 15, 30, 60, 90, 120 minutes). **E.** Analysis of the area under the curve of the GTT. Results are expressed as mean ± SEM; n=60 for NCD and n=70 for HFD. Unpaired t test with Welch's correction for B and D; ****p<0.0001.

To validate the presence of EVs in the gut of the mouse model in study, we stained gut cross sections for CD81 as a commonly used EV-marker and the presence of EVs was detected in the intestine lumen in both conditions (Fig.17A). Moreover, western blot was performed to detected the enrichment of CD63 in GDE, in fact, CD63 was only detected in the GDEs, in comparison with gut tissue (Fig.17B). Both markers did not show differences in terms of amounts between the groups. Inclusively, we did not find any particular topographic profile looking to the CD81 signal in the gut, but that is something we would like to look into detail in the future.

Gut EVs were characterized by nanoparticle tracking analysis (NTA) and total amount of protein was quantified by BCA. The mean size of the particles obtained by NTA, in both conditions, was around 100 nm, what is consistent with the expected size of small EVs, specifically exosomes (Fig.17C). The only reason why we do not call our EVs exosomes is because we did not investigate their intracellular origin, namely endosomal origin. To be conservative we opted for referring to it as EVs. Moreover, it should be noted the presence, although in much smaller proportion, of larger vesicles (around 200 nm in diameter). While the number of particles did not change with diet (Fig.17D), protein cargo was higher in GDEs isolated from HFD-fed mice (HFD-GDE) than in the ones isolated from NCD-fed mice (NCD-GDE) (Fig.17D; E). The ratio of the two parameters gives the amount of protein per EV. Interestingly, GDEs isolated from prediabetic mice are packed with more protein when compared to controls (Fig.17F).

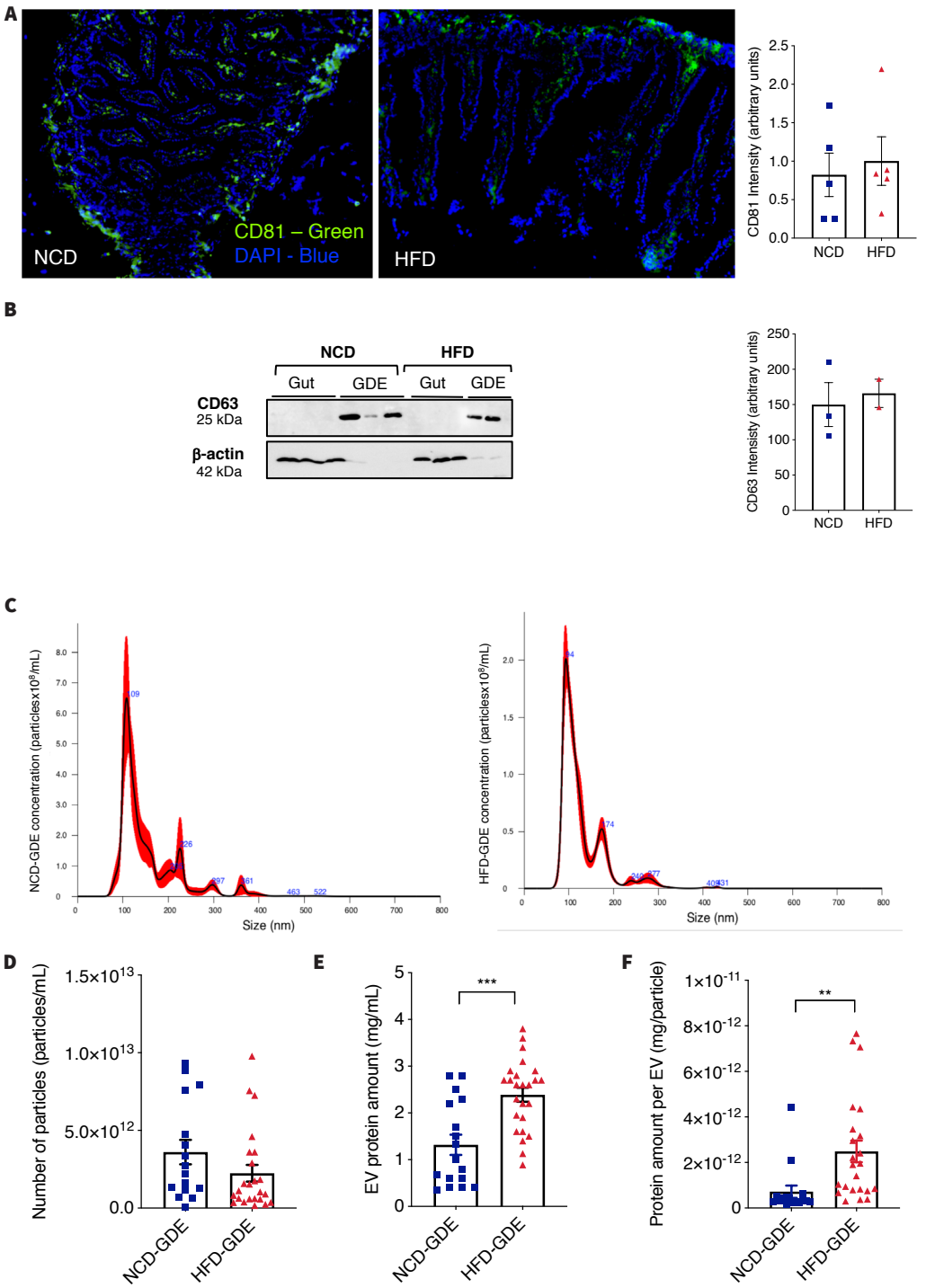

Figure 17. Prediabetes increases protein content/cargo in gut-derived EV. A. EVs labelled in green (CD81) and nuclei in blue (DAPI). NCD gut tissue in the left and HFD gut tissue in the right. Analysis of the CD81 quantification in the gut of injected animals. **B.** Immunoblotting of gut tissue and gut-derived EV (GDE) in NCD conditions and HFD. Protein extracts prepared from mice gut (10 µg) and from mice GDE (15 µg) were analyzed by western blotting using antibodies against EV marker CD63 or protein marker of other subcellular compartments (β-actin). Analysis of CD63 quantification of immunoblotting. **C.** Size and concentration distribution of GDE determined by nanoparticle tracking analysis (NTA). A representative NTA graph of GDE of mice fed with NCD (NCD-GDE) (left) and HFD (HFD-GDE) (right). **D.** Analysis of the number of particles per mL of sample. **E.** Protein quantification in GDE in mg per mL of sample, obtained by BCA. **F.** Protein content per each GDE, represented in mg of protein per particle. Results are expressed as mean ± SEM; n=17 forNCD-GDE and n=25 for HFD-GDE. Unpaired t test with Welch's correction (A, B, D, E, F); ***p<0.0005, **p<0.005.

The technological advance in equipment and in methods analysis are leading to a more precise understanding of multiple pathophysiological mechanisms. One of the research approaches that have been flourishing is proteomics. Importantly, EVs protein cargo provides innumerous information regarding the cellular environment where EVs were produced (Kalra, Drummen, and Mathivanan 2016). EVs proteomic studies have been applied to dig into cell biological and pathophysiological functions and demonstrated to be a rich source for identification of novel biomarker candidates for diseases (Brown 2008; Raimondo et al. 2011). The gold-standard in proteomics is mass spectrometry (MS) and, it is vastly used in EV studies with great success (Conde-Vancells et al. 2008). Essentially, the proteome is digested into peptides, followed by chromatographic separation and MS-based analysis, yielding a list of detected peaks characterized by their retention time (Matthiesen 2013).

We proposed that a diet induced dysmetabolism environment influences the protein composition of GDEs. Thus, to identify the impact of this milieu to GDE protein cargo, we isolated EVs from the guts of 20 mice under HFD and respective controls. GDEs were pooled in order to obtain enough material for further analysis by MS. The EVs pool was divided in three. Each technical sample was run three times, giving us a total of nine technical replicates. Obtained data was quantified and analyzed with bioinformatic tools (Fig. 18A).

Because we wanted to study the impact of gut in particular, without the effect of microbiota, we first evaluated if the isolated EVs were indeed coming from gut cells, and not from gut colonizing bacteria. In fact, we observed that almost every protein identified were from *Mus musculus*, with the other bars counting for homologous proteins (Fig.18B). In addition, by streaking an agar petri dish, in the absence of antibiotics, with the culture media where the guts were deposited overnight, we did not observe any bacterial growth, indicating that the isolated EVs were GDEs and not biota derived EVs (Fig.18C).

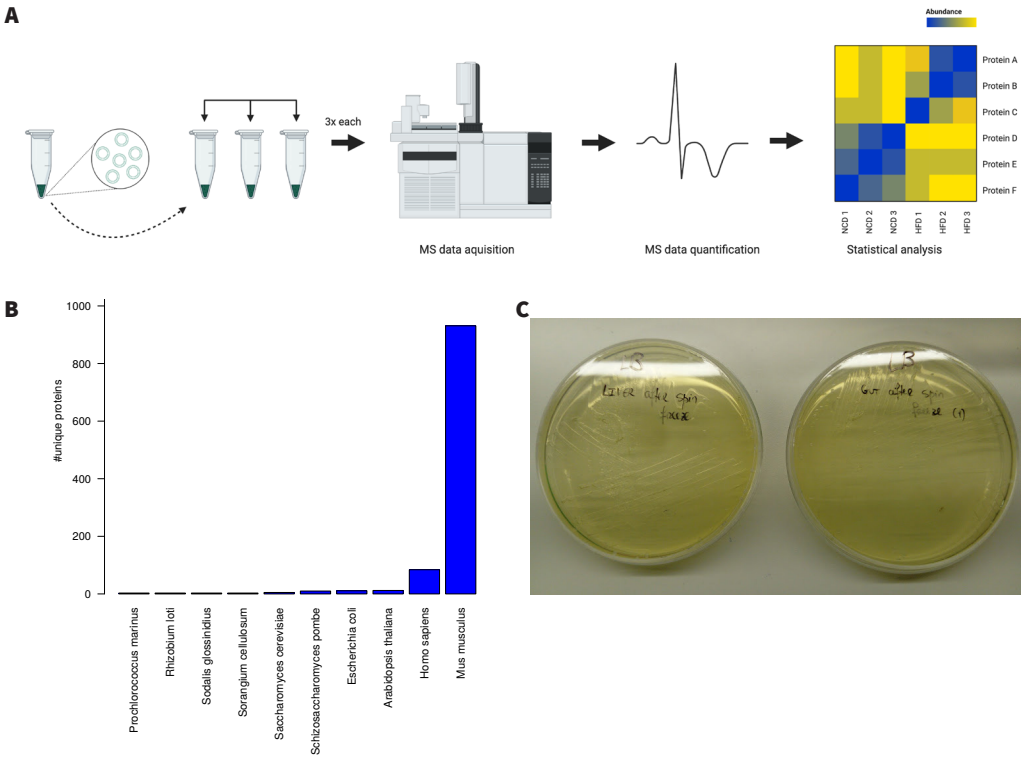

Figure 18. Study flow of proteomic approach for characterization of gut-derived EV protein cargos. **A.** Schematic representation of the experimental process of analysis of gut-derived EV (GDE). **B.** Bar plot indicating the number of proteins uniquely identified from different species when searched against all proteins from all species in UniProt. **C.** Picture of LB-agar (without antibiotics) petri dish after 24 after hours of inoculation with media where guts were deposit overnight at 37ºC prior to EVs isolation.

After filtrating the identified proteins from reverse proteins and possible contaminating proteins lead to a total of 2467 identified proteins, with 217 proteins predominantly identified in the NCD group and 422 in the HFD group. Excluding proteins with missing quantification values resulted in 2156 proteins. The raw data was then submitted to normalization (Fig.19A). We started by excluding every protein with missing values. The missing values are acquisition values of zero, among the same replica. In addition, we evaluated every protein in each group, and established that a protein is classified as unique in one group, based on abundance, importantly it does not exclude its expression in the other group. The Venn Diagram on Figure 19A represents the number of protein identification from each of the two sample conditions. After excluding proteins with missing quantitative values all the remaining proteins were identified in both conditions, so the two circles of the Venn Diagram culminated in one with a final list of 2156 identified proteins (Appendix Document). Subsequently, we distinguished between identified and regulated proteins. In the present study, we defined regulated proteins which reflect the difference between the two groups, as the ones that are at least two-fold of regulated and with an adj. p-value < 0.05. After applying the aforementioned criteria to our data set, we obtained a list of robustly regulated 558 proteins, suggesting that diet-induced prediabetes alters the abundance of many proteins in GDEs (Fig.19A). All data, before applying the filtering criteria, is represented in a volcano plot that describes the level of significance and magnitude of changes observed, comparing the HFD with the NCD group (Fig.19B). The dotted line in the plot represents the threshold of adj.p-value<0.05, and from that line above each individual dot represents a protein within the 558 regulated ones. Moreover, on the left the down-regulated proteins are grouped and, on the right, the up-regulated ones. We observed a similar number of down and up regulated proteins.

Afterwards, bioinformatics analysis was performed on the 588 regulated proteins. Gene Ontology (GO) and Kyoto Encyclopedia for Genes and Genomes (KEGG) enrichment analysis revealed that altered proteins are involved on distinct molecular functions, and consistently the vast majority are closely related with metabolism. In terms of molecular function, enzyme activity shows up in the top of list, isomerases for example catalyze reactions such as glycolysis and carbohydrate metabolism, while hydrolases are very common in lipid metabolism. Furthermore, oxidoreductase proteins are also up-regulated, these are mediators of an oxidation-reduction reaction, where the oxidation state of an atom within a molecule is altered (Fig.19C). Most of the enriched pathways for GO biological process emphasized lipid metabolism, highlighting FA β-oxidation. Curiously, glycolysis-related and proteolysis in cellular protein catabolic processes-related proteins are mostly down-regulated (Fig.19D). Considering KEGG pathways enrichment analysis, the affected proteins belong primarily to FA, carbohydrate and amino acid metabolism. Interestingly, alcoholism-related proteins show up with great significance (Fig.19E). In terms of down-regulate proteins, based on the KEGG analysis the proteasome and focal adhesions are markedly down-regulated. Finally, to assess sub-cellular localization of the GDE protein cargo regulated by diet we used GO cellular component analysis and found that the majority of altered proteins are mitochondrial, followed by the cytosolic ones. Once again, proteasome related proteins show up as down-regulated (Fig.19F).

For a more detailed characterization of GDE proteome, we looked into the subset of proteins that were overly altered among groups. For that, we established an adj.p-value<0.0001 as cut-off (Fig.20A). The proteins with that significance are represented in the heatmap. We found a variety of proteins that are up-regulated and others down-regulated in GDEs from prediabetic mice compared with control animals, suggesting that altogether these proteins can change the metabolism of the recipient cells upon EV uptake (Fig.20B).

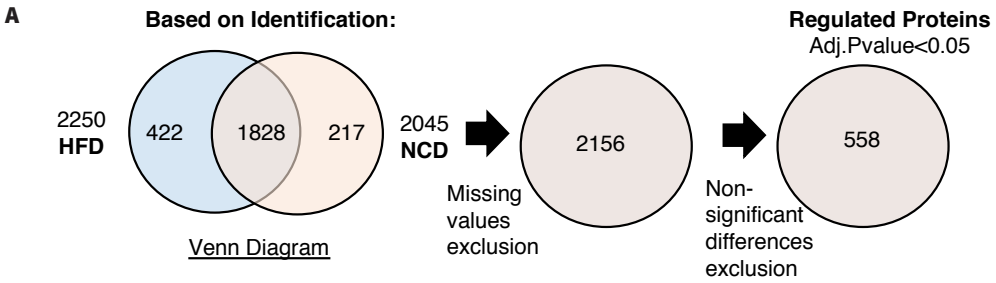
A
Based on Identification:
Regulated Proteins
Adj.Pvalue<0.05
2250
HFD
422
1828
217
2045
NCD
2156
558
Missing values exclusion
Non-significant differences exclusion
Venn Diagram

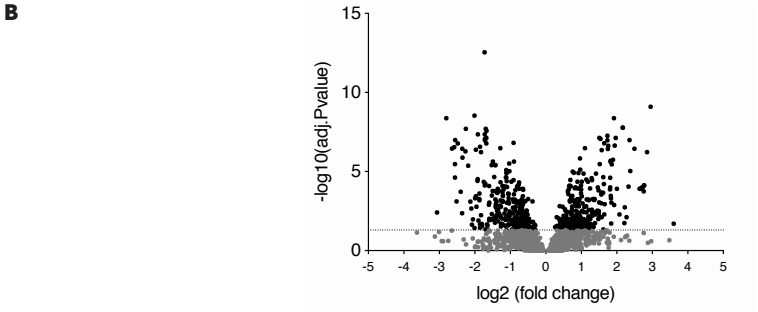
B
-log10(adj.Pvalue)
log2 (fold change)

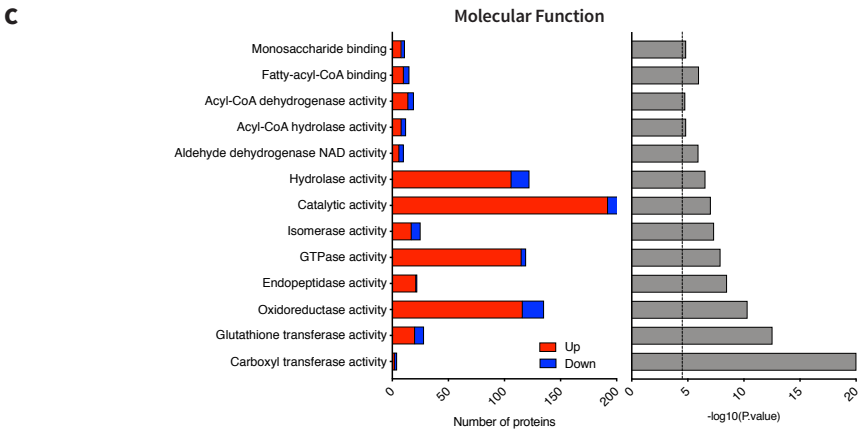
C
Molecular Function
Monosaccharide binding
Fatty-acyl-CoA binding
Acyl-CoA dehydrogenase activity
Acyl-CoA hydrolase activity
Aldehyde dehydrogenase NAD activity
Hydrolase activity
Catalytic activity
Isomerase activity
GTPase activity
Endopeptidase activity
Oxidoreductase activity
Glutathione transferase activity
Carboxyl transferase activity
Up
Down
Number of proteins
-log10(P.value)

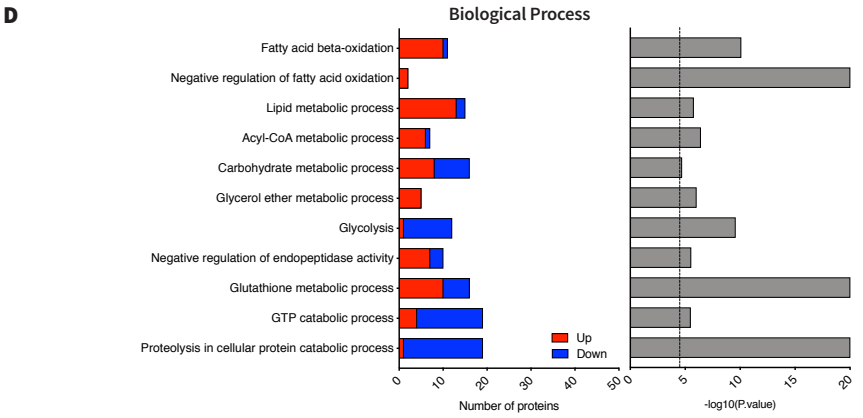
D
Biological Process
Fatty acid beta-oxidation
Negative regulation of fatty acid oxidation
Lipid metabolic process
Acyl-CoA metabolic process
Carbohydrate metabolic process
Glycerol ether metabolic process
Glycolysis
Negative regulation of endopeptidase activity
Glutathione metabolic process
GTP catabolic process
Proteolysis in cellular protein catabolic process
Up
Down
Number of proteins
-log10(P.value)

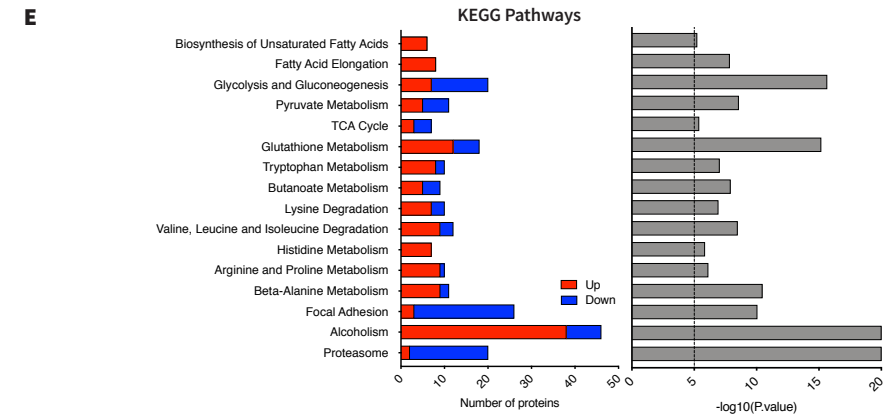
E
KEGG Pathways
Biosynthesis of Unsaturated Fatty Acids
Fatty Acid Elongation
Glycolysis and Gluconeogenesis
Pyruvate Metabolism
TCA Cycle
Glutathione Metabolism
Tryptophan Metabolism
Butanoate Metabolism
Lysine Degradation
Valine, Leucine and Isoleucine Degradation
Histidine Metabolism
Arginine and Proline Metabolism
Beta-Alanine Metabolism
Focal Adhesion
Alcoholism
Proteasome
Up
Down
Number of proteins
-log10(P.value)

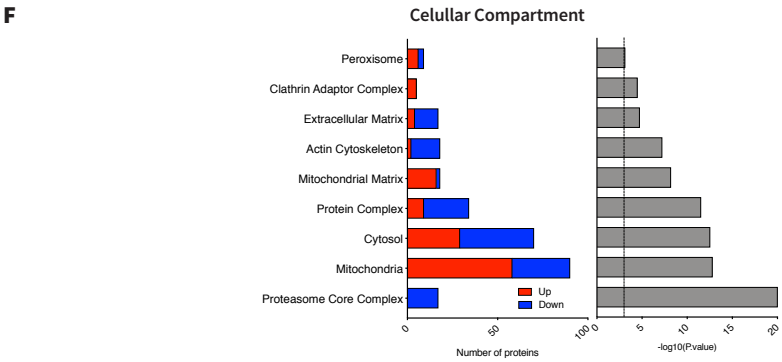

Figure 19. Characterization of prediabetic gut-derived EV by GO and KEGG enrichment analysis directly against mouse annotation, according to GO terms. **A.** Strategy used for selection of proteins to be analyzed with confidence. **B.** Volcano plot representing the fold change and adj.p-value in the gut-derived EV (GDE) isolated from prediabetic mice and control groups. x-axis represents fold change, and y-axis adj.p-value. Dotted line sets the threshold of adj.p-value<0.05. In grey are the non-regulated proteins, in black the 558 regulated proteins. **C.** Molecular function analysis of the GDE identified proteins. GO enrichment analysis according to Molecular Function. **D.** Analysis of the main biological regulated by the proteins identified in the GDE. GO enrichment analysis according to Biological Process. **E.** KEGG enrichment analysis for KEGG pathway. **F.** GO enrichment analysis according to Cellular Compartment. For C, D, E and F; on the left panel, changes are displayed as the number of proteins with increased (red) or decreased (blue) levels (horizontal axis). On the right panel, the horizontal axis indicates the significance -log10 (p-value) of the functional association, which is dependent on the number of submitted proteins in the class, the number of proteins annotated in the class, the total number of submitted proteins and the total number of mouse proteins.

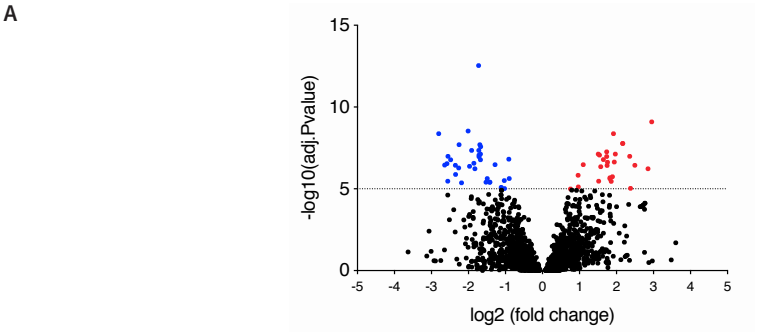

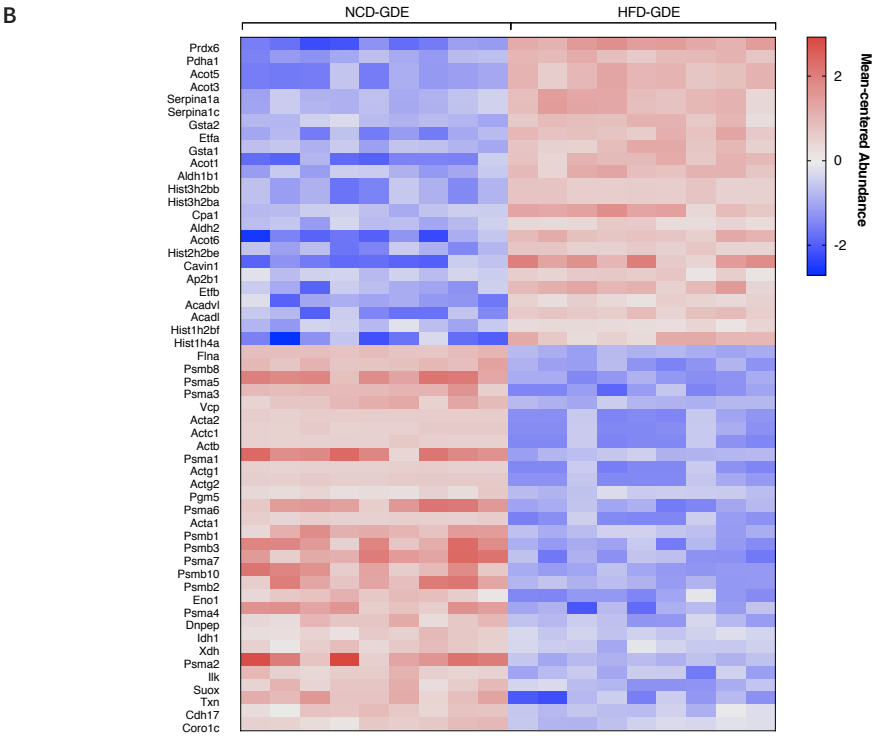

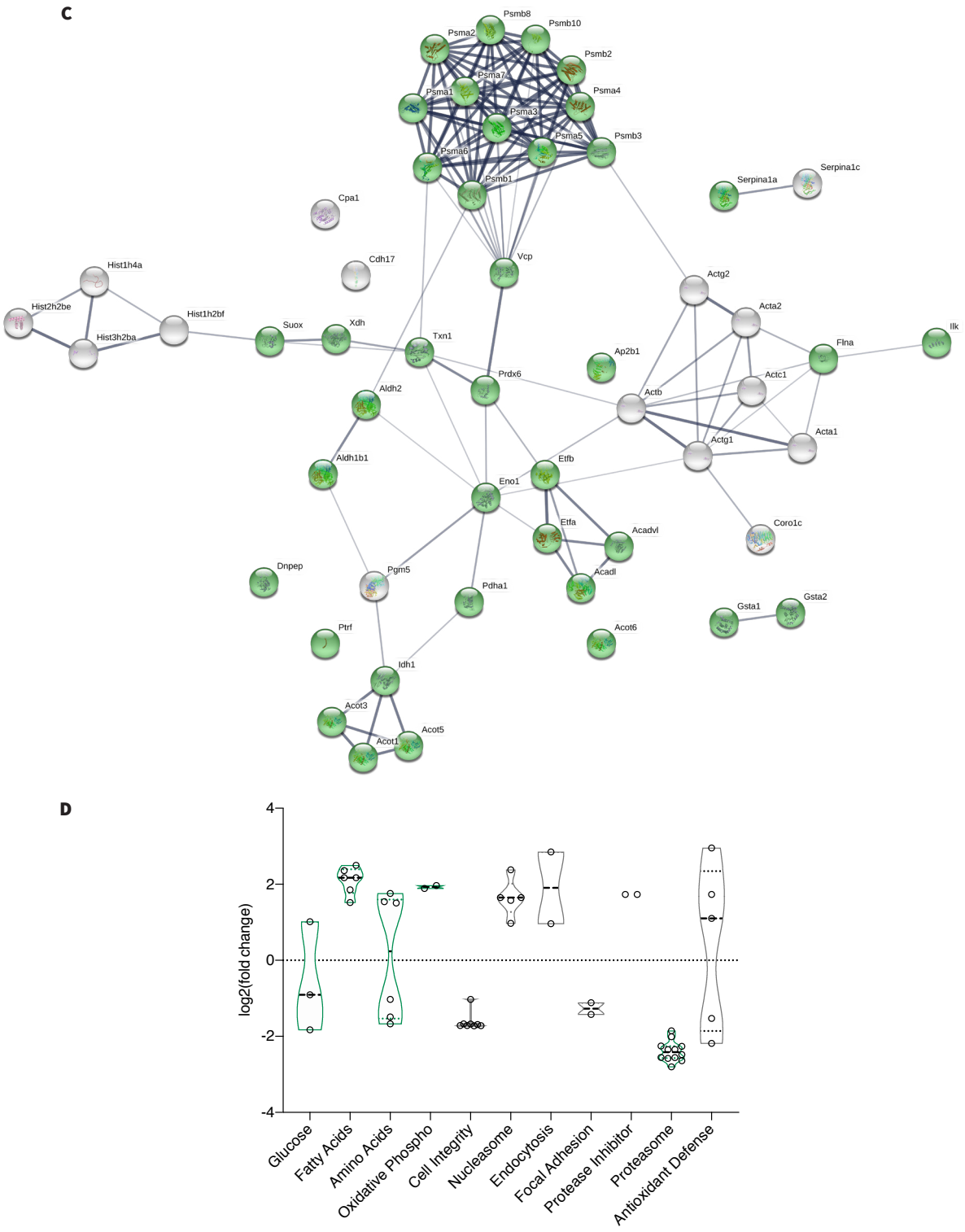

Figure 20. Cluster analysis of the top50 altered proteins of gut-derived EV in prediabetic mice. A. Volcano plot representing the fold change and adj.p-value of gut-derived EV (GDE) proteins isolated from prediabetic mice and control groups. x-axis represents fold change, and y-axis adj.p-value. Dotted line sets the threshold of adj.p-value<0.0001, highlighting the most altered proteins in GDE from HFD comparing with GDE from NCD. In blue are the most down-regulated proteins and in red the most up-regulated. **B.** Heatmap representing mean-centered abundance of the nine technical replicas for the most altered proteins decorated in the previous volcano plot. **C.** Protein-protein interaction network. The network was built using the STRING online software with a medium confidence level (0.4). Each circle represents one protein. The line thickness indicates the strength of the evidence, with thicker connections indicating higher confidence in the protein-protein interaction. Green circles represent the proteins belonging to cellular metabolic process according to GO enrichment analysis for biological processes. **D.** Violin plot demonstrating the fold changes of the most altered proteins and correspondent cellular functions. Cellular metabolic process (GO) represented in green.

To gain insight into protein-protein interaction of GDE identified protein cargo, we used the STRING software to link some of the altered proteins and to display the level of relationship between them. The proteins that demonstrate higher level of interaction are the ones related with the proteasome, both α subunits (PSMA) and β (PSMB). Actin related proteins which function is to maintain cellular integrity (ACTA1, ACTA2, ACTB, ACTC1, ACTG1, ACTG2, CORO1C, FLNA, MYL6, MYL6B) also display relevant interaction. Moreover, network analysis highlights strong bias towards metabolic-related proteins, which are represented by green circles (Fig.20C). The fold change of all altered proteins varied up to an approximately 2-fold difference in abundance when comparing HFD with NCD EVs content. Importantly, looking into metabolic pathways, the altered proteins are mainly involved in nutrient metabolic pathways, such as glucose, FA and amino acid, being the FA pathway represented only by up-regulated proteins, on the contrary, cell integrity, focal adhesion and proteasome-related proteins are all down-regulated (Fig.20D).

For proper visualization of subcellular origin of the key proteins regulated by the diet and packaged inside GDE, Figure 21A illustrates the most altered ones according to their fold change. Data is displayed in terms of HFD compared with NCD, meaning that when a certain protein is up or down regulated, this is in the HFD-GDE versus NCD-GDE. These observations demonstrate that, in fact, GDEs mirror the environment of the cells of origin. In Figure 21B it is represented the significant fold change for each protein in the image, according to its most associated pathway. Naturally, there is some level of functional homology, since the same protein can play role in diverse pathways. Noteworthy to mention, carbohydrate metabolism, which ensures the supply of energy to the cells, has several proteins affected but mainly down-regulated (PFKL, ALDOA, ALDOB, PGAM2, ENO1, PGM5). Contrary to the proteins related with lipid homeostasis (ACOT1, ACOT2, ACOT3, ACOT5, ACOT6), FA mitochondrial β-oxidation (HDHA, ACADVL, ACADL, ECHS1, ACAA2) and very-long chain FA peroxisomal β-oxidation (ECH1, ACOX1) that are all up-regulated. On the other hand, proteins involved in TCA cycle are down-regulated (DLST, IDH1). Moreover, cholesterol homeostasis related proteins are down-regulated (ACAT1, ACAT2). Metabolic pathways of amino acids are also greatly affected, namely glutathione (GSTA1, GSTA2). In the trafficking front, endocytic proteins are being up-regulated, namely AP2B and CAVIN1. Proteasomal proteins are consistently down-regulated, with a big portion of proteins altered, and all of them significantly down-regulated (PSMA1, PSMA2, PSMA3, PSMA4, PSMA5, PSMA6, PSMA7, PSMB1, PSMB2, PSMB3, PSMB8, PSMB10). Finally, proteins related with antioxidant defense are majorly up-regulated (ALDH2, ALDH1B1, PRDX6, GSTA4, GSTM2). Table 1 describes all the proteins up- and down-regulated according to its biological function.

In summary, our proteomics approach revealed that in GDEs isolated from a diet-induced prediabetic mouse model, the top regulated pathways are the metabolic, particularly pathways related with nutrient sensing and utilization.

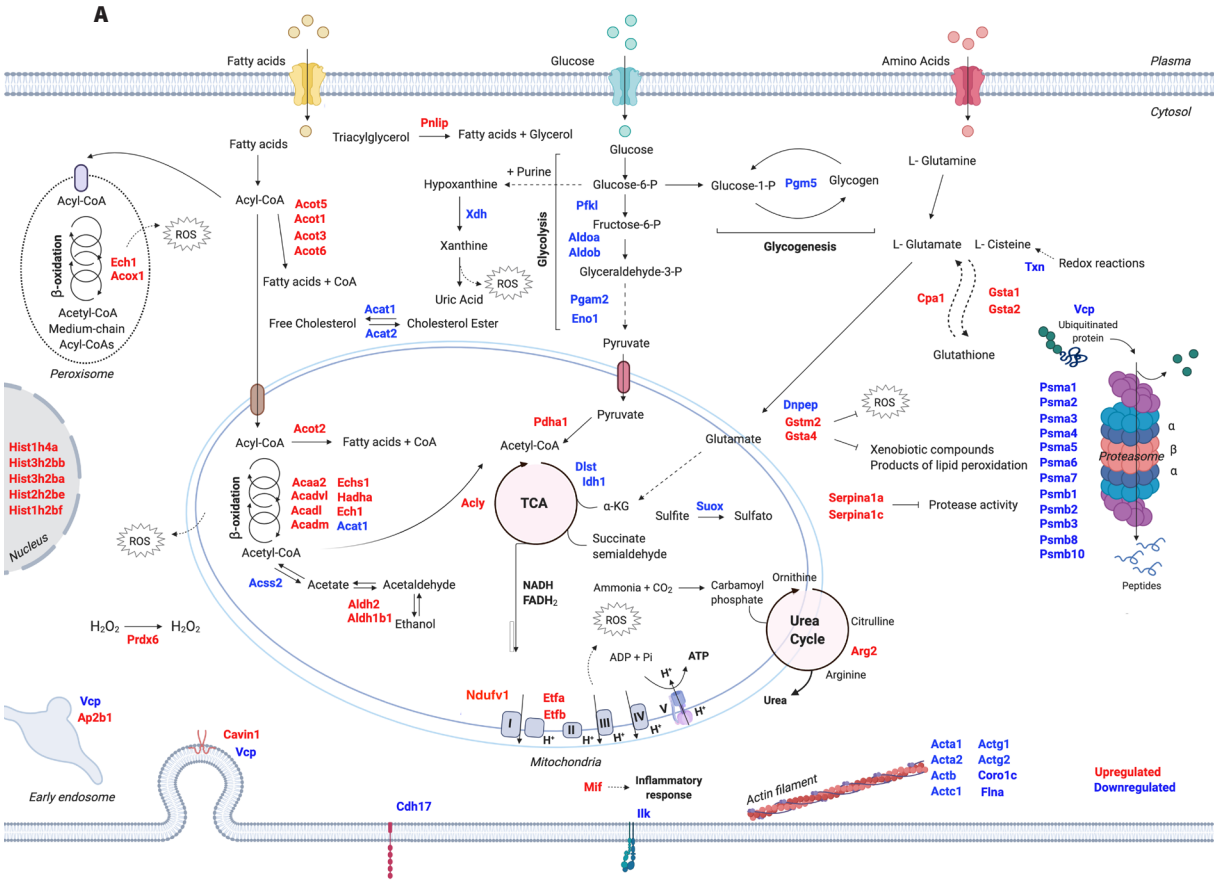
A
Fatty acids
Glucose
Amino Acids
Plasma
Cytosol
Triacylglycerol
Pnlip
Fatty acids + Glycerol
Acyl-CoA
Acot5
Acot1
Acot3
Acot6
Fatty acids + CoA
β-oxidation
Ech1
Acox1
ROS
Acetyl-CoA
Medium-chain
Acyl-CoAs
Peroxisome
Free Cholesterol
Acat1
Acat2
Cholesterol Ester
Hypoxanthine
+ Purine
Xdh
Xanthine
Uric Acid
Glycolysis
Glucose-6-P
Pfkl
Fructose-6-P
Aldoa
Aldob
Glyceraldehyde-3-P
Pgam2
Eno1
Pyruvate
Glucose-1-P
Pgm5
Glycogen
Glycogenesis
L- Glutamine
L- Glutamate
L- Cysteine
Redox reactions
Txn
Cpa1
Gsta1
Gsta2
Glutathione
Vcp
Ubiquitinated protein
Psma1
Psma2
Psma3
Psma4
Psma5
Psma6
Psma7
Psmb1
Psmb2
Psmb3
Psmb8
Psmb10
Proteasome
Peptides
Hist1h4a
Hist3h2bb
Hist3h2ba
Hist2h2be
Hist1h2bf
Nucleus
Acot2
Pdha1
Acetyl-CoA
Glutamate
Dnpep
Gstm2
Gsta4
Xenobiotic compounds
Products of lipid peroxidation
Serpina1a
Serpina1c
Protease activity
Acaa2
Acadvl
Acadl
Acadm
Echs1
Hadha
Ech1
Acat1
Acly
TCA
Dlst
Idh1
α-KG
Sulfite
Suox
Sulfato
Succinate semialdehyde
Acss2
Acetate
Acetaldehyde
Aldh2
Aldh1b1
Ethanol
NADH
FADH2
Ammonia + CO2
Carbamoyl phosphate
Ornithine
Urea Cycle
Citrulline
Arg2
Arginine
Urea
H2O2
Prdx6
ADP + Pi
ATP
Ndufv1
Etfa
Etfb
Mitochondria
Vcp
Ap2b1
Early endosome
Cavin1
Vcp
Cdh17
Mif
Inflammatory response
Ilk
Actin filament
Acta1
Acta2
Actb
Actc1
Actg1
Actg2
Coro1c
Flna
Upregulated
Downregulated
B
log2(fold change)
Eno1
Pfkl
Aldoa
Aldob
Pgam2
Pgm5
Pdha1
Glucose
Acot1
Acot5
Acot3
Acot6
Acadl
Acadvl
Hadha
Echs1
Ech1
Acat1
Acat2
Acly
Pnlip
Fatty acids
Vcp
Gsta1
Gsta2
Cpa1
Dnpep
Xdh
Amino acids
Dlst
Idh1
TCA cycle
Etfa
Etfb
Ndufv1
Oxidative phosphorilation
Aldh2
Aldh1b1
Prdx6
Gsta4
Gstm2
Txn
Suox
Antioxidant defense
Psma3
Psmb2
Psma4
Psmb1
Psma6
Psma1
Psma2
Psmb3
Psma7
Psma5
Proteasome

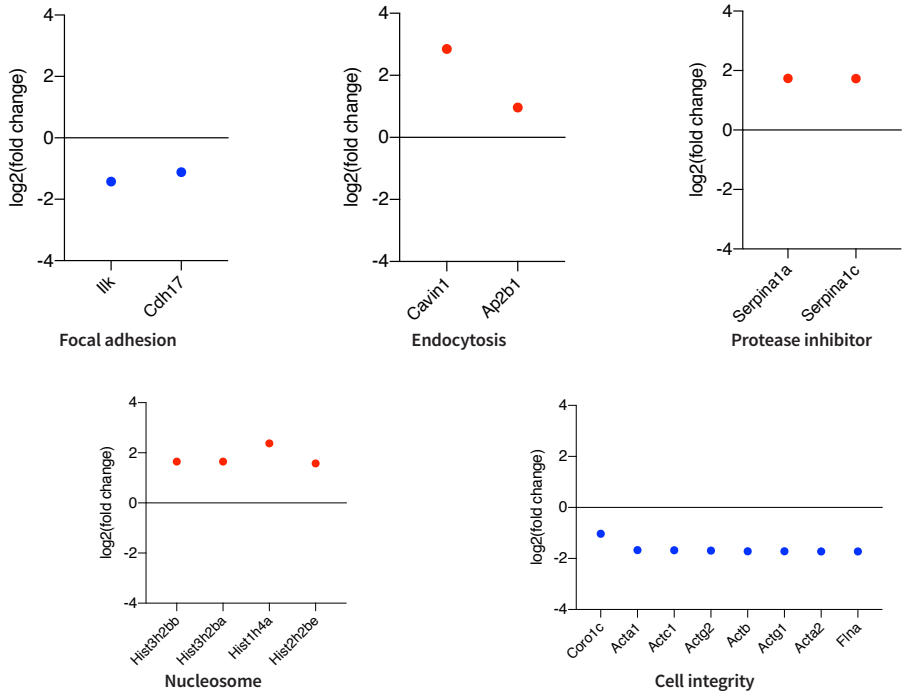

Figure 21. Overview of prediabetes impact on gut-derived EV proteome. A. The identified proteins with higher differential expression are represented in the image according to their function and estimated subcellular localization. Red color for proteins up-regulated and blue color for proteins down-regulated in gut-derived EV of mice fed with HFD compared with controls, mice fed with NCD. ROS, reactive oxygen species; α-KC, α-ketoglutarate; TCA, tricarboxylic acid cycle; I, II, IV and V, complexes of mitochondrial oxidative phosphorylation (I-IV: respiratory chain complexes; V: ATP synthase complex); Pi, inorganic phosphate; ADP, adenosine diphosphate; ATP, adenosine triphosphate; α and ß, proteasome subunits. The detailed description of protein names is shown in Abbreviations List. **B.** Data plots demonstrating the log fold changes of each protein in the image in accordance to its related pathway.

Biological Function	Up	Down
Glucose metabolism		
Glycolysis		PFKL; ALDOA; ALDOB; PGAM2; ENO1; PGM5
Conversion of pyruvate to acetyl-CoA	PDHA1	
Amino acid metabolism		
Glutathione metabolism	GSTA1; GSTA2	
C-terminal amino acid release	CPA1	
Protein degradation		VCP
Peptide metabolism		DNPEP
Purine metabolism		XDH
Lipid metabolism		
Mitochondrial ß-oxidation	HADHA; ACADVL; ACADL; ECH1; ECHS1	
Peroxisome ß-oxidation	ECH1; ACOX1	
Lipid homeostasis	ACOT1; ACOT2; ACOT3; ACOT5; ACOT6	ACSS2
Lipid biosynthesis	ACLY	
Cholesterol metabolism		ACAT1; ACAT2
Triglyceride metabolism	PNLIP; ACOT	
Tricarboxylic acid cycle		DLST; IDH1
Oxidative phosphorylation	ETFA; ETFB; NDUFV1	

Biological Function	Up	Down
Sulfur oxidative degradation		SUOX
Urea cycle	ARG2	
Antioxidant defense	PRDX6; GSTA4; GSTM2; ALDH2; ALDH1B1	TXN
Proteasome complex		PSMA1; PSMA2; PSMA3; PSMA4; PSMA5; PSMA6; PSMA7; PSMB1; PSMB2; PSMB3; PSMB8; PSMB10
Protease inhibitor	SERPINA1A; SERPINA1C	
Cell integrity		ACTA1; ACTA2; ACTB; ACTC1; ACTG1; ACTG2; CORO1C; FLNA
Nucleosome	HIST1H4A; HIST3H2BB; HIST3H2BA; HIST2H2BE; HIST1H2BF	
Endocytosis		
Caveolar endocytosis	CAVIN1	
Clathrin-dependent endocytosis	AP2B1	
Focal adhesion		ILK; CDH17
Inflammatory response	MIF	

Table 1. Biological function of the main up- and down- regulated proteins in HFD-GDE compared with NCD-GDE by proteomics. The detailed description of protein names is shown in Abbreviations list.

1.2. Proteomic comprehensions on plasma EV of prediabetic mice

Once the route used by EV for mobilization is the circulatory system, next we studied how much of the proteome of EV traveling in the blood meet the one from GDEs. Therefore, we isolated plasma EVs from the same prediabetic mice model and respective controls. Blood is first fractioned into plasma (Fig.22A). Plasma EVs were analyzed in the NTA, that revealed increased number of particles in HFD mice (Fig.22B), and the BCA protein quantification also demonstrated that the same mice had increased amount of protein (Fig.22C), that culminated in similar average amount of protein per EV in both groups (Fig.22D).

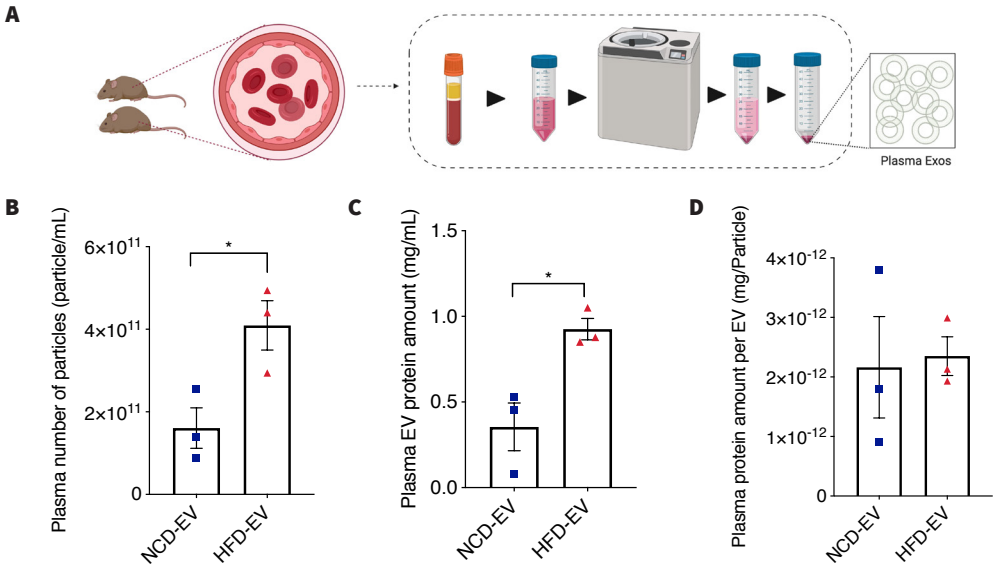

Figure 22. EV isolation and quantification in plasma of mice fed with NCD and HFD. A. Schematic representation of plasma EVs isolation. **B.** Quantification of the number of EVs per mL of plasma. **C.** Quantification of amount of protein in plasma EVs, in mg per mL of sample. **D.** Representation of the amount of protein per EVs of plasma, resulting from the ratio of B and C. Results are expressed as mean ± SEM; Each n is a pool of 20, n=3 for NCD and HFD. Unpaired t test with Welch's correction. *p<0.05

MS studies were performed in plasma EV in order to trace the proteome profile and link with gut observations. Using the same exclusion criteria of gut EV, 161 proteins were identified in plasma EV. From those, 129 proteins were in common with gut (Fig.23A). The co-expressed proteins are highlighted in red in the volcano plot (Fig.23B).

An analysis of the distribution of biological processes related with all proteins identified was done by PANTHER software, based on GO annotations, for plasma EV (Fig.23C) and for gut EV (Fig.23D), in order they could be compared side-by-side. We can see that in both tissues the EV proteins are predominantly related with metabolic processes, with a small increment in the case of gut EVs (Fig.23C). The level of significance for our plasma EV data was much inferior to the gut. One of the reasons is because we only had two replica of plasma EVs. Therefore, we established a threshold of p-value<0.9 for regulated proteins. By studying the overlap between regulated proteins in plasma and gut, the list of proteins with similar variance are plotted in Figure 23D.

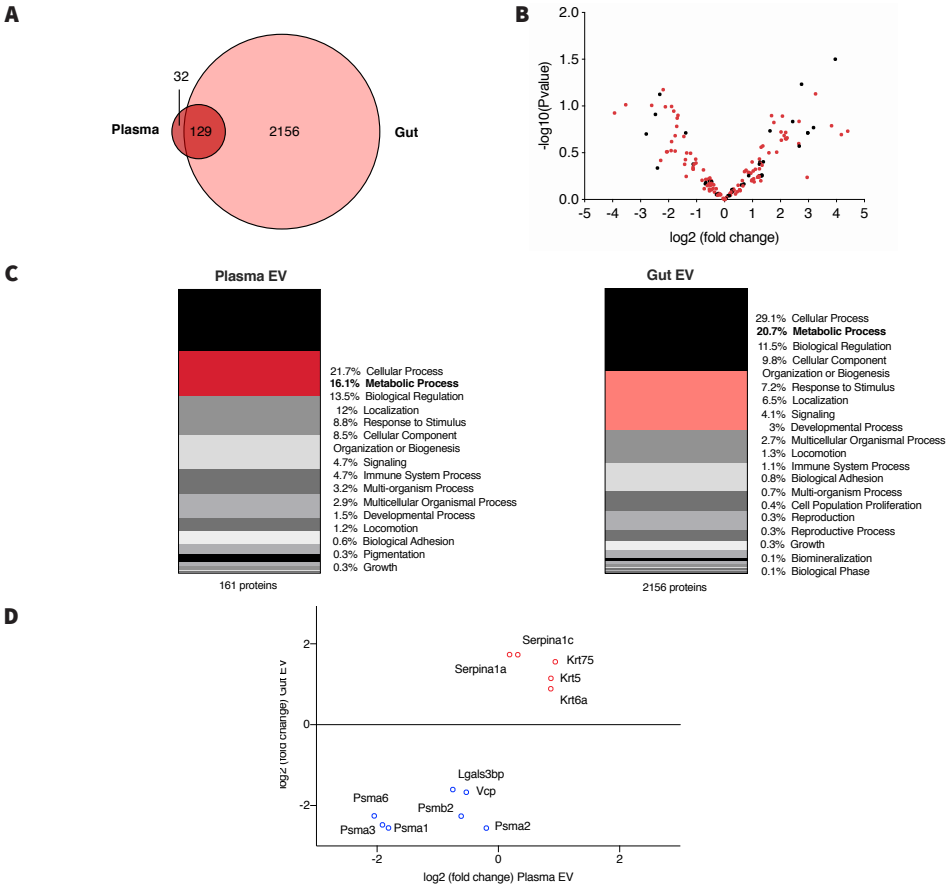

Figure 23. Proteome analysis of plasma EV. A. Venn diagram demonstrating the intersection of plasma EV-identified proteins with gut EV-identified proteins. **B.** Univariate, significance (p-value) vs. fold change analyses representing all identified proteins in plasma EVs. Each dot symbolizes a protein. The red dots represent the proteins identified in both tissues. **C.** Percental distribution of biological processes related with proteins identified in plasma EV (left). Percental distribution of biological processes related with proteins identified in gut EV (right). Analysis performed using the PANTHER online tool, based on GO annotations for biological processes. **D.** Relation of fold change variation of regulated proteins in plasma EVs and gut EVs. Red circles highlight up-regulated proteins on EV of both tissues in HFD scenario and blue circles highlight down-regulated proteins on EV of both tissues in the same condition. The detailed description of protein names is shown in Abbreviations list.

Discussion

Today's modern society has witnessed a profound change in lifestyle and diet. In fact, changes have been seen towards the over-consumption of processed fatty and sugary foods, combined with a decreased intake of fruits and vegetables. These changes in dietary habits are widely accepted as the so-called western diet, viewed as one of the main culprits in the exponentially increased of obesity rates. Moreover, western diet consumption is strongly associated with a general pro-inflammatory state with deleterious consequences in organismal homeostasis (Losacco et al. 2018).Therefore, the relationship between dietary habits and the incidence of multiple metabolic disorders is one of the main public health concerns. One of the first organs to contact with food and its derivates is the gut, as a consequence it is where the first organismal response should be found. Fundamentally, the gut is the first sensing organ to exogenous energy sources (Abumrad and Davidson 2012). The impact of diet on gut microbiota and consequently in its metabolites is well described in the literature (Zhang and Yang 2016). Likewise, western diet-induced obesity considerably alters intestinal flora (David et al. 2014) resulting in IR and metabolic diseases (Saad, Santos, and Prada 2016). How western diet-induced obesity mechanistically trigger prediabetes, partially independent of gut microbiota, is still elusive. Here, we report, for the first time, that GDE isolated from animals fed with HFD have a distinct proteome that strongly reflects the intestinal dysmetabolic milieu.

The present findings show that the GDE proteome reflects the capability of the intestine to sense dietary regimens and mirrors its metabolic alterations. Interestingly, in GDE from prediabetic animals, we found numerous pathways associated with macronutrients altered. Several lines of evidence support a model in which the metabolic alterations induced by the HFD are translated into alterations in GDE protein cargo. For simplicity, we will discuss it by relevant groups in metabolic profiles.

Carbohydrate metabolism

Our data revealed that glucose metabolism is disturbed, in particular glycolysis, the enzymes participating in the first steps of the pathway were found downregulated, namely phosphofructokinase (PFKL); phosphoglycerate mutase (PGAM2), aldolase A and B (ALDOA and ALDOB), β-enolase (ENO1) (Tarnopolsky 2018) (Fig.21). However, down the glycolysis pathway, pyruvate dehydrogenase (PDHA1) was upregulated, indicating a possible compensation in the pathway given the importance of acetyl-CoA for the TCA cycle and in many other biochemical reactions in protein and lipid metabolism. From the enrichment analysis we observed that both glycolysis-gluconeogenesis pathway and pyruvate pathway appear in the top of the most affected routes (Fig.19D; E).

The decreased in glycolysis might be explained by the low amount of fibers provided by the diet; since the percentage of fibers in HFD is considerably reduced and in part replaced by sucrose. In accordance, fibers have a beneficial effect on NCD mice, by improving intestinal integrity, enhancing energy expenditure and reducing inflammation (Jangra et al. 2019)(. In fact, because HFD has increased sucrose, we envisage that sucrose is being directed to an alternative pathway, such as DNL, known to also occur in the gut (Hoffman, Alvares, and Adeli 2019).

Amino acid metabolism

The gut is the place where amino acids are digested from dietary protein. Even though GDE were released exclusively from intestinal cells (Fig.18B; C), we cannot exclude the impact of gut microbiota

metabolites in the cell. Thus, this might explain why we see proteins classically related with bacterial metabolites pathways being affected in the GDE (Gu et al. 2019). That is the case of short-chain fatty acids (SCFA) and amino acids that derive from bacterial activity in the gut (Neis, Dejong, and Rensen 2015). The KEGG analysis revealed several pathways associated to essential and non-essential amino acids to be affected (Fig.19E). Amino acids are particularly important in the survival and growth of bacteria, but also controlling energy and protein homeostasis (Neis, Dejong, and Rensen 2015). Upon uptake by bacteria, amino acids can be directly assimilated into bacterial cells or catabolized. Lysine, whose pathway we see affected in HFD-GDE, is greatly used by bacteria (Stoll et al. 1998); alternatively it intermediates protein biosynthesis, such as carnitine, a key factor in FA metabolism (Azevedo and Saiardi 2016). Interestingly, carnitine deficiency due to poor lysine diet induces triglycerides accumulation (Khan and Bamji 1979).

The amino acids derived from microbial protein fermentation can also serve as precursors of SCFA synthesis, for example lysine fermentation pathway leads to the production of butanoate (Van Nielen et al. 2014; Kreimeyer et al. 2007) that we also see, in our analysis, to have its related metabolic proteins greatly affected. Butanoate is absorbed by the intestinal epithelium and is used by liver cells for gluconeogenesis and cholesterol synthesis (Neis, Dejong, and Rensen 2015).

In HFD-induced obesity and T2D there is a marked increase in the portal concentrations of several essential amino acids, particularly the branched-chain amino acids (BCAA), valine, leucine and isoleucine (Lian et al. 2015; J. Wang et al. 2019). From our data we cannot ascertain amino acids and SCFA levels; however their pathways are definitely affected in HFD mice, one more evidence of diet impact on intestinal microenvironment (Oliphant and Allen-Vercoe 2019) (Fig.19E).

Lipid metabolism

In accordance with lipidic diet content, we observed that the lipid metabolism is massively altered, especially with many proteins being upregulated. Not only GO and KEGG enrichment analysis revealed a dominant number of pathways related with lipid metabolism, such as biosynthesis of unsaturated FA and FA elongation, but also among the top 50 most affected proteins are many lipid related-ones.

The excess of fat in the diet is known to cause increased uptake of FA into the cells, which can be either metabolized for the production of energy or, when in excess, will be stored. Our findings that several proteins inside the HFD-GDE involved in mitochondrial β-oxidation (HADHA, ACADVL, ACADL, ECH1, ECHS1) and peroxisome β-oxidation (ECH1, ACOX1) are upregulated, suggest that fatty acids are favored as energy source over glucose. Over-activation of those lipid metabolism related pathways is a common feature of obesity and T2D, leading to a state of hyperglycemia (Deng et al. 2010; Kanuri et al. 2018; Knebel et al. 2015)(Fig.21). Additionally, we identified a family of acyl-CoA thiosterases (ACOTs) particularly up-regulated. The FA, upon entry in the cell, can be directed to the TCA cycle, and produce ATP, or alternatively can be stored. ACOT are intermediaries in that decision, directing FA to be stored (Wang et al. 2018; Steensels et al. 2020). In this crossroad, ACSS2 is the protein that conducts FA to the TCA cycle pathway, and that we found downregulated in HFD-GDE. In addition, we saw that PDHA1, responsible for pyruvate degradation and sending it to TCA cycle, is upregulated. Altogether, this fits the idea that HFD regimen shifts the burden of energy provision from carbohydrates toward fat derived from diet, since ACSS2 is downregulated and PDHA1 is upregulated in order to ensure the energetic need of the cell. Based on recent literature, obesity-induced activation of ACOTs directs FA towards TG synthesis for incorporation into chylomicrons or VLDL particles (Alves-Bezerra et al. 2019; Ersoy et al. 2018). Indeed, from our results we conclude that intestinal cells are facing an overload of FA leading

to over-activation of lipid related metabolic pathways. Interestingly, some studies consider activation of ACOT protective against FA over-supply, slowing the flux of FA to downstream metabolic pathways (Yamaguchi et al. 2007; Fujita et al. 2011; Franklin, Sathyanarayan, and Mashek 2017). Whether this is the case or not needs to be further explored.

Additionally, intestinal cells in the HFD model appear to prioritize production of energy from FA, instead of carbohydrates. This is shown by the upregulation of ATP-citrate lyase (ACLY), an enzyme responsible for the conversion of citrate to acetyl-CoA – the first step in DNL.

Oxidative milieu

Increased FA oxidation promotes mitochondrial dysfunction, as well as FA peroxidation and glucose dysmetabolism, altogether leading to reactive oxygen species (ROS) accumulation to pernicious levels (Kuschner 2017). The excessive release of ROS, superior to the endogenous antioxidant capacity, is an indicator of oxidative stress. Oxidative stress causes macromolecular damage and is implicated in various disease states such as atherosclerosis, cancer, neurodegeneration, and diabetes (Luo et al. 2017). Coincidently we observed several proteins involved in antioxidant defense mechanisms such as removal of free radicals (PRDX6) and elimination of xenobiotic compounds and products of lipids peroxidation (GSTA4, GSTM2) up-regulated in HFD-GDE (Fig.21). It is widely recognized that intracellular hyperglycemia, which we speculate to occur in gut cells due to the diet, promotes production of ROS (Volpe et al. 2018), therefore the observed activation of an antioxidant response to fight ROS elevation in such cells.

Surprisingly, by KEGG analysis it was possible to observe profound alterations in alcohol related pathways, namely the upregulation of the numerous isoforms of the aldehyde dehydrogenase (ALDH) family. ALDHs are a family of oxidizing enzymes responsible for cellular detoxification, differentiation and drug resistance by oxidation of biogenic and xenogenic aldehydes (Yang et al. 2017), commonly associated with ethanol consumption. Consistent with our model, ALDHs are responsible for detoxifying aldehydes that accumulate through metabolism, to which we are exposed from the environment or in certain disease states, such as diabetes (Chen et al. 2014). In particular, ALDH1B1 role was highlighted since its ability to metabolize acetaldehyde enables the maintenance of glucose homeostasis (Singh et al. 2015). Of interest, ALDH2 has been explored as a pharmacological target, due to its role in cellular damage defense against oxidative stress induced by pathological conditions, for instances high glucose (Chen et al. 2014). This piece of information led us to disclose that, in fact, food choices may be as toxifying as alcohol, and the organism uses the same weapons to fight both damaging effects. Besides, it is known that in absence of oxygen and as a result of yeast fermentation, production of ethanol from glucose is observed (Aslankoohi et al. 2015). Whether the biota has a role in the modulation of ALDH family needs to be unveiled.

Proteasome

Lastly, evidence that the HFD not only induced obesity, but also a pathological state arises from the massive alteration of proteasome-related proteins. In fact, these proteins were all indisputably down-regulated (Fig.20). The proteasome recognizes unfolded and damaged proteins eliminating them by degradation, therefore gained attention as an important target in many diseases (Amir, Weber, Beard, Bomyea 2008). By degrading several cellular proteins, the proteasome controls many other processes,

e.g. cell cycle, transcription, signaling, trafficking, protein quality control and amino acid homeostasis (Rousseau and Bertolotti 2018). Normally, dietary amino acids constitute 20% of the amino acid supply to build the proteins an adult requires, and the remaining 80% of amino acids comes from the recycling of amino acids following protein degradation (Kaushik and Cuervo 2018). Our data clearly shows the proteasome to be impaired what results in a defective degradation of proteins, an hallmark of disease (Rousseau and Bertolotti 2018). However, it is necessary to further validate if the alterations in GDE are truly mirrored in the cell.

We conclude that diet composition is definitely a game-changer on the cell's background. Furthermore, diet composition will be mirrored on metabolic/proteomic profile of the GDE that are continuously being produced. Overall, from the observed alteration in GDEs we speculate that in the gut upon HFD glucose metabolism is jeopardized in favor of FA metabolism; there is an impairment on amino acid synthesis that results in increased oxidative stress inside the cell; and to counteract this oxidative stress one would expect the proteasome to be upregulated but this is not the case, probably if we had analyzed an early time point of diet we would have observed an up-regulation of proteasome components. The down regulation of proteasome proteins suggests an inability to detoxify the cell of misfolded proteins, leading to increased accumulation of toxic molecules and disease progression.

Plasma EVs

Parallel to GDE proteome characterization, we tested the possibility of using plasma EVs as liquid biopsies in prediabetes. This would allow us to predict gut malfunction, thus providing an early biomarker of the disease. Considering EVs' role as communication vehicles, we hypothesize that enterocytes sense and translate the energetic clues given by the diet into alterations in GDE protein cargo. Changes in GDE protein cargo will propagate the diabetogenic message to other organs, thus promoting disease progression. Therefore, we evaluated which of the proteins present in GDE overlap with the ones in plasma EVs. In a preliminary approach, we searched for a biomarker of dysmetabolic features by performing a comprehensive and comparative analysis of the proteome of HFD plasma EVs to the ones derived from control animals. Interestingly, we observed an altered metabolic footprint in plasma EVs from HFD mice, when compared with NCD plasma EVs (Fig.25).

We found a small group of proteins that were similarly altered in GDE and plasma EVs. The Serpin family (SERPINA1A, SERPINA1C) and Keratin family (KRT5, KRT6A, KRT75) were both upregulated. Serpins are protease inhibitors, with some of its family members presenting proteolytic activity against insulin. In particular serpinB1 was proposed to mediate hyperinsulinemia, an hallmark of prediabetes (Glicksman et al. 2017; Xu et al. 2019), highlighting the idea that EV mirror the metabolic state of the organism.

Keratins are fibrous structural proteins giving stability and protection from cell stress (Xu et al. 2019). Keratins' upregulation in EVs may be counteracting the oxidative stress to which cells are exposed, helping to reshape the cell. While the particular keratins found altered in the present study have not been associated to diabetes, keratin 8 is known to be responsive to glucose and participates in the regulation of pancreatic β cells, in T2D phenotypes (Alam et al. 2013).

On the contrary, we found down-regulated, valosin containing protein (VCP), galectin 3 binding protein (LGALS3BP) and several proteasome proteins (PSMA1, PSMA2, PSMA3, PSMA6, PSMB2). VCP is related

with vesicle budding and ubiquitin-dependent sorting to the proteasome. Interestingly, evidences link it to diabetes, for being an apoptotic regulator and fundamental target of Akt signaling, and activating the insulin-like growth factor receptor (IGF-R) signaling; also, it was demonstrated that the loss of VCP causes polyubiquitinated cellular proteins accumulation (Vandermoere et al. 2006; Lu et al. 2008) that, together with inhibited proteasome, increases the accumulation of proteins to be degraded and ultimately also increases oxidative stress. LGALS3BP promotes integrin-mediated cell adhesion that is thought to be activated in immune response to cell toxicity (Xu et al. 2019), which in fact matches the GDE general behavior in terms of focal adhesion. Overall, the downregulation of proteasome components appears to be a common feature among plasma EV and GDE.

In summary, we have found that protein composition of plasma EVs does not fully match the one seen in GDEs. However, plasma EVs derived from diet induced obese mice had a disturbed metabolic setting. It is not surprising that plasma EVs do not fully correspond to gut EVs, since plasma EVs carry information from many tissues and systems. Nonetheless, more detailed information still needs to be addressed in future studies.

In toto, our study highlights the importance of understanding the intestine as a metabolically active organ that may be targeted in the future and the importance of GDE as mediators of prediabetes.

2. Gut extracellular vesicles follow gut-liver axis towards macrophages leaving a metabolic footprint

2.1. Gut extracellular vesicles biodistribution

Metabolic homeostasis is achieved by a complex, multidirectional crosstalk between key metabolic tissues, inclusively gut and liver. This crosstalk, conventionally intermediated by hormones and metabolites, becomes dysregulated in diseases such as obesity and diabetes. A recently discovered alternative way of cells communicate is by secreting EVs, which became well-known for mediating local and systemic cell communication through horizontal transfer of genetic, protein and lipidic information. EVs carry on their surface proteins that are exposed to the extracellular environment, targeting them to specific recipient cells (Are 2016). The function of these cells is modulated upon EVs content incorporation; for instance some cells may even differentiate or become activated, according to the material delivered by the EVs (Rana et al. 2012).

In the previous chapter we examined the effect of prediabetes in GDEs protein cargo, revealing a significant change in 588 GDEs proteins due to high fat and sugar diet and the concomitant glucose intolerance and fat accumulation in the liver, hallmarks of prediabetes (Campbell et al. 2020). Interestingly, we observed alteration in glucose and lipid pathways related proteins. Our results suggest that the prediabetic environment in the gut induces marked alterations in the GDEs proteome. However, it remains unknown how prediabetic GDEs modulate disease progression. To test the biological role of GDEs in insulin and glucose sensitivity in the periphery, as well as in cholesterol and TG levels in liver, we started by studying the uptake of labelled-GDEs in different organs and to study the metabolic changes induced by the prediabetic GDEs in healthy animals.

In summary, in the present chapter we addressed whether GDEs from prediabetic mice can induce some of the disease hallmarks on a healthy animal and on the other side, can healthy GDEs alleviate or even revert some of the prediabetic hallmarks. To do so, we developed a model, based on the prosperous discovery of EV function in cancer metastasis (Costa-Silva et al. 2015), and adapted it to answer our question. Detailed optimization will be exposed in the next section.

First, to explore which organs capture the GDEs and thus evaluate biodistribution, near-infrared (nIR) labelled GDEs were retro-orbitally injected into *wild-type* (WT) mice and PBS was used as control. Equal amount of protein of GDE from NCD-fed mice and HFD-fed mice were injected in WT mice and tissues were collected 24h after. Quantification of nIR signal revealed that GDEs were preferentially localized in the liver (Fig.24B). To evaluate whether biodistribution is altered by time, we evaluated it at different times after injection, 1, 3, 6 and 24 hours post-injection and no difference was observed (Fig.24C; D and Supplementary Fig.1).

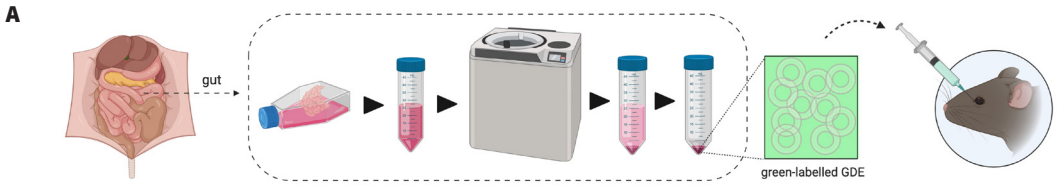

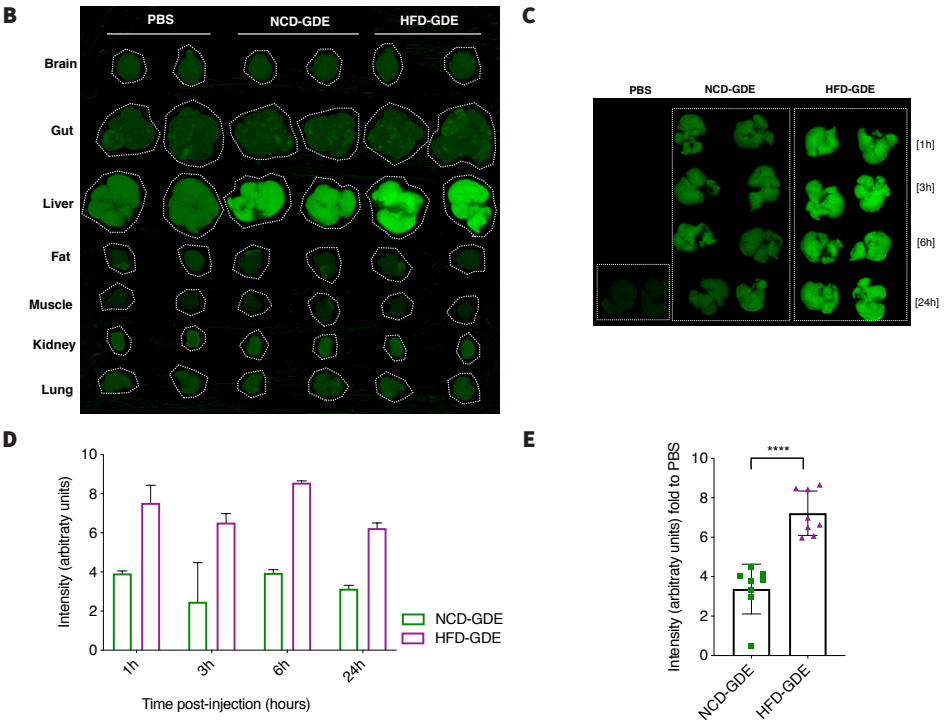

Figure 24. Gut-derived EV are preferentially captured by the liver. Biodistribution after retro-orbital injection in WT mice. A. Schematic representation of gut-derived EV (GDE) isolation and subsequent retro-orbital injection in mice. **B.** Intensity of near infra-red signal detection in several tissues from the injected mice, acquired in Odyssey imaging system (LI-COR Biosciences). Groups: mice injected with PBS, mice injected with GDE from NCD-fed mice (NCD-GDE) and mice injected with GDE from HFD-fed mice (HFD-GDE). **C.** Liver signal detection at different time-points after injection (1, 3, 6 and 24 hours). **D.** Analysis of liver signal detection quantification at different time-points after injection (1, 3, 6 and 24 hours), n=2 for PBS, NCD-GDE and HFD-GDE. **E.** Statistical analysis of liver signal detection, independently of time-point. Values normalized to PBS. n=2 for PBS and n=8 for NCD-GDE and HFD-GDE. Results are expressed as mean ± SEM. Unpaired t test with Welch's correction. ****p<0.0001

Being the liver a particularly heterogeneous organ in terms of cell types, we next aimed to evaluate the specific cells that take up GDE. The macrophages, for its phagocytic ability, have been already described as cells that uptake EVs (Feng et al. 2010; Costa-Silva et al. 2015) so we started by looking at Kupffer cells (KC).

For this purpose, we used fluorescently labelled GDE from NCD-fed mice and HFD-fed mice and injected retro-orbitally in WT mice. 24 hours after injection the frequency of EV+ cells in liver slides was assessed (Fig.25A); we found that over 70% of liver cells that take up EVs were F4/80+ by immunofluorescence, indicating KC to be the potential targets of EVs, confirming our prospects (Fig.25B).

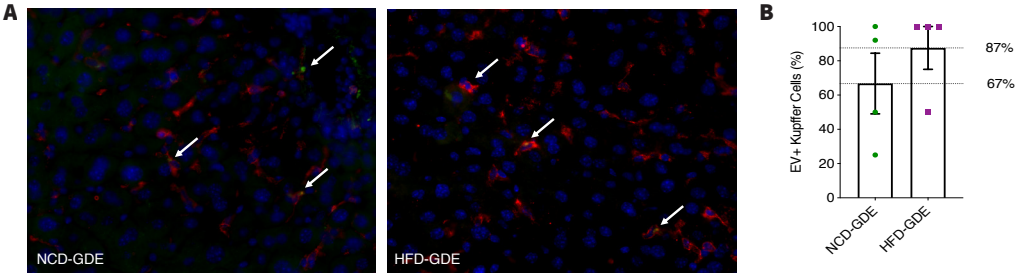

Figure 25. Co-localization of gut-derived EV with Kupffer cells. 24 hours after injection with green-labelled gut-derived EV (GDE) from different diets into WT mice animals were sacrificed and livers were fixed and then processed for immunohistochemistry. Kupffer cells (KC) are stained in red with anti-F4/80 antibody; GDE are labelled in green with PKH67; nuclei with DAPI in blue. **A.** Liver cross-section of a mice injected with GDE from NCD mice (NCD-GDE) (left). Liver cross-section of a mice injected with GDE from HFD-mice (HFD-GDE) (right). Arrows indicate KC EV positive. **B.** Statistical analysis of EVs co-localized with KC; n=4 for NCD-GDE and HFD-GDE. Results are expressed as mean ± SEM. Unpaired t test with Welch's correction.

To further confirm the results obtained in the immunohistochemistry experiments, next we performed flow cytometry analysis using the same animal protocol as before. The liver of green-labelled injected mice was analyzed by flow cytometry, stained with CD45, Ly6c, CD11b and F4/80. CD45 is the leukocyte common antigen, typically used to identify immune cells (Altin and Sloan 1997). Ly6c is a marker of recruitment of macrophages (Ramachandran et al. 2012). CD11b or Mac-1 (macrophage-1 antigen) is other common marker of macrophages, amongst other immune cells, it is an integrin that mediates inflammation by regulating adhesion and migration of the cell (Ye and Boulay 1997). Finally, F4/80 is a specific marker for KC, that are CD45+ Ly6c- CD11b+ F4/80+.

From this experiment, we observed that over 50% of EV+ cells were CD11b+F4/80+, inside the CD45+Ly6c- population, a phenotype consistent with KC (Fig.26E). The abundance of CD45- (Fig.26F) in these cells can be explained by the protocol we used, where cells were isolated from the whole liver through mechanical smashing, without any previous treatment, only red blood cells were depleted, so we were expecting to find excess of debris.

When looking to the white blood cell population (CD45+) they seem to increase in EV-injected mice (Fig.26G), the same way as KC (Fig.26H), which increment is more relevant in the mice injected with GDE from NCD mice (NCD-GDE mice). The percentage of KC that take up EV in NCD-GDE mice are around 30% and 15% in mice injected with GDE from HFD mice (HFD-GDE mice) (Fig.26I). Ly6c enables us to distinguish the resident macrophages, the KC (CD45+ Ly6c- CD11b+ F4/80+), from the recruited (recruited hepatic macrophages, RHM), that are known for promoting inflammation (CD45+ Ly6c+ CD11b+ F4/80low) (Holt, Cheng, and Ju 2008). RHM are not very frequent and seem to be increased with EV-injection, but with statistical difference (Fig.26J).

By microscopy we observed that 70-90% of KC were receiving EV while by flow cytometry the numbers were slightly decreased, in an average of 50-60%, that we believe to be related with processing of the samples that must be different for each protocol. Also, by flow cytometry we were able to use more markers specific of KC. However, it is clear that KC are predominantly engulfing GDE, in comparison to remainder cells. That evidence corroborates the literature also for the crucial role that KC have demonstrated in several aspects of metabolic syndrome (Dixon et al. 2016).

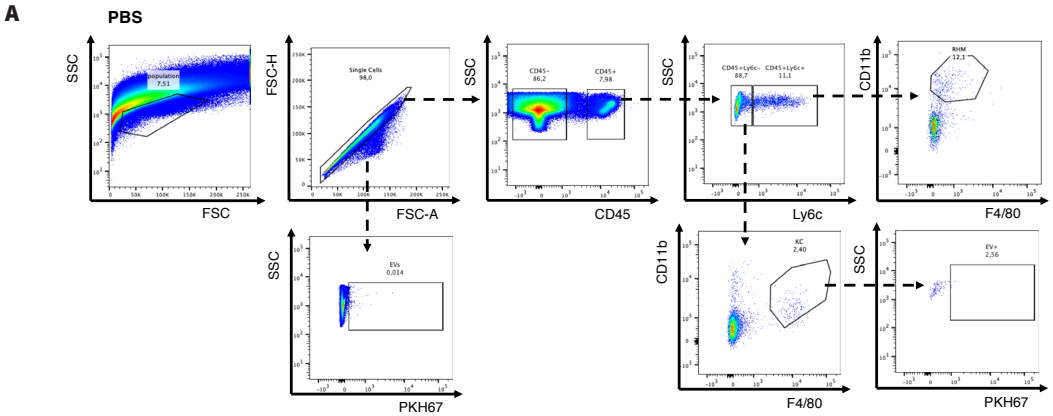

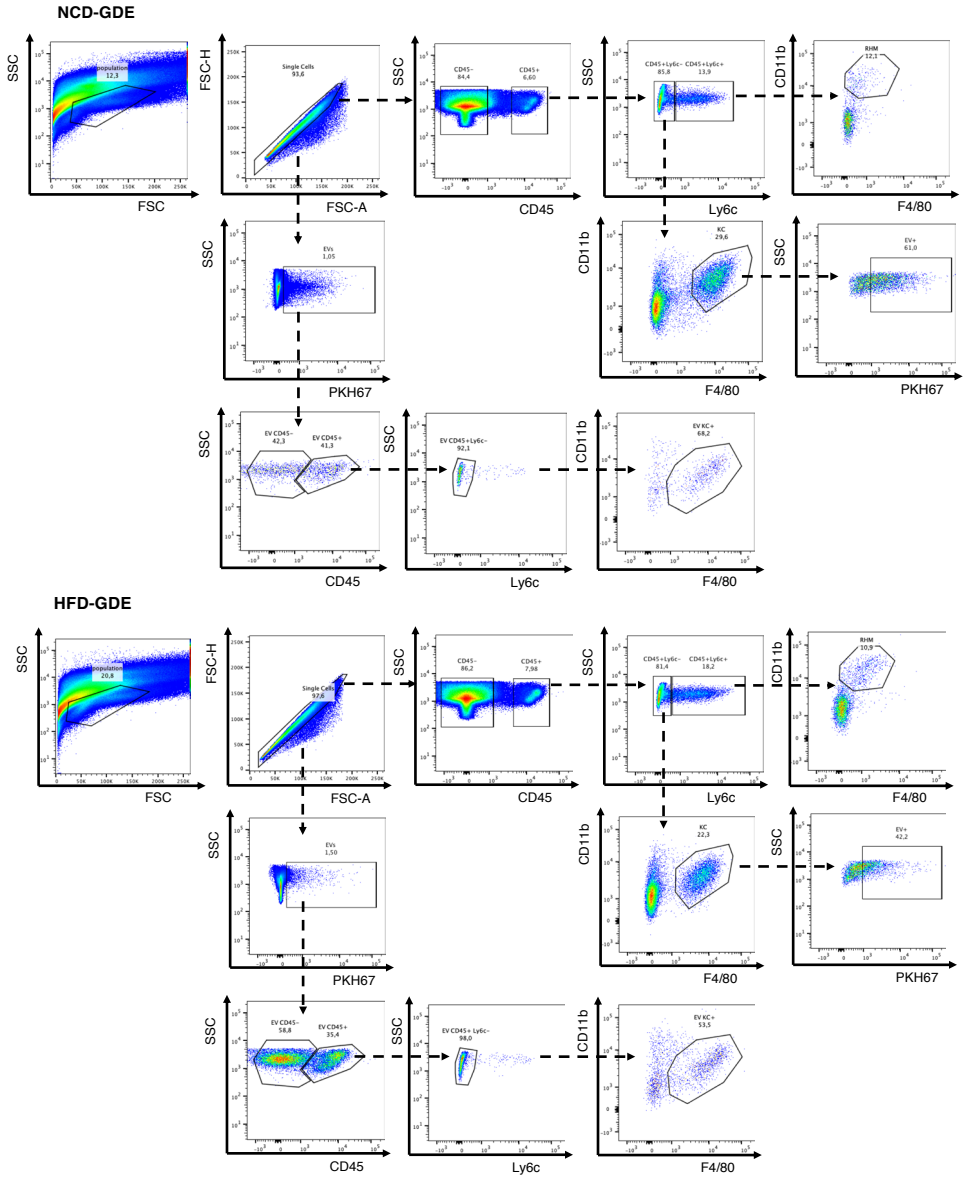
NCD-GDE
SSC
FSC
FSC-H
FSC-A
CD45
Ly6c
CD11b
F4/80
PKH67
HFD-GDE

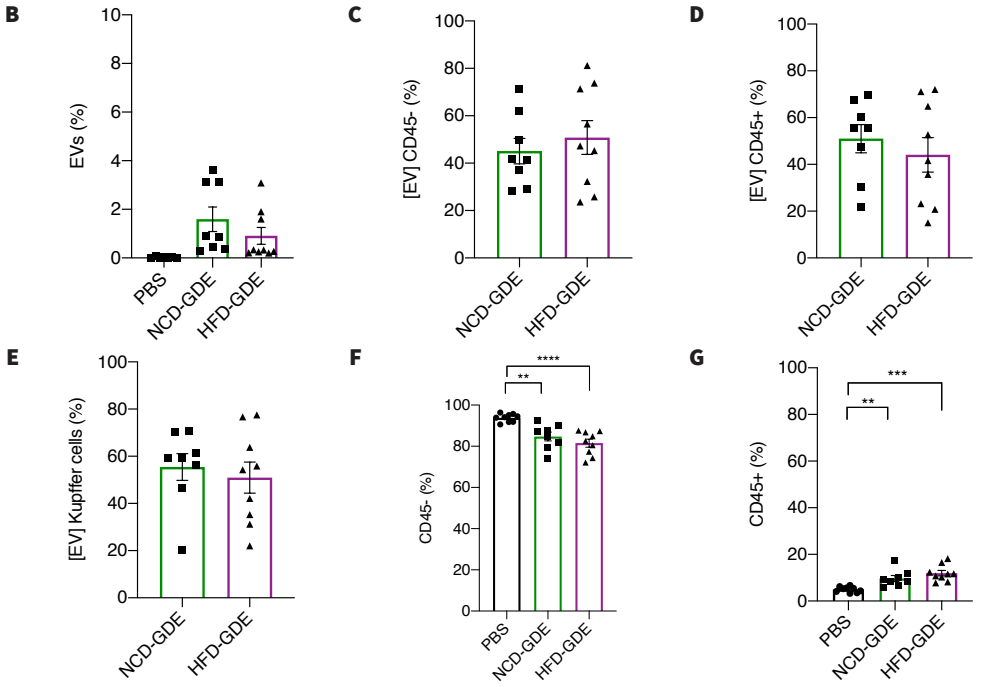
B
EVs (%)
C
[EV] CD45- (%)
D
[EV] CD45+ (%)
E
[EV] Kupffer cells (%)
F
CD45- (%)
G
CD45+ (%)
PBS
NCD-GDE
HFD-GDE

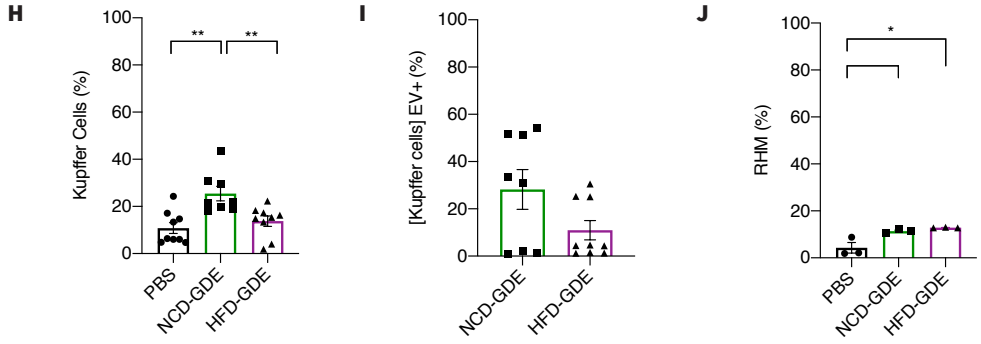

Figure 26. Kupffer cells favorably uptake gut-derived EV. 24 hours post injection with green-labelled gut-derived EV (GDE) animals were sacrificed and liver cells were isolated and prepared for flow cytometry staining. **A.** Flow cytometry plots with the gating strategy used for the analysis of mice injected with PBS (PBS), mice injected with GDE from NCD fed mice (NCD-GDE) and mice injected with GDE from HFD fed mice (HFD-GDE). **B.** Analysis of the percentage of EVs. **C.** Analysis of the percentage of CD45- cells among EVs. **D.** Analysis of the percentage of CD45+ cells among EVs. **E.** Analysis of the percentage of Kupffer Cells (KC) (CD45+ Ly6c-CD11b+ F4/80+) among EVs. **F.** Analysis of the percentage of CD45- cells. **G.** Analysis of the percentage of CD45+ cells. **H.** Analysis of the percentage of KC. **I.** Analysis of the percentage of EV+ cells among KC. **J.** Analysis of the percentage of recruited hepatic macrophages (RHM) (CD45+Ly6c+CD11b+F4/80low). Results are expressed as mean ± SEM; n=8 for PBS, NCD-GDE and HFD-GDE. Unpaired t test with Welch's correction (C, D, E); ANOVA multiple comparisons (B, F, G, H, I, J); *p<0.05, **p<0.005, ***p<0.0005, ****p<0.0001.

2.2. Gut extracellular vesicles biological effect

Next, we evaluated the biological impact of GDEs isolated from our prediabetic mice model, by studying whether those play a role in the induction of the disease. First, we implemented a model, based on the prosperous discovery of EV function in cancer metastasis (Costa-Silva et al. 2015) and adapted it to our setting of metabolic disorders. Briefly, this model is based in the "education" of WT mice with our EVs of interest, achieved by injecting WT mice with GDE isolated from prediabetic animals. In the dictionary education is defined as the process of receiving or giving systematic instruction. In our case the instructions are given by the EVs cargo and then we evaluate if the animal is following those instructions by analyzing the diabetic phenotype of the animals after education. In summary, we intend to test whether the phenotype of the EV producing animal can be induced in the recipient one. We knew that GDEs were carrying many metabolism related proteins altered in prediabetes. We started by determining the GDEs dosage and frequency, the education length and assessing the diabetic phenotype. All technical adjustments and phenotype characterization are represented in Figure 27.

As before, WT mice were retro-orbitally injected with GDE from NCD fed mice and GDE from HFD fed mice for a prolonged period, in a process defined as education. Our first approach was to evaluate if GDEs had any biological effect on healthy mice. Based on the evidence that GDE protein amount was altered in prediabetic mice (Fig. 17B), we calculated that 5 µg of NCD-GDE were equivalent to 3 µg of HFD-GDE, by number of EV. All doses were diluted to a final volume of 100 µl. In Education 1, WT mice, fed *ad libitum* with NCD, were retro-orbitally injected with 5 µg of NCD-GDE, 3 µg of HFD-GDE, and 100 µl of PBS, every other day, for three weeks. After three weeks of education, we did not observe any differences neither in the glucose tolerance, that we evaluated through the GTT, nor in terms of lipid accumulation in the liver (Supplementary Fig.2).

Since we did not see any effect of either NCD-GDE or HFD-GDE education of WT mice, next we fixed the dose to 5 µg of both NCD-GDE and HFD-GDE and increased the time of the education to six weeks. The GTT was performed at week 5 and lipids in the liver were measured after sacrifice. We did not observe any differences in glucose tolerance (Fig.27B). While cholesterol levels in the liver were not affected by the education, mice injected with HFD-GDE had significantly increased levels of TG in the liver (Fig.27D).

For the third education we duplicated the dosage and kept the six weeks duration, which we considered, at the time, to be the minimum time required to alter the metabolism of mice. Education 3 consisted on a dosage of 10 µg of NCD-GDE and HFD-GDE, for six weeks, injected in WT mice fed *ad libitum* with NCD. We observed that glucose tolerance of educated mice was altered only in the post-prandial state at 90-minutes post glucose bolus (Fig.27E). In terms of lipids in the liver, consistent with education 2, cholesterol did not change upon education and TG showed a trend to increase from PBS to GDE injected animals, however it did not reach statistical significance (Fig.27F; G). Noteworthy to mention, the distribution of the cholesterol values is much more disperse than in education 2.

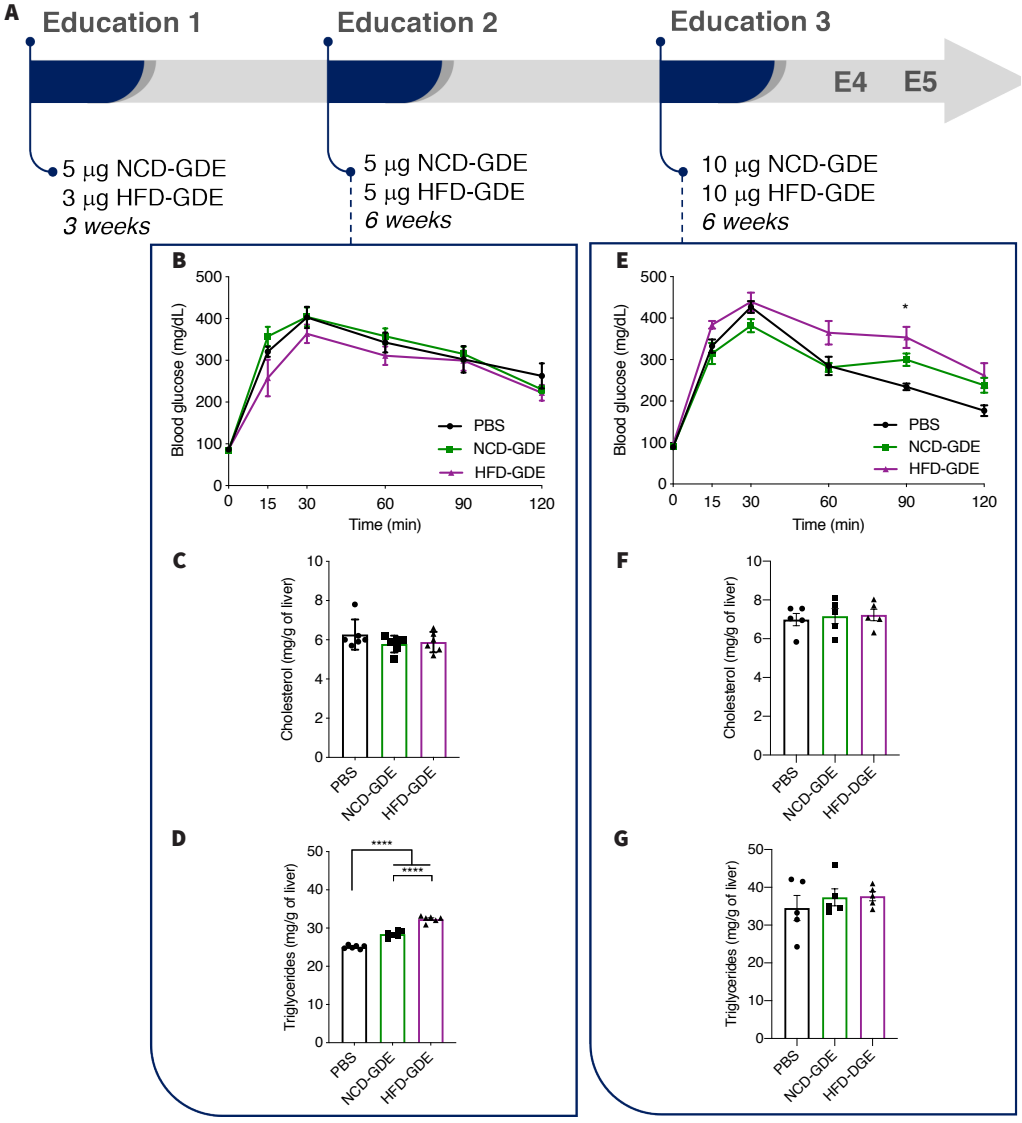

Figure 27. Scheme of the education optimization process. Education 1 - Mice were injected with 5 µg of gut-derived EV (GDE) from NCD-fed mice (NCD-GDE) and 3 µg of GDE from HFD-fed mice (HFD-GDE) for three weeks. **Education 2** - Mice were injected with 5 µg of NCD-GDE and 5 µg of HFD-GDE for six weeks. **Education 3** - Mice were injected with 10 µg of NCD-GDE and 10 µg of HFD-GDE for six weeks. **A.** Time-line of education's evolution. **B.** Glucose tolerance test (GTT) at different time points (0, 15, 30, 60, 90, 120 minutes) of mice from education 2. **C.** Analysis of cholesterol levels in the liver of mice from education 2. **D.** Analysis of triglyceride (TG) levels in the liver of mice from education 2. **E.** GTT at different time points (0, 15, 30, 60, 90, 120 minutes) of mice from education 3. **F.** Analysis of cholesterol levels in the liver mice from education 3. **G.** Analysis of TG levels in the liver of mice from education 3. Cholesterol and TG represented in milligram per gram of liver tissue. Results are expressed as mean ± SEM; n=4 for PBS, n=7 for NCD-GDE and HFD-GDE. ANOVA multiple comparisons. *p<0.05, ***p<0.0005.

Despite of not a complete recapitulation of the GDE producer mice phenotype upon education, our data was indicating at least some metabolic alteration induced by the prediabetic GDE. Anyhow, we were not expecting with our model a 100% mimicking of the prediabetic phenotype, relying uniquely on GDE the transmission of disease.

Given the route of administration of the GDE, retro-orbital injection into the blood flow, we wanted to make sure that we were giving enough EVs to overtake the normal levels in circulation. Next, the dosage was calculated based on the number of EVs in systemic circulation and we kept the six weeks duration. Plasma EV analysis showed that NCD mice had an average of 0.35 µg of EV protein per µL of plasma (Fig.22 and Supplementary Fig.3). This means that in 100 µL of plasma, mice have about 35 µg of EV protein. 100 µL is the maximum volume that can be injected in the orbital sinus. Ideally, we would inject a dose of 35 µg of GDE, but due to limitation of GDE availability, we established the six weeks as a favorable time window for the metabolism alterations, and we fixed the dosage to 20 µg. Therefore, WT mice fed *ad libitum* with NCD were injected with 20 µg of NCD-GDE and HFD-GDE, every other day, for six weeks (Fig.28A). We observed that HFD-GDE mice had significantly higher weight gain, in comparison with the PBS group (Fig.28B). GTT glycemic curves did not show overall glucose tolerance alterations upon education (Fig.28C). Regarding the AUC, while it did not reach statistically relevance, it revealed a slightly increase from the PBS to the groups educated with the GDEs (Fig.28D). In contrary to what we did in previous educations, where GDE from the same diets were all pooled together and then divided into the defined doses to be injected; in this education GDE were pooled just enough to educate a single recipient mouse. This way, we could track the donor of the recipient mice and correlate phenotypes. Importantly, we observed a positive correlation of the GTT AUC of donor mice with the GTT AUC of the correspondent recipient mice, i.e. injected with GDE from that donor (Fig.28E). Insulin tolerance test (ITT) was performed at week 4 of education, the ITT informs us about insulin resistance. We perceived that HFD-GDE educated mice were displaying some degree of resistance, however it was not statically significative. In addition, in terms of insulin resistance quantified by the area above the curve, mice injected with NCD-GDE showed a trend to be more resistant than PBS ones, and the ones injected with HFD-GDE, also showed a trend to be even more resistant than the NCD-GDE injected ones; however, ANOVA of multiple comparisons did not show any statistical differences (Fig.28F, G). Finally, cholesterol levels did not change either in NCD-GDE or HFD-GDE educated mice in relation to controls (Fig.28H). Consistent with the previous educations, TG are increased in educated mice, in a step-wise manner from PBS to HFD-GDE injected animals (Fig.28I).

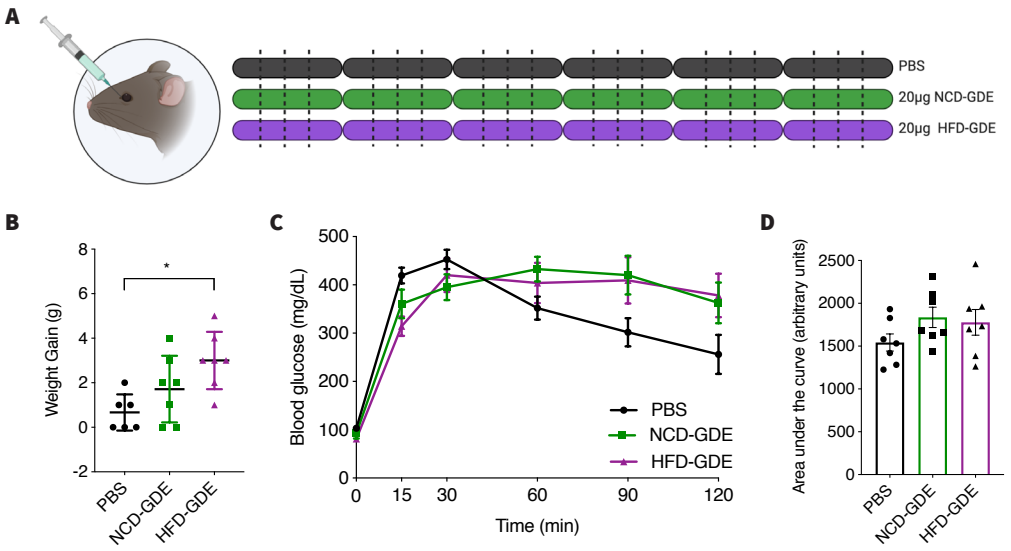

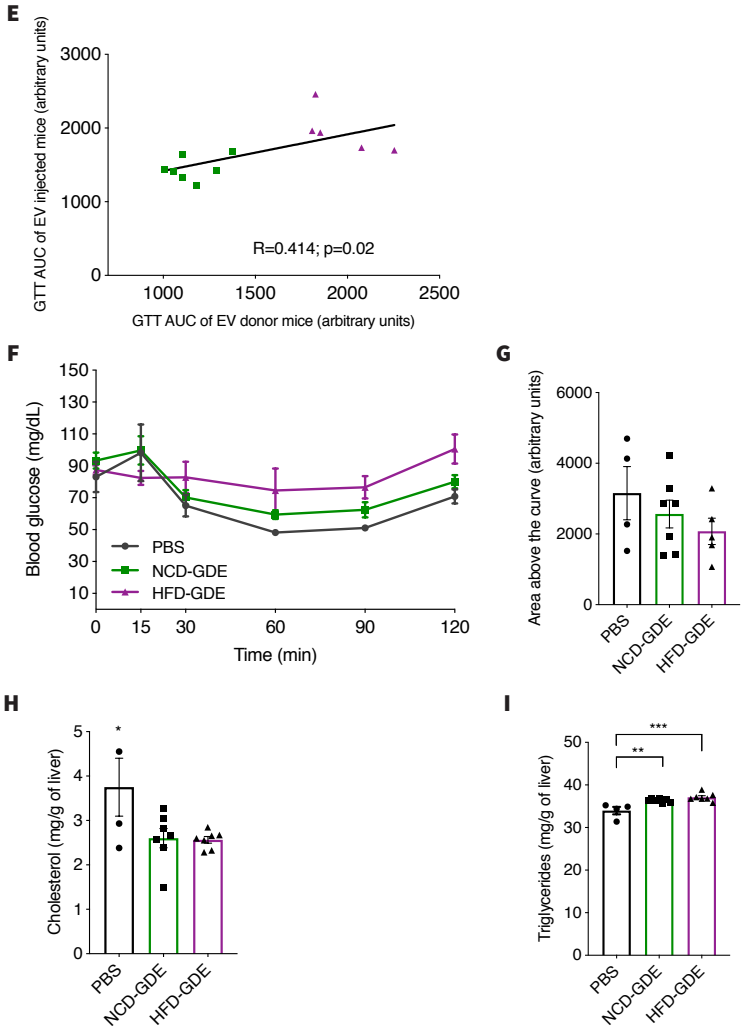

Figure 28. Gut-derived EV induce an increase in liver triglycerides when administered to WT mice under a control diet. A. Schematic representation of Education 4: Mice were retro-orbitally injected, every other day, with 20 µg of gut-derived EV (GDE) from NCD-fed mice (NCD-GDE), 20 µg of gut-derived EV from HFD-fed mice (HFD-GDE) and PBS, for six weeks and fed with NCD. Individual doses were calculated for 100 µl of volume. **B.** Analysis of weight gain of treated mice after education. **C.** Glucose tolerance test (GTT) at different time points (0, 15, 30, 60, 90, 120 minutes). **D.** Analysis of the area under the curve (AUC) of the GTT. **E.** Positive correlation between the EV-donor mice GTT AUC and correspondent EV-recipient mice GTT AUC. **F.** Insulin tolerance test (ITT) of mice at different time points (0, 15, 30, 60, 90, 120 minutes) **G.** Analysis of the area above the curve of the ITT. **H.** Analysis of cholesterol levels in the liver of educated mice. **I.** Analysis of triglyceride (TG) levels in the liver of educated mice. Cholesterol and TG are represented in milligram per gram of liver tissue. Results are expressed as mean ± SEM; n=4 for PBS, n=7 for NCD-GDE and HFD-GDE. ANOVA multiple comparisons. *p<0.05, **p<0.005, ***p<0.0005.

Altogether, our results indicate that GDEs are carrying a metabolic message with particular impact on FA synthesis. Hypothesizing that GDEs are auxiliary in the organismal adjustment to signals from the environment – the diet, in our case – we added a stimulus to the education. Assuming GDEs are mediators of the complex system that diabetes is, we wanted to see their behavior with the HFD background. Therefore, we followed exactly the same protocol as education 4, WT mice injected, as before, with 20 µg of NCD-GDE and 20 µg of HFD-GDE and simultaneously fed with HFD for six weeks duration of the education (Fig. 29A). In terms of weight gain, we did not see any differences (Fig.29B). GTT was done at week 5 of education and, despite not significantly different, we observed a trend for glucose intolerance in the HFD-GDE educated mice, as expected from our hypothesis (Fig.29C; D). ITT was performed at week 4, again the differences did not reach statistical relevance, however HFD-GDE injected mice appear to be more resistant to insulin than PBS and NCD-GDE (Fig.29E; F). Considering cholesterol levels, no

statistical differences were observed, while there is a trend for gradual increase from PBS, to NCD-GDE and HFD-GDE (Fig.29G). Importantly, TG levels consistently demonstrate significative increased in NCD-GDE mice and even more in HFD-GDE mice (Fig.29H). Nevertheless, liver histology analysis of these mice did not show any evidence of steatosis at this point yet (Supplementary Fig.4).

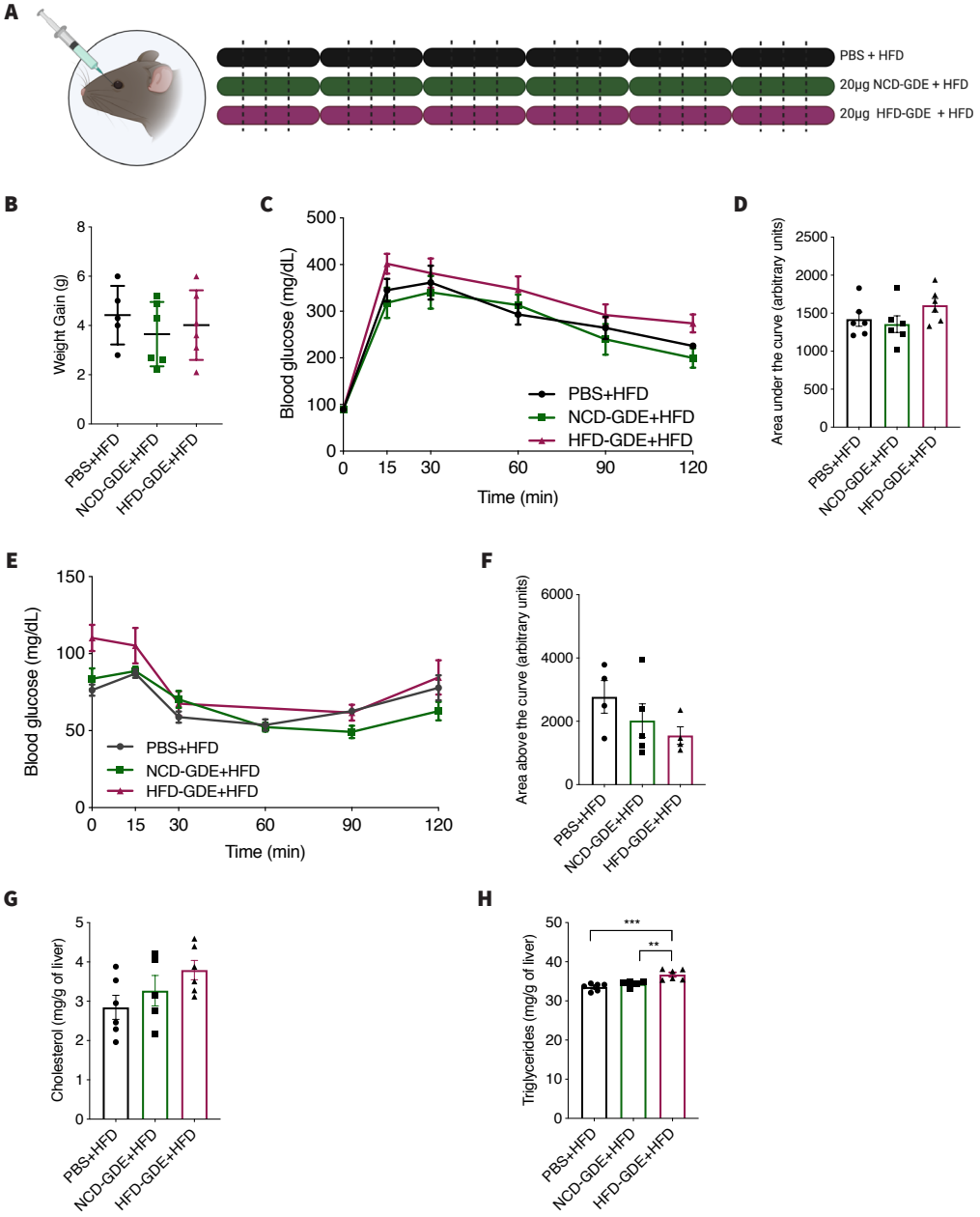

Figure 29. Gut-derived EV induce an increase in liver triglycerides when administered to WT mice under an HFD. A. Schematic representation of Education 5: mice were retro-orbitally injected with 20 µg of gut-derived EV (GDE) from NCD-fed mice (NCD-GDE) and 20 µg of gut-derived EV from HFD-fed mice (HFD-GDE) every other day for six weeks and fed with HFD. Every dose was calculated for a total volume of 100 µl. **B.** Weight gain of injected mice after education. **C.** Glucose tolerance test (GTT) of mice at different time points (0, 15, 30, 60, 90, 120 minutes). **D.** Analysis of the area under the curve of the GTT. **E.** Insulin tolerance test (ITT) of mice at different time points (0, 15, 30, 60, 90, 120 minutes). **F.** Analysis of the area above the curve of the ITT. **G.** Analysis of the cholesterol levels in the liver of injected mice. **H.** Analysis of triglyceride (TG) levels in the liver of injected mice. Cholesterol and TG are represented in milligram per gram of liver tissue. Results are expressed as mean ± SEM; n=4 for PBS, n=7 for NCD-GDE and HFD-GDE. ANOVA multiple comparisons. *p<0.05, **p<0.005, ***p<0.0005.

From the single retro-orbital injection of GDE in WT mice we observed that those GDE were directed preferentially to the KC (Fig.26). However, we also observed that GDE provoked alterations in the livers of injected mice, after six weeks of injections, specifically on the amount of fat stored, what have effects on tissue morphology and probably in the cellularity. So, aiming to learn about the distribution of these EVs in the different hepatic cell populations after six weeks of every other day injections, we performed flow cytometry analysis of liver tissue (Fig.30A). To that end, livers of educated mice (education 5) were perfused, non-parenchymal cells were enriched through a Percoll gradient (Duarte et al. 2018) and stained for CD45, Ly6c, CD11b and F4/80. The uptake of EVs is visible from the differences between the PBS-injected group and the other two groups, but the levels were not very expressive, about 3% of the cells seemed to take up EV. Anyway, HFD-GDE injected mice showed up with increased EVs than NCD-GDE (Fig.30B). Replicating the previously observed pattern of only one injection of GDE, EVs were predominantly going to the KC (Fig.30E). Meanwhile, the population of KC looked to be diminished in educated mice, with no statistically difference (Fig.30H) importantly almost every KC was EV+, indicating great activation of these cells by EV (Fig.30I). The RHM (CD45+ Ly6c+ CD11b+ F4/80low), arise has being decreased in injected mice compared with PBS (Fig.30J).

Tissue-resident macrophages adapt to perform specific functions vital for tissue homeostasis (Davies et al. 2014). Besides, KC are particularly dynamic, recruited when necessary from monocytes, normally derived from bone marrow (Scott et al. 2016). In order to have more information about the effect of GDE on cell recruitment, we analyzed the bone marrow (Supplementary Fig.5) of the educated mice. However, the proportions of GDE positivity in that tissue was very few, the observed frequency of EV was about ~0.5%.

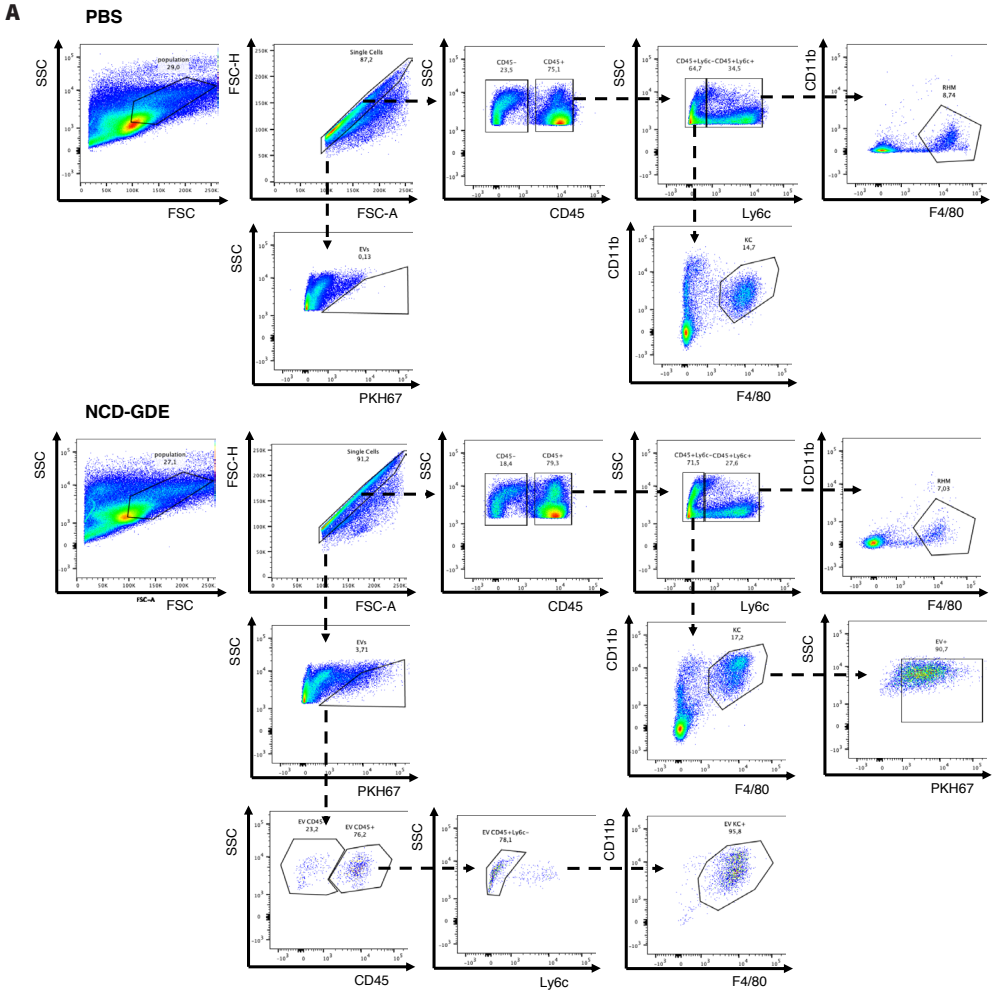

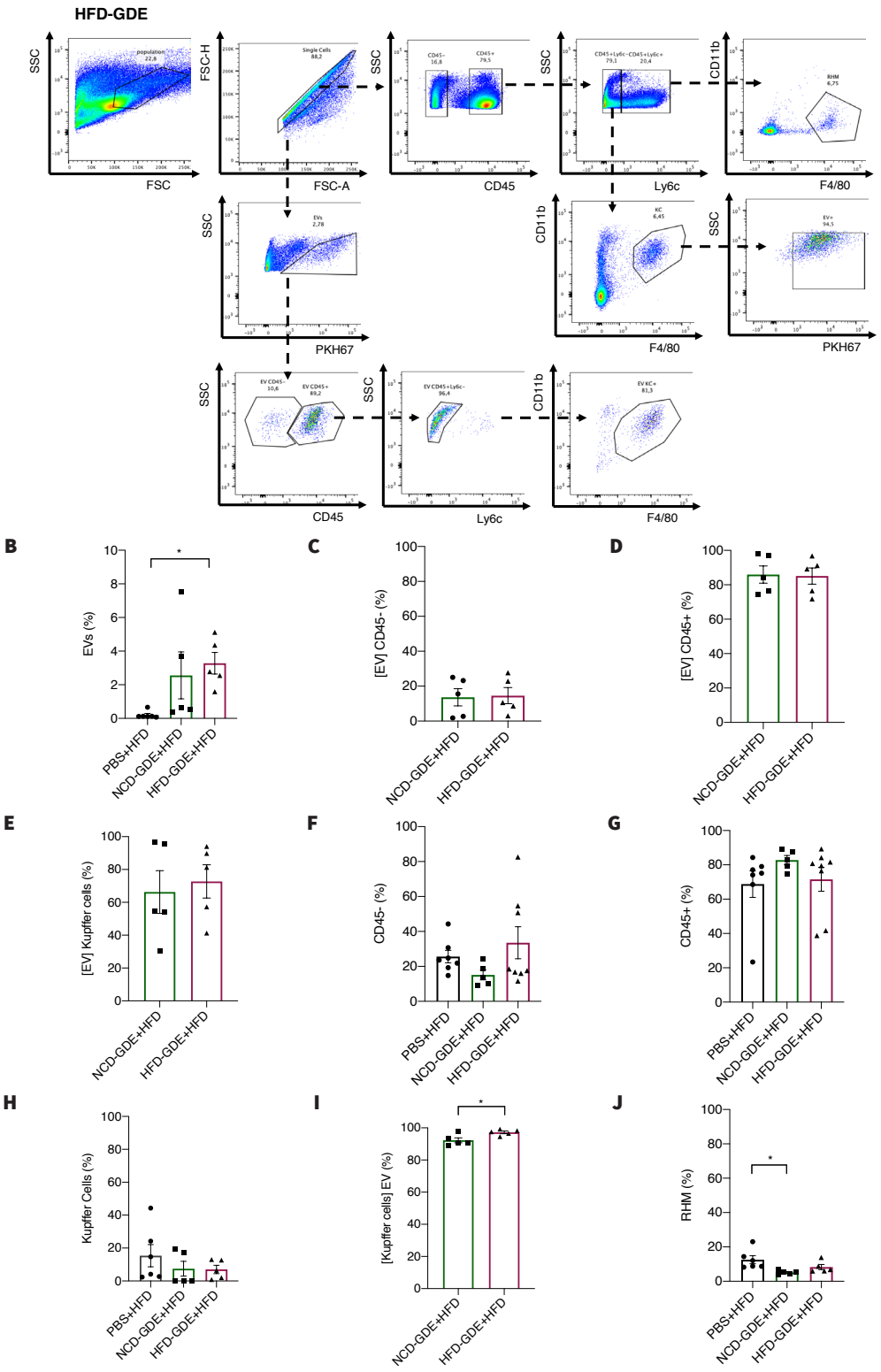

Figure 30. Kupffer cells favorably take up gut-derived EV after six weeks of injections. Mice were fed with HFD for 6 weeks and during the same period were injected with 20 µg of fluorescent-labelled gut-derived EV (GDE) from NCD-fed mice (NCD-GDE) and 20 µg of fluorescent-labelled gut-derived EV from HFD-fed mice (HFD-GDE). **A.** Flow cytometry plots with gating strategy for the analysis of PBS-injected group, NCD-GDE and HFD-GDE. **B.** Analysis of the percentage of EVs. **C.** Analysis of the percentage of CD45 negative (CD45-) cells among EVs. **D.** Analysis of the percentage of CD45 positive (CD45+) cells among EVs. **E.** Analysis of the percentage of Kupffer cells (KC) among EVs, KC are CD45+Ly6c-CD11b+F4/80. **F.** Analysis of the percentage of CD45- cells. **G.** Analysis of the percentage of CD45+ cells; **H.** Analysis of the percentage of KC. **I.** Analysis of the percentage of EV+ cells among KC. **J.** Analysis of the percentage of recruited hepatic macrophages (RHM). RHM are CD45+Ly6c+CD11b+F4/80low. Results are expressed as mean ± SEM, n=7 for PBS and n=5 for NCD-GDE and HFD-GDE; Unpaired t test with Welch's correction (C, D, E); ANOVA multiple comparisons (B, F, G, H, I, J); *p<0.05.

Discussion

The concept of tissue-derived EVs playing a role in metabolic diseases arose in recent years (Huang-Doran, Zhang, and Vidal-Puig 2017). Deng et al. observed that by administering EVs isolated from the adipose tissue of obese mice into healthy ones, glucose intolerance and insulin resistance developed (Deng et al. 2009). In humans, distinct EV miRNA profiles for metabolic syndrome, T2D, hypercholesterolemia and hypertension were identified (Karolina et al. 2012). From mice to humans we find great relevance for EVs in metabolism and whole-body homeostasis. However, the role of GDE in metabolic disorders has not been fully addressed. We previously described that GDE proteome is highly altered by high-fat diet. Here we investigated the fate of HFD-GDE in non-obese WT mice, both in terms of organ as well as cellular population; and whether they trigger dysmetabolism in healthy mice. Our findings clearly show that GDE were directed to the liver (Fig.24), and in great extent, specifically to the KC (Fig.25;26). In terms of metabolic alterations, non-obese WT mice injected with HFD-GDE display elevated levels of hepatic TG. In contrast, glucose and insulin homeostasis was not affected.

The bidirectional relationship between the gut and the liver classical described by the anatomy, is here for the first time further highlighted by the uptake of GDE exclusively by the liver (DeSesso and Jacobson 2001). Most interestingly, HFD-GDE mice livers' display a more intense signal than NCD-GDE (Figure 24C), suggesting HFD-GDE to have higher specificity for the liver or increased charge, or even both. It is noteworthy that KC are the primary innate immune defense against foreign components from the diet absorbed in the intestinal tract (Parker and Picut 2005; Remmerie and Scott 2018). Along with our observation that GDE are preferentially going to KC, these results suggest that GDE derived from healthy animals may work as a detoxifying system by carrying toxic products from the diet and targeting them to KC in order to trigger a defense response. In addition, when animals are fed for prolonged time with an HFD regimen, KC can no longer detoxify the excess of lipids coming from the diet and dysmetabolism arises in the liver. Metabolomics studies over the near future may shed light on this important question.

We proceeded to test the hypothesis that chronic exposure of healthy mice to HFD-GDE triggers a prediabetic obese phenotype. The complexity of optimizing a protocol within the metabolic field, since there are innumerous parameters to take into account, is quite challenging; nevertheless we started with the protocol described in the cancer field, where EVs content is particularly aggressive (Costa-Silva et al. 2015). While this was a starting point, we have to keep in mind that the metabolic system is predefined to be highly adaptative and to be continuously under adjustments, well-illustrated by the intermittent feeding regimen.

According to Heydemann, who did an overview on the development of T2D in the HFD model, mice start to become glucose intolerants and IR around 8 weeks post HFD feeding (Heydemann 2016). Taken into account we treated healthy lean mice only with GDE, in a dose that does not surpass plasma EVs concentration evaluated in HFD mice, it is not surprising that no differences were observed in glucose and insulin resistance.

It is thus likely that, at six weeks of injections every other day with GDE, the animals' immune and antioxidant systems are still capable to counteract the pro-diabetogenic and pro-inflammatory effects carried by the HFD-GDE from the gut to the KC. Therefore, one would not expect to see marked changes in glucose tolerance and insulin resistance, at this age and time of treatment, yet we observed a difference on the GTT curves from PBS to GDE injected mice, but with no statistic meaning (Fig.27B, E;

28C). These data raise the possibility that by increasing the time of treatment with GDE, the observed trend would become more pronounced and gain statistical power. In addition, ITT from education 4 (Fig.28F; G) shows a trend to increased insulin resistance from PBS to NCD-GDE, and from those to HFD-GDE. In the same line of evidence, again, with no statistical meaning, it is curious to observe that animals educated with NCD-GDE and simultaneously fed an HFD display decreased glucose tolerance in relation to PBS, indicating that "healthy" GDE might also have a protective effect in a scenario of disease (Fig.29D). Nevertheless, to fully understand the impact of HFD-GDE on whole-body glucose and insulin homeostasis further studies are of the uttermost importance. We anticipate that by administering HFD-GDE to mice previously exposed to an HFD we would be able to observe a fastest progression of metabolic disorders, such as diabetes and obesity. Furthermore, even in lean healthy mice, if the treatment with GDE from diet induced obese animals would be prolonged a pathophysiological effect of those on liver and peripherical glucose metabolism would be expected.

Interestingly, increased levels of hepatic TG in HFD-GDE versus NCD-GDE, and PBS (Fig.27D; 28; 29) were observed, further strengthening the GDE proteomics characterization, that revealed an upregulation of lipid metabolism related proteins in HFD-GDE. Considering GDE tropism to KC, and the role of KC in hepatic lipid accumulation and inflammation, it is acceptable that hepatic lipid content is altered upon administration of HFD-GDE. This result and the fact that overload of specific lipid species derived from diet activates KC in models of NAFLD and steatohepatitis indicates that GDEs might be vehicles of lipid transport to the KC, where these lipids suffer remodeling and are posteriorly sent to the hepatocytes (Dixon et al. 2016).

The previous idea is further supported by the fact that KCs gene expression profile is enriched in genes involved in the uptake, processing and export of excess cholesterol to be transported to hepatocytes (Scott et al. 2016). It would be interesting to test whether KC also mediate the export of excessive TG or their building blocks, the FFAs, via EVs or other alternative pathways. In the case of NAFLD, the characteristic inflammatory state is triggered by the activation of KC that rapidly secretes cytokines and chemokines such as IL-1β and TNFα contributing to a paracrine activation of protective or apoptotic signaling pathways in hepatocytes and the recruitment of other immune cells (Duarte et al. 2015). A different study also showed that, under HFD or upon FFA treatment, KCs are activated producing high levels of proinflammatory cytokines(Leroux et al. 2012). Interestingly, KCs from mice exposed to HFD were shown to accumulate increased amount of DAG and FA as consequence of activated lipolysis (Gordon and Plüddemann 2017; Huang et al. 2014). Thus, lipid sensing by KCs may condition its sensitivity to proinflammatory triggers. Most importantly, McGettigan demonstrated that dietary lipids alter specifically the transcriptome of KC in NAFLD (McGettigan et al. 2019). Not only, McGettigan, but also Tabas and Bornfeldt demonstrated KC to have a transcriptional profile highly specialized on lipid metabolism, that are acquired by dealing with lipids of dying cells they phagocytize (Tabas and Bornfeldt 2016; Scott et al. 2016). Further analysis needs to be done to test the molecular effects of GDE in KC, particularly at the inflammatory level in order to identify potential early steps of disease.

Briefly, GDEs promote changes in lipid metabolism, seen in vivo by the increase hepatic TG. Thus, we conjecture that intestinal cells are overloaded with lipids coming from the diet, hindering a message that is encapsulated in GDEs which in turn are delivered to the liver. No doubt, obesity is associated with a spectrum of liver alterations, being one of them increased hepatic TG. This idea is supported by the increase in weight gain in HFD-GDE mice. However, we need to understand if there is lipid accumulation

in other tissues, namely in white adipose tissue, and/or a hormonal dysregulation controlling their eating behavior; for that it would be important to monitor food intake as well. Additionally, our preliminary lipidomics data comparing liver derived EV with GDE showed that the latter had an enrichment in ceramides, which are highly pro-inflammatory (results not shown) (Meeusen et al. 2018).

The fact that we observed an increase in hepatic TG induced by HFD-GDEs expands our understanding of how EVs modulate body metabolic homeostasis and opens new doors for future studies in the applicably of using healthy EV to revert metabolic diseases phenotype.

Chapter V

Final Discussion and Future Perspectives

Final Discussion and Future Perspectives

Prediabetes precedes T2D, which is a multisystemic disease and represents the end stage of several metabolic impairments (e.g. hyperglycemia, insulin resistance) being associated with obesity and dyslipidemia (Hinder et al. 2017). The vast network of metabolic organs participating in the disease suggests the existence of more than one mode of communication. EVs emerged in the last few years as novel mediators of cell-to-cell and organ-to-organ interaction. Owing to their ubiquitous presence and stability in several human biofluids they demonstrate to be extremely relevant targets in multiple diseases (Feng et al. 2010). Recent studies show that in obesity, insulin resistance, NAFLD and diabetes, the number of circulating EVs increases, suggesting an important role for these vesicles in pathophysiological mechanisms (Huang-Doran, Zhang, and Vidal-Puig 2017).

We have explored the role of GDE in prediabetes, since dysbiosis has emerged as a strong diabetogenic factor (Shen, Obin, and Zhao 2013). In fact, metabolic surgery is the only known intervention that leads to diabetes remission, prior to and largely independent of weight loss (Batterham and Cummings 2016). Therefore, our aim was to understand if GDE proteome was affected by dysmetabolism, specifically in a setting of diet induced obesity and prediabetes. Additionally, we aimed at understanding if GDE could be used as surrogate markers of disease progression and prognosis. With these goals in mind, we started by analyzing the effect of HFD feeding in the proteome of GDE. We observed, for the first time, that GDE protein cargoes are altered both in terms of concentration and profile from a healthy balanced diet to a western diet mimicking one. Consistent with previous reports, our results suggest that GDE mirrored the milieu of parent cells (Vileigas et al. 2019). We clearly observed variations in the expression of proteins related with carbohydrate, fat and protein metabolism. Plus, we observed the up-regulation of some protector proteins in ROS responsiveness pathways for food derived metabolites. Furthermore, the fact that many proteasomal proteins were down-regulated, indicates that we are dealing with an initial pathologic state.

In order to understand if the unique cargoes in NCD-GDE vs. HFD-GDE impact on the development of metabolic disorders in vivo we administered GDE from NCD or HFD fed mice to lean healthy mice. First, we aimed at determining the tropism of these vesicles; secondly, we studied the effect of a prolonged exposure to these vesicles on the development of metabolic dysfunction. One single injection of GDEs in lean healthy mice showed that GDE are mainly target to the liver, in particular to its resident macrophages, Kupffer cells (Fig.25;26). KCs are particularly relevant in certain pathologies, such as NAFLD that is closely associated to the development of T2D. NAFLD is triggered by fat accumulation in the liver due to LPS uptake from blood by KC (Wenfeng et al. 2014). Cardiovascular diseases, such as atherosclerosis, are another example where the interaction of lipids with KC worsens a pathophysiological state (Remmerie and Scott 2018). The specific mechanisms through which lipids activate macrophages are not completely known (Méndez-Sánchez et al. 2020), data gathered in this dissertation is thought-provoking. Observing that GDE derived from obese animals are favorably going to KC raises the question of a potential inflammatory activation. If this is the case, how do HFD-GDE activate the inflammatory response? Although the proteomics characterization did not reveal any relevant alterations in inflammation related proteins, other studies showed that microRNA delivered by EVs modulate the inflammatory response (Karolina et al. 2012). In order to clarify this point, first, one would expose primary KC to GDE and assess whether or not there is induction of inflammation. At that point, we would be ready to dissect the underlying molecular mechanism.

Do HFD-GDE per se induce prediabetic hallmarks? Indeed, we saw an accumulation of TG in the

liver of HFD-GDE injected mice. Note that in the liver, the production and secretion of TG is closely linked to nutrient availability and insulin levels. Interestingly, in our experimental settings those animals which displayed increased accumulation of hepatic TG were not exposed either to an HFD, or to hyperinsulinemia, thus suggesting that HFD-GDE carry lipids from the gut to the liver and are per se the inducers of the observed phenotype. TG constitute the biggest store of lipids from diet (Jensen-Urstad and Semenkovich 2012), again those mice were not under an HFD regimen, they were uniquely injected with HFD-GDE. And yet, elevated levels of TG are observed in the liver while the EV were isolated from gut. Other than that, these data is consistent with the proteomic analysis where many proteins related with lipid pathways were impressively up-regulated. We highlight a particular family of proteins considerably up-regulated in HFD-GDE (Fig.20B), the ACOTs enzymes, which are described in the literature to be directly associated with the synthesis of TG, directing FFA to be stored into the form of TG (Alves-Bezerra and Cohen 2018). In summary, we suggest a role for GDE in promoting ectopic lipid accumulation, a hallmark of NAFLD pathogenesis (Xia, Bian, and Gao 2019).

Finally, regarding other prediabetic hallmarks, every other day injections of GDE throughout 6 weeks, did not have a clear impact on glucose tolerance or insulin resistance; however as discussed on the second section, we see a trend for that phenotype alongside with educations (Fig.27B, E; Fig.28C). Moreover, we were not expecting to observe such alteration, reasons exposed in detail on the second section. Importantly, in a very clear and consistent way, educated mice showed increase levels of hepatic TG (Fig.27D, G; 28I).

Keeping on the lipid front, hepatic cholesterol levels in educated mice did not show alterations (Fig.27C,F; 28H). We can related it with the fact that acyl-coenzyme A: cholesterol acyltransferase enzymes (ACAT1 and ACAT2) are down-regulated in HFD-GDE (Fig.21; Table 1). Those proteins are described as responsible for storage of cholesterol in cytosolic droplets (Cohen and Fisher 2013). According to the literature ACAT2 demonstrated to be a major cholesterol-esterification enzyme in mouse small intestine and liver by observing that in ACAT2-deficient mice, fed with HFD, profound resistance to hypercholesterolemia and cholesterol store formations were evident. Hence, inhibition of ACAT by pharmacological intermediation or deletion of ACAT2 significantly demonstrated to reduce the rate of cholesterol absorption (Chen et al. 2001). This might be a feature of the mild phenotype window that we are targeting, where the cell is still able to develop some counteracting behaviors to the excess of fat.

Linking proteomic data with the outcomes from the education we have gathered strong evidence supporting the idea that GDEs are carriers of diet derived lipids from the gut to the liver to be stored in the form of TG. The idea of specific lipids as main components of EVs, is not new and there are studies demonstrating that they play an important role in their biology (Zhang et al. 2019). Inclusively, EVs exhibit particular lipids ordered in its membrane and carry FA binding proteins, meaning that they are transporting bioactive lipids (Record et al. 2014; Skotland et al. 2019). Nevertheless, in preliminary results we found that GDE are enriched in a specific types of ceramides (data not shown), which are known for being pro-inflammatory lipids (Hait and Maiti 2017), indicating that GDE might be an alternative mean of inflammation activation.

The scientific interest in EVs has been growing, considering their importance in cell-to-cell and cell-to-organism communication and their potential in therapeutics, due to efficient transfer of components into selective targets. With this study we highlight an important cargo that has not been well noticed, the lipids. The characteristics of EV such as stability and capacity to protect its loads from degradation, with the ability to target specific cells, made EVs good candidates for delivery tools both in health and

disease (Johnsen et al. 2014). The present dissertation has revealed crucial information for the role of extracellular vesicles in the gut-liver axis, in the context of metabolic disorders such as obesity, diabetes and NAFLD. However, a number of questions remain to be addressed:

1. How do GDE propagate diet alterations? On one side, we learned that their proteome is largely altered upon high fat and high sucrose feeding. In addition, preliminary results show that certain ceramides, toxic lipids, are enriched in HFD-GDE. It remains to be explored their miRNA content. In terms the route taken by the GDE, since chylomicrons transport exogenous lipids in the lymph, should we expect GDE transporting dietary lipid shipments to use that route as well? That could be one possible explanation for the lack of FA-related proteins in plasma EVs from HFD mice. Whether GDE can be found in the lymph is an interesting question to be addressed in the future.

2. Why do GDE mediate the accumulation of TG in particular? Since there is no alteration in terms of hepatic cholesterol, nor hepatic lipid droplets accumulation in HFD-GDE educated mice, the detailed mechanism regarding the accumulation of TG remains to be disclose. For that, we plan to validate, initially by western blot, the levels of ACOT and ACAT enzymes, in the tissues, both gut and liver.

3. What kind of relationship have KC and GDE? The interaction between KC and GDE is another aspect we want to dissect in an upcoming project, specifically the exact mechanisms by which KC are activated upon uptake of HFD-GDEs.

Perhaps the most important and intriguing question that rests is whether GDE per se are effectively able to diffuse all the prediabetic hallmarks and ultimately induce diabetes. Our results strongly suggest that we are in the right path to observe such induction.

We believe that by educating the animals for longer time and on a daily frequency will likely induce a more pronounced phenotype. In addition, injecting GDE from frank diabetic mice, would be an alternative approach to achieve diabetes solely by GDE education. In terms of treatment, we would explore the fact that healthy GDEs could revert some of the prediabetic hallmarks.

However, the challenge for the future will be to apply our findings in a more translational setting, namely in patients. In particular, it will be very interesting to analyze GDE from samples of patients that were submitted to bariatric surgery. I

In any case, from today's findings to tomorrow's applications a lot needs to be understood. The idea of using EVs as liquid biopsies is still one of our long term achievements. In the immediate future, we plan to do lipidomics analysis on plasma EVs and GDE. Additionally, with the help of scientific advance we would like to track in vivo in real time GDE travelling in the blood. Moreover, there are some examples of high-tech approaches to assay multiple EV markers at the same time such as microfluidics biochips (Shao et al. 2015) and proximity barcoding assays, designed to analyze surface proteins of individual EVs, employing a combination antibody-DNA conjugates with next-generation sequencing (Wu et al. 2019).

In conclusion, we set a new viewpoint of prediabetes that underlines on GDEs and lipid metabolism giving a great contribute for the field of EVs in the diabetogenic scene and, thus providing a base for future studies

Chapter VI

References

References

Abumrad, Nada A., and Nicholas O. Davidson. 2012. “Role of the Gut in Lipid Homeostasis.” Physiological Reviews 92 (3): 1061–85.

Afonso, Ricardo A., Joana M. Gaspar, Iva Lamarão, W. Wayne Lautt, and M. Paula Macedo. 2016. “Postprandial Insulin Action Relies on Meal Composition and Hepatic Parasympathetics: Dependency on Glucose and Amino Acids. Meal, Parasympathetics & Insulin Action.” Journal of Nutritional Biochemistry 27: 70–78.

Aguilar-Olivos, Nancy E., Paloma Almeda-Valdes, Carlos A. Aguilar-Salinas, Misael Uribe, and Nahum Méndez-Sánchez. 2016. “The Role of Bariatric Surgery in the Management of Nonalcoholic Fatty Liver Disease and Metabolic Syndrome.” Metabolism: Clinical and Experimental 65 (8): 1196–1207.

Alam, Catharina M., Jonas S.G. Silvander, Ebot N. Daniel, Guo Zhong Tao, Sofie M. Kvarnström, Parvez Alam, M. Bishr Omary, Arno Hänninen, and Diana M. Toivola. 2013. “Keratin 8 Modulates B-Cell Stress Responses and Normoglycaemia.” Journal of Cell Science 126 (24): 5635–44.

Alfa, Ronald W., Sangbin Park, Kathleen Rose Skelly, Gregory Poffenberger, Nimit Jain, Xueying Gu, Lutz Kockel, et al. 2015. “Suppression of Insulin Production and Secretion by a Decretin Hormone.” Cell Metabolism 21 (2): 323–34.

Altin, Joseph G., and Erica K. Sloan. 1997. “The Role of CD45 and CD45-Associated Molecules in T Cell Activation.” Immunology and Cell Biology 75 (5): 430–45.

Alves-Bezerra, Michele, Yingxia Li, Mariana Acuña, Anna A. Ivanova, Kathleen E. Corey, Eric A. Ortlund, and David E. Cohen. 2019. “Thioesterase Superfamily Member 2 Promotes Hepatic VLDL Secretion by Channeling Fatty Acids Into Triglyceride Biosynthesis.” Hepatology 70 (2): 496–510.

Are, Where We. 2016. “Review Communication by Extracellular Vesicles : Where We Need to Go.”

Aron Fisher “Peroxiredoxin 6 in the repair of peroxidized cell membranes and cell signaling” Arch Biochem Biophys. 2017. 617:68-83.

Aron-Wisnewsky, Judith, Chloé Vigliotti, Julia Witjes, Phuong Le, Adriaan G. Holleboom, Joanne Verheij, Max Nieuwdorp, and Karine Clément. 2020. “Gut Microbiota and Human NAFLD: Disentangling Microbial Signatures from Metabolic Disorders.” Nature Reviews Gastroenterology & Hepatology, 1–19.

Ashburner, Michael, Catherine A. Ball, Judith A. Blake, David Botstein, Heather Butler, J. Michael Cherry, Allan P. Davis, et al. 2000. “The Gene Ontology Consortium, Michael Ashburner1, Catherine A. Ball3, Judith A. Blake4, David Botstein3, Heather Butler1, J. Michael Cherry3, Allan P. Davis4, Kara Dolinski3, Selina S. Dwight3, Janan T. Eppig4, Midori A. Harris3, David P. Hill4, Laurie Is.” Nature Genetics 25 (1): 25–29.

Aslankoohi, Elham, Mohammad Naser Rezaei, Yannick Vervoort, Christophe M. Courtin, and Kevin J. Verstrepen. 2015. “Glycerol Production by Fermenting Yeast Cells Is Essential for Optimal Bread Dough Fermentation.” PLoS ONE 10 (3).

Aswad, Hala, Alexis Forterre, Oscar P B Wiklander, Guillaume Vial, Emmanuelle Danty-Berger, Audrey Jalabert, Antonin Lamazi??re, et al. 2014. “Exosomes Participate in the Alteration of Muscle

Homeostasis during Lipid-Induced Insulin Resistance in Mice." Diabetologia 57 (10): 2155–64.

Azevedo, Cristina, and Adolfo Saiardi. 2016. "Why Always Lysine? The Ongoing Tale of One of the Most Modified Amino Acids." Advances in Biological Regulation 60: 144–50.

Badoud, Flavia, Karen P. Lam, Alicia Dibattista, Maude Perreault, Michael A. Zulyniak, Bradley Cattrysse, Susan Stephenson, Philip Britz-Mckibbin, and David M. Mutch. 2014. "Serum and Adipose Tissue Amino Acid Homeostasis in the Metabolically Healthy Obese." Journal of Proteome Research 13 (7): 3455–66.

Barnett, Richard. 2018. "Type 1 Diabetes." The Lancet 391 (10117): 195.

Batterham, Rachel L., and David E. Cummings. 2016. "Mechanisms of Diabetes Improvement Following Bariatric/Metabolic Surgery." Diabetes Care 39 (6): 893–901.

Bedinger, Daniel H., and Sean H. Adams. 2015. "Metabolic, Anabolic, and Mitogenic Insulin Responses: A Tissue-Specific Perspective for Insulin Receptor Activators." Molecular and Cellular Endocrinology 415: 143–56.

Ben-Moshe, Shani, and Shalev Itzkovitz. 2019. "Spatial Heterogeneity in the Mammalian Liver." Nature Reviews Gastroenterology and Hepatology 16 (7): 395–410.

Buchwald, Henry, Rhonda Estok, Kyle Fahrbach, Deirdre Banel, Michael D. Jensen, Walter J. Pories, John P. Bantle, and Isabella Sledge. 2009. "Weight and Type 2 Diabetes after Bariatric Surgery: Systematic Review and Meta-Analysis." American Journal of Medicine 122 (3): 248-256.e5.

Buhman, Kimberly K., Michel Accad, Sabine Novak, Rebekah S. Choi, Jinny S. Wong, Robert L. Hamilton, Stephen Turley, and Robert V. Farese. 2000. "Resistance to Diet-Induced Hypercholesterolemia and Gallstone Formation in ACAT2-Deficient Mice." Nature Medicine 6 (12): 1341–47.

Bunce, Catey, and Richard Wormald. 2006. "Leading Causes of Certification for Blindness and Partial Sight in England & Wales." BMC Public Health 6: 1–7.

Burcelin, Rémy, Matteo Serino, Chantal Chabo, Vincent Blasco-Baque, and Jacques Amar. 2011. "Gut Microbiota and Diabetes: From Pathogenesis to Therapeutic Perspective." Acta Diabetologica 48 (4): 257–73.

Campbell, Matthew D., Thirunavukkarasu Sathish, Paul Z. Zimmet, Kavumpurathu R. Thankappan, Brian Oldenburg, David R. Owens, Jonathan E. Shaw, and Robyn J. Tapp. 2020. "Benefit of Lifestyle-Based T2DM Prevention Is Influenced by Prediabetes Phenotype." Nature Reviews Endocrinology.

Castillo-Armengol, Judit, Lluis Fajas, and Isabel C Lopez-Mejia. 2019. "Inter-organ Communication: A Gatekeeper for Metabolic Health." EMBO Reports 20 (9): 1–16.

Chang, Xin, Shu Ling Wang, Sheng Bing Zhao, Yi Hai Shi, Peng Pan, Lun Gu, Jun Yao, Zhao Shen Li, and Yu Bai. 2020. "Extracellular Vesicles with Possible Roles in Gut Intestinal Tract Homeostasis and IBD." Mediators of Inflammation 2020.

Chatelier, Emmanuelle Le, Trine Nielsen, Junjie Qin, Edi Prifti, Falk Hildebrand, Gwen Falony, Mathieu Almeida, et al. 2013. "Richness of Human Gut Microbiome Correlates with Metabolic Markers." Nature 500 (7464): 541–46.

Chelakkot, Chaithanya, Youngwoo Choi, Dae Kyum Kim, Hyun T. Park, Jaewang Ghim, Yonghoon Kwon, Jinseong Jeon, et al. 2018. “Akkermansia Muciniphila-Derived Extracellular Vesicles Influence Gut Permeability through the Regulation of Tight Junctions.” Experimental and Molecular Medicine 50 (2): e450-11.

Chen, Che Hong, Julio Cesar Batista Ferreira, Eric R. Gross, and Daria Mochly-Rosen. 2014. “Targeting Aldehyde Dehydrogenase 2: New Therapeutic Opportunities.” Physiological Reviews 94 (1): 1–34.

Chen, Li, Ruju Chen, Sherri Kemper, and David R. Brigstock. 2018. “Pathways of Production and Delivery of Hepatocyte Exosomes.” Journal of Cell Communication and Signaling.

Chen, M. I.N., Yingkui Yang, Evan Braunstein, Keith E. Georgeson, and Carroll M. Harmon. 2001. “Gut Expression and Regulation of FAT/CD36: Possible Role in Fatty Acid Transport in Rat Enterocytes.” American Journal of Physiology - Endocrinology and Metabolism 281 (5 44-5): 916–23.

Choi, Dong Sic, Dae Kyum Kim, Yoon Keun Kim, and Yong Song Gho. 2013. “Proteomics, Transcriptomics and Lipidomics of Exosomes and Ectosomes.” Proteomics 13 (10–11): 1554–71.

Clarke, Gerard, Roman M. Stilling, Paul J. Kennedy, Catherine Stanton, John F. Cryan, and Timothy G. Dinan. 2014. “Minireview: Gut Microbiota: The Neglected Endocrine Organ.” Molecular Endocrinology 28 (8): 1221–38.

Cifarelli, Vincenza, and Nada A. Abumrad. 2018. “Intestinal CD36 and Other Key Proteins of Lipid Utilization: Role in Absorption and Gut Homeostasis.” Comprehensive Physiology 8 (2): 493–507.

Clearfield MB. A novel therapeutic approach to dyslipidemia. J Am Osteopath Assoc. 2003;103(1 Suppl 1):S16-S20.

Clementi, Alicia H., Allison M. Gaudy, Nico van Rooijen, Robert H. Pierce, and Robert A. Mooney. 2009. “Loss of Kupffer Cells in Diet-Induced Obesity Is Associated with Increased Hepatic Steatosis, STAT3 Signaling, and Further Decreases in Insulin Signaling.” Biochimica et Biophysica Acta - Molecular Basis of Disease 1792 (11): 1062–72.

Cohen, David E., and Edward A. Fisher. 2013. “Lipoprotein Metabolism, Dyslipidemia, and Nonalcoholic Fatty Liver Disease.” Seminars in Liver Disease 33 (4): 380–88.

Colombo, Marina, Graça Raposo, and Clotilde Théry. 2014. “Biogenesis, Secretion, and Intercellular Interactions of Exosomes and Other Extracellular Vesicles.” Annual Review of Cell and Developmental Biology 30 (1): 255–89.

Conde-Vancells, Javier, Eva Rodriguez-Suarez, Nieves Embade, David Gil, Rune Matthiesen, Mikel Valle, Felix Elortza, Shelly C. Lu, Jose M. Mato, and Juan Manuel Falcon-Perez. 2008. “Characterization and Comprehensive Proteome Profiling of Exosomes Secreted by Hepatocytes.” Journal of Proteome Research 7 (12): 5157–66.

Coresh, Josef, Brad C. Astor, Tom Greene, Garabed Eknoyan, and Andrew S. Levey. 2003. “Prevalence of Chronic Kidney Disease and Decreased Kidney Function in the Adult US Population: Third National Health and Nutrition Examination Survey.” American Journal of Kidney Diseases 41 (1): 1–12.

Costa-Silva, Bruno, Nicole M Aiello, Allyson J Ocean, Swarnima Singh, Haiying Zhang, Basant Kumar Thakur, Annette Becker, et al. 2015. “Pancreatic Cancer Exosomes Initiate Pre-Metastatic Niche Formation in the Liver.” Nature Cell Biology 17 (6): 1–7.

David, Lawrence A., Corinne F. Maurice, Rachel N. Carmody, David B. Gootenberg, Julie E. Button, Benjamin E. Wolfe, Alisha V. Ling, et al. 2014. “Diet Rapidly and Reproducibly Alters the Human Gut Microbiome.” Nature 505 (7484): 559–63.

Davies, Luke C, Stephen J Jenkins, Judith E Allen, and Philip R Taylor. 2014. “Europe PMC Funders Group Tissue-Resident Macrophages.” Nature Immunol 14 (10): 986–95.

Davies, Mark, Sinead Brophy, Rhys Williams, and Ann Taylor. 2006. “The Prevalence, Severity, and Impact of Painful Diabetic Peripheral Neuropathy in Type 2 Diabetes.” Diabetes Care 29 (7): 1518–22.

Defronzo, Ralph A. 2009. “From the Triumvirate to the Ominous Octet: A New Paradigm for the Treatment of Type 2 Diabetes Mellitus.” Diabetes 58 (4): 773–95.

DeFronzo, Ralph A., and Ele Ferrannini. 2015. Regulation of Intermediary Metabolism During Fasting and Feeding. Endocrinology: Adult and Pediatric. Seventh Ed. Vol. 1–2. Elsevier Inc.

Deng, Wen Jun, Song Nie, Jie Dai, Jia Rui Wu, and Rong Zeng. 2010. “Proteome, Phosphoproteome, and Hydroxyproteome of Liver Mitochondria in Diabetic Rats at Early Pathogenic Stages.” Molecular and Cellular Proteomics 9 (1): 100–116.

Deng, Zhong-bin, Anton Poliakov, Robert W Hardy, Ronald Clements, Cunren Liu, Yuelong Liu, Jianhua Wang, et al. 2009. “Adipose Tissue Exosome-Like Vesicles Mediate Activation of Macrophage-Induced Insulin Resistance” 58 (November).

Deregibus, Maria Chiara, Vincenzo Cantaluppi, Raffaele Calogero, Marco Lo Iacono, Ciro Tetta, Luigi Biancone, Stefania Bruno, Benedetta Bussolati, and Giovanni Camussi. 2007. “Endothelial Progenitor Cell - Derived Microvesicles Activate an Angiogenic Program in Endothelial Cells by a Horizontal Transfer of MRNA.” Blood 110 (7): 2440–48.

DeSesso, J. M., and C. F. Jacobson. 2001. “Anatomical and Physiological Parameters Affecting Gastrointestinal Absorption in Humans and Rats.” Food and Chemical Toxicology 39 (3): 209–28.

Dixon, Laura J, Mark Barnes, Hui Tang, Michele T Pritchard, E Laura, and Cleveland Clinic. 2016. “Kupffer Cells in the Liver.” Compr Physiology 3 (2): 785–97.

Drover, Victor A., Mohammad Ajmal, Fatiha Nassir, Nicholas O. Davidson, Andromeda M. Nauli, Daisy Sahoo, Patrick Tso, and Nada A. Abumrad. 2005. “CD36 Deficiency Impairs Intestinal Lipid Secretion and Clearance of Chylomicrons from the Blood.” Journal of Clinical Investigation 115 (5): 1290–97.

Duarte, Nádia, Inês Coelho, Denys Holovanchuk, Joana Inês Almeida, Carlos Penha-Gonçalves, and Maria Paula Macedo. 2018. “Dipeptidyl Peptidase-4 Is a Pro-Recovery Mediator During Acute Hepatotoxic Damage and Mirrors Severe Shifts in Kupffer Cells.” Hepatology Communications 2 (9): 1080–94.

Duarte, Nádia, Inês C. Coelho, Rita S. Patarrão, Joana I. Almeida, Carlos Penha-Gonçalves, and M. Paula Macedo. 2015. “How Inflammation Impinges on NAFLD: A Role for Kupffer Cells.” BioMed Research International 2015.

Elia, Ilaria, Dorien Broekaert, Stefan Christen, Ruben Boon, Enrico Radaelli, Martin F. Orth, Catherine Verfaillie, Thomas G.P. Grünewald, and Sarah Maria Fendt. 2017. "Proline Metabolism Supports Metastasis Formation and Could Be Inhibited to Selectively Target Metastasizing Cancer Cells." Nature Communications 8 (May): 1–11.

Ersoy, Baran A., Kristal M. Maner-Smith, Yingxia Li, Ipek Alpertunga, and David E. Cohen. 2018. "Thioesterase-Mediated Control of Cellular Calcium Homeostasis Enables Hepatic ER Stress." Journal of Clinical Investigation 128 (1): 141–56.

Evers, Simon S., Darleen A. Sandoval, and Randy J. Seeley. 2017. "The Physiology and Molecular Underpinnings of the Effects of Bariatric Surgery on Obesity and Diabetes." Annual Review of Physiology 79 (1): 313–34.

Falony, Gwen, Marie Joossens, Sara Vieira-Silva, Jun Wang, Youssef Darzi, Karoline Faust, Alexander Kurilshikov, et al. 2016. "Population-Level Analysis of Gut Microbiome Variation." Science 352 (6285): 560–64.

Fang, Lei, George Karakiulakis, and Michael Roth. 2020. "Are Patients with Hypertension and Diabetes Mellitus at Increased Risk for COVID-19 Infection?" The Lancet Respiratory 2600 (20): 30116.

Fargion, S., P. Dongiovanni, A. Guzzo, S. Colombo, L. Valenti, and A. L. Fracanzani. 2005. "Iron and Insulin Resistance." Alimentary Pharmacology and Therapeutics, Supplement 22 (2): 61–63.

Feng, Du, Wen Long Zhao, Yun Ying Ye, Xiao Chen Bai, Rui Qin Liu, Lei Fu Chang, Qiang Zhou, and Sen Fang Sui. 2010. "Cellular Internalization of Exosomes Occurs through Phagocytosis." Traffic 11 (5): 675–87.

Ferrannini, Ele, Amalia Gastaldelli, and Patricia Iozzo. 2011. "Pathophysiology of Prediabetes." Medical Clinics of North America 95 (2): 327–39.

Ferrannini, Ele, Monica Nannipieri, Ken Williams, Clicerio Gonzales, Steve M. Haffner, and Michael P. Stern. 2004. "Mode of Onset of Type 2 Diabetes from Normal or Impaired Glucose Tolerance." Diabetes 53 (1): 160–65.

Ferrere, Gladys, Anne Leroux, Laura Wrzosek, Virginie Puchois, Francoise Gaudin, Dragos Ciocan, Marie Laure Renoud, Sylvie Naveau, Gabriel Perlemuter, and Anne Marie Cassard. 2016. "Activation of Kupffer Cells Is Associated with a Specific Dysbiosis Induced by Fructose or High Fat Diet in Mice." PLoS ONE 11 (1): 1–16.

Forman, Henry Jay, Rinna, Alessandra. 2009. "Glutathione: Overview of its Protective Roles, Measurement, and Biosynthesis" Mol Aspects Med. 30:1-12.

Frayn, Keith N. 2010. Metabolic Regulation: A Human Perspective. 3rd Edition

Kadiu, Irena, Narayanasamy Prabagaran, Daash, Prasanta K., Zhang Wei, Gendelman, Howard. 2012. "Biochemical and Biological Characterization of Exosomes and Microvesicles as Facilitators of HIV-1 Infection in Macrophages" J Immunol. 189(2):744-754.

Franklin, Mallory P., Aishwarya Sathyanarayan, and Douglas G. Mashek. 2017. "Acyl-CoA Thioesterase 1 (ACOT1) Regulates PPARα to Couple Fatty Acid Flux with Oxidative Capacity during Fasting." Diabetes 66 (8): 2112–23.

Freeman, David W., Nicole Noren Hooten, Erez Eitan, Jamal Green, Nicolle A. Mode, Monica Bodogai, Yongqing Zhang, et al. 2018. “Altered Extracellular Vesicle Concentration, Cargo, and Function in Diabetes.” Diabetes 67 (11): 2377–88.

Fujita, Mariko, Atsushi Momose, Takayuki Ohtomo, Azusa Nishinosono, Kouichi Tanonaka, Hiroo Toyoda, Masako Morikawa, and Junji Yamada. 2011. “Upregulation of Fatty Acyl-CoA Thioesterases in the Heart and Skeletal Muscle of Rats Fed a High-Fat Diet.” Biological and Pharmaceutical Bulletin 34 (1): 87–91.

Gaudet, Daniel, Jean Philippe Drouin-Chartier, and Patrick Couture. 2017. “Lipid Metabolism and Emerging Targets for Lipid-Lowering Therapy.” Canadian Journal of Cardiology 33 (7): 872–82.

Ge, Qian, Xin Xin Xie, Xiaoqiu Xiao, and Xi Li. 2019. “Exosome-like Vesicles as New Mediators and Therapeutic Targets for Treating Insulin Resistance and β -Cell Mass Failure in Type 2 Diabetes Mellitus.” Journal of Diabetes Research 2019.

Gerstein, Hertzel C. 2015. “Diabetes: Dysglycaemia as a Cause of Cardiovascular Outcomes.” Nature Reviews Endocrinology 11 (9): 508–10.

Glicksman, Michael, Asha Asthana, Brent S. Abel, Mary F. Walter, Monica C. Skarulis, and Ranganath Muniyappa. 2017. “Plasma SerpinB1 Is Related to Insulin Sensitivity but Not Pancreatic β-Cell Function in Non-Diabetic Adults.” Physiological Reports 5 (5): 1–5.

Gordon, Siamon, and Annette Plüddemann. 2017. “Tissue Macrophages: Heterogeneity and Functions.” BMC Biology 15 (1): 1–18.

Gray, Lawrence R., Sean C. Tompkins, and Eric B. Taylor. 2014. “Regulation of Pyruvate Metabolism and Human Disease.” Cellular and Molecular Life Sciences 71 (14): 2577–2604.

Grill, Harvey J., and Matthew R. Hayes. 2012. “Hindbrain Neurons as an Essential Hub in the Neuroanatomically Distributed Control of Energy Balance.” Cell Metabolism 16 (3): 296–309.

Gu, Yu, Can Liu, Ningning Zheng, Wei Jia, Weidong Zhang, and Houkai Li. 2019. “Metabolic and Gut Microbial Characterization of Obesity-Prone Mice under a High-Fat Diet.” Journal of Proteome Research 18 (4): 1703–14.

Guay, Claudiane, and Romano Regazzi. 2017. “Exosomes as New Players in Metabolic Organ Cross-Talk.” Diabetes, Obesity and Metabolism 19 (May): 137–46.

Gurung, Manoj, Zhipeng Li, Hannah You, Richard Rodrigues, Donald B. Jump, Andrey Morgun, and Natalia Shulzhenko. 2020. “Role of Gut Microbiota in Type 2 Diabetes Pathophysiology.” EBioMedicine 51: 102590.

Hait, Nitai C., and Aparna Maiti. 2017. “The Role of Sphingosine-1-Phosphate and Ceramide-1-Phosphate in Inflammation and Cancer.” Mediators of Inflammation 2017.

Hamdy, Osama, Mhd Wael Tasabehji, Taha Elseaidy, Shaheen Tomah, Sahar Ashrafzadeh, and Adham Mottalib. 2018. “Fat Versus Carbohydrate-Based Energy-Restricted Diets for Weight Loss in Patients With Type 2 Diabetes.” Current Diabetes Reports 18 (12).

Hansen, Torben. 2002. “Genetics of Type 2 Diabetes.” Current Science 83 (12): 1477–82.

Henry, Robert R. 1998. “Type 2 Diabetes Care: The Role of Insulin-Sensitizing Agents and Practical

Implications for Cardiovascular Disease Prevention." American Journal of Medicine 105 (1 A).

Heydemann, Ahlke. 2016. "An Overview of Murine High Fat Diet as a Model for Type 2 Diabetes Mellitus." Journal of Diabetes Research 2016.

Hinder, Lucy M., Phillipe D. O'Brien, John M. Hayes, Carey Backus, Andrew P. Solway, Catrina Sims-Robinson, and Eva L. Feldman. 2017. "Dietary Reversal of Neuropathy in a Murine Model of Prediabetes and Metabolic Syndrome." DMM Disease Models and Mechanisms 10 (6): 717–25.

Hobson, R. M., B. Saunders, G. Ball, R. C. Harris, and C. Sale. 2012. "Effects of β-Alanine Supplementation on Exercise Performance: A Meta-Analysis." Amino Acids 43 (1): 25–37.

Hoffman, Simon, Danielle Alvares, and Khosrow Adeli. 2019. "Intestinal Lipogenesis: How Carbs Turn on Triglyceride Production in the Gut." Current Opinion in Clinical Nutrition and Metabolic Care 22 (4): 284–88.

Holst, Jens Juul, Fiona Gribble, Michael Horowitz, and Chris K. Rayner. 2016. "Roles of the Gut in Glucose Homeostasis." Diabetes Care 39 (6): 884–92.

Horton, Jay D, Joseph L Goldstein, and Michael S Brown. 2002. "SREBPs." Most 109 (9): 1125–31.

Horváth, ViktorJózsef, Zsuzsanna Putz, Ferenc Izbéki, Anna Erzsébet Körei, László Gerő, Csaba Lengyel, Péter Kempler, and Tamás Várkonyi. 2015. "Diabetes-Related Dysfunction of the Small Intestine and the Colon: Focus on Motility." Current Diabetes Reports 15 (11).

Hoshino, Ayuko, Bruno Costa-Silva, Tang-Long Shen, Goncalo Rodrigues, Ayako Hashimoto, Milica Tesic Mark, Henrik Molina, et al. 2015. "Tumour Exosome Integrins Determine Organotropic Metastasis." Nature 527 (7578): 329–35.

Hospital, Steno Memorial, and Infectious Diseases. 1990. "Diabetologia," 15–23.

Hu, Guoku, Ai Yu Gong, Amanda L. Roth, Bing Q. Huang, Honorine D. Ward, Guan Zhu, Nicholas F. LaRusso, Nancy D. Hanson, and Xian Ming Chen. 2013. "Release of Luminal Exosomes Contributes to TLR4-Mediated Epithelial Antimicrobial Defense." PLoS Pathogens 9 (4).

Huang-Doran, Isabel, Chen Yu Zhang, and Antonio Vidal-Puig. 2017. "Extracellular Vesicles: Novel Mediators of Cell Communication In Metabolic Disease." Trends in Endocrinology and Metabolism 28 (1): 3–18.

Huang, Stanley Ching Cheng, Bart Everts, Yulia Ivanova, David O'Sullivan, Marcia Nascimento, Amber M. Smith, Wandy Beatty, et al. 2014. "Cell-Intrinsic Lysosomal Lipolysis Is Essential for Alternative Activation of Macrophages." Nature Immunology 15 (9): 846–55.

Huang, Wan, Anantha Metlakunta, Nikolaos Dedousis, Pili Zhang, Ian Sipula, John J. Dube, Donald K. Scott, and Robert M. O'Doherty. 2010. "Depletion of Liver Kupffer Cells Prevents the Development of Diet-Induced Hepatic Steatosis and Insulin Resistance." Diabetes 59 (2): 347–57.

Hudgins, Lisa C., Marc K. Hellerstein, Cynthia E. Seidman, Richard A. Neese, Jolanta D. Tremaroli, and Jules Hirsch. 2000. "Relationship between Carbohydrate-Induced Hypertriglyceridemia and Fatty Acid Synthesis in Lean and Obese Subjects." Journal of Lipid Research 41 (4): 595–604.

Hudgins, Lisa Cooper, Marc Hellerstein, Cynthia Seidman, Richard Neese, Jolanta Diakun, and Jules Hirsch. 1996. "Human Fatty Acid Synthesis Is Stimulated by a Eucaloric Low Fat, High

Carbohydrate Diet." Journal of Clinical Investigation 97 (9): 2081–91.

Hyo, Sun Lee, Jaeho Jeong, and Kong Joo Lee. 2009. "Characterization of Vesicles Secreted from Insulinoma NIT-1 Cells." Journal of Proteome Research 8 (6): 2851–62.

IDF. 2019. IDF Diabetes Atlas Ninth. Dunia : IDF.

Ii, Type. n.d. "Molecular Pathways in the Pathogenesis of Type II Diabetes."

Iqbal, Jahangir, and M. Mahmood Hussain. 2009. "Intestinal Lipid Absorption." American Journal of Physiology - Endocrinology and Metabolism 296 (6).

Jalabert, Audrey, Guillaume Vial, Claudiane Guay, Oscar P B Wiklander, Joel Z Nordin, Hala Aswad, Alexis Forterre, et al. 2016. "Exosome-like Vesicles Released from Lipid-Induced Insulin-Resistant Muscles Modulate Gene Expression and Proliferation of Beta Recipient Cells in Mice."

Jan, Arif Tasleem, Mudasir A. Malik, Safikur Rahman, Hye R. Yeo, Eun J. Lee, Tasduq S. Abdullah, and Inho Choi. 2017. "Perspective Insights of Exosomes in Neurodegenerative Diseases: A Critical Appraisal." Frontiers in Aging Neuroscience 9 (SEP): 1–8.

Jangra, Surender, Shekar K. Raja, Raj Kumar Sharma, Ramesh Pothuraju, and A. K. Mohanty. 2019. "Ameliorative Effect of Fermentable Fibres on Adiposity and Insulin Resistance in C57BL/6 Mice Fed a High-Fat and Sucrose Diet." Food and Function 10 (6): 3696–3705.

Janowska-Wieczorek, Anna, Marcin Majka, Jacek Kijowski, Monika Baj-Krzyworzeka, Ryan Reca, A. Robert Turner, Janina Ratajczak, Steven G. Emerson, M. Anna Kowalska, and Mariusz Z. Ratajczak. 2001. "Platelet-Derived Microparticles Bind to Hematopoietic Stem/Progenitor Cells and Enhance Their Engraftment." Blood 98 (10): 3143–49.

Jensen-Urstad, Anne P.L., and Clay F. Semenkovich. 2012. "Fatty Acid Synthase and Liver Triglyceride Metabolism: Housekeeper or Messenger?" Biochimica et Biophysica Acta - Molecular and Cell Biology of Lipids 1821 (5): 747–53.

Johnsen, Kasper Bendix, Johann Mar Gudbergsson, Martin Najbjerg Skov, Linda Pilgaard, Torben Moos, and Meg Duroux. 2014. "A Comprehensive Overview of Exosomes as Drug Delivery Vehicles - Endogenous Nanocarriers for Targeted Cancer Therapy." Biochimica et Biophysica Acta - Reviews on Cancer 1846 (1): 75–87.

Johnstone, R. M., M. Adam, J. R. Hammond, L. Orr, and C. Turbide. 1987. "Vesicle Formation during Reticulocyte Maturation. Association of Plasma Membrane Activities with Released Vesicles (Exosomes)." Journal of Biological Chemistry 262 (19): 9412–20.

Jr., Tobias C. Walther and Robert V. Farese. 2012. "FS-SOC-Prelim.Pdf." Annual Review of Biochemistry 81: 687–714.

Kagnoff, Martin F. 1993. "Immunology of the Intestinal Tract." Gastroenterology 105 (5): 1275–80.

Kahn, S. E. 2003. "The Relative Contributions of Insulin Resistance and Beta-Cell Dysfunction to the Pathophysiology of Type 2 Diabetes." Diabetologia 46 (1): 3–19.

Kalluri, Raghu, and Valerie S LeBleu. 2020. "The Biology, Function, and Biomedical Applications of Exosomes." Science (New York, N.Y.) 367 (6478).

Kalra, Hina, Gregor P.C. Drummen, and Suresh Mathivanan. 2016. "Focus on Extracellular Vesicles:

Introducing the next Small Big Thing." International Journal of Molecular Sciences 17 (2).

Kang, Insoo, and Richard Bucala. 2019. "The Immunobiology of MIF: Function, Genetics and Prospects for Precision Medicine." Nature Reviews Rheumatology 15 (7): 427–37.

Kanuri, Babu Nageswararao, Sanjay C. Rebello, Priya Pathak, Hobby Agarwal, Jitendra S. Kanshana, Deepika Awasthi, Anand P. Gupta, Jiaur R. Gayen, Kumaravelu Jagavelu, and Madhu Dikshit. 2018. "Glucose and Lipid Metabolism Alterations in Liver and Adipose Tissue Pre-Dispose P47phox Knockout Mice to Systemic Insulin Resistance." Free Radical Research 52 (5): 568–82.

Karolina, Dwi Setyowati, Subramaniam Tavintharan, Arunmozhiarasi Armugam, Sugunavathi Sepramaniam, Sharon Li Ting Pek, Michael T.K. Wong, Su Chi Lim, Chee Fang Sum, and Kandiah Jeyaseelan. 2012. "Circulating MiRNA Profiles in Patients with Metabolic Syndrome." Journal of Clinical Endocrinology and Metabolism 97 (12): 2271–76.

Kashyap, Sangeeta R., Patrick Gatmaitan, Stacy Brethauer, and Philip Schauer. 2010. "Bariatric Surgery for Type 2 Diabetes: Weighing the Impact for Obese Patients." Cleveland Clinic Journal of Medicine 77 (7): 468–76.

Kaushik, Susmita, and Ana Maria Cuervo. 2018. "The Coming of Age of Chaperone-Mediated Autophagy." Nature Reviews Molecular Cell Biology 19 (6): 365–81.

Kawano, Yuki, and David E. Cohen. 2013. "Mechanisms of Hepatic Triglyceride Accumulation in Non-Alcoholic Fatty Liver Disease." Journal of Gastroenterology 48 (4): 434–41.

Keller, Matthew D., Krystal L. Ching, Feng Xia Liang, Avantika Dhabaria, Kayan Tam, Beatrix M. Ueberheide, Derya Unutmaz, Victor J. Torres, and Ken Cadwell. 2020. "Decoy Exosomes Provide Protection against Bacterial Toxins." Nature 579 (7798): 260–64.

Kelley, David E. 2005. "Skeletal Muscle Fat Oxidation: Timing and Flexibility Are Everything." Journal of Clinical Investigation 115 (7): 1699–1702.

Khan, Latifa, and Mahtab S. Bamji. 1979. "Tissue Carnitine Deficiency Due to Dietary Lysine Deficiency: Triglyceride Accumulation and Concomitant Impairment in Fatty Acid Oxidation." The Journal of Nutrition 109 (1): 24–31.

Khan, Niamat, and Abdul R. Asif. 2015. "Transcriptional Regulators of Claudins in Epithelial Tight Junctions." Mediators of Inflammation 2015 (1).

Kim, Wook, and Josephine M. Egan. 2008. "The Role of Incretins in Glucose Homeostasis and Diabetes Treatment." Pharmacological Reviews 60 (4): 470–512.

King, Aileen J.F. 2012. "The Use of Animal Models in Diabetes Research." British Journal of Pharmacology 166 (3): 877–94.

Knebel, Birgit, Sonja Hartwig, Jutta Haas, Stefan Lehr, Simon Goeddeke, Franciscus Susanto, Lothar Bohne, et al. 2015. "Peroxisomes Compensate Hepatic Lipid Overflow in Mice with Fatty Liver." Biochimica et Biophysica Acta - Molecular and Cell Biology of Lipids 1851 (7): 965–76.

Koliaki, Chrysi, Stavros Liatis, Carel W. le Roux, and Alexander Kokkinos. 2017. "The Role of Bariatric Surgery to Treat Diabetes: Current Challenges and Perspectives." BMC Endocrine Disorders 17 (1): 50.

Koppers-Lalic, Danijela, Michael Hackenberg, Irene V. Bijnsdorp, Monique A.J. van Eijndhoven, Payman Sadek, Daud Sie, Nicoletta Zini, et al. 2014. “Nontemplated Nucleotide Additions Distinguish the Small RNA Composition in Cells from Exosomes.” Cell Reports 8 (6): 1649–58.

Kowalski, Greg M., and Clinton R. Bruce. 2014. “The Regulation of Glucose

Metabolism: Implications and Considerations for the Assessment of Glucose Homeostasis in Rodents.” American Journal of Physiology - Endocrinology and Metabolism 307 (10): E859–71.

Kralj-Iglic, Veronika. 2012. “Stability of Membranous Nanostructures: A Possible Key Mechanism in Cancer Progression.” International Journal of Nanomedicine 7: 3579–96.

Kranendonk, Mariëtte E.G., Frank L.J. Visseren, Joost A. Van Herwaarden, Esther N.M. Nolte-’t Hoen, Wilco De Jager, Marca H.M. Wauben, and Eric Kalkhoven. 2014. “Effect of Extracellular Vesicles of Human Adipose Tissue on Insulin Signaling in Liver and Muscle Cells.” Obesity 22 (10): 2216–23.

Kreimeyer, Annett, Alain Perret, Christophe Lechaplais, David Vallenet, Claudine Médigue, Marcel Salanoubat, and Jean Weissenbach. 2007. “Identification of the Last Unknown Genes in the Fermentation Pathway of Lysine.” Journal of Biological Chemistry 282 (10): 7191–97.

Hirsova, P., Ibrahim, S. H., Krishnan, A., Verma, V. K., Bronk, S. F., Werneburg, N. W., Charlton, M. R., Shah, V. H., Malhi, H., & Gores, G. J. (2016). Lipid-Induced Signaling Causes Release of Inflammatory Extracellular Vesicles From Hepatocytes. Gastroenterology, 150(4), 956–967.

Lakhter, Alexander J., and Emily K. Sims. 2015. “Minireview: Emerging Roles for Extracellular Vesicles in Diabetes and Related Metabolic Disorders.” Molecular Endocrinology (Baltimore, Md.) 29 (11): 1535–48.

Lanthier, Nicolas. 2015. “Targeting Kupffer Cells in Non-Alcoholic Fatty Liver Disease/ Non-Alcoholic Steatohepatitis: Why and How?” World Journal of Hepatology 7 (19): 2184–88.

Lavoie, J. M., and M. S. Gauthier. 2006. “Regulation of Fat Metabolism in the Liver: Link to Non-Alcoholic Hepatic Steatosis and Impact of Physical Exercise.” Cellular and Molecular Life Sciences 63 (12): 1393–1409.

Lázaro-Ibáñez, Elisa, Andres Sanz-Garcia, Tapio Visakorpi, Carmen Escobedo-Lucea, Pia Siljander, Ángel Ayuso-Sacido, and Marjo Yliperttula. 2014. “Different GDNA Content in the Subpopulations of Prostate Cancer Extracellular Vesicles: Apoptotic Bodies, Microvesicles, and Exosomes.” Prostate 74 (14): 1379–90.

Lee, Yun Kyung, and Sarkis K. Mazmanian. 2010. “Has the Microbiota Played a Critical Role in the Evolution of the Adaptive Immune System?” Science 330 (6012): 1768–73.

Leroux, Anne, Gladys Ferrere, Vanessa Godie, Frédéric Cailleux, Marie Laure Renoud, Françoise Gaudin, Sylvie Naveau, et al. 2012. “Toxic Lipids Stored by Kupffer Cells Correlates with Their Pro-Inflammatory Phenotype at an Early Stage of Steatohepatitis.” Journal of Hepatology 57 (1): 141–49.

Leroux, Anne, Gladys Ferrere, Vanessa Godie, Frédéric Cailleux, Marie Laure Renoud, Françoise Gaudin, Sylvie Naveau, et al. 2012. “Toxic Lipids Stored by Kupffer Cells Correlates with Their Pro-Inflammatory Phenotype at an Early Stage of Steatohepatitis.” Journal of Hepatology 57 (1): 141–49.

Lian, Kun, Chaosheng Du, Yi Liu, Di Zhu, Wenjun Yan, Haifeng Zhang, Zhibo Hong, et al. 2015. “Impaired Adiponectin Signaling Contributes to Disturbed Catabolism of Branched-Chain Amino Acids in Diabetic Mice.” Diabetes 64 (1): 49–59.

Little, Tanya J., Selena Doran, James H. Meyer, Andre J.P.M. Smout, Deirdre G. O’Donovan, Keng Liang Wu, Karen L. Jones, et al. 2006. “The Release of GLP-1 and Ghrelin, but Not GIP and CCK, by Glucose Is Dependent upon the Length of Small Intestine Exposed.” American Journal of Physiology - Endocrinology and Metabolism 291 (3): 647–55.

Liu, Huici, Zhang, Min, Ma, Qingyu, Tian, Baoming, Nie, Chenxi, Chen, Zhifei, Li, Juxiu. 2020. “Health Beneficial Effects of Resistant Starch on Diabetes and Obesity via Regulation of Gut Miccrobiota: A Review”. Food Funct.

Luo, Hanzhi, Hou Hsien Chiang, Makensie Louw, Albert Susanto, and Danica Chen. 2017. “Nutrient Sensing and the Oxidative Stress Response.” Trends in Endocrinology and Metabolism 28 (6): 449–60.

Hongato, Liu, You, Shujie, Xu, Jian. 2012. “Enhamcement of 26S Proteasome Functionality Connects Oxidative Stress and Vascular Endothelial Inflammatory Response in Diabetes”. Arterioscler Throm Vasc Biol. 32(9):2131-2140.

Losacco, Mariana Cerqueira, Carolina Fernanda Theodora de Almeida, Andressa Harumi Torelli Hijo, Paula Bargi-Souza, Patricia Gama, Maria Tereza Nunes, and Francemilson Goulart-Silva. 2018. “High-Fat Diet Affects Gut Nutrients Transporters in Hypo and Hyperthyroid Mice by PPAR-a Independent Mechanism.” Life Sciences 202 (February): 35–43.

Lu, Hongfang, Ying Yang, Emman M. Allister, Nadeeja Wijesekara, and Michael B. Wheeler. 2008. “The Identification of Potential Factors Associated with the Development of Type 2 Diabetes: A Quantitative Proteomics Approach.” Molecular and Cellular Proteomics 7 (8): 1434–51.

Luo, Wenjing, Qinyu Xu, Qi Wang, Huimin Wu, and Jing Hua. 2017. “Effect of Modulation of PPAR-γ Activity on Kupffer Cells M1/M2 Polarization in the Development of Non-Alcoholic Fatty Liver Disease.” Scientific Reports 7 (March): 1–13.

Lutchmansingh, Fallon K., Jean W. Hsu, Franklyn I. Bennett, Asha V. Badaloo, McFarlane Anderson Norma, M. Gordon Strachan Georgiana, A. Wright Pascoe Rosemarie, Farook Jahoor, and Michael S. Boyne. 2018. “Glutathione Metabolism in Type 2 Diabetes and Its Relationship with Microvascular Complications and Glycemia.” PLoS ONE 13 (6): 1–12.

Macedo, Maria Paula, Ines S. Lima, Joana M. Gaspar, Ricardo A. Afonso, Rita S. Patarrao, Young Bum Kim, and Rogerio T. Ribeiro. 2014. “Risk of Postprandial Insulin Resistance: The Liver/Vagus Rapport.” Reviews in Endocrine and Metabolic Disorders 15 (1): 67–77.

MacParland, Sonya A., Jeff C. Liu, Xue Zhong Ma, Brendan T. Innes, Agata M. Bartczak, Blair K. Gage, Justin Manuel, et al. 2018. “Single Cell RNA Sequencing of Human Liver Reveals Distinct Intrahepatic Macrophage Populations.” Nature Communications 9 (1): 1–21.

Macpherson, Andrew J., and Nicola L. Harris. 2004. “Interactions between Commensal Intestinal Bacteria and the Immune System.” Nature Reviews Immunology 4 (6): 478–85.

Maia, Joana, Sergio Caja, Maria Carolina Strano Moraes, Nuno Couto, and Bruno Costa-Silva. 2018. “Exosome-Based Cell-Cell Communication in the Tumor Microenvironment.” Frontiers in Cell

and Developmental Biology 6 (FEB): 1–19.

Malarkey, David E., Kennita Johnson, Linda Ryan, Gary Boorman, and Robert R. Maronpot. 2005. "New Insights into Functional Aspects of Liver Morphology." Toxicologic Pathology 33 (1): 27–34.

Mallegol, J., G. Van Niel, and M. Heyman. 2005. "Phenotypic and Functional Characterization of Intestinal Epithelial Exosomes." Blood Cells, Molecules, and Diseases 35 (1): 11–16.

Mallegol, Julia, Guillaume Van Niel, Corinne Lebreton, Yves Lepelletier, Céline Candalh, Christophe Dugave, Joan K. Heath, Graça Raposo, Nadine Cerf-Bensussan, and Martine Heyman. 2007. "T84-Intestinal Epithelial Exosomes Bear MHC Class II/Peptide Complexes Potentiating Antigen Presentation by Dendritic Cells." Gastroenterology 132 (5): 1866–76.

Manuscript, Author. 2013. "NIH Public Access." Hepatol Res. 43 (1): 51–64.

Marín-Peñalver, Juan José, Iciar Martín-Timón, Cristina Sevillano-Collantes, and Francisco Javier del Cañizo-Gómez. 2016. "Update on the Treatment of Type 2 Diabetes Mellitus." World Journal of Diabetes 7 (17): 354.

Mathieu, Mathilde, Lorena Martin-Jaular, Grégory Lavieu, and Clotilde Théry. 2019. "Specificities of Secretion and Uptake of Exosomes and Other Extracellular Vesicles for Cell-to-Cell Communication." Nature Cell Biology 21 (1): 9–17.

Matthiesen, Rune. 2013. Mass Spectrometry Data Analysis in Proteomics. Methods in Molecular Biology. Vol. 1007.

Matyash, Vitali, Gerhard Liebisch, Teymuras V. Kurzchalia, Andrej Shevchenko, and Dominik Schwudke. 2008. "Lipid Extraction by Methyl-Terf-Butyl Ether for High-Throughput Lipidomics." Journal of Lipid Research 49 (5): 1137–46.

Maxson & Mitchell. 2016. "Energy Metabolism in the Liver." Physiology & Behavior 176 (1): 139–48.

McGettigan, Brett, Rachel McMahan, David Orlicky, Matthew Burchill, Thomas Danhorn, Prashanth Francis, Lin Ling Cheng, Lucy Golden-Mason, Claudia V. Jakubzick, and Hugo R. Rosen. 2019. "Dietary Lipids Differentially Shape Nonalcoholic Steatohepatitis Progression and the Transcriptome of Kupffer Cells and Infiltrating Macrophages." Hepatology 70 (1): 67–83.

Meeusen, Jeffrey W., Leslie J. Donato, Sandra C. Bryant, Linnea M. Baudhuin, Peter B. Berger, and Allan S. Jaffe. 2018. "Plasma Ceramides a Novel Predictor of Major Adverse Cardiovascular Events after Coronary Angiography." Arteriosclerosis, Thrombosis, and Vascular Biology 38 (8): 1933–39.

Méndez-Sánchez, Nahum, Alejandro Valencia-Rodríguez, Carlos Coronel-Castillo, Alfonso Vera-Barajas, Jocelyn Contreras-Carmona, Guadalupe Ponciano-Rodríguez, and Daniel Zamora-Valdés. 2020. "The Cellular Pathways of Liver Fibrosis in Non-Alcoholic Steatohepatitis." Annals of Translational Medicine 8 (6): 400–400.

Mingrone, Geltrude, and Lidia Castagneto-Gissey. 2014. "Type 2 Diabetes Mellitus in 2013: A Central Role of the Gut in Glucose Homeostasis." Nature Reviews Endocrinology 10 (2): 73–74.

Mithieux, Gilles. 2009. "A Novel Function of Intestinal Gluconeogenesis: Central Signaling in Glucose and Energy Homeostasis." Nutrition 25 (9): 881–84.

Mittelbrunn, María, Cristina Gutiérrez-Vázquez, Carolina Villarroya-Beltri, Susana González, Fátima

Sánchez-Cabo, Manuel Ángel González, Antonio Bernad, and Francisco Sánchez-Madrid. 2011. "Unidirectional Transfer of MicroRNA-Loaded Exosomes from T Cells to Antigen-Presenting Cells." Nature Communications 2 (1).

Moxey, P. W., P. Gogalniceanu, R. J. Hinchliffe, I. M. Loftus, K. J. Jones, M. M. Thompson, and P. J. Holt. 2011. "Lower Extremity Amputations - a Review of Global Variability in Incidence." Diabetic Medicine 28 (10): 1144–53.

Muller, Laurent, Sylvia Muller-Haegele, Masato Mitsuhashi, William Gooding, Hideho Okada, and Theresa L. Whiteside. 2015. "Exosomes Isolated from Plasma of Glioma Patients Enrolled in a Vaccination Trial Reflect Antitumor Immune Activity and Might Predict Survival." OncoImmunology 4 (6): 1–8.

Murata, Chisato, Yoshihiko Suzuki, Taro Muramatsu, Matsuo Taniyama, Yoshihito Atsumi, Kempei Matsuoka, Tetsu Watanabe, and Isao Okazaki. 2000. "Inactive Aldehyde Dehydrogenase 2 Worsens Glycemic Control in Patients With Type 2 Diabetes Mellitus Who Drink Low to Moderate Amounts of Alcohol." Alcoholism: Clinical and Experimental Research 24 (4): 5S-11S.

Najjar, Sonia M., and Germán Perdomo. 2019. "Hepatic Insulin Clearance: Mechanism and Physiology." Physiology (Bethesda, Md.) 34 (3): 198–215.

Narita, Masami. 2020. "The Gut Microbiome as a Target for Prevention of Allergic Diseases." Japanese Journal of Allergology 69 (1): 19–22.

Nauck, Michael A., and Juris J. Meier. 2018. "Incretin Hormones: Their Role in Health and Disease." Diabetes, Obesity and Metabolism 20 (September 2017): 5–21.

Neis, Evelien P.J.G., Cornelis H.C. Dejong, and Sander S. Rensen. 2015. "The Role of Microbial Amino Acid Metabolism in Host Metabolism." Nutrients 7 (4): 2930–46.

Niel, Guillaume Van, Gisela D'Angelo, and Graça Raposo. 2018. "Shedding Light on the Cell Biology of Extracellular Vesicles." Nature Reviews Molecular Cell Biology 19 (4): 213–28.

Nielen, Monique Van, Edith J.M. Feskens, Marco Mensink, Ivonne Sluijs, Esther Molina, Pilar Amiano, Eva Ardanaz, et al. 2014. "Dietary Protein Intake and Incidence of Type 2 Diabetes in Europe: The EPIC-InterAct Case-Cohort Study." Diabetes Care 37 (7): 1854–62.

Nolte'T Hoen, Esther N.M., Henk P.J. Buermans, Maaike Waasdorp, Willem Stoorvogel, Marca H.M. Wauben, and Peter A.C. 'T Hoen. 2012. "Deep Sequencing of RNA from Immune Cell-Derived Vesicles Uncovers the Selective Incorporation of Small Non-Coding RNA Biotypes with Potential Regulatory Functions." Nucleic Acids Research 40 (18): 9272–85.

Nordestgaard, Børge G., M. John Chapman, Kausik Ray, Jan Borén, Felicita Andreotti, Gerald F. Watts, Henry Ginsberg, et al. 2010. "Lipoprotein(a) as a Cardiovascular Risk Factor: Current Status." European Heart Journal 31 (23): 2844–53.

Observatório Nacional da Diabetes. 2016. Diabetes: Factos e Números - O Ano 2015. Relatório Anual Do Observatório Nacional Da Diabetes.

Odenwald, Matthew A., and Jerrold R. Turner. 2017. "The Intestinal Epithelial Barrier: A Therapeutic Target?" Nature Reviews Gastroenterology and Hepatology 14 (1): 9–21.

Oliphant, Kaitlyn, and Emma Allen-Vercoe. 2019. "Macronutrient Metabolism by the Human Gut

Microbiome: Major Fermentation by-Products and Their Impact on Host Health." Microbiome 7 (1): 1–15.

Ortega-Prieto, Paula, and Catherine Postic. 2019. "Carbohydrate Sensing through the Transcription Factor ChREBP." Frontiers in Genetics 10 (JUN): 1–9.

Palmisano, Giuseppe, Søren Skov Jensen, Marie Catherine Le Bihan, Jeanne Lainé, James N. McGuire, Flemming Pociot, and Martin Røssel Larsen. 2012. "Characterization of Membrane-Shed Microvesicles from Cytokine-Stimulated β-Cells Using Proteomics Strategies." Molecular and Cellular Proteomics 11 (8): 230–43.

Paneni, Francesco, Joshua A. Beckman, Mark A. Creager, and Francesco Cosentino. 2013. "Diabetes and Vascular Disease: Pathophysiology, Clinical Consequences, and Medical Therapy: Part I." European Heart Journal 34 (31): 2436–46.

Papackova, Zuzana, Eliska Palenickova, Helena Dankova, Jana Zdychova, Vojtech Skop, Ludmila Kazdova, and Monika Cahova. 2012. "Kupffer Cells Ameliorate Hepatic Insulin Resistance Induced by High-Fat Diet Rich in Monounsaturated Fatty Acids: The Evidence for the Involvement of Alternatively Activated Macrophages." Nutrition and Metabolism 9: 1–15.

Pareek, Manan, Philip R. Schauer, Lee M. Kaplan, Lawrence A. Leiter, Francesco Rubino, and Deepak L. Bhatt. 2018. "Metabolic Surgery: Weight Loss, Diabetes, and Beyond." Journal of the American College of Cardiology 71 (6): 670–87.

Parker, George A., and Catherine A. Picut. 2005. "Liver Immunobiology." Toxicologic Pathology 33 (1): 52–62.

Pearson-Stuttard, Jonathan, Bin Zhou, Vasilis Kontis, James Bentham, Marc J. Gunter, and Majid Ezzati. 2018. "Worldwide Burden of Cancer Attributable to Diabetes and High Body-Mass Index: A Comparative Risk Assessment." The Lancet Diabetes and Endocrinology 6 (6): e6–15.

Penhoat, Armelle, Laetitia Fayard, Anne Stefanutti, Gilles Mithieux, and Fabienne Rajas. 2014. "Intestinal Gluconeogenesis Is Crucial to Maintain a Physiological Fasting Glycemia in the Absence of Hepatic Glucose Production in Mice." Metabolism: Clinical and Experimental 63 (1): 104–11.

Perakis, Samantha, and Michael R. Speicher. 2017. "Emerging Concepts in Liquid Biopsies." BMC Medicine 15 (1): 1–12.

Perry, Rachel J., Varman T. Samuel, Kitt F. Petersen, and Gerald I. Shulman. 2014. "The Role of Hepatic Lipids in Hepatic Insulin Resistance and Type 2 Diabetes." Nature 510 (7503): 84–91.

Petersen, Max C., and Gerald I. Shulman. 2018. "Mechanisms of Insulin Action and Insulin Resistance." Physiological Reviews 98 (4): 2133–2223.

Phillips, Liza K., Adam M. Deane, Karen L. Jones, Chris K. Rayner, and Michael Horowitz. 2015. "Gastric Emptying and Glycaemia in Health and Diabetes Mellitus." Nature Reviews Endocrinology 11 (2): 112–28.

Phillips, Michael C. 2014. "Molecular Mechanisms of Cellular Cholesterol Efflux." Journal of Biological Chemistry 289 (35): 24020–29.

Qi, Lu, Marilyn C. Cornelis, Cuilin Zhang, Rob M. Van Dam, and Frank B. Hu. 2009. "Genetic Predisposition, Western Dietary Pattern, and the Risk of Type 2 Diabetes in Men." American Journal of Clinical

Nutrition 89 (5): 1453–58.

Raimondo, Francesca, Lavinia Morosi, Clizia Chinello, Fulvio Magni, and Marina Pitto. 2011. “Advances in Membranous Vesicle and Exosome Proteomics Improving Biological Understanding and Biomarker Discovery.” Proteomics 11 (4): 709–20.

Ramachandran, Prakash, Antonella Pellicoro, Madeleine A. Vernon, Luke Boulter, Rebecca L. Aucott, Aysha Ali, Stephen N. Hartland, et al. 2012. “Differential Ly-6C Expression Identifies the Recruited Macrophage Phenotype, Which Orchestrates the Regression of Murine Liver Fibrosis.” Proceedings of the National Academy of Sciences of the United States of America 109 (46).

Ramírez-Pérez, Oscar, Vania Cruz-Ramón, Paulina Chinchilla-López, and Nahum Méndez-Sánchez. 2017. “The Role of the Gut Microbiota in Bile Acid Metabolism.” Annals of Hepatology 16: S21–26.

Rana, Sanyukta, Shijing Yue, Daniela Stadel, and Margot Zöller. 2012. “Toward Tailored Exosomes: The Exosomal Tetraspanin Web Contributes to Target Cell Selection.” International Journal of Biochemistry and Cell Biology 44 (9): 1574–84.

Raposo, Graça, and Willem Stoorvogel. 2013. “Extracellular Vesicles: Exosomes, Microvesicles, and Friends.” Journal of Cell Biology 200 (4): 373–83.

Raposo, Graça, Hans W. Nijman, Willem Stoorvogel, Richtje Leijendekker, Clifford V. Harding, Cornelis J.M. Melief, and Hans J. Geuze. 1996. “B Lymphocytes Secrete Antigen-Presenting Vesicles.” Journal of Experimental Medicine 183 (3): 1161–72.

Record, Michel, Kevin Carayon, Marc Poirot, and Sandrine Silvente-Poirot. 2014. “Exosomes as New Vesicular Lipid Transporters Involved in Cell-Cell Communication and Various Pathophysiologies.” Biochimica et Biophysica Acta - Molecular and Cell Biology of Lipids 1841 (1): 108–20.

Record, Michel, Kevin Carayon, Marc Poirot, and Sandrine Silvente-Poirot. 2014. “Exosomes as New Vesicular Lipid Transporters Involved in Cell-Cell Communication and Various Pathophysiologies.” Biochimica et Biophysica Acta - Molecular and Cell Biology of Lipids 1841 (1): 108–20.

Remmerie, Anneleen, and Charlotte L. Scott. 2018. “Macrophages and Lipid Metabolism.” Cellular Immunology 330 (February): 27–42.

Reuter, Tanja Y. 2007. “Diet-Induced Models for Obesity and Type 2 Diabetes.” Drug Discovery Today: Disease Models 4 (1): 3–8.

Richard, Dawn M., Michael A. Dawes, Charles W. Mathias, Ashley Acheson, Nathalie Hill-Kapturczak, and Donald M. Dougherty. 2009. “L-Tryptophan: Basic Metabolic Functions, Behavioral Research and Therapeutic Indications.” International Journal of Tryptophan Research 2 (1): 45–60.

Rivellese, Angela A., Claudia Natale, And Stefania Lilli. 2006. “Type of Dietary Fat and Insulin Resistance.” Annals of the New York Academy of Sciences 967 (1): 329–35.

Rodrigues, Reena. 2016. “A Comprehensive Review: The Use of Animal Models in Diabetes Research.” Journal of Analytical & Pharmaceutical Research 3 (6).

Rousseau, Adrien, and Anne Bertolotti. 2018. “Regulation of Proteasome Assembly and Activity in Health and Disease.” Nature Reviews Molecular Cell Biology 19 (11): 697–712.

Roy, Claude C., C. Lawrence Kien, Lise Bouthillier, and Emile Levy. 2006. “Short-Chain Fatty Acids: Ready for Prime Time?” Nutrition in Clinical Practice 21 (4): 351–66.

Rubino, Francesco. 2008. “Is Type 2 Diabetes an Operable Intestinal Disease? A Provocative yet Reasonable Hypothesis.” Diabetes Care 31 Suppl 2.

Saad, M. J.A., A. Santos, and P. O. Prada. 2016. “Linking Gut Microbiota and Inflammation to Obesity and Insulin Resistance.” Physiology 31 (4): 283–93.

Sadri, Parissa, Maria A. G. Reid, Ricardo A. Afonso, Joshua Schafer, Dallas J. Legare, M. Paula Macedo, and W. Wayne Lautt. 2006. “Meal-Induced Insulin Sensitization in Conscious and Anaesthetized Rat Models Comparing Liquid Mixed Meal with Glucose and Sucrose.” British Journal of Nutrition 95 (2): 288–95.

Sanders, Francis W.B., and Julian L. Griffin. 2016. “De Novo Lipogenesis in the Liver in Health and Disease: More than Just a Shunting Yard for Glucose.” Biological Reviews 91 (2): 452–68.

Sarmento, Bruno (2015). Concepts and Models for Drug Permeability Studies: Cell and Tissue based In Vitro Culture Models. Woodhead Publishing. pp. 57–58.

Saxena, Richa, Benjamin F. Voight, Valeriya Lyssenko, Noël P. Burtt, Paul I.W. De Bakker, Hong Chen, Jeffrey J. Roix, et al. 2007. “Genome-Wide Association Analysis Identifies Loci for Type 2 Diabetes and Triglyceride Levels.” Science 316 (5829): 1331–36.

Schroeder, Bjoern O., and Fredrik Bäckhed. 2016. “Signals from the Gut Microbiota to Distant Organs in Physiology and Disease.” Nature Medicine 22 (10): 1079–89.

Scott, Charlotte L., Fang Zheng, Patrick De Baetselier, Liesbet Martens, Yvan Saeys, Sofie De Prijck, Saskia Lippens, et al. 2016. “Bone Marrow-Derived Monocytes Give Rise to Self-Renewing and Fully Differentiated Kupffer Cells.” Nature Communications 7: 1–10.

Senoo, Haruki. 2017. “The Stellate Cell System (Vitamin A-Storing Cell System).” Anatomical Science International 92 (4): 387–455.

Seo, Wonhyo, and Won Il Jeong. 2016. “Hepatic Non-Parenchymal Cells: Master Regulators of Alcoholic Liver Disease?” World Journal of Gastroenterology 22 (4): 1348–56.

Shao, Huilin, Jaehoon Chung, Kyungheon Lee, Leonora Balaj, Changwook Min, Bob S. Carter, Fred H. Hochberg, Xandra O. Breakefield, Hakho Lee, and Ralph Weissleder. 2015. “Chip-Based Analysis of Exosomal MRNA Mediating Drug Resistance in Glioblastoma.” Nature Communications 6 (May): 1–9.

Silva, João C P, Cátia Marques, Fátima O Martins, Ivan Viegas, Ludgero Tavares, Maria Paula, and John G Jones. 2019. “Determining Contributions of Exogenous Glucose and Fructose to de Novo Fatty Acid and Glycerol Synthesis in Liver and Adipose Tissue.” Metabolic Engineering 56 (August): 69–76.

Singh, Awadhesh Kumar, Ritu Singh, and Sunil Kumar Kota. 2015. “Bariatric Surgery and Diabetes Remission: Who Would Have Thought It?” Indian Journal of Endocrinology and Metabolism 19 (5): 563–76.

Singh, Surendra, Ying Chen, Akiko Matsumoto, David J. Orlicky, Hongbin Dong, David C. Thompson, and Vasilis Vasiliou. 2015. “ALDH1B1 Links Alcohol Consumption and Diabetes.” Biochemical and

Biophysical Research Communications 463 (4): 768–73.

Sirwi, Alaa, and M. Mahmood Hussain. 2018. “Lipid Transfer Proteins in the Assembly of ApoB-Containing Lipoproteins.” Journal of Lipid Research 59 (7): 1094–1102.

Skotland, Tore, Nina P. Hessvik, Kirsten Sandvig, and Alicia Llorente. 2019. “Exosomal Lipid Composition and the Role of Ether Lipids and Phosphoinositides in Exosome Biology.” Journal of Lipid Research 60 (1): 9–18.

Smythies, Lesley E., and John R. Smythies. 2014. “Exosomes in the Gut.” Frontiers in Immunology 5 (MAR): 2–5.

Squadrito, Mario Leonardo, Caroline Baer, Frédéric Burdet, Claudio Maderna, Gregor D. Gilfillan, Robert Lyle, Mark Ibberson, and Michele De Palma. 2014. “Endogenous RNAs Modulate MicroRNA Sorting to Exosomes and Transfer to Acceptor Cells.” Cell Reports 8 (5): 1432–46.

Steensels, Sandra, Jixuan Qiao, Yanzhen Zhang, Kristal M. Maner-Smith, Nourhan Kika, Corey D. Holman, Kathleen E. Corey, W. Clay Bracken, Eric A. Ortlund, and Baran A. Ersoy. 2020. “ Acot9 Traffics Mitochondrial Short-chain Fatty Acids towards de Novo Lipogenesis and Glucose Production in the Liver .” Hepatology, 0–3.

Steinke, Julia M. 2009. “The Natural Progression of Kidney Injury in Young Type 1 Diabetic Patients.” Current Diabetes Reports 9 (6): 473–79.

Stephens, Richard W., Lidia Arhire, and Mihai Covasa. 2018. “Gut Microbiota: From Microorganisms to Metabolic Organ Influencing Obesity.” Obesity 26 (5): 801–9.

Stilling, Roman M., Marcel van de Wouw, Gerard Clarke, Catherine Stanton, Timothy G. Dinan, and John F. Cryan. 2016. “The Neuropharmacology of Butyrate: The Bread and Butter of the Microbiota-Gut-Brain Axis?” Neurochemistry International 99: 110–32.

Stoll, Barbara, Joseph Henry, Peter J. Reeds, Hung Yu, Farook Jahoor, and Douglas G. Burrin. 1998. “Catabolism Dominates the First-Pass Intestinal Metabolism of Dietary Essential Amino Acids in Milk Protein-Fed Piglets.” The Journal of Nutrition 128 (3): 606–14.

Tabák, Adam G., Christian Herder, Wolfgang Rathmann, Eric J. Brunner, and Mika Kivimäki. 2012. “Prediabetes: A High-Risk State for Diabetes Development.” The Lancet 379 (9833): 2279–90.

Tabas, Ira, and Karin E. Bornfeldt. 2016. “Macrophage Phenotype and Function in Different Stages of Atherosclerosis.” Circulation Research 118 (4): 653–67.

Takahashi, Yuki, Makiya Nishikawa, Haruka Shinotsuka, Yuriko Matsui, Saori Ohara, Takafumi Imai, and Yoshinobu Takakura. 2013. “Visualization and in Vivo Tracking of the Exosomes of Murine Melanoma B16-BL6 Cells in Mice after Intravenous Injection.” Journal of Biotechnology 165 (2): 77–84.

Tarnopolsky, Mark A. 2018. “Myopathies Related to Glycogen Metabolism Disorders.” Neurotherapeutics 15 (4): 915–27.

Théry, Clotilde, Kenneth W. Witwer, Elena Aikawa, Maria Jose Alcaraz, Johnathon D. Anderson, Ramaroson Andriantsitohaina, Anna Antoniou, et al. 2018. “Minimal Information for Studies of Extracellular Vesicles 2018 (MISEV2018): A Position Statement of the International Society for Extracellular Vesicles and Update of the MISEV2014 Guidelines.” Journal of Extracellular Vesicles 7 (1).

Théry, Clotilde, Laurence Zitvogel, and Sebastian Amigorena. 2002. “Exosomes: Composition, Biogenesis and Function.” Nature Reviews. Immunology 2 (8): 569–79.

Thomas, Charles, Roberto Pellicciari, Mark Pruzanski, Johan Auwerx, and Kristina Schoonjans. 2008. “Targeting Bile-Acid Signalling for Metabolic Diseases.” Nature Reviews Drug Discovery 7 (8): 678–93.

Tsilidis, Konstantinos K., John C. Kasimis, David S. Lopez, Evangelia E. Ntzani, and John P.A. Ioannidis. 2015. “Type 2 Diabetes and Cancer: Umbrella Review of Meta-Analyses of Observationlal Studies.” BMJ (Online) 350 (January): 1–11.

Ussar, Siegfried, Max Felix Haering, Shiho Fujisaka, Dominik Lutter, Kevin Y. Lee, Ning Li, Georg K. Gerber, Lynn Bry, and C. Ronald Kahn. 2017. “Regulation of Glucose Uptake and Enteroendocrine Function by the Intestinal Epithelial Insulin Receptor.” Diabetes 66 (4): 886–96.

Vandermoere, Franck, Ikram El Yazidi-Belkoura, Christian Slomianny, Yohann Demont, Gabriel Bidaux, Eric Adriaenssens, Jérôme Lemoine, and Hubert Hondermarck. 2006. “The Valosin-Containing Protein (VCP) Is a Target of Akt Signaling Required for Cell Survival.” Journal of Biological Chemistry 281 (20): 14307–13.

Vileigas, Danielle F., Victoria M. Harman, Paula P. Freire, Cecília L.C. Marciano, Paula G. Sant’Ana, Sérgio L.B. de Souza, Gustavo A.F. Mota, et al. 2019. “Landscape of Heart Proteome Changes in a Diet-Induced Obesity Model.” Scientific Reports 9 (1): 18050.

Vily-Petit, Justine, Maud Soty-Roca, Marine Silva, Margaux Raffin, Amandine Gautier-Stein, Fabienne Rajas, and Gilles Mithieux. 2020. “Intestinal Gluconeogenesis Prevents Obesity-Linked Liver Steatosis and Non-Alcoholic Fatty Liver Disease.” Gut, gutjnl-2019-319745.

Volpe, Caroline Maria Oliveira, Pedro Henrique Villar-Delfino, Paula Martins Ferreira Dos Anjos, and José Augusto Nogueira-Machado. 2018. “Cellular Death, Reactive Oxygen Species (ROS) and Diabetic Complications Review-Article.” Cell Death and Disease 9 (2).

Wang, Fang, Jingyi Wu, Zhichao Qiu, Xiaosong Ge, Xingxiang Liu, Chun Zhang, Wenhuan Xu, et al. 2018. “ACOT1 Expression Is Associated with Poor Prognosis in Gastric Adenocarcinoma.” Human Pathology 77: 35–44.

Wang, Ji, Yunxia Liu, Kun Lian, Xinyi Shentu, Junwei Fang, Jing Shao, Mengping Chen, Yibin Wang, Meiyi Zhou, and Haipeng Sun. 2019. “BCAA Catabolic Defect Alters Glucose Metabolism in Lean Mice.” Frontiers in Physiology 10 (September): 1–14.

Wenfeng, Zhang, Wu Yakun, Mu Di, Gong Jianping, Wu Chuanxin, and Huang Chun. 2014. “Kupffer Cells: Increasingly Significant Role in Nonalcoholic Fatty Liver Disease.” Annals of Hepatology 13 (5): 489–95.

World Health Organization. 2015. “Tool for the Assessment of Diabetic Retinopathy and Diabetes Management Systems,” 34.

Wu, Di, Junhong Yan, Xia Shen, Yu Sun, Måns Thulin, Yanling Cai, Lotta Wik, et al. 2019. “Profiling Surface Proteins on Individual Exosomes Using a Proximity Barcoding Assay.” Nature Communications 10 (1): 1–10.

Wu, Hao, Eduardo Esteve, Valentina Tremaroli, Muhammad Tanweer Khan, Robert Caesar, Louise

Mannerås-Holm, Marcus Ståhlman, et al. 2017. “Metformin Alters the Gut Microbiome of Individuals with Treatment-Naive Type 2 Diabetes, Contributing to the Therapeutic Effects of the Drug.” Nature Medicine 23 (7): 850–58.

Xia, Ming Feng, Hua Bian, and Xin Gao. 2019. “NAFLD and Diabetes: Two Sides of the Same Coin? Rationale for Gene-Based Personalized NAFLD Treatment.” Frontiers in Pharmacology 10 (JULY): 1–11.

Xu, Gang, Zhangchuan Xia, Feiyan Deng, Lin Liu, Qiming Wang, Yi Yu, Fubing Wang, et al. 2019. “Inducible LGALS3BP/90K Activates Antiviral Innate Immune Responses by Targeting TRAF6 and TRAF3 Complex.” PLoS Pathogens 15 (8): 1–22.

Yamaguchi, Kanji, Liu Yang, Shannon McCall, Jiawen Huang, Xian Yu Xing, Sanjay K. Pandey, Sanjay Bhanot, Brett P. Monia, Yin Xiong Li, and Anna Mae Diehl. 2007. “Inhibiting Triglyceride Synthesis Improves Hepatic Steatosis but Exacerbates Liver Damage and Fibrosis in Obese Mice with Nonalcoholic Steatohepatitis.” Hepatology 45 (6): 1366–74.

Yáñez-Mó, María, Pia R-M Siljander, Zoraida Andreu, Apolonija Bedina Zavec, Francesc E Borràs, Edit I Buzas, Krisztina Buzas, et al. 2015. “Biological Properties of Extracellular Vesicles and Their Physiological Functions.” Journal of Extracellular Vesicles 4: 27066.

Yang, Cheng Kun, Xiang Kun Wang, Xi Wen Liao, Chuang Ye Han, Ting Dong Yu, Wei Qin, Guang Zhi Zhu, et al. 2017. “Aldehyde Dehydrogenase 1 (ALDH1) Isoform Expression and Potential Clinical Implications in Hepatocellular Carcinoma.” PLoS ONE 12 (8): 1–13.

Yang, Zhongyue, and Shengfa F. Liao. 2019. “Physiological Effects of Dietary Amino Acids on Gut Health and Functions of Swine.” Frontiers in Veterinary Science 6 (JUN): 1–13.

Ye, Richard D., and François Boulay. 1997. “Structure and Function of Leukocyte Chemoattractant Receptors.” Advances in Pharmacology 39 (C): 221–89.

Zeggini, Eleftheria, Michael N Weedon, Cecilia M Lindgren, M Timothy, Katherine S Elliott, Hana Lango, Nicholas J Timpson, et al. 2007. “Multiple Type 2 Diabetes Susceptibility Genes Following Genome- Wide Association Scan in UK Samples.” Science 316 (5829): 1336–41.

Zhang, Husen, John K. DiBaise, Andrea Zuccolo, Dave Kudrna, Michele Braidotti, Yeisoo Yu, Prathap Parameswaran, et al. 2009. “Human Gut Microbiota in Obesity and after Gastric Bypass.” Proceedings of the National Academy of Sciences of the United States of America 106 (7): 2365–70.

Zhang, Jian, Sha Li, Lu Li, Meng Li, Chongye Guo, Jun Yao, and Shuangli Mi. 2015. “Exosome and Exosomal MicroRNA: Trafficking, Sorting, and Function.” Genomics, Proteomics and Bioinformatics 13 (1).

Zhang, Mei, and Xiao Jiao Yang. 2016. “Effects of a High Fat Diet on Intestinal Microbiota and Gastrointestinal Diseases.” World Journal of Gastroenterology 22 (40): 8905–9.

Zhang, Yuan, Yunfeng Liu, Haiying Liu, and Wai Ho Tang. 2019. “Exosomes: Biogenesis, Biologic Function and Clinical Potential.” Cell and Bioscience 9 (1): 1–18.

Chapter VII

Supplementary Data

Supplementary Data

1. Odyssey images of gut-derived EV biodistribution for all tissues separately

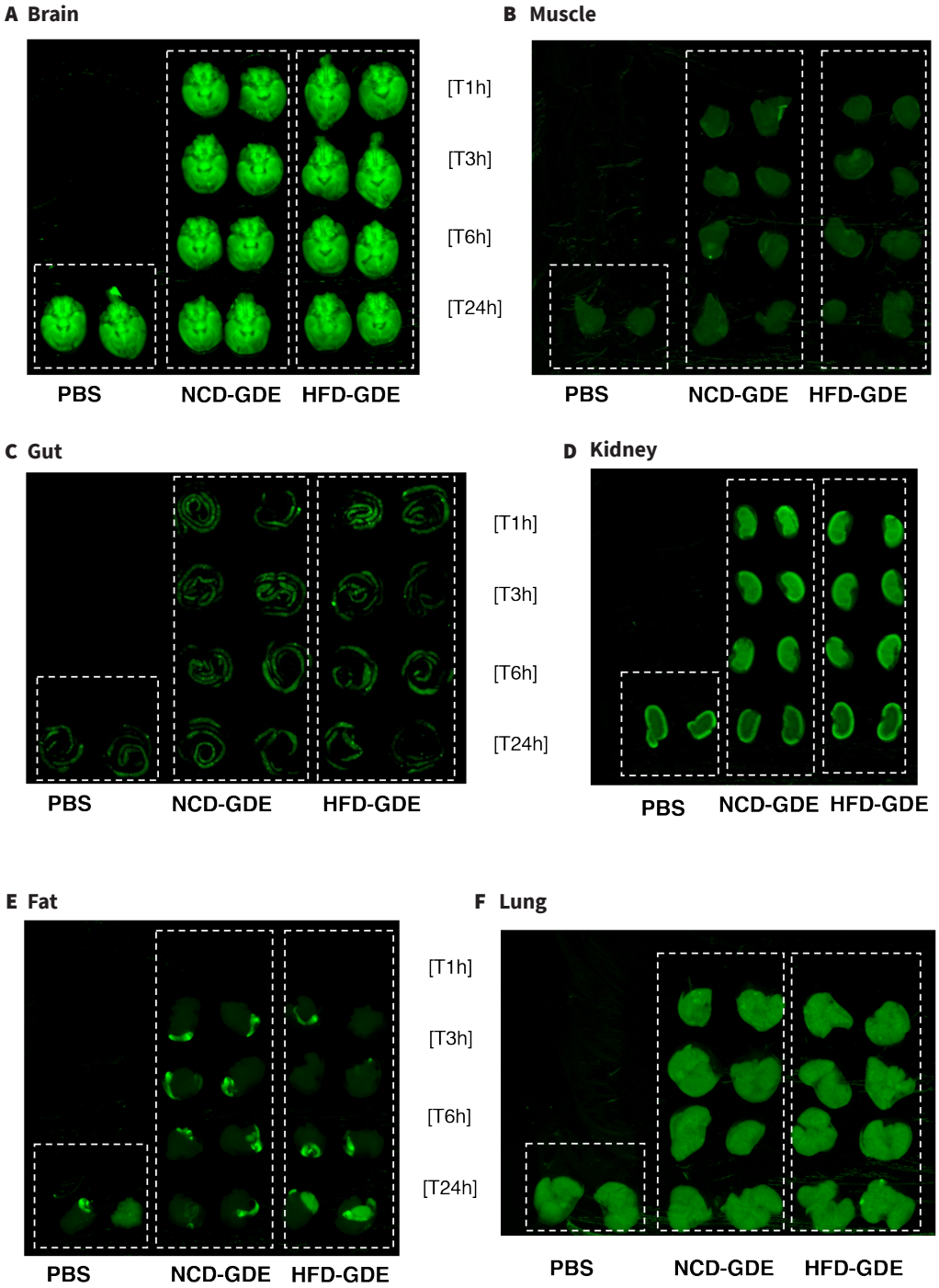

Supplementary Fig.1.Gut-derived EV tracking after retro-orbital injection in healthy mice. Intensity of near infra-red signal detection of several tissues from mice with PBS (PBS), injected with gut-derived EV (GDE) from NCD-fed mice (NCD-GDE) and mice injected with GDE from HFD-fed mice (HFD-GDE), in different time-points after injection (1, 3, 6 and 24 hours). **A.** Infra-red signal detection of brain. **B.** Infra-red signal detection of muscle. **C.** Infra-red signal detection of gut. **D.** Infra-red signal detection of kidney. **E.** Infra-red signal detection of fat /white adipose tissue. **F.** Infra-red signal detection of lung. Images obtained from Odyssey Image System (LI-COR).

2. Education 1

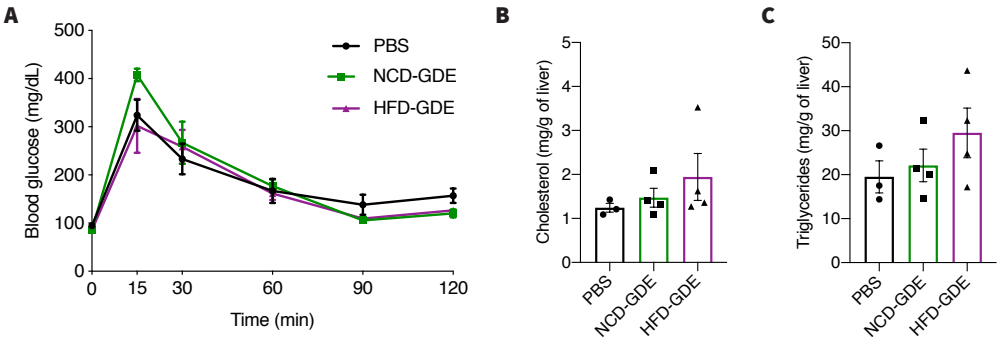

Supplementary Fig.2. Education 1: Mice were injected with 5 µg of gut-derived EV from NCD-fed mice (NCD-GDE) and 3 µg of gut-derived EV from HFD-fed mice (HFD-GDE) for three weeks. A. Glucose tolerance test of mice at different time points (0, 15, 30, 60, 90, 120 minutes); **B.** Analysis of cholesterol levels in the liver of injected mice. **C.** Analysis of triglyceride (TG) levels in the liver of injected mice. Cholesterol and TG are represented in mg per gram of liver tissue. Results are expressed as mean ± SEM; n=3 for PBS, n=4 for NCD-GDE and HFD-GDE. ANOVA multiple comparisons.

3. Plasma EV protein amount in healthy and prediabetic mice

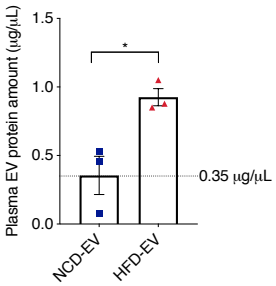

Supplementary Fig.3. EV quantification in plasma of mice fed with NCD and HFD. Quantification of amount of protein in plasma EVs, in mg per mL of sample, by Nanosight (NTA). Dotted line highlighting the protein concentration in the plasma of a WT mice, in normal conditions. Results are expressed as mean ± SEM; Each n is a pool of 20, n=3 for NCD and HFD. Unpaired t test with Welch's correction. *p<0.05

4. Liver histology: diet mice versus educated mice fed with NCD

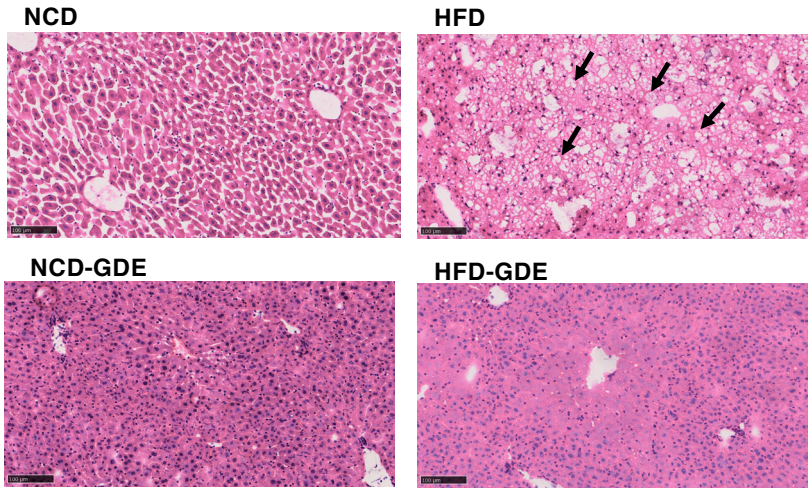

Supplementary Fig.4. Liver hematoxylin-eosin staining of NCD-fed and HFD-fed mice (top) and NCD-GDE and HFD-GDE injected mice (bottom). Liver of HFD mice reveals steatosis, evidenced by the dominance of the lipid droplets (black arrows) compared with the NCD mice liver (top). Mice were retro-orbitally injected, every other day, with 20 µg of gut-derived EV from NCD-fed mice (NCD-GDE), 20 µg of gut-derived EV from HFD-fed mice (HFD-GDE) and PBS for six weeks and fed with NCD (bottom). There is no steatosis observed in the livers of injected mice after six weeks of education.

5. Flow cytometry analysis of bone marrow of educated mice fed with HFD

Considering our preliminary studies on bone marrow cells and gut-derived EV potential interaction, and despite the low frequencies of GDE detected in the tissue, there are some aspects to mention. We observed that lymphocytes were increased in HFD-GDE mice (Supplementary Fig.5B), in opposite to monocytes and granulocytes that did not show any alteration in their population (Supplementary Fig.5D; F), what might indicate an initial phase of an adaptive inflammatory response, since lymphocytes are the first ones to be activated (Burger and Dayer 2002). In terms of EV in this tissue, we could see some traces of EV in the lymphocytes and monocytes but not in the granulocytes, what is in accordance with literature, since there is no record, so far, of granulocytes act as recipient of EV from other cell types, while lymphocytes and macrophages are demonstrated to react to EVs (Chan et al. 2019) (Supplementary Fig.5C; E; G).

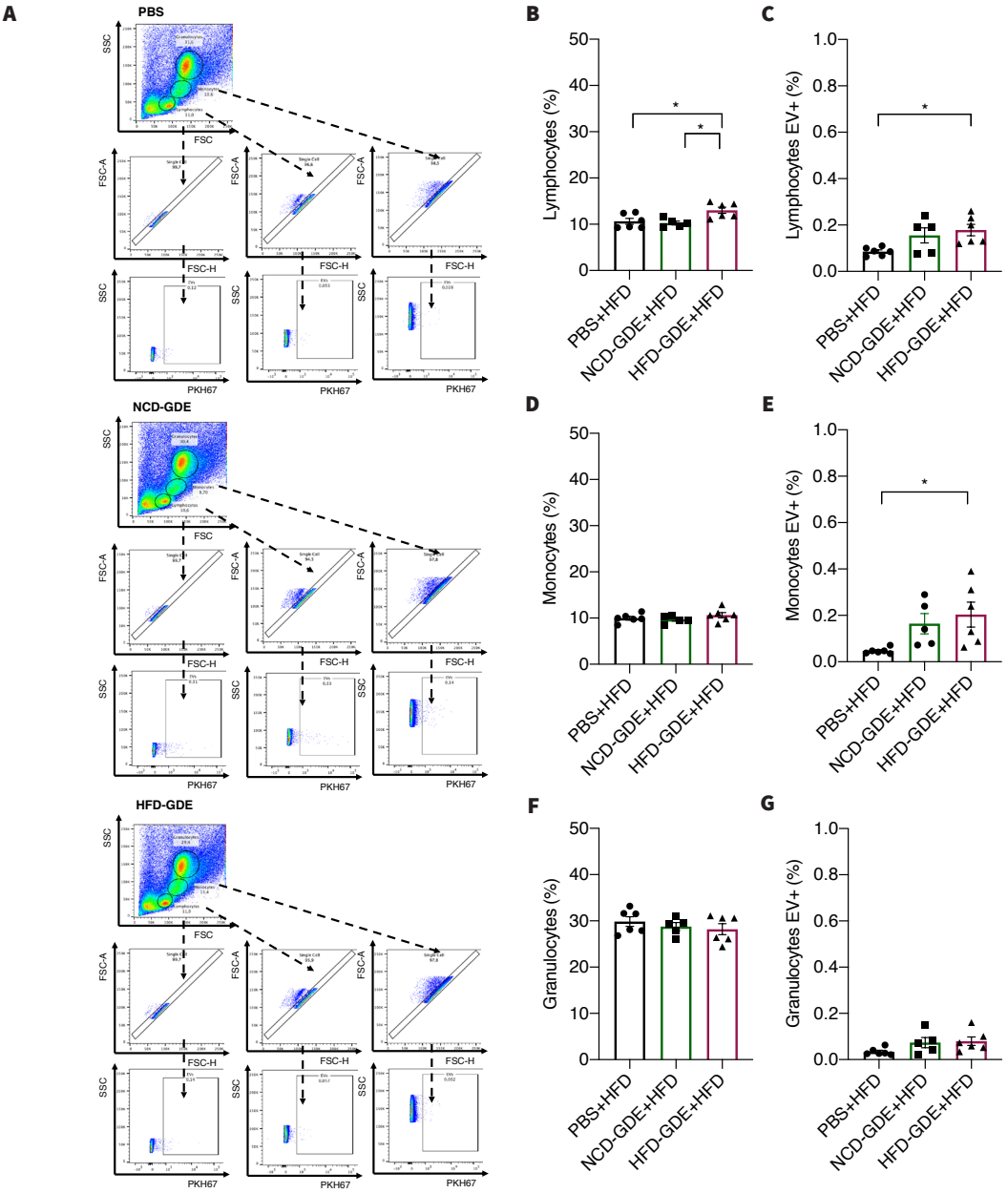

Supplementary Fig.5. Bone marrow analysis of educated mice fed with HFD. Bone marrow, collected from femur of mice fed with HFD and injected with PBS, 20 µg of GDE from NCD-fed mice (NCD-GDE) and 20 µg of GDE from HFD-fed mice (HFD-GDE) every other day, for six weeks, was analyzed by flow. **A.** Flow cytometry plot with gating strategy for EV tracking in the bone marrow. **B.** Analysis of the percentage of lymphocytes. **C.** Analysis of the percentage of EVs among lymphocytes. **D.** Analysis of the percentage of monocytes. **E.** Analysis of the percentage of EV among monocytes. F. Analysis of the percentage of granulocytes. G. Analysis of the percentage of EV among granulocytes. Results are expressed as mean ± SEM; n=6 for PBS and HFD-GDE and n=5 for NCD-GDE. ANOVA multiple comparisons, *p<0.05.

Chapter VIII

Appendix Document

Proteomic raw data with all the proteins identified in gut-derived EV. In red is highlighted the up-regulated proteins; in blue the down-regulated proteins and in purple the missing values; when two colors are present is because one protein was identified as up or down-regulated but it had an acquisition of zero, therefore it was excluded. Description by columns: Pro - protein headers; Sample names - 18 columns with quantitative values named with sample names (9 columns of NCD sample replicas, 9 columns of HFD sample replicas); mean_C - mean expression for controls (NCD-GDE); mean_T - mean expression for treated (HFD-GDE); GN – gene name; logFC – log2fold change; AveExp – average expression; t – t value; P.Value – Pvalue; adj.P.Val – adjusted P value using BH; B – B-value.

pro	G..data	G..data	G..data	G..data	G..data	G..data	G..dat	G..dat	G..da	G..data	G..dat	G..dat	G..data	G..data	G..dat	G..dat	G..data	G..data	mean_C	mean_T	GN	logFC	AveExp	t	P.Value	adj.P.Val	B
>sp|Q06185|ATP5I_	0	0	0	0	0	0	0	0	0	19,5	20	19	19,9	19,8	19	19	19,4	17,4	0.00000	19,2605	Atp5i	19,3	9,63	76,77	2E-22	7E-19	36
>sp|Q8BTM8|FLNA_	23,86	23,9	23,9	23,8	23,9	23,8	24	24	24	22,3	22	22	22,3	22,2	22	22	22	22,1	23,872	22,1496	Flna	-1,7	23	-33,3	2E-16	3E-13	27
>sp|O08709|PRDX6_	22,71	22,6	22,1	22,1	23	22,5	23	23	23	25,5	25	26	26	25,7	26	25	25,3	25,7	22,652	25,6068	Prdx6	2,95	24,1	19,76	8E-13	8E-10	20
>sp|P28063|PSB8_M	25,1	24,8	25,2	24,8	24,9	24,9	25	25	25	23,3	23	23	23,4	22,8	23	23	23,3	22,8	25,016	23,0073	Psmb8	-2	24	-17,9	4E-12	3E-09	18
>sp|Q9Z2U1|PSA5_M	28,33	28,1	28,2	27,1	28,1	27,7	28	28	28	25,4	25	25	25,1	25,5	25	25	25,1	25,4	28,01	25,2089	Psma5	-2,8	26,6	-17,1	7E-12	4E-09	18
>sp|Q8BWT1|THIM_M	22,94	23,2	23,1	23,4	23,8	23,5	23	24	24	25,4	25	26	25,2	25	25	25	25,5	25,1	23,415	25,3358	Acaa2	1,92	24,4	16,99	8E-12	4E-09	17
>sp|Q9DCG6|PBLD1_	19,27	19,7	19,1	19,5	19,3	19,2	19	20	19	21,6	22	21	21,6	21,6	22	21	21,1	21,7	19,336	21,523	Pbld1	2,19	20,4	15,18	5E-11	2E-08	16
>sp|Q6Q2Z6|ACOT5_I	16,25	16,2	16,2	17,2	16,2	16,9	17	17	17	18,8	18	19	19,1	18,8	19	18	18,6	18,9	16,582	18,7521	Acot5	2,17	17,7	15,15	5E-11	2E-08	16
>sp|Q9QYR7|ACOT3_I	16,25	16,2	16,2	17,2	16,2	16,9	17	17	17	18,8	18	19	19,1	18,8	19	18	18,6	18,9	16,582	18,7521	Acot3	2,17	17,7	15,15	5E-11	2E-08	16
>sp|P63268|ACTH_M	28,76	28,8	28,8	28,8	28,8	28,8	29	29	29	26,9	27	28	26,8	26,8	27	28	27,3	27	28,801	27,1108	Actg2	-1,7	28	-14,8	6E-11	2E-08	15
>sp|O70435|PSA3_M	27,65	27,6	27,7	27,6	27,7	27,7	28	28	27	25,2	25	26	24,8	25,6	26	25	25,4	25,7	27,692	25,4363	Psma3	-2,3	26,6	-14,8	7E-11	2E-08	15
>sp|Q01853|TERA_M	25,05	25,3	25,3	25,6	25,8	25,9	25	26	26	23,9	24	24	24,1	23,8	24	24	23,8	23,8	25,489	23,8189	Vcp	-1,7	24,7	-14,4	1E-10	3E-08	15
>sp|Q60605|MYL6_M	23,54	23,9	24,3	24,2	24,3	23,6	25	24	24	21,9	22	22	22,1	22,5	22	22	21,8	22,3	23,993	22,0779	Myl6	-1,9	23	-13,8	2E-10	4E-08	14
>sp|P62737|ACTA_M	28,76	28,7	28,8	28,8	28,8	28,8	29	29	29	26,8	27	28	26,7	26,8	27	28	27,1	26,9	28,75	27,0282	Acta2	-1,7	27,9	-13,8	2E-10	4E-08	14
>sp|P58404|STRN4_I	14,62	15,7	16,6	18,7	16,4	16	15	18	15	21,8	22	22	22,6	22,6	23	22	22,1	22	16,288	22,2578	Strn4	5,97	19,3	13,75	2E-10	4E-08	14
>sp|P97315|CSRP1_	23,46	23,9	23,8	23,9	24,3	23,8	24	24	24	22,2	22	22	21,1	21,8	22	21	21,6	21,6	23,931	21,736	Csrp1	-2,2	22,8	-13,5	3E-10	5E-08	14
>sp|P07758|A1AT1_	21,84	22,4	22,1	22	22,3	22	22	22	23	23,8	24	24	24,2	23,8	24	24	24	23,3	22,164	23,8969	Serpina1a	1,73	23	13,45	3E-10	5E-08	14
>sp|Q00896|A1AT3_	21,95	22,5	22,2	22,1	22,3	22	22	22	23	23,9	24	24	24,3	23,8	24	24	24	23,4	22,254	23,986	Serpina1c	1,73	23,1	13,15	4E-10	7E-08	14
>sp|P10648|GSTA2_I	22,59	22,6	22,9	23,1	22,6	22,5	23	23	22	24	24	24	24,2	24,4	24	24	24,4	23,6	22,657	24,1651	Gsta2	1,51	23,4	13,01	5E-10	7E-08	13
>sp|Q99LC5|ETFA_MC	23,3	23,5	22,7	23,7	22,7	23,1	23	23	24	25,3	25	25	25	24,9	25	25	25,6	24,9	23,188	25,1571	Etfa	1,97	24,2	13,01	5E-10	7E-08	13
>sp|P68033|ACTC_M	28,66	28,6	28,8	28,6	28,7	28,7	29	29	29	26,8	27	28	26,7	26,7	27	28	27,2	26,8	28,693	27,017	Actc1	-1,7	27,9	-13	5E-10	7E-08	13
>sp|P60710|ACTB_M	28,6	28,6	28,6	28,6	28,6	28,8	29	29	29	26,7	27	28	26,6	26,7	27	28	26,8	26,7	28,625	26,9102	Actb	-1,7	27,8	-12,8	6E-10	9E-08	13
>sp|P13745|GSTA1_I	23,18	23,3	23	23,3	22,7	23,2	23	23	23	24,6	24	24	24,7	25,1	25	25	24,8	24,3	23,087	24,6294	Gsta1	1,54	23,9	12,78	6E-10	9E-08	13
>sp|O55137|ACOT1_	19,03	18,9	20	19	18,9	19,3	19	19	20	21,6	21	22	21,7	21,7	22	21	21,9	21,8	19,35	21,7063	Acot1	2,36	20,5	12,58	8E-10	1E-07	13
>sp|Q9R1P4|PSA1_M	28,15	27,5	27,6	28,2	27,7	26,2	28	28	27	24,7	25	25	25,2	25,4	25	25	25	25	27,588	25,0342	Psma1	-2,6	26,3	-12,6	8E-10	1E-07	13
>sp|Q9CZS1|AL1B1_M	22,14	22,8	22,2	22,8	22,8	22,4	22	22	23	24,2	24	24	24,6	24,1	24	24	24,4	24	22,482	24,2166	Aldh1b1	1,73	23,3	12,5	9E-10	1E-07	13
>sp|P42669|PURA_M	18,03	18,1	18	17,7	17,6	18,2	18	18	17	20,4	20	20	19,9	20,5	20	20	20	18,9	17,806	20,025	Pura	2,22	18,9	12,47	9E-10	1E-07	13
>sp|P63260|ACTG_M	28,58	28,5	28,6	28,6	28,6	28,6	29	29	29	26,7	27	28	26,5	26,7	27	28	26,8	26,6	28,593	26,8766	Actg1	-1,7	27,7	-12,4	9E-10	1E-07	13
>sp|Q8BZF8|PGM5_M	23,17	23,1	23,2	23	23,1	23	23	23	23	22,1	22	22	22,6	22,3	22	22	22,3	22,1	23,165	22,2585	Pgm5	-0,9	22,7	-12,1	1E-09	2E-07	12
>sp|Q8CGP0|H2B3B_	26,99	26,5	26,8	25,9	26,1	27,1	27	26	27	28,4	28	28	28,2	28,2	28	28	28,1	28,1	26,575	28,2228	Hist3h2b	1,65	27,4	12	2E-09	2E-07	12
>sp|Q9D2U9|H2B3A_	26,99	26,5	26,8	25,9	26,1	27,1	27	26	27	28,4	28	28	28,2	28,2	28	28	28,1	28,1	26,575	28,2228	Hist3h2b	1,65	27,4	12	2E-09	2E-07	12
>sp|Q9QUM9|PSA6_M	26,73	27,5	27,6	27,5	26,6	27,7	28	28	28	25	25	25	25	25,2	24	25	25,1	25,3	27,515	25,0362	Psma6	-2,5	26,3	-11,9	2E-09	2E-07	12
>sp|P68134|ACTS_M	28,62	28,5	28,6	28,5	28,5	28,6	29	29	29	26,5	27	28	26,7	26,6	27	28	26,9	26,8	28,582	26,9087	Acta1	-1,7	27,7	-11,9	2E-09	2E-07	12
>sp|Q9CQF3|CPSF5_M	18,69	18,6	19,3	18,9	18,2	18,9	19	19	18	21,1	20	21	20,7	20,5	21	21	20,4	20,8	18,755	20,6963	Nudt21	1,94	19,7	11,65	2E-09	2E-07	12
>sp|Q7TPZ8|CBPA1_I	21,33	21,4	21,6	21,7	21,4	21,1	21	22	22	23,4	23	23	23,8	23,4	24	22	23	22,8	21,485	23,2433	Cpa1	1,76	22,4	11,6	3E-09	2E-07	12
>sp|O35955|PSB10_	23,83	24,6	25,2	24,6	24,7	24,5	24	25	25	22,8	23	23	23,1	23,1	23	23	22,3	22,6	24,625	22,7693	Psmb10	-1,9	23,7	-11,5	3E-09	3E-07	12
>sp|P36368|EGFB2_I	21,5	21,3	21,1	21,4	21,3	20,8	22	22	22	19,4	20	20	19,3	19,7	20	20	19,7	19,7	21,371	19,7418	Egfbp2	-1,6	20,6	-11,4	3E-09	3E-07	11
>sp|Q9R1P1|PSB3_M	27,66	27,6	27,3	26,2	27,7	26,5	27	28	28	24,9	25	25	24,7	25,2	24	25	24,6	24,4	27,272	24,6933	Psmb3	-2,6	26	-11,4	3E-09	3E-07	11
>sp|Q04857|CO6A1_	21,19	21,4	21,1	21,5	21,4	20,7	22	22	22	20,1	20	20	20,2	19,9	20	20	20,2	20,2	21,337	20,0566	Col6a1	-1,3	20,7	-11,2	4E-09	3E-07	11
>sp|P47738|ALDH2_	22,88	23	22,4	23,2	22,8	22,9	23	23	23	23,9	24	24	24,2	24,2	24	24	24	23,9	22,858	23,9612	Aldh2	1,1	23,4	11,23	4E-09	3E-07	11
>sp|Q9Z2U0|PSA7_M	27,63	26,7	27,4	27,2	28,2	27,6	27	28	28	25,5	24	25	24,8	25,5	25	25	24,8	24,5	27,66	25,02	Psma7	-2,6	26,3	-11,2	4E-09	4E-07	11
>sp|Q32Q92|ACOT6_	16,16	17,2	16,8	17	16,8	17,5	16	18	18	19,6	20	20	19,4	19,5	19	19	19,9	19,7	17,092	19,5882	Acot6	2,5	18,3	11,13	5E-09	4E-07	11
>sp|P62242|RS8_MC	15,28	15,6	15,7	16,5	15,5	16,5	16	16	16	19	19	20	18,1	18,5	18	19	19,3	18,2	15,879	18,689	Rps8	2,81	17,3	11,11	5E-09	4E-07	11
>sp|O09061|PSB1_M	27,92	27,7	27,4	26,4	27,1	26,4	27	28	26	24,8	25	25	25,1	24,8	25	25	24,6	24,6	27,054	24,7028	Psmb1	-2,4	25,9	-11,1	5E-09	4E-07	11
>sp|Q8R1G2|CMBL_M	20,64	20,4	19,9	20,3	20,4	20,6	20	20	20	22,2	21	22	22	21,9	22	22	22,2	22,5	20,295	22,0417	Cmbl	1,75	21,2	11,06	5E-09	4E-07	11
>sp|Q8CI43|MYL6B_M	21,9	22,3	22,1	22,1	21,8	21,9	22	22	22	19,6	20	20	20,5	20,6	20	20	19	19,9	21,914	19,9422	Myl6b	-2	20,9	-11	6E-09	4E-07	11
>sp|Q64524|H2B2E_	27,13	26,6	27	26	26,2	27,2	27	26	27	28,4	28	28	28,2	28,3	28	28	28,2	28,2	26,712	28,2872	Hist2h2b	1,58	27,5	10,91	6E-09	4E-07	11

>sp|Q9R1P3|PSB2_M	25,96	27,4	26,7	26,1	26,7	26,2	27	28	27	24,6	25	25	24,7	24,6	24	25	24,2	24,2	26,767	24,5053	Psmb2	-2,3	25,6	-10,8	8E-09	5E-07	11
>sp|O54724|CAVN1_	18,38	19	18,7	18,5	18,5	18,4	18	20	20	22,3	22	22	21,3	22,3	21	21	21,8	22	18,81	21,6616	Cavin1	2,85	20,2	10,65	9E-09	6E-07	10
>sp|P17182|ENOA_M	27,95	28,2	28,3	28,7	28,2	28,5	28	28	28	26,1	26	26	26,4	26,1	27	27	26,4	26,2	28,229	26,4014	Eno1	-1,8	27,3	-10,6	9E-09	6E-07	10
>sp|Q9DBH5|LMAN2_	18,34	18,3	18,2	18,8	18,5	18,4	19	18	18	19,4	20	19	19,7	19,6	20	19	19,1	19,3	18,437	19,4108	Lman2	0,97	18,9	10,17	2E-08	1E-06	9,7
>sp|Q9R1P0|PSA4_M	27,56	27,6	27,2	27,5	26,5	26,7	26	28	27	24,9	25	24	25,2	24,1	25	25	24,8	25,3	27,17	24,8223	Psma4	-2,3	26	-10	2E-08	1E-06	9,5
>sp|P52624|UPP1_M	24,33	24,6	24	23,8	24,4	23,9	24	25	24	22,6	22	22	22,6	22,6	23	23	23	23	24,194	22,7463	Upp1	-1,4	23,5	-10	2E-08	1E-06	9,5
>sp|Q9DBG3|AP2B1_	19,97	19,4	19,7	19,8	19,4	19,7	19	20	20	20,7	21	21	20,8	20,7	21	20	20,7	20,3	19,652	20,617	Ap2b1	0,96	20,1	9,923	2E-08	1E-06	9,4
>sp|Q9DCW4|ETFB_M	23,91	23,4	22,5	23,9	23,7	23,5	23	23	24	25,3	26	26	25,4	25,5	25	25	25,9	24,8	23,48	25,3712	Etfb	1,89	24,4	9,761	3E-08	2E-06	9,1
>sp|P45952|ACADM_	22,4	22,1	23,4	22,2	22,4	21,7	22	22	22	23,8	24	24	24,2	24,3	24	24	23,8	24,3	22,207	24,0331	Acadm	1,83	23,1	9,658	4E-08	2E-06	9
>sp|Q9Z2W0|DNPEP_	25,06	25	25,7	25,4	25,4	25,9	25	25	26	24,1	24	24	24	23,4	23	24	23,9	23,5	25,368	23,878	Dnpep	-1,5	24,6	-9,56	4E-08	2E-06	8,8
>sp|O88844|IDHC_M	24,85	24,8	25,1	24,8	25,2	25,1	26	25	25	24,3	24	24	24	24,2	24	24	24,4	24,3	25,104	24,206	Idh1	-0,9	24,7	-9,56	4E-08	2E-06	8,8
>sp|D3Z6P0|PDIA2_M	22,77	21,6	21,5	22,2	21,8	22	21	22	22	24,3	24	24	23,6	23,2	23	24	23,9	23,5	21,958	23,7817	Pdia2	1,82	22,9	9,519	4E-08	2E-06	8,8
>sp|Q00519|XDH_M(	22,99	22,6	23,1	23,4	22,9	23,2	23	23	23	22,2	22	22	21,5	22,4	22	22	22	22,1	23,069	22,0396	Xdh	-1	22,6	-9,34	6E-08	3E-06	8,5
>sp|P49722|PSA2_M	28,22	27,5	26,2	28,3	26	26,7	27	28	27	24,9	24	25	24,6	24,7	25	25	24,6	24,8	27,23	24,6727	Psma2	-2,6	26	-9,25	7E-08	3E-06	8,4
>sp|P50544|ACADV_	21,11	19,4	20,3	20,4	20,3	20,4	20	20	20	21,8	22	22	21,7	21,5	22	22	21,7	21,8	20,2	21,7207	Acadvl	1,52	21	9,251	7E-08	3E-06	8,4
>sp|P36369|K1B26_	21,62	21,4	21,2	22,2	22	21	22	22	22	19,5	20	20	19,8	20,1	20	20	19,9	20,2	21,719	20,0259	Klk1b26	-1,7	20,9	-9,24	7E-08	3E-06	8,3
>sp|P51174|ACADL_	24,4	24,2	23	24,5	23,5	23,2	23	24	24	25,6	26	26	25,5	25,8	25	26	25,9	25,5	23,758	25,6142	Acadl	1,86	24,7	9,219	7E-08	3E-06	8,3
>sp|O55222|ILK_MOI	22,91	22,4	22,3	22,5	22,5	23	22	22	22	20,9	21	21	20,9	21,5	21	20	21,5	20,8	22,535	21,1097	Ilk	-1,4	21,8	-9,13	8E-08	4E-06	8,2
>sp|Q8JZQ5|AOC1_M	22,32	21,9	21,5	21,6	21,7	21,2	22	22	22	20,5	20	20	20,4	20,6	21	20	20,6	20	21,762	20,3426	Aoc1	-1,4	21,1	-9,11	8E-08	4E-06	8,1
>sp|Q8R086|SUOX_M	20,12	20,7	20,1	20,4	20,4	20,9	20	20	21	19,3	19	19	18,9	18,4	18	18	18,7	19,1	20,368	18,841	Suox	-1,5	19,6	-9,11	8E-08	4E-06	8,1
>sp|P97855|G3BP1_	19,4	19,2	19,3	19,4	19,3	19,5	19	19	20	20,1	20	20	20,6	20,3	21	21	20,1	20	19,391	20,2743	G3bp1	0,88	19,8	9,056	9E-08	4E-06	8,1
>sp|O88851|RBBP9_	17,89	16,7	14,3	14,4	15,3	14,5	16	16	17	0	14	0	0	0	0	0	0	0	15,804	1.535247	Rbbp9	-14	8,67	-9,05	9E-08	4E-06	8
>sp|Q6P1B1|XPP1_M	24,12	23,4	23,8	23,6	24	24,3	24	24	24	23	23	23	22,8	22,7	23	22	22,7	22,9	23,944	22,8069	Xpnpep1	-1,1	23,4	-9,05	9E-08	4E-06	8
>sp|P10639|THIO_M(	24,7	24,4	25,1	24,3	24,3	24,7	24	24	25	21,5	21	23	23,1	22	23	22	22,8	22,2	24,51	22,3246	Txn	-2,2	23,4	-9,02	9E-08	4E-06	8
>sp|Q9JJU8|SH3L1_M	17,1	16,9	16,5	16,7	16,4	16,8	17	17	17	15,1	16	16	15,6	15,4	16	16	15,9	15,9	16,796	15,6863	Sh3bgrl	-1,1	16,2	-8,96	1E-07	5E-06	7,9
>sp|A3KMP2|TTC38_	21,49	20,8	21,2	21,1	21,4	21,4	21	21	21	22,6	22	22	22	22,1	22	22	22,1	22,4	21,251	22,1692	Ttc38	0,92	21,7	8,865	1E-07	5E-06	7,8
>sp|Q91X79|CELA1_I	24,46	23,8	23,2	23,1	23,4	23,5	24	24	24	25,6	25	25	25,4	25,2	26	25	25,6	25,7	23,803	25,4407	Cela1	1,64	24,6	8,766	1E-07	6E-06	7,6
>sp|P48036|ANXA5_	21	20,5	21,2	21	19,5	21	20	21	21	22,9	23	22	23,6	22,3	23	24	23,1	23,9	20,666	23,1607	Anxa5	2,49	21,9	8,643	2E-07	7E-06	7,4
>sp|P10853|H2B1F_	27,49	27,1	27,9	27,9	27,5	28,1	28	27	28	28,6	29	29	28,6	28,6	29	29	28,4	28,7	27,632	28,6028	Hist1h2b	0,97	28,1	8,574	2E-07	8E-06	7,3
>sp|Q64478|H2B1H_	27,49	27,1	27,9	27,9	27,5	28,1	28	27	28	28,6	29	29	28,6	28,6	29	29	28,4	28,7	27,632	28,6028	Hist1h2b	0,97	28,1	8,574	2E-07	8E-06	7,3
>sp|Q6ZWY9|H2B1C_	27,49	27,1	27,9	27,9	27,5	28,1	28	27	28	28,6	29	29	28,6	28,6	29	29	28,4	28,7	27,632	28,6028	Hist1h2b	0,97	28,1	8,574	2E-07	8E-06	7,3
>sp|Q8CGP1|H2B1K_	27,49	27,1	27,9	27,9	27,5	28,1	28	27	28	28,6	29	29	28,6	28,6	29	29	28,4	28,7	27,632	28,6028	Hist1h2b	0,97	28,1	8,574	2E-07	8E-06	7,3
>sp|Q9R100|CAD17_	21,24	21	21,7	21,7	21,8	21,6	21	22	22	20,4	20	20	20,3	20,3	21	20	20,9	20,7	21,535	20,4209	Cdh17	-1,1	21	-8,54	2E-07	8E-06	7,2
>sp|P62806|H4_MOI	26,31	25,1	26,5	27,3	25,7	26,1	28	26	26	29,1	28	28	28,3	28,1	29	29	28,8	28,8	26,276	28,6552	Hist1h4a	2,38	27,5	8,431	2E-07	9E-06	7,1
>sp|Q9WUM4|COR1C	22,96	22,9	22,7	22,6	23,1	23	23	23	23	21,9	22	22	21,8	22,1	22	22	22,3	22,3	23,025	21,9979	Coro1c	-1	22,5	-8,42	2E-07	9E-06	7
>sp|Q9JLJ2|AL9A1_M	23,14	23,3	22,8	23	23,2	23	23	23	23	24,1	24	24	23,9	23,9	24	24	24,2	23,8	23,125	23,8858	Aldh9a1	0,76	23,5	8,36	3E-07	1E-05	6,9
>sp|P02089|HBB2_M	28,83	28,8	28,7	28,8	28,8	28,6	29	29	29	27,9	27	28	27,4	27,2	27	28	27,9	28	28,705	27,5945	Hbb-b2	-1,1	28,1	-8,25	3E-07	1E-05	6,8
>sp|O08601|MTP_M(	22,89	23	23,3	23	23	23,2	23	23	23	24,1	24	24	23,8	23,9	24	24	24	24,3	23,142	23,9363	Mttp	0,79	23,5	8,245	3E-07	1E-05	6,7
>sp|P83877|TXN4A_	0	0	16,2	0	0	0	0	0	0	16,4	16	16	16,1	16,6	16	17	16,2	17	1.79630	16,4438	Txnl4a	14,6	9,12	8,226	3E-07	1E-05	6,7
>sp|P10854|H2B1M	27,49	27,1	27,9	27,9	27,5	28,1	28	27	28	28,6	29	29	28,4	28,6	29	29	28,4	28,6	27,632	28,5524	Hist1h2b	0,92	28,1	8,201	3E-07	1E-05	6,7
>sp|Q64475|H2B1B_	27,49	27,1	27,9	27,9	27,5	28,1	28	27	28	28,6	29	29	28,4	28,6	29	29	28,4	28,6	27,632	28,5524	Hist1h2b	0,92	28,1	8,201	3E-07	1E-05	6,7
>sp|Q64525|H2B2B_	27,49	27,1	27,9	27,9	27,5	28,1	28	27	28	28,6	29	29	28,4	28,6	29	29	28,4	28,6	27,632	28,5524	Hist2h2b	0,92	28,1	8,201	3E-07	1E-05	6,7
>sp|Q8CGP2|H2B1P_	27,49	27,1	27,9	27,9	27,5	28,1	28	27	28	28,6	29	29	28,4	28,6	29	29	28,4	28,6	27,632	28,5524	Hist1h2b	0,92	28,1	8,201	3E-07	1E-05	6,7
>sp|Q9EQP2|EHD4_M	20,22	20,4	20,1	20,7	20,2	19,9	21	21	21	19	20	19	19,6	18,9	20	19	19,4	19,2	20,373	19,2683	Ehd4	-1,1	19,8	-8,18	4E-07	1E-05	6,6
>sp|P53026|RL10A_	22,85	23,2	22,6	22,7	22,6	23	23	23	24	24	24	24	24,1	24	24	24	24	23,9	22,895	23,9588	Rpl10a	1,06	23,4	8,121	4E-07	1E-05	6,5
>sp|Q6P8U6|LIPP_M(	19,65	20	19,9	19	19,4	19,3	19	20	19	21,6	21	21	20,6	20,1	21	21	21	21	19,46	20,8729	Pnlip	1,41	20,2	8,12	4E-07	1E-05	6,5
>sp|Q9R0G6|COMP_I	21,71	21,6	21,3	22,1	22,6	21,7	22	22	22	20,1	20	20	20,8	20,6	21	21	20,3	20,1	21,833	20,3808	Comp	-1,5	21,1	-7,81	6E-07	2E-05	6
>sp|P70696|H2B1A_	26,63	25,4	26,7	26,2	25,9	27,4	26	26	27	28,2	27	28	28	28,1	28	28	28	27,8	26,32	27,9415	Hist1h2b	1,62	27,1	7,793	7E-07	2E-05	6

>sp|Q9QYB5|ADDG_M	0	0	0	0	14,5	0	0	0	0	14	15	14	14,2	14,7	14	13	13,5	13,9	1.61435	14,1152	Add3	12,5	7,86	7,77	7E-07	2E-05	5,9
>sp|Q8QZR5|ALAT1_M	22,78	23,4	22,1	22,8	22,9	23,1	23	23	23	22	21	21	22	21,8	22	22	22	21,9	22,957	21,8304	Gpt	-1,1	22,4	-7,77	7E-07	2E-05	5,9
>sp|P99026|PSB4_M	25,28	27,6	27,6	27,5	26,8	28,4	27	26	26	24,2	24	25	23,8	23,6	23	24	24,6	24,7	26,898	24,1155	Psma2	-2,6	25,5	-7,74	7E-07	2E-05	5,9
>sp|Q6GQT1|A2MG_M	23,95	24,6	24,3	23,5	23,7	23,5	24	24	24	22,4	23	23	23	22,6	23	23	22,6	23	23,83	22,7152	A2m	-1,1	23,3	-7,73	7E-07	2E-05	5,9
>sp|O54865|GCYB1_	17,29	15,9	17,3	16,1	16,2	17,2	16	17	17	18,4	18	18	18,4	18,6	19	18	18,5	19	16,614	18,4302	Gucy1b3	1,82	17,5	7,71	8E-07	2E-05	5,8
>sp|P56480|ATPB_M	22,36	22,5	22,7	22,5	22,7	22,7	23	23	23	24,4	24	24	23,8	24,6	24	24	23,5	24,3	22,738	24,0316	Atp5b	1,29	23,4	7,68	8E-07	3E-05	5,8
>sp|P62071|RRAS2_	20,36	19,7	19,9	20,3	20,2	19,9	21	21	21	19,5	19	18	18	18,2	18	18	18,2	18,9	20,299	18,3788	Rras2	-1,9	19,3	-7,59	9E-07	3E-05	5,6
>sp|P97371|PSME1_	20,2	20,2	19,7	20,5	20,8	20	21	21	20	21,8	21	21	21,7	21,4	22	21	21,3	21,5	20,273	21,4147	Psme1	1,14	20,8	7,539	1E-06	3E-05	5,5
>sp|Q9QZQ8|H2AY_M	21,49	21,4	21,5	21,6	21,6	21,2	22	22	22	22,4	22	22	22,1	22,2	22	22	22,4	22,4	21,571	22,2641	H2afy	0,69	21,9	7,513	1E-06	3E-05	5,5
>sp|Q9DCM0|ETHE1_I	20,53	21,2	21,2	21,5	21,2	21,3	22	21	22	23	22	23	22,2	22,7	23	23	23,3	22,1	21,285	22,5897	Ethe1	1,3	21,9	7,483	1E-06	3E-05	5,4
>sp|Q8QZT1|THIL_MOI	23,1	23,2	22,8	22,6	22,6	22,8	23	22	23	21,7	22	22	22	22,1	22	22	22	21,9	22,819	21,9106	Acat1	-0,9	22,4	-7,48	1E-06	3E-05	5,4
>sp|P01867|IGG2B_I	17,02	17,2	18,3	18,5	18,2	18,6	19	18	17	15,7	17	17	15,8	16,3	16	15	16,2	15,7	17,992	16,0677	Igh-3	-1,9	17	-7,4	1E-06	4E-05	5,3
>sp|Q9WUU7|CATZ_M	21,88	22,2	21,9	22,1	22,1	22,2	22	22	21	20,6	21	21	20,9	21	22	21	20,9	20,6	21,945	20,8427	Ctsz	-1,1	21,4	-7,38	1E-06	4E-05	5,3
>sp|P70695|F16P2_	23,78	23,4	22,7	22,9	22,9	23,4	23	23	23	24,3	24	25	24,2	24	24	25	24,1	24,2	23,208	24,2242	Fbp2	1,02	23,7	7,331	1E-06	4E-05	5,2
>sp|Q9DBJ1|PGAM1_	22,63	23,3	22,5	23,1	22,3	23	23	23	23	22	21	22	22,1	22,1	22	22	21,9	21,5	22,844	21,8718	Pgam1	-1	22,4	-7,33	1E-06	4E-05	5,2
>sp|Q9EQH2|ERAP1_I	19,99	19,4	19,4	19,2	19,6	19,4	19	19	19	20,4	20	20	20,2	20	21	20	20,4	20,5	19,417	20,3098	Erap1	0,89	19,9	7,317	2E-06	4E-05	5,1
>sp|P50247|SAHH_M	24,74	24,9	24,5	24,8	25,2	24,6	25	25	25	25,8	26	26	26,2	25,9	26	27	26,1	25,9	24,904	26,0921	Ahcy	1,19	25,5	7,315	2E-06	4E-05	5,1
>sp|P01837|IGKC_M	24,84	24,6	25,4	24,3	24,7	25	25	25	25	23,5	23	22	22,3	23,8	23	23	23,3	22,1	24,798	23,0514	>sp|P018	-1,7	23,9	-7,29	2E-06	5E-05	5,1
>sp|Q9D2G2|ODO2_M	20,67	21	20,7	20,9	20,7	20,8	21	21	21	19,5	20	19	20,1	20	20	19	19,9	18,7	20,873	19,5999	Dlst	-1,3	20,2	-7,25	2E-06	5E-05	5
>sp|P26039|TLN1_M	22,51	22,5	22	21,8	22,2	22,3	22	22	22	21,7	21	21	21,5	21,5	22	21	21,4	21,1	22,187	21,4347	Tln1	-0,8	21,8	-7,23	2E-06	5E-05	5
>sp|P02104|HBE_MO	28,55	28,6	28,5	28,4	28,1	27,7	28	28	28	27	26	27	26	25,8	26	28	27	26,4	28,241	26,5381	Hbb-y	-1,7	27,4	-7,11	2E-06	6E-05	4,8
>sp|Q9QYR9|ACOT2_I	18,45	18,7	19,6	18,3	18,4	18,9	19	19	20	21,4	21	20	20,5	20,2	21	20	20,6	20,5	18,959	20,5943	Acot2	1,64	19,8	7,098	2E-06	6E-05	4,8
>sp|Q9D7Z6|CLCA1_I	24,26	23,8	23,7	23,6	23,4	23,8	24	24	24	23,4	23	23	23	22,9	23	23	23,1	23,2	23,893	23,1303	Clca1	-0,8	23,5	-7,03	2E-06	7E-05	4,6
>sp|Q3TNA1|XYLB_MO	15,67	15,4	16,4	16,4	16,7	16,8	17	17	16	14,5	15	14	14,4	15,1	15	15	13,5	15,1	16,325	14,6051	Xylb	-1,7	15,5	-6,96	3E-06	8E-05	4,5
>sp|Q8VHP7|ILEUB_M	19,97	20,5	20,5	19,6	20,5	19,8	20	20	20	21,1	21	21	21,6	20,9	22	21	21,4	20,9	20,205	21,1946	Serpinb1b	0,99	20,7	6,951	3E-06	8E-05	4,5
>sp|P0C0S6|H2AZ_M	24,88	25,2	24,2	24,5	24,5	24,8	25	24	22	27,2	27	27	27,2	27,3	27	26	26,7	27,2	24,22	26,9903	H2afz	2,77	25,6	6,948	3E-06	8E-05	4,5
>sp|Q3THW5|H2AV_M	24,88	25,2	24,2	24,5	24,5	24,8	25	24	22	27,2	27	27	27,2	27,3	27	26	26,7	27,2	24,22	26,9903	H2afv	2,77	25,6	6,948	3E-06	8E-05	4,5
>sp|O08691|ARGI2_I	22,69	23	22,9	22,4	22,4	23,1	23	23	23	23,4	23	23	23,5	23,4	23	24	23,7	23,7	22,82	23,4947	Arg2	0,67	23,2	6,941	3E-06	8E-05	4,5
>sp|Q6PHZ2|KCC2D_	16,89	17,3	16,9	17,5	17,1	17,1	16	17	17	16	16	15	16,3	16	16	16	15,7	16	17,037	15,8178	Camk2d	-1,2	16,4	-6,9	3E-06	8E-05	4,4
>sp|O35643|AP1B1_	19,94	19,8	19,8	20,4	20,2	19,8	20	20	20	20,6	21	21	20,5	20,8	21	21	20,9	20,4	20,048	20,7076	Ap1b1	0,66	20,4	6,885	3E-06	8E-05	4,4
>sp|P01644|KV5AB_	20,09	20,1	20,9	20,2	20,9	20,4	20	21	20	19,5	20	19	19	17,7	19	18	18,8	18,5	20,384	18,7852	>sp|P016	-1,6	19,6	-6,88	3E-06	8E-05	4,4
>sp|P01645|KV5AC_	20,09	20,1	20,9	20,2	20,9	20,4	20	21	20	19,5	20	19	19	17,7	19	18	18,8	18,5	20,384	18,7852	>sp|P016	-1,6	19,6	-6,88	3E-06	8E-05	4,4
>sp|P01646|KV5AD_	20,09	20,1	20,9	20,2	20,9	20,4	20	21	20	19,5	20	19	19	17,7	19	18	18,8	18,5	20,384	18,7852	>sp|P016	-1,6	19,6	-6,88	3E-06	8E-05	4,4
>sp|Q9R0H0|ACOX1_	21,87	22,1	21,8	21,7	21,9	21,6	22	22	22	22,8	23	23	22,6	22,3	22	23	22,9	22,6	21,931	22,6362	Acox1	0,7	22,3	6,862	3E-06	8E-05	4,3
>sp|Q9QZ25|VNN3_M	17,44	17,3	17,8	17,3	17,6	17,8	17	17	17	15,8	16	17	16,6	16,4	15	16	16,2	16,3	17,373	16,1832	Vnn3	-1,2	16,8	-6,86	3E-06	8E-05	4,3
>sp|Q60847|COCA1_	19,23	19,3	18,8	19,1	18,7	18,9	19	19	19	18,1	18	18	18,4	18	18	19	18,6	18,1	19,019	18,2101	Col12a1	-0,8	18,6	-6,83	4E-06	9E-05	4,3
>sp|P16858|G3P_MO	26,15	25,2	26	25,9	25,4	26,1	26	26	26	24,8	25	25	24,5	24,5	24	25	24,7	24,6	25,845	24,7118	Gapdh	-1,1	25,3	-6,82	4E-06	9E-05	4,2
>sp|P21765|GPX5_M	18,61	17,8	16,4	19,4	17,6	19,4	18	19	18	20,3	21	21	20,3	20	20	21	20,8	21,3	18,292	20,6218	Gpx5	2,33	19,5	6,812	4E-06	9E-05	4,2
>sp|Q8BH35|CO8B_M	17,57	18	17,9	17,5	17,3	17,4	18	18	17	0	16	0	0	0	0	12	0	0	17,585	3.20267	C8b	-14	10,4	-6,78	4E-06	9E-05	4,2
>sp|P01592|IGJ_MOU	21,43	21,3	22,2	22,2	22,5	21,9	22	22	22	20,6	21	21	21,1	20,5	21	21	21,2	20,6	21,945	20,8515	Jchain	-1,1	21,4	-6,77	4E-06	1E-04	4,1
>sp|Q9CPV4|GLOD4_	19,54	19,7	20,5	20,2	19,8	20	21	20	21	22,1	22	22	22	21,5	22	21	21,7	21,2	20,186	21,648	Glod4	1,46	20,9	6,729	4E-06	0,0001	4,1
>sp|Q8CCK0|H2AW_I	19,41	19,4	18,8	19	18,3	19,5	20	21	20	21,6	22	22	21,1	21,1	21	21	21,4	21,1	19,495	21,3118	H2afy2	1,82	20,4	6,729	4E-06	0,0001	4,1
>sp|Q64523|H2A2C_	25,41	25,7	24,6	24,9	24,8	25,2	25	24	22	27,5	28	27	27,5	27,5	28	26	27,7	27,4	24,657	27,3753	Hist2h2ac	2,72	26	6,726	4E-06	0,0001	4,1
>sp|Q6GSS7|H2A2A_I	25,41	25,7	24,6	24,9	24,8	25,2	25	24	22	27,5	28	27	27,5	27,5	28	26	27,7	27,4	24,657	27,3753	Hist2h2aa	2,72	26	6,726	4E-06	0,0001	4,1
>sp|P14869|RLA0_M	23,25	23	22,8	23,2	23,6	23,7	23	23	24	24,2	24	24	24,4	23,9	24	24	24,3	24,4	23,307	24,1433	Rplp0	0,84	23,7	6,722	4E-06	0,0001	4,1
>sp|Q9DB29|IAH1_M	21,65	21,7	21,5	21,4	21,4	21,4	21	22	22	22,6	22	23	22,5	22,8	22	22	22	22,6	21,593	22,4069	Iah1	0,81	22	6,66	5E-06	0,0001	3,9
>sp|Q8CGP5|H2A1F_	24,91	25,2	24,3	24,6	24,5	24,9	25	24	22	27,3	27	27	27,1	27,4	27	26	26,7	27,3	24,263	26,9554	Hist1h2af	2,69	25,6	6,655	5E-06	0,0001	3,9
>sp|O35855|BCAT2_	19,77	20,3	20,3	20,1	20,3	20,3	20	20	20	21,4	20	21	21,5	21,2	21	21	21,1	21,2	20,17	21,0676	Bcat2	0,9	20,6	6,634	5E-06	0,0001	3,9

>sp|P05208|CEL2A_I	24,55	25	25,4	25,4	25,3	25,6	26	25	25	25,9	26	27	26,8	26,5	26	27	26,2	26,1	25,206	26,4518	Cela2a	1,25	25,8	6,628	5E-06	0,0001	3,9
>sp|Q71LX4|TLN2_M(	18,87	18,8	18,9	18,1	18,4	18,7	18	19	19	17,8	18	18	17,6	17,9	18	18	17,7	17,8	18,558	17,812	Tln2	-0,7	18,2	-6,59	6E-06	0,0001	3,8
>sp|Q9WV32|ARC1B	22,74	22,8	22,3	22,5	22,8	22,7	23	23	23	22,2	22	22	22	21,8	22	22	21,9	22	22,694	22,0457	Arpc1b	-0,6	22,4	-6,58	6E-06	0,0001	3,8
>sp|Q02788|CO6A2_	20,69	21,1	21,3	21,7	21,7	21,5	21	21	21	20,3	20	19	20,5	19,7	20	19	19,4	20,5	21,19	19,8399	Col6a2	-1,4	20,5	-6,58	6E-06	0,0001	3,8
>sp|Q8R1M2|H2AJ_M	25,44	25,7	24,8	25	24,9	25,4	25	24	22	27,5	28	27	27,5	27,7	28	26	27,6	27,6	24,73	27,3693	H2afj	2,64	26	6,563	6E-06	0,0001	3,8
>sp|Q61425|HCDH_M	21,47	22	23,9	22,9	23,4	23,1	23	22	22	24,2	24	25	24,8	25,1	25	24	24,6	24,9	22,621	24,6227	Hadh	2	23,6	6,552	6E-06	0,0001	3,7
>sp|C0HKE1|H2A1B_	25,64	26,1	24,8	25,1	25	25,4	25	24	22	27,6	28	27	27,6	27,7	28	27	27,6	27,6	24,838	27,5075	Hist1h2al	2,67	26,2	6,53	6E-06	0,0001	3,7
>sp|C0HKE2|H2A1C_	25,64	26,1	24,8	25,1	25	25,4	25	24	22	27,6	28	27	27,6	27,7	28	27	27,6	27,6	24,838	27,5075	Hist1h2ac	2,67	26,2	6,53	6E-06	0,0001	3,7
>sp|C0HKE3|H2A1D_	25,64	26,1	24,8	25,1	25	25,4	25	24	22	27,6	28	27	27,6	27,7	28	27	27,6	27,6	24,838	27,5075	Hist1h2ac	2,67	26,2	6,53	6E-06	0,0001	3,7
>sp|C0HKE4|H2A1E_I	25,64	26,1	24,8	25,1	25	25,4	25	24	22	27,6	28	27	27,6	27,7	28	27	27,6	27,6	24,838	27,5075	Hist1h2ae	2,67	26,2	6,53	6E-06	0,0001	3,7
>sp|C0HKE5|H2A1G_	25,64	26,1	24,8	25,1	25	25,4	25	24	22	27,6	28	27	27,6	27,7	28	27	27,6	27,6	24,838	27,5075	Hist1h2ag	2,67	26,2	6,53	6E-06	0,0001	3,7
>sp|C0HKE6|H2A1I_M	25,64	26,1	24,8	25,1	25	25,4	25	24	22	27,6	28	27	27,6	27,7	28	27	27,6	27,6	24,838	27,5075	Hist1h2ai	2,67	26,2	6,53	6E-06	0,0001	3,7
>sp|C0HKE7|H2A1N_	25,64	26,1	24,8	25,1	25	25,4	25	24	22	27,6	28	27	27,6	27,7	28	27	27,6	27,6	24,838	27,5075	Hist1h2ar	2,67	26,2	6,53	6E-06	0,0001	3,7
>sp|C0HKE8|H2A1O_	25,64	26,1	24,8	25,1	25	25,4	25	24	22	27,6	28	27	27,6	27,7	28	27	27,6	27,6	24,838	27,5075	Hist1h2ac	2,67	26,2	6,53	6E-06	0,0001	3,7
>sp|C0HKE9|H2A1P_	25,64	26,1	24,8	25,1	25	25,4	25	24	22	27,6	28	27	27,6	27,7	28	27	27,6	27,6	24,838	27,5075	Hist1h2ap	2,67	26,2	6,53	6E-06	0,0001	3,7
>sp|Q8BFU2|H2A3_M	25,64	26,1	24,8	25,1	25	25,4	25	24	22	27,6	28	27	27,6	27,7	28	27	27,6	27,6	24,838	27,5075	Hist3h2a	2,67	26,2	6,53	6E-06	0,0001	3,7
>sp|Q8CGP6|H2A1H_	25,64	26,1	24,8	25,1	25	25,4	25	24	22	27,6	28	27	27,6	27,7	28	27	27,6	27,6	24,838	27,5075	Hist1h2ah	2,67	26,2	6,53	6E-06	0,0001	3,7
>sp|Q8CGP7|H2A1K_	25,64	26,1	24,8	25,1	25	25,4	25	24	22	27,6	28	27	27,6	27,7	28	27	27,6	27,6	24,838	27,5075	Hist1h2ak	2,67	26,2	6,53	6E-06	0,0001	3,7
>sp|P29758|OAT_MC	23,56	23,2	22,7	22,9	23,2	23,8	23	24	23	24	24	25	24,4	23,6	24	24	24,1	24,3	23,263	24,241	Oat	0,98	23,8	6,507	6E-06	0,0001	3,7
>sp|Q8C0E2|VP26B_	17,19	17,1	16,3	16,2	15,4	16,9	15	16	15	18,4	17	18	17,6	18,4	18	18	18,2	18,3	16,239	18,0475	Vps26b	1,81	17,1	6,487	7E-06	0,0001	3,6
>sp|P17426|AP2A1_	20,87	20,7	21,4	21	20,9	21,1	21	21	21	21,7	22	22	21,6	21,9	22	21	21,5	21,2	20,963	21,6124	Ap2a1	0,65	21,3	6,477	7E-06	0,0001	3,6
>sp|P63038|CH60_M	22,09	22	22,3	22,8	22,2	22,4	22	22	22	23,3	24	24	23	22,7	23	23	23,3	24	22,291	23,2871	Hspd1	1	22,8	6,466	7E-06	0,0001	3,6
>sp|P01878|IGHA_M	23,08	23,5	23,4	24	23,6	24,3	24	24	24	22,9	22	22	22,9	23	23	22	22,8	22,3	23,846	22,6565	>sp|P018	-1,2	23,3	-6,45	7E-06	0,0001	3,6
>sp|Q8BPB5|FBLN3_I	20,26	19,8	20,3	20	20,3	20,4	20	20	20	19,4	20	19	19,5	19,3	19	20	19,5	19,8	20,121	19,4832	Efemp1	-0,6	19,8	-6,43	7E-06	0,0001	3,5
>sp|Q8R146|APEH_M	22,2	22,2	22	22	22,1	22,4	22	22	23	21,7	21	22	21,3	21,6	21	21	21,2	21,8	22,238	21,3814	Apeh	-0,9	21,8	-6,4	8E-06	0,0002	3,5
>sp|P48771|CX7A2_	18,72	19,7	19,5	18,7	18,2	19,3	19	20	20	20,7	20	20	21,3	21	21	20	20,7	20,6	19,169	20,6572	Cox7a2	1,49	19,9	6,378	8E-06	0,0002	3,4
>sp|P0DP26|CALM1_	22	22,6	22,4	22	21,8	21,8	23	23	23	21	21	21	21,5	21,1	21	22	21	20,7	22,388	21,0692	Calm1	-1,3	21,7	-6,33	9E-06	0,0002	3,3
>sp|P0DP27|CALM2_	22	22,6	22,4	22	21,8	21,8	23	23	23	21	21	21	21,5	21,1	21	22	21	20,7	22,388	21,0692	Calm2	-1,3	21,7	-6,33	9E-06	0,0002	3,3
>sp|P0DP28|CALM3_	22	22,6	22,4	22	21,8	21,8	23	23	23	21	21	21	21,5	21,1	21	22	21	20,7	22,388	21,0692	Calm3	-1,3	21,7	-6,33	9E-06	0,0002	3,3
>sp|P49182|HEP2_M	23,65	22,9	22,6	23,1	23,1	23	23	23	23	20,7	22	21	21,6	21,6	22	22	20,6	21,9	22,998	21,5029	Serpind1	-1,5	22,3	-6,32	9E-06	0,0002	3,3
>sp|Q9DBR7|MYPT1_	20,32	20,7	20,3	19,2	20,5	20,4	20	20	20	18,5	19	20	18,6	18,8	19	19	18,8	18,3	20,259	18,8394	Ppp1r12:	-1,4	19,5	-6,3	9E-06	0,0002	3,3
>sp|P08113|ENPL_M	21,63	21,6	21,8	21,7	21	21,5	22	22	22	22,2	22	22	22,2	22,1	22	22	22,1	22,1	21,596	22,216	Hsp90b1	0,62	21,9	6,284	1E-05	0,0002	3,2
>sp|P27661|H2AX_M	24,62	24,9	23,9	24,2	24,1	24,5	25	23	21	26,7	27	26	27	27,1	27	25	26,5	26,7	23,888	26,6464	H2afx	2,76	25,3	6,283	1E-05	0,0002	3,2
>sp|P29699|FETUA_M	27,67	28,2	28,4	27,5	27,6	27,6	28	28	27	25,1	23	25	25,8	26,2	26	26	25,8	24,8	27,652	25,2573	Ahsg	-2,4	26,5	-6,26	1E-05	0,0002	3,2
>sp|Q9CR35|CTRB1_	22,73	22,8	23,3	22,3	22,9	23,1	22	23	23	21,6	22	22	21,8	21,7	21	20	21,1	21,1	22,787	21,4363	Ctrb1	-1,4	22,1	-6,24	1E-05	0,0002	3,1
>sp|Q9Z1T2|TSP4_MC	21,52	21,2	20,7	21,5	21	20,4	21	20	21	20,3	20	20	19,3	19,8	20	19	19,3	19,2	20,885	19,6639	Thbs4	-1,2	20,3	-6,22	1E-05	0,0002	3,1
>sp|Q923G2|RPAB3_	18,49	17,9	19,6	18,7	19,4	19	18	19	18	20,3	20	20	19,9	21,1	20	20	19,9	20,5	18,672	20,2398	Polr2h	1,57	19,5	6,176	1E-05	0,0002	3
>sp|Q9D1H9|MFAP4_	18,66	18,4	19,2	17,9	17,9	19,3	18	19	19	20,2	21	20	19,7	20,8	21	20	19,5	19,4	18,597	20,2126	Mfap4	1,62	19,4	6,166	1E-05	0,0002	3
>sp|P06330|HVM51	22,44	23	22,4	22,7	22,3	22,2	22	23	23	21,9	21	21	20,3	21,5	22	22	21,5	21,1	22,605	21,2357	>sp|P063	-1,4	21,9	-6,15	1E-05	0,0002	3
>sp|P52196|THTR_M	20,52	19,5	20,7	19,9	20	19,6	20	21	21	21,1	21	21	21,2	21	21	21	21,4	21	20,173	21,1654	Tst	0,99	20,7	6,116	1E-05	0,0002	2,9
>sp|Q9WVA4|TAGL2_	22,48	23,5	23,8	24	23,3	24	23	23	24	22,3	22	22	22,5	22,3	23	23	22,5	22,9	23,553	22,4933	Tagln2	-1,1	23	-6,09	1E-05	0,0002	2,9
>sp|Q9CWH6|PSA7L_	24,66	23,7	25,3	25	25,8	25	25	26	26	24,5	23	23	23,5	22,6	23	24	23,2	23	25,165	23,2964	Psma8	-1,9	24,2	-6,09	1E-05	0,0002	2,9
>sp|P62774|MTPN_M	21,27	21,9	21,1	22,1	21,3	22,4	22	22	22	21	20	20	20,5	20,5	21	21	20,7	20,7	21,659	20,6113	Mtpn	-1	21,1	-6,05	2E-05	0,0003	2,8
>sp|Q8K0C9|GMDS_M	24,21	24,2	23,9	24,3	24,5	24,5	24	25	25	25	25	25	25,1	25,2	25	25	25,2	25	24,389	25,0248	Gmds	0,64	24,7	6,039	2E-05	0,0003	2,8
>sp|Q9JKX6|NUDT5_I	20,8	20,7	20,9	20	21,1	20,5	20	21	21	20	19	20	20	19,8	20	20	19,8	19,5	20,712	19,8146	Nudt5	-0,9	20,3	-6,03	2E-05	0,0003	2,7
>sp|Q9CVB6|ARPC2_	21,81	22,5	22,5	22,4	22,8	22,3	23	23	23	24,3	23	24	24,4	24,5	24	23	24,5	24,5	22,487	24,0496	Arpc2	1,56	23,3	6,001	2E-05	0,0003	2,7
>sp|P57776|EF1D_M	19,91	20,1	20,2	19,9	20,3	20,2	20	20	19	19,1	20	19	17,8	18,8	18	19	18,7	18,8	19,974	18,7681	Eef1d	-1,2	19,4	-5,95	2E-05	0,0003	2,6
>sp|Q61398|PCOC1_	17,3	16,9	17,7	17,2	17,3	18,1	17	17	17	14,4	16	16	15,6	16,7	16	16	16,2	15,2	17,335	15,8162	Pcolce	-1,5	16,6	-5,93	2E-05	0,0003	2,5

>sp|Q99LD4|CSN1_M	20,11	20,2	19,4	19,7	20,2	18,9	20	20	20	21,3	22	22	22,1	22,1	22	20	21,6	21,8	19,845	21,6768	Gps1	1,83	20,8	5,89	2E-05	0,0004	2,5
>sp|P37040|NCPR_M	21,39	21	21,1	21,2	21,2	20,7	21	21	21	22,3	22	22	21,9	21,8	22	22	21,4	21,9	21,153	21,8972	Por	0,74	21,5	5,885	2E-05	0,0004	2,5
>sp|Q6PDN3|MYLK_M	23,29	24	22,5	23	23,3	23,1	23	23	23	23,1	22	22	21,6	21,7	21	22	22	21,8	23,11	21,9003	Mylk	-1,2	22,5	-5,88	2E-05	0,0004	2,4
>sp|P62631|EF1A2_I	23,99	24,2	24	24,4	24	24,4	24	24	25	23,4	23	24	23,9	23,7	24	24	23,4	23,5	24,26	23,6129	Eef1a2	-0,6	23,9	-5,85	2E-05	0,0004	2,4
>sp|Q91VI7|RINI_MOI	24,14	24,3	24,2	24	24,4	24,1	24	24	25	22,1	23	22	23,9	23,3	21	21	21,7	22,2	24,261	22,2907	Rnh1	-2	23,3	-5,85	2E-05	0,0004	2,4
>sp|Q60928|GGT1_M	16,44	17,2	17,4	17,6	17,2	17,5	17	18	18	18,4	18	18	18,8	18,7	18	18	18,1	18,7	17,339	18,3517	Ggt1	1,01	17,8	5,845	2E-05	0,0004	2,4
>sp|Q9CZU6|CISY_MO	23,74	23,6	24,3	23,8	24,1	23,8	24	24	24	24,4	25	25	24,6	24,8	25	25	24,8	24,4	24,003	24,715	Cs	0,71	24,4	5,803	2E-05	0,0004	2,3
>sp|Q61754|K1B24_	18,78	18,3	19,3	18,5	18,5	19,2	20	19	19	17,7	18	18	17,4	17,8	18	18	17,7	18,2	18,906	17,8565	Klk1b24	-1	18,4	-5,72	3E-05	0,0005	2,1
>sp|Q60759|GCDH_M	19,62	19,5	20,3	19	19	19,5	19	20	21	20,9	23	22	21,9	21,5	22	20	21,3	21,3	19,692	21,5303	Gcdh	1,84	20,6	5,701	3E-05	0,0005	2,1
>sp|P07724|ALBU_M	27,82	25,4	26,8	25,7	26,7	26,8	26	27	28	25,2	25	25	23,6	24,5	24	25	25,1	25,2	26,688	24,6943	Alb	-2	25,7	-5,7	3E-05	0,0005	2,1
>sp|Q9Z2I8|SUCB2_M	0	0	15	0	0	0	0	0	16	16,2	17	17	16,3	15,5	16	15	16,9	16,8	3.43960	16,2299	Suclg2	12,8	9,83	5,65	3E-05	0,0005	2
>sp|Q8VDQ1|PTGR2_	20,48	21,4	21,6	19,7	21	20,4	21	21	21	21,9	22	22	22,4	21,7	23	22	22,4	22,7	20,883	22,2086	Ptgr2	1,33	21,5	5,636	3E-05	0,0005	2
>sp|Q922D4|PP6R3_	15,61	15,4	15,3	14,8	14,7	13,8	15	15	14	15,9	16	15	16,1	16,2	17	16	16,1	16,4	14,746	16,1196	Ppp6r3	1,37	15,4	5,633	3E-05	0,0005	1,9
>sp|Q99L20|GSTT3_M	21,04	21,2	21,4	21,1	21,3	21,3	21	22	21	20,7	21	21	21	20,9	21	21	20,8	20,6	21,296	20,7976	Gstt3	-0,5	21	-5,63	3E-05	0,0005	1,9
>sp|Q9CZ42|NNRD_M	21,15	21	20,9	20,8	20,6	20,8	20	21	21	22,5	22	22	22,1	21,9	22	22	21,2	21,6	20,845	21,7895	Naxd	0,94	21,3	5,625	3E-05	0,0005	1,9
>sp|Q9CQ71|RFA3_M	19,57	18,7	18,8	17,4	20,4	19,8	19	19	19	17,7	17	17	16,8	17,3	17	17	18,5	16,8	19,077	17,2029	Rpa3	-1,9	18,1	-5,62	4E-05	0,0005	1,9
>sp|O55023|IMPA1_	19,68	19	20,2	19,9	20,1	19,8	20	20	20	21,1	22	22	21	20,9	21	21	20,9	20,7	19,845	21,1919	Impa1	1,35	20,5	5,605	4E-05	0,0006	1,9
>sp|P50446|K2C6A_	22,12	21,7	21,7	21,7	22,1	22,1	21	22	22	22,2	23	22	22,5	22,7	22	23	23,1	23,2	21,791	22,68	Krt6a	0,89	22,2	5,599	4E-05	0,0006	1,9
>sp|Q91ZJ5|UGPA_M	22,23	22,3	22,2	22	21,8	21,8	22	22	22	21,6	21	22	21,6	20,8	21	21	21,2	21,4	22,053	21,3773	Ugp2	-0,7	21,7	-5,6	4E-05	0,0006	1,9
>sp|P09542|MYL3_M	19,66	19,5	19,2	20,1	20,5	20,5	21	20	20	18	18	18	18,3	19	19	19	19,5	18,9	20,03	18,6132	Myl3	-1,4	19,3	-5,59	4E-05	0,0006	1,9
>sp|Q8VCI0|PLBL1_M	18,92	18,7	19	18,4	18,5	18,7	18	20	19	18,2	18	18	17,6	18,2	18	17	17,4	17,9	18,802	17,8724	Plbd1	-0,9	18,3	-5,58	4E-05	0,0006	1,8
>sp|Q8BK48|EST2E_M	21,55	21,1	21,7	20,3	21,9	21	22	22	21	22,6	23	22	22,7	22,6	23	22	23,1	21,9	21,397	22,5478	Ces2e	1,15	22	5,571	4E-05	0,0006	1,8
>sp|P05064|ALDOA_	26,7	25,1	25,6	25,4	25,4	25,8	26	26	25	24,9	25	25	24,8	24,8	25	25	24,9	24,5	25,647	24,775	Aldoa	-0,9	25,2	-5,56	4E-05	0,0006	1,8
>sp|Q62426|CYTB_M	19,99	20,5	20,3	20,2	19,8	20,5	21	20	21	21,8	21	22	22,5	22,1	22	22	21	21,2	20,404	21,6103	Cstb	1,21	21	5,558	4E-05	0,0006	1,8
>sp|P30115|GSTA3_I	23,15	23,1	22,9	22,5	21,9	22,4	23	22	22	23,6	23	23	24,3	24,5	24	24	24,4	24,2	22,551	23,9144	Gsta3	1,36	23,2	5,519	4E-05	0,0006	1,7
>sp|P01844|LAC2_M	0	0	16,5	0	0	0	0	0	18	17,3	18	17	17,6	17,3	18	17	17,2	17,9	3.79146	17,5028	Iglc2	13,7	10,6	5,516	4E-05	0,0006	1,7
>sp|P01845|LAC3_M	0	0	16,5	0	0	0	0	0	18	17,3	18	17	17,6	17,3	18	17	17,2	17,9	3.79146	17,5028	Iglc3	13,7	10,6	5,516	4E-05	0,0006	1,7
>sp|P01746|HVM02	21,05	19,9	21,4	21,1	20,7	20,4	21	21	21	18,2	18	20	19,8	17,8	18	19	20	19,6	20,86	18,9902	>sp|P017	-1,9	19,9	-5,51	4E-05	0,0006	1,7
>sp|P01747|HVM03	21,05	19,9	21,4	21,1	20,7	20,4	21	21	21	18,2	18	20	19,8	17,8	18	19	20	19,6	20,86	18,9902	>sp|P017	-1,9	19,9	-5,51	4E-05	0,0006	1,7
>sp|Q8JZV9|BDH2_M	17,61	16,5	17,2	17,3	17,6	17,6	17	17	17	18,1	17	18	18	18,4	19	18	18,2	18	17,201	18,1156	Bdh2	0,91	17,7	5,502	4E-05	0,0006	1,7
>sp|Q9CPU0|LGUL_M	22,9	23,1	22,9	22,8	22,7	22,7	23	22	24	23,2	24	24	23,8	23,9	24	23	23,3	23,9	22,858	23,6283	Glo1	0,77	23,2	5,501	4E-05	0,0006	1,7
>sp|P11352|GPX1_M	23,6	23,5	24	24,2	24,6	23,3	23	23	24	25	25	25	24,4	24,4	24	26	25	25,2	23,748	24,9611	Gpx1	1,21	24,4	5,492	5E-05	0,0007	1,7
>sp|P08003|PDIA4_I	21,57	21,7	21,1	20,8	20,5	20,6	21	21	21	21,6	22	22	21,7	21,8	22	22	21,8	21,7	20,974	21,7509	Pdia4	0,78	21,4	5,477	5E-05	0,0007	1,6
>sp|Q8VCN5|CGL_MO	21,91	21,9	21,9	22,2	21,9	21,8	22	22	22	22,2	23	23	22,8	23	23	22	22,2	22,9	21,966	22,639	Cth	0,67	22,3	5,475	5E-05	0,0007	1,6
>sp|Q60676|PPP5_M	22,6	21,9	21,5	22,4	21,6	21,4	22	21	21	20,3	20	20	19,9	19,9	20	21	20,8	20,9	21,677	20,4005	Ppp5c	-1,3	21	-5,47	5E-05	0,0007	1,6
>sp|Q922R8|PDIA6_I	19,09	19,3	18,9	19,2	18,8	19	19	20	19	20,5	20	20	19,9	20	20	19	20,2	20,1	19,114	19,9934	Pdia6	0,88	19,6	5,446	5E-05	0,0007	1,6
>sp|P19221|THRB_M	23,92	24,1	23,3	23,7	23,7	23,4	24	24	24	23,2	23	23	23,2	22,9	23	23	23,1	23,5	23,818	23,1258	F2	-0,7	23,5	-5,44	5E-05	0,0007	1,6
>sp|Q8K1J6|TRNT1_M	17,17	17,5	18,1	17,1	17,6	17,9	18	18	18	18,5	18	18	18,6	18,6	19	19	18,9	19,3	17,678	18,6136	Trnt1	0,94	18,1	5,436	5E-05	0,0007	1,6
>sp|P10493|NID1_M	20,07	20,2	19,7	19,4	20,2	20,2	20	20	20	19,5	20	19	19,1	19	20	19	19,4	19,3	19,955	19,3828	Nid1	-0,6	19,7	-5,43	5E-05	0,0007	1,5
>sp|P62874|GBB1_M	22,54	22,5	23,1	22,3	22	23,2	22	23	23	22,1	21	22	20,9	21,5	21	21	21,7	21,6	22,59	21,3804	Gnb1	-1,2	22	-5,41	5E-05	0,0007	1,5
>sp|Q68FD5|CLH1_M	21,63	21,9	21,4	21,6	21,6	21,8	22	22	22	21,2	21	21	21,4	21,4	21	21	21,5	21,1	21,661	21,286	Cltc	-0,4	21,5	-5,39	6E-05	0,0008	1,5
>sp|Q9JKS4|LDB3_M(	19,45	19,6	19	18,7	18,4	18,7	19	19	19	18,4	18	18	18,4	18	18	18	18,2	17,9	18,98	18,2007	Ldb3	-0,8	18,6	-5,38	6E-05	0,0008	1,4
>sp|Q9R098|HGFA_M	18,24	18,5	19,1	18,6	18,3	18,6	18	19	18	18,1	17	18	17,9	17,8	18	18	17,9	18	18,559	17,8673	Hgfac	-0,7	18,2	-5,38	6E-05	0,0008	1,4
>sp|Q61207|SAP_MO	21,35	21,6	22	22,4	20,1	21,7	21	19	21	18,6	19	18	18,9	18,8	20	17	18,6	18	21,085	18,5698	Psap	-2,5	19,8	-5,38	6E-05	0,0008	1,4
>sp|P07628|K1KB8_	20,5	20,1	19,4	21,5	20,9	19,3	22	20	21	17,2	18	19	18,2	18,8	17	19	19	19,4	20,508	18,3832	Klk1b8	-2,1	19,4	-5,37	6E-05	0,0008	1,4
>sp|O55111|DSG2_M	18,28	18,2	18,2	17,9	19,1	18,7	19	19	19	17,4	18	18	17,9	17,6	18	16	17,2	17,2	18,5	17,4481	Dsg2	-1,1	18	-5,36	6E-05	0,0008	1,4
>sp|Q9JKA5|GPA33_	17,59	17,9	17,7	17,7	17,4	17,8	17	18	18	18,5	19	18	18,6	18,6	19	18	17,7	17,9	17,687	18,3662	Gpa33	0,68	18	5,36	6E-05	0,0008	1,4
>sp|P56399|UBP5_M	21,01	21,4	21,4	20,5	21,3	20,6	21	21	21	20,3	20	20	20,1	19,9	19	20	20,4	20,1	21,029	20,1279	Usp5	-0,9	20,6	-5,35	6E-05	0,0008	1,4

>sp|Q91Y97|ALDOB_I	28,1	28,4	27,6	27,6	27,3	27,6	28	27	27	26	27	26	26,1	26,2	26	28	26,1	26,1	27,575	26,3638	Aldob	-1,2	27	-5,34	6E-05	0,0008	1,4
>sp|Q9D1J1|NECP2_I	0	0	0	0	0	0	0	0	0	0	16	0	15,7	16,1	16	16	15	14,6	0.00000	12,1883	Necap2	12,2	6,09	5,337	6E-05	0,0008	1,3
>sp|Q61838|PZP_MC	24,37	24,1	24,2	24,1	24,4	24,1	24	25	25	23,9	24	24	24	23,7	24	23	23,4	23,4	24,368	23,6406	Pzp	-0,7	24	-5,33	6E-05	0,0008	1,3
>sp|P05977|MYL1_M	19,93	19,8	19,4	20,3	20,7	20,8	21	20	21	18,3	18	19	18,6	19,3	19	19	19,8	19,1	20,292	18,8997	Myl1	-1,4	19,6	-5,32	6E-05	0,0008	1,3
>sp|Q8QZR3|EST2A_M	21,12	19,5	20,6	18,3	20,1	20,4	20	21	20	21,4	22	21	21,6	21,3	22	22	22	21,4	20,095	21,5981	Ces2a	1,5	20,8	5,294	7E-05	0,0009	1,3
>sp|P30677|GNA14_	14,65	16,8	16,9	17,1	17,3	16,9	16	15	16	18,3	18	18	17,9	17,7	19	18	18,8	18,5	16,319	18,1655	Gna14	1,85	17,2	5,281	7E-05	0,0009	1,2
>sp|Q9ET54|PALLD_M	18,84	18,4	19,2	18,4	19,1	18,9	18	19	19	17,9	18	18	18,2	18,5	18	18	17,8	17,8	18,762	18,0169	Palld	-0,7	18,4	-5,28	7E-05	0,0009	1,2
>sp|P01872|IGHM_M	22,48	22,7	22,3	22,7	22,4	22,7	23	22	23	22,1	22	22	22,4	22,2	22	22	22,1	21,5	22,605	21,9771	Ighm	-0,6	22,3	-5,27	7E-05	0,0009	1,2
>sp|P35700|PRDX1_	27,6	27,7	25,8	26,1	25,7	26,8	27	25	26	24,7	25	24	25,4	24,9	25	25	24,9	24,8	26,387	24,7965	Prdx1	-1,6	25,6	-5,27	7E-05	0,0009	1,2
>sp|Q9Z2X1|HNRPF_I	20,2	20	19,5	19,9	19,5	19,1	19	19	19	17,8	18	19	18,5	18,5	19	19	18,9	18,2	19,537	18,4464	Hnrnpf	-1,1	19	-5,25	7E-05	0,001	1,2
>sp|Q61703|ITIH2_M	24,48	24,2	25	24,4	24,7	24,8	24	25	25	23,4	24	24	24,1	23,6	24	24	23,4	23,3	24,591	23,7696	Itih2	-0,8	24,2	-5,25	7E-05	0,001	1,2
>sp|Q8BGZ7|K2C75_	21,15	20	20,8	19,8	20,1	20,5	20	20	20	21	22	21	21,2	21,6	21	23	22,5	22,5	20,144	21,7006	Krt75	1,56	20,9	5,229	8E-05	0,001	1,1
>sp|P21279|GNAQ_M	16,86	17,6	17,8	17,8	17,6	17,4	16	17	17	18,4	18	18	17,9	17,9	18	18	19	18,6	17,303	18,3381	Gnaq	1,03	17,8	5,212	8E-05	0,001	1,1
>sp|Q60854|SPB6_M	23,88	23,2	23,5	24	23,4	23,7	24	23	24	22,6	22	22	22,5	22,7	23	23	23	22,7	23,568	22,5308	Serpinb6	-1	23	-5,2	8E-05	0,001	1,1
>sp|Q63836|SBP2_M	23,11	23	22,8	22	23	22,8	23	23	23	22,5	22	22	21,8	21,9	22	22	21,9	22,5	22,79	22,0577	Selenbp2	-0,7	22,4	-5,19	8E-05	0,001	1,1
>sp|Q9CXN7|PBLD2_	21,45	21,3	22,2	21,8	22,6	22,1	22	22	22	22,8	23	23	22,7	22,7	23	23	22,8	22,9	21,981	22,803	Pbld2	0,82	22,4	5,19	8E-05	0,0011	1
>sp|O35206|COFA1_	16,15	16,9	16	16,5	16,6	16,9	17	17	17	19,4	19	19	17	17,5	17	19	18,2	18,2	16,687	18,3437	Col15a1	1,66	17,5	5,148	9E-05	0,0011	1
>sp|Q9QZH3|PPIE_MC	17,94	17,7	17,9	18,2	17,7	17,8	18	18	18	17,1	15	17	17	15,1	17	17	16,4	17,1	17,885	16,4773	Ppie	-1,4	17,2	-5,13	9E-05	0,0012	0,9
>sp|O54891|LEG6_M	19,35	18,2	18,9	18,1	18,2	19,1	19	19	19	19,7	19	20	19,5	19,1	19	20	20	20,1	18,682	19,5908	Lgals6	0,91	19,1	5,111	1E-04	0,0012	0,9
>sp|Q07797|LG3BP_	22,12	21,5	21,5	21,4	21,5	21,1	21	20	22	20,1	20	21	19,3	19,5	18	20	19,2	20,2	21,36	19,7555	Lgals3bp	-1,6	20,6	-5,1	1E-04	0,0013	0,9
>sp|P68368|TBA4A_	25,12	24,7	24,4	24,3	24,8	24,4	24	25	25	24,1	24	24	24,1	23,8	24	24	24	24,1	24,699	24,0433	Tuba4a	-0,7	24,4	-5,09	1E-04	0,0013	0,8
>sp|P21995|EMB_M(	16,02	16,6	14,4	16,2	14,8	16,3	15	16	14	17,7	17	17	17,8	17,4	18	16	18,1	16,2	15,409	17,3347	Emb	1,93	16,4	5,076	1E-04	0,0013	0,8
>sp|Q9R0Q7|TEBP_M	22,16	21,6	21,4	20,9	21,9	21,1	20	22	22	20,6	21	21	19,5	19,2	20	20	19,9	19,9	21,432	20,1448	Ptges3	-1,3	20,8	-5,03	1E-04	0,0014	0,7
>sp|Q8BKC5|IPO5_M	20,48	20,5	20,9	20,4	20,9	20,6	21	21	21	21,2	21	21	20,8	21,1	21	21	21,2	21,2	20,643	21,0321	Ipo5	0,39	20,8	4,991	1E-04	0,0015	0,6
>sp|E9Q414|APOB_M	17,25	16,7	17,3	17,5	17,1	17	17	17	17	17,8	17	18	18,5	18,7	18	18	17,9	17,6	17,117	17,9705	Apob	0,85	17,5	4,987	1E-04	0,0015	0,6
>sp|Q9QZB9|DCTN5_I	17,12	18,2	18,9	17,9	17,4	18,5	18	19	19	19	19	19	19,9	19,5	19	19	19,1	18,8	18,176	19,312	Dctn5	1,14	18,7	4,98	1E-04	0,0016	0,6
>sp|Q91YT0|NDUV1_I	20,41	20,1	21	20,1	20,7	20,8	20	20	21	21,7	22	21	20,7	21,1	21	21	21,7	21,6	20,432	21,3607	Ndufv1	0,93	20,9	4,962	1E-04	0,0016	0,6
>sp|Q06890|CLUS_M	20,31	20,3	19,6	20,3	21	20,2	20	20	20	21,1	21	21	21,1	21,1	21	21	21	20,7	20,237	20,9783	Clu	0,74	20,6	4,945	1E-04	0,0017	0,5
>sp|Q3UEB3|PUF60_I	17,75	17,6	17,4	17,7	17,4	17,4	17	17	18	17,4	17	16	17,1	16,6	17	16	16,7	16,6	17,485	16,7471	Puf60	-0,7	17,1	-4,94	1E-04	0,0017	0,5
>sp|P09103|PDIA1_I	22,46	22,3	22,4	21,9	22,2	22,3	23	22	23	22,9	23	23	22,5	22,7	23	23	23	22,6	22,353	22,8305	P4hb	0,48	22,6	4,939	1E-04	0,0017	0,5
>sp|P62962|PROF1_	26,78	27,6	26,3	26,9	27,6	28,4	27	28	28	26,2	25	26	25,9	26	26	27	26	25,7	27,397	25,985	Pfn1	-1,4	26,7	-4,94	1E-04	0,0017	0,5
>sp|Q88545|CSN6_M	21,92	21,9	21,6	22,1	22,1	22,1	22	22	22	21,3	20	20	20,6	20,9	21	21	19,8	21,5	22,002	20,7374	Cops6	-1,3	21,4	-4,93	1E-04	0,0017	0,5
>sp|P55292|DSC2_M	20,3	19,9	20	19,5	20,4	20,6	21	20	21	19,3	19	19	19,3	19,5	20	20	19,3	19,4	20,297	19,4454	Dsc2	-0,9	19,9	-4,93	1E-04	0,0017	0,5
>sp|P28076|PSB9_M	24,54	24,5	25	25,3	25,4	25,2	22	26	24	22,9	23	22	23,2	22,5	23	23	23,2	22,2	24,678	22,7277	Psmb9	-2	23,7	-4,92	1E-04	0,0017	0,5
>sp|P53811|PIPNB_I	17,42	17,6	16,4	17,6	17,6	18,2	18	18	17	18,8	18	18	18,8	18,3	19	19	19	19	17,552	18,6361	Pitpnb	1,08	18,1	4,898	2E-04	0,0018	0,4
>sp|Q99KR8|FUCO2_	19,52	17,5	18	20,6	20,4	20,7	21	21	18	21,8	22	22	21,8	22	22	22	21,8	21,8	19,666	21,8925	Fuca2	2,23	20,8	4,887	2E-04	0,0018	0,4
>sp|P19157|GSTP1_I	26,47	25,4	27,7	26,7	27,6	27,5	26	28	27	26	26	26	25,5	24,8	25	26	25,7	25,5	26,95	25,5541	Gstp1	-1,4	26,3	-4,87	2E-04	0,0019	0,4
>sp|P17563|SBP1_M	23,21	23,1	22,9	22,1	23,1	22,9	23	23	23	22,6	22	22	21,8	22,2	22	22	22,1	22,7	22,911	22,2415	Selenbp1	-0,7	22,6	-4,86	2E-04	0,0019	0,4
>sp|Q9R0P5|DEST_M(	26,4	25,5	25,9	26,4	26,2	24,9	26	25	25	24,8	24	25	24,9	24,7	25	25	24,9	24,7	25,736	24,8086	Dstn	-0,9	25,3	-4,84	2E-04	0,002	0,3
>sp|P63005|LIS1_MC	24,18	23,8	23,5	23,6	24,4	23,9	24	24	24	23,1	22	23	23,2	23,1	23	24	23,1	23,4	23,862	23,1326	Pafah1b1	-0,7	23,5	-4,81	2E-04	0,0021	0,3
>sp|O70251|EF1B_M	21,22	21,5	20,4	20,9	21	21	21	20	21	20,3	20	19	18,9	18,7	16	19	18,8	19,5	20,896	18,801	Eef1b	-2,1	19,8	-4,79	2E-04	0,0022	0,2
>sp|Q8CH72|TRI32_M	0	0	0	0	0	0	0	15	15	16,7	14	15	15,1	12,8	14	14	12,3	13,3	3.37632	14,1433	Trim32	10,8	8,76	4,783	2E-04	0,0022	0,2
>sp|P61087|UBE2K_	19,84	20,4	19,7	20	19,9	19,7	20	20	21	20,5	20	21	20,5	20,7	21	21	20,5	20,4	20,01	20,5485	Ube2k	0,54	20,3	4,747	2E-04	0,0024	0,1
>sp|P61290|PSME3_	21	20,8	20,9	21,5	21,4	21,6	21	22	22	22,4	23	22	22,1	21,4	22	22	21,9	22,2	21,304	22,0393	Psme3	0,74	21,7	4,718	2E-04	0,0025	0,1
>sp|P01756|HVM12	22,55	22,9	22,2	22,7	22	21,9	22	23	23	22	21	20	19,9	21,7	21	22	21,5	20,9	22,501	21,1588	>sp|P017	-1,3	21,8	-4,72	2E-04	0,0025	0,1
>sp|P01757|HVM13	22,55	22,9	22,2	22,7	22	21,9	22	23	23	22	21	20	19,9	21,7	21	22	21,5	20,9	22,501	21,1588	>sp|P017	-1,3	21,8	-4,72	2E-04	0,0025	0,1
>sp|Q62159|RHOC_M	22,27	22,5	22,3	23,4	21,9	23,1	23	22	22	22,3	21	21	21,4	21,4	22	21	21	21,4	22,495	21,3634	Rhoc	-1,1	21,9	-4,71	2E-04	0,0025	0
>sp|P34884|MIF_MO	24,11	23,8	23,5	23,7	23,5	23,4	24	25	25	25,1	26	25	25,4	25,9	26	25	24,9	25,2	24,055	25,3545	Mif	1,3	24,7	4,699	2E-04	0,0026	0

>sp|Q8R2Y2|MUC18_	14,13	15,8	14,7	14,5	15,4	13,7	15	15	16	16,1	16	17	16,6	16	16	16	16,1	15,7	14,879	16,0887	Mcam	1,21	15,5	4,683	2E-04	0,0026	-0
>sp|P12382|PFKAL_I	20,91	20,8	20,2	20,8	20,6	20,5	21	21	21	20,3	19	20	20,3	19,9	20	20	20,3	19,5	20,777	19,8928	Pfkl	-0,9	20,3	-4,68	2E-04	0,0026	-0
>sp|P09528|FRIH_M(	28,48	28,4	27,6	28,5	28,3	28,5	29	29	28	27,4	28	28	27,9	26,9	28	28	27,8	27,9	28,374	27,6774	Fth1	-0,7	28	-4,63	3E-04	0,0029	-0
>sp|Q08943|SSRP1_I	19,24	18,9	19,1	18,9	19,2	16,8	19	19	19	17,7	18	17	16,6	16,9	17	18	17,6	17,6	18,739	17,3627	Ssrp1	-1,4	18,1	-4,62	3E-04	0,003	-0
>sp|Q91UZ5|IMPA2_I	18,49	18,3	20,5	19,5	20,4	20,6	20	20	21	20,9	22	21	21,7	21,6	21	21	21,5	21,3	19,92	21,3747	Impa2	1,45	20,6	4,617	3E-04	0,003	-0
>sp|P10126|EF1A1_I	24,59	24,7	25	24,7	24,8	25,2	25	25	26	24,4	24	24	24,5	24,5	24	24	24,4	24,6	24,982	24,439	Eef1a1	-0,5	24,7	-4,62	3E-04	0,003	-0
>sp|P00688|AMYP_M	25,18	25,3	24,9	26,3	25,9	25,7	26	25	25	25	24	24	24,5	24,4	25	25	25	24,7	25,473	24,6114	Amy2	-0,9	25	-4,61	3E-04	0,003	-0
>sp|Q9CQ60|6PGL_M	22,18	22,2	22,1	21,5	21,5	22	22	22	22	22,5	22	22	22,6	22,1	23	22	22,5	22,6	21,94	22,4994	Pgls	0,56	22,2	4,599	3E-04	0,0031	-0
>sp|Q9CPW4|ARPC5	20,06	20,2	21,4	21,1	20,9	21,4	21	22	21	22,4	22	21	22,1	22,2	22	22	21,8	21,7	20,979	21,9968	Arpc5	1,02	21,5	4,594	3E-04	0,0031	-0
>sp|P16045|LEG1_M	23,23	23,1	23,1	23,4	23,1	23,1	23	23	23	22,6	23	22	22,8	22,4	23	22	22,9	23,2	23,173	22,6379	Lgals1	-0,5	22,9	-4,59	3E-04	0,0031	-0
>sp|Q9D8I3|GLOD5_M	20,71	20	20	20,2	20,6	20,7	21	21	21	22	21	22	21,4	21,2	22	22	20,8	21,3	20,528	21,3813	Glod5	0,85	21	4,588	3E-04	0,0031	-0
>sp|Q9DB16|CB39L_	19,05	18,2	16,9	17,1	16,9	16,9	18	17	17	18,7	20	19	18,3	18,4	18	19	18,9	19,4	17,461	18,9525	Cab39l	1,49	18,2	4,579	3E-04	0,0032	-0
>sp|P20918|PLMN_M	22,25	22,5	22,3	22,5	21,3	22,2	22	22	22	21,2	21	21	21,7	21,8	21	21	21,5	21,4	22,083	21,4173	Plg	-0,7	21,8	-4,56	3E-04	0,0033	-0
>sp|O70209|PDLI3_M	17,03	17,2	17,5	17,5	16,5	17,5	17	17	16	15,7	16	16	16,1	15,8	17	17	16,6	16	17,101	16,0836	Pdlim3	-1	16,6	-4,55	3E-04	0,0033	-0
>sp|Q5SW19|CLU_MC	21,06	21,3	21,9	21,6	21,5	21,6	22	22	21	20,6	21	21	20,7	21,1	21	21	21,2	21,2	21,57	20,9592	Cluh	-0,6	21,3	-4,53	3E-04	0,0034	-0
>sp|O08738|CASP6_	22,3	22,3	21,8	22,2	22,2	22,4	23	22	22	21,5	21	21	22,2	21,5	22	22	21,8	21,7	22,358	21,683	Casp6	-0,7	22	-4,52	3E-04	0,0035	-0
>sp|Q812C9|AOC2_M	20,46	19,9	19,6	19,6	20,2	20,1	20	20	20	18,9	20	20	18,9	19,6	19	19	19,4	19,7	20,012	19,3845	Aoc2	-0,6	19,7	-4,51	3E-04	0,0036	-0
>sp|Q91XD2|LIMS2_M	20,78	20,6	21	21,1	20,8	20,8	21	21	21	20,4	20	19	20,7	20,1	20	21	20,1	20	20,984	20,2334	Lims2	-0,8	20,6	-4,51	3E-04	0,0036	-0
>sp|Q9JM62|REEP6_I	16,75	16,9	16	15,5	16,7	17,3	17	17	17	18,9	18	17	17,6	17,5	17	19	17,7	18,8	16,63	17,9916	Reep6	1,36	17,3	4,505	3E-04	0,0036	-0
>sp|Q9QUR6|PPCE_M	21,96	22,1	21,4	22	22,4	21,7	22	22	22	23	23	23	22,2	22,3	22	23	23	23	21,995	22,7191	Prep	0,72	22,4	4,504	3E-04	0,0036	-0
>sp|Q02248|CTNB1_	20,41	20,2	20,7	20,8	20,5	20,4	21	21	20	20,8	21	21	20,8	20,9	21	22	21,3	21,6	20,507	21,1267	Ctnnb1	0,62	20,8	4,496	3E-04	0,0037	-0
>sp|Q8CJ53|CIP4_M(	18,83	19,1	19,5	18,9	19	18,9	19	19	19	19,9	19	21	20,5	20,2	20	19	20,2	20,3	19,017	20,0825	Trip10	1,07	19,5	4,491	4E-04	0,0037	-0
>sp|Q9CXW3|CYBP_M	20,85	19,6	21,1	20,8	20	21,4	21	20	20	21,7	21	22	21,5	21,3	21	22	21,7	21,2	20,574	21,4699	Cacybp	0,9	21	4,482	4E-04	0,0037	-0
>sp|P50543|S10AB_	17,68	21	20,9	22	17,5	18,2	20	21	19	19,1	17	15	15,8	15,4	17	16	17,3	16,5	19,625	16,563	S100a11	-3,1	18,1	-4,47	4E-04	0,0038	-0
>sp|Q9CZ13|QCR1_M	20,38	22,8	20,1	20,5	20,4	20,3	20	20	22	21,9	22	22	21,9	21,9	22	22	22,4	22,4	20,72	22,0901	Uqcrc1	1,37	21,4	4,466	4E-04	0,0038	-0
>sp|Q922U2|K2C5_M	22,19	21,8	22,6	21,8	22,1	22,1	22	21	22	22,5	23	22	22,4	23,3	22	24	23,7	24,1	21,964	23,1103	Krt5	1,15	22,5	4,465	4E-04	0,0038	-0
>sp|Q60668|HNRPD_	18,07	19,3	18,4	18,5	19,3	19,2	19	19	19	18,2	21	20	20,5	19,9	21	20	20,4	20,2	18,82	20,1255	Hnrnpd	1,31	19,5	4,429	4E-04	0,0041	-1
>sp|P10107|ANXA1_	16,01	20,9	19,4	20,2	18,6	18,2	20	19	20	16,3	18	17	17,2	16,9	16	16	16,7	16,3	19,202	16,8446	Anxa1	-2,4	18	-4,41	4E-04	0,0043	-1
>sp|P54265|DMPK_I	19,25	19,4	19,9	18,7	18,7	18,8	19	19	19	18,5	18	18	18,6	18,6	19	19	18,4	18,1	19,116	18,4453	Dmpk	-0,7	18,8	-4,4	4E-04	0,0044	-1
>sp|P53808|PPCT_M	15,43	17	16,2	14,9	16,9	17,7	17	17	16	18,2	19	18	18,1	17,9	18	17	17,6	18,1	16,547	18,038	Pctp	1,49	17,3	4,389	4E-04	0,0044	-1
>sp|Q9QUI0|RHOA_M	22,25	22,7	22,9	23,4	22	23,2	23	23	22	22,6	21	22	21,5	21,7	22	21	21,4	21,4	22,652	21,6598	Rhoa	-1	22,2	-4,38	4E-04	0,0045	-1
>sp|Q8R0Y6|AL1L1_M	23,75	23,5	23,1	23,1	23,3	23,1	23	23	24	23,2	22	23	23	22,4	23	22	22,7	23,2	23,397	22,7099	Aldh1l1	-0,7	23,1	-4,38	4E-04	0,0045	-1
>sp|P97447|FHL1_M	22,52	21,9	22,3	21,9	23,1	23	23	23	23	21,3	20	22	21	21,7	21	22	22,3	20,7	22,557	21,3905	Fhl1	-1,2	22	-4,38	4E-04	0,0045	-1
>sp|Q8BFZ3|ACTBL_M	27,62	27,6	26,1	27,7	27,6	27,6	28	26	26	25,7	26	26	25,5	25,4	26	27	26,2	26,2	27,269	25,9551	Actbl2	-1,3	26,6	-4,37	4E-04	0,0045	-1
>sp|P26369|U2AF2_	17,48	17,2	17,6	16,6	17,1	17,7	17	18	18	16,3	17	17	15,8	16,1	17	17	16,5	16,3	17,415	16,4951	U2af2	-0,9	17	-4,37	4E-04	0,0045	-1
>sp|P59235|NUP43_	0	0	0	0	0	14	15	16	0	16,1	17	16	15,3	14,8	17	16	17,8	16	5.07405	16,1413	Nup43	11,1	10,6	4,37	5E-04	0,0045	-1
>sp|Q64467|G3PT_M	22,2	22,5	22,8	23,1	22	22,8	23	23	23	21,4	22	22	21,8	22,3	22	22	21,2	22	22,628	21,8354	Gapdhs	-0,8	22,2	-4,37	5E-04	0,0046	-1
>sp|Q99JI4|PSMD6_M	18,29	18,8	20,5	18,6	19,1	19,4	20	21	19	17	19	18	17,9	16,9	18	18	18,1	18	19,38	17,862	Psmd6	-1,5	18,6	-4,34	5E-04	0,0048	-1
>sp|P62307|RUXF_M	19,82	17,9	19,3	20	19,5	19,5	20	20	20	20,8	20	20	21,6	21,3	22	21	21	21	19,435	20,8261	Snrpf	1,39	20,1	4,335	5E-04	0,0048	-1
>sp|Q11011|PSA_MC	21,83	22,2	21,3	21,9	21,6	21,6	22	23	22	23,1	23	23	23	22,8	23	23	22,9	22,7	22,036	22,9337	Npepps	0,9	22,5	4,33	5E-04	0,0049	-1
>sp|Q91W89|MA2C1	20,14	20	19,5	20,3	19,8	19,9	20	20	20	19,6	20	19	18,9	19	19	19	19,8	19,6	19,931	19,344	Man2c1	-0,6	19,6	-4,32	5E-04	0,005	-1
>sp|Q9DBG6|RPN2_M	16,98	17,6	18	17,9	17,8	18	18	18	19	18,9	18	19	18,5	18,7	19	18	18,6	18,8	17,897	18,6191	Rpn2	0,72	18,3	4,305	5E-04	0,0051	-1
>sp|O88958|GNPI1_I	20,26	20	19,7	19,4	19,8	19,7	20	20	20	21,8	19	22	21,8	21,3	22	21	21,1	21,5	19,857	21,2578	Gnpda1	1,4	20,6	4,303	5E-04	0,0051	-1
>sp|Q9DD02|HIKES_M	0	0	16	0	0	0	0	16	16	15,7	16	17	16,7	17,4	17	17	16,6	16,7	5.33152	16,6739	Hikeshi	11,3	11	4,298	5E-04	0,0051	-1
>sp|Q9JI48|PLAC8_M	21,13	21,7	21,2	21,1	23,6	21,1	22	22	22	23,9	24	23	22,3	23,3	22	23	24,3	24,3	21,802	23,4471	Plac8	1,64	22,6	4,296	5E-04	0,0051	-1
>sp|P06151|LDHA_M	24,29	24,2	23,6	24,4	24,6	24,4	24	25	25	24	23	23	23,1	23,7	24	24	23,8	24,1	24,314	23,6747	Ldha	-0,6	24	-4,3	5E-04	0,0051	-1
>sp|Q8C570|RAE1L_I	21,98	22,7	23,1	23,6	23,7	22,5	23	23	23	22,5	23	22	21,3	22	22	22	22	21,2	23,031	21,9875	Rae1	-1	22,5	-4,29	5E-04	0,0051	-1
>sp|Q93092|TALDO_I	23,07	24	22,3	22,3	22,7	22,1	23	22	23	23,9	23	23	24,1	23,5	24	24	23,9	23,4	22,72	23,6698	Taldo1	0,95	23,2	4,294	5E-04	0,0051	-1

>sp|Q8CHR6|DPYD_M	20,53	20,3	20,5	19,7	19,8	19,9	20	20	20	22,9	23	23	23	22,8	23	19	19,9	22,9	20,108	22,1853	Dpyd	2,08	21,1	4,291	5E-04	0,0051	-1
>sp|Q9DCV7|K2C7_M	20,55	20	20,1	19,8	19,9	19,7	19	20	19	21,7	21	22	20,2	20,6	20	22	21,1	21,4	19,732	21,0337	Krt7	1,3	20,4	4,286	5E-04	0,0052	-1
>sp|O88428|PAPS2_	21,89	22,1	22,3	22,4	22,3	22,2	22	23	23	21,7	22	22	21,9	21,8	22	22	21,7	21,8	22,343	21,8261	Papss2	-0,5	22,1	-4,27	6E-04	0,0053	-1
>sp|P43275|H11_MO	19,16	19,3	18,7	18,6	19,3	18,6	18	19	18	17	19	18	18	18	18	17	15,8	16,7	18,759	17,3788	Hist1h1a	-1,4	18,1	-4,24	6E-04	0,0056	-1
>sp|Q9CQC2|COL_MO	22,87	22,6	23	22,9	22,7	23,1	22	22	22	21,5	22	22	22,1	22,5	22	22	22,1	22,1	22,677	21,989	Clps	-0,7	22,3	-4,23	6E-04	0,0057	-1
>sp|Q921M7|FA49B_	20,56	20	20,3	20,2	20,4	19,8	20	20	20	20,2	19	20	19,4	19,6	20	20	19,2	19,4	20,19	19,6119	Fam49b	-0,6	19,9	-4,22	6E-04	0,0058	-1
>sp|Q5SQX6|CYFP2_M	17,08	16,4	16,8	15,5	16,3	15,7	16	17	16	15,7	14	15	15,2	12,1	14	15	14,9	15,4	16,449	14,6241	Cyfip2	-1,8	15,5	-4,22	6E-04	0,0058	-1
>sp|Q9JK81|MYG1_M	21,03	21,5	21,3	21,3	21,2	21,5	21	22	22	22	22	22	22,1	21,9	22	22	21,7	21,9	21,468	22,044	Myg1	0,58	21,8	4,221	6E-04	0,0058	-1
>sp|P61021|RAB5B_	22,34	21,6	20,6	21,4	21,3	21,6	21	21	21	22,3	22	22	22,2	21,7	22	22	22,2	22,1	21,352	22,1428	Rab5b	0,79	21,7	4,201	6E-04	0,0061	-1
>sp|Q8BP67|RL24_M	18,48	17,8	17,6	17,6	17,5	18,3	18	17	16	19,1	18	19	18,2	19,6	20	19	19,1	19,4	17,708	19,0276	Rpl24	1,32	18,4	4,191	7E-04	0,0062	-1
>sp|P70412|CUZD1_	20,24	20,3	19,9	20	19,8	19,5	20	20	20	20,1	21	20	20,1	20,4	21	20	20,6	20,7	19,933	20,4331	Cuzd1	0,5	20,2	4,184	7E-04	0,0063	-1
>sp|Q8R4V5|OIT3_MO	17,06	17,6	17,5	17,1	16,9	16,6	17	17	16	16,6	15	17	15,2	15,8	15	16	16,2	16,2	17,002	15,9801	Oit3	-1	16,5	-4,18	7E-04	0,0063	-1
>sp|P15864|H12_MO	18,77	18,9	18,3	18,1	18,9	18,2	18	18	18	16,6	18	18	17,5	17,6	17	16	15,4	16,3	18,346	16,9656	Hist1h1c	-1,4	17,7	-4,17	7E-04	0,0064	-1
>sp|P43274|H14_MO	18,77	18,9	18,3	18,1	18,9	18,2	18	18	18	16,6	18	18	17,5	17,6	17	16	15,4	16,3	18,346	16,9656	Hist1h1e	-1,4	17,7	-4,17	7E-04	0,0064	-1
>sp|P43277|H13_MO	18,57	18,8	18,2	18	18,7	18,1	18	18	18	16,4	18	18	17,4	17,4	17	16	15,1	16,1	18,183	16,7915	Hist1h1d	-1,4	17,5	-4,16	7E-04	0,0065	-1
>sp|Q920M5|CORO6	19,86	19,2	20,7	19,4	20,9	20,6	21	21	21	19	19	19	19,4	19,7	20	19	19,4	19,2	20,5	19,2238	Coro6	-1,3	19,9	-4,16	7E-04	0,0065	-1
>sp|Q8BH86|GLUCM_	19,7	19,8	20,6	20,8	20,5	20,8	20	21	21	21,8	21	22	21,5	21,3	21	21	20,8	20,8	20,441	21,247	Dglucy	0,81	20,8	4,16	7E-04	0,0065	-1
>sp|P70697|DCUP_M	20,13	19,1	19,3	19,1	18,9	19,2	19	19	20	20,6	20	20	19,7	19,9	20	20	20,6	20,5	19,317	20,0835	Urod	0,77	19,7	4,129	8E-04	0,0069	-1
>sp|O70258|SGCE_M	18,24	18,3	17,7	16,6	15,8	16,9	17	18	17	17,9	19	18	18,3	18,9	19	18	18,7	18,2	17,187	18,3936	Sgce	1,21	17,8	4,119	8E-04	0,007	-1
>sp|Q9DCG9|TR112_	0	15,7	0	0	14,7	0	0	0	0	16,1	0	17	16,8	17,1	18	17	17,8	17,7	3.37681	15,2566	Trmt112	11,9	9,32	4,084	8E-04	0,0075	-1
>sp|Q91VM9|IPYR2_M	17,41	18,5	17,3	18,5	19,2	18,7	19	20	20	20,7	20	20	20	19,7	20	20	19,6	19,7	18,628	19,8424	Ppa2	1,21	19,2	4,079	8E-04	0,0076	-1
>sp|Q05144|RAC2_M	21,26	21,5	22,7	21,9	21,8	20,6	22	22	21	20,6	21	20	21,1	21,2	20	19	20,7	20,6	21,636	20,5564	Rac2	-1,1	21,1	-4,08	8E-04	0,0076	-1
>sp|Q4KML4|ABRAL_	17,33	17,3	17,2	16,6	17,2	17,8	16	17	17	19,3	19	19	17,2	16,6	19	19	19,1	18,8	17,03	18,5355	Abracl	1,51	17,8	4,071	9E-04	0,0077	-1
>sp|P08030|APT_MO	21,24	21,7	21,7	21,9	21,6	21,5	21	22	22	22,3	22	22	22,5	22,1	22	22	21,7	22,2	21,608	22,1249	Aprt	0,52	21,9	4,07	9E-04	0,0077	-1
>sp|Q91VR5|DDX1_M	20,37	19,9	20,1	20,8	20,2	20,4	20	20	21	20,2	20	19	19,5	19,4	20	20	20	20,1	20,358	19,7537	Ddx1	-0,6	20,1	-4,07	9E-04	0,0077	-1
>sp|Q9JHR7|IDE_MOL	21,29	21,6	21,6	21,4	21,6	21,7	22	22	22	22,2	22	22	22,1	22	22	22	21,9	21,7	21,56	21,8678	Ide	0,31	21,7	4,068	9E-04	0,0077	-1
>sp|P29788|VTNC_M	17,77	17,9	19,6	17,6	17,9	17,8	18	18	18	19,6	20	20	18,6	19,9	20	18	19,2	18,2	18,045	19,2939	Vtn	1,25	18,7	4,065	9E-04	0,0077	-1
>sp|P70195|PSB7_M	24,76	23,8	23,8	23,8	24,3	23,5	24	23	23	23,1	23	23	22,4	23,3	23	23	23,4	22,5	23,82	22,989	Psmb7	-0,8	23,4	-4,06	9E-04	0,0078	-1
>sp|P97298|PEDF_M	21,7	23,1	21,9	21,8	23,1	23,6	23	23	24	21,9	22	21	21,8	20,9	22	22	21,5	22	22,73	21,6122	Serpinf1	-1,1	22,2	-4,06	9E-04	0,0078	-1
>sp|Q06138|CAB39_	19,34	19,1	17,8	18,9	17,9	17,5	19	20	19	19,9	20	20	19,4	19,6	20	20	19,7	20,3	18,723	19,928	Cab39	1,21	19,3	4,053	9E-04	0,0078	-1
>sp|P29391|FRIL1_M	27,75	27,5	25,8	28,2	28,5	27,3	27	28	28	26,5	26	26	26,5	26,4	26	27	25,7	26,4	27,59	26,322	Ftl1	-1,3	27	-4,05	9E-04	0,0078	-1
>sp|Q9Z1T1|AP3B1_M	15,48	16,3	15,5	15,6	15,3	15,2	16	16	15	16,2	17	16	16,4	16,6	17	17	16,2	15,3	15,568	16,3545	Ap3b1	0,79	16	4,05	9E-04	0,0078	-1
>sp|Q91WC0|SETD3_M	18,41	18,5	19	18,4	18,1	18,2	18	19	19	18,3	19	19	19,3	18,7	20	20	19,7	19,7	18,484	19,2972	Setd3	0,81	18,9	4,045	9E-04	0,0078	-1
>sp|Q91VS7|MGST1_M	16,65	17,3	17,7	17,4	16,8	16,6	17	16	17	17,1	18	18	17,7	18	18	17	18,2	17,9	16,946	17,8075	Mgst1	0,86	17,4	4,045	9E-04	0,0078	-1
>sp|P15626|GSTM2_	23,5	24,3	24,4	24,1	24,1	24,3	24	24	24	24,4	25	25	24,1	25	25	25	24,5	24,6	24,057	24,6011	Gstm2	0,54	24,3	4,044	9E-04	0,0078	-1
>sp|Q9WUM3|COR1B	21,72	21,6	22,1	22,1	22,2	22,3	22	22	22	21,2	21	21	22	21,4	22	22	21,3	21,3	22,037	21,3889	Coro1b	-0,6	21,7	-4,04	9E-04	0,0078	-1
>sp|P41105|RL28_M	16,41	17,4	18,4	17,9	18,5	17,2	18	18	18	17,4	19	20	20,5	19,6	19	20	18,5	19,8	17,751	19,3246	Rpl28	1,57	18,5	4,043	9E-04	0,0078	-1
>sp|Q8C0E3|TRI47_M	15,27	14,7	15,5	0	0	15,3	0	15	15	0	0	0	0	0	0	0	0	0	10,005	0.0000	Trim47	-10	5	-4,04	9E-04	0,0078	-1
>sp|Q8BMS1|ECHA_M	15,9	14	16,8	15,1	13,5	13,8	15	14	14	16,9	19	19	16,7	16,6	16	16	17	15,8	14,673	16,9458	Hadha	2,27	15,8	4,042	9E-04	0,0078	-1
>sp|Q61879|MYH10_	19,94	20,3	19,2	19,8	18,9	20,9	19	19	20	20,5	20	21	21	20,5	21	21	20,4	20,7	19,7	20,6821	Myh10	0,98	20,2	4,042	9E-04	0,0078	-1
>sp|O88312|AGR2_M	23,71	22,8	23	23,2	23,2	22,9	23	24	24	23,3	22	23	22,4	22,4	22	23	22	22,1	23,316	22,4406	Agr2	-0,9	22,9	-4,03	9E-04	0,008	-1
>sp|Q99J77|SIAS_MO	22,74	22,2	21,7	22,1	22,5	22,4	22	22	22	21,5	21	22	22,1	21,7	22	22	22	20,9	22,302	21,6611	Nans	-0,6	22	-4,03	9E-04	0,008	-1
>sp|P06345|HB2S_M	18,2	16,9	15,9	17,7	17	17,4	18	17	17	16,1	15	16	15,9	15,8	17	17	16,2	14	17,227	15,7881	H2-Ab1	-1,4	16,5	-4,03	9E-04	0,008	-1
>sp|P17427|AP2A2_	20,95	20,6	20,4	20,7	20,7	20,6	21	21	22	21,3	22	22	22,1	21	22	22	21,2	21,1	20,811	21,5797	Ap2a2	0,77	21,2	4,024	9E-04	0,008	-1
>sp|Q8BH95|ECHM_M	22,44	22,8	23,4	22,4	24	23,5	23	23	23	23,8	24	23	23,7	24,1	24	24	23,9	24	23,039	23,8127	Echs1	0,77	23,4	3,975	0,001	0,0089	-2
>sp|Q9Z331|K2C6B_	22,04	21,3	21,5	21,2	21,6	21,7	21	21	21	21,7	22	22	22	22,3	22	23	23	22,9	21,362	22,2542	Krt6b	0,89	21,8	3,949	0,001	0,0094	-2
>sp|P06745|G6PI_MO	24,44	23,9	23,9	24,5	24,2	24,5	24	25	24	24,7	25	25	24,7	24,5	25	25	24,8	24,9	24,336	24,7053	Gpi	0,37	24,5	3,942	0,001	0,0095	-2
>sp|Q9D0M5|DYL2_M	22,73	22,8	23,2	22,4	22,7	22,7	23	23	23	23,1	23	23	23,8	23,4	23	23	23,2	23	22,812	23,3087	Dynll2	0,5	23,1	3,942	0,001	0,0095	-2

>sp|Q9ESN6|TRIM2_M	0	0	0	0	0	0	0	13	14	15,5	14	14	14,2	14,1	14	15	15	0	2.96169	12,8567	Trim2	9,89	7,91	3,94	0,001	0,0095	-2
>sp|Q8K1R3|PNPT1_	0	0	0	0	0	0	0	0	0	9,01	13	14	13,8	12,2	14	0	0	0	0	8,43525	Pnpt1	8,44	4,22	3,937	0,001	0,0095	-2
>sp|Q99LB6|MAT2B_	19,75	19,8	19,9	19,9	19,6	19,9	20	20	20	20,8	21	21	20,5	20,3	20	20	20,1	20,4	19,98	20,5013	Mat2b	0,52	20,2	3,937	0,001	0,0095	-2
>sp|P07356|ANXA2_	24,17	24,1	23,8	23,8	23,9	24,1	24	25	25	21,3	24	24	22,9	22,8	23	23	23,1	21	24,153	22,7569	Anxa2	-1,4	23,5	-3,94	0,001	0,0095	-2
>sp|P51150|RAB7A_	23,43	22,9	22,9	23,7	22,2	22,8	23	23	23	22,4	22	22	22,5	21,7	23	22	22,6	22,5	22,955	22,2735	Rab7a	-0,7	22,6	-3,93	0,001	0,0095	-2
>sp|P63001|RAC1_M	21,97	22,2	23,1	22,4	22,8	21,8	22	22	22	21,5	22	22	21,9	22	21	21	21,4	21,4	22,373	21,616	Rac1	-0,8	22	-3,93	0,001	0,0095	-2
>sp|P14602|HSPB1_	21,31	21,6	20,6	20,7	20,7	20,6	21	21	20	19,8	20	20	20,5	20,4	21	20	20,3	20	20,844	20,1348	Hspb1	-0,7	20,5	-3,93	0,001	0,0095	-2
>sp|Q64285|CEL_MO	20,18	20,1	19,5	20,4	20,3	20,7	20	20	20	20,8	21	21	21,2	21,4	21	21	20,4	20,3	20,234	20,837	Cel	0,6	20,5	3,928	0,001	0,0095	-2
>sp|Q61133|GSTT2_M	24,28	24,4	23	24,5	24,1	23,6	24	24	24	23	23	23	23,7	23,5	23	24	23,4	23	24,023	23,2203	Gstt2	-0,8	23,6	-3,93	0,001	0,0095	-2
>sp|P80314|TCPB_M	22,85	21,1	22	20,7	22,5	21,6	22	22	21	21,5	20	20	20,6	20,3	20	20	20,4	20,7	21,698	20,47	Cct2	-1,2	21,1	-3,93	0,001	0,0095	-2
>sp|Q62267|SPR1B_	19,85	20,7	18,5	19,7	19,7	19,8	21	21	20	18,4	19	17	17,6	19,7	17	19	19,1	18,8	19,982	18,3884	Sprr1b	-1,6	19,2	-3,92	0,001	0,0096	-2
>sp|Q9DC50|OCTC_M	20,16	20,1	19,8	20,3	20,1	20,1	20	21	21	21,7	21	20	20,8	21,8	21	21	20,9	20,9	20,211	20,9735	Crot	0,76	20,6	3,918	0,001	0,0097	-2
>sp|Q9WVK4|EHD1_M	20,62	23,3	22,9	20,5	20,8	20,5	21	20	21	19,9	19	19	19,7	19,3	20	19	19,9	20,1	21,149	19,6521	Ehd1	-1,5	20,4	-3,92	0,001	0,0097	-2
>sp|Q7TPR4|ACTN1_I	23,16	22,8	22,4	22,6	22,7	22,8	23	23	23	22,4	22	23	22,4	22,4	23	22	22,6	22,3	22,856	22,3833	Actn1	-0,5	22,6	-3,91	0,001	0,0097	-2
>sp|Q6Q899|DDX58_	15,05	15,2	16,4	14,2	14,3	14,4	14	15	14	16	16	16	16,7	16,1	18	15	16	15,9	14,703	16,1848	Ddx58	1,48	15,4	3,902	0,001	0,0099	-2
>sp|Q8BK67|RCC2_M	21,22	20,7	20,5	21,8	21,8	21,4	22	21	21	21,9	22	22	22,1	22,1	22	22	21,9	21,3	21,23	21,9308	Rcc2	0,7	21,6	3,899	0,001	0,01	-2
>sp|P68372|TBB4B_	24,11	23,6	24,7	24	24,1	24,3	25	25	25	23,8	24	24	23,6	23,8	23	24	23,8	24,1	24,352	23,7504	Tubb4b	-0,6	24,1	-3,88	0,001	0,0103	-2
>sp|B2RQC6|PYR1_M	18,35	17,3	18	17,7	17,2	17	18	17	16	17,9	19	19	19	18,2	19	18	18	18,4	17,354	18,4221	Cad	1,07	17,9	3,878	0,001	0,0103	-2
>sp|Q9CR09|UFC1_M	20,88	21,2	20,5	21,1	20,8	20,2	20	20	21	22	21	21	22,4	22	22	22	20,6	22,3	20,706	21,6842	Ufc1	0,98	21,2	3,878	0,001	0,0103	-2
>sp|O88533|DDC_MO	20,07	20,8	20,7	19,6	20,5	20,3	21	21	21	21,1	21	21	21	21	21	21	21,6	21	20,532	21,1803	Ddc	0,65	20,9	3,875	0,001	0,0104	-2
>sp|P24472|GSTA4_I	23,44	23,8	21,9	23,6	23,1	23,1	23	24	23	24,8	22	24	24,9	25,1	25	25	24,8	24,5	23,19	24,4424	Gsta4	1,25	23,8	3,874	0,001	0,0104	-2
>sp|P05213|TBA1B_	25,25	24,8	25,4	24,5	25,3	24,9	25	26	25	24,6	25	24	25	24,6	24	24	24,2	24,7	25,1	24,535	Tuba1b	-0,6	24,8	-3,87	0,001	0,0104	-2
>sp|Q9CQE1|NPS3B_I	19,05	19,3	18,8	19,3	18,7	19	18	18	19	18,1	18	18	18,3	18,4	17	18	18,6	18,3	18,862	18,1533	Nipsnap3	-0,7	18,5	-3,87	0,001	0,0104	-2
>sp|P51881|ADT2_M	20,56	20	19,1	16,6	20,6	19,1	16	19	18	17,6	16	17	16,9	16,8	17	17	17,2	16,5	18,865	16,8139	Slc25a5	-2,1	17,8	-3,87	0,001	0,0104	-2
>sp|Q61316|HSP74_	21,34	21,1	20,8	21,2	21,1	21,7	21	21	21	21,6	21	22	21,6	21,3	22	22	22,4	22,4	21,23	21,8666	Hspa4	0,64	21,5	3,864	0,001	0,0105	-2
>sp|Q8BH64|EHD2_M	21,66	22	22	21,4	21,7	21,5	21	22	22	21,2	20	22	21,4	21,3	21	21	21,1	21	21,731	21,1225	Ehd2	-0,6	21,4	-3,86	0,001	0,0107	-2
>sp|Q99K28|ARFG2_	15,8	16,6	14,9	15,4	14,1	15	15	16	16	13,5	14	14	14,9	14,3	15	14	14,3	14,7	15,364	14,2603	Arfgap2	-1,1	14,8	-3,85	0,001	0,0107	-2
>sp|Q62318|TIF1B_M	17,87	19	16,7	19,2	16,7	17,4	19	19	19	16,2	16	17	17,1	17,2	17	17	16,8	16,3	18,3	16,7758	Trim28	-1,5	17,5	-3,85	0,001	0,0107	-2
>sp|Q62219|TGFI1_M	18,36	18,3	18,9	18,4	18,7	18,1	16	18	18	16,8	17	16	17,5	17,2	17	17	17,5	17,3	18,178	17,1257	Tgfb1i1	-1,1	17,7	-3,85	0,001	0,0107	-2
>sp|Q8BFW7|LPP_MO	20,55	20,6	19,9	19,9	20,5	20,9	20	20	20	17,9	20	21	17,8	18,1	18	19	18,8	18,2	20,309	18,7986	Lpp	-1,5	19,6	-3,85	0,001	0,0108	-2
>sp|Q64674|SPEE_M(	21,7	21,9	22	21,9	21,5	22	22	22	22	21,5	21	22	21,7	21,6	21	22	20,9	21,5	21,986	21,502	Srm	-0,5	21,7	-3,83	0,001	0,0111	-2
>sp|Q80XC2|TRM61_	20,79	0	15,7	0	0	0	0	0	16	16,2	17	17	16,1	16,7	17	18	17,5	17,2	5.80543	16,9671	Trmt61a	11,2	11,4	3,829	0,001	0,0111	-2
>sp|Q99KR3|LACB2_	22,6	22,1	21,8	21,7	22,3	22,1	22	22	23	20,2	22	21	20	21,4	22	22	21,3	20,2	22,196	21,0578	Lactb2	-1,1	21,6	-3,83	0,001	0,0111	-2
>sp|Q08091|CNN1_M	22,26	23	21,1	22,2	21,9	22	22	22	22	21,7	20	21	21,5	20,5	21	22	21,2	21,2	22,062	21,136	Cnn1	-0,9	21,6	-3,82	0,001	0,0112	-2
>sp|Q9D0F9|PGM1_M	22,75	22,5	22,3	22,1	22,6	22,2	22	22	23	22,5	23	23	23,2	23,1	23	23	22,9	22,6	22,38	22,8307	Pgm1	0,45	22,6	3,818	0,001	0,0113	-2
>sp|P18528|HVM57	19,73	20,4	20,3	20,6	20,5	19,9	20	21	20	19,8	19	20	20,2	19,7	19	19	18,9	17,7	20,325	19,3416	>sp|P185	-1	19,8	-3,81	0,001	0,0116	-2
>sp|Q9DBC7|KAP0_M	19,04	18,8	18,9	18,5	20	19,2	19	20	19	18,5	19	18	18,2	17,8	18	18	19,1	18	19,128	18,2631	Prkar1a	-0,9	18,7	-3,79	0,002	0,0119	-2
>sp|P84091|AP2M1_	21,42	21	20,1	20,9	19,7	20,7	23	21	21	22,1	21	22	22,4	22,2	23	22	22,5	21,9	20,877	22,0506	Ap2m1	1,17	21,5	3,785	0,002	0,012	-2
>sp|Q62351|TFR1_M	17,56	16,5	17,1	16,7	16,7	16,9	16	15	15	15,4	17	16	14	14,6	15	15	14,1	15	16,463	15,0481	Tfrc	-1,4	15,8	-3,78	0,002	0,012	-2
>sp|O70250|PGAM2_	20,4	22,2	21	22,4	19,4	21	22	20	20	19,6	18	20	20,6	18,7	19	20	18,4	19,7	20,989	19,394	Pgam2	-1,6	20,2	-3,78	0,002	0,0121	-2
>sp|Q64737|PUR2_M	20,76	21,2	19,7	19,6	20,5	19,4	21	21	21	19,2	19	19	19,5	19,2	20	20	19,1	20	20,356	19,4411	Gart	-0,9	19,9	-3,78	0,002	0,0121	-2
>sp|Q6ZWM4|LSM8_M	18,76	19,3	20,2	19,2	18,5	19,5	20	20	20	20,7	21	21	20,4	20,8	21	20	20,5	19,3	19,49	20,4945	Lsm8	1	20	3,772	0,002	0,0122	-2
>sp|P16015|CAH3_M	22,13	22,4	22,9	22,4	22,9	23,1	22	23	23	23,4	23	23	23,4	23,4	23	23	23,6	22,8	22,647	23,1686	Ca3	0,52	22,9	3,764	0,002	0,0124	-2
>sp|Q9CSH3|RRP44_	14,15	14,1	15,5	14,9	14,6	14,8	16	14	14	15,4	16	16	15,9	15,4	16	15	15,2	15,9	14,709	15,5763	Dis3	0,87	15,1	3,762	0,002	0,0125	-2
>sp|Q9D6P8|CALL3_I	20,75	21	20,5	20,9	20,3	20,3	20	20	20	18,9	15	19	19,7	19,9	18	20	19,4	17,8	20,534	18,6353	Caml3	-1,9	19,6	-3,76	0,002	0,0126	-2
>sp|Q99020|ROAA_M	18,75	18,5	20,3	20,4	20,3	19,7	20	20	20	20	21	21	21,1	20,4	21	21	21,3	20,9	19,809	20,8189	Hnrnpab	1,01	20,3	3,751	0,002	0,0127	-2
>sp|Q99L47|F10A1_I	20,83	20,8	20,7	20,5	20,7	20,5	20	21	20	21,3	22	21	20,6	21,7	21	22	21,1	20,9	20,549	21,1614	St13	0,61	20,9	3,741	0,002	0,0129	-2
>sp|P01636|KV5A4_	18,42	0	14,6	17	15,7	18,2	0	18	17	16	0	0	0	0	0	0	0	0	13,155	1.776523	>sp|P016	-11	7,47	-3,74	0,002	0,013	-2

>sp|Q5SV42|ILEUC_M	18,22	20	20,7	19,1	20,5	19,7	20	20	20	20,5	21	21	21,4	20,7	22	21	21	20,7	19,847	20,9279	Serpinb1c	1,08	20,4	3,733	0,002	0,0131	-2
>sp|Q80X90|FLNB_M	20,59	20,7	20,2	20,6	20,4	20,7	20	20	20	19,7	20	20	19,8	20,1	20	20	19,6	20	20,325	19,8375	Flnb	-0,5	20,1	-3,73	0,002	0,0131	-2
>sp|P42125|ECI1_M(	20,7	20,4	19,3	20,1	19,3	20,1	21	20	20	19,4	20	19	19,7	18,2	19	20	19,7	19,4	20,161	19,2828	Eci1	-0,9	19,7	-3,73	0,002	0,0132	-2
>sp|Q8CDN6|TXNL1_I	20,78	21,1	20,5	20,7	20,6	20,7	20	21	21	21,2	21	22	20,8	21,3	21	21	21,1	20,8	20,719	21,2515	Txnl1	0,53	21	3,724	0,002	0,0133	-2
>sp|Q9D1A2|CNDP2_	23,86	24	24,1	24,1	24,2	24,2	24	24	25	24,7	24	25	24,5	24,5	25	24	24,5	24,8	24,15	24,5471	Cndp2	0,4	24,3	3,721	0,002	0,0133	-2
>sp|P01899|HA11_M	20,32	20,2	20,4	20,5	20,6	20,4	21	20	20	20,1	20	19	20,2	20,2	20	20	19,7	19,5	20,464	19,923	H2-D1	-0,5	20,2	-3,71	0,002	0,0135	-2
>sp|P08071|TRFL_M(	18	16,9	17,9	14,2	17,6	17,9	17	16	16	8,98	16	17	0	9,17	0	11	12,6	9,17	16,812	9.305669	Ltf	-7,5	13,1	-3,71	0,002	0,0136	-2
>sp|P07759|SPA3K_	21,07	21,1	20,2	20,5	20,5	20,4	20	21	21	21,9	21	21	21,1	20,8	21	21	21,5	21,6	20,677	21,2673	Serpina3k	0,59	21	3,705	0,002	0,0137	-2
>sp|P63085|MK01_I	21,81	22,2	22,6	21,7	22	22,2	23	22	22	21,9	21	21	21,9	21,9	21	21	21,6	21,8	22,256	21,5891	Mapk1	-0,7	21,9	-3,7	0,002	0,0137	-2
>sp|P09055|ITB1_M(	21,26	21,3	20,5	22,9	22,8	22,5	23	22	21	21,4	21	20	20,1	20,2	20	20	20,3	21,5	21,92	20,569	Itgb1	-1,4	21,2	-3,7	0,002	0,0138	-2
>sp|Q8CG76|ARK72_	22,68	22,1	21,6	22	21,4	21,1	22	22	22	22,1	23	24	23,5	21,8	24	23	22,6	23,6	21,893	22,9132	Akr7a2	1,02	22,4	3,691	0,002	0,014	-2
>sp|O35344|IMA4_M	18,51	17,5	17,2	17,4	16,9	19,1	17	18	18	19,4	19	19	18,8	18,6	19	19	18,7	19,3	17,873	18,8681	Kpna3	1	18,4	3,689	0,002	0,014	-2
>sp|Q9Z2V4|PCKGC_	18,79	18,4	17,5	17,9	17,6	18,5	17	18	18	16,6	17	17	17,9	16,9	17	16	16,9	17,7	17,963	17,0178	Pck1	-0,9	17,5	-3,68	0,002	0,0142	-2
>sp|Q3UX10|TBAL3_I	22,26	22,3	22	21,4	21,9	22,1	22	22	22	20,8	22	21	21,8	21,9	22	21	21,6	20,7	22,023	21,4327	Tubal3	-0,6	21,7	-3,68	0,002	0,0143	-2
>sp|P62880|GBB2_M	22,66	22,4	22,5	22,2	21	22,6	22	23	22	21,8	21	21	21,2	21,6	21	21	21,6	21,7	22,19	21,3684	Gnb2	-0,8	21,8	-3,66	0,002	0,0147	-2
>sp|Q80W21|GSTM7_	23,4	24,2	24,5	24,1	24,1	24,3	24	24	23	24,4	25	24	24	24,8	25	25	24,5	24,7	24,006	24,5594	Gstm7	0,55	24,3	3,654	0,002	0,015	-2
>sp|Q9DBE0|CSAD_M	19,83	19,6	19,3	19,3	19,9	19,3	20	20	19	19,8	20	20	20,1	20,5	20	20	19,8	20,2	19,624	20,0534	Csad	0,43	19,8	3,644	0,002	0,0153	-2
>sp|P60843|IF4A1_M	22,83	23,1	23,2	23,1	23,4	23,4	23	23	24	23,1	23	23	23	22,9	23	23	22,8	23,1	23,281	22,922	Eif4a1	-0,4	23,1	-3,64	0,002	0,0154	-2
>sp|P11688|ITA5_M(	0	15,1	14,3	14	14,4	13,5	14	15	13	8,73	0	13	0	0	0	0	11,9	0	12,654	3.727559	Itga5	-8,9	8,19	-3,64	0,002	0,0154	-2
>sp|O88986|KBL_MC	20,03	20,5	20,8	20,7	20,1	21	21	22	22	21,7	22	22	22	21,3	22	21	20,9	21,9	20,75	21,5402	Gcat	0,79	21,1	3,636	0,002	0,0154	-2
>sp|P00756|K1KB3_	19,79	19,6	19,3	19,3	19,2	18,7	19	19	19	19,8	19	20	19,6	19,8	20	20	20,2	19,6	19,219	19,7457	Klk1b3	0,53	19,5	3,635	0,002	0,0154	-2
>sp|Q91YR9|PTGR1_I	22,14	22,1	22,3	22,1	22,1	22,1	22	22	22	21,5	22	22	21,7	22	22	22	21,5	21,2	22,206	21,7826	Ptgr1	-0,4	22	-3,63	0,002	0,0155	-2
>sp|Q8BJY1|PSMD5_I	21,71	21,2	22,3	22	22,3	22,2	22	22	22	22,2	22	23	23,2	23,3	23	22	22,3	22,4	21,977	22,7121	Psmd5	0,73	22,3	3,619	0,002	0,0159	-2
>sp|Q61702|ITIH1_M	19,25	17,9	18,3	18,8	18,9	18	19	19	19	19,6	19	19	19,8	18,6	20	20	19,5	19,2	18,613	19,3557	Itih1	0,74	19	3,611	0,002	0,0161	-2
>sp|P14094|AT1B1_	20,67	20,2	19,6	20,2	19,9	19,8	20	20	20	20,7	20	21	20,5	20,2	21	20	20,8	20,6	19,983	20,4904	Atp1b1	0,51	20,2	3,609	0,002	0,0162	-2
>sp|P10518|HEM2_M	21,17	22	21,9	21,6	23	22	22	22	21	19,4	19	20	20,6	21,5	22	21	21,6	19,5	21,916	20,4869	Alad	-1,4	21,2	-3,58	0,002	0,0173	-2
>sp|Q99PT1|GDIR1_M	23,73	23,5	23,7	23,7	22,5	23,4	23	23	23	23,8	23	24	24	24	24	24	24	24,3	23,222	23,9116	Arhgdia	0,69	23,6	3,561	0,003	0,0178	-2
>sp|P62317|SMD2_M	20,62	19	18,3	18,6	21,6	19,3	18	19	19	21,3	19	19	23	22,8	20	22	22,5	22,8	19,275	21,4897	Snrpd2	2,21	20,4	3,552	0,003	0,0181	-2
>sp|Q99M73|KRT84_	19,51	17	19,3	18,4	18,6	19,5	19	19	18	18,9	19	20	20,4	20,1	20	21	21	20,9	18,59	19,9734	Krt84	1,38	19,3	3,548	0,003	0,0183	-2
>sp|A1L317|K1C24_	0	15,1	0	0	0	0	15	16	16	16,3	16	18	13,9	15	17	18	18,8	19,1	7.01761	16,9698	Krt24	9,95	12	3,543	0,003	0,0184	-2
>sp|P01901|HA1B_M	20,29	20,7	20,8	20,8	20,5	20,5	20	21	21	20,1	21	18	19,8	19,8	20	20	20,1	19,9	20,587	19,8308	H2-K1	-0,8	20,2	-3,54	0,003	0,0185	-2
>sp|Q3TCH7|CUL4A_I	14,78	14,9	15,1	14,6	13,9	14,4	14	15	14	9,17	12	0	0	10,9	14	0	11,2	11,4	14,45	7.63234	Cul4a	-6,8	11	-3,52	0,003	0,0191	-2
>sp|Q8BVI4|DHPR_M	22,41	22,6	22,6	22,4	23,3	22,8	23	23	23	23	23	24	23,4	23,5	23	23	22,8	23,5	22,769	23,2514	Qdpr	0,48	23	3,522	0,003	0,0191	-2
>sp|O08663|MAP2_I	18,57	19,9	18,9	19,7	20,4	19,8	20	19	19	22,4	19	19	22,3	19,9	23	22	22	22	19,403	21,2461	Metap2	1,84	20,3	3,52	0,003	0,0192	-2
>sp|Q9QXG4|ACSA_M	20,02	19,9	20,4	20,1	20	20,4	20	21	19	19,6	19	20	19,5	18,5	19	20	19,3	18,8	20,028	19,241	Acss2	-0,8	19,6	-3,52	0,003	0,0193	-2
>sp|P42225|STAT1_M	20,19	19,5	19,1	18,9	19,5	19,6	19	20	19	18,7	19	18	19	17,8	18	20	18,9	18,2	19,432	18,7009	Stat1	-0,7	19,1	-3,51	0,003	0,0196	-3
>sp|Q5SGK3|AOXB_M	17,81	17,5	17,7	17,2	16,6	17,2	17	16	16	16,2	15	17	16,4	16,5	17	16	16,2	16,1	17,046	16,247	Aox2	-0,8	16,6	-3,51	0,003	0,0196	-3
>sp|Q9CYW4|HDHD3_	20,29	20,7	20,9	18,4	20,7	20	20	20	20	21	21	21	21,1	21,5	22	21	21,2	20,7	20,152	21,069	Hdhd3	0,92	20,6	3,505	0,003	0,0196	-3
>sp|O35343|IMA3_M	15,45	16,6	19	16,9	16,7	17,2	18	17	18	18,7	18	18	18,4	18,2	18	19	18,5	19	17,218	18,4129	Kpna4	1,19	17,8	3,504	0,003	0,0196	-3
>sp|Q9D8U3|ERP27_	19,07	20,7	20,2	18,5	19,2	20,1	18	20	20	20,8	21	21	20,9	20,4	20	21	20,1	20,4	19,48	20,5788	Erp27	1,1	20	3,502	0,003	0,0196	-3
>sp|Q9Z1F9|SAE2_MC	16,54	15,7	16,7	16,3	21	16,1	16	16	21	21,1	22	21	21,6	21,7	22	22	21,7	14,9	17,231	20,8362	Uba2	3,6	19	3,502	0,003	0,0196	-3
>sp|O08807|PRDX4_	23,68	23,2	22,9	23	21,4	23,2	23	24	24	22,2	22	20	22,7	22,2	21	22	21,9	22	23,099	21,8359	Prdx4	-1,3	22,5	-3,5	0,003	0,0198	-3
>sp|P10649|GSTM1_	24,32	24,9	25,1	24,7	24,7	25	25	25	25	25	25	25	25	25,6	26	25	25,2	25,4	24,819	25,23	Gstm1	0,41	25	3,495	0,003	0,0198	-3
>sp|O35459|ECH1_M	17,07	19,6	18,8	19	18,3	18,9	18	20	20	21,4	20	20	19,9	19,8	20	20	19,5	20	18,829	20,0711	Ech1	1,24	19,5	3,495	0,003	0,0198	-3
>sp|Q8VC28|AK1CD_	24,35	24,2	24,6	23,9	24,4	23,9	24	25	25	25,1	25	25	24,9	24,9	25	25	24,7	25	24,378	24,8959	Akr1c13	0,52	24,6	3,485	0,003	0,0202	-3
>sp|Q8BWF0|SSDH_M	24,22	24,9	25	24,5	24,9	23,9	24	24	25	23,6	24	23	23,2	18,9	22	23	23,7	23,1	24,532	22,7287	Aldh5a1	-1,8	23,6	-3,48	0,003	0,0202	-3
>sp|P09411|PGK1_M	26,1	25,1	26,6	26,5	26,5	27,6	26	28	26	25,7	26	26	25,2	25,3	25	26	25,4	25,8	26,477	25,5134	Pgk1	-1	26	-3,47	0,003	0,0209	-3
>sp|Q9Z0T9|ITB6_MO	16,84	17,2	17,1	16,8	16,3	17	17	17	17	14,8	17	17	15,6	14,6	16	16	15,7	13,7	16,795	15,577	Itgb6	-1,2	16,2	-3,46	0,003	0,021	-3

>sp|P60229|EIF3E_M	19,38	19,5	19,5	19,8	19,7	20	19	20	19	20,2	19	20	20,5	20,4	20	20	20,3	20,5	19,606	20,1297	Eif3e	0,52	19,9	3,462	0,003	0,021	-3
>sp|Q91YI0|ARLY_MO	21	20,6	19,9	21,1	20,1	20,4	21	20	21	21,2	23	23	21,8	20,4	22	21	21,7	21,5	20,56	21,5724	Asl	1,01	21,1	3,456	0,003	0,0213	-3
>sp|P14115|RL27A_	18,12	15,9	17	17	16,9	17,1	17	18	18	18,5	19	18	18,5	18,4	18	18	17,5	17,3	17,227	18,14	Rpl27a	0,91	17,7	3,453	0,003	0,0213	-3
>sp|Q91V76|CK054_	20,62	21,4	21,7	21,2	21,4	20,7	21	21	21	20,7	21	20	20	20,6	20	21	20,6	20,5	21,094	20,5581	>sp|Q91V	-0,5	20,8	-3,45	0,003	0,0214	-3
>sp|O35621|PMM1_	20,35	20,3	20,1	21,1	21,1	21,3	20	21	21	21,2	21	21	21,8	21,4	21	21	21,4	21,3	20,676	21,3069	Pmm1	0,63	21	3,439	0,003	0,0218	-3
>sp|Q91YR1|TWF1_M	20,39	20,9	20,9	20,6	20,9	20,7	21	21	21	21,4	21	22	21,5	21,2	22	21	22,1	21,1	20,892	21,4169	Twf1	0,53	21,2	3,438	0,003	0,0218	-3
>sp|P12265|BGLR_M	18,51	18,5	18,8	21	19,1	18,3	18	19	19	17,5	18	18	18,3	17,7	18	18	17,5	17,4	18,854	17,8012	Gusb	-1,1	18,3	-3,44	0,003	0,0218	-3
>sp|Q9Z2R6|U119A_	15,18	15	15,6	15,9	16,4	15,7	14	15	15	16,1	16	17	16	15,3	17	16	16,3	16,9	15,451	16,2873	Unc119	0,84	15,9	3,437	0,003	0,0218	-3
>sp|Q8N7N5|DCAF8_	17,52	17,5	16,2	17,9	17,6	18,1	18	17	17	16	16	17	16,3	16,4	16	17	16,3	17,2	17,373	16,4534	Dcaf8	-0,9	16,9	-3,44	0,003	0,0218	-3
>sp|P14211|CALR_M	21,85	21,3	22,1	21,6	22,4	22	21	22	22	20,6	21	21	21,7	21	21	22	20,9	21	21,721	21,0887	Calr	-0,6	21,4	-3,44	0,003	0,0218	-3
>sp|P60764|RAC3_M	21,45	21,6	22,8	22,1	22,3	21,3	22	22	22	21	22	21	21,4	21,6	20	20	21	21	21,952	21,1318	Rac3	-0,8	21,5	-3,43	0,003	0,0222	-3
>sp|P18572|BASI_M(	17	16,1	18	18,6	18,1	18,4	16	18	18	16,9	17	17	16,5	16,7	15	17	13,6	15,1	17,655	15,9938	Bsg	-1,7	16,8	-3,42	0,003	0,0222	-3
>sp|Q3UKJ7|SMU1_M	20,34	17,6	17,8	17,7	19,6	17,4	21	21	20	16,7	19	17	17,6	17	17	17	16,8	17,2	19,115	17,2629	Smu1	-1,9	18,2	-3,42	0,003	0,0223	-3
>sp|P50518|VATE1_I	23,58	23,4	20,2	23,3	23,6	20,9	24	23	20	18,8	21	21	19,5	21,1	20	20	20	20,3	22,393	20,3122	Atp6v1e1	-2,1	21,4	-3,4	0,004	0,0231	-3
>sp|P19096|FAS_MO	23,11	23,6	22,9	23,3	23,2	23,1	23	23	23	23,1	23	23	23,1	23,1	23	23	22,9	22,8	23,207	22,8908	Fasn	-0,3	23	-3,4	0,004	0,0231	-3
>sp|Q6WVG3|KCD12	18,77	19	18	19	18,6	19,2	18	19	19	16,4	17	18	18,4	17,9	19	17	17,9	18	18,734	17,8344	Kctd12	-0,9	18,3	-3,4	0,004	0,0233	-3
>sp|P14431|HA19_M	19,01	19,1	19,4	19,1	19	18,9	19	19	18	17,7	18	18	18,7	17,8	19	18	18,6	17,1	18,858	18,0722	H2-Q9	-0,8	18,5	-3,39	0,004	0,0235	-3
>sp|Q60870|REEP5_I	19,98	19,7	20,3	19,2	19,4	20,2	17	19	18	20,5	20	20	20,6	20,4	21	20	21,1	20,3	19,167	20,4584	Reep5	1,29	19,8	3,392	0,004	0,0236	-3
>sp|Q60997|DMBT1_	20,01	20,4	18,2	19,6	18,2	18,3	17	18	18	19,7	20	20	20,8	20	20	19	19,8	19,6	18,623	19,9408	Dmbt1	1,32	19,3	3,388	0,004	0,0237	-3
>sp|Q61753|SERA_M	20	20,5	19,6	19,7	20,2	19,6	20	20	20	20,2	21	20	21	20,5	21	20	20,3	20,3	19,982	20,527	Phgdh	0,55	20,3	3,378	0,004	0,0242	-3
>sp|P97379|G3BP2_	16,61	16,7	16,4	17,3	16,6	17,5	17	17	16	17,3	17	19	18,5	17,2	18	19	17,3	17,4	16,797	17,7028	G3bp2	0,91	17,2	3,365	0,004	0,0248	-3
>sp|Q9Z0X1|AIFM1_M	19,17	19	18,6	20,2	19,8	18,2	19	18	19	17,7	18	18	18,2	18,5	18	18	18,2	17,9	18,984	18,1759	Aifm1	-0,8	18,6	-3,36	0,004	0,0248	-3
>sp|P28654|PGS2_M	20,46	21	21,9	20,7	20,8	22	21	21	20	22	22	21	21,9	21,9	22	21	21,7	21,5	20,965	21,7644	Dcn	0,8	21,4	3,363	0,004	0,0248	-3
>sp|Q9D6Y9|GLGB_M	21,35	20,6	20,7	20,5	21,3	20,3	21	21	21	19	19	19	19,9	19,6	20	22	20,7	19,9	20,944	19,8814	Gbe1	-1,1	20,4	-3,35	0,004	0,0255	-3
>sp|P10833|RRAS_M	24,15	23,5	23,6	21,7	21,6	21,7	22	23	24	20,7	21	20	20,8	21,8	21	24	20,4	20,5	22,843	21,202	Rras	-1,6	22	-3,35	0,004	0,0255	-3
>sp|P49312|ROA1_M	22,37	21,2	21,8	21,1	21,2	21,5	21	22	21	21,8	22	21	23,3	23,4	23	23	21,3	23,8	21,463	22,6033	Hnrnpa1	1,14	22	3,339	0,004	0,0259	-3
>sp|Q3UPL0|SC31A_I	20,31	20,3	19,6	19,8	19,7	19,8	20	20	19	20,2	20	20	20,3	20,2	20	20	20,2	20,5	19,811	20,2138	Sec31a	0,4	20	3,338	0,004	0,0259	-3
>sp|O08638|MYH11_	22,47	22,2	21,7	21,3	21,4	22,1	22	22	22	22,2	22	22	22,3	22,4	22	22	22	22,2	21,781	22,2402	Myh11	0,46	22	3,338	0,004	0,0259	-3
>sp|Q571I9|A16A1_I	22,43	22,7	22,7	22,9	22,3	22,4	23	23	23	22,1	22	22	22,3	22,1	23	22	22,4	22,3	22,602	22,3042	Aldh16a1	-0,3	22,5	-3,34	0,004	0,0259	-3
>sp|Q8CAY6|THIC_MC	21,56	21,8	20,6	20,3	21,1	20,1	20	21	22	20,7	21	20	19,9	19,8	20	20	20	19,9	20,993	20,1428	Acat2	-0,9	20,6	-3,33	0,004	0,0262	-3
>sp|Q9JHW9|AL1A3_	21,6	22,1	21,2	22,1	22	21,5	21	21	22	21,9	22	23	22,8	22,2	23	22	21,8	22	21,506	22,2297	Aldh1a3	0,72	21,9	3,328	0,004	0,0263	-3
>sp|P46412|GPX3_M	22,13	20,2	20,9	20,8	21,9	22,4	21	22	22	22,2	22	23	22,1	22,3	22	23	22,6	22,8	21,453	22,4506	Gpx3	1	22	3,327	0,004	0,0263	-3
>sp|Q91V92|ACLY_M	22,59	22,9	22,7	22,5	22,9	22,9	23	23	23	22,4	23	22	21,9	22	22	22	22,9	22,4	22,784	22,2853	Acly	-0,5	22,5	-3,32	0,004	0,0264	-3
>sp|Q3UMY5|EMAL4_	19,31	19,3	19,4	19,5	19,6	19,1	19	19	19	18,6	19	19	19,1	19,2	19	19	19,2	19	19,341	19,017	Eml4	-0,3	19,2	-3,32	0,004	0,0264	-3
>sp|Q8R574|KPRB_M	17,33	15,4	17,4	16,4	16,9	15,8	17	18	18	15,1	16	16	15,5	15,7	16	17	14,9	15,2	16,853	15,7034	Prpsap2	-1,1	16,3	-3,32	0,004	0,0264	-3
>sp|P48453|PP2BB_	20,02	19,6	19,1	20,4	20,4	19,8	20	20	20	18,5	20	19	19,1	19,1	19	20	19,9	19	19,922	19,2647	Ppp3cb	-0,7	19,6	-3,31	0,004	0,0268	-3
>sp|Q9R0Y5|KAD1_M	19,36	19,3	19,4	18,7	19,3	19,3	19	19	20	18,2	19	19	19	19,4	18	18	17,9	18,6	19,275	18,6547	Ak1	-0,6	19	-3,31	0,004	0,0271	-3
>sp|Q505B7|ARCH_M	17,83	18,4	18,4	18,4	19,6	18,6	19	19	18	19,3	19	19	19,1	19,1	20	19	19,6	19,6	18,479	19,2221	Zbtb8os	0,74	18,9	3,303	0,004	0,0274	-3
>sp|Q99JW2|ACY1_M	20,86	20,1	20,4	20,1	20,9	20,3	21	20	20	20,9	21	21	21,2	20,3	21	21	21	21,1	20,311	20,8947	Acy1	0,58	20,6	3,3	0,004	0,0275	-3
>sp|P11725|OTC_MC	21,37	21,4	21,5	21,2	21,1	21,9	21	22	21	21,5	22	22	22,3	21,7	22	22	21,8	21,6	21,364	21,7538	Otc	0,39	21,6	3,298	0,004	0,0276	-3
>sp|Q9CWJ9|PUR9_M	22,31	22,4	21,9	22,5	22,2	22,8	22	22	22	23,1	23	23	22,5	22,4	23	23	22,7	22,6	22,344	22,6754	Atic	0,33	22,5	3,292	0,004	0,0279	-3
>sp|P17879|HS71B_	23,2	23,7	23,6	23,4	23,5	23,4	23	23	23	23,7	23	24	23,7	24	24	24	23,7	23,7	23,368	23,6837	Hspa1b	0,32	23,5	3,289	0,005	0,0279	-3
>sp|Q61696|HS71A_	23,2	23,7	23,6	23,4	23,5	23,4	23	23	23	23,7	23	24	23,7	24	24	24	23,7	23,7	23,368	23,6837	Hspa1a	0,32	23,5	3,289	0,005	0,0279	-3
>sp|Q9CWK8|SNX2_M	18,16	17,8	17,8	17,4	17,7	18,4	18	18	19	16,3	17	17	18,1	16,8	18	17	17,7	16,3	18,034	17,1436	Snx2	-0,9	17,6	-3,28	0,005	0,0284	-3
>sp|Q8BXK9|CLIC5_M	19,55	20	19	19,9	19	20,8	21	21	22	17,7	20	18	17,4	17,7	18	17	20,4	19,6	20,261	18,4658	Clic5	-1,8	19,4	-3,28	0,005	0,0284	-3
>sp|Q99JY9|ARP3_M	23,41	23,6	23,5	23,1	23,7	23,4	23	24	24	23,2	23	23	22,5	23,3	23	23	23,2	23,2	23,517	23,0131	Actr3	-0,5	23,3	-3,28	0,005	0,0285	-3
>sp|Q6ZQL4|WDR43_	17,99	17,7	17,4	16,7	17,1	17,4	17	18	18	17,7	18	18	18,4	18,2	18	18	18,1	18,1	17,367	17,9704	Wdr43	0,6	17,7	3,268	0,005	0,029	-3
>sp|Q64261|CDK6_M	18,47	18,1	18,3	18,5	19,7	18,9	19	18	20	19,2	18	16	18,2	17,6	17	18	17,7	16,8	18,727	17,4646	Cdk6	-1,3	18,1	-3,26	0,005	0,0294	-3

>sp|Q9D142|NUD14_	16,72	18,9	17,9	18,2	18,1	18,3	19	18	18	19,1	18	19	19,3	19,9	20	19	19,4	18,3	18,164	19,1408	Nudt14	0,98	18,7	3,251	0,005	0,03	-3
>sp|O55234|PSB5_M	23,84	24	23,7	23,3	23,7	23,2	24	24	23	23	23	23	23,3	23,2	23	23	23,5	23,4	23,657	23,2049	Psmb5	-0,5	23,4	-3,25	0,005	0,03	-3
>sp|P42567|EPS15_	0	0	0	0	0	0	0	14	15	16,8	12	12	13,2	0	13	11	14,7	14,1	3.27187	11,8993	Eps15	8,63	7,59	3,246	0,005	0,0301	-3
>sp|Q8K0D5|EFGM_M	15,39	15	16,3	14	15,9	14,8	15	15	16	16,4	16	17	15,9	16	15	17	16,1	16,3	15,244	16,1725	Gfm1	0,93	15,7	3,245	0,005	0,0301	-3
>sp|Q91X72|HEMO_M	15,85	15,9	16,9	16,8	15,9	16,3	17	16	16	16,5	16	18	16,8	17,7	17	17	17,3	17	16,379	17,069	Hpx	0,69	16,7	3,239	0,005	0,0305	-3
>sp|Q9CV28|MINY3_M	0	0	0	16,6	15,5	16,5	16	0	0	16,5	15	16	16,4	16,4	16	17	15,7	16,6	7.16342	16,2095	MINDY3	9,05	11,7	3,223	0,005	0,0315	-3
>sp|Q922Q8|LRC59_M	19,17	18,1	18,1	17,2	18,1	19,2	20	19	20	20,4	21	20	18,6	19,4	20	21	20,4	20,8	18,821	20,1706	Lrrc59	1,35	19,5	3,218	0,005	0,0317	-3
>sp|Q64442|DHSO_M	22,15	22,4	22,7	22,5	22,2	22,3	23	23	23	22,3	22	22	22,3	21,8	22	22	22	21,8	22,456	22,1056	Sord	-0,4	22,3	-3,22	0,005	0,0317	-3
>sp|P70349|HINT1_M	23,19	21,8	23,1	21,7	23,2	22,6	22	22	22	23,3	23	22	23,1	23,4	23	23	23,4	23,7	22,419	23,2093	Hint1	0,79	22,8	3,205	0,005	0,0326	-3
>sp|Q9D8N0|EF1G_M	22,66	22,9	22,5	22,6	22,7	22,7	23	23	23	22,9	23	23	22,8	23,1	23	23	23	22,6	22,706	22,9713	Eef1g	0,27	22,8	3,2	0,005	0,0328	-3
>sp|Q6PE01|SNR40_M	19,46	20,5	19,7	20,5	21,2	20,2	21	20	19	19,8	20	19	19,5	19,8	20	19	19,2	19,3	20,236	19,5045	Snrnp40	-0,7	19,9	-3,19	0,006	0,0333	-3
>sp|Q80UY1|CARME_M	0	0	0	0	0	0	0	0	0	16,7	0	15	0	0	17	18	17,2	0	0	9,4147	Carnmt1	9,41	4,71	3,188	0,006	0,0335	-3
>sp|Q9D662|SC23B_M	19,64	19,8	20,2	19,2	19,5	19,8	20	20	20	20,5	20	20	20	20	20	20	20,1	20	19,732	20,1118	Sec23b	0,38	19,9	3,187	0,006	0,0335	-3
>sp|Q8BK62|OLFL3_M	16,93	16,9	16,5	17	17,7	16,8	17	17	17	16,9	16	16	16,3	15,6	16	17	16,7	16,5	16,981	16,379	Olfml3	-0,6	16,7	-3,18	0,006	0,0339	-3
>sp|P42208|SEPT2_M	19,56	19	21,7	19,1	20,2	19,7	20	20	20	21,2	21	23	20,7	20,1	20	21	21	20,9	19,868	21,0012	Sept2	1,13	20,4	3,17	0,006	0,0346	-3
>sp|O08547|SC22B_M	20,04	20,1	17,7	19,4	20	20	19	20	19	15,8	17	16	19,6	19,9	17	17	16,6	19,7	19,476	17,6205	Sec22b	-1,9	18,5	-3,17	0,006	0,0348	-3
>sp|Q91VZ6|SMAP1_M	17,2	17,9	17,3	17,7	17	17,4	18	18	18	18,5	18	19	18	18,4	17	19	18,5	17,6	17,554	18,1659	Smap1	0,61	17,9	3,163	0,006	0,035	-3
>sp|Q9D967|MGDP1_M	18,48	19	17,8	20	19,8	17,4	19	19	19	19,8	20	19	20,1	19,8	20	20	20,1	21	18,88	19,895	Mdp1	1,02	19,4	3,155	0,006	0,0356	-3
>sp|Q3TJD7|PDLI7_M	20,98	21,3	20,7	21,9	20,8	20,1	21	21	21	20,5	20	21	20,3	20,8	20	20	19,6	20,5	21,046	20,3972	Pdlim7	-0,6	20,7	-3,15	0,006	0,0356	-3
>sp|P46664|PURA2_M	21,42	21,1	21,6	21,2	21,5	21,5	22	22	22	22,3	22	22	21,6	21,8	22	22	22,1	22,2	21,544	21,9605	Adss	0,42	21,8	3,147	0,006	0,036	-3
>sp|P48455|PP2BC_M	19,48	18,8	19	20,3	20,1	19,8	19	19	20	18,3	19	18	18,8	19	19	19	19,5	18,5	19,615	18,8237	Ppp3cc	-0,8	19,2	-3,15	0,006	0,036	-3
>sp|P12970|RL7A_M	19,33	18,8	19,2	19	19	18	19	18	19	17,9	18	19	17,7	18,4	19	18	18,3	18,1	18,814	18,1971	Rpl7a	-0,6	18,5	-3,15	0,006	0,036	-3
>sp|Q8R5C5|ACTY_M	20,54	21,2	20,7	20,4	20,2	20,1	20	20	20	21,2	21	21	20,8	21	21	21	20,7	20,9	20,47	20,8889	Actr1b	0,42	20,7	3,145	0,006	0,036	-3
>sp|O55106|STRN_M	19,31	19,1	19,1	18,8	18,7	18,6	19	18	19	19	19	19	18,6	19,6	20	20	19,8	19,5	18,869	19,39	Strn	0,52	19,1	3,137	0,006	0,0365	-3
>sp|P37804|TAGL_M	22,43	22,6	23,1	22,1	22,4	22,9	23	23	23	23	23	23	23,1	23,6	23	23	23,3	22,8	22,759	23,2453	Tagln	0,49	23	3,136	0,006	0,0365	-3
>sp|Q8CIN4|PAK2_M	16,19	17,8	17,4	16,6	16	17,1	16	17	16	17,1	18	17	18,1	16,5	18	18	18	17,8	16,687	17,5741	Pak2	0,89	17,1	3,133	0,006	0,0367	-3
>sp|Q9D0W5|PPIL1_M	20,06	19,4	19,8	19,4	19	19,8	19	19	19	21,2	21	22	19,7	21,5	22	19	19,2	19,8	19,386	20,6143	Ppil1	1,23	20	3,133	0,006	0,0367	-3
>sp|O35841|API5_M	20,59	20,6	20,7	20,8	20,5	20,8	21	21	21	19,9	20	20	15,6	15,1	20	20	19,9	19,4	20,745	18,738	Api5	-2	19,7	-3,13	0,006	0,0371	-3
>sp|P47968|RPIA_M	15,62	15,3	16,3	16,3	15,9	16,5	16	17	16	17,2	17	18	16,4	17,6	16	17	16,7	17	16,102	16,9094	Rpia	0,81	16,5	3,122	0,006	0,0374	-3
>sp|Q61247|A2AP_M	14,91	15,2	15,8	14,9	13,4	16	16	16	15	16,4	15	16	15,6	17,1	15	17	16,5	16,8	15,142	16,1827	Serpinf2	1,04	15,7	3,114	0,007	0,038	-3
>sp|P17742|PPIA_M	26,36	27,7	26,4	26,7	26,4	26,7	27	28	26	25,8	25	26	25,9	26,1	25	27	25,7	25,9	26,793	25,9333	Ppia	-0,9	26,4	-3,1	0,007	0,039	-3
>sp|P18531|HVM60	0	18,2	18,4	19	18,8	19	19	18	18	17,6	0	0	0	0	0	18	0	16,6	16,581	5.744353	Ighv3-6	-11	11,2	-3,09	0,007	0,0396	-3
>sp|P68373|TBA1C_M	24,97	24,5	25,4	24,3	25,1	24,6	25	25	25	24,5	25	24	24,9	24,6	24	24	24,1	24,6	24,922	24,4468	Tuba1c	-0,5	24,7	-3,09	0,007	0,0401	-3
>sp|P26262|KLKB1_M	17,9	18,3	18,9	18,2	18,8	18,7	19	18	19	16,6	17	18	16,7	18,4	19	18	18,1	17,5	18,463	17,6346	Klkb1	-0,8	18	-3,08	0,007	0,0405	-3
>sp|Q01768|NDKB_M	22,44	22,3	22	22,6	22,7	22,1	22	22	22	22,7	23	23	23,3	23	23	23	23,4	22,3	22,298	22,768	Nme2	0,47	22,5	3,058	0,007	0,0422	-3
>sp|Q63844|MK03_M	22,45	22,3	21,6	21,4	21,6	21,8	22	22	22	21,6	22	21	21,5	21,8	21	21	21,3	21,4	21,891	21,4731	Mapk3	-0,4	21,7	-3,06	0,007	0,0422	-3
>sp|P35486|ODPA_M	20,47	20,7	19,4	19,6	18,5	19,3	20	19	19	20,4	20	20	20,7	20,5	20	22	21,4	21,8	19,625	20,6425	Pdha1	1,02	20,1	3,057	0,007	0,0422	-3
>sp|Q99MN1|SYK_MO	21,34	21,5	21,4	21,8	21,8	21,7	22	22	22	22,3	22	22	22	21,8	22	22	21,8	21,9	21,702	22,0257	Kars	0,32	21,9	3,056	0,007	0,0422	-3
>sp|P02301|H3C_MO	25,32	27,9	27,5	27,6	27,8	27,5	28	28	28	28	28	28	28,8	28,8	29	28	28,6	28,3	27,434	28,3538	H3f3c	0,92	27,9	3,055	0,007	0,0422	-3
>sp|P84244|H33_MO	25,32	27,9	27,5	27,6	27,8	27,5	28	28	28	28	28	28	28,8	28,8	29	28	28,6	28,3	27,434	28,3538	H3f3a	0,92	27,9	3,055	0,007	0,0422	-3
>sp|P68369|TBA1A_M	25,02	24,5	25,4	24,4	25,2	24,7	25	25	25	24,5	25	24	24,9	24,6	24	24	24,2	24,6	24,97	24,484	Tuba1a	-0,5	24,7	-3,05	0,007	0,0423	-3
>sp|Q9ZQE6|GBP2_M	18,69	19,1	19,9	19,3	19,3	18,7	19	19	20	18,6	19	19	19,1	19	19	18	18,4	18,7	19,247	18,7869	Gbp2	-0,5	19	-3,05	0,007	0,0424	-3
>sp|P13020|GELS_MO	23,99	24	24,5	23,9	24,2	24,5	24	24	24	23	24	24	23,8	24,2	24	23	23,7	23,3	24,101	23,6219	Gsn	-0,5	23,9	-3,05	0,007	0,0424	-3
>sp|P55264|ADK_MO	23,14	23,3	22,6	22,8	23,1	22,7	23	23	24	22,8	23	23	22,3	22,3	22	23	22,7	22,5	23,092	22,6251	Adk	-0,5	22,9	-3,04	0,008	0,0429	-3
>sp|O55135|IF6_MOU	23,67	23,6	23,4	23,3	23,4	23,3	24	24	24	23,6	23	23	23,3	22,7	23	23	22,7	23,4	23,547	23,1195	Eif6	-0,4	23,3	-3,04	0,008	0,0429	-3
>sp|Q8K419|LEG4_MO	23,26	23,3	22,8	23,6	23,3	23,5	24	23	24	23,4	24	24	24,1	24,2	24	24	23,7	24	23,397	23,7773	Lgals4	0,38	23,6	3,041	0,008	0,043	-3
>sp|P39053|DYN1_M	15,89	16,1	15,9	15,5	15,2	15,4	14	16	16	15,4	15	15	14,7	15,1	15	14	14,2	15,4	15,531	14,8031	Dnm1	-0,7	15,2	-3,04	0,008	0,043	-3
>sp|Q91VR2|ATPG_M	18,18	18,5	19,8	18,3	20,4	19,6	20	19	20	20,4	20	20	20,7	20,8	20	19	20	20,1	19,268	20,1394	Atp5c1	0,87	19,7	3,032	0,008	0,0437	-3

>sp|Q99J09|MEP50_	20,77	21,1	21	20,7	20,4	20,7	21	21	21	20,4	20	21	20,3	20,6	21	20	20,7	20,5	20,865	20,4676	Wdr77	-0,4	20,7	-3,01	0,008	0,0453	-4
>sp|P38060|HMGCL_	20,64	21,2	19,8	20,6	20,9	20,6	21	21	21	20,2	20	20	20,1	19,8	21	20	20,2	20,8	20,745	20,2164	Hmgcl	-0,5	20,5	-3,01	0,008	0,0455	-4
>sp|Q91VF2|HNMT_M	14,86	17,1	19,1	18,6	18,4	18,9	15	18	18	18,5	19	19	19,1	19,4	19	19	18,8	19,4	17,517	19,139	Hnmt	1,62	18,3	3,008	0,008	0,0456	-4
>sp|Q9EQ06|DHB11_	17,26	17,8	17,3	17,2	15,3	17,4	17	18	18	13,5	17	18	14,1	16,5	15	14	16,5	16,2	17,257	15,5624	Hsd17b1	-1,7	16,4	-3,01	0,008	0,0456	-4
>sp|P68433|H31_MC	25,37	28	27,5	27,6	27,9	27,5	28	28	28	28,2	28	28	29	29	29	28	28,8	28,4	27,52	28,4678	Hist1h3a	0,95	28	3,007	0,008	0,0456	-4
>sp|P84228|H32_MC	25,37	28	27,5	27,6	27,9	27,5	28	28	28	28,2	28	28	29	29	29	28	28,8	28,4	27,52	28,4678	Hist1h3b	0,95	28	3,007	0,008	0,0456	-4
>sp|P06684|CO5_MC	20,28	20,2	19,9	20,8	21	20	21	20	20	19,6	19	20	19,8	20,2	20	20	19,2	19,9	20,301	19,6694	C5	-0,6	20	-3	0,008	0,0461	-4
>sp|P16125|LDHB_M	23,03	23,2	22,4	22,9	22,9	23	23	23	23	20,6	22	21	20,8	23	23	22	21,2	22,5	22,85	21,9	Ldhb	-1	22,4	-3	0,008	0,0463	-4
>sp|P61957|SUMO2_	20,99	17,9	17,9	21,3	21,1	18	22	21	21	18,4	18	19	17,4	19,1	18	18	18,7	18,5	20,054	18,4233	Sumo2	-1,6	19,2	-2,99	0,009	0,0473	-4
>sp|Q9QXS1|PLEC_MC	19,67	19,4	19,1	19,2	19,5	19,7	19	19	19	19	19	19	19,2	19,1	19	19	18,8	19	19,367	19,0718	Plec	-0,3	19,2	-2,99	0,009	0,0473	-4
>sp|O70589|CSKP_M	17,84	18,8	18,5	18,6	19,4	18,8	19	19	19	16,9	18	18	17,1	18,2	19	19	17,1	18	18,693	17,8679	Cask	-0,8	18,3	-2,99	0,009	0,0473	-4
>sp|P07901|HS90A_	23,58	23,7	23,9	23,7	23,7	23,9	24	23	24	24	24	24	24,2	24,1	24	24	24,1	24,1	23,733	24,0842	Hsp90aa1	0,35	23,9	2,98	0,009	0,0477	-4
>sp|P14206|RSSA_M	22,22	22,6	21,8	21,3	21,8	21,5	22	22	22	23,3	23	22	22,6	22,1	22	22	22,4	22,6	21,976	22,5035	Rpsa	0,53	22,2	2,975	0,009	0,0482	-4
>sp|Q8K0U4|HS12A_	16,19	16,4	17,2	16,5	16,1	16,1	16	17	16	17,2	18	17	17,4	17	17	17	16,3	16,6	16,337	16,9867	Hspa12a	0,65	16,7	2,971	0,009	0,0485	-4
>sp|O08532|CA2D1_	16,38	16,7	16,8	17,4	17,6	16,1	17	17	16	15,8	16	16	16,4	16,4	16	16	16,2	16,4	16,791	16,1872	Cacna2d1	-0,6	16,5	-2,97	0,009	0,0485	-4
>sp|P17892|LIPR2_M	17,82	18,1	18,5	17,7	18,1	18,4	18	17	18	17,6	18	18	18,8	18,5	19	19	18,1	19,1	17,8	18,5708	Pnliprp2	0,77	18,2	2,967	0,009	0,0487	-4
>sp|P54923|ADPRH_	20,43	20,9	20,3	20,1	19,9	20	20	20	20	19,6	20	20	20,3	19,4	20	19	19,6	19,8	20,219	19,7505	Adprh	-0,5	20	-2,96	0,009	0,0491	-4
>sp|P46425|GSTP2_M	24,99	24,8	27,6	25,7	26,8	27,4	26	27	26	25,4	25	25	24,8	23,9	25	26	25,3	25,1	26,211	25,1025	Gstp2	-1,1	25,7	-2,96	0,009	0,0496	-4
>sp|P05063|ALDOC_	20,68	20,3	19,8	20,1	20,8	20,4	21	21	21	20,8	20	20	19,5	19,4	20	19	20,1	19,2	20,512	19,8428	Aldoc	-0,7	20,2	-2,94	0,01	0,0517	-4
>sp|Q9ES74|NEK7_MC	14,46	15,5	14,4	15,1	14,4	14,4	15	14	12	0	0	13	0	13,5	14	0	13,9	12,7	14,379	7.469924	Nek7	-6,9	10,9	-2,94	0,01	0,0517	-4
>sp|O55229|CHKB_M	20,75	20,9	20,2	21,1	20,1	19,4	20	20	20	21,4	21	21	21,1	21,1	21	21	20,7	20,7	20,383	20,94	Chkb	0,56	20,7	2,934	0,01	0,0518	-4
>sp|Q9Z172|SUMO3_	20,6	17,6	17,5	21	20,8	17,7	21	21	20	18,1	18	18	17,1	18,8	18	18	18,4	18,2	19,701	18,1003	Sumo3	-1,6	18,9	-2,93	0,01	0,0522	-4
>sp|Q9Z130|HNRDL_M	16,57	16,5	17,7	17,8	17,6	16	18	17	18	16,5	19	20	19,9	15,8	20	20	20	19,7	17,252	18,9525	Hnrnpdl	1,7	18,1	2,929	0,01	0,0522	-4
>sp|Q8BFY9|TNPO1_M	16,97	18,4	17,8	18	17,7	17,8	18	18	17	17,7	19	17	18,5	18,6	19	20	20,3	19,3	17,745	18,85	Tnpo1	1,1	18,3	2,922	0,01	0,0528	-4
>sp|P20029|GRP78_	24,16	24,3	24,2	24,7	24,8	24,5	24	25	25	24,6	25	25	24,5	24,8	25	25	25,1	25,2	24,476	24,7959	Hspa5	0,32	24,6	2,914	0,01	0,0536	-4
>sp|Q8BTW3|EXOS6_M	19,35	19,4	18,2	22,8	23,1	23	23	22	22	22,4	17	18	18,2	18,2	18	18	16,7	21,9	21,351	18,703	Exosc6	-2,6	20	-2,91	0,01	0,0536	-4
>sp|Q9D6F9|TBB4A_M	23,37	23	24,1	23,5	23,4	23,6	24	24	24	23,5	23	23	22,6	23,1	22	23	23,2	23,6	23,704	23,1279	Tubb4a	-0,6	23,4	-2,91	0,01	0,0536	-4
>sp|P97384|ANX11_	19,35	19	19	18,1	20	17,7	19	19	19	18,2	18	18	17,4	16,6	18	19	18,6	18,6	18,983	18,037	Anxa11	-0,9	18,5	-2,91	0,01	0,0538	-4
>sp|P68181|KAPCB_	23,39	24,5	23,2	21,9	21,3	22,6	23	23	23	22,3	20	20	22,6	22,5	22	21	21,8	20,6	22,801	21,4493	Prkacb	-1,4	22,1	-2,91	0,01	0,0539	-4
>sp|Q6ZWN5|RS9_MC	18,65	18,4	18,8	15,5	16,8	18,7	18	19	15	19,1	18	20	20,4	19,5	19	19	19,9	20,3	17,664	19,3933	Rps9	1,73	18,5	2,899	0,01	0,055	-4
>sp|Q9CQF9|PCYOX_M	17,74	17	16,8	13,8	16,4	16,5	16	17	16	12,3	16	16	15	14,3	15	14	15	14,5	16,37	14,7804	Pcyox1	-1,6	15,6	-2,89	0,01	0,0554	-4
>sp|Q5SV66|CCD42_	19,87	20,3	19,9	20,1	19,9	20	20	21	18	21,3	21	21	21,2	20,6	21	20	20,6	20	19,876	20,751	ACP6	0,88	20,3	2,891	0,01	0,0557	-4
>sp|O55131|SEPT7_M	20,39	20,4	20,8	20,5	20,5	22,8	20	20	20	22	22	22	20,3	22,3	22	21	21,6	21,7	20,717	21,6391	Sept7	0,92	21,2	2,888	0,011	0,056	-4
>sp|Q64449|MRC2_M	17,01	16,9	18,3	18	18,2	18,3	19	19	18	16,9	17	17	17,3	17,8	18	17	17,2	17,5	18,025	17,3149	Mrc2	-0,7	17,7	-2,89	0,011	0,0561	-4
>sp|P51660|DHB4_M	21,9	21,9	20,2	22,3	21,8	20,4	22	22	20	21,7	19	20	20,6	20,2	20	21	20,2	20,2	21,361	20,2427	Hsd17b4	-1,1	20,8	-2,88	0,011	0,0573	-4
>sp|Q9CPY7|AMPL_M	24,03	24,1	24,5	24,3	23,9	24,3	25	25	25	24,2	24	24	23,7	23,9	24	24	23,9	24	24,419	23,9725	Lap3	-0,4	24,2	-2,86	0,011	0,0587	-4
>sp|P28661|SEPT4_M	16,38	16,3	16	13,8	13,6	12,6	16	17	17	17,3	18	18	15,3	15,7	18	17	16,9	17,5	15,295	17,0045	Sept4	1,71	16,1	2,855	0,011	0,0595	-4
>sp|Q8K4L3|SVIL_MO	18,45	16,1	15,5	18,4	16	16,2	16	16	16	15,6	15	15	15,7	15,4	16	16	15,4	15,8	16,536	15,402	Svil	-1,1	16	-2,85	0,011	0,0595	-4
>sp|Q9JIF7|COPB_MC	20,16	20,7	22,3	20,1	20,4	21,8	22	21	21	20,4	20	20	20	20,9	20	20	20,2	20,2	20,989	20,248	Copb1	-0,7	20,6	-2,85	0,011	0,0597	-4
>sp|P30275|KCRU_M	26,19	24,9	25,5	24,9	25,6	25,7	26	26	26	25,2	25	25	25,3	24,7	25	26	24,7	25	25,594	25,0705	Ckmt1	-0,5	25,3	-2,85	0,011	0,0601	-4
>sp|Q00612|G6PD1_	23,01	22,5	22,4	23	22,3	22,7	23	23	23	22,8	22	22	22,4	22,3	22	22	22,2	22,3	22,671	22,3872	G6pdx	-0,3	22,5	-2,85	0,011	0,0601	-4
>sp|P60766|CDC42_	20,4	21,6	22,2	22,4	21,5	20,7	21	21	21	20,4	21	20	20,9	21,1	21	20	20,2	20,1	21,3	20,5087	Cdc42	-0,8	20,9	-2,85	0,011	0,0601	-4
>sp|P97449|AMPN_M	22,62	22,3	23,1	23,5	23,5	22,3	23	22	23	21,9	21	23	21,9	21,8	22	22	22,2	23,2	22,859	22,1072	Anpep	-0,8	22,5	-2,85	0,011	0,0601	-4
>sp|Q8VDP3|MICA1_	14,82	14,5	15,8	15,7	16,3	15,5	15	16	15	14,5	16	15	14,5	14,2	15	14	14,2	14,7	15,395	14,6002	Mical1	-0,8	15	-2,84	0,012	0,0601	-4
>sp|Q9DCL9|PUR6_M	21,32	18,8	20	21,7	21,5	21,6	21	18	21	18,6	19	19	18,7	18,7	21	18	20,8	17,6	20,627	19,0464	Paics	-1,6	19,8	-2,84	0,012	0,0602	-4
>sp|Q8R1Q9|RBSK_M	18,52	18,2	17,9	16,3	16,8	16,5	17	17	18	19,6	18	18	18,4	18,3	20	20	16,6	17,8	17,294	18,6176	Rbks	1,32	18	2,842	0,012	0,0603	-4
>sp|P80313|TCPH_M	19,44	19,7	19,4	19,8	20	19,4	20	20	20	20,3	21	20	20,5	19,7	21	20	20,6	19,6	19,701	20,1904	Cct7	0,49	19,9	2,835	0,012	0,0611	-4
>sp|P14824|ANXA6_	21,58	21,4	21,3	21,9	21,8	21,9	22	22	22	21,8	23	22	22,1	22,1	22	22	22,2	22,2	21,713	22,1827	Anxa6	0,47	21,9	2,832	0,012	0,0613	-4

>sp|P56395|CYB5_M	15,89	18,3	17,7	19,3	18,8	18,8	18	18	18	19	18	19	19,6	19,4	20	19	19,1	19,2	18,086	19,1161	Cyb5a	1,03	18,6	2,831	0,012	0,0613	-4
>sp|P60670|NPL4_M	19,39	19,1	18,5	19	18,2	18,4	19	18	19	16,8	19	18	18,2	17,5	17	18	18,1	18,9	18,709	17,9813	Nploc4	-0,7	18,3	-2,82	0,012	0,062	-4
>sp|Q61937|NPM_M	16,46	16,9	16,6	17,5	17,5	16,6	16	17	17	17,7	17	17	17,9	16,7	17	18	18	17,6	16,78	17,406	Npm1	0,63	17,1	2,825	0,012	0,062	-4
>sp|P35979|RL12_M	24,53	24,2	25,2	25,3	25,7	25,1	25	26	26	25,7	26	26	25,7	25,7	26	25	25,4	25,6	25,119	25,6313	Rpl12	0,51	25,4	2,819	0,012	0,0626	-4
>sp|Q7TMM9|TBB2A_	23,82	23,4	24,4	23,7	23,9	23,8	24	24	24	23,6	24	24	23,3	23,7	23	24	23,6	23,7	24,009	23,5917	Tubb2a	-0,4	23,8	-2,82	0,012	0,0629	-4
>sp|Q8VED5|K2C79_	21,53	20,6	21,2	20,4	20,8	20,9	21	20	20	20,2	23	21	21,2	21,3	21	23	22,6	23	20,715	21,776	Krt79	1,06	21,2	2,815	0,012	0,0629	-4
>sp|O88587|COMT_M	19,9	19,7	20,6	20,5	20,7	20,6	21	21	21	19,9	21	20	17,7	19,4	20	20	20	20	20,564	19,6666	Comt	-0,9	20,1	-2,81	0,012	0,063	-4
>sp|Q63918|CAVN2_	17,37	17,3	16,6	17	17,2	16,2	16	17	17	17,2	21	21	18,1	17,5	18	18	17,8	17,4	16,823	18,4042	Cavin2	1,58	17,6	2,812	0,012	0,0631	-4
>sp|P01898|HA10_M	20,14	19,6	19,8	19,7	19,4	19,7	20	20	20	20,6	21	20	19,9	20,3	20	20	20	19,7	19,798	20,195	H2-Q10	0,4	20	2,808	0,012	0,0636	-4
>sp|Q9DAK9|PHP14_	20,11	21,8	21	21,2	21,1	21	21	21	21	20,5	21	21	20,6	20,8	21	20	20,6	20,3	21,053	20,5874	Phpt1	-0,5	20,8	-2,81	0,012	0,0637	-4
>sp|Q6P8M1|TATD1_	15,24	15,9	17,3	17,4	17,2	17,4	17	17	18	17,5	18	18	18,4	18,3	18	18	17,9	16,4	16,956	17,8983	Tatdn1	0,94	17,4	2,805	0,012	0,0637	-4
>sp|P28798|GRN_M(	17,2	17,3	18	17,5	17,8	17,1	18	18	18	16,7	16	17	17,2	17,4	18	17	17,4	15,6	17,666	16,8997	Grn	-0,8	17,3	-2,8	0,013	0,0644	-4
>sp|P97461|RS5_MC	21,11	17,7	19,2	19,8	18,7	19	19	19	19	19,9	21	20	19,4	19,9	20	21	19,9	20,4	19,188	20,1934	Rps5	1,01	19,7	2,797	0,013	0,0644	-4
>sp|Q91ZA3|PCCA_M	20,74	22,3	21,9	21,7	21,7	21,8	22	22	21	21	22	21	21,1	20,9	21	21	20,6	21,5	21,661	21,1405	Pcca	-0,5	21,4	-2,8	0,013	0,0644	-4
>sp|Q99KQ4|NAMPT_	19,93	21,6	21	22,9	22,6	20,7	22	22	22	20,8	21	21	20,6	20,9	21	21	20,7	20,6	21,611	20,7417	Nampt	-0,9	21,2	-2,8	0,013	0,0644	-4
>sp|Q9CWS0|DDAH1_	18,58	19,2	18,9	19,3	19,1	19,4	19	20	19	19,4	19	20	19,8	19,6	20	19	19,2	19,3	19,094	19,4695	Ddah1	0,38	19,3	2,793	0,013	0,0648	-4
>sp|Q8BIW1|PRUN1_	22,08	22,2	15,4	20,7	19,7	15,9	22	19	16	13,8	15	15	15,1	17,1	17	19	15,9	17,1	19,146	16,1383	Prune1	-3	17,6	-2,79	0,013	0,0656	-4
>sp|Q8BWZ3|NAA25_	15,25	15,8	14,7	14,4	14,8	16,2	15	16	16	15,9	17	16	16,4	15,9	16	16	15,2	16,1	15,347	16,0869	Naa25	0,74	15,7	2,779	0,013	0,0666	-4
>sp|Q9WUA2|SYFB_M	20,1	19,9	20	20,9	20,6	20,3	21	21	21	19,8	20	20	19,4	20,4	20	21	19,7	20,3	20,489	19,9496	Farsb	-0,5	20,2	-2,78	0,013	0,0667	-4
>sp|Q08857|CD36_M	17,38	18	17,5	17,5	17,2	17,3	18	17	17	16,7	16	17	17,1	16,8	17	17	17,3	17,5	17,405	16,9726	Cd36	-0,4	17,2	-2,77	0,013	0,0677	-4
>sp|P62852|RS25_M	20,31	20,4	22,7	21,7	19,8	22,5	23	23	23	22,7	23	23	23,2	23	23	23	22,6	22,8	21,766	22,9441	Rps25	1,18	22,4	2,768	0,014	0,0678	-4
>sp|P62814|VATB2_	21,32	21,8	21,7	21,5	21,6	21,6	21	22	22	20,9	21	22	20,8	21,2	20	22	21,4	21,6	21,616	21,1642	Atp6v1b2	-0,5	21,4	-2,77	0,014	0,068	-4
>sp|Q9CYH2|F213A_M	0	0	15,2	13,9	0	15,5	0	15	14	15,4	16	14	15,8	13	13	16	17,7	17,7	8.17249	15,41	Fam213a	7,24	11,8	2,757	0,014	0,0692	-4
>sp|P62830|RL23_M	22,8	22,5	21,3	22,3	22,1	20,5	22	22	22	23,7	23	24	22,7	22,7	25	24	23,9	20,7	22,054	23,2856	Rpl23	1,23	22,7	2,752	0,014	0,0698	-4
>sp|Q9Z1D1|EIF3G_M	16,27	16,6	16,4	17,1	15,7	14,9	16	16	16	16,6	17	17	16,9	16,9	16	17	16,5	16,6	16,054	16,6598	Eif3g	0,61	16,4	2,751	0,014	0,0698	-4
>sp|P35441|TSP1_M	22,05	22	21,9	22	21,7	21,5	21	22	22	21,6	22	21	20,9	21,5	21	21	21,7	21,4	21,761	21,3931	Thbs1	-0,4	21,6	-2,74	0,014	0,0717	-4
>sp|Q8BLY2|SYTC2_M	21,2	21,8	17,9	21,4	17,6	13,8	17	13	14	9,05	14	14	15,7	15,6	15	15	14	12,5	17,471	13,8419	Tarsl2	-3,6	15,7	-2,74	0,014	0,0717	-4
>sp|Q8BK64|AHSA1_	18,61	19,3	19,7	20	19,5	19,5	19	20	19	18,9	22	22	22,7	19,2	19	22	22,5	19,1	19,33	20,8857	Ahsa1	1,56	20,1	2,733	0,015	0,0721	-4
>sp|Q80VJ3|DNPH1_	17,14	17,2	19,4	16,9	16,1	17,6	17	17	16	17,4	21	18	21,1	17,9	18	18	18	21,2	17,171	18,9692	Dnph1	1,8	18,1	2,73	0,015	0,0725	-4
>sp|P31428|DPEP1_	16,8	17,1	17,7	18,5	18,5	19,2	18	18	20	21,6	21	18	18	18,3	21	20	21	21,4	18,218	19,8989	Dpep1	1,68	19,1	2,727	0,015	0,0726	-4
>sp|Q50H33|KCTD8_	16,89	17,8	15,4	17,7	16	15,7	16	16	15	14,3	15	16	15,4	15,8	15	15	15	15,2	16,284	15,2753	Kctd8	-1	15,8	-2,73	0,015	0,0726	-4
>sp|P70389|ALS_M	0	0	14,5	0	0	13,4	14	12	15	13,9	14	17	14,2	14,8	15	13	13,7	14,3	7.70735	14,3969	Igfals	6,69	11,1	2,726	0,015	0,0727	-4
>sp|Q7TNG5|EMAL2_M	20,92	20,8	22,2	21,1	20,9	21,4	21	21	21	20,1	21	21	21,1	20,9	20	21	20,9	20,5	21,241	20,7589	Eml2	-0,5	21	-2,72	0,015	0,0727	-4
>sp|Q640N1|AEBP1_	17,34	16,4	17,7	17,8	18,5	18	17	17	17	17,2	17	17	16,2	16,6	16	16	16,5	17,4	17,447	16,7429	Aebp1	-0,7	17,1	-2,72	0,015	0,0727	-4
>sp|P14069|S10A6_	20,01	20,9	20,1	20,8	21,1	21,7	21	20	19	18,7	19	19	20	19,9	20	20	20,1	20,2	20,495	19,6783	S100a6	-0,8	20,1	-2,72	0,015	0,0727	-4
>sp|Q5MJS3|FA20C_M	17,24	15,7	17,3	16,9	17,1	17,3	17	17	17	16,9	16	16	15,8	17,1	18	15	15,5	15,3	17,039	16,0427	Fam20c	-1	16,5	-2,72	0,015	0,0727	-4
>sp|P24823|PPBN_M	17,58	16,6	16,2	17,4	17,1	17,4	19	18	18	20,9	21	20	21	18,2	18	18	17,7	17,6	17,555	19,2056	Alppl2	1,65	18,4	2,722	0,015	0,0727	-4
>sp|Q08ED0|B2L15_M	18,9	19,1	19,4	19,3	19,5	19,3	19	19	20	19,1	19	18	18,6	18,8	19	19	19,4	19	19,297	18,8573	Bcl2l15	-0,4	19,1	-2,72	0,015	0,0727	-4
>sp|Q91ZX7|LRP1_M	19,52	19,6	19,9	20	19,5	19,4	20	20	20	18,9	20	19	19,1	18,9	19	20	19,6	19,6	19,738	19,3283	Lrp1	-0,4	19,5	-2,72	0,015	0,0733	-4
>sp|Q6IMF0|KRT87_M	20,05	19	19,5	19,5	19,6	19,5	19	19	18	19,5	19	20	20,5	20,9	19	21	20,9	21,2	19,216	20,2113	Krt87	1	19,7	2,707	0,015	0,0747	-4
>sp|Q9D154|ILEUA_M	24,08	23,4	25,3	23,8	22,8	23,4	24	23	23	24,7	25	24	23,9	24,1	24	25	24,8	25	23,669	24,5038	Serpinb1a	0,83	24,1	2,704	0,015	0,075	-4
>sp|P17225|PTBP1_	22,29	21,6	21,2	22,3	22	21	23	22	23	21,3	23	21	18,7	20,5	20	21	21,8	20,1	21,975	20,839	Ptbp1	-1,1	21,4	-2,7	0,015	0,075	-4
>sp|Q64522|H2A2B_	24,79	25,1	24	24,3	24,5	24,9	25	23	17	26,6	27	27	26,9	27	27	22	26,6	26,7	23,563	26,3206	Hist2h2ab	2,76	24,9	2,698	0,016	0,0758	-4
>sp|P47754|CAZA2_	23,59	22,9	23,5	23,6	23,8	23,7	24	24	24	23,6	24	24	22,8	22,6	23	23	23,3	23,1	23,618	23,1841	Capza2	-0,4	23,4	-2,7	0,016	0,0758	-4
>sp|Q9CR68|UCRI_M	15,06	15,7	15,8	17,1	16,1	18,7	16	18	17	18	17	18	18,3	17,8	17	17	16,9	18,5	16,529	17,6995	Uqcrfs1	1,17	17,1	2,697	0,016	0,0758	-4
>sp|Q7TPD2|F185A_M	15,3	15,4	15,6	15,9	15	14,3	15	15	15	12	14	14	0	14,5	0	14	13,1	0	15,242	9.131965	Fam185a	-6,1	12,2	-2,68	0,016	0,0775	-4
>sp|Q78JT3|3HAO_M	19,08	19	18,1	16,7	18,7	19,6	20	19	19	16,7	18	17	17,5	19	18	17	16,8	18,3	18,685	17,612	Haao	-1,1	18,1	-2,68	0,016	0,0781	-4
>sp|Q99PS0|K1C23_	15,15	15,6	15,8	15,7	15,8	14,8	16	15	15	14,9	15	16	16,5	16,4	17	19	19	18,4	15,419	16,8659	Krt23	1,45	16,1	2,679	0,016	0,0781	-4

>sp|Q5SUR0|PUR4_M	20,47	20,2	19,5	20,5	20	20	20	20	20	20,6	22	20	20,2	22,2	21	21	20,7	20,5	20,078	20,8701	Pfas	0,79	20,5	2,679	0,016	0,0781	-4
>sp|P01897|HA1L_M	19,87	19,9	20,3	20	20,2	20,1	20	20	20	19,8	20	19	20	20,1	20	20	19,4	19,2	20,12	19,6666	H2-L	-0,5	19,9	-2,68	0,016	0,0781	-4
>sp|P47791|GSHR_M	22,51	22,7	22,4	20,4	22,5	22,1	22	23	23	18,8	18	22	22,2	19,3	20	22	22,1	21,6	22,314	20,6547	Gsr	-1,7	21,5	-2,68	0,016	0,0781	-4
>sp|Q11136|PEPD_M	22,68	22,8	22,1	22,3	22,9	23,1	22	23	23	22,8	23	23	22,7	23,7	23	23	22,8	23,3	22,622	23,0137	Pepd	0,39	22,8	2,677	0,016	0,0781	-4
>sp|Q61598|GDIB_M	24,59	24,5	24,6	24,6	24,3	24,6	25	25	25	24,6	24	25	24,5	24,5	24	24	24,3	24,5	24,636	24,4037	Gdi2	-0,2	24,5	-2,67	0,016	0,0787	-4
>sp|Q9D898|ARP5L_	17,08	17,2	16,1	16,6	16,1	17,6	17	18	18	18,3	17	18	17,6	17,5	17	18	18,5	19,6	17,075	17,9638	Arpc5l	0,89	17,5	2,671	0,016	0,0788	-4
>sp|Q8C0M9|ASGL1_	0	0	0	0	0	15	0	0	15	14,8	15	15	15,3	14,5	15	15	0	0	3.35320	11,5762	Asrgl1	8,22	7,46	2,669	0,017	0,079	-4
>sp|O35737|HNRH1_	21,44	21,6	19,1	20,5	18,9	20,8	21	21	21	18,9	19	19	18,1	19,2	19	20	20,9	20,2	20,506	19,3402	Hnrnph1	-1,2	19,9	-2,66	0,017	0,0796	-4
>sp|P70168|IMB1_M	21,43	21,5	21,9	22,2	21,7	21,8	22	21	22	21,6	21	21	21,5	21,2	22	21	21,5	21,3	21,706	21,2976	Kpnb1	-0,4	21,5	-2,66	0,017	0,0796	-4
>sp|Q9D0L8|MCES_M	14,99	15,3	14,8	14,9	14,6	14,6	15	15	14	16,9	16	16	14,1	14,4	16	17	16,1	15,7	14,877	15,7672	Rnmt	0,89	15,3	2,663	0,017	0,0796	-4
>sp|Q8BMJ2|SYLC_M	17,71	18,2	18,1	16,1	16,4	16,8	17	17	16	18,5	19	18	18,1	17,9	18	18	16,6	17,8	17,143	18,0033	Lars	0,86	17,6	2,654	0,017	0,0809	-4
>sp|P70296|PEBP1_	20,22	20,8	20,3	20,1	19,8	20,5	20	21	20	20,6	20	20	19	19,5	19	19	19,8	19,3	20,315	19,7635	Pebp1	-0,6	20	-2,65	0,017	0,0809	-4
>sp|Q9ZDS1|BPNT1_M	24,94	24,1	24,4	24,3	24	24,2	24	25	25	24,8	25	25	24,2	24,6	25	25	24,6	25,3	24,352	24,7316	Bpnt1	0,38	24,5	2,65	0,017	0,0815	-4
>sp|Q8VDM4|PSMD2	19,12	19,2	22,4	20,7	20,8	20,7	20	20	20	20,9	22	22	20,7	22	21	21	20,9	21,6	20,383	21,3128	Psmd2	0,93	20,8	2,647	0,017	0,0817	-4
>sp|P12815|PDCD6_	19,04	19	18,7	19,1	19,6	18,8	19	20	20	19,2	19	19	17,9	18	16	19	18,8	18,6	19,227	18,3483	Pdcd6	-0,9	18,8	-2,64	0,017	0,082	-4
>sp|E9PV24|FIBA_MC	20,93	21,4	21,9	21,4	21,2	19,5	20	20	19	20	19	20	18,7	20,7	20	19	18,9	18,9	20,57	19,4683	Fga	-1,1	20	-2,64	0,017	0,082	-4
>sp|Q920A5|RISC_M	18,31	17,9	18,7	18,5	18,5	18,5	19	18	18	17,4	19	18	17,6	18,1	18	18	18,1	18,2	18,387	17,9935	Scpep1	-0,4	18,2	-2,64	0,018	0,0828	-4
>sp|P26231|CTNA1_	18,84	18,5	18,9	19,7	18,8	19	20	19	19	19,4	18	18	18,1	18,3	18	19	18,4	18,4	19,021	18,4245	Ctnna1	-0,6	18,7	-2,64	0,018	0,0828	-4
>sp|Q9DBL1|ACDSB_I	16,94	16,5	17,6	16	15,8	17	17	16	16	18,4	19	16	16,6	18,2	16	18	17,9	18,2	16,592	17,6555	Acadsb	1,06	17,1	2,637	0,018	0,0828	-4
>sp|Q9WV85|NDK3_I	15,87	17,1	16,9	15,7	17,6	17	16	17	16	17,2	17	17	17,8	17	18	17	16,7	17,1	16,638	17,273	Nme3	0,63	17	2,624	0,018	0,085	-4
>sp|Q9D8E6|RL4_MO	15,52	14,8	14,9	15,8	16,9	15,6	0	12	0	17,1	18	19	17,3	17,6	17	19	17	17	11,772	17,6679	Rpl4	5,9	14,7	2,623	0,018	0,085	-4
>sp|Q9EST5|AN32B_M	20,65	19,3	23,4	20,2	20,1	19,7	20	21	20	22,4	22	23	22,8	22,5	23	20	20,6	20,4	20,438	21,8164	Anp32b	1,38	21,1	2,622	0,018	0,085	-4
>sp|P01863|GCAA_M	17,87	17,9	18,2	17,5	17,8	17,9	18	18	15	16,9	17	16	16,2	17,3	15	17	16,8	16,4	17,575	16,4811	Ighg	-1,1	17	-2,62	0,018	0,085	-4
>sp|P14430|HA18_M	19,63	19,8	19,9	19,8	19,6	19,7	20	20	20	19,3	20	18	19,6	19,4	20	19	19,1	18,9	19,706	19,1782	H2-Q8	-0,5	19,4	-2,62	0,018	0,0853	-4
>sp|Q9EPL8|IPO7_MC	17,1	16,9	18,2	18,4	17	17,2	17	17	17	17,3	20	18	17,6	18	18	19	17,5	17,5	17,196	18,1275	Ipo7	0,93	17,7	2,618	0,018	0,0854	-4
>sp|O35598|ADA10_	17,09	17,1	17,9	18,3	18	17,2	17	17	18	16,8	17	17	17,4	17	17	16	16,3	16,1	17,483	16,793	Adam10	-0,7	17,1	-2,61	0,019	0,0862	-4
>sp|P14429|HA17_M	19,7	19,9	20	19,9	19,7	19,7	20	20	20	19,4	20	18	19,6	19,5	20	19	19,2	19	19,797	19,2735	H2-Q7	-0,5	19,5	-2,61	0,019	0,0862	-4
>sp|P62257|UBE2H_	18,42	17,7	17,5	17,4	18	18	17	17	18	18,7	19	18	18,4	18,5	19	17	18,3	17,9	17,687	18,3132	Ube2h	0,63	18	2,611	0,019	0,0862	-4
>sp|P52480|KPYM_M	26,83	25,7	26,1	25,7	26,7	25,1	26	27	27	25,7	26	26	25,8	25,7	25	26	25,6	25,5	26,207	25,616	Pkm	-0,6	25,9	-2,61	0,019	0,0865	-4
>sp|Q07113|MPRI_M	16,88	16	14,4	16,5	16,7	15,1	17	15	17	14	16	16	13,5	13,1	14	14	16	15,9	16,139	14,7081	Igf2r	-1,4	15,4	-2,61	0,019	0,0867	-4
>sp|Q9CQZ5|NDUA2_	16,66	18,8	19,2	17,4	17,1	17,6	19	19	19	18,4	21	21	18,7	19,8	19	19	19	19,3	18,173	19,3075	Ndufa2	1,13	18,7	2,605	0,019	0,0867	-4
>sp|P62983|RS27A_	21,09	20,4	20,6	21,5	21,4	21,2	22	21	21	21	21	21	21,2	20,6	19	20	20,4	20,8	21,136	20,5469	Rps27a	-0,6	20,8	-2,61	0,019	0,0867	-4
>sp|P62984|RL40_M	21,09	20,4	20,6	21,5	21,4	21,2	22	21	21	21	21	21	21,2	20,6	19	20	20,4	20,8	21,136	20,5469	Uba52	-0,6	20,8	-2,61	0,019	0,0867	-4
>sp|Q91WS4|BHMT2_	15,71	16,1	15,3	15,4	15,6	15,6	16	16	16	15,4	15	16	15,5	15,4	16	15	15,7	14,8	15,764	15,3806	Bhmt2	-0,4	15,6	-2,6	0,019	0,0867	-4
>sp|P01865|GCAM_I	17,45	17,5	17,7	17,1	17,5	17,5	17	18	15	16,6	17	15	15,8	16,8	14	17	16,4	16	17,152	16,0729	Igh-1a	-1,1	16,6	-2,6	0,019	0,0867	-4
>sp|Q9JHU4|DYHC1_I	18,34	18,6	18,6	17,9	18,6	19,4	18	18	18	19,3	19	18	18,9	19,1	19	19	18,9	19	18,437	18,9478	Dync1h1	0,51	18,7	2,603	0,019	0,0867	-4
>sp|O88569|ROA2_M	19,98	20,1	20,5	19,9	20,4	19,6	20	19	20	18,7	19	19	19,9	20	19	20	19,8	19,7	20,039	19,5298	Hnrnpa2b	-0,5	19,8	-2,6	0,019	0,0867	-4
>sp|P11679|K2C8_M	22,12	21,5	22,3	21,5	21,9	22,1	22	22	22	22	23	22	22	22	22	23	23	23	21,995	22,5674	Krt8	0,57	22,3	2,601	0,019	0,0867	-4
>sp|Q9QZ73|DCNL1_I	18,73	18,9	19,1	18,8	19,4	18,6	19	19	19	19,5	19	20	19,3	20	20	19	19,3	19,2	18,931	19,4329	Dcun1d1	0,5	19,2	2,601	0,019	0,0867	-4
>sp|Q9JLV5|CUL3_M	22,06	20,3	20,1	21,1	22,2	22,4	20	22	22	18,8	19	19	21,3	20,9	20	20	21,2	21	21,327	19,988	Cul3	-1,3	20,7	-2,6	0,019	0,0868	-4
>sp|Q8R081|HNRPL_	18,9	18,9	19,7	20,1	20,1	19,9	20	19	19	20,1	20	20	19,9	20,5	21	20	19,5	19,8	19,49	20,0407	Hnrnpl	0,55	19,8	2,599	0,019	0,0869	-4
>sp|Q9WU78|PDC6I_	21,57	22,4	21	21,8	22	21,1	22	21	22	20,9	21	21	21,7	21,1	22	21	21,6	20,9	21,732	21,1781	Pdcd6ip	-0,6	21,5	-2,59	0,019	0,0878	-4
>sp|P61205|ARF3_M	22,93	24,7	22,8	22,7	22,7	22,5	23	24	24	23,1	23	23	22,9	21,6	21	22	22,4	22,1	23,185	22,3218	Arf3	-0,9	22,8	-2,59	0,02	0,0883	-4
>sp|P84078|ARF1_M	22,93	24,7	22,8	22,7	22,7	22,5	23	24	24	23,1	23	23	22,9	21,6	21	22	22,4	22,1	23,185	22,3218	Arf1	-0,9	22,8	-2,59	0,02	0,0883	-4
>sp|P62492|RB11A_	22,65	22,8	20,3	22,6	22,3	21,3	22	21	21	21	22	21	20,8	20,5	21	21	21	20,7	21,764	20,9649	Rab11a	-0,8	21,4	-2,59	0,02	0,0884	-4
>sp|P97821|CATC_M	20,94	21,3	18,6	21,5	21,6	20,9	21	20	21	19,8	16	17	20,9	19,1	20	20	20,5	17,2	20,687	19,0073	Ctsc	-1,7	19,8	-2,59	0,02	0,0886	-4
>sp|P16301|LCAT_M	19,44	18,9	19,9	20,5	19,8	19,7	20	20	20	19	19	19	19,4	19,4	19	20	18,3	19,8	19,736	19,1434	Lcat	-0,6	19,4	-2,59	0,02	0,0886	-4
>sp|Q62000|MIME_M	19,68	20,6	20,3	21,2	20,8	20,8	21	21	21	22,4	20	22	22	21,9	21	22	21	21,2	20,764	21,4985	Ogn	0,73	21,1	2,58	0,02	0,0893	-4

>sp|Q8VDD5|MYH9_M	19,62	20	20,7	20,8	19,9	20,2	20	20	20	21	20	20	20,2	20,6	20	21	20,5	20,6	20,109	20,5123	Myh9	0,4	20,3	2,579	0,02	0,0894	-4
>sp|Q9JK88|SPI2_MC	18,02	17,8	18,1	17,6	17,8	19,1	18	18	19	17,2	18	18	17,2	16,9	18	19	17,1	17,3	18,171	17,5546	Serpini2	-0,6	17,9	-2,57	0,02	0,0904	-4
>sp|Q5NCQ5|DPH1_M	16,32	15,9	16,7	14,5	14,7	15,6	16	16	15	17,3	16	17	17,5	16,2	16	16	17,8	16,3	15,687	16,6054	Dph1	0,92	16,1	2,572	0,02	0,0904	-4
>sp|P70333|HNRH2_	21,54	21,7	19,1	20,6	18,8	20,9	21	21	21	19,1	19	19	18,3	19,3	19	20	20,9	20,3	20,589	19,4491	Hnrnph2	-1,1	20	-2,57	0,02	0,0904	-4
>sp|Q9WUA3|PFKAP_	21,95	21,5	22,1	21,5	21,5	21,4	22	22	22	21,4	21	21	21,5	21,4	22	22	21,6	20,7	21,751	21,3589	Pfkp	-0,4	21,6	-2,57	0,02	0,0904	-4
>sp|Q5M8N0|CNRP1	15,2	16,4	16,7	16,5	16,7	17,1	17	15	15	16,9	16	17	17,1	17	17	17	16,9	16,9	16,133	16,9584	Cnrip1	0,83	16,5	2,569	0,02	0,0906	-4
>sp|P62301|RS13_M	21,25	19,2	19,9	19	19,2	19,4	19	19	20	19,1	21	20	22,6	20	23	20	22,7	20,2	19,559	20,9502	Rps13	1,39	20,3	2,563	0,021	0,0916	-4
>sp|Q99KI0|ACON_M	23,89	23,9	24	24,8	24,2	24,2	25	24	25	24,5	25	25	24,6	24,3	24	25	25,1	25,1	24,281	24,7232	Aco2	0,44	24,5	2,559	0,021	0,0924	-4
>sp|P32261|ANT3_M	24,26	24	24,3	23,9	24,4	24,7	24	24	25	24	24	24	24,2	24	24	24	24,2	23,8	24,341	24,0597	Serpinc1	-0,3	24,2	-2,56	0,021	0,0925	-4
>sp|Q01730|RSU1_M	19,87	21,4	20,1	21,4	21,1	21,8	20	21	22	22	23	22	21,8	21,6	21	21	21,6	21,8	20,935	21,7646	Rsu1	0,83	21,3	2,556	0,021	0,0925	-4
>sp|Q9ZDL8|GGH_MO	18,2	19,3	18,8	17,5	17	19,1	19	19	19	17,7	18	18	17,2	17,7	18	17	17,5	18,2	18,594	17,7761	Ggh	-0,8	18,2	-2,56	0,021	0,0925	-4
>sp|P97300|NPTN_M	0	16,2	14,8	14	0	0	15	0	0	0	0	0	0	0	0	0	0	0	6,6372	0	Nptn	-6,6	3,32	-2,55	0,021	0,0931	-4
>sp|Q8BVF2|PDCL3_M	19,72	19,9	20,9	19,4	20,1	19,8	20	20	20	20,9	20	21	21,2	20,7	21	21	20,2	19,8	20,016	20,5474	Pdcl3	0,53	20,3	2,547	0,021	0,0939	-4
>sp|Q07417|ACADS_	20,87	21,5	21,6	22,1	22	21,4	22	21	22	21,3	21	21	20,9	21,6	22	21	21,1	21	21,621	21,1698	Acads	-0,5	21,4	-2,54	0,021	0,0944	-4
>sp|Q8CID3|FA20A_M	16,84	14,6	17,1	16,8	16,8	17,1	17	17	17	16,9	15	15	15,2	16,8	17	13	14,6	14,5	16,753	15,4481	Fam20a	-1,3	16,1	-2,54	0,021	0,0944	-4
>sp|Q99KR7|PPIF_M(	18,03	20	19,9	19,4	18	18,7	20	18	19	19,4	20	20	20,3	20,4	19	19	20	20,3	19,015	19,8529	Ppif	0,84	19,4	2,541	0,022	0,0947	-4
>sp|Q9ERE2|KRT81_M	20,25	19,7	19,6	19,6	19,9	19,7	19	19	18	19,6	19	20	20,6	21	20	21	21,1	21,4	19,458	20,3769	Krt81	0,92	19,9	2,539	0,022	0,0949	-4
>sp|O08810|U5S1_M	19,58	19,4	19	20,7	18,2	19,9	19	19	19	19,7	20	19	20,4	20,5	22	20	19,7	19,8	19,311	20,2316	Eftud2	0,92	19,8	2,536	0,022	0,0955	-4
>sp|P14131|RS16_M	20,96	21,3	20,8	21,3	22,4	22	21	21	22	22	22	22	21,3	21,8	22	22	22,3	22,1	21,436	21,9422	Rps16	0,51	21,7	2,534	0,022	0,0957	-4
>sp|P97861|KRT86_	20,2	19,6	19,6	19,6	19,8	19,6	19	19	18	19,6	19	20	20,6	21	20	21	21	21,3	19,405	20,3174	Krt86	0,91	19,9	2,532	0,022	0,096	-4
>sp|Q8VCH0|THIKB_M	15,47	17,6	17,4	17,7	17	17	17	17	18	18	19	19	17,2	18,3	18	17	17,4	19	17,123	18,012	Acaa1b	0,89	17,6	2,53	0,022	0,096	-4
>sp|Q921H8|THIKA_M	15,47	17,6	17,4	17,7	17	17	17	17	18	18	19	19	17,2	18,3	18	17	17,4	19	17,123	18,012	Acaa1a	0,89	17,6	2,53	0,022	0,096	-4
>sp|Q60692|PSB6_M	23,24	24,5	24,7	24,8	25,2	25,1	25	25	25	24,3	24	24	24,4	24,6	24	24	23,8	23,5	24,723	24,111	Psmb6	-0,6	24,4	-2,53	0,022	0,0965	-4
>sp|Q8C4B4|U119B_	17,42	18,4	16,1	16,6	16,9	16,6	16	17	17	17,7	18	18	17,5	16,9	17	19	17,6	17,5	16,825	17,6687	Unc119b	0,84	17,2	2,515	0,023	0,0987	-5
>sp|P05214|TBA3_M	24,78	24,3	25,2	24	24,7	24,4	25	25	25	24,3	25	24	24,6	24,4	24	24	24	24,5	24,7	24,2985	Tuba3a	-0,4	24,5	-2,51	0,023	0,0987	-5
>sp|Q9JK23|PSMG1_	19,9	19,1	18,2	18,9	19,2	20,2	19	20	22	20,1	22	21	20,6	20,4	22	21	20,1	20,1	19,666	20,8312	Psmg1	1,16	20,2	2,51	0,023	0,0994	-5
>sp|P0CG50|UBC_M(	18,19	17,3	17,7	18,5	18,3	18,4	18	18	18	17,9	17	18	18,2	17,6	16	17	17,5	17,9	18,114	17,531	Ubc	-0,6	17,8	-2,5	0,023	0,1005	-5
>sp|P41216|ACSL1_I	19,42	20	19,2	19,4	18,9	18,8	19	19	19	18,5	18	19	18,8	18,4	19	19	18,3	19,5	19,221	18,7	Acsl1	-0,5	19	-2,5	0,023	0,1011	-5
>sp|P06728|APOA4_	22,91	21,6	23	23,3	23	23,7	22	22	22	23,4	24	24	23,2	23,7	23	23	23	23,1	22,623	23,3026	Apoa4	0,68	23	2,495	0,024	0,1022	-5
>sp|Q8JZQ9|EIF3B_M(	20,44	20,6	20,3	20,6	20,6	20,3	21	21	20	21,2	21	21	20,5	20,8	21	21	20,6	21	20,586	20,889	Eif3b	0,3	20,7	2,493	0,024	0,1025	-5
>sp|A2AQ19|RTF1_M	16,92	15	15,6	17,2	16,9	14,5	14	17	17	18	15	16	18,2	17,4	18	17	17,3	17,7	15,989	17,2158	Rtf1	1,23	16,6	2,488	0,024	0,1032	-5
>sp|Q99KD5|UN45A_	16,29	15,1	16,8	14,5	16,7	15,2	16	15	17	17,3	18	0	0	13,9	0	14	0	17,1	15,874	8.856617	Unc45a	-7	12,4	-2,49	0,024	0,1035	-5
>sp|P06339|HA15_M	17,62	17,5	18,4	17,7	17,7	17,3	17	17	17	16,2	17	16	17,4	16,5	18	17	17,3	15,5	17,473	16,7055	H2-T23	-0,8	17,1	-2,48	0,024	0,1037	-5
>sp|Q9D6R2|IDH3A_I	21,06	21,3	21	21,2	21	21,2	21	21	21	22,1	21	22	21,5	21,2	22	21	21,3	21,3	21,172	21,4996	Idh3a	0,33	21,3	2,48	0,024	0,1046	-5
>sp|Q91XF0|PNPO_M	19,94	20,7	21,2	20,5	21,7	21,9	20	21	21	21,8	21	22	21,5	21,7	22	21	20,8	22,4	20,88	21,5562	Pnpo	0,68	21,2	2,479	0,024	0,1046	-5
>sp|Q9JHI5|IVD_MOU	21,91	21,6	21,7	22,1	21,6	22,3	22	22	22	21,5	22	21	22,3	21,2	22	21	21,7	21,5	21,957	21,514	Ivd	-0,4	21,7	-2,47	0,025	0,1054	-5
>sp|Q62261|SPTB2_I	21,02	21,1	19,9	20,9	21	21	21	21	19	19,2	19	19	20,3	18,9	20	20	21,3	19,8	20,648	19,8484	Sptbn1	-0,8	20,2	-2,47	0,025	0,1056	-5
>sp|P35802|GPM6A	18,21	18,7	20,4	17,7	18,4	18,4	18	17	18	19,8	19	19	20,1	20,3	20	20	19,1	17,4	18,318	19,3518	Gpm6a	1,03	18,8	2,472	0,025	0,1057	-5
>sp|P0CG49|UBB_M(	19,41	18,7	19	19,8	19,7	19,5	20	19	19	19,3	19	19	19,6	19	17	19	18,8	19,2	19,43	18,8594	Ubb	-0,6	19,1	-2,46	0,025	0,108	-5
>sp|P70372|ELAV1_I	15,3	15,4	16,2	16,5	16,1	16,4	17	16	16	15,7	0	15	0	0	15	15	15,2	15	16,147	10,0341	Elavl1	-6,1	13,1	-2,46	0,026	0,1089	-5
>sp|P23506|PIMT_M	19,67	19,7	18,4	19,2	19,1	18,6	19	19	19	19,2	20	20	19,8	21,9	20	20	19	19,6	19,163	19,9426	Pcmt1	0,78	19,6	2,445	0,026	0,1109	-5
>sp|P55288|CAD11_	15,01	14,2	15,5	0	14,5	13,9	15	15	14	0	15	13	13,4	13,2	0	0	0	0	13,037	6.030909	Cdh11	-7	9,53	-2,44	0,026	0,1109	-5
>sp|P21107|TPM3_M	16,83	18,7	15,6	16	15,4	18,2	18	16	18	19,9	16	20	19,5	18,6	18	18	18,4	18,8	16,981	18,4822	Tpm3	1,5	17,7	2,444	0,026	0,1109	-5
>sp|P58771|TPM1_M	16,83	18,7	15,6	16	15,4	18,2	18	16	18	19,9	16	20	19,5	18,6	18	18	18,4	18,8	16,981	18,4822	Tpm1	1,5	17,7	2,444	0,026	0,1109	-5
>sp|P58774|TPM2_M	16,83	18,7	15,6	16	15,4	18,2	18	16	18	19,9	16	20	19,5	18,6	18	18	18,4	18,8	16,981	18,4822	Tpm2	1,5	17,7	2,444	0,026	0,1109	-5
>sp|Q9WVQ5|MTNB_I	18,91	18,8	19,4	19,3	19,3	19,6	19	18	18	19,3	20	19	19,9	20	20	19	19	19,3	18,963	19,5265	Apip	0,56	19,2	2,443	0,026	0,111	-5
>sp|Q9JJK2|LANC2_M	18,83	18,6	19,5	17	20,2	17,5	17	17	17	16,4	19	16	17,2	15,6	16	18	15,3	16,6	18,129	16,7302	Lancl2	-1,4	17,4	-2,44	0,026	0,1117	-5
>sp|Q6P069|SORCN_	20,15	20,4	21,3	19,7	19,2	19,9	20	20	19	18,6	20	20	19,1	19,5	19	19	18,7	19	19,952	19,2394	Sri	-0,7	19,6	-2,44	0,027	0,1119	-5

>sp|Q9DA19|CIR1_M	17,56	20,4	19,6	19,5	19,4	19,8	20	20	20	20	20	20	20,7	20,5	20	20	19,9	20	19,514	20,1908	Cir1	0,68	19,9	2,43	0,027	0,1135	-5
>sp|P62911|RL32_M	0	0	16,8	18,1	17,9	16,8	0	16	0	17,1	15	16	17,5	15,7	17	18	17,6	17	9.55232	16,8567	Rpl32	7,3	13,2	2,427	0,027	0,114	-5
>sp|Q9WVP6|PAPOB	16,54	17,1	16,3	15,8	15,6	14,6	15	15	15	14,3	15	16	15,5	14,6	15	14	15,3	15,5	15,749	14,9889	Papolb	-0,8	15,4	-2,42	0,027	0,1143	-5
>sp|A6H630|ARMT1_	18,38	17,4	17,4	15	16,6	17	17	18	18	17,3	18	19	17,7	18,1	18	17	18,7	17,4	17,081	17,9488	Armt1	0,87	17,5	2,424	0,027	0,1143	-5
>sp|Q9Z0P5|TWF2_M	18,81	19	21,8	19,1	18,6	21,7	21	21	22	19,2	24	25	25	19,6	24	19	23,1	24,1	20,372	22,6633	Twf2	2,29	21,5	2,418	0,028	0,1157	-5
>sp|P48774|GSTM5_	21,96	23,8	23,6	23,5	23,3	23,3	24	24	22	23,8	24	24	23,6	23,7	24	24	23,7	23,8	23,225	23,7642	Gstm5	0,54	23,5	2,417	0,028	0,1157	-5
>sp|Q9D0M1|KPRA_I	20,61	20,7	20,3	20,6	20	20,1	21	20	20	19	19	19	20,4	20,4	20	20	20,2	20,5	20,447	19,9018	Prpsap1	-0,5	20,2	-2,41	0,028	0,1163	-5
>sp|Q60973|RBBP7_	21,79	21,9	21,6	21,6	21,7	21,9	22	22	22	22,2	22	22	22,2	22,2	22	23	21,6	22	21,852	22,1317	Rbbp7	0,28	22	2,411	0,028	0,1168	-5
>sp|Q64G17|AN32C_	19,67	19,4	19,4	19,6	19,8	19,6	20	19	19	18,3	18	19	19,3	19,4	20	19	19,4	19,1	19,546	19,0314	Anp32c	-0,5	19,3	-2,41	0,028	0,117	-5
>sp|Q9Z2T6|KRT85_M	20,15	19,1	19,6	19,7	20	19,8	19	19	18	19,7	19	20	20,5	20,9	20	21	21	21,3	19,441	20,2846	Krt85	0,84	19,9	2,401	0,029	0,1186	-5
>sp|Q3UV17|K22O_M	20,5	20,8	21,3	20,4	20,5	20	19	20	20	20,2	20	20	20,9	21	21	22	22,2	22,3	20,234	21,1153	Krt76	0,88	20,7	2,401	0,029	0,1186	-5
>sp|Q9CRB3|HIUH_M	19,13	18,6	22	21,8	22,5	22	19	22	22	22,9	22	22	22,6	22,5	23	20	22,6	22,9	20,925	22,3539	Urah	1,43	21,6	2,4	0,029	0,1186	-5
>sp|Q8VE62|PAIP1_M	18,51	18,2	17,3	18,5	17,9	18	18	19	18	17,7	19	19	19,3	19,2	19	19	18,5	18,6	18,169	18,6998	Paip1	0,53	18,4	2,4	0,029	0,1186	-5
>sp|Q99KP6|PRP19_	22,07	22	21,2	22,1	21	20,2	20	21	21	22	22	22	22,7	22,1	22	22	21,3	20,9	21,215	21,9385	Prpf19	0,72	21,6	2,398	0,029	0,1188	-5
>sp|P12710|FABPL_I	16,13	18,8	19	18,5	18,7	18,9	19	19	19	19,3	18	19	19,8	19,3	20	20	19,7	18,9	18,47	19,2807	Fabp1	0,81	18,9	2,398	0,029	0,1188	-5
>sp|P46737|BRCC3_	15,41	15,7	17,4	16,8	16,9	19,1	17	17	17	17,1	19	19	19	18	18	17	17,1	17,8	16,896	17,8959	Brcc3	1	17,4	2,392	0,029	0,12	-5
>sp|Q61035|SYHC_M	19,69	19,6	19,1	19	19,3	18,8	19	19	19	19,3	19	19	19,4	19,5	20	20	19,6	19,5	19,17	19,4742	Hars	0,3	19,3	2,391	0,029	0,1202	-5
>sp|P49429|HPPD_M	18,31	18,1	17,9	18,4	17,7	17,6	18	19	18	18,4	15	17	17,6	17,3	16	18	17,2	17,9	18,065	17,1093	Hpd	-1	17,6	-2,39	0,029	0,1209	-5
>sp|Q9ERK4|XPO2_M	20,4	20,6	20,6	20,8	20,7	20,4	21	21	18	24,3	18	18	24,3	24	24	24	23,6	23,6	20,371	22,6363	Cse1l	2,27	21,5	2,382	0,03	0,1219	-5
>sp|Q9JJZ2|TBA8_MC	23,93	23,8	23,4	23,3	23,9	23,3	24	24	24	23,8	24	23	23,6	23,3	23	23	23,4	22,8	23,709	23,3571	Tuba8	-0,4	23,5	-2,38	0,03	0,1223	-5
>sp|Q9R0N0|GALK1_	20,33	20,5	20,9	21,2	21,4	20,9	21	21	20	22,1	21	21	22,4	22,5	23	22	20,2	21,7	20,831	21,6215	Galk1	0,79	21,2	2,379	0,03	0,1225	-5
>sp|Q8BVG4|DPP9_M	17,04	17,2	17,3	16,4	16,7	17,1	16	17	16	16	17	18	17,5	17,7	18	18	17,6	17,5	16,762	17,3532	Dpp9	0,59	17,1	2,373	0,03	0,1237	-5
>sp|Q05895|TSP3_M	21,02	21	21	21,2	20,9	19,9	20	20	18	19,2	19	19	19,4	19,6	20	20	19,2	19,9	20,297	19,4745	Thbs3	-0,8	19,9	-2,37	0,03	0,1239	-5
>sp|Q9WV92|E41L3_	15,38	14,2	0	13,1	15,6	13,9	14	14	14	14,2	13	12	0	0	0	0	0	14,6	12,625	5.945647	Epb41l3	-6,7	9,29	-2,37	0,031	0,1247	-5
>sp|Q9CX80|CYGB_M	16,74	19,2	16,7	17,1	18	16,4	18	21	20	21,5	19	20	19,2	18,9	19	19	19,5	19,4	18,145	19,5452	Cygb	1,4	18,8	2,366	0,031	0,125	-5
>sp|Q60675|LAMA2_	14,26	14,1	13,8	13,8	13,6	12,8	14	13	13	10,6	12	14	13,4	12,9	14	13	13,3	12,4	13,638	12,7709	Lama2	-0,9	13,2	-2,37	0,031	0,1251	-5
>sp|Q9JI46|NUDT3_M	19,45	17,5	18,6	17,8	17,3	17,3	16	18	18	15	17	17	17	17,5	17	17	17	17,3	17,763	16,8665	Nudt3	-0,9	17,3	-2,36	0,031	0,1263	-5
>sp|P38647|GRP75_	21,46	20,8	21,2	21,6	21,3	21,1	21	21	21	21,1	21	21	20,6	20,9	21	20	21,1	21	21,139	20,8447	Hspa9	-0,3	21	-2,36	0,031	0,1263	-5
>sp|P09671|SODM_M	22,64	24	23,6	23,3	24	23,7	25	26	25	23,4	23	23	23,6	22,9	23	24	22,7	23,6	24,065	23,3157	Sod2	-0,7	23,7	-2,36	0,031	0,1269	-5
>sp|Q63932|MP2K2_	21,44	21,4	21,2	21,2	21	20,3	21	21	21	20,9	20	19	20,7	20,9	21	21	19,4	20,9	21,008	20,4236	Map2k2	-0,6	20,7	-2,35	0,031	0,127	-5
>sp|Q99L45|IF2B_MC	18,88	15,7	15,4	18,4	17,9	16,2	19	16	15	15,6	15	16	17,4	15,6	16	14	15,5	15,7	16,926	15,6102	Eif2s2	-1,3	16,3	-2,35	0,031	0,1272	-5
>sp|Q9Z1Q5|CLIC1_M	22,54	20,8	22,1	21,6	21,9	22,3	22	22	22	22	21	21	21,7	21,2	21	21	21,4	21	21,846	21,385	Clic1	-0,5	21,6	-2,35	0,032	0,128	-5
>sp|Q8VCF0|MAVS_M	19,72	16,1	19,3	19,9	16,2	19,3	19	18	18	17,4	18	17	16	15,2	17	18	18,1	17	18,474	17,0937	Mavs	-1,4	17,8	-2,35	0,032	0,1282	-5
>sp|Q61496|DDX4_M	15,49	14,1	15,3	16,1	15,1	14,4	15	14	16	15,6	15	15	15,6	15,7	16	16	15,8	15,7	15,037	15,5946	Ddx4	0,56	15,3	2,348	0,032	0,1282	-5
>sp|P61222|ABCE1_	19,8	19,7	19,7	19,4	19,8	20	19	19	20	20,2	20	21	20,2	20,8	21	19	19,5	19,7	19,59	20,141	Abce1	0,55	19,9	2,344	0,032	0,1289	-5
>sp|Q6NT99|DUS23_I	16,28	17,2	15,2	16,1	16,2	14,7	16	15	15	16,7	16	16	17,8	16	17	16	16,6	16,8	15,755	16,5745	Dusp23	0,82	16,2	2,344	0,032	0,1289	-5
>sp|P00342|LDHC_M	22,21	22,7	19,4	22,5	22,4	22,4	22	22	22	20,1	19	20	19,9	22,3	22	22	19,8	21,9	22,058	20,7805	Ldhc	-1,3	21,4	-2,34	0,032	0,1297	-5
>sp|P62245|RS15A_	28,39	28,3	20,2	27,4	22,8	20,2	22	20	19	20,7	20	21	21,4	20,5	21	19	17,1	20,2	23,182	20,0562	Rps15a	-3,1	21,6	-2,34	0,032	0,1302	-5
>sp|Q62009|POSTN_I	21,25	19,9	22,6	22,1	22,6	22,7	23	22	22	20,6	23	22	20,8	20,9	21	21	21,3	21	22,054	21,1831	Postn	-0,9	21,6	-2,34	0,033	0,1304	-5
>sp|O70423|AOC3_M	21,97	21,9	23,3	23,4	23,2	23	22	23	23	21,7	21	23	22,7	22,9	23	21	22,5	21,1	22,77	22,0006	Aoc3	-0,8	22,4	-2,34	0,033	0,1304	-5
>sp|Q3TIU4|PDE12_M	15,5	16,5	16,8	16,4	15,7	16,3	16	16	16	16,5	16	17	16,7	16,8	17	16	16,7	17	16,121	16,5828	Pde12	0,46	16,4	2,33	0,033	0,1316	-5
>sp|Q08652|RET2_M	19,89	23,7	23,8	19,3	20	20,5	21	23	21	22,7	24	25	22,8	22,6	22	22	24,3	22	21,319	22,9455	Rbp2	1,63	22,1	2,328	0,033	0,132	-5
>sp|P0C7N9|PSMG4_	0	0	0	14,7	0	0	18	16	17	17,7	18	18	16,9	16,9	17	0	16,4	17	7.32801	15,3537	Psmg4	8,03	11,3	2,325	0,033	0,1327	-5
>sp|P15331|PERI_M(	14,22	17,5	16,1	17,6	17,7	16,1	17	17	14	21,1	20	21	17	15,7	17	17	17,3	17	16,315	18,2274	Prph	1,91	17,3	2,323	0,033	0,1329	-5
>sp|P01804|HVM35	16,45	16,7	18,2	19,4	14,5	14,8	16	18	17	18,5	17	18	19,8	18,1	17	19	17,9	17,8	16,803	18,1923	>sp|P018	1,39	17,5	2,316	0,034	0,1348	-5
>sp|Q9CSN1|SNW1_M	17,74	17,4	15,8	18,1	17,9	17,7	18	17	17	18,9	16	20	19,8	16,3	20	20	19,5	19,6	17,46	18,7979	Snw1	1,34	18,1	2,313	0,034	0,1352	-5
>sp|Q78PY7|SND1_M	20,16	20,5	22	20,8	21,2	21,7	21	21	21	21,3	22	22	21,2	22,1	22	21	21,4	21,3	20,973	21,5308	Snd1	0,56	21,3	2,312	0,034	0,1352	-5
>sp|Q9ZDX4|PDE3A_I	16,6	14,2	15,4	15,7	15,1	16,4	15	15	16	14,6	16	14	14,3	15,1	14	16	14,8	15	15,532	14,8358	Pde3a	-0,7	15,2	-2,31	0,034	0,1352	-5

>sp|P19324|SERPH_I	18,31	18,8	19,3	19,1	19,2	19,2	19	19	20	20,3	20	19	19,8	19,6	19	20	20,5	20,4	19,231	19,8256	Serpinh1	0,59	19,5	2,307	0,034	0,1365	-5
>sp|P02468|LAMC1_	19,74	20,3	22,3	22,8	22,8	20,9	22	22	23	22,8	23	22	23,1	22,6	23	22	22,3	22,6	21,736	22,6331	Lamc1	0,9	22,2	2,303	0,035	0,1373	-5
>sp|P26041|MOES_M	22,86	22,5	22,3	22,7	22,3	22,9	23	22	23	23	23	23	22,4	22,4	23	23	23,1	23,3	22,561	22,8506	Msn	0,29	22,7	2,302	0,035	0,1376	-5
>sp|P04071|K1B16_	21,67	21,5	21,3	21,8	21,6	21,2	22	21	22	21,3	20	21	21,4	21,4	22	21	21,3	21,1	21,548	21,1409	Klk1b16	-0,4	21,3	-2,3	0,035	0,1383	-5
>sp|P24527|LKHA4_	21,92	22,2	22,4	22,6	22,5	22,8	22	22	23	22,3	22	22	22,3	22,1	22	22	21,9	21,7	22,385	22,1095	Lta4h	-0,3	22,2	-2,3	0,035	0,1388	-5
>sp|P20060|HEXB_M	19,53	19,6	18,5	18,4	18,4	18,1	19	19	18	17,8	18	18	18,3	18,8	19	18	18	18,2	18,769	18,2392	Hexb	-0,5	18,5	-2,29	0,035	0,1389	-5
>sp|Q60597|ODO1_M	21,38	20,8	20,4	20,6	19,9	20,6	21	21	21	21,3	20	21	21,4	20,5	21	21	21,6	21,5	20,649	21,0892	Ogdh	0,44	20,9	2,292	0,036	0,1396	-5
>sp|Q8K157|GALM_M	19,49	19	18,6	19,1	20,3	20,6	20	20	20	20	20	19	21,2	20,7	21	20	20,7	19,9	19,662	20,3541	Galm	0,69	20	2,29	0,036	0,14	-5
>sp|Q45VN2|DFA20_	24,09	25,6	26,2	25,5	25,7	26	25	25	25	24,8	25	24	24,9	25,4	25	25	24,9	24,8	25,388	24,8428	Defa20	-0,5	25,1	-2,29	0,036	0,14	-5
>sp|P27048|RSMB_M	18,92	19,5	18,5	19	18,5	18,6	18	19	18	19,2	19	19	19	19,4	19	19	18,5	19,3	18,647	19,0925	Snrpb	0,45	18,9	2,287	0,036	0,1402	-5
>sp|Q9DCS3|MECR_M	17,03	18,6	22,8	24,1	18,7	18,6	23	24	23	23,8	23	21	23,7	23,8	24	24	23,6	23,9	21,087	23,3215	Mecr	2,23	22,2	2,287	0,036	0,1402	-5
>sp|Q05BC3|EMAL1_	19,34	17,1	17,4	16,9	17,1	17	17	17	17	16,6	17	17	16,3	17,2	17	16	17,3	15,5	17,269	16,4907	Eml1	-0,8	16,9	-2,28	0,036	0,1407	-5
>sp|Q9WVJ9|FBLN4_I	20,88	19,8	19,3	20,7	20,8	20,7	21	18	21	18,2	21	19	20,1	18,6	18	20	18,1	20,2	20,223	19,1585	Efemp2	-1,1	19,7	-2,28	0,036	0,142	-5
>sp|Q91VA1|CTL4_M	19,55	17,9	18,6	17,6	14,9	17,4	17	16	17	17	15	14	15,5	15,9	18	17	15,4	15,4	17,255	15,9253	Slc44a4	-1,3	16,6	-2,27	0,037	0,1433	-5
>sp|P63163|RSMN_M	18,8	19,4	18,4	18,9	18,4	18,5	18	18	18	19,1	19	19	18,9	19,2	19	19	18,4	19,2	18,517	18,9617	Snrpn	0,44	18,7	2,274	0,037	0,1433	-5
>sp|P02088|HBB1_M	29,06	29,1	29,1	29,1	29,1	29,1	29	29	29	28,8	29	29	28,1	27,5	27	29	29,1	29,1	29,061	28,55	Hbb-b1	-0,5	28,8	-2,27	0,037	0,1436	-5
>sp|P01631|KV2A7_	21,29	18,6	17,3	15,8	18,7	0	17	22	20	21,1	18	0	0	0	0	0	15,7	17,6	16,71	7.999455	>sp|P016	-8,7	12,4	-2,27	0,037	0,1436	-5
>sp|Q9ESX5|DKC1_M	18,76	18,9	14,2	18,6	18,3	14,5	18	18	18	15,2	16	16	16,3	16,5	16	16	16,5	16,4	17,546	16,1539	Dkc1	-1,4	16,9	-2,27	0,037	0,1444	-5
>sp|Q8BML9|SYQ_MO	18,25	18,2	18	17,8	18,2	18,4	18	18	19	18,5	18	19	18,3	18,1	18	18	18,5	18,5	18,161	18,4003	Qars	0,24	18,3	2,262	0,038	0,1458	-5
>sp|Q9Z1Z2|STRAP_M	23,34	23,4	23,8	24,5	24,2	23,6	24	24	24	23,6	23	23	23,5	23,5	24	23	23,3	23,5	23,812	23,474	Strap	-0,3	23,6	-2,26	0,038	0,1459	-5
>sp|P19639|GSTM3_	23,69	23,7	24	23,9	23,9	24,2	24	23	24	23,9	24	24	23,5	24,4	24	24	24,3	24,4	23,738	24,1194	Gstm3	0,38	23,9	2,254	0,038	0,1479	-5
>sp|Q8BJD1|ITIH5_M	0	13,5	0	14,7	14,9	15,4	16	11	12	15,7	15	15	15,9	16,2	16	16	15,7	15,6	10,87	15,5836	Itih5	4,71	13,2	2,253	0,038	0,1479	-5
>sp|Q920B9|SP16H_	19,14	19,2	19,3	20,2	20	19,6	21	20	20	19,9	20	20	20,7	20	21	21	20,3	20,8	19,837	20,3597	Supt16h	0,52	20,1	2,252	0,038	0,148	-5
>sp|Q8VDG3|PARN_M	19,49	0	13,3	20	0	0	0	0	0	0	15	15	15,2	15,3	14	19	14,9	14	5.86640	13,6337	Parn	7,77	9,75	2,251	0,038	0,1481	-5
>sp|Q5EBG6|HSPB6_I	19,49	20,9	20,7	20,9	20,7	21,1	21	20	21	20,8	21	21	21,6	21,3	21	21	21	20,9	20,602	21,1234	Hspb6	0,52	20,9	2,251	0,038	0,1481	-5
>sp|P62897|CYC_MO	0	0	18,4	0	17	18,3	17	18	18	18,4	17	20	19,2	19,6	20	17	17,1	19,5	11,884	18,5819	Cycs	6,7	15,2	2,25	0,039	0,1481	-5
>sp|Q9ESL4|M3K20_I	19,19	18,5	18,7	18,5	17,6	18,5	19	18	19	18,8	20	19	18,9	18,4	20	19	18,7	19	18,494	18,971	Map3k20	0,48	18,7	2,247	0,039	0,1488	-5
>sp|Q8VCA8|SCRN2_	22,53	21,7	19,6	20,4	20,3	20,4	20	20	21	20,5	19	20	19,5	20	20	20	19,9	20	20,658	19,8793	Scrn2	-0,8	20,3	-2,25	0,039	0,1491	-5
>sp|Q9R069|BCAM_I	17,92	15,9	15,2	16,6	19,9	14,9	15	15	16	16,5	14	16	14,5	14,1	15	15	15,3	14,4	16,248	14,8953	Bcam	-1,4	15,6	-2,24	0,039	0,1498	-5
>sp|Q7TQI3|OTUB1_M	22,18	22	21,3	21,3	22,3	21,1	22	22	22	21,8	21	21	21,3	21	21	22	21,5	20,9	21,733	21,3399	Otub1	-0,4	21,5	-2,24	0,039	0,1498	-5
>sp|Q8BJW6|EIF2A_M	21,12	21,1	21,3	21,4	22,3	21	22	21	21	21,2	20	21	21,2	21,1	20	20	21,3	21,1	21,322	20,8747	Eif2a	-0,4	21,1	-2,24	0,039	0,1498	-5
>sp|Q8VHX6|FLNC_M	20,89	20,7	20,8	20,3	21,3	20,7	20	20	20	19,4	20	20	20,1	20,2	20	20	19,8	20,4	20,448	19,9847	Flnc	-0,5	20,2	-2,24	0,039	0,1505	-5
>sp|Q3UXZ6|FA81A_I	15,35	17,4	16,6	16,5	17,4	18	16	16	16	14	14	16	0	14,9	0	15	15,7	15,5	16,605	11,6733	Fam81a	-4,9	14,1	-2,24	0,04	0,1508	-5
>sp|P26443|DHE3_M	22,96	23,1	23,3	23,1	23,3	22,2	23	23	23	22,1	23	23	22,5	23,1	23	22	22,7	22,7	23,044	22,6287	Glud1	-0,4	22,8	-2,24	0,04	0,1508	-5
>sp|Q8VDQ8|SIR2_M(	16,8	18	18,6	18,9	18,3	18,4	19	16	17	18,3	20	19	19,1	18,5	18	18	18,3	18,3	17,896	18,6827	Sirt2	0,79	18,3	2,234	0,04	0,1513	-5
>sp|Q9R0P9|UCHL1_	19,95	19,8	20,4	20,1	19,9	19,9	20	20	20	20	21	21	20,4	20,6	21	20	20,5	20,1	20,042	20,4231	Uchl1	0,38	20,2	2,232	0,04	0,1515	-5
>sp|Q61081|CDC37_	19,46	19,8	20,1	19,4	19,3	19,8	19	19	20	18,4	19	19	19,6	19	20	19	19,5	19,2	19,567	19,2088	Cdc37	-0,4	19,4	-2,23	0,04	0,1515	-5
>sp|Q9QYJ0|DNJA2_M	20,58	21,1	17,4	20,4	18,3	18,3	20	19	20	17,2	17	17	18,4	18,3	19	20	18,6	18,7	19,411	18,2311	Dnaja2	-1,2	18,8	-2,23	0,04	0,1518	-5
>sp|O89053|COR1A_	21,98	22,9	22	23,2	22,7	23,2	23	23	23	21,6	20	22	22,7	22,7	23	22	21,2	22,2	22,718	21,9478	Coro1a	-0,8	22,3	-2,23	0,04	0,1518	-5
>sp|Q8VIJ6|SFPQ_MO	19,58	18,9	19,1	19,1	19,6	19,4	20	19	20	21	20	21	20,4	19,7	20	19	19,1	19,6	19,463	20,0338	Sfpq	0,57	19,7	2,229	0,04	0,1518	-5
>sp|Q3UFY7|5NT3B_M	19,25	16,5	18,4	18,2	17,5	18	19	18	18	17,1	17	17	17,4	17,2	18	18	18,3	17,2	18,1	17,4361	Nt5c3b	-0,7	17,8	-2,22	0,041	0,1535	-5
>sp|Q6ZQI3|MLEC_MO	22,93	22,8	22,1	23	23	21,8	23	23	23	21,2	22	22	19,2	21,1	21	23	23,3	22,9	22,713	21,7394	Mlec	-1	22,2	-2,22	0,041	0,1549	-5
>sp|Q3UQ28|PXDN_M	20,04	19,9	19,8	20,1	19,9	20,2	21	20	20	19,4	19	20	20,1	18,8	20	20	18,9	18,8	20,136	19,5875	Pxdn	-0,5	19,9	-2,22	0,041	0,1549	-5
>sp|Q64514|TPP2_M	21,75	21,9	21,8	22	21,9	21,7	22	22	22	21,8	22	22	21,3	21,4	22	22	21,7	21,5	21,822	21,6595	Tpp2	-0,2	21,7	-2,21	0,041	0,1554	-5
>sp|P29387|GBB4_M	22,47	22,2	22	21,9	19,4	22,3	21	23	20	20,8	19	21	20,4	20,7	20	20	21,1	21,1	21,508	20,5516	Gnb4	-1	21	-2,21	0,042	0,1561	-5
>sp|P16627|HS71L_I	23,49	23,7	23,4	23,8	23,6	24	23	23	24	23,6	23	24	24,1	23,8	24	24	24,4	24,5	23,602	23,9249	Hspa1l	0,32	23,8	2,211	0,042	0,1561	-5
>sp|Q8VHQ9|ACO11_	17,75	16,1	20	19,2	17,3	18	20	19	19	17,5	16	18	18,3	18,2	16	18	16,9	16,7	18,462	17,3319	Acot11	-1,1	17,9	-2,21	0,042	0,1569	-5
>sp|P34914|HYES_M(	21,84	21,8	20,8	21,6	22,3	21,8	23	22	22	22	22	21	21	21,2	21	22	21,3	21,7	21,905	21,4435	Ephx2	-0,5	21,7	-2,2	0,042	0,1588	-5

>sp|Q8BSL7|ARF2_M(	22,89	24,7	22,6	22,4	22,2	22,4	22	23	24	22,9	23	23	22,8	21,5	21	22	22,2	21,9	22,931	22,1439	Arf2	-0,8	22,5	-2,2	0,042	0,159	-5
>sp|O88990|ACTN3_	19,75	19,8	19,8	19,4	19,9	19,5	20	20	20	19,3	18	18	19,7	19,3	19	20	19,9	19,1	19,74	19,1772	Actn3	-0,6	19,5	-2,2	0,043	0,1595	-5
>sp|Q9D6Z1|NOP56_	17,25	17,4	16,4	16,1	16,3	16,6	17	16	16	16,5	15	16	15,3	16,3	16	15	15,8	16,7	16,494	15,9092	Nop56	-0,6	16,2	-2,19	0,043	0,1604	-5
>sp|Q3TYX3|SMYD5_M	17,39	17,4	18,2	16,1	17,3	16,7	17	17	18	17	18	17	16,1	15,9	16	16	17,4	15,8	17,208	16,5249	Smyd5	-0,7	16,9	-2,19	0,043	0,1613	-5
>sp|Q99LN9|DOHH_M	17,48	17	17,1	15,1	15,2	16,7	16	16	17	15,6	16	16	15,2	15,5	16	17	14,6	15,6	16,365	15,6134	Dohh	-0,8	16	-2,19	0,043	0,1613	-5
>sp|P07742|RIR1_M	19,68	20,6	20,6	19,3	19,7	20,8	21	21	21	20,8	21	21	20,7	20,7	21	21	21,1	21,2	20,433	20,9626	Rrm1	0,53	20,7	2,19	0,043	0,1613	-5
>sp|Q6P4T2|U520_M	19,59	19,4	18,1	19,3	17,5	18,3	20	18	19	18,5	19	20	20,2	19,3	21	20	19,9	18,8	18,72	19,5054	Snrnp200	0,79	19,1	2,185	0,044	0,1624	-5
>sp|P62746|RHOB_M	20,72	20,8	21,1	20,5	20,3	20,7	21	21	17	20,8	17	20	17	17	17	0	0	20,4	20,363	14,3199	Rhob	-6	17,3	-2,18	0,044	0,1627	-5
>sp|Q9QXD6|F16P1_	22,76	22,1	21,4	21,9	21,7	22,3	22	23	23	22,8	23	23	22,2	22,7	23	23	22,4	22,8	22,184	22,626	Fbp1	0,44	22,4	2,18	0,044	0,1637	-5
>sp|Q91Z53|GRHPR_	21,58	22,1	22,3	21,8	22,5	21,3	22	22	22	22,7	22	22	22,7	22,4	22	22	22,3	22,7	21,963	22,335	Grhpr	0,37	22,1	2,174	0,045	0,1657	-5
>sp|P63101|1433Z_	24,75	26,7	24,9	26,5	24,7	24,6	25	25	25	24,1	25	25	24,5	24,1	25	25	25	24,1	25,238	24,5955	Ywhaz	-0,6	24,9	-2,17	0,045	0,167	-5
>sp|Q8CJG1|AGO1_M	17,92	18,7	18,5	17,7	19,3	17	21	19	20	19,9	19	17	16,8	16,6	17	17	16,8	17,9	18,651	17,5008	Ago1	-1,2	18,1	-2,17	0,045	0,167	-5
>sp|Q61301|CTNA2_	17,57	17,3	17,7	18,9	16,5	16,7	19	18	16	15,4	16	17	16,1	16,2	15	19	17,1	17,1	17,562	16,5739	Ctnna2	-1	17,1	-2,17	0,045	0,1672	-5
>sp|Q9DAW9|CNN3_I	20,85	21,1	19,8	19,5	20,1	20,7	18	20	19	18,6	16	18	19,8	18,6	17	20	20,1	19,9	19,897	18,6598	Cnn3	-1,2	19,3	-2,17	0,045	0,1674	-5
>sp|Q9Z2M7|PMM2_	21,89	21,8	21,5	21,8	22,1	22	21	22	22	21,5	22	22	22,2	22,4	22	22	22,4	21,9	21,745	22,041	Pmm2	0,3	21,9	2,165	0,046	0,1676	-5
>sp|P54071|IDHP_M	22,75	22,4	22,6	21,9	22,8	22,5	23	23	23	23,2	23	23	23,5	23,1	23	23	22,9	23,1	22,722	23,0863	Idh2	0,36	22,9	2,162	0,046	0,1684	-5
>sp|P07310|KCRM_I	23,46	22,9	23,9	23,6	23	22,7	23	23	23	23,2	23	23	21,8	23,2	22	23	22,7	22	23,202	22,7124	Ckm	-0,5	23	-2,16	0,046	0,1684	-5
>sp|P97390|VPS45_	22,83	21,6	18	22,2	22,3	22,1	20	22	17	17,3	21	20	19,2	19,1	20	18	18,7	20,4	20,928	19,3115	Vps45	-1,6	20,1	-2,16	0,046	0,1686	-5
>sp|Q7TSI3|PP6R1_M	14,29	13,6	14,8	15,1	15,2	14,2	15	15	15	15,5	14	16	15,7	15,7	16	15	14,8	15,2	14,688	15,2679	Ppp6r1	0,58	15	2,157	0,046	0,1692	-5
>sp|Q8CF98|COL10_I	16,28	16,6	21,8	17,3	21,5	21,6	22	21	21	18,5	19	17	19,2	18,8	19	17	14,5	18,5	19,954	17,8936	Colec10	-2,1	18,9	-2,16	0,046	0,1692	-5
>sp|P00375|DYR_MC	19,18	19,2	20,9	20,3	20,2	17,1	21	20	19	16,2	16	20	19,8	16,6	21	15	18,6	19	19,711	17,9662	Dhfr	-1,7	18,8	-2,16	0,046	0,1692	-5
>sp|Q60817|NACA_M	17,25	18,5	19,2	17,3	19,9	19,5	19	21	20	19,6	20	21	19,7	20,1	19	20	20,3	20,3	19,072	19,9969	Naca	0,92	19,5	2,155	0,046	0,1692	-5
>sp|P61164|ACTZ_M	23,63	23,9	21,2	22,7	22	21,3	21	23	21	21,7	22	21	21,1	21,6	21	22	21,4	21,5	22,236	21,4522	Actr1a	-0,8	21,8	-2,15	0,046	0,1692	-5
>sp|Q6IFZ6|K2C1B_M	22,11	22,3	22,5	21,9	21,6	21,7	22	22	22	22,1	23	22	22	21,7	22	24	23,9	23,6	22,012	22,6774	Krt77	0,67	22,3	2,154	0,046	0,1692	-5
>sp|P47911|RL6_MC	17,66	18,1	20,9	20,9	19,7	20,8	21	18	17	17,7	18	18	18	18,6	18	18	18,2	18,3	19,342	18,1955	Rpl6	-1,1	18,8	-2,15	0,047	0,1693	-5
>sp|Q9CWF2|TBB2B_	23,63	23,2	24,4	23,7	23,9	23,8	24	24	24	23,6	24	24	23,3	23,7	23	24	23,6	23,7	23,957	23,5958	Tubb2b	-0,4	23,8	-2,15	0,047	0,1693	-5
>sp|P98064|MASP1_	14,71	15,5	17,1	15,5	17,1	17	14	14	15	16,9	17	18	17,7	18	18	15	16,1	14,9	15,609	16,8088	Masp1	1,2	16,2	2,151	0,047	0,1699	-5
>sp|Q9WVH9|FBLN5_	19,11	19,1	18,6	19,1	18,7	17,3	18	19	18	18,3	18	18	17,1	17,9	19	18	18,2	17,4	18,559	18,0206	Fbln5	-0,5	18,3	-2,15	0,047	0,1701	-5
>sp|Q8BZW8|NHLC2_	21,48	19,7	24,3	22,7	21,7	21,1	22	21	21	21,8	22	24	21,9	23,9	22	24	22,6	22,7	21,61	22,7269	Nhlrc2	1,12	22,2	2,149	0,047	0,1701	-5
>sp|Q80W22|THNS2_	14,37	15,2	13,4	14,1	14,1	13,7	14	14	13	14,9	16	16	14,3	14,4	14	14	13,8	14,7	13,886	14,6776	Thnsl2	0,79	14,3	2,144	0,047	0,1715	-5
>sp|Q9JIF0|ANM1_M(	21,8	21,3	21	21,2	21,4	21,5	21	21	22	22,2	22	21	22,4	21,6	21	22	21,8	21,8	21,431	21,7427	Prmt1	0,31	21,6	2,143	0,047	0,1715	-5
>sp|Q62266|SPR1A_	15,16	15,4	16,1	14,7	19	18,9	0	15	14	18,6	18	19	17,9	19,2	18	18	17,7	17,9	14,231	18,221	Sprr1a	3,99	16,2	2,143	0,047	0,1715	-5
>sp|P46061|RAGP1_	20,24	20,3	19,7	20,1	20,3	19,4	20	20	20	20	19	20	19,4	19,7	20	19	19	19,6	19,894	19,5182	Rangap1	-0,4	19,7	-2,14	0,048	0,1717	-5
>sp|P97807|FUMH_M	19,86	20,2	20,3	19,8	20,5	20,4	20	20	21	20,5	21	21	20,7	20,1	20	21	20,1	20,2	20,211	20,5387	Fh	0,33	20,4	2,139	0,048	0,1724	-5
>sp|O35405|PLD3_M	17,3	17,1	16	16,9	16,1	16,5	17	17	15	17,5	15	18	18,4	17,9	17	17	17,3	17,3	16,581	17,359	Pld3	0,78	17	2,136	0,048	0,1731	-5
>sp|P16460|ASSY_M(	20	20,3	19,8	20	20,7	20,1	21	20	21	19,2	20	19	19,5	19,7	22	20	19	18,8	20,281	19,6322	Ass1	-0,6	20	-2,14	0,048	0,1733	-5
>sp|P63168|DYL1_M	22,7	22,8	23,1	22,2	22,5	22,6	23	22	23	22,9	23	23	23,5	23,1	23	23	22,9	22,5	22,74	23,0378	Dynll1	0,3	22,9	2,134	0,048	0,1734	-5
>sp|Q9CRC8|LRC40_	14,54	14,3	13,7	14,3	13,7	16,2	14	14	14	14,8	13	14	14	13,4	14	14	12,4	13,6	14,402	13,7032	Lrrc40	-0,7	14,1	-2,13	0,048	0,1735	-5
>sp|Q8BJU0|SGTA_M(	18,71	18,4	21,6	19,9	19	20	20	18	20	21,1	20	21	19,6	21,8	21	19	20,3	20,6	19,586	20,5616	Sgta	0,98	20,1	2,132	0,048	0,1736	-5
>sp|Q5XJY5|COPD_M	21,68	20,8	23	22,6	22,4	22,8	22	22	22	23	22	21	21,6	19,9	21	21	21,9	21,7	22,183	21,4445	Arcn1	-0,7	21,8	-2,13	0,048	0,1736	-5
>sp|Q8BLF1|NCEH1_M	14,75	13,8	14,4	14,5	14	0	0	16	16	15,5	15	0	0	11,9	0	0	0	0	11,463	4.688075	Nceh1	-6,8	8,08	-2,13	0,049	0,1738	-5
>sp|Q91YN5|UAP1_M	19,4	19,3	18,9	21,2	19,9	19,6	21	20	20	19	19	20	19,3	18,9	19	20	19,4	19,2	19,916	19,3045	Uap1	-0,6	19,6	-2,13	0,049	0,1748	-5
>sp|P97326|CADH6_	15,86	17,3	18	19,6	20,3	17,7	15	18	15	15,9	20	20	20,6	21	21	18	18	18,5	17,556	19,3056	Cdh6	1,75	18,4	2,12	0,05	0,1772	-5
>sp|P01798|HVM29	18,64	19	0	17,9	0	0	19	18	18	19,5	18	19	18,8	18,9	19	19	18,6	18,7	12,276	18,7147	>sp|P017	6,44	15,5	2,118	0,05	0,1776	-5
>sp|O35969|GAMT_M	19,08	18,9	18,6	17,6	18,2	18,6	18	19	19	19,7	19	19	19,3	18,9	19	19	18,3	19,1	18,636	19,0845	Gamt	0,45	18,9	2,113	0,05	0,1789	-5
>sp|Q9CQ52|CEL3B_I	24,81	23,3	23,3	24,7	24,5	23,3	25	24	24	24,9	25	25	24,3	24,1	24	24	25,4	25,6	24,142	24,7581	Cela3b	0,62	24,5	2,113	0,05	0,1789	-5
>sp|Q7TMC8|FUK_MC	20,53	20,9	19,4	20,9	21,1	19	21	19	19	18,5	19	18	19,1	19,7	20	20	19,7	19,7	20,04	19,2824	Fuk	-0,8	19,7	-2,11	0,05	0,1792	-5
>sp|Q3U1J4|DDB1_M	19,15	19,6	19,6	19,6	19,2	21	22	20	21	19,7	19	19	19,4	19,4	19	19	19,4	20	20,05	19,381	Ddb1	-0,7	19,7	-2,11	0,051	0,1792	-5

>sp|P61922|GABT_M	20,36	20,1	19,9	20,1	20,6	20,8	20	20	20	20,5	20	21	20,3	20,7	20	21	20,3	20,4	20,164	20,446	Abat	0,28	20,3	2,106	0,051	0,1807	-5
>sp|Q9WUM5|SUCA_I	18,28	17,4	20,5	18,4	17,2	18,6	18	19	18	19,1	20	19	19	19,1	19	19	19,1	18,8	18,365	19,0619	Suclg1	0,7	18,7	2,104	0,051	0,1813	-5
>sp|Q9R1T2|SAE1_M(	18,07	17,6	17,6	18,1	18	18	17	19	17	17,5	18	18	17,3	17	17	18	17,5	17,3	17,845	17,4449	Sae1	-0,4	17,6	-2,1	0,051	0,1814	-5
>sp|P27773|PDIA3_I	21,5	21,9	22,1	21	21,2	21,4	21	22	21	22,1	21	22	22,2	22,2	22	21	22	22	21,528	21,9057	Pdia3	0,38	21,7	2,102	0,051	0,1815	-5
>sp|P18242|CATD_M	22,32	23,4	24,2	23,2	22,5	22,9	23	24	24	23,3	23	22	22,6	20,3	23	23	23,2	22,6	23,241	22,4885	Ctsd	-0,8	22,9	-2,1	0,051	0,1815	-5
>sp|O88947|FA10_M	20,35	18,7	18,9	17,4	19,1	17,9	17	20	19	16,5	16	19	17,9	17,4	19	19	15,8	18,4	18,752	17,6393	F10	-1,1	18,2	-2,1	0,052	0,1826	-5
>sp|P17918|PCNA_M	20,98	21,2	21,8	20,9	20,8	21,9	22	22	20	22,1	22	22	21,8	20,9	22	21	21,7	22	21,272	21,7058	Pcna	0,43	21,5	2,097	0,052	0,1827	-5
>sp|P61600|NAA20_	18,93	17,9	17,8	19,2	18,1	19,1	19	19	16	15,7	19	19	16,1	16,8	17	20	15,6	16,5	18,408	17,1756	Naa20	-1,2	17,8	-2,09	0,052	0,1838	-5
>sp|Q02053|UBA1_M	22,08	22,1	22	23,1	23	22,2	22	22	22	22	22	22	22,1	21,6	22	23	21,8	21,8	22,336	21,9491	Uba1	-0,4	22,1	-2,09	0,052	0,1838	-5
>sp|P68037|UB2L3_	19,36	19,2	22,4	23,8	23,9	21,5	24	23	24	23,6	21	24	24,1	24,2	24	24	24	24,5	22,289	23,7656	Ube2l3	1,48	23	2,092	0,052	0,184	-5
>sp|Q9DCH4|EIF3F_M	19,18	20,1	19,6	20,3	19,4	20,3	20	20	20	20,3	20	20	20,1	20,5	20	20	20,4	21,5	19,885	20,3382	Eif3f	0,45	20,1	2,091	0,052	0,184	-5
>sp|Q9DBB9|CPN2_M	22,06	20,5	20,4	21,5	20,5	19,7	21	22	21	21,4	22	19	18,8	18,5	20	19	21,2	19,8	20,906	19,9067	Cpn2	-1	20,4	-2,09	0,053	0,184	-5
>sp|P36552|HEM6_M	19,24	19	19	18,9	18,7	19,1	19	19	18	17,9	15	18	19	18,8	19	18	18,6	18,4	18,954	17,9992	Cpox	-1	18,5	-2,09	0,053	0,1841	-5
>sp|Q8K411|PREP_M	18,57	18,6	18,2	19	18,1	19,4	19	19	19	18,7	18	18	19,1	19	18	18	18	18,2	18,859	18,4045	Pitrm1	-0,5	18,6	-2,09	0,053	0,1852	-5
>sp|P01629|KV2A4_	18,43	18,8	0	18,4	17,9	17,9	19	17	0	0	19	0	0	0	0	0	16,3	17,6	14,138	5.902734	>sp|P016	-8,2	10	-2,09	0,053	0,1852	-5
>sp|Q922B1|MACD1	19,65	16,3	16,1	15,8	15,9	16,3	16	16	17	17,9	16	19	18,2	16,7	18	18	17,5	16,8	16,565	17,5473	Macrod1	0,98	17,1	2,084	0,053	0,1854	-5
>sp|P62315|SMD1_M	21,14	20,5	23,9	25,5	20,7	24,2	24	25	25	22,4	25	25	25,7	25,3	25	25	24,9	25,1	23,352	24,8835	Snrpd1	1,53	24,1	2,082	0,053	0,1861	-5
>sp|Q9Z0K8|VNN1_M	17,6	17,1	17,5	17,7	17,1	17,2	16	17	17	15,7	18	17	16,7	17	16	16	16,9	16	17,153	16,5727	Vnn1	-0,6	16,9	-2,08	0,054	0,1867	-5
>sp|P61327|MGN_M	20,66	20,2	20	19,6	21,2	20,3	20	20	20	21,1	23	21	21,4	21,4	21	21	20,8	18,6	20,197	21,0611	Magoh	0,86	20,6	2,074	0,054	0,1884	-5
>sp|Q3UW68|CAN13	18,68	18,1	19	18,4	17,9	18,7	19	19	19	17,9	16	18	18,4	18,2	19	17	18,5	16	18,542	17,7391	Capn13	-0,8	18,1	-2,07	0,054	0,1888	-5
>sp|O55060|TPMT_M	19,91	20,2	20,1	19,8	20,1	19,9	20	20	19	20	19	20	20,4	20,6	21	20	19,9	20,2	19,835	20,1639	Tpmt	0,33	20	2,072	0,054	0,1888	-5
>sp|Q8C0C7|SYFA_M(	19,46	18,7	17	18,2	16,9	16,7	18	18	18	16,4	18	17	17,4	17,8	18	17	16,5	16,9	17,959	17,2048	Farsa	-0,8	17,6	-2,07	0,055	0,189	-5
>sp|Q8CC86|PNCB_M	19,44	20	20,7	19,9	18,8	19,8	20	20	20	19,2	20	19	19,6	19,2	20	19	19,7	19,6	19,834	19,4575	Naprt	-0,4	19,6	-2,07	0,055	0,19	-5
>sp|Q922H9|ZN330_	18,33	18,9	16,6	16,2	15,2	16,1	19	17	16	14,9	16	16	15,4	16,2	15	17	14,8	17,4	17,015	15,8542	Znf330	-1,2	16,4	-2,07	0,055	0,19	-5
>sp|Q6PAV2|HERC4_	16,82	17,2	16,1	17,1	16,5	15,9	17	16	16	15,3	18	16	16,3	15,8	16	15	15,7	15	16,495	15,8897	Herc4	-0,6	16,2	-2,07	0,055	0,19	-5
>sp|Q8VE37|RCC1_M	15,23	14,9	16,2	16,2	15,4	15,4	15	14	15	14,1	14	15	14,9	14,9	15	15	15,4	14,8	15,351	14,8017	Rcc1	-0,5	15,1	-2,07	0,055	0,1902	-5
>sp|Q9QZ06|TOLIP_M	15,77	16	15,9	16,5	16,4	16,9	17	17	17	16,8	17	16	15,2	16	16	16	15,9	15,7	16,526	16,0197	Tollip	-0,5	16,3	-2,06	0,056	0,1916	-5
>sp|P62141|PP1B_M	24,19	24,1	24,1	23,9	23,3	24,1	24	24	24	24,1	24	24	23,3	23,8	23	24	23,9	24,1	24,065	23,7753	Ppp1cb	-0,3	23,9	-2,06	0,056	0,1916	-5
>sp|Q61001|LAMA5_	15,6	15,3	14,3	14,4	14,7	14,2	15	14	15	15,4	15	15	15,5	15	15	15	15,1	15	14,656	15,0605	Lama5	0,4	14,9	2,059	0,056	0,1918	-5
>sp|Q99J99|THTM_M	20,93	20,3	20,6	21,4	20,2	20,3	20	20	20	20,4	21	19	18,6	19,8	19	20	19,9	19,7	20,376	19,8127	Mpst	-0,6	20,1	-2,05	0,057	0,1945	-5
>sp|Q8R2U6|NUDT4_	19,64	19,5	17,6	19,4	19,2	19,6	19	19	19	18,2	18	15	18,7	18,2	19	19	18,9	19,1	19,123	18,2348	Nudt4	-0,9	18,7	-2,05	0,057	0,1955	-5
>sp|Q99JX4|EIF3M_M	18,25	18,6	18,7	18,3	18,3	18,4	18	19	19	19,2	19	20	18,9	18,9	19	19	19,2	18,2	18,525	18,897	Eif3m	0,37	18,7	2,046	0,057	0,1959	-5
>sp|Q8VDK1|NIT1_M(	21,27	21,3	20,8	21	21,2	21,3	21	21	21	20,6	20	21	21,6	20,8	21	21	21,2	21,1	21,158	20,8701	Nit1	-0,3	21	-2,04	0,058	0,1973	-5
>sp|Q8CJG0|AGO2_M	19,35	19,5	19	19,3	19,8	18,8	21	19	20	20,3	19	19	18,5	18,6	19	19	18,7	19,3	19,591	19,0126	Ago2	-0,6	19,3	-2,04	0,058	0,1977	-5
>sp|Q80Y86|MK15_M	18,39	16,5	18,5	18,2	18,4	18,3	18	18	18	9,77	13	14	19,2	19,2	14	15	18,8	18,7	18,084	15,7693	Mapk15	-2,3	16,9	-2,04	0,058	0,1986	-5
>sp|Q62148|AL1A2_	21,38	22,1	20,6	22	22,1	21,6	21	21	22	21,7	20	22	22,7	22,1	22	22	22,5	22,1	21,424	22,0421	Aldh1a2	0,62	21,7	2,033	0,059	0,2	-5
>sp|O35945|AL1A7_	24,05	24	23,7	24,1	24,2	24	24	24	24	24,2	24	24	24,3	24,1	24	24	24,1	24,4	24,059	24,2302	Aldh1a7	0,17	24,1	2,032	0,059	0,2001	-5
>sp|Q03311|CHLE_M	19,19	18,8	16,4	16,6	16,4	17,9	17	14	18	15,6	15	16	17,3	16,3	17	15	14,8	14	17,019	15,6974	Bche	-1,3	16,4	-2,03	0,059	0,2001	-5
>sp|P61979|HNRPK_	21,33	21,1	21,6	21,6	20,8	22,3	22	22	22	21,2	22	21	21	21,2	21	21	21,3	21	21,509	21,1929	Hnrnpk	-0,3	21,4	-2,03	0,059	0,2009	-5
>sp|Q8K1M6|DNM1L	17,75	17,5	17,8	16,8	17,7	17,1	17	17	18	16,3	17	15	17	17,5	18	17	17,7	17	17,447	16,89	Dnm1l	-0,6	17,2	-2,03	0,059	0,2018	-5
>sp|Q9JJF3|RIOX1_M	0	0	0	0	0	0	0	0	0	13,7	0	0	0	0	0	14	0	14,1	0	4,60961	Riox1	4,61	2,3	2,023	0,06	0,2028	-5
>sp|Q8BZM1|GLMN_M	0	0	0	0	0	0	0	0	0	0	0	0	0	0	0	17	16	17,7	0	5,60446	Glmn	5,6	2,8	2,021	0,06	0,2035	-5
>sp|Q9Z0H4|CELF2_M	16,86	0	0	0	14,9	15,5	0	0	0	0	0	0	0	0	0	0	0	0	5,2578	0	Celf2	-5,3	2,63	-2,02	0,06	0,2038	-5
>sp|Q9CRC9|GNPI2_M	16,41	16,9	17,8	17,5	17,8	17,2	19	18	18	18,7	19	19	18,2	18,3	18	18	17,3	17,7	17,649	18,2796	Gnpda2	0,63	18	2,016	0,061	0,2047	-5
>sp|Q9CPR4|RL17_M	0	0	0	0	13,9	0	0	16	16	0	0	0	0	0	0	0	0	0	5,1561	0	Rpl17	-5,2	2,58	-2,02	0,061	0,2047	-5
>sp|Q6URW6|MYH14	19,45	19,5	18	18,3	17,9	20,6	19	19	19	20,3	19	20	20,4	19,8	18	20	19,6	20,3	18,967	19,7516	Myh14	0,78	19,4	2,015	0,061	0,2047	-5
>sp|Q8VDW0|DX39A	21,33	20,2	20	19,8	20,4	19,9	20	20	20	20,7	23	20	20,1	20,4	21	21	20,8	21,2	20,124	20,847	Ddx39a	0,72	20,5	2,011	0,061	0,206	-5
>sp|P50580|PA2G4_	22,92	22,8	22,7	22,8	22,4	22,3	23	23	23	22,4	22	24	24	24,2	24	23	22,6	24,1	22,733	23,3331	Pa2g4	0,6	23	2,01	0,061	0,2063	-5

>sp|O70194|EIF3D_M	20,76	21	21,6	21,1	21,1	21,2	21	22	19	22,9	20	23	22,1	22,1	23	22	19,8	22,6	21,032	21,9539	Eif3d	0,92	21,5	2,009	0,061	0,2063	-5
>sp|Q8VEK3|HNRPU_	20,26	20,4	20,3	20,1	20,7	20,1	20	20	20	19,7	19	20	20,3	19,6	20	20	19,9	20,7	20,321	19,9929	Hnrnpu	-0,3	20,2	-2,01	0,061	0,2063	-5
>sp|O88398|AVIL_MC	16,78	15,6	17,1	15,3	16,4	15,3	15	0	0	15,6	16	16	0	0	0	0	0	0	12,434	5.355725	Avil	-7,1	8,89	-2,01	0,062	0,2074	-5
>sp|Q9QWL7|K1C17_	21,93	21,9	21,4	21,7	21,1	21,4	21	21	22	20,5	24	22	21,5	22,1	21	23	22,9	23,8	21,606	22,4393	Krt17	0,83	22	2,005	0,062	0,2075	-5
>sp|Q9JL62|GLTP_MC	19,39	20,3	19,8	20,7	19,5	18,9	17	18	18	19,4	19	14	15,9	0	13	16	18,3	19	19,08	14,9787	Gltp	-4,1	17	-2	0,062	0,2084	-5
>sp|P15948|K1B22_	17,49	15,5	18,2	18	18,9	17,7	18	18	18	18,6	19	19	17,8	18,5	18	18	18,4	18,6	17,793	18,4527	Klk1b22	0,66	18,1	2,001	0,062	0,2086	-5
>sp|Q64471|GSTT1_M	23,97	23,6	23,2	24	23,8	23,3	24	24	24	23,5	23	23	23,8	23,5	24	24	23,5	23,5	23,707	23,4412	Gstt1	-0,3	23,6	-2	0,063	0,2097	-5
>sp|P84084|ARF5_M	22,28	24,3	22	22,2	22,1	21,6	22	23	23	22,6	23	22	22,6	21,1	21	22	21,9	21,7	22,56	21,8828	Arf5	-0,7	22,2	-2	0,063	0,2103	-5
>sp|Q8CJF9|AGO3_M	17,77	18,6	18,4	17,2	19,2	16,7	21	18	20	19,9	19	16	16,5	16,3	17	17	16,7	18	18,527	17,3343	Ago3	-1,2	17,9	-1,99	0,064	0,2122	-5
>sp|Q8VCN9|TBCC_M	16,75	17	17,6	17,6	16,8	16,7	17	18	18	17,2	17	17	16,7	17,2	17	17	15,5	16	17,274	16,7566	Tbcc	-0,5	17	-1,99	0,064	0,213	-5
>sp|Q8R0G9|NU133_	16,63	18,1	17,7	17,5	17	17,3	18	18	18	17	18	18	18,9	18,4	19	18	17,5	18,3	17,596	18,1086	Nup133	0,51	17,9	1,986	0,064	0,2133	-5
>sp|Q76MZ3|2AAA_M	22,24	22,1	22,1	22,9	22,8	22,6	23	23	23	23	22	22	21,9	22	22	23	22,4	22,5	22,573	22,2135	Ppp2r1a	-0,4	22,4	-1,98	0,064	0,2139	-5
>sp|P18653|KS6A1_	15,19	16	15,5	15,4	14,1	15,7	14	16	15	14,9	18	16	14,9	19,7	16	15	16,1	16,1	15,277	16,3987	Rps6ka1	1,12	15,8	1,984	0,064	0,2139	-5
>sp|O54949|NLK_MC	18,7	16,8	18,9	18,5	18,8	18,6	19	18	18	15,4	14	14	19,5	19,5	14	16	19,1	19	18,417	16,7024	Nlk	-1,7	17,6	-1,98	0,065	0,2145	-5
>sp|Q9DCV4|RMD1_M	17,05	19,8	18,1	16,4	20,3	20,3	17	21	18	22,7	22	22	16,2	20,5	16	22	22,8	22,8	18,563	20,6827	Rmdn1	2,12	19,6	1,981	0,065	0,2145	-5
>sp|P32921|SYWC_M	23,48	23,3	22,8	22,7	22,1	21	22	22	22	23,1	23	20	22	22,6	21	21	20,9	20,6	22,369	21,5032	Wars	-0,9	21,9	-1,98	0,065	0,2145	-5
>sp|P46638|RB11B_	22,57	22,8	20,2	22,5	22,3	21,4	22	21	21	21,1	22	21	20,8	20,6	21	21	21	20,8	21,755	21,1076	Rab11b	-0,6	21,4	-1,98	0,065	0,2145	-5
>sp|Q9WTN0|GGPPS_	18,73	19	18,4	17,8	19,4	18,5	18	19	19	18,1	18	18	18,9	17,5	18	19	18,6	18,7	18,694	18,2529	Ggps1	-0,4	18,5	-1,98	0,065	0,2145	-5
>sp|O54774|AP3D1_	18,83	17,9	18,9	17,9	18,5	19,1	18	19	18	18,1	17	19	17,6	16,6	18	18	17	19,8	18,483	17,7981	Ap3d1	-0,7	18,1	-1,98	0,065	0,2145	-5
>sp|O08553|DPYL2_M	23,9	23,6	23,4	23,4	23,4	23,6	23	23	23	23,3	23	23	23,3	23	23	23	23,3	23,1	23,378	23,1199	Dpysl2	-0,3	23,2	-1,98	0,065	0,2146	-5
>sp|P31001|DESM_M	22,79	21,8	23	22,3	23,1	22,3	23	22	22	22,1	23	22	21,1	21,1	22	21	23,1	21,7	22,469	21,9082	Des	-0,6	22,2	-1,98	0,065	0,2148	-5
>sp|Q9D3X9|MFA3L_	17,95	17,2	18,3	17,5	17,5	17,6	18	18	18	16,8	17	17	17,3	17,8	18	17	17,4	17,4	17,662	17,3695	Mfap3l	-0,3	17,5	-1,98	0,065	0,215	-5
>sp|P12960|CNTN1_	19,32	19,7	19,7	19,6	19,3	19,6	20	19	19	18,4	19	19	18,9	19,4	20	18	19,3	19,6	19,493	19,0236	Cntn1	-0,5	19,3	-1,98	0,065	0,2151	-5
>sp|Q9CY64|BIEA_MC	22,02	22,1	21,9	22,2	21,6	21,6	22	21	22	21,8	22	22	21,2	21,5	22	21	21,7	20,8	21,906	21,5807	Blvra	-0,3	21,7	-1,97	0,065	0,2152	-5
>sp|P99024|TBB5_M	23,55	23	24,1	23,6	23,9	23,6	24	24	24	23,5	24	24	23,1	23,6	23	24	23,6	23,7	23,813	23,5023	Tubb5	-0,3	23,7	-1,97	0,065	0,2152	-5
>sp|Q8CG16|C1RA_M	18,99	18,3	19	16,2	19,3	15,1	19	19	19	15,6	15	15	19	15,9	15	19	19,4	14,7	18,166	16,5316	C1ra	-1,6	17,3	-1,97	0,066	0,2152	-5
>sp|Q9R0P3|ESTD_M(	24,14	24,1	23,8	24,1	23,7	23,4	24	24	24	24,5	24	24	23,1	22,8	24	23	23,7	23,8	24,018	23,6368	Esd	-0,4	23,8	-1,97	0,066	0,2157	-6
>sp|Q811J3|IREB2_M	0	14,4	0	0	0	0	0	14	0	14,3	14	14	0	0	0	14	12,2	14,2	3,1394	9,18911	Ireb2	6,05	6,16	1,971	0,066	0,2158	-6
>sp|Q8CJF8|AGO4_M	17,43	18,4	18,5	16,8	19,1	15,9	21	18	20	19,9	19	15	15,6	15,7	16	16	16,3	17,9	18,313	16,8715	Ago4	-1,4	17,6	-1,97	0,066	0,2158	-6
>sp|Q04736|YES_MOI	18,01	19,6	18,5	17,6	19,7	18,6	19	19	19	19,3	19	17	18	18,5	17	18	18,2	18,1	18,712	18,0976	Yes1	-0,6	18,4	-1,97	0,066	0,2158	-6
>sp|Q925E7|2ABD_M	0	0	0	0	0	0	0	15	16	14,2	0	0	14,6	15,8	15	16	15,1	0	3.46018	10,1131	Ppp2r2d	6,65	6,79	1,969	0,066	0,2158	-6
>sp|P26043|RADI_M	22,36	21,9	22,2	22,4	22	22,5	22	22	22	22,6	22	22	22,1	22	23	22	22,8	22,9	22,196	22,4455	Rdx	0,25	22,3	1,969	0,066	0,2158	-6
>sp|P01802|HVM33	19,18	19,5	16,6	20,2	14,7	15,1	19	19	19	20,2	19	19	20,5	19,3	19	20	19,2	19,1	18,093	19,4813	>sp|P018	1,39	18,8	1,961	0,067	0,2186	-6
>sp|Q8VCT3|AMPB_M	23	23	22,4	22,1	22,5	22,7	22	22	22	22,4	22	22	22,3	22	22	22	22,8	22	22,481	22,1662	Rnpep	-0,3	22,3	-1,96	0,067	0,2187	-6
>sp|Q6PEB6|PHOCN_	18,53	19,4	20	20,5	20	20,3	21	20	20	20,3	21	20	20,4	20,1	20	20	20,5	20,2	19,933	20,3538	Mob4	0,42	20,1	1,959	0,067	0,219	-6
>sp|Q5SWU9|ACACA_	16,51	15,8	19,2	19,4	19,6	19,5	20	19	18	19,4	18	19	15,9	16	15	16	15,5	18,6	18,534	17,1355	Acaca	-1,4	17,8	-1,96	0,067	0,2191	-6
>sp|Q9JKV1|ADRM1_	18,2	20,6	19,4	18,4	19,1	18,2	19	19	19	18,8	17	17	17,9	18,5	18	19	18,7	18,7	18,903	18,2882	Adrm1	-0,6	18,6	-1,96	0,068	0,2195	-6
>sp|Q91YQ5|RPN1_M	15,36	15,6	14,5	14,8	14,2	0	14	0	14	14,9	16	16	16,4	16,5	17	15	14,7	15,1	11,408	15,6146	Rpn1	4,21	13,5	1,954	0,068	0,2205	-6
>sp|Q8CFG9|C1RB_M	19,13	18,5	19,2	16,4	19,4	15,4	19	19	19	15,7	15	15	19,2	16,1	15	19	19,6	14,8	18,338	16,7135	C1rb	-1,6	17,5	-1,95	0,068	0,2205	-6
>sp|P49945|FRIL2_M	25,86	25,6	25,1	27,4	28,4	26,9	26	27	27	26,1	26	26	26,4	25,7	26	26	25,5	26	26,558	25,8863	Ftl2	-0,7	26,2	-1,95	0,068	0,2214	-6
>sp|P61982|1433G_	23,98	25,3	22,8	25,4	22,8	23,3	24	24	23	25,1	24	25	24,3	23,6	25	26	25,7	23,6	23,809	24,6418	Ywhag	0,83	24,2	1,947	0,069	0,2227	-6
>sp|Q91VT4|CBR4_M	17,02	15,9	16,9	17	17,1	16,7	15	15	16	16,3	18	18	17,3	17,8	16	17	16,3	16,8	16,358	17,0181	Cbr4	0,66	16,7	1,946	0,069	0,2229	-6
>sp|Q8BG07|PLD4_M	0	16	17,2	16,8	14,7	15,7	16	16	16	17,9	16	18	18	17,3	18	18	18	18,1	14,272	17,753	Pld4	3,48	16	1,946	0,069	0,2229	-6
>sp|P24369|PPIB_M	20,85	21,2	24,4	24,3	21,4	20,5	24	21	25	24,3	23	24	23,3	24,7	23	24	23,2	23,1	22,543	23,7675	Ppib	1,22	23,2	1,943	0,069	0,2237	-6
>sp|Q99J08|S14L2_M	17,62	18,3	18,6	19,1	18,2	18,4	19	19	19	18,4	19	19	18,2	18	18	18	17,8	17,7	18,581	18,1747	Sec14l2	-0,4	18,4	-1,94	0,069	0,2237	-6
>sp|P45878|FKBP2_	15,97	16,9	17,1	16,9	17	17,2	17	17	17	17,3	19	17	17,3	17,2	18	17	16,7	16,5	16,804	17,3512	Fkbp2	0,55	17,1	1,94	0,07	0,2239	-6
>sp|P01796|HVM27	18,95	19,2	16,3	19,9	14,5	14,8	19	19	19	19,9	18	19	20,3	19	19	20	18,9	18,9	17,829	19,214	>sp|P017	1,38	18,5	1,939	0,07	0,2239	-6
>sp|P01797|HVM28	18,95	19,2	16,3	19,9	14,5	14,8	19	19	19	19,9	18	19	20,3	19	19	20	18,9	18,9	17,829	19,214	>sp|P017	1,38	18,5	1,939	0,07	0,2239	-6

>sp|P01799|HVM30	18,95	19,2	16,3	19,9	14,5	14,8	19	19	19	19,9	18	19	20,3	19	19	20	18,9	18,9	17,829	19,214	>sp|P017	1,38	18,5	1,939	0,07	0,2239	-6
>sp|P01800|HVM31	18,95	19,2	16,3	19,9	14,5	14,8	19	19	19	19,9	18	19	20,3	19	19	20	18,9	18,9	17,829	19,214	>sp|P018	1,38	18,5	1,939	0,07	0,2239	-6
>sp|P01801|HVM32	18,95	19,2	16,3	19,9	14,5	14,8	19	19	19	19,9	18	19	20,3	19	19	20	18,9	18,9	17,829	19,214	>sp|P018	1,38	18,5	1,939	0,07	0,2239	-6
>sp|P61089|UBE2N_	20,91	21,5	21,3	20,7	21,4	21,4	21	22	23	24,2	23	22	22	21,8	22	22	21,4	21,5	21,509	22,2455	Ube2n	0,74	21,9	1,937	0,07	0,2242	-6
>sp|Q8K1B8|URP2_M	20,19	18,7	19,6	18,8	18,7	19,2	18	20	19	19,8	20	19	19,5	19,4	19	19	19,3	19,7	19,118	19,5033	Fermt3	0,39	19,3	1,937	0,07	0,2242	-6
>sp|Q9Z1K5|ARI1_M(	18,04	18,3	18,1	17,9	17,9	17,7	18	17	18	17,6	17	18	17,5	17,6	18	18	17,8	17,8	17,878	17,6211	Arih1	-0,3	17,7	-1,94	0,07	0,2245	-6
>sp|Q8VDM6|HNRL1_	15,99	17	18,2	17,8	17,8	17,8	18	18	18	18,1	18	18	17,4	18,5	18	18	18,3	18,6	17,661	18,1756	Hnrnpul1	0,51	17,9	1,931	0,071	0,2261	-6
>sp|Q99LD8|DDAH2_	21,38	21,6	20,6	21,7	21,7	21,6	22	22	20	19,9	21	21	21,1	20,7	21	22	21,6	20,4	21,364	20,8725	Ddah2	-0,5	21,1	-1,93	0,071	0,2261	-6
>sp|Q9D110|MTHFS_I	18,83	18,2	20,3	19,6	20,1	20,4	20	18	20	18,8	18	19	19,1	19,3	19	19	18,6	18,6	19,501	18,7868	Mthfs	-0,7	19,1	-1,93	0,071	0,2266	-6
>sp|P62743|AP2S1_	20,81	18,6	19,4	18,6	20,6	20,2	21	20	19	20,2	18	18	20,1	18,6	19	19	19,2	18,4	19,727	18,9165	Ap2s1	-0,8	19,3	-1,92	0,072	0,2285	-6
>sp|Q91V41|RAB14_	21,77	22	21,9	22,5	22,7	22,3	22	21	22	21,4	22	22	21,8	21,9	21	22	21,8	21,8	22,104	21,7921	Rab14	-0,3	21,9	-1,92	0,072	0,2294	-6
>sp|Q8BH59|CMC1_I	0	0	0	0	0	0	0	15	15	14	14	15	13,9	14,1	0	0	13,9	0	3,3235	9,4592	Slc25a12	6,14	6,39	1,921	0,072	0,2294	-6
>sp|P62889|RL30_M	22,02	20,8	20,6	22,1	21,8	21,2	21	21	21	21,9	21	21	22,1	21,7	22	21	21,8	22,1	21,339	21,7418	Rpl30	0,4	21,5	1,92	0,072	0,2297	-6
>sp|Q99KE1|MAOM_I	22,27	22,6	22,1	22,8	22,9	22,1	22	22	23	22,3	22	22	22,5	22,4	23	22	22,3	22	22,488	22,2778	Me2	-0,2	22,4	-1,92	0,073	0,2311	-6
>sp|Q8CBY8|DCTN4_I	17,65	16,8	17,4	16,7	16,9	17,6	16	17	17	18	18	17	17,1	16,6	17	18	17,6	18,7	17,064	17,6106	Dctn4	0,55	17,3	1,914	0,073	0,2317	-6
>sp|O54804|CHKA_M	14,57	13,9	13,8	14,1	13,4	13,2	14	12	12	12,6	14	14	14,7	14,8	15	15	13,7	14,4	13,474	14,1846	Chka	0,71	13,8	1,913	0,073	0,2317	-6
>sp|Q61781|K1C14_	22,76	22,3	21,8	21,4	21,2	20,8	21	21	22	20,3	24	22	22,7	22	21	24	23,2	23,5	21,648	22,5194	Krt14	0,87	22,1	1,913	0,073	0,2317	-6
>sp|P27612|PLAP_M	20,23	20	22,1	20	20,3	22,3	20	20	20	21,5	22	22	21,8	22	22	20	20,3	20,1	20,503	21,2875	Plaa	0,78	20,9	1,913	0,073	0,2317	-6
>sp|P07744|K2C4_M	19,89	17,5	19,6	18,7	19	19,4	19	19	17	19,3	18	20	20	20,6	17	21	21	21,7	18,669	19,8235	Krt4	1,15	19,2	1,911	0,074	0,232	-6
>sp|P63280|UBC9_M	21,08	22,3	21,7	21,6	21,4	21	22	21	21	20,7	22	21	21,7	21,1	21	21	20,8	21,3	21,501	21,1563	Ube2i	-0,3	21,3	-1,91	0,074	0,2326	-6
>sp|Q7TSV4|PGM2_M	21,2	21,2	21,9	21,8	21,8	21,9	21	21	22	22,1	22	21	21,6	21,5	22	22	21,9	21,6	21,542	21,8024	Pgm2	0,26	21,7	1,905	0,074	0,2342	-6
>sp|P08103|HCK_M(	17,78	19,4	18,2	17,2	19,4	18,3	18	18	19	19,2	18	16	17,9	18,1	17	17	17,7	17,8	18,429	17,7301	Hck	-0,7	18,1	-1,9	0,075	0,2345	-6
>sp|Q61599|GDIR2_I	18,96	18,7	18,6	18,3	18,8	18,2	17	20	20	20,6	21	19	19	19,4	19	19	19,3	18,5	18,721	19,457	Arhgdib	0,74	19,1	1,903	0,075	0,2345	-6
>sp|Q8R2K1|FUCM_M	18,23	17,8	18,5	23,5	19,1	23,6	23	23	17	23,4	23	23	16,2	24	24	24	23,8	23,8	20,456	22,8066	Fuom	2,35	21,6	1,9	0,075	0,2356	-6
>sp|B8ZKI1|QTRT2_M	15,96	0	17,5	15,3	15,1	15,8	0	15	15	15,9	18	19	15,9	14,4	19	16	15,9	16,1	12,191	16,649	Qtrt2	4,46	14,4	1,899	0,075	0,236	-6
>sp|P50171|DHB8_M	18,37	19	18,7	18	15,2	17,5	18	17	18	16,4	17	18	17,8	16,1	18	15	17,2	14,5	17,643	16,617	Hsd17b8	-1	17,1	-1,9	0,076	0,2368	-6
>sp|Q14CH1|MOCOS_	16,95	17,2	19,9	17,4	16,5	16,9	17	17	16	17,1	21	21	17,9	18,1	18	17	17,4	18	17,249	18,4319	Mocos	1,18	17,8	1,894	0,076	0,2376	-6
>sp|Q9DCZ1|GMPR1_	20,28	21,2	20,4	20,7	20,8	20	20	21	21	19,6	20	21	18,9	20,4	21	20	20,1	20,4	20,516	20,0844	Gmpr	-0,4	20,3	-1,89	0,076	0,2376	-6
>sp|P61358|RL27_M	20,92	21,5	21,6	20,1	20,3	20,6	20	22	21	21	22	22	21,5	21,5	21	21	20,7	21,7	20,858	21,3193	Rpl27	0,46	21,1	1,892	0,076	0,238	-6
>sp|Q3UDE2|TTL12_M	20,89	19,7	19,7	21,1	19,4	19,8	22	21	21	21,1	21	21	21,8	21,9	21	20	20,8	21,7	20,565	21,2375	Ttll12	0,67	20,9	1,891	0,076	0,238	-6
>sp|P01029|CO4B_M	20,34	20,7	19,8	19,6	18,7	20,1	20	20	20	20,6	20	20	21	20	21	20	20,2	20,8	19,877	20,3691	C4b	0,49	20,1	1,891	0,076	0,238	-6
>sp|Q9R045|ANGL2_	17,59	17,6	13,9	16,9	16,9	0	16	0	0	15,9	14	15	16,5	17,2	17	17	16,5	16,8	10,945	16,1584	Angptl2	5,21	13,6	1,891	0,076	0,238	-6
>sp|Q9JKF1|IQGA1_M	19,23	19	19,4	19,2	19	19,6	19	19	19	19,7	20	20	19,2	19,7	19	19	19,2	19,2	19,221	19,4552	Iqgap1	0,23	19,3	1,887	0,077	0,2393	-6
>sp|P54869|HMCS2_	18,92	19,7	19,8	17,6	19,5	19	19	20	20	19,7	20	20	19,8	19,2	20	20	19,6	19,5	19,21	19,721	Hmgcs2	0,51	19,5	1,885	0,077	0,24	-6
>sp|Q8BGF3|WDR92_	14,93	20	17,9	19,5	19	18,6	19	18	21	20,6	18	18	20,8	21,2	20	21	20,8	20,2	18,71	20,0159	Wdr92	1,31	19,4	1,882	0,078	0,2412	-6
>sp|O70370|CATS_	17,12	15	18,2	15,7	17,2	17	17	16	17	17,5	15	14	14,1	0	13	16	14,4	16,6	16,711	13,4364	Ctss	-3,3	15,1	-1,88	0,078	0,2413	-6
>sp|Q6PAM1|TXLNA_	15,11	15,1	18,4	18,2	18,5	18,4	18	17	17	15,8	17	15	16,6	17	17	16	16,3	16,7	17,26	16,3381	Txlna	-0,9	16,8	-1,88	0,078	0,2414	-6
>sp|Q9DC11|PXDC2_	18,08	17,4	17,6	21,7	21,5	21,9	22	22	22	17	17	17	20,2	20,1	20	20	19,7	17,5	20,389	18,7749	Plxdc2	-1,6	19,6	-1,88	0,078	0,2419	-6
>sp|P47857|PFKAM_	21,59	21,2	21	19,5	20,9	21,1	20	20	21	20,7	21	21	19,8	19,7	19	20	20,6	19,7	20,775	20,1765	Pfkm	-0,6	20,5	-1,88	0,078	0,2425	-6
>sp|Q91W50|CSDE1_	14,4	14,7	14,2	15,4	13,6	12,6	14	13	13	11,9	14	12	13,6	0	14	12	11,7	10,2	13,843	11,0946	Csde1	-2,7	12,5	-1,87	0,079	0,2439	-6
>sp|Q8K183|PDXK_M	22,05	22,1	22,1	22,3	21,7	21,8	22	22	23	22,3	23	23	22,9	22	22	23	22,3	22,3	22,172	22,4294	Pdxk	0,26	22,3	1,872	0,079	0,2441	-6
>sp|Q3UMT1|PP12C_	14,23	14	15,1	13,3	15,5	13,6	14	14	15	10,9	13	15	14,1	12,7	15	13	13,8	13,1	14,295	13,4019	Ppp1r12c	-0,9	13,8	-1,87	0,079	0,2441	-6
>sp|Q8R3G9|TSN8_M	21,36	21,7	21	21,3	21,5	21,2	22	21	21	20,7	21	21	21,2	20,6	21	21	20,8	20,4	21,266	20,9607	Tspan8	-0,3	21,1	-1,87	0,08	0,2456	-6
>sp|Q8BZA9|TIGAR_M	16,17	16,7	17,2	17,1	16,8	17,3	16	17	17	16,8	17	17	16,6	16,6	17	16	16,1	16,6	16,875	16,5804	Tigar	-0,3	16,7	-1,87	0,08	0,2456	-6
>sp|Q8CFI7|RPB2_M(	15,68	16,2	16,7	15,5	17,1	15,2	16	16	17	17,1	17	16	17,2	16,7	16	16	16,3	16,6	16,042	16,5539	Polr2b	0,51	16,3	1,867	0,08	0,2456	-6
>sp|Q80SW1|SAHH2_	22,1	22,8	22,4	23,2	22,1	21,9	23	22	23	22,9	23	23	23	22,9	23	23	22,5	22,5	22,484	22,762	Ahcyl1	0,28	22,6	1,862	0,081	0,2474	-6
>sp|P28652|KCC2B_	14,75	15,8	15,3	16,4	15,9	15,7	15	15	15	13,1	14	0	14,7	14,3	14	15	12,6	14,9	15,409	12,4798	Camk2b	-2,9	13,9	-1,86	0,081	0,2474	-6
>sp|Q64321|ZBT7B_I	17,89	18	15,9	18,6	17,9	16,9	17	17	15	15	16	17	17	16,2	17	17	16,3	16,9	17,176	16,4014	Zbtb7b	-0,8	16,8	-1,86	0,081	0,2478	-6

>sp|P10630|IF4A2_M	23,03	22,8	23,7	23,2	23,8	23,6	24	24	24	23,2	23	24	23,5	23,2	23	23	23	23	23,581	23,2563	Eif4a2	-0,3	23,4	-1,86	0,081	0,2479	-6
>sp|P18525|HVM54	17,93	18,5	18,1	17,8	18,6	18,4	19	19	18	17,4	18	0	17,3	17,9	17	17	17,1	0	18,336	13,6045	>sp|P185	-4,7	16	-1,86	0,081	0,2484	-6
>sp|P19001|K1C19_	23,32	22,3	23,1	22	21,6	22,4	21	22	22	21,3	23	23	22,8	23,2	22	23	22,5	23,4	22,192	22,788	Krt19	0,6	22,5	1,855	0,082	0,2496	-6
>sp|P50096|IMDH1_	0	0	18,6	0	0	0	0	18	21	0	21	15	14,8	14,4	14	13	13,8	12,2	6.41331	13,2077	Impdh1	6,79	9,81	1,854	0,082	0,2496	-6
>sp|Q68FL4|SAHH3_M	21,94	22,7	22,4	23,3	22	21,8	22	22	23	22,8	23	23	23	22,8	23	22	22,6	22,5	22,415	22,7107	Ahcyl2	0,3	22,6	1,854	0,082	0,2496	-6
>sp|P23116|EIF3A_M	19,28	19,9	18,3	19,2	18,4	18,2	19	19	19	19,5	18	18	17,7	17,7	17	19	19,6	17,7	18,99	18,3734	Eif3a	-0,6	18,7	-1,85	0,082	0,2496	-6
>sp|Q99KK2|NEUA_M	20,46	21,2	21	21,1	20,8	20	20	21	21	20,5	20	20	20	20,7	21	21	20,9	19,8	20,764	20,401	Cmas	-0,4	20,6	-1,85	0,082	0,2504	-6
>sp|Q9JMD3|STA10_M	17,86	19,3	16,2	19,8	19,7	19,4	21	19	19	16,8	17	16	18,8	17,3	19	19	19,9	17,5	19,107	18,0179	Stard10	-1,1	18,6	-1,85	0,082	0,2504	-6
>sp|Q8BMB3|IF4E2_M	0	15,2	14,6	15,9	15,8	15,4	17	15	16	16,8	17	17	19	16,7	18	17	16,7	16,7	13,956	17,2022	Eif4e2	3,25	15,6	1,848	0,083	0,2513	-6
>sp|Q6DYE8|ENPP3_M	19	19,1	20,7	19,8	21,1	19,6	20	16	21	19,6	19	20	18,4	18,4	16	19	16,4	19,1	19,656	18,4707	Enpp3	-1,2	19,1	-1,85	0,083	0,2513	-6
>sp|Q64374|RGN_MO	18,56	18,7	17,7	18,7	18,7	18,5	18	18	18	18,4	18	19	17,3	18,1	17	18	18,4	18,1	18,424	18,0557	Rgn	-0,4	18,2	-1,85	0,083	0,2516	-6
>sp|P06801|MAOX_M	21,4	21	21,1	22,5	21,2	22	21	21	23	23,4	24	22	22,3	21,4	21	22	22,5	22,3	21,591	22,3648	Me1	0,77	22	1,846	0,083	0,2516	-6
>sp|Q9D6J6|NDUV2_M	16,07	15,3	15,2	14,9	15,9	16,4	16	17	16	16,4	17	18	15,4	16,2	16	16	16,5	16	15,856	16,4384	Ndufv2	0,58	16,1	1,845	0,083	0,2521	-6
>sp|Q9DCN2|NB5R3_M	18,56	18,5	20	18,8	19,4	19,2	19	20	19	19,8	20	19	19,1	19,9	19	20	20,8	20,5	19,186	19,7022	Cyb5r3	0,52	19,4	1,843	0,083	0,2525	-6
>sp|Q62179|SEM4B_M	17,76	18	17,6	17,2	17,3	17,2	17	17	17	15,6	16	17	17,7	16,7	18	16	16,4	16,5	17,216	16,625	Sema4b	-0,6	16,9	-1,84	0,084	0,2531	-6
>sp|Q922P9|GLYR1_M	17,84	18	15,9	18	15,5	15,5	18	16	16	17,8	15	16	15,9	16	16	16	15,2	15,3	16,736	15,9014	Glyr1	-0,8	16,3	-1,84	0,084	0,2535	-6
>sp|Q9CWZ3|RBM8A	17,17	16,6	18,1	17,2	17,4	15,1	15	17	17	17,2	18	16	18,1	18,1	18	17	17,5	17,3	16,833	17,5178	Rbm8a	0,68	17,2	1,839	0,084	0,2537	-6
>sp|Q91ZE0|TMLH_MO	19,4	21,8	21,5	21,4	18,2	22	22	22	22	20,1	18	20	20,9	20,8	21	18	20,9	20,4	21,153	20,01	Tmlhe	-1,1	20,6	-1,83	0,085	0,2557	-6
>sp|Q9DAW6|PRP4_M	16,94	15,8	16,4	14,4	16	17	15	15	16	16,8	17	16	17,3	15,9	16	16	16,6	17,4	15,88	16,5395	Prpf4	0,66	16,2	1,833	0,085	0,2559	-6
>sp|Q8BHG2|CA123_M	19,02	18,9	19,7	20,5	20,8	20,1	20	20	20	19,8	20	19	19,1	19,5	20	19	19,2	18,9	19,911	19,4436	>sp|Q8BH	-0,5	19,7	-1,83	0,086	0,2575	-6
>sp|Q9QZD9|EIF3I_MO	21,07	21	21,4	20,7	20,9	20,8	21	21	21	20,7	21	21	21,1	21,5	21	21	21,1	21	20,946	21,143	Eif3i	0,2	21	1,829	0,086	0,2576	-6
>sp|Q3THS6|METK2_M	20,93	21,2	24,1	21	22,2	22,3	22	22	21	22,3	24	23	22,3	22,6	24	22	22	22,4	21,93	22,6526	Mat2a	0,72	22,3	1,828	0,086	0,2576	-6
>sp|P59326|YTHD1_M	15,4	16,3	17	15,8	16,3	14,9	17	16	14	16	16	16	15,5	17,1	17	17	16,4	17	15,842	16,4538	Ythdf1	0,61	16,1	1,827	0,086	0,2576	-6
>sp|P39061|COIA1_M	0	14,7	15	14,3	14,5	14,9	15	15	14	15,6	16	16	16,4	16,5	16	16	15,5	16	13,07	16,0409	Col18a1	2,97	14,6	1,827	0,086	0,2576	-6
>sp|Q9CWG8|NDUF7_M	15,92	16,2	17	16,3	15,8	16,2	15	15	14	16,3	16	16	16,9	16,3	17	16	15,9	15,7	15,591	16,2662	Ndufaf7	0,68	15,9	1,826	0,086	0,2576	-6
>sp|Q924M7|MPI_MO	21,61	21,1	21,3	21,4	21,6	20,6	22	21	22	20,6	21	21	21,5	20,8	22	22	20,1	20,3	21,365	20,9156	Mpi	-0,4	21,1	-1,83	0,086	0,2576	-6
>sp|P40336|VP26A_M	20,12	18,9	19,6	19,5	20,4	20,5	21	21	19	21,1	20	20	21	20,9	21	21	20,7	20,3	20,005	20,5485	Vps26a	0,54	20,3	1,824	0,087	0,2585	-6
>sp|Q923T9|KCC2G_M	14,86	15,9	15,4	16,5	16	15,9	15	15	15	13,5	14	0	14,8	14,4	14	15	12,8	15	15,517	12,6244	Camk2g	-2,9	14,1	-1,82	0,087	0,2587	-6
>sp|Q99KC8|VMA5A_M	18,98	18,1	23,5	18,6	23,7	23,4	19	23	24	18,1	21	20	17,7	18,3	22	17	18,4	21,9	21,32	19,4152	Vwa5a	-1,9	20,4	-1,82	0,087	0,2594	-6
>sp|Q9ERD7|TBB3_MO	23,29	22,7	23,9	23,1	23	23,2	24	24	24	23,4	23	23	22,4	22,8	22	23	23,2	23,6	23,409	23,0116	Tubb3	-0,4	23,2	-1,82	0,087	0,2602	-6
>sp|Q8BWG8|ARRB1_M	18,21	17,6	18,9	18,7	18,6	18,1	19	19	18	17,4	18	18	18,8	18,7	18	18	17,3	18,3	18,439	18,0375	Arrb1	-0,4	18,2	-1,81	0,088	0,2619	-6
>sp|Q922F4|TBB6_MO	23,57	23	24,1	23,1	23,3	23,4	24	24	24	23,5	24	23	22,8	23,2	23	23	23,2	23,6	23,591	23,2626	Tubb6	-0,3	23,4	-1,81	0,088	0,2624	-6
>sp|Q8BG32|PSD11_M	19,37	19,4	20	20,6	20,6	20,2	18	20	20	20,4	21	20	20,8	21,1	21	20	20,2	19,8	19,876	20,4695	Psmd11	0,59	20,2	1,811	0,089	0,263	-6
>sp|Q6DFW4|NOP58_M	0	16	15,1	0	15,1	14,9	0	14	0	15,8	16	16	16,5	16,1	16	0	15,6	15,4	8.39530	14,1093	Nop58	5,71	11,3	1,811	0,089	0,263	-6
>sp|P26883|FKB1A_M	19,02	19	18,9	18,1	19,8	19,2	19	18	19	18,5	18	18	18,8	19,1	19	17	17,9	17,1	18,811	18,2619	Fkbp1a	-0,5	18,5	-1,81	0,089	0,2632	-6
>sp|Q91X20|ASH2L_M	0	13,3	0	13,3	0	15,3	0	0	15	0	12	0	0	0	0	0	0	0	6,3212	1,28323	Ash2l	-5	3,8	-1,81	0,089	0,2632	-6
>sp|Q7TMK9|HNRPQ_M	21,53	20,5	19,4	21,6	21,5	21,4	21	21	18	20,1	19	20	21,2	20,4	20	21	18,4	19,5	20,699	19,8455	Syncrip	-0,9	20,3	-1,81	0,089	0,2632	-6
>sp|P31230|AIMP1_M	15,17	16,3	16,1	16	17	16,3	15	16	16	15,3	15	16	15,1	14,3	15	15	15,4	16,5	15,897	15,3868	Aimp1	-0,5	15,6	-1,81	0,089	0,2632	-6
>sp|P20612|GNAT1_M	17,73	17,7	17,4	18,7	19,2	18,8	19	18	17	16,7	18	19	19,4	19,1	19	19	19,7	19,6	18,116	18,8635	Gnat1	0,75	18,5	1,807	0,089	0,2632	-6
>sp|Q3V3I2|GNAT3_M	17,73	17,7	17,4	18,7	19,2	18,8	19	18	17	16,7	18	19	19,4	19,1	19	19	19,7	19,6	18,116	18,8635	Gnat3	0,75	18,5	1,807	0,089	0,2632	-6
>sp|P08207|S10AA_M	20,25	19,5	20,5	20,3	20,5	21	19	20	20	18,8	20	20	18,9	20,4	20	19	19,4	20,1	20,076	19,6011	S100a10	-0,5	19,8	-1,8	0,09	0,264	-6
>sp|P01843|LAC1_MO	19,64	20	19,5	20,3	20,5	20,5	21	20	20	19	17	20	19,8	20,1	20	20	19,7	20,1	20,208	19,5336	>sp|P018	-0,7	19,9	-1,8	0,09	0,264	-6
>sp|P01896|HA1Z_MO	20,14	20,4	20,4	20,4	20,1	20,3	20	20	20	20,1	20	18	20,1	20,2	20	20	19,6	19,8	20,324	19,7922	>sp|P018	-0,5	20,1	-1,8	0,09	0,264	-6
>sp|P70122|SBDS_MO	18,06	20,3	19,1	20,4	18,7	19,9	18	21	19	19,1	21	20	20,3	19,9	20	21	20,1	19,6	19,327	20,0139	Sbds	0,69	19,7	1,803	0,09	0,2641	-6
>sp|Q3ULJ0|GPD1L_M	21,1	21,7	19,9	19,7	19,5	20	20	20	20	19,1	19	20	20,6	19,1	20	20	19,4	20,6	20,253	19,7202	Gpd1l	-0,5	20	-1,8	0,09	0,2649	-6
>sp|Q91YP3|DEOC_MO	21,81	22,4	22,3	20,9	22,4	23	22	22	23	22,3	22	22	21,7	20,7	21	22	22,3	22,1	22,194	21,7137	Dera	-0,5	22	-1,8	0,09	0,2649	-6
>sp|P50149|GNAT2_M	17,63	17,6	17,3	18,6	19,1	18,7	19	18	17	16,7	18	19	19,3	19	19	19	19,6	19,5	18,026	18,7671	Gnat2	0,74	18,4	1,8	0,09	0,2649	-6
>sp|Q8VDP4|CCAR2_M	22,08	19,3	16,1	17,9	18	14,7	19	15	16	18,6	17	16	15,8	16,1	16	16	13,9	15,2	17,602	16,0456	Ccar2	-1,6	16,8	-1,8	0,09	0,2649	-6

>sp|P33434|MMP2_	15,45	18	14	18,4	19	16,3	16	18	16	17,7	17	15	0	13,8	14	16	13	14,7	16,731	13,4541	Mmp2	-3,3	15,1	-1,8	0,091	0,2649	-6
>sp|Q6PDG5|SMRC2_	14,66	14,3	14,2	14,3	14	14,2	15	12	14	13,9	15	15	15,7	13,6	15	15	15,1	14,6	14,083	14,651	Smarcc2	0,57	14,4	1,799	0,091	0,2649	-6
>sp|Q07968|F13B_M	16,4	16,7	14,4	15,5	16,2	18,1	18	17	17	17,3	15	16	15,7	15,2	15	16	16	16,2	16,623	15,7765	F13b	-0,8	16,2	-1,8	0,091	0,2654	-6
>sp|P97470|PP4C_M	21,65	20,5	20,5	22,8	20,8	21,6	21	21	21	20,6	22	21	20,3	20,2	20	21	20,7	20,8	21,283	20,7331	Ppp4c	-0,5	21	-1,8	0,091	0,2661	-6
>sp|P55002|MFAP2_	15,94	16,5	17,3	19	18,2	18,5	18	18	17	18,2	19	19	17,7	17,9	18	19	17,9	18,4	17,583	18,1989	Mfap2	0,62	17,9	1,789	0,092	0,2687	-6
>sp|Q8BYK6|YTHD3_M	15,37	16,2	16,9	15,8	16,2	14,8	17	16	14	15,9	16	16	15,5	16,9	17	17	16,3	16,9	15,777	16,3765	Ythdf3	0,6	16,1	1,789	0,092	0,2687	-6
>sp|Q9CQD1|RAB5A_	20,9	21,2	19,2	21,2	20,9	20,5	21	21	21	21,5	21	21	21,2	21	21	21	20,9	21	20,76	21,1553	Rab5a	0,4	21	1,788	0,092	0,2687	-6
>sp|Q8CFX1|G6PE_M	15,11	13,8	20,1	16,8	20,6	20	15	15	14	16,5	19	19	18,9	19,2	19	18	16,6	19,4	16,684	18,4525	H6pd	1,77	17,6	1,786	0,093	0,2695	-6
>sp|P61967|AP1S1_	19,38	18,6	17,3	18,1	18	17,7	18	19	18	18,8	19	19	18,6	18,6	18	18	18,8	18,1	18,239	18,6848	Ap1s1	0,45	18,5	1,786	0,093	0,2695	-6
>sp|P01783|HVM16	17,7	17,6	17,9	17,6	17,6	17,3	18	18	17	16,1	17	0	17	17,2	17	17	16,8	0	17,614	13,2052	>sp|P017	-4,4	15,4	-1,78	0,093	0,27	-6
>sp|P18527|HVM56	18,2	18	18,4	18	18	17,9	18	18	18	16,6	18	0	17,5	17,6	17	18	17,3	0	18,112	13,5812	>sp|P185	-4,5	15,8	-1,78	0,093	0,27	-6
>sp|O35658|C1QBP_	18,98	18,3	18,1	18,4	19	18,9	18	20	20	18,8	18	18	14,3	0	0	18	19,1	18,6	18,776	14,019	C1qbp	-4,8	16,4	-1,78	0,093	0,27	-6
>sp|Q91W90|TXND5_	23,85	23,8	19,8	20,4	20,2	20,6	21	21	20	20,3	20	19	20,1	20,4	21	20	20,6	20,4	21,186	20,2302	Txndc5	-1	20,7	-1,78	0,093	0,27	-6
>sp|O89112|LANC1_	19,83	19,8	21	20,3	19,6	20,9	20	20	20	20,7	20	21	20,3	20,3	21	20	20,4	20,7	20,201	20,5162	Lancl1	0,32	20,4	1,782	0,093	0,27	-6
>sp|Q8BH00|AL8A1_	0	0	17,8	18,3	18,8	17,9	15	18	18	18	16	20	19,9	18,6	19	18	18	18,5	13,778	18,4442	Aldh8a1	4,67	16,1	1,782	0,093	0,27	-6
>sp|P04444|HBBZ_M	20,11	20,7	20,3	20,3	21,3	21,3	15	20	20	0	20	21	21,2	15,7	17	17	17,3	14,2	19,943	16,011	Hbb-bh1	-3,9	18	-1,78	0,094	0,271	-6
>sp|P18526|HVM55	17,93	17,8	18,1	17,8	17,8	17,6	18	18	18	16,3	18	0	17,3	17,4	17	17	17,1	0	17,834	13,3816	>sp|P185	-4,5	15,6	-1,78	0,094	0,271	-6
>sp|P18529|HVM58	17,93	17,8	18,1	17,8	17,8	17,6	18	18	18	16,3	18	0	17,3	17,4	17	17	17,1	0	17,834	13,3816	>sp|P185	-4,5	15,6	-1,78	0,094	0,271	-6
>sp|Q9Z1R3|APOM_M	23,27	22,4	20,7	21,7	22,8	20,4	23	23	21	22,1	23	22	16,4	16,4	17	23	22,8	20,2	22,043	20,2363	Apom	-1,8	21,1	-1,78	0,094	0,2712	-6
>sp|P51655|GPC4_M	18,03	18,6	18,4	17,3	17	17,2	17	18	18	18,5	20	20	18	17,8	17	18	17,7	19,3	17,672	18,4079	Gpc4	0,74	18	1,773	0,095	0,2729	-6
>sp|Q80Y81|RNZ2_M	16,69	17,6	16,9	17,5	17,7	16,8	17	17	17	18,6	17	18	16,9	16,3	17	18	18,3	19	17,006	17,5986	Elac2	0,59	17,3	1,773	0,095	0,2729	-6
>sp|Q3UL36|ARGL1_I	15,09	17,8	15	18,4	18,5	18,8	17	15	20	20	21	16	12,9	9,77	0	10	15,9	16,4	17,346	13,4974	Arglu1	-3,8	15,4	-1,77	0,095	0,2732	-6
>sp|Q9EQH3|VPS35_I	21,28	22,2	19,9	20,9	23,1	22,9	21	23	20	22,5	23	23	23,2	22,9	23	23	22,8	20	21,665	22,541	Vps35	0,88	22,1	1,771	0,095	0,2732	-6
>sp|Q61768|KINH_M	15,13	15	14,6	15,3	14,4	16	15	16	15	15,7	17	17	14,4	14,6	15	15	15,4	17,5	15,129	15,8775	Kif5b	0,75	15,5	1,77	0,095	0,2734	-6
>sp|Q8VED9|LEGL_MO	15,54	18,2	17,6	15,3	17,5	18	18	18	18	18,1	18	18	18,2	18,2	0	0	0	17,8	17,384	12,0698	Lgalsl	-5,3	14,7	-1,77	0,096	0,2748	-6
>sp|P28843|DPP4_M	21,84	22	20,3	20,3	20,3	20,3	20	20	21	20,4	21	20	20,2	20,3	21	20	19,9	20,1	20,75	20,3004	Dpp4	-0,4	20,5	-1,76	0,097	0,2776	-6
>sp|E9Q557|DESP_MO	17,23	18	17,4	15,9	16,3	16,5	16	16	17	17,2	17	17	16,4	19,2	20	16	19,1	16,5	16,659	17,5659	Dsp	0,91	17,1	1,754	0,098	0,2806	-6
>sp|P56546|CTBP2_	18,65	19,2	17,6	18,2	18,4	18,8	18	19	19	19,4	20	20	18,6	19,6	19	18	19,5	17,8	18,534	19,1257	Ctbp2	0,59	18,8	1,753	0,098	0,2808	-6
>sp|Q9DBB4|NAA16_	20,28	13,4	19,7	18,8	13,5	19,8	19	15	19	15	15	17	16	15,4	15	18	18	12	17,695	15,7746	Naa16	-1,9	16,7	-1,75	0,098	0,281	-6
>sp|O08710|THYG_M	17,47	17,4	13,6	17	17,5	14,6	17	17	17	14,3	0	12	16	12,5	16	16	16,5	16,9	16,531	13,3658	Tg	-3,2	14,9	-1,75	0,098	0,281	-6
>sp|Q80WB5|NTAQ1_	0	0	16,9	16,5	17	15,8	16	15	15	15,7	16	17	16,4	18,8	19	16	16,4	15,4	12,542	16,7255	Wdyhv1	4,18	14,6	1,749	0,099	0,2821	-6
>sp|Q9Z1B5|MD2L1_	0	0	15,7	16,2	16,3	16,8	16	16	17	15,7	15	18	17,2	17,6	17	16	17	17,2	12,635	16,8191	Mad2l1	4,18	14,7	1,748	0,099	0,2824	-6
>sp|Q9D6N1|CAH13_	15,41	0	14,7	14,8	16,6	16	15	17	17	17,6	18	18	16,8	16,8	16	16	15,9	16,8	13,947	17,0337	Ca13	3,09	15,5	1,745	0,1	0,2837	-6
>sp|Q8C5P5|NT5D1_	13,99	14,8	13,9	14,6	14,1	15,5	15	14	13	0	15	14	14,1	13,4	13	14	13,7	0	14,345	10,8013	Nt5dc1	-3,5	12,6	-1,74	0,1	0,2837	-6
>sp|Q8BP47|SYNC_M	21,39	20,3	20,9	21	20,2	21,1	20	20	21	20,6	21	20	20,3	20,6	21	21	19,3	19,4	20,678	20,2116	Nars	-0,5	20,4	-1,74	0,101	0,2875	-6
>sp|P04186|CFAB_M	20,44	21,1	21,6	21,4	21,4	21,3	21	21	21	20,9	22	21	21,3	21,3	22	22	21,4	21	21,077	21,3395	Cfb	0,26	21,2	1,736	0,101	0,2879	-6
>sp|Q9JK38|GNA1_M	19	19,7	20,7	20,4	19,8	19,8	20	20	20	20	20	19	18	18,1	18	20	20,3	20,2	19,986	19,3571	Gnpnat1	-0,6	19,7	-1,73	0,102	0,2883	-6
>sp|P29416|HEXA_M	20,55	19,6	18,9	20	18,4	18,9	20	19	20	18,9	19	19	17,8	18,5	19	20	19,6	18,8	19,45	18,9062	Hexa	-0,5	19,2	-1,73	0,102	0,289	-6
>sp|Q501J6|DDX17_	19,27	19,3	20,8	19,2	19,3	19,2	19	20	20	19,2	20	20	19,3	19	19	19	18,9	19,1	19,544	19,196	Ddx17	-0,3	19,4	-1,73	0,102	0,2893	-6
>sp|Q91YT7|YTHD2_M	15,44	15,9	16,8	0	15,9	0	16	14	14	15,4	16	16	15,1	16,8	16	16	15,7	15,1	11,976	15,8883	Ythdf2	3,91	13,9	1,729	0,103	0,2905	-6
>sp|P97865|PEX7_M	19,72	20,3	19,9	19,1	18,9	19,2	20	20	20	20,7	20	21	20,3	19,4	21	20	19,9	19,7	19,708	20,1272	Pex7	0,42	19,9	1,726	0,103	0,2916	-6
>sp|P24452|CAPG_M	14,33	13,6	13	12,9	12,7	12,5	0	0	0	0	0	0	0	11,2	13	0	0	9,77	8,794	3,80674	Capg	-5	6,3	-1,72	0,104	0,2929	-6
>sp|Q8BGR6|ARL15_	19,23	19,1	18,9	18,2	18,5	19	16	15	15	17,3	18	17	0	17,1	0	17	16,1	16,5	17,624	13,239	Arl15	-4,4	15,4	-1,72	0,104	0,2936	-6
>sp|P59279|RAB2B_	19,81	19,5	19,2	19,5	19,1	19,9	19	20	20	19,8	20	20	19,7	19,7	20	20	19,9	19,9	19,631	19,8781	Rab2b	0,25	19,8	1,719	0,105	0,2947	-6
>sp|P23591|FCL_MO	21,13	21,4	20,8	21	20,7	21	21	21	21	21,2	22	22	21,9	21,4	21	21	21,4	20,8	21,086	21,4062	Tsta3	0,32	21,2	1,718	0,105	0,2948	-6
>sp|P61750|ARF4_M	22,28	24,4	22	22	21,6	22,1	22	23	23	22,5	23	22	22,6	21,3	21	21	21,9	21,5	22,428	21,8164	Arf4	-0,6	22,1	-1,71	0,106	0,299	-6
>sp|O88322|NID2_M	19,12	19	19,3	19,1	18,3	19,5	19	19	19	18,9	19	19	19,4	19,5	19	19	18,9	19,5	19,053	19,2771	Nid2	0,22	19,2	1,709	0,106	0,299	-6
>sp|Q99KJ8|DCTN2_I	16,68	17,3	19,2	0	15,7	18,7	15	15	0	17,7	18	18	18,5	18,8	19	15	14,7	15,6	13,005	17,3452	Dctn2	4,34	15,2	1,708	0,106	0,299	-6

>sp|Q6P5F9|XPO1_M	20,42	20,6	22,2	20,1	19	20,6	21	21	21	20,7	19	20	20,2	20,1	20	20	21,2	19,9	20,746	20,1543	Xpo1	-0,6	20,4	-1,71	0,107	0,3001	-6
>sp|P0C605|KGP1_M	20,58	20,3	19,8	20,1	20,4	20,9	20	21	21	19,8	21	20	20,4	19,2	19	20	20,3	20	20,455	19,9684	Prkg1	-0,5	20,2	-1,7	0,107	0,301	-6
>sp|Q91WP0|MASP2	16,35	16,6	16,7	20,5	20,6	20,2	20	16	16	20,9	20	16	21,6	20,3	21	21	21,5	16	18,092	19,8113	Masp2	1,72	19	1,702	0,108	0,3014	-6
>sp|P97290|IC1_MO	17,73	19,6	24,2	20	19,7	24,2	20	25	24	20,4	24	24	24,3	24,3	24	24	20,3	24,2	21,573	23,3556	Serping1	1,78	22,5	1,702	0,108	0,3014	-6
>sp|Q8BND5|QSOX1_	19,86	20,4	19,8	19,8	20,1	21,9	20	21	17	16,8	17	20	19,7	19,1	20	20	19,6	19,1	20,007	19,0123	Qsox1	-1	19,5	-1,7	0,108	0,3014	-6
>sp|P84096|RHOG_M	16,01	17,9	21,6	21,4	19,2	19	19	18	19	18,5	18	16	18,8	18,8	19	15	14,3	19,2	19,039	17,6132	Rhog	-1,4	18,3	-1,7	0,108	0,303	-6
>sp|Q9D819|IPYR_MO	24,82	24,2	28,4	24,4	28,4	24,2	25	25	28	25,5	26	24	23,7	24,1	24	24	24,3	24	25,779	24,581	Ppa1	-1,2	25,2	-1,7	0,109	0,3034	-6
>sp|Q14AT2|TEX11_M	15,73	15,5	15,4	15,3	16,1	14,3	15	13	16	13,9	14	14	15,7	14,4	16	14	14,7	14,1	15,166	14,506	Tex11	-0,7	14,8	-1,7	0,109	0,3034	-6
>sp|Q9CQJ6|COTL1_M	24,96	23	23,3	23	23,5	23,6	24	23	23	23,1	23	23	23,4	22,9	23	23	22,9	23	23,427	23,0482	Cotl1	-0,4	23,2	-1,7	0,109	0,3034	-6
>sp|P97372|PSME2_	21,28	21,4	21,2	21,3	21,7	21,8	21	22	22	20,7	20	21	21,1	21	21	21	21,7	22,3	21,459	21,1054	Psme2	-0,4	21,3	-1,7	0,109	0,3034	-6
>sp|O35678|MGLL_M	20,52	20,8	18,1	19	18,8	18,7	18	19	19	18,9	18	18	19,4	18,7	17	19	18,7	18,4	19,133	18,5243	Mgll	-0,6	18,8	-1,69	0,109	0,3044	-6
>sp|O35660|GSTM6_	22,79	23,1	23,3	22,7	23	23,3	23	21	23	22,9	24	23	21,6	23,9	24	24	23,7	23,4	22,825	23,3708	Gstm6	0,55	23,1	1,692	0,11	0,3046	-6
>sp|O08992|SDCB1_	17,81	16,5	18,2	17,6	17,8	17,5	17	18	18	17,3	18	18	16,6	16,8	18	17	16,8	17,7	17,577	17,2196	Sdcbp	-0,4	17,4	-1,69	0,11	0,3046	-6
>sp|Q61414|K1C15_	22,52	22,3	21,6	21,6	20,8	19,7	21	21	22	20	22	22	22,6	21,8	21	23	23,4	23,9	21,341	22,2072	Krt15	0,87	21,8	1,691	0,11	0,3046	-6
>sp|Q8VCS0|PGRP2_	20,54	20,6	20,4	18,6	20,6	20,5	21	21	20	20,4	17	20	20,1	19,7	20	20	19,6	20	20,349	19,5919	Pglyrp2	-0,8	20	-1,69	0,11	0,3047	-6
>sp|Q5SSZ5|TENS3_M(	15,61	16,7	17,1	15,7	17,4	17,2	17	17	17	16,3	16	16	16,5	16,6	17	16	16,6	15,4	16,735	16,317	Tns3	-0,4	16,5	-1,69	0,11	0,3049	-6
>sp|P97760|RPB3_M	18,84	18,8	16,4	18,6	18,4	18,8	19	19	19	19,3	18	17	19,6	19,6	20	20	19,7	19,9	18,481	19,2193	Polr2c	0,74	18,9	1,685	0,111	0,3073	-6
>sp|Q9QXF8|GNMT_M	0	15,5	15,5	16,9	17,2	15,1	15	17	17	17,5	18	18	18,1	17,7	17	17	18,4	15,5	14,335	17,3956	Gnmt	3,06	15,9	1,684	0,111	0,3075	-6
>sp|Q3UZZ6|ST1D1_M	18,13	17,7	18,1	17,7	17,7	17,8	18	18	17	18,4	17	18	18	17,5	18	19	19	17,6	17,801	18,1307	Sult1d1	0,33	18	1,681	0,112	0,3089	-6
>sp|Q9CR21|ACPM_M	19,31	20,4	18,9	20,8	21,2	17,5	18	19	19	17,4	17	19	18,9	19	19	18	18,5	18,7	19,356	18,5439	Ndufab1	-0,8	18,9	-1,68	0,112	0,3094	-6
>sp|O35350|CAN1_M	19,94	21,5	21,7	21	20,7	21,9	22	22	22	21,5	22	21	20,7	20,9	21	20	20,9	20,9	21,348	20,928	Capn1	-0,4	21,1	-1,68	0,113	0,3103	-6
>sp|P09470|ACE_MO	18,83	19,2	21	19,1	20,3	20,2	19	20	20	19,7	20	20	19,1	19,5	19	19	19,3	19,2	19,779	19,3547	Ace	-0,4	19,6	-1,68	0,113	0,3106	-6
>sp|P42227|STAT3_M	18,62	18,5	19,7	18	18,6	18,5	18	18	18	17,4	19	19	18,3	17,4	19	18	18,5	17,2	18,501	18,0627	Stat3	-0,4	18,3	-1,67	0,113	0,3111	-6
>sp|Q08879|FBLN1_M	21,41	21,6	20,8	21,2	21,8	21,4	21	21	21	20,6	21	21	19,2	20	21	22	22,1	21,6	21,336	20,8193	Fbln1	-0,5	21,1	-1,67	0,113	0,3111	-6
>sp|Q9DC51|GNAI3_M	18,11	18,2	16,6	18,9	19,4	19,2	19	18	19	18,3	17	19	19,3	21,6	19	20	19,8	19,5	18,478	19,2734	Gnai3	0,8	18,9	1,674	0,113	0,3111	-6
>sp|P20152|VIME_M	21,15	21,1	21,3	21	21,1	21,2	20	21	20	21,9	21	22	20,8	21,4	20	21	21,2	21,6	20,888	21,2926	Vim	0,41	21,1	1,665	0,115	0,3154	-6
>sp|Q99JW4|LIMS1_M	20,55	21	21	21,1	20,9	20,7	21	21	21	20,2	20	20	20,9	20,4	21	21	20,7	20,6	20,883	20,651	Lims1	-0,2	20,8	-1,66	0,116	0,3173	-6
>sp|Q07456|AMBP_I	14,2	14	14	13,7	14,9	13,6	14	14	14	13,8	13	16	15,1	13,9	15	14	14	14,8	14,023	14,5034	Ambp	0,48	14,3	1,656	0,117	0,3198	-6
>sp|Q9JHS3|LTOR2_M	19,91	19,7	19,7	19,8	19,6	20	20	20	19	20	21	20	19,4	19,4	21	20	20,4	20,1	19,747	20,0703	Lamtor2	0,32	19,9	1,656	0,117	0,3198	-6
>sp|Q61391|NEP_MO	18,91	18,5	18,7	18,3	19,1	18,5	19	19	19	19	19	19	18,7	18,9	19	19	19,4	18,8	18,726	18,9187	Mme	0,19	18,8	1,655	0,117	0,3199	-6
>sp|P60122|RUVB1_	0	0	17,4	16,3	16,5	16,1	16	16	17	17,9	19	16	16,3	16,5	16	16	16,5	17,4	12,847	16,8535	Ruvbl1	4,01	14,9	1,653	0,117	0,3208	-6
>sp|Q8BH61|F13A_M	17,64	19,3	21,2	19,7	21,2	21,4	20	21	21	19,8	22	22	20,8	22,3	21	22	21,7	18,9	20,137	21,0368	F13a1	0,9	20,6	1,653	0,117	0,3209	-6
>sp|Q9Z1N5|DX39B_	21,52	20,7	20,9	20,5	21	20,6	21	20	20	21,2	23	20	20,6	21	21	21	21,3	21,5	20,723	21,2155	Ddx39b	0,49	21	1,65	0,118	0,3221	-6
>sp|O89020|AFAM_M	18,1	18,7	19	14,2	18,1	18,1	19	0	0	18,3	18	18	18,5	18	19	18	17,7	17,8	13,861	18,2049	Afm	4,34	16	1,649	0,118	0,3224	-6
>sp|P01027|CO3_MO	24,38	24,5	24,3	24,6	23,5	23,9	24	25	24	24,1	24	24	24,5	23	24	24	24,1	23,3	24,187	23,8471	C3	-0,3	24	-1,65	0,118	0,3224	-6
>sp|Q9JMH6|TRXR1_	19,71	19,5	19,8	19,9	19,9	19,8	20	20	20	19,9	19	19	19,9	19,5	20	20	19,2	19,8	19,775	19,5529	Txnrd1	-0,2	19,7	-1,65	0,118	0,3224	-6
>sp|Q6NVF9|CPSF6_M	0	15,4	14,3	15,7	16,1	15,9	16	15	17	16,4	16	17	17,1	16,9	18	17	16,5	16,5	13,967	16,8445	Cpsf6	2,88	15,4	1,648	0,118	0,3224	-6
>sp|Q60710|SAMH1_	21,4	21,2	21,1	20,6	21,8	21,5	22	22	22	21,3	22	21	20,2	23,2	23	22	23,5	23,3	21,465	22,1593	Samhd1	0,69	21,8	1,646	0,119	0,3228	-6
>sp|Q6P8K8|CBPA4_	18,26	17	15,7	16,8	16	18,5	19	15	16	16,6	17	18	15,7	15,9	15	15	15,7	15,6	16,868	16,0449	Cpa4	-0,8	16,5	-1,64	0,119	0,3236	-6
>sp|Q9QUH0|GLRX1_	21,69	21,8	22,2	21,8	22,1	21,8	22	21	20	21,4	21	21	21,7	20,4	22	20	21	21,9	21,662	21,1745	Glrx	-0,5	21,4	-1,64	0,119	0,3236	-6
>sp|Q9QY76|VAPB_M	17,95	18,3	18,9	18,4	18,1	18,4	18	19	19	17,4	18	19	13,9	18,1	18	18	18	17,4	18,416	17,6105	Vapb	-0,8	18	-1,64	0,12	0,3243	-6
>sp|Q922X9|ANM7_M	15,81	16,8	0	15,4	15,6	13,3	0	0	0	16	0	14	16,6	14,5	16	16	16,2	14,5	8.55122	13,8015	Prmt7	5,25	11,2	1,642	0,12	0,3244	-6
>sp|Q06806|TIE1_MO	15,58	15,9	16,5	15,7	15,6	15,5	15	15	13	15,1	0	13	15	11,4	15	15	15,1	14,8	15,382	12,677	Tie1	-2,7	14	-1,64	0,12	0,3244	-6
>sp|P70336|ROCK2_	15,88	17	17,2	16,8	15,9	15,7	16	16	16	16	16	16	15,9	16,3	16	16	16,6	15,7	16,321	15,9574	Rock2	-0,4	16,1	-1,64	0,12	0,3254	-6
>sp|B1AR13|CISD3_M	20,57	21	21,4	21,3	20,9	21,4	21	20	20	20	21	21	20,7	21	21	21	19,8	20,4	20,894	20,5596	Cisd3	-0,3	20,7	-1,64	0,12	0,3255	-6
>sp|Q9EQU5|SET_MOU	24,02	23,6	18	17,6	17,7	19,6	17	18	20	18,1	19	18	18,3	18,3	18	18	18,4	17,6	19,534	18,1488	Set	-1,4	18,8	-1,63	0,121	0,3274	-6
>sp|Q99LL5|PWP1_M	19,57	18,7	19,3	19	18,4	18,7	18	18	19	18,6	20	19	20,1	20,2	20	18	18,8	18,6	18,765	19,2393	Pwp1	0,47	19	1,634	0,121	0,3274	-6
>sp|P67871|CSK2B_	18,22	18	18,6	18,8	17,1	18,1	18	19	18	18,6	19	21	18	18,5	18	18	18,4	18,9	18,184	18,8001	Csnk2b	0,62	18,5	1,634	0,121	0,3274	-6

>sp|Q9DCJ5|NDUA8_	19,22	19,2	16,6	16	17,9	17,9	17	17	16	16,1	19	17	16,1	16,2	16	17	16,4	16,2	17,466	16,5958	Ndufa8	-0,9	17	-1,63	0,122	0,3284	-6
>sp|Q8K023|AKC1H_	20,69	20,2	20,5	21,4	21,2	20,8	21	21	21	21,1	21	21	20,7	21	22	22	20,9	21,4	20,856	21,1809	Akr1c18	0,33	21	1,631	0,122	0,3284	-6
>sp|Q9QXY6|EHD3_M	18,94	19,3	20,4	19,2	19,6	18,5	20	20	20	18	19	21	18,2	20,3	19	19	18,3	18,5	19,643	18,967	Ehd3	-0,7	19,3	-1,63	0,122	0,3289	-6
>sp|Q91VM3|WIPI4_I	16,85	16,6	16,8	17,8	16,9	16,9	16	16	16	16,1	16	17	16,1	16,2	17	16	16,9	15,9	16,723	16,3858	Wdr45	-0,3	16,6	-1,62	0,124	0,3317	-6
>sp|P26928|HGFL_M	18,53	20,2	21,6	21,3	20,3	20	21	20	20	21,5	20	22	20,4	20,5	22	21	20,7	20,4	20,324	20,8885	Mst1	0,56	20,6	1,624	0,124	0,3317	-6
>sp|Q9ERF3|WDR61_	19,63	20,6	19,9	18,5	19,9	19,5	20	20	20	20,2	21	19	20,6	20,1	20	20	19,3	20,2	19,785	20,1994	Wdr61	0,41	20	1,62	0,124	0,3333	-6
>sp|A0AUP1|CC112_	17,08	17,1	15,2	17	18,7	18,8	18	14	18	15,4	15	16	17	16,2	16	17	17,2	16,9	17,129	16,2217	Ccdc112	-0,9	16,7	-1,62	0,124	0,3333	-6
>sp|Q9WTL7|LYPA2_M	22,62	22,7	23,2	22,8	23,8	23,3	23	23	24	23,7	24	23	22,3	22,4	22	22	22,1	23,3	23,181	22,7849	Lypla2	-0,4	23	-1,62	0,125	0,3337	-6
>sp|Q8BVA4|LMOD1_	20,82	21,2	20,9	21	21	20,8	20	21	21	21,3	22	22	21	21,5	21	20	20,8	21	20,866	21,257	Lmod1	0,39	21,1	1,618	0,125	0,3337	-6
>sp|P59325|IF5_MOI	18,79	17,7	20,9	18	18,1	19,9	20	21	19	20,1	18	19	20,5	20,4	20	20	20,2	20,5	19,25	19,9786	Eif5	0,73	19,6	1,618	0,125	0,3337	-6
>sp|Q8QZS1|HIBCH_M	19,73	19,9	19,9	20,4	20,3	20	20	20	20	20,3	20	20	20,3	19,7	21	21	20,3	20,4	20,023	20,2373	Hibch	0,21	20,1	1,615	0,125	0,3351	-6
>sp|Q6IFX2|K1C42_M	21,7	21,4	21,1	20,9	20,8	20,5	21	21	22	20,4	22	22	21	21,9	21	23	22,1	23,2	21,18	21,7635	Krt42	0,58	21,5	1,614	0,126	0,3351	-6
>sp|Q9EQK5|MVP_M(	22,26	22,6	22	22,2	22,7	22,9	22	23	22	22,5	22	23	22,8	22,7	23	22	22,6	22,4	22,385	22,5664	Mvp	0,18	22,5	1,614	0,126	0,3351	-6
>sp|P70297|STAM1_	15,63	14,6	15,2	14,3	15,6	14,8	15	15	14	13,7	15	15	14	14,2	14	16	14,6	13,9	14,967	14,4822	Stam	-0,5	14,7	-1,61	0,126	0,3351	-6
>sp|P53657|KPYR_M	24,13	23,4	23,1	24,2	24,1	24	24	23	24	24	24	24	24,4	24,5	24	24	23,9	23,7	23,742	24,0556	Pklr	0,31	23,9	1,613	0,126	0,3351	-6
>sp|Q91WP6|SPA3N_	20,04	20,2	19,1	19,5	18,9	19,4	19	19	19	20	20	20	19,9	19,7	19	20	19,6	19,5	19,346	19,6625	Serpina3n	0,32	19,5	1,61	0,127	0,3365	-6
>sp|Q8BG02|2ABG_M	19,66	19,4	20,1	21,7	21,9	22,4	18	15	16	20,7	20	20	21,1	21,4	21	21	20,8	20,8	19,406	20,7666	Ppp2r2c	1,36	20,1	1,61	0,127	0,3365	-6
>sp|P21981|TGM2_M	21,95	21,8	20,6	21,9	22,1	22	21	22	21	20,3	20	22	21,7	21,7	20	20	21,7	20,7	21,5	20,9771	Tgm2	-0,5	21,2	-1,61	0,127	0,3366	-6
>sp|P05132|KAPCA_	24,02	24,4	23,2	21,9	21,2	22,5	23	23	24	22,3	20	23	22,7	24,3	22	21	21,9	20,6	22,928	22,0277	Prkaca	-0,9	22,5	-1,61	0,127	0,3366	-6
>sp|B2RSH2|GNAI1_M	18,11	18,2	17,1	18,9	19,5	19,3	19	18	19	18,3	17	19	19,3	21,6	19	20	19,8	19,5	18,538	19,2734	Gnai1	0,73	18,9	1,608	0,127	0,3369	-6
>sp|P00687|AMY1_M	22,77	23,7	24,1	24,6	24,3	24,1	23	24	25	23,7	24	24	23,1	23	23	24	23,5	23,1	23,831	23,3971	Amy1	-0,4	23,6	-1,61	0,128	0,3377	-6
>sp|Q8BGC4|PTGR3_	15,03	15,4	14,4	14,7	14,7	15,6	14	14	15	14,8	16	16	14,7	14,8	15	16	15	14,6	14,721	15,1629	Zadh2	0,44	14,9	1,605	0,128	0,3377	-6
>sp|Q9CYT6|CAP2_M	22,56	22,3	22,2	21,8	21,7	22	20	22	22	22,8	22	22	22,6	22,7	23	22	21,9	21,6	21,885	22,2852	Cap2	0,4	22,1	1,604	0,128	0,3377	-6
>sp|P01787|HVM18	18,59	18,6	0	18,8	18,2	17,7	19	18	17	19,3	19	19	19,7	19,7	20	20	19,3	19,3	16,235	19,4674	>sp|P017	3,23	17,9	1,603	0,128	0,3377	-6
>sp|P01788|HVM19	18,59	18,6	0	18,8	18,2	17,7	19	18	17	19,3	19	19	19,7	19,7	20	20	19,3	19,3	16,235	19,4674	>sp|P017	3,23	17,9	1,603	0,128	0,3377	-6
>sp|P01790|HVM21	18,59	18,6	0	18,8	18,2	17,7	19	18	17	19,3	19	19	19,7	19,7	20	20	19,3	19,3	16,235	19,4674	>sp|P017	3,23	17,9	1,603	0,128	0,3377	-6
>sp|P01791|HVM22	18,59	18,6	0	18,8	18,2	17,7	19	18	17	19,3	19	19	19,7	19,7	20	20	19,3	19,3	16,235	19,4674	>sp|P017	3,23	17,9	1,603	0,128	0,3377	-6
>sp|P01794|HVM25	18,59	18,6	0	18,8	18,2	17,7	19	18	17	19,3	19	19	19,7	19,7	20	20	19,3	19,3	16,235	19,4674	>sp|P017	3,23	17,9	1,603	0,128	0,3377	-6
>sp|P01642|KV5A9_	21,16	21,7	18,8	18,2	18,6	18,8	19	18	19	15,9	17	16	17,7	17,3	18	17	23,8	17,1	19,193	17,7737	Gm10881	-1,4	18,5	-1,6	0,128	0,3378	-6
>sp|P08752|GNAI2_I	18,02	18,2	17	18,8	19,4	19,2	19	18	19	18,2	17	19	19,2	21,5	19	19	19,7	19,4	18,451	19,1823	Gnai2	0,73	18,8	1,598	0,129	0,3399	-6
>sp|O70325|GPX41_	23,09	20,8	21	21,4	20,9	22,8	22	21	23	20,6	21	23	21,4	21,2	21	21	20,4	20,9	21,749	21,1435	Gpx4	-0,6	21,4	-1,59	0,13	0,3415	-6
>sp|Q8BWP8|B4GA1	18,29	20,2	19,9	19,4	19,1	19,6	19	19	19	20,6	19	21	18,1	21,1	21	21	19,6	19,2	19,375	20,035	B4gat1	0,66	19,7	1,594	0,13	0,3416	-6
>sp|P32020|NLTP_M	16,6	16,7	18,3	20,7	20,6	21,2	21	18	0	20,7	21	21	21,1	21,5	21	19	19,5	19,3	17,05	20,5608	Scp2	3,51	18,8	1,589	0,131	0,3441	-6
>sp|P52432|RPAC1_	0	0	14,5	14,4	15	14	15	15	15	14,4	15	15	15	14,8	15	15	14,4	15	11,371	14,7519	Polr1c	3,38	13,1	1,589	0,131	0,3441	-6
>sp|Q8BWN8|ACOT4_	19,82	20,8	20,6	21,1	20,9	20,7	21	21	21	21,3	21	21	21	21,4	21	21	20,3	20,8	20,725	21,0058	Acot4	0,28	20,9	1,588	0,131	0,3442	-6
>sp|P54310|LIPS_MC	16,56	16,8	15	16,2	16,3	15,8	16	16	15	17,1	17	17	16	15,5	16	16	17	16,4	16,008	16,4231	Lipe	0,42	16,2	1,587	0,132	0,3444	-6
>sp|Q8BYC6|TAOK3_I	16,74	16,8	0	16,1	16,1	16,4	16	16	0	11,4	16	15	18,2	17,7	18	18	17,7	17,7	12,68	16,6101	Taok3	3,93	14,6	1,584	0,132	0,346	-6
>sp|Q6ZWR4|2ABB_M	19,47	19,3	20,1	21,7	21,9	22,4	18	15	15	20,6	20	20	21	21,4	21	21	20,6	20,7	19,18	20,6777	Ppp2r2b	1,5	19,9	1,584	0,132	0,346	-6
>sp|Q9QWR8|NAGAB	18,66	20,4	20,8	21,4	21,3	18,7	21	18	20	20,9	20	21	20,5	20,6	21	21	20,7	20,8	20,038	20,6725	Naga	0,63	20,4	1,583	0,133	0,3461	-6
>sp|Q64727|VINC_M	23,28	23,2	21,8	23,3	23,8	23,8	23	23	23	22	22	22	23,7	22,2	24	23	23,1	22,1	23,134	22,6336	Vcl	-0,5	22,9	-1,58	0,134	0,3495	-6
>sp|Q91VC3|IF4A3_M	21,92	21,9	21,4	21,3	22,4	21,9	22	22	22	21,9	21	22	22,6	22,3	22	22	22,4	22,6	21,813	22,1021	Eif4a3	0,29	22	1,575	0,134	0,3502	-6
>sp|Q8BHN3|GANAB_	21,29	20,9	21,7	20,9	21,2	21,2	21	21	23	21,4	23	23	21,4	21,8	22	21	21,4	21,5	21,338	21,77	Ganab	0,43	21,6	1,573	0,135	0,3506	-6
>sp|Q99JT9|MTND	0	15,3	14,8	0	0	13,9	0	0	15	15,3	16	16	0	16,2	0	15	15,4	14,5	6.61326	12,0072	Adi1	5,39	9,31	1,573	0,135	0,3506	-6
>sp|P03987|IGHG3_I	17,51	17,4	17,2	17,7	16,7	18	18	18	17	19	16	17	15,7	16	16	17	17,3	17,2	17,439	16,8108	>sp|P039	-0,6	17,1	-1,57	0,135	0,3506	-6
>sp|P12367|KAP2_M	21,82	19,7	19,5	21,3	21,7	21,3	22	20	22	20,5	19	19	21,3	18,9	21	21	20,7	20,8	20,982	20,2667	Prkar2a	-0,7	20,6	-1,57	0,135	0,3506	-6
>sp|P47934|CACP_M	18,1	18,1	19,3	20,8	17,7	18,1	18	19	17	19,2	19	19	19,2	18,5	18	20	18,2	18,6	18,359	19,0329	Crat	0,67	18,7	1,569	0,136	0,3527	-6
>sp|P17897|LYZ1_M(	21,01	23,1	23,3	22,7	22,8	21	23	21	23	23	23	23	23,5	23,4	24	22	22,8	22,8	22,451	23,0625	Lyz1	0,61	22,8	1,568	0,136	0,3529	-6
>sp|Q9D0I9|SYRC_MC	21,27	20,9	21,4	21,8	21,4	21,7	22	21	21	21,8	21	21	21,5	21,7	22	22	21,8	21,5	21,416	21,5915	Rars	0,18	21,5	1,564	0,137	0,3549	-6

>sp|P07607|TYSY_MC	17,15	16,8	16	15,7	16,6	17,4	16	16	18	17,6	19	17	16,8	16,3	15	17	19	18,8	16,692	17,4515	Tyms	0,76	17,1	1,563	0,137	0,3552	-6
>sp|Q99JY3|GIMA4_M	18,4	19,9	19	18,5	21,5	21,5	22	18	19	18	19	18	22,3	22,5	22	22	21,9	22,3	19,7	20,9366	Gimap4	1,24	20,3	1,563	0,137	0,3552	-6
>sp|P28650|PURA1_	0	0	16,2	16,1	16,3	16,5	16	16	16	15,3	16	17	16,7	17	17	15	15,8	16,1	12,512	16,1773	Adssl1	3,67	14,3	1,562	0,137	0,3552	-6
>sp|Q8C878|UBA3_M	19,56	19,1	19	21,5	21,4	21,3	22	20	19	18,7	19	21	19,4	19	21	19	18,8	19,1	20,186	19,4363	Uba3	-0,7	19,8	-1,56	0,137	0,3552	-6
>sp|Q6ZQ38|CAND1_	22,82	23,6	23,3	23,5	23,5	23,7	24	23	24	22,7	22	24	22,4	22,5	22	24	23,8	23,7	23,379	23,0054	Cand1	-0,4	23,2	-1,56	0,138	0,3565	-6
>sp|P47199|QOR_MO	19,1	20	20,5	18,6	20,2	18,4	18	18	18	19,3	19	21	18,4	17,6	18	17	18,3	17,8	19,138	18,4534	Cryz	-0,7	18,8	-1,56	0,139	0,3574	-6
>sp|P62702|RS4X_M	20,82	22	19,6	22,3	22,1	21,8	19	19	19	25,2	18	20	19,3	25,1	25	25	19,1	24,9	20,664	22,4487	Rps4x	1,78	21,6	1,556	0,139	0,358	-6
>sp|Q60737|CSK21_	16,37	16,2	21	16,8	15,5	19,6	16	16	15	17,8	24	23	16,6	16,8	18	16	19,2	17,1	16,985	18,7366	Csnk2a1	1,75	17,9	1,553	0,139	0,3592	-6
>sp|Q9QUR8|SEM7A_	15,32	15,6	16,9	16,9	16,4	14	15	15	13	17,3	17	15	17,7	17,8	18	14	17,9	13,8	15,388	16,5079	Sema7a	1,12	15,9	1,553	0,14	0,3592	-6
>sp|Q9D404|OXSM_M	17,1	17,2	17,7	15,6	17,6	17,1	17	17	17	17,1	17	18	16,1	17,9	16	16	15,6	16,2	17,067	16,5234	Oxsm	-0,5	16,8	-1,55	0,141	0,3624	-6
>sp|P62254|UB2G1_	16,88	17,2	16,2	16,6	15,6	17,6	17	18	17	17,6	14	16	15,8	16	16	16	17,1	17,4	16,96	16,2675	Ube2g1	-0,7	16,6	-1,55	0,141	0,3627	-6
>sp|P14152|MDHC_I	26,53	25,2	25,7	24,9	25,4	24,6	26	26	25	25,4	25	25	25,6	24,8	25	25	25,3	25,4	25,542	25,1973	Mdh1	-0,3	25,4	-1,54	0,142	0,3636	-6
>sp|Q8R0I0|ACE2_MO	18,63	15,7	14,5	18,2	17	14,7	15	16	15	17	18	17	16,7	17,1	17	17	15,9	16,4	16,109	16,9373	Ace2	0,83	16,5	1,544	0,142	0,3636	-6
>sp|Q7TT45|RRAGD_I	15,95	15,5	14,7	15,6	16,6	14,9	0	17	17	16,6	16	16	16,2	17,2	17	17	17,7	16,6	14,108	16,8456	Rragd	2,74	15,5	1,542	0,142	0,3642	-6
>sp|P08249|MDHM_	27,24	26,7	26,4	26,8	26,4	26,3	27	27	27	26,3	26	26	26,2	26,4	26	28	26	26,3	26,637	26,363	Mdh2	-0,3	26,5	-1,54	0,142	0,3647	-6
>sp|O09159|MA2B1_	15,96	16,9	20,7	16,6	17,3	16,7	18	17	16	17,8	21	21	17,7	18	18	18	17,7	16,8	17,288	18,2687	Man2b1	0,98	17,8	1,539	0,143	0,3659	-6
>sp|Q99K70|RRAGC_	16,09	15,6	14,9	15,7	16,7	15	0	17	17	16,7	16	16	16,3	17,3	18	18	17,9	16,7	14,235	16,9884	Rragc	2,75	15,6	1,538	0,143	0,3659	-6
>sp|Q8CGB6|TNS2_M	14,11	15,6	15,1	13,7	16,3	16	16	16	15	13,4	0	15	15,2	15,1	15	14	14	13,1	15,287	12,7871	Tns2	-2,5	14	-1,54	0,143	0,3659	-6
>sp|Q61759|K1B21_	18,96	18,6	20,5	20	19,5	19,3	19	20	20	18,8	19	19	19,1	19,6	18	19	19,2	19,8	19,487	19,069	Klk1b21	-0,4	19,3	-1,54	0,143	0,3659	-6
>sp|Q8BMF4|ODP2_M	21,62	21,4	20	20,4	20,3	21,3	20	21	21	19,9	21	21	20,6	20,8	20	20	20	20,6	20,734	20,4069	Dlat	-0,3	20,6	-1,54	0,143	0,3659	-6
>sp|Q61823|PDCD4_	20,07	20,1	20,2	20,2	21,9	20,2	20	19	21	15,3	21	21	16,2	20,5	21	20	20,3	15,7	20,301	18,9766	Pdcd4	-1,3	19,6	-1,53	0,144	0,3676	-6
>sp|Q9D832|DNJB4_	20,84	18,5	18,6	17,5	17,3	17,9	19	19	18	16,9	19	17	18,4	18,4	18	16	18,8	16,7	18,44	17,6695	Dnajb4	-0,8	18,1	-1,53	0,144	0,3677	-6
>sp|Q9D3U0|PUS10_	16,15	16,3	13,9	16,4	16,1	16	15	15	14	13,4	0	14	15	14,8	15	15	14,5	15,3	15,498	12,973	Pus10	-2,5	14,2	-1,53	0,144	0,3677	-6
>sp|Q920E5|FPPS_MO	20,04	20,9	21,3	20,9	21	20,8	21	21	21	20,5	20	20	20,8	20,9	21	21	20,4	20,3	20,768	20,4898	Fdps	-0,3	20,6	-1,53	0,145	0,3681	-6
>sp|P15535|B4GT1_	18,88	23,9	24,5	24,2	24,3	24,4	24	24	24	23,3	23	23	17,5	23,5	23	23	17,5	23,2	23,59	22,0197	B4galt1	-1,6	22,8	-1,53	0,146	0,37	-6
>sp|Q9D2R0|AACS_M	18,52	18	17	16,9	17,3	17,3	19	18	18	17,7	17	17	17	17,4	17	18	16,9	17,7	17,734	17,385	Aacs	-0,3	17,6	-1,53	0,146	0,37	-6
>sp|Q9R062|GLYG_M	18,75	18,1	18,6	19,3	19,4	19,2	18	20	19	18,7	19	19	19,8	19,8	19	19	19,1	19,4	18,902	19,2445	Gyg1	0,34	19,1	1,526	0,146	0,3706	-6
>sp|O70133|DHX9_M	24,04	24	23,4	23,5	24	23,8	24	23	21	22,5	23	23	23,4	22,3	23	23	22,7	22,5	23,39	22,8486	Dhx9	-0,5	23,1	-1,53	0,146	0,3706	-6
>sp|Q6P3D0|NUD16_	14,63	14,9	13,5	0	13,8	15,1	14	16	16	16,5	14	17	14,6	14,7	16	17	15,3	15,5	13,077	15,6133	Nudt16	2,54	14,3	1,523	0,147	0,3719	-6
>sp|P80316|TCPE_M	20,21	19,9	21,1	19,6	20	20,1	20	20	20	21,2	20	21	21	20,1	21	20	19,9	19,9	20,069	20,4461	Cct5	0,38	20,3	1,522	0,147	0,3723	-6
>sp|Q923B0|GGACT_	21,05	19	19,2	18,6	19,7	19	21	19	18	18,4	19	19	19,3	19,5	19	19	19	18,8	19,448	18,9807	Ggact	-0,5	19,2	-1,52	0,147	0,3723	-6
>sp|Q6NTA4|RRAGB_	19,42	19,7	16,2	18,8	18,7	16,5	18	15	15	14,7	16	15	15,8	16,6	16	19	18,4	15,4	17,429	16,2515	Rragb	-1,2	16,8	-1,52	0,147	0,3726	-6
>sp|P26638|SYSC_MO	20,75	21,1	20,9	20,6	20,7	20,5	21	21	21	21,1	22	22	21,4	20,8	21	21	20,4	20,9	20,832	21,0882	Sars	0,26	21	1,519	0,148	0,3734	-6
>sp|Q8BGY2|IF5A2_M	22,1	22,1	21,1	21,7	21,7	21,4	21	22	22	21	21	21	21,5	21,7	22	21	21,3	21,3	21,64	21,3602	Eif5a2	-0,3	21,5	-1,51	0,149	0,3757	-6
>sp|Q9JLV6|PNKP_M	0	0	15,6	14,8	14,7	14,5	15	14	15	14,1	14	15	15,1	14,9	16	14	14,4	14,9	11,432	14,6906	Pnkp	3,26	13,1	1,514	0,149	0,376	-6
>sp|Q9JIW9|RALB_MO	17,38	16,5	17,8	16,3	15,9	17,6	17	16	16	16,6	16	20	17,9	17,5	18	16	17,5	16,1	16,627	17,3591	Ralb	0,73	17	1,513	0,149	0,3762	-6
>sp|Q8BX09|RBBP5_	21,11	21,5	19,8	21,8	20,7	21,4	21	21	20	21,5	19	20	18,5	17,9	21	21	21,2	20,5	20,939	20,1953	Rbbp5	-0,7	20,6	-1,51	0,149	0,3762	-6
>sp|Q5F2E8|TAOK1_M	16,61	16,6	0	16	16	16,3	16	16	0	10,2	16	15	18,1	17,6	18	18	17,6	17,6	12,595	16,3705	Taok1	3,78	14,5	1,511	0,15	0,3769	-6
>sp|Q9WUL7|ARL3_M	18,71	18,2	18,3	18	17,5	18,6	18	19	19	18,6	17	19	17,4	17,5	17	18	17,6	18,8	18,386	17,9833	Arl3	-0,4	18,2	-1,51	0,15	0,3777	-6
>sp|Q64105|SPRE_M	23,33	22,6	23	22,9	23,8	24,8	23	24	24	24,1	24	24	23,9	23,9	23	24	23,7	24	23,524	23,9035	Spr	0,38	23,7	1,504	0,152	0,381	-6
>sp|Q9D0E1|HNRPM_	17,02	16,8	18,7	17,1	16,8	16,7	18	17	17	17,2	17	15	17	17,5	15	17	17,2	17	17,27	16,7282	Hnrnpm	-0,5	17	-1,5	0,152	0,3814	-6
>sp|P21300|ALD1_M	22,07	21,8	22,8	22	22,2	22	22	22	22	22,9	21	23	21,9	23,3	22	23	21,8	23,1	22,111	22,4842	Akr1b7	0,37	22,3	1,497	0,153	0,3847	-6
>sp|P14576|SRP54_	16,18	17,5	18,4	16,5	16,2	18	16	17	18	18	18	18	18,1	17,8	18	18	18,1	15,2	17,036	17,6737	Srp54	0,64	17,4	1,497	0,154	0,3847	-6
>sp|Q9CQL1|MGN2_M	20,6	20,1	19,9	19,5	21,2	20,1	20	20	20	20,9	23	20	21,3	21,3	21	21	20,6	17,4	20,055	20,8266	Magohb	0,77	20,4	1,496	0,154	0,3851	-6
>sp|O88712|CTBP1_	19,38	19,6	19	19,3	19,9	19,7	19	20	19	19,7	21	20	19,6	20	20	19	20	18,7	19,413	19,7316	Ctbp1	0,32	19,6	1,491	0,155	0,3876	-6
>sp|P49935|CATH_M	0	14,2	14,8	15,4	0	17,3	15	17	17	18	18	16	15,6	15,2	14	16	14,4	15,7	12,368	15,9244	Ctsh	3,56	14,1	1,49	0,155	0,3885	-6
>sp|Q9CQE6|ASF1A_M	17,09	16,6	19,5	15,8	16,9	0	0	15	17	17,4	17	17	15,6	17,6	17	17	16,8	16,7	13,148	16,8504	Asf1a	3,7	15	1,485	0,157	0,3913	-6
>sp|Q3UGR5|HDHD2_	18,7	16,3	18	17,5	18,3	18,4	18	18	18	19,6	20	19	16,6	16,7	17	20	19,4	20	17,796	18,6228	Hdhd2	0,83	18,2	1,48	0,158	0,3944	-6

>sp|P19253|RL13A_	17,31	18,2	18,2	18,4	17,8	18,3	19	18	18	19,9	18	21	18,5	18,2	19	18	17,7	18,5	18,187	18,733	Rpl13a	0,55	18,5	1,477	0,159	0,3956	-6
>sp|Q9WVL0|MAAI_M	21,3	21,5	21,1	21,2	20,9	21,1	20	21	20	20,9	21	21	21,3	21,4	21	21	21,3	21,1	20,945	21,1666	Gstz1	0,22	21,1	1,475	0,159	0,3966	-6
>sp|P51432|PLCB3_	21,13	21,6	21,1	21	21,3	20,9	21	21	21	20,9	21	21	21,1	21,1	21	21	21,1	21	21,166	21,0459	Plcb3	-0,1	21,1	-1,47	0,16	0,3979	-6
>sp|Q91V12|BACH_M	21,2	21	20,8	21	21,1	21	21	22	22	21,5	22	22	21,6	21,2	22	21	20,8	21,3	21,239	21,4718	Acot7	0,23	21,4	1,471	0,16	0,3988	-6
>sp|Q8BP48|MAP11	18,97	19,2	19	19,3	19,7	19,3	19	20	19	18,9	20	19	19	19,7	19	18	18,8	18,5	19,197	18,9307	Metap1	-0,3	19,1	-1,47	0,161	0,3992	-6
>sp|Q05920|PYC_MC	17,17	17,3	18,3	17,5	17,9	18,5	18	18	18	18	18	18	17,7	17,7	18	16	16,9	16,8	17,774	17,4143	Pc	-0,4	17,6	-1,47	0,161	0,4004	-6
>sp|A2A8Z1|OSBL9_M	17,24	0	16,5	15,2	0	16,4	17	14	0	14,4	15	12	13,1	13,8	17	20	18,8	10,6	10,751	14,9433	Osbpl9	4,19	12,8	1,466	0,162	0,4012	-6
>sp|Q9DD03|RAB13_	21,59	21,4	21,5	22,3	21,7	21,8	22	22	22	18,2	19	23	18,8	22,7	20	22	22,3	22,2	21,832	20,888	Rab13	-0,9	21,4	-1,47	0,162	0,4012	-6
>sp|Q61183|PAPOA_	13,86	13,1	12,9	12,9	12,7	14	14	14	13	14,7	11	14	13,5	9,61	13	15	0	9,61	13,424	11,1758	Papola	-2,2	12,3	-1,46	0,162	0,4016	-6
>sp|Q78ZA7|NP1L4_I	23,8	22,6	20,9	21,5	23,3	21,8	21	23	23	23	21	21	21,2	20,9	22	21	20,5	23	22,239	21,5678	Nap1l4	-0,7	21,9	-1,46	0,162	0,4017	-6
>sp|Q99KN2|CIAO1_I	14,84	15,2	14,8	0	14,3	15,2	15	0	15	14,8	15	15	14,8	14,6	16	15	14,1	13,9	11,582	14,7608	Ciao1	3,18	13,2	1,463	0,162	0,4017	-6
>sp|P57780|ACTN4_	22,1	21,8	21,9	22	22	22,1	22	22	22	21,6	21	22	22	22,3	22	22	21,8	22	22,064	21,8771	Actn4	-0,2	22	-1,46	0,162	0,4017	-6
>sp|Q9WU28|PFD5_M	15,4	19,7	21	18	18,4	18,3	19	20	21	17,2	20	20	15,4	20,6	18	16	15,8	15,7	19,014	17,673	Pfdn5	-1,3	18,3	-1,46	0,163	0,4017	-6
>sp|Q8K2I1|FNTB_MC	18,16	16	15,9	15,5	17,2	16,3	17	16	15	15,9	17	15	16,1	15,8	16	16	15,4	16	16,342	15,8665	Fntb	-0,5	16,1	-1,46	0,163	0,402	-6
>sp|P16675|PPGB_M	20,17	19,7	21,4	21,2	21	21,5	21	21	21	20,5	21	19	20,7	20,8	21	21	20,5	20,5	20,855	20,4436	Ctsa	-0,4	20,6	-1,46	0,163	0,4024	-6
>sp|O35864|CSN5_M	23,73	22,5	19,5	20,1	23,2	23	21	20	23	22,9	20	21	20,4	20,5	21	21	20,1	21,5	21,752	20,8755	Cops5	-0,9	21,3	-1,46	0,163	0,4025	-6
>sp|Q9DBR1|XRN2_M	15,78	16	17,7	15,8	15	17,9	18	17	17	15,4	18	16	18,3	18,7	19	18	18,2	15,7	16,671	17,4723	Xrn2	0,8	17,1	1,458	0,164	0,4033	-6
>sp|A6BLY7|K1C28_I	22,45	21,8	20,6	20,4	20,1	19,9	20	21	21	19,5	21	19	22,7	21,9	21	24	23,5	23,8	20,877	21,7968	Krt28	0,92	21,3	1,457	0,164	0,4037	-6
>sp|Q9CXS4|CENPV_I	21,86	15,1	0	16,8	16,5	16	17	0	0	16	15	16	15,9	15,3	16	16	14,8	15,7	11,468	15,7003	Cenpv	4,23	13,6	1,457	0,164	0,4038	-6
>sp|O09174|AMACR	18,25	18,3	14,2	15,4	0	14,4	17	18	0	17,1	16	17	15,8	15,5	16	17	16	16,3	12,801	16,364	Amacr	3,56	14,6	1,453	0,165	0,4059	-6
>sp|Q8C3K6|SC5A1_	15,09	17,8	16,6	15	15,4	14,3	16	14	16	16,2	16	17	16,7	16,9	17	16	15,8	15	15,546	16,1874	Slc5a1	0,64	15,9	1,452	0,165	0,4064	-6
>sp|Q80XL6|ACD11_	18,37	18,7	17	17,4	17,6	16,6	17	17	17	18,6	18	18	16,5	17,9	18	18	18,2	18,1	17,473	17,8996	Acad11	0,43	17,7	1,446	0,167	0,4098	-6
>sp|Q6PGB6|NAA50_	18,12	18,5	17,3	17,4	17,5	16,6	18	19	19	17	19	18	16,2	17,2	17	17	17,9	18	17,928	17,3801	Naa50	-0,5	17,7	-1,44	0,167	0,4107	-6
>sp|P97333|NRP1_M	14,5	15,7	16,6	14,9	14,8	15,9	17	16	16	15,7	16	15	16,7	16,4	16	16	15,7	16,3	15,65	16,0782	Nrp1	0,43	15,9	1,444	0,168	0,4109	-6
>sp|P07146|TRY2_M	25,9	24,7	25,5	26,8	25,5	25,2	25	26	25	25,6	26	25	25,4	25,4	25	25	25,2	24,9	25,605	25,2992	Prss2	-0,3	25,5	-1,44	0,17	0,4152	-6
>sp|P11276|FINC_MC	21,21	20,8	21,2	21,2	21,1	21,6	21	21	21	20,2	22	22	20,3	21,9	21	20	20,1	20,1	21,147	20,7704	Fn1	-0,4	21	-1,44	0,17	0,4161	-6
>sp|P62196|PRS8_M	18,23	18,2	19,8	17,1	17,4	17,8	18	17	18	19,4	19	18	18,1	18,1	18	18	18,7	17,9	17,936	18,3997	Psmc5	0,46	18,2	1,435	0,17	0,4161	-6
>sp|P08730|K1C13_	21,79	21,7	21,3	21,8	21,1	20,7	21	21	22	20,5	22	22	21,3	22,1	21	23	22,2	23,3	21,4	21,8977	Krt13	0,5	21,6	1,434	0,17	0,4162	-6
>sp|Q91VK1|BZW2_M	19,07	15,7	17,5	18,2	15,2	17,2	18	18	18	15,2	17	15	18,5	15,3	18	18	15	15,6	17,391	16,4862	Bzw2	-0,9	16,9	-1,43	0,17	0,4162	-6
>sp|P28656|NP1L1_	17,9	19,8	19,1	17,4	19,4	18,7	18	18	18	18,1	19	18	17,3	18,4	17	17	19,3	17,3	18,45	17,9265	Nap1l1	-0,5	18,2	-1,43	0,171	0,4162	-6
>sp|Q80YA7|DPP8_M	17,58	16,6	16,4	15,8	16,1	16,6	16	16	16	16,6	17	17	16,1	16,9	16	17	16,7	16,6	16,331	16,6368	Dpp8	0,31	16,5	1,432	0,171	0,4167	-6
>sp|Q9CXW4|RL11_M	21,53	22,2	22,4	23,3	23,2	22,3	22	21	21	22,2	20	22	21,7	22,2	22	21	21,5	21,3	22,08	21,5785	Rpl11	-0,5	21,8	-1,43	0,172	0,418	-6
>sp|Q149F3|ERF3B_M	20,47	20,2	18,3	20	19,9	19,4	20	19	19	18,1	17	17	20,2	19,1	20	19	19,1	20,6	19,634	18,9533	Gspt2	-0,7	19,3	-1,43	0,172	0,418	-6
>sp|P97429|ANXA4_	22,17	22	22,2	20,5	20,9	22,5	20	20	22	21,3	23	20	21	20,3	20	20	21	20	21,447	20,8298	Anxa4	-0,6	21,1	-1,43	0,172	0,418	-6
>sp|Q60972|RBBP4_	22,29	22,2	21,9	22,1	22,2	22,4	22	22	22	22,5	22	23	22,5	22,4	22	23	22	22,2	22,224	22,3639	Rbbp4	0,14	22,3	1,428	0,172	0,418	-6
>sp|Q8K182|CO8A_M	14,35	17,4	15,7	16,4	16,6	16,6	14	16	16	15,9	16	15	15,9	15	15	16	12	15,9	15,936	15,1388	C8a	-0,8	15,5	-1,43	0,172	0,418	-6
>sp|Q9WTX5|SKP1_M	16,56	16,7	15,7	16,5	16,2	18,3	16	17	17	16,5	16	16	0	14,8	15	15	16,3	16,4	16,621	14,09	Skp1	-2,5	15,4	-1,43	0,172	0,418	-6
>sp|P16331|PH4H_M	13,92	13,4	0	13,1	0	12,3	13	13	14	15,8	16	0	15,6	14,4	17	17	14,6	17,1	10,314	14,0496	Pah	3,74	12,2	1,427	0,172	0,418	-6
>sp|O35226|PSMD4_	16,48	17,1	16,6	17,7	16,7	16,2	16	16	16	16,4	0	16	16,8	16,3	16	15	14,7	16,2	16,667	14,1472	Psmd4	-2,5	15,4	-1,43	0,173	0,4189	-6
>sp|Q99MD9|NASP_M	0	0	15,4	14,6	15,3	15,3	15	14	15	14,9	14	15	15,2	15	15	15	14,8	14,2	11,62	14,7218	Nasp	3,1	13,2	1,424	0,173	0,4194	-6
>sp|P70677|CASP3_	19,57	20	21,1	20,6	20,8	21,1	21	21	20	20,5	20	20	20,4	20,2	21	20	20,5	20,5	20,554	20,2404	Casp3	-0,3	20,4	-1,42	0,173	0,4196	-6
>sp|Q9CR25|DPH2_M	14,97	15,5	15	0	15,1	14,3	16	15	15	15,4	16	16	15,9	16	16	16	16,2	15,6	13,466	15,8428	Dph2	2,38	14,7	1,421	0,174	0,4208	-6
>sp|P60335|PCBP1_	21,22	21,4	21,3	21	21,7	21,6	22	22	22	21,4	20	21	21,7	21,6	21	21	21,6	21,4	21,572	21,3024	Pcbp1	-0,3	21,4	-1,42	0,174	0,4208	-6
>sp|P61202|CSN2_M	20,73	19,6	18,4	20	18,6	18,9	20	20	19	19,2	21	20	20,7	21	20	19	19,3	19,5	19,417	19,9217	Cops2	0,51	19,7	1,42	0,174	0,421	-6
>sp|Q9CX56|PSMD8_	20,73	19,2	18,6	20,4	19,2	19,4	21	19	21	18,3	20	19	18,7	19,6	20	20	19,9	18,9	19,728	19,2722	Psmd8	-0,5	19,5	-1,42	0,175	0,421	-6
>sp|Q61024|ASNS_M	21,12	21,2	22,6	22,3	22,4	22,1	22	22	21	22,1	22	22	23	22	22	23	22,6	22,5	21,982	22,3115	Asns	0,33	22,1	1,413	0,177	0,4254	-6
>sp|P05480|SRC_MC	18,01	19,7	18,2	18,3	18	18,5	18	18	17	18,1	18	17	17,5	18,1	18	17	18,2	18,3	18,246	17,8911	Src	-0,4	18,1	-1,41	0,177	0,4254	-6
>sp|Q8R180|ERO1A_	16,39	18,3	18	18,2	20,2	17,2	19	18	18	19,1	18	19	19	19,6	19	18	18,4	18,4	18,11	18,6798	Ero1a	0,57	18,4	1,41	0,177	0,4264	-6

>sp|Q921F2|TADBP_I	16,31	16,4	14,9	16,7	16,6	15,5	16	16	16	14,7	16	16	14,4	15,1	0	16	15,6	15,5	16,091	13,6763	Tardbp	-2,4	14,9	-1,41	0,177	0,4264	-6
>sp|Q8BUV3|GEPH_M	20,63	21,3	19,1	20,7	21,2	18,6	19	19	19	20,9	19	19	19,3	22,1	22	22	21,4	21,5	19,973	20,7411	Gphn	0,77	20,4	1,41	0,177	0,4264	-6
>sp|Q99L27|GMPR2_	19,88	19,8	19,5	18,8	20	19,7	20	19	18	17,6	18	18	19,9	19,2	20	19	18,5	19,2	19,348	18,8207	Gmpr2	-0,5	19,1	-1,41	0,178	0,4273	-6
>sp|P70451|FER_MO	16,72	16,5	14,9	17,3	17,1	16,8	17	16	16	18	15	15	18,9	15,3	19	19	18,6	18,6	16,565	17,4613	Fer	0,9	17	1,404	0,179	0,4292	-6
>sp|P24270|CATA_M	22,01	23,4	23,7	23	23,6	23,8	24	24	24	23,8	24	24	23,4	23,4	24	24	23,8	24,1	23,367	23,652	Cat	0,28	23,5	1,404	0,179	0,4292	-6
>sp|Q3TCJ1|ABRX2_I	19,22	19,5	19,1	19,1	19,8	19,7	20	18	18	19,8	20	19	19,5	19,5	20	19	19,7	18,7	19,207	19,5223	Abraxas2	0,32	19,4	1,401	0,18	0,4314	-6
>sp|Q8VDD8|WASH1_	14,44	17,4	14,1	17,3	17,4	17,6	15	14	19	18,7	19	15	0	14,1	0	14	18,3	15,1	16,27	12,7058	Washc1	-3,6	14,5	-1,4	0,18	0,4322	-6
>sp|P05201|AATC_M	17,68	18,9	18,8	18,3	18,8	18,7	19	19	19	18,9	20	20	18,4	18,9	19	19	18,8	18,3	18,614	18,9079	Got1	0,29	18,8	1,398	0,181	0,4322	-6
>sp|Q9D051|ODPB_M	20,1	20,1	19,8	21	20,5	20,3	21	21	21	21,6	21	21	20,2	20,1	20	21	21,4	20,8	20,475	20,8046	Pdhb	0,33	20,6	1,398	0,181	0,4323	-6
>sp|O70456|1433S_	23,76	25,4	21,2	25,4	22,4	22,9	24	23	23	23,7	24	25	24,3	23,3	25	24	24,5	23,4	23,419	24,0934	Sfn	0,67	23,8	1,398	0,181	0,4323	-6
>sp|Q9QWG7|ST1B1_	19,76	20,4	20,7	21,1	20,9	21,1	21	21	20	20,9	20	21	20,5	18,8	21	20	20,1	19,8	20,595	20,2342	Sult1b1	-0,4	20,4	-1,4	0,181	0,4325	-6
>sp|Q9JLT4|TRXR2_M	18,34	18,1	18,6	18,2	18	18,4	19	18	19	19,3	18	18	18	14,2	18	19	14,5	18,7	18,356	17,5016	Txnrd2	-0,9	17,9	-1,4	0,182	0,4333	-6
>sp|P63276|RS17_M	19,63	19,5	20,2	20	20,2	20,3	20	20	20	20,2	20	20	20,1	20,7	21	20	20,4	19,4	19,939	20,1804	Rps17	0,24	20,1	1,393	0,182	0,4345	-6
>sp|Q80UM3|NAA15	23,96	23,6	23,8	24,1	24	21,3	24	24	21	22,4	22	19	23,4	23,5	24	23	23,2	19,7	23,275	22,3283	Naa15	-0,9	22,8	-1,39	0,183	0,4351	-6
>sp|Q8CI94|PYGB_M(	22,58	22,6	22,5	22,5	22,3	22,6	23	23	23	22,8	23	23	22,4	22,4	22	22	22,3	22,4	22,621	22,4588	Pygb	-0,2	22,5	-1,39	0,183	0,4368	-6
>sp|P46460|NSF_MO	19,21	17,9	18,6	18,2	18,2	18,4	17	18	18	17,9	18	18	18,2	18,4	18	18	17,6	18	18,258	18,0002	Nsf	-0,3	18,1	-1,39	0,184	0,4389	-6
>sp|Q9ET01|PYGL_MC	22,84	22,9	21,5	20,9	20,5	20,7	20	20	21	21	21	21	20,6	20,8	21	20	20,5	21	21,239	20,7668	Pygl	-0,5	21	-1,38	0,186	0,4429	-6
>sp|Q9CX34|SGT1_M	18,55	21,1	18	18,2	17,8	20,8	18	18	17	17,5	18	18	18,2	17,9	19	18	17,8	18,2	18,694	18,0691	Sugt1	-0,6	18,4	-1,38	0,187	0,4452	-6
>sp|P50516|VATA_M	21,46	21,4	21,5	21,6	22,4	21,1	22	21	22	22,1	22	21	21,7	21,4	22	22	22,3	22	21,593	21,8565	Atp6v1a	0,26	21,7	1,374	0,188	0,4459	-6
>sp|P25911|LYN_MO	17,55	16,8	17,2	17	19,3	18	18	18	19	19	18	16	17,6	17,4	16	17	16,9	16,8	17,782	17,1905	Lyn	-0,6	17,5	-1,37	0,188	0,4465	-6
>sp|P62305|RUXE_M	19,73	18,1	17,3	18,3	17,7	18,4	0	18	18	17,4	20	19	16,6	17,1	19	20	21,6	21,5	16,161	19,0356	Snrpe	2,87	17,6	1,373	0,188	0,4465	-6
>sp|P97364|SPS2_M	18,48	18,5	18,8	18,7	19,1	19	19	19	19	18,9	18	18	18,6	18,5	19	19	18,7	19,1	18,861	18,6549	Sephs2	-0,2	18,8	-1,37	0,19	0,4492	-6
>sp|Q9CZY3|UB2V1_I	21,86	24,1	21,6	21,7	24,1	24,8	22	22	22	21,6	22	22	21,1	24,4	21	21	21,5	21,4	22,554	21,7953	Ube2v1	-0,8	22,2	-1,37	0,19	0,4506	-6
>sp|Q9DBZ5|EIF3K_M	19,99	19,6	19,7	19,1	19,8	19,6	20	19	19	20,3	20	21	19,6	19,7	20	20	19,5	19,1	19,592	19,8432	Eif3k	0,25	19,7	1,364	0,191	0,452	-6
>sp|O35286|DHX15_	19,85	18,9	18,9	19,5	19,5	20,1	20	20	19	18,8	19	19	19,8	19,5	20	19	19,2	19,5	19,52	19,248	Dhx15	-0,3	19,4	-1,36	0,192	0,4546	-6
>sp|O54734|OST48_I	20,95	17,4	15,4	20	19,7	18,8	20	14	16	18,9	18	18	21,9	19,9	20	18	20,4	17,9	18,059	19,3184	Ddost	1,26	18,7	1,358	0,193	0,4552	-6
>sp|Q8VCK7|SYCN_M	17,38	17,3	17,1	16,6	17,4	17,7	18	17	16	18,4	18	17	17	19,1	19	14	18,7	18,4	17,126	17,8539	Sycn	0,73	17,5	1,357	0,193	0,4556	-6
>sp|Q9D868|PPIH_M	21,64	20,3	20,3	20,5	20,6	20,6	21	20	19	19,7	21	21	19,9	19	19	20	20,6	20,6	20,454	20,076	Ppih	-0,4	20,3	-1,35	0,195	0,4592	-6
>sp|Q99K48|NONO_M	24,41	22,6	18,8	24,5	18,1	24,4	25	25	24	23,3	17	17	23,4	23,5	23	21	17,7	23,6	22,923	21,1568	Nono	-1,8	22	-1,35	0,195	0,4598	-6
>sp|Q60749|KHDR1_	16,67	18	18,1	19	18	18,2	18	18	17	17,9	16	18	17,6	17,6	18	18	17,7	18,1	17,965	17,5455	Khdrbs1	-0,4	17,8	-1,35	0,195	0,4599	-6
>sp|P06683|CO9_M(	19,43	19,8	19,6	19,6	19,6	20	20	20	19	18,2	19	18	18,4	20,3	20	16	20,4	19,6	19,606	18,9134	C9	-0,7	19,3	-1,35	0,195	0,4599	-6
>sp|P19467|MUC13	19,95	20,1	19,4	19,6	20,1	20,2	20	21	20	19	20	20	19,8	20	20	20	19,9	19,2	19,993	19,7454	Muc13	-0,2	19,9	-1,35	0,197	0,4623	-6
>sp|Q3V132|ADT4_M	15,42	16,2	15,9	16,2	16,2	16,5	16	16	16	15,7	15	16	16,3	16	16	15	16,2	15,8	16,034	15,8346	Slc25a31	-0,2	15,9	-1,35	0,197	0,4624	-6
>sp|Q9DCJ9|NPL_MO	18,99	18	18,5	17,7	19,9	18,2	20	19	19	19,1	17	20	19,5	19,2	20	19	20,6	20,1	18,741	19,3122	Npl	0,57	19	1,342	0,198	0,4635	-6
>sp|P01637|KV5A5_	16,77	17,6	17	17	16,2	17,8	17	17	17	16,2	16	16	0	15,7	16	17	16,4	16,8	16,995	14,5646	>sp|P016	-2,4	15,8	-1,34	0,198	0,4635	-6
>sp|P01638|KV5A6_	16,77	17,6	17	17	16,2	17,8	17	17	17	16,2	16	16	0	15,7	16	17	16,4	16,8	16,995	14,5646	>sp|P016	-2,4	15,8	-1,34	0,198	0,4635	-6
>sp|P06240|LCK_MC	17,13	19,3	18,3	15,9	19,3	17	18	18	19	19	18	16	17,7	18	16	17	17,5	17,2	17,963	17,2933	Lck	-0,7	17,6	-1,34	0,198	0,4635	-6
>sp|Q9D1E6|TBCB_M	19	19,2	17,4	19,4	14,6	17,4	18	17	17	20	17	17	20,3	14	20	20	19,9	20	17,636	18,7816	Tbcb	1,15	18,2	1,342	0,198	0,4635	-6
>sp|Q8BFW4|TRI65_M	15,07	14,9	0	14,5	14	14,4	15	13	11	8,68	15	0	0	15,1	14	13	0	13,6	12,532	8.821844	Trim65	-3,7	10,7	-1,34	0,199	0,4649	-6
>sp|Q9DBB8|DHDH_M	20,83	18,4	16,5	19,9	19,2	19,6	20	18	22	21,3	21	20	20,1	19,6	20	20	19,1	19,8	19,387	20,1697	Dhdh	0,78	19,8	1,338	0,199	0,4657	-6
>sp|P97324|G6PD2_	22,61	21,3	21,4	22,3	21	21,7	22	21	22	21,9	22	21	21,4	21,1	21	22	21,4	21,4	21,671	21,3931	G6pd2	-0,3	21,5	-1,34	0,2	0,4659	-6
>sp|Q9QZ88|VPS29_I	22,81	22,6	22,5	23,1	23,4	22,8	23	22	23	22,1	22	22	23,7	21,9	23	23	22,3	22,3	22,769	22,4754	Vps29	-0,3	22,6	-1,34	0,2	0,4659	-6
>sp|Q6P9R2|OXSR1_	0	13,9	15,1	14	0	17,7	13	17	17	16,7	17	0	14	0	0	17	0	0	11,964	7.130908	Oxsr1	-4,8	9,55	-1,34	0,2	0,4659	-6
>sp|Q3TFQ1|SPRY7_M	17,47	17,9	17,3	17,7	17,9	18,4	17	18	16	16,4	17	18	18	14,3	18	16	17,2	17,2	17,542	16,9288	Spryd7	-0,6	17,2	-1,33	0,201	0,4681	-6
>sp|Q9DBF1|AL7A1_I	20,12	20,7	20,1	20,6	20,4	20,7	21	20	20	20,4	20	20	20	19,8	20	21	20,1	20,2	20,392	20,1925	Aldh7a1	-0,2	20,3	-1,33	0,201	0,4688	-6
>sp|B1AVD1|XPP2_M	19,81	19,3	16,2	16,3	15,7	16,8	17	16	17	16,8	16	17	17	15,5	16	16	16,3	17,1	17,114	16,4246	Xpnpep2	-0,7	16,8	-1,33	0,202	0,4697	-6
>sp|Q8BWU5|OSGEP_	20,73	20,3	20,2	19,6	18,7	19,9	19	20	20	19,8	21	21	20,6	20,4	20	20	19,5	19,7	19,855	20,1865	Osgep	0,33	20	1,329	0,202	0,4697	-6
>sp|A2AQ07|TBB1_M	21,83	21,7	22,8	22	21,9	22,2	22	23	23	22,5	23	23	22,2	22,8	22	23	22,6	22	22,23	22,4577	Tubb1	0,23	22,3	1,329	0,202	0,4697	-6

>sp|Q8VBW6|ULA1_M	18,71	18,8	19,6	18,7	18,5	19,2	19	19	19	20,5	21	18	19	19,2	19	19	18,8	19,1	18,981	19,373	Nae1	0,39	19,2	1,328	0,202	0,4697	-6
>sp|Q8CGR7|UPP2_M	15,72	17,2	15,5	15,5	15,4	16	15	19	19	18,1	17	18	14,6	14,9	0	15	14,3	14	16,507	13,9813	Upp2	-2,5	15,2	-1,33	0,202	0,4697	-6
>sp|P11499|HS90B_	24,68	24,3	24,5	24,7	24,9	24,6	24	25	25	24,5	25	24	24,6	24,7	25	24	24,5	24,5	24,654	24,5534	Hsp90ab1	-0,1	24,6	-1,33	0,203	0,4715	-6
>sp|O08740|RPB11_	0	15,1	16	16,6	13,8	0	0	18	18	16,6	18	0	17,2	17,7	18	17	14,9	15,9	10,748	15,0978	Polr2j	4,35	12,9	1,323	0,204	0,4727	-6
>sp|Q8CIG8|ANM5_M	22,36	21,2	22,1	22,2	22,6	22,8	22	22	23	21,8	22	22	22	22,4	22	22	22,2	22,2	22,235	21,9831	Prmt5	-0,3	22,1	-1,32	0,204	0,4735	-6
>sp|Q8R4N0|CLYBL_M	20,41	18,3	18,1	18,4	18,5	17,5	18	18	18	16,9	17	18	18,6	18,3	19	18	18,5	17,8	18,45	17,9897	Clybl	-0,5	18,2	-1,32	0,205	0,4736	-6
>sp|P62715|PP2AB_	24,09	23,5	23,4	23,7	23,5	22,6	23	23	23	23,5	24	23	22,2	22,3	22	23	23,4	23,4	23,352	23,0143	Ppp2cb	-0,3	23,2	-1,32	0,205	0,4736	-6
>sp|Q9JLI6|SCLY_MOL	20,25	19,9	20,1	20,3	20	19,7	20	20	20	20,1	20	20	20,5	20,3	20	20	20	19,9	19,937	20,087	Scly	0,15	20	1,319	0,205	0,4736	-6
>sp|P00757|K1KB4_	19,15	18,9	19,3	18,6	19,3	19,1	19	19	19	16,9	19	20	19,4	19,1	21	19	20,7	20,6	18,989	19,535	Klk1b4	0,55	19,3	1,319	0,205	0,4736	-6
>sp|Q9CXT8|MPPB_M	21,08	21	20,6	20	20,2	20,9	21	21	20	20,3	21	21	21,1	20,5	21	21	20,7	20,5	20,574	20,8179	Pmpcb	0,24	20,7	1,319	0,205	0,4736	-6
>sp|Q9Z2Z9|GFPT2_M	15,74	14,3	17,1	16,8	16,3	16,7	17	17	17	17,6	17	17	17,5	16,7	17	16	16,2	17,2	16,445	16,9323	Gfpt2	0,49	16,7	1,319	0,205	0,4736	-6
>sp|Q8R059|GALE_M	20,82	21,3	22,5	22,4	18,6	22,5	18	22	22	22,4	22	22	18	23	23	23	22,9	22,7	21,157	22,154	Gale	1	21,7	1,318	0,206	0,4739	-6
>sp|Q91XL9|OSBL1_M	16,45	14,8	16,1	13,8	14,6	16,7	16	16	17	17,8	19	16	13,7	12,3	13	12	15,4	11,9	15,783	14,5767	Osbpl1a	-1,2	15,2	-1,32	0,206	0,4739	-6
>sp|Q99J45|NRBP_M	0	0	18,8	0	0	0	0	14	0	12,8	17	17	14,5	0	0	0	14,3	0	3,6626	8,39882	Nrbp1	4,74	6,03	1,316	0,206	0,4747	-6
>sp|Q9CQM5|TXD17_	22,39	22,4	23,2	22,8	22,4	22,4	23	23	23	17,1	25	25	17,5	25,3	18	18	17,3	25,2	22,753	20,9792	Txndc17	-1,8	21,9	-1,31	0,208	0,4772	-6
>sp|Q8BVQ5|PPME1_	18,8	18,9	18	18,6	18,4	18,2	18	19	18	18,9	19	20	18,2	18	19	19	19,3	18,4	18,511	18,7953	Ppme1	0,28	18,7	1,311	0,208	0,4774	-6
>sp|P57759|ERP29_	19,08	16,2	13,9	19,9	20,1	19	21	0	0	17,2	17	16	18,2	19	19	17	19,2	18,8	14,295	17,9409	Erp29	3,65	16,1	1,311	0,208	0,4774	-6
>sp|P45377|ALD2_M	23,1	21,8	23	23,3	23,4	23,3	22	23	22	23,2	22	23	23,4	24,1	23	23	22,2	23,7	22,811	23,172	Akr1b8	0,36	23	1,311	0,208	0,4774	-6
>sp|Q91WT9|CBS_MO	23,06	18,7	18,3	18,7	18,4	18,8	18	19	20	19,5	20	20	19,9	20,2	20	20	19,6	19,5	19,209	19,8705	Cbs	0,66	19,5	1,309	0,209	0,4779	-6
>sp|Q8CE96|TRM6_M	15,34	16	16,4	16	15,3	16,4	16	15	16	16,4	15	17	16,9	16,4	16	16	15,3	16,4	15,839	16,1623	Trmt6	0,32	16	1,309	0,209	0,4779	-6
>sp|Q8K2C6|SIR5_MO	15,82	16,8	17,3	17,3	16,8	16,8	17	16	17	16,7	16	17	16,8	16,4	17	16	16,5	16,4	16,754	16,528	Sirt5	-0,2	16,6	-1,31	0,209	0,4783	-6
>sp|P26040|EZRI_MO	22,49	22	22,3	22,5	22,2	22,5	22	22	22	22,6	22	23	22	22	23	22	22,8	22,9	22,3	22,4699	Ezr	0,17	22,4	1,307	0,209	0,4783	-6
>sp|O35295|PURB_M	18,64	18,4	18,7	17,4	17,2	18,8	19	18	19	18	18	19	19,3	19,4	19	19	18,3	18,2	18,345	18,7056	Purb	0,36	18,5	1,307	0,209	0,4783	-6
>sp|P02535|K1C10_	22,7	23	22,4	21,5	22,2	21	22	22	22	21,6	22	22	23	22,1	22	24	23,9	24,1	22,144	22,6506	Krt10	0,51	22,4	1,306	0,21	0,4788	-6
>sp|P28658|ATX10_	0	14,5	14,7	14,3	14,3	13,8	14	15	14	14,6	15	15	14,7	15,4	15	14	14,3	14,5	12,709	14,7709	Atxn10	2,06	13,7	1,305	0,21	0,4788	-6
>sp|Q8BRF7|SCFD1_M	17,8	17,6	20,4	17,3	18,2	19,1	17	19	20	20,8	20	20	20,2	20,4	21	17	17	17,2	18,464	19,3028	Scfd1	0,84	18,9	1,305	0,21	0,4788	-6
>sp|Q61704|ITIH3_M	23,41	22,4	22,1	23,5	23,1	23,4	24	24	24	22,6	22	23	22,9	23,8	23	23	22,2	23,1	23,264	22,9172	Itih3	-0,3	23,1	-1,3	0,211	0,4807	-6
>sp|P35278|RAB5C_	21,76	21,3	20,3	23,2	21,2	20,9	21	22	21	21,9	22	21	21,6	21,4	22	23	22,1	21,6	21,42	21,8024	Rab5c	0,38	21,6	1,302	0,211	0,4807	-6
>sp|Q9D1M0|SEC13_	21,18	20,9	21,4	20,9	21,5	21,7	20	21	21	21,9	22	22	21	21,5	21	21	21,4	21,3	21,187	21,433	Sec13	0,25	21,3	1,301	0,211	0,4807	-6
>sp|P59999|ARPC4_	22,98	23,1	23,4	22,7	23,2	23,7	23	23	23	23,7	23	23	23,7	23,2	23	24	23,1	23	23,159	23,364	Arpc4	0,21	23,3	1,3	0,211	0,4811	-6
>sp|Q9JMD0|ZN207_	20,16	20,3	20,4	20	17,9	20	20	21	21	15,6	20	20	20,3	20,3	20	19	20	18,3	20,096	19,3137	Znf207	-0,8	19,7	-1,3	0,212	0,4821	-6
>sp|Q64324|STXB2_M	15,83	14,7	16,7	14,8	15,1	16,6	0	17	17	17,6	15	17	17,1	17,1	17	15	17,1	16,7	14,251	16,6193	Stxbp2	2,37	15,4	1,297	0,213	0,4829	-6
>sp|P49138|MAPK2_	15,83	16,2	16,5	14,6	14,4	14,3	16	15	14	15,5	16	15	16,5	16,5	15	16	16,2	14,7	15,204	15,7445	Mapkapk2	0,54	15,5	1,296	0,213	0,4832	-6
>sp|Q71RI9|KAT3_MO	19,1	19,6	19,9	19,5	18,7	19,2	20	20	20	20,7	19	21	20,1	18,9	20	19	20,9	21,1	19,521	19,9988	Kyat3	0,48	19,8	1,295	0,213	0,4843	-7
>sp|Q80V85|TRI62_M	18,02	15,5	15,1	18	17,6	14,6	18	14	18	11,7	14	14	14,1	13,9	14	19	19,7	15,1	16,473	15,1495	Trim62	-1,3	15,8	-1,29	0,214	0,4855	-7
>sp|Q01320|TOP2A_	13,82	13,1	0	13	12,8	0	13	11	0	8,76	12	12	12,9	10,6	13	12	10,6	11,2	8.59271	11,4007	Top2a	2,81	10	1,289	0,215	0,488	-7
>sp|Q9WTX6|CUL1_M	18,32	19,2	19,2	18,3	20	19,3	18	19	19	19,4	19	18	18,8	19,3	19	18	18	18,7	19,013	18,6997	Cul1	-0,3	18,9	-1,29	0,216	0,4888	-7
>sp|Q8R3D1|TBC13_	17,71	17,4	17,1	17,3	17	17,5	17	19	19	18,7	17	17	17,2	16,9	16	17	18,3	16,5	17,657	17,1982	Tbc1d13	-0,5	17,4	-1,29	0,216	0,4888	-7
>sp|Q9QY36|NAA10_	15,87	16,4	15,7	15,6	15,7	15,8	0	15	16	14,5	15	15	0	14,4	0	16	15,1	0	13,995	10,0839	Naa10	-3,9	12	-1,29	0,216	0,4888	-7
>sp|Q3TMQ6|ANG4_M	19,17	18	18,9	18,4	18,6	18,6	19	18	18	16	21	0	17,9	18,1	17	18	17,4	17,3	18,509	15,9159	Ang4	-2,6	17,2	-1,29	0,217	0,4892	-7
>sp|P22599|A1AT2_	23,94	24	23,3	22,1	21,9	24,1	24	24	24	24,5	24	24	23,9	23,5	24	24	24,5	23,2	23,547	23,9795	Serpina1b	0,43	23,8	1,284	0,217	0,4897	-7
>sp|Q91X52|DCXR_M	17,29	15,9	16,5	16,6	15,2	16,6	16	15	16	14,7	15	15	16,8	15,9	17	15	16	16,2	16,177	15,7531	Dcxr	-0,4	16	-1,28	0,218	0,4918	-7
>sp|P35293|RAB18_	19,74	20,2	19,1	19,1	18,8	19,2	20	19	21	21	21	21	19,3	20,2	20	19	19,6	19	19,556	19,987	Rab18	0,43	19,8	1,279	0,219	0,4932	-7
>sp|P28660|NCKP1_	18,24	17,2	17,9	18,3	18	18,1	18	17	17	18	17	18	17,8	17,5	18	17	17,4	17,8	17,833	17,6123	Nckap1	-0,2	17,7	-1,28	0,219	0,4932	-7
>sp|Q3UX61|NAA11_	16,21	16,8	16,1	15,9	16	16,2	0	15	16	15	16	16	0	14,7	0	16	15,5	0	14,334	10,3506	Naa11	-4	12,3	-1,28	0,219	0,4935	-7
>sp|P47753|CAZA1_	21,78	21,4	21,8	21,2	22	21,7	23	22	22	22,1	22	22	21,5	21,2	21	22	21,2	21,7	21,917	21,6531	Capza1	-0,3	21,8	-1,27	0,221	0,4975	-7
>sp|P39688|FYN_MO	17,42	19,4	18,5	16,9	19,5	18,2	18	18	19	19,2	19	17	17,9	18,5	17	17	18	17,9	18,402	17,9113	Fyn	-0,5	18,2	-1,27	0,221	0,4975	-7
>sp|P48962|ADT1_M	15,66	16,4	16,2	16,4	16,4	16,8	16	16	16	15,9	16	16	16,6	16,2	16	16	16,4	16,1	16,245	16,058	Slc25a4	-0,2	16,2	-1,27	0,221	0,4975	-7

>sp|Q9CQW5|LEG2_M	23,47	23,7	23	23,2	23	23,3	23	22	23	23,5	24	23	23,7	23,7	23	23	22,9	22,8	23,069	23,2974	Lgals2	0,23	23,2	1,271	0,222	0,4976	-7
>sp|Q9Z2I9|SUCB1_M	19,06	19,1	21,8	19,7	18,3	21,5	19	20	20	20,9	21	21	21,3	21,3	21	19	19,3	18,4	19,752	20,4258	Sucla2	0,67	20,1	1,268	0,223	0,4996	-7
>sp|P50608|FMOD_M	21,73	22	20,7	21,6	21,4	20,3	20	22	22	20,6	21	22	21,7	19,9	20	20	22	19,7	21,298	20,7991	Fmod	-0,5	21	-1,26	0,224	0,5018	-7
>sp|Q9D9M5|PHOP2	17,11	17	17,8	16,2	16,9	16,2	17	18	16	18,5	15	18	18,5	14,7	19	18	18,2	18,3	16,898	17,6166	Phospho	0,72	17,3	1,264	0,224	0,5018	-7
>sp|Q9CZ44|NSF1C_M	16,81	16,3	16,9	15,9	0	16,3	18	18	18	17,7	19	19	17,6	18,7	18	16	17	15,9	15,162	17,6011	Nsfl1c	2,44	16,4	1,26	0,225	0,5046	-7
>sp|O35345|IMA7_M	21,37	21,8	19,7	17	19,3	20,4	18	21	21	17,9	20	21	18,2	20,7	21	17	16,6	17,6	19,912	18,9317	Kpna6	-1	19,4	-1,26	0,226	0,5049	-7
>sp|Q91XE4|ACY3_M	19,32	19,9	18,7	17,8	18,4	18,5	17	18	18	17,6	19	19	16,9	18,4	19	18	17,1	18,1	18,45	17,9974	Acy3	-0,5	18,2	-1,26	0,226	0,5051	-7
>sp|P63158|HMGB1	23,67	20,4	21	21,1	21,9	21,1	24	21	21	20,9	20	21	21,7	21,8	22	21	21,5	21	21,687	21,1182	Hmgb1	-0,6	21,4	-1,26	0,226	0,5058	-7
>sp|P35980|RL18_M	19,33	19,5	19,4	19,3	21	20,3	20	20	20	19,9	20	20	20,2	20,1	20	20	21,4	20,5	19,907	20,2316	Rpl18	0,32	20,1	1,256	0,227	0,5062	-7
>sp|Q8K354|CBR3_M	20,51	20,8	22,5	19,8	20,3	20,1	19	23	24	19,6	21	21	20,4	20,9	20	20	20,1	20,2	21,137	20,4492	Cbr3	-0,7	20,8	-1,25	0,227	0,5068	-7
>sp|Q64133|AOFA_M	0	19,3	18,4	14	18,1	18,1	18	20	20	20,4	20	20	19,7	19	14	18	19,1	18,6	16,168	18,8828	Maoa	2,71	17,5	1,249	0,229	0,5107	-7
>sp|Q9CQJ3|GMFB_M	20,93	20,8	21,1	20,7	21,2	20,6	21	21	22	21,4	21	20	20,2	21,3	22	20	20,4	20,6	21,09	20,7813	Gmfb	-0,3	20,9	-1,25	0,23	0,5122	-7
>sp|Q99LX0|PARK7_	21,48	20,9	21,5	21,4	21,6	21,2	20	21	21	21,6	21	21	20,8	20,1	20	21	21,4	20,3	21,17	20,8458	Park7	-0,3	21	-1,24	0,231	0,5141	-7
>sp|Q8R5H1|UBP15_	14,45	14,7	16,1	15,9	16,1	15,9	15	15	16	15,8	16	16	15,7	16,4	16	16	15,8	14,9	15,453	15,7638	Usp15	0,31	15,6	1,241	0,232	0,5164	-7
>sp|P62754|RS6_MO	15,93	0	18,8	16,7	15,9	16,5	19	19	17	17,8	17	18	18,6	18,3	18	17	17,4	17,4	15,405	17,832	Rps6	2,43	16,6	1,24	0,232	0,5165	-7
>sp|Q60960|IMA5_M	15,65	16,1	15,8	15,8	15,8	16,2	16	17	16	15,6	16	16	16,2	15,8	15	15	15,6	15,8	16,011	15,8147	Kpna1	-0,2	15,9	-1,24	0,233	0,5173	-7
>sp|Q9JHI7|EXOS9_M	17,91	18,1	17,2	16,2	17	18,2	18	17	18	17,5	18	18	18,4	17,8	18	18	18,6	17	17,505	17,8388	Exosc9	0,33	17,7	1,239	0,233	0,5173	-7
>sp|Q9JMA1|UBP14_	21,31	18,5	19,7	18,7	18,4	19,6	21	18	19	18,4	20	19	19,2	19	19	19	18,2	18,6	19,38	18,8399	Usp14	-0,5	19,1	-1,24	0,234	0,5185	-7
>sp|Q9D7J7|CPNS2_I	18,17	15,5	18,1	19,1	18,8	18,1	18	18	18	15,2	19	19	17,2	15,3	16	14	18,8	19,2	18,007	17,0568	Capns2	-1	17,5	-1,24	0,234	0,5185	-7
>sp|Q8C196|CPSM_M	23,34	22,9	22,6	22,6	23	22,6	23	23	23	22,4	23	23	22,9	22,7	22	23	22,6	22,9	22,817	22,6846	Cps1	-0,1	22,8	-1,23	0,235	0,5208	-7
>sp|Q91V64|ISOC1_M	20,45	21,1	21,3	21,5	22,1	22,5	22	22	21	21,7	22	22	21,6	21,4	21	22	22,3	22,6	21,526	21,8246	Isoc1	0,3	21,7	1,229	0,236	0,5233	-7
>sp|Q61011|GBB3_M	17,79	18,4	19,6	18,5	18,3	19,3	18	19	19	18,8	17	19	20	20,2	20	18	19,5	18,6	18,593	19,0566	Gnb3	0,46	18,8	1,229	0,236	0,5233	-7
>sp|P83940|ELOC_M	23,31	22,3	21,9	22,1	22,6	22	22	22	21	21,5	22	22	22,1	22,1	22	22	21,9	21,7	22,219	21,9674	Eloc	-0,3	22,1	-1,23	0,237	0,5233	-7
>sp|Q91YJ3|THYN1_M	16,55	16,9	17,2	17,1	17,7	17,3	18	18	18	18,2	16	18	18,7	18,3	16	18	18,6	18,6	17,307	17,821	Thyn1	0,51	17,6	1,224	0,238	0,5267	-7
>sp|P17047|LAMP2_	14,1	15,5	16,1	0	0	13,1	14	16	12	15,5	12	16	14	12	13	11	15,2	16,3	11,139	13,8509	Lamp2	2,71	12,5	1,22	0,24	0,5295	-7
>sp|Q61990|PCBP2_	20,05	19,6	20	20,3	20,7	20,1	21	20	20	19,7	20	20	20,3	20,2	20	20	20,1	19	20,157	19,912	Pcbp2	-0,2	20	-1,22	0,241	0,5319	-7
>sp|Q8CAA7|PGM2L_	17,55	17,5	18	14,9	17,7	17,4	18	17	18	17,4	17	17	15,3	17	17	16	18,2	17,5	17,388	16,8644	Pgm2l1	-0,5	17,1	-1,21	0,242	0,5333	-7
>sp|Q8VEJ9|VPS4A_M	15,75	16	15,4	15,6	15,5	16,2	16	16	16	15,2	0	14	17,1	14,6	18	15	14,6	14,8	15,735	13,6273	Vps4a	-2,1	14,7	-1,21	0,243	0,5345	-7
>sp|Q78JN3|ECI3_MO	19,83	20,2	21,1	19,5	19,5	17,1	16	21	22	16,7	17	24	17,1	16,7	17	20	17,1	20,7	19,611	18,3572	Eci3	-1,3	19	-1,21	0,244	0,5362	-7
>sp|Q99K23|UFSP2_I	17,46	18,4	18,1	17,9	18,3	18,6	19	19	18	18,7	19	19	18,6	18,3	18	18	18,5	18,5	18,299	18,5235	Ufsp2	0,22	18,4	1,209	0,244	0,5362	-7
>sp|Q61847|MEP1B_	20,49	20,8	20,4	20,2	20,5	20,5	21	21	20	20,4	20	20	20,4	20,5	21	20	20,7	20,6	20,526	20,4104	Mep1b	-0,1	20,5	-1,21	0,244	0,5362	-7
>sp|Q91VC4|PLVAP_	20,64	18	17,6	16,8	21,3	21,4	18	16	17	17	16	17	21,1	17,3	18	17	16,9	16,8	18,472	17,4784	Plvap	-1	18	-1,21	0,244	0,5362	-7
>sp|Q61239|FNTA_M	18,87	19,4	19,2	18,8	18	19	19	19	19	19,5	20	19	19,2	18,8	19	19	19	19	18,956	19,1634	Fnta	0,21	19,1	1,208	0,244	0,5365	-7
>sp|P70460|VASP_M	20,13	19,3	19,4	19,2	19,3	19,6	20	20	20	19,4	20	20	20	19,9	20	19	19	19,7	19,556	19,7544	Vasp	0,2	19,7	1,207	0,245	0,5365	-7
>sp|Q9CQE8|RTRAF_M	17,58	17,7	16,5	17,1	16,5	15,6	16	17	17	17,1	17	18	18,5	15,6	18	17	16,6	17,9	16,757	17,2202	RTRAF	0,46	17	1,207	0,245	0,5365	-7
>sp|Q9CXF0|KYNU_M	14,16	15,2	15	0	14,6	14,5	15	14	14	15,3	14	14	0	0	0	14	14,6	14,7	13,04	9.581108	Kynu	-3,5	11,3	-1,2	0,246	0,538	-7
>sp|Q6P5E4|UGGG1_	17,3	20,3	20,5	19,6	20,6	19,7	19	20	20	19,2	18	18	19,9	20,3	20	19	19,9	18,6	19,718	19,1401	Uggt1	-0,6	19,4	-1,2	0,246	0,538	-7
>sp|Q99PL5|RRBP1_	13,84	14,2	19,5	19	18,8	19	14	12	12	7,76	13	12	13,5	18,3	18	18	10,2	12,6	15,707	13,7201	Rrbp1	-2	14,7	-1,2	0,246	0,538	-7
>sp|Q01514|GBP1_M	17,7	18,1	18,9	18,9	19,1	18,7	18	19	19	18,3	19	19	18,8	19	19	19	18,8	18,4	18,501	18,7274	Gbp1	0,23	18,6	1,203	0,246	0,538	-7
>sp|P24822|PPBI_M	23,06	22,2	23	22,9	22,8	22	22	22	22	22,8	22	22	23,2	22,5	23	23	22,6	22,4	22,452	22,6863	Iap	0,23	22,6	1,203	0,246	0,538	-7
>sp|P31532|SAA4_M	18,69	18,5	16,6	21,3	21,5	22	18	21	21	20,8	18	21	21	21,6	21	21	21,1	20,9	19,85	20,6881	Saa4	0,84	20,3	1,192	0,25	0,5471	-7
>sp|Q99JW5|EPCAM_	20,19	21,9	23,5	19,8	20,1	22,2	22	22	21	24,4	24	23	15,7	17,6	0	17	18,7	24,2	21,386	18,3364	Epcam	-3	19,9	-1,19	0,251	0,5471	-7
>sp|Q8R3B1|PLCD1_	17,91	17,8	19,1	19	18,3	18,5	20	19	19	18,6	19	18	18,7	18	19	18	18,1	18,3	18,684	18,3769	Plcd1	-0,3	18,5	-1,19	0,251	0,5473	-7
>sp|P09041|PGK2_M	23,25	23,5	24	23,5	23,4	23,3	23	24	24	23,6	24	24	23,4	23	23	23	23,3	22,9	23,649	23,3903	Pgk2	-0,3	23,5	-1,19	0,251	0,5478	-7
>sp|P62267|RS23_M	16,42	16,1	17,4	16,3	16,8	17,3	16	17	17	17,4	16	18	15,7	17,9	18	17	17,8	15,8	16,63	17,0367	Rps23	0,41	16,8	1,186	0,253	0,5505	-7
>sp|P62281|RS11_M	19,78	20,3	25,6	20,2	24	24,1	24	25	25	20,8	24	24	20,5	21	21	21	23,4	24	23,208	22,0895	Rps11	-1,1	22,6	-1,18	0,253	0,5507	-7
>sp|Q8BPB0|MOB1B	20,96	20	21,2	20,2	21,5	21,3	21	20	21	20,7	21	20	21,3	21,2	21	23	21,1	21,2	20,758	21,1257	Mob1b	0,37	20,9	1,184	0,253	0,5507	-7
>sp|Q921Y0|MOB1A_	20,96	20	21,2	20,2	21,5	21,3	21	20	21	20,7	21	20	21,3	21,2	21	23	21,1	21,2	20,758	21,1257	Mob1a	0,37	20,9	1,184	0,253	0,5507	-7

>sp|P04104|K2C1_M	22,24	22,4	22,2	21,8	21,5	21,1	21	21	21	21,2	21	21	22,1	21,8	22	23	23,7	23	21,654	22,0925	Krt1	0,44	21,9	1,184	0,253	0,5507	-7
>sp|Q9D939|ST1C2_I	15,72	15,9	15	16,5	15,7	16,5	15	16	16	15,4	16	17	16,6	16,4	16	15	16	16	15,816	16,0927	Sult1c2	0,28	16	1,18	0,255	0,5532	-7
>sp|P97328|KHK_MO	20,86	20,4	22	21,6	21,3	21,5	22	21	21	21,6	22	21	20,9	21,3	21	21	22,2	21,7	21,249	21,4953	Khk	0,25	21,4	1,179	0,255	0,5538	-7
>sp|Q8VEE0|RPE_MOI	17,44	16,8	17,6	17,8	17	17,3	18	20	20	20,3	19	18	23,1	17,8	18	18	17,7	17,1	17,942	18,8039	Rpe	0,86	18,4	1,178	0,256	0,554	-7
>sp|Q9CQT1|MTNA_M	19,26	21,7	21,1	19,8	20,5	21,8	21	21	20	21	20	21	20	21,5	22	21	21,6	21,6	20,618	21,0524	Mri1	0,43	20,8	1,178	0,256	0,554	-7
>sp|Q9R111|GUAD_M	21,9	22,3	21,5	22,7	21,9	22,1	22	22	21	22,2	22	22	22,5	22,4	23	22	22,3	21,4	21,953	22,1781	Gda	0,23	22,1	1,174	0,257	0,5568	-7
>sp|Q9D1H7|GET4_M	15,84	0	0	16,1	15,5	15,9	16	16	0	16,5	0	16	16,9	15,3	16	15	16,7	16,6	10,54	14,2341	Get4	3,69	12,4	1,172	0,258	0,5583	-7
>sp|Q9WV60|GSK3B_	22,97	23,4	18,6	19,9	19,4	19,5	21	21	22	19,4	19	19	19,8	19,7	20	24	19,4	19,6	20,841	19,9334	Gsk3b	-0,9	20,4	-1,17	0,258	0,5586	-7
>sp|P24547|IMDH2_	18,43	21	19,1	19,1	20,4	20,7	19	20	19	19,8	19	19	18,6	19,2	19	20	19,2	19,4	19,633	19,2416	Impdh2	-0,4	19,4	-1,17	0,259	0,5586	-7
>sp|P61963|DCAF7_	17,78	22,5	26,5	21,9	21,9	26,4	22	17	17	17,9	25	18	20,7	20,8	18	20	18,3	20,4	21,566	19,9774	Dcaf7	-1,6	20,8	-1,17	0,259	0,5586	-7
>sp|Q8R050|ERF3A_I	21,03	20,8	18,7	20,1	20,1	19,4	20	20	19	22,7	18	19	19,9	19,3	24	19	23	23,3	19,873	20,8134	Gspt1	0,94	20,3	1,17	0,259	0,5586	-7
>sp|Q5BKQ4|LIPR1_M	21,66	19,8	20,5	21,3	21,5	20,5	21	21	22	20,5	21	21	21,8	21,4	22	22	22,5	20,9	21,081	21,4491	Pnliprp1	0,37	21,3	1,167	0,26	0,5606	-7
>sp|Q9D9V3|ECHD1_	19,12	17,9	18,1	17,5	17,4	17,3	17	20	20	18,6	21	20	18,5	18,4	18	18	18,2	18,3	18,243	18,819	Echdc1	0,58	18,5	1,166	0,26	0,5608	-7
>sp|Q9WUB3|PYGM_I	21,65	21,3	22,7	21,6	21	22,8	22	21	22	22,7	23	23	21,7	22,9	22	21	21,5	21,9	21,736	22,0827	Pygm	0,35	21,9	1,164	0,261	0,5624	-7
>sp|Q810D6|GRWD1	15,42	18,4	18,7	14,7	14	18,6	18	18	19	16,1	15	19	16,9	16,6	17	16	16,2	16	17,252	16,414	Grwd1	-0,8	16,8	-1,16	0,261	0,5624	-7
>sp|Q9D281|NXP20_	17,07	15,3	14,6	15,1	0	0	15	0	15	0	15	14	0	12,6	14	0	0	0	10,24	6.170266	Fam114a1	-4,1	8,2	-1,16	0,263	0,5649	-7
>sp|O54984|ASNA_M	19,79	19,8	19,1	19,6	19,5	18,6	18	18	18	18,9	17	18	18,6	18,4	17	19	20,3	18,4	18,931	18,4166	Asna1	-0,5	18,7	-1,16	0,263	0,5655	-7
>sp|P15945|K1KB5_	20,86	20	20,8	20,3	20,5	20,8	21	21	21	20,5	20	21	20,9	20,6	22	21	21,4	21,4	20,614	20,8474	Klk1b5	0,23	20,7	1,154	0,265	0,5688	-7
>sp|Q04447|KCRB_M	24,5	23,9	24,4	25,2	24,6	24,9	24	26	26	25,4	25	24	24,6	25	24	24	24,3	24,8	24,808	24,5129	Ckb	-0,3	24,7	-1,15	0,265	0,5688	-7
>sp|Q9D8T2|GSDMD_	15,86	18,5	15,6	18,4	18,4	18,1	18	18	18	17,9	18	18	18,6	17,4	18	18	18,3	18,3	17,578	18,0204	Gsdmdc1	0,44	17,8	1,153	0,265	0,5692	-7
>sp|Q99JF5|MVD1_M	16,93	0	17,8	0	16,4	16,4	14	16	17	16,4	15	14	13,7	0	0	0	16,9	0	12,642	8.509784	Mvd	-4,1	10,6	-1,15	0,266	0,57	-7
>sp|P84099|RL19_M	15,65	15,4	16	15,6	15,5	15,9	16	20	20	15,7	18	16	15,8	15,6	17	16	0	16	16,545	14,3747	Rpl19	-2,2	15,5	-1,15	0,266	0,571	-7
>sp|Q9JJN5|CBPN_M	19,48	19	19,8	19,6	19,4	19,5	19	19	19	19,2	19	20	19,6	19,8	20	19	19,7	18,9	19,276	19,4592	Cpn1	0,18	19,4	1,147	0,268	0,5733	-7
>sp|P55065|PLTP_M	21,47	22	18,5	21,6	21,6	16,4	22	22	22	21,5	19	16	16,2	21,9	22	21	17,5	21,1	20,807	19,6482	Pltp	-1,2	20,2	-1,15	0,268	0,5742	-7
>sp|Q99MQ4|ASPN_M	18,05	20,6	18,1	20,3	17,9	17,4	19	19	20	16,6	20	12	16,5	18,6	18	18	20,6	19,8	18,937	17,8928	Aspn	-1	18,4	-1,15	0,269	0,5742	-7
>sp|P50396|GDIA_M	24,07	23,9	24,1	24,1	23,8	24,2	24	24	24	23,9	24	24	24,4	24,2	24	24	23,8	23,9	24,023	23,9192	Gdi1	-0,1	24	-1,14	0,269	0,5757	-7
>sp|Q8BG05|ROA3_M	18,26	18,5	18,8	18	17,7	18,9	19	19	18	18,8	17	18	18,7	18,8	17	18	18,1	18	18,412	18,1422	Hnrnpa3	-0,3	18,3	-1,14	0,271	0,5796	-7
>sp|P16381|DDX3L_	18,53	19,1	19,4	19,2	18,8	19,2	19	19	19	18,8	20	20	18,6	18,9	19	19	19	18,6	19,156	18,9736	D1Pas1	-0,2	19,1	-1,14	0,272	0,5796	-7
>sp|Q3TCN2|PLBL2_M	15,76	15,6	16,4	16,4	15,5	15,8	16	16	15	12,7	18	14	15,4	16,1	16	14	14,5	16,6	15,801	15,2209	Plbd2	-0,6	15,5	-1,14	0,272	0,5796	-7
>sp|Q61292|LAMB2_	20,17	20,1	19,5	19,9	18,8	19,7	20	20	19	19,6	20	19	20	19,1	20	20	18,4	19,5	19,708	19,4583	Lamb2	-0,2	19,6	-1,14	0,273	0,5802	-7
>sp|P70699|LYAG_M	16,33	16,4	16,5	16,4	17,5	17,3	17	15	16	16,7	17	17	16,9	17,3	17	16	16,9	17	16,502	16,8183	Gaa	0,32	16,7	1,135	0,273	0,5802	-7
>sp|P68510|1433F_	24,24	25,5	22,7	25,5	23,1	23,7	24	24	24	24,2	25	25	24,5	23,7	25	25	24,5	23,9	24,072	24,4718	Ywhah	0,4	24,3	1,134	0,273	0,5802	-7
>sp|Q8CIB5|FERM2_M	22,33	22,5	22,1	22,3	22,4	22,3	23	23	23	22,3	22	22	22,8	22,5	22	22	22,5	22,5	22,495	22,356	Fermt2	-0,1	22,4	-1,13	0,273	0,5802	-7
>sp|O09106|HDAC1_	19,76	20	17,1	18,1	18,3	17,5	18	18	17	18,1	18	19	19,6	19,5	19	18	17,9	19,5	18,235	18,7088	Hdac1	0,47	18,5	1,134	0,273	0,5802	-7
>sp|P28271|ACOC_M	26,24	25	22,8	24,9	23,7	22,1	24	23	23	23,2	23	23	23,1	23	23	23	23,5	23,3	23,76	23,2479	Aco1	-0,5	23,5	-1,13	0,273	0,5802	-7
>sp|P07361|A1AG2_	17,35	0	18,5	16,1	15,6	15,1	17	18	17	18,2	19	19	16,4	15,6	17	16	15,5	16,9	14,863	17,0381	Orm2	2,17	16	1,13	0,275	0,5825	-7
>sp|Q60590|A1AG1_	17,35	0	18,5	16,1	15,6	15,1	17	18	17	18,2	19	19	16,4	15,6	17	16	15,5	16,9	14,863	17,0381	Orm1	2,17	16	1,13	0,275	0,5825	-7
>sp|Q2NL51|GSK3A_I	22,81	23,3	17,5	17,6	17,1	17,2	17	17	22	16,6	18	17	16,3	17,1	17	24	16,9	17,5	19,151	17,7904	Gsk3a	-1,4	18,5	-1,13	0,275	0,5825	-7
>sp|O70475|UGDH_M	21,63	21,7	21,7	21,7	21,3	22	22	22	22	21,8	22	22	21,1	21	21	22	22,1	21,4	21,751	21,5495	Ugdh	-0,2	21,7	-1,13	0,275	0,5825	-7
>sp|P54822|PUR8_M	21,58	21,3	20,8	21,4	21,2	19,9	21	21	21	20,5	22	21	20	19,3	21	21	21,1	20,4	20,966	20,6502	Adsl	-0,3	20,8	-1,13	0,276	0,5831	-7
>sp|Q9WTI7|MYO1C_I	15,6	17	15,6	16,6	17,2	17,8	18	18	17	16,9	15	16	17,2	16	18	17	15,5	16,9	16,949	16,4946	Myo1c	-0,5	16,7	-1,13	0,276	0,5831	-7
>sp|P01789|HVM20	18,59	18,6	0	18,8	18,2	17,7	19	18	17	18,3	18	18	18,8	18,8	19	18	18,4	17,7	16,235	18,5095	>sp|P017	2,27	17,4	1,127	0,276	0,5831	-7
>sp|P01792|HVM23	18,59	18,6	0	18,8	18,2	17,7	19	18	17	18,3	18	18	18,8	18,8	19	18	18,4	17,7	16,235	18,5095	>sp|P017	2,27	17,4	1,127	0,276	0,5831	-7
>sp|P01793|HVM24	18,59	18,6	0	18,8	18,2	17,7	19	18	17	18,3	18	18	18,8	18,8	19	18	18,4	17,7	16,235	18,5095	>sp|P017	2,27	17,4	1,127	0,276	0,5831	-7
>sp|Q8R2E9|ERO1B_I	19,5	20,1	16,9	18	20,3	17,1	19	17	18	19,1	19	19	19,2	19,3	19	19	18,1	18,6	18,465	18,9765	Ero1b	0,51	18,7	1,124	0,277	0,585	-7
>sp|P18654|KS6A3_	16,24	16,1	16,9	16,4	16,6	16,8	17	18	18	16,9	16	17	16,2	16,6	16	17	16,1	17,4	16,83	16,5496	Rps6ka3	-0,3	16,7	-1,12	0,278	0,5855	-7
>sp|Q68FH4|GALK2_I	18,21	19,6	20,1	18,1	18,3	19,2	18	21	20	20,8	20	21	17,7	19,3	18	20	20	21,3	19,177	19,7663	Galk2	0,59	19,5	1,123	0,278	0,5855	-7
>sp|Q711T7|NADE_M	18,46	19	18,9	18,9	18,9	18,7	19	19	19	18,6	19	19	18,8	19,1	19	18	18,6	18,9	18,882	18,7501	Nadsyn1	-0,1	18,8	-1,12	0,28	0,5886	-7

>sp|P31938|MP2K1	22,35	22,7	21,7	23,1	21,6	21,5	21	22	21	22,1	22	22	21,1	23	23	22	22,4	22,4	21,943	22,2504	Map2k1	0,31	22,1	1,117	0,28	0,5886	-7
>sp|Q8BMF3|MAON_I	16,5	18,9	19,3	17,1	17	16,6	14	14	14	12,5	15	15	16	14,8	15	15	16,1	19,3	16,373	15,3673	Me3	-1	15,9	-1,12	0,28	0,5886	-7
>sp|Q9WV80|SNX1_M	17,98	19,4	18,1	19,7	20,1	20,3	20	20	20	18,6	19	19	19,2	19,2	20	19	18,9	19,3	19,437	19,1081	Snx1	-0,3	19,3	-1,12	0,28	0,5886	-7
>sp|P51569|AGAL_M	17,89	18,5	15,1	16	18,1	17,4	19	19	16	17,4	17	16	16	18,1	18	16	16,8	16,2	17,364	16,7823	Gla	-0,6	17,1	-1,12	0,28	0,5886	-7
>sp|Q5U3K5|RABL6_	14,51	15,4	15,4	0	15	15,3	14	15	15	15	15	15	16	15,2	15	15	14,1	15,2	13,314	15,166	Rabl6	1,85	14,2	1,116	0,28	0,5886	-7
>sp|Q8VDG7|PAFA2_	0	14,9	15,3	15,2	14,8	13,6	15	13	15	12,9	15	15	14,9	15,8	16	15	14,8	14,4	13,042	14,8847	Pafah2	1,84	14	1,116	0,281	0,5887	-7
>sp|Q9D8W5|PSD12_	18,89	18,6	19,5	18,2	18,2	18,7	19	18	19	17,8	19	18	18,7	18,2	19	18	18,6	18,4	18,616	18,3556	Psmd12	-0,3	18,5	-1,11	0,281	0,5891	-7
>sp|P01630|KV2A6_	20,87	20,9	19,3	19,1	19,1	18	18	19	19	18,4	18	19	18,8	19,6	19	19	17,4	18	19,232	18,7571	>sp|P016	-0,5	19	-1,11	0,282	0,5915	-7
>sp|Q78JE5|FBX22_M	20,62	17,8	21,6	21,9	20	21,4	19	19	21	19	19	21	21,1	19,1	21	19	18,6	18,6	20,322	19,6528	Fbxo22	-0,7	20	-1,11	0,283	0,5921	-7
>sp|Q8C7R4|UBA6_M	0	13,2	13,6	0	13,8	12,7	14	13	15	12,2	13	14	13,9	12,2	14	12	11,5	11,9	10,532	12,7517	Uba6	2,22	11,6	1,109	0,284	0,5931	-7
>sp|Q60864|STIP1_M	14,61	14,4	14,8	16,3	15,6	15,6	15	16	16	15,5	16	15	14,6	14	15	15	14,8	15,1	15,362	15,0562	Stip1	-0,3	15,2	-1,11	0,284	0,5931	-7
>sp|Q9CZX8|RS19_M	17,76	17,1	16,3	16,9	16,9	16	18	18	17	18,6	18	16	15	15,4	0	18	16,5	17	17,067	14,9588	Rps19	-2,1	16	-1,11	0,284	0,5935	-7
>sp|Q8BKG3|PTK7_M	16,11	19,6	17,9	18,3	19,7	20,1	20	18	18	17,6	19	20	19,5	20,1	20	18	19,5	18,9	18,605	19,1378	Ptk7	0,53	18,9	1,106	0,285	0,5943	-7
>sp|Q91WL0|ES8L3_M	20,17	20,8	20,7	19,9	19,7	19,9	21	20	17	20	17	20	17,5	19,8	20	20	19,7	19,4	19,832	19,1934	Eps8l3	-0,6	19,5	-1,11	0,285	0,5948	-7
>sp|Q9EPU0|RENT1_M	19,97	20,2	24,6	24,1	24,5	24,5	20	20	21	23,5	24	23	24	23,9	24	21	20,6	24	22,099	23,0647	Upf1	0,97	22,6	1,103	0,286	0,5969	-7
>sp|Q8VHN8|TIRR_M(	19,26	18,8	15,9	18,1	18,3	19,1	19	19	16	17,7	17	18	17,7	18,2	18	18	17,2	16,7	18,226	17,7175	Nudt16l1	-0,5	18	-1,1	0,286	0,5972	-7
>sp|Q60865|CAPR1_	0	0	0	0	14,1	0	14	12	0	0	15	15	0	15,8	0	15	0	12,8	4,4819	8,24337	Caprin1	3,76	6,36	1,101	0,287	0,5973	-7
>sp|O88544|CSN4_M	20,18	19,8	19,2	19,8	19,9	19,4	20	20	20	20,7	20	20	19,6	19,5	19	19	19,5	19,7	19,811	19,6039	Cops4	-0,2	19,7	-1,1	0,287	0,5979	-7
>sp|O08529|CAN2_M	21,14	21,1	21,8	20,2	22	21,6	20	21	22	21,7	21	21	21,4	21,5	22	21	21,9	21,8	21,158	21,447	Capn2	0,29	21,3	1,099	0,288	0,5983	-7
>sp|Q6P5C5|SMUG1_	18,82	18,6	19,1	18,4	20,6	18,3	18	18	19	17	20	20	18,3	17,1	18	18	18,1	18	18,765	18,2644	Smug1	-0,5	18,5	-1,1	0,288	0,5997	-7
>sp|Q9Z2K1|K1C16_	22,67	22	22,6	21	20,4	21,5	20	21	21	20,4	22	21	22,3	22,2	20	23	23	23,2	21,385	21,9352	Krt16	0,55	21,7	1,097	0,289	0,5998	-7
>sp|Q9Z2Q6|SEPT5_M	18,67	19	21,1	20,5	18,9	19	20	19	21	19,2	19	20	19,3	19,3	20	19	19,1	19,1	19,696	19,3207	Sept5	-0,4	19,5	-1,1	0,289	0,6007	-7
>sp|Q7TQE6|MACOI_M	16,04	15,3	16,6	15,1	15,7	16,4	17	16	16	16	16	16	0	15,5	16	15	15,7	15,3	15,929	14,0206	Maco1	-1,9	15	-1,09	0,29	0,6016	-7
>sp|Q8K370|ACD10_	18,43	18,5	18,1	18,8	19,5	18,1	19	19	18	18,8	18	18	19,6	19,6	19	20	18,6	19,2	18,624	18,9534	Acad10	0,33	18,8	1,093	0,29	0,6016	-7
>sp|Q9CQR6|PPP6_M	22,09	22,5	21,6	21,5	22	21,7	22	22	22	21,8	22	22	21,9	21,7	23	22	21,8	22,3	21,886	22,041	Ppp6c	0,15	22	1,09	0,291	0,6039	-7
>sp|P54775|PRS6B_	16,95	18,1	18,7	17,5	18,2	18,8	18	18	18	18,3	18	19	18,9	18,2	18	19	17,8	18,5	18,034	18,2836	Psmc4	0,25	18,2	1,089	0,292	0,6046	-7
>sp|P56677|ST14_M	17,97	17	18,9	18,2	19,1	18,8	19	19	19	18,3	19	18	18	18,3	19	18	18	18,4	18,522	18,2541	St14	-0,3	18,4	-1,09	0,293	0,6056	-7
>sp|P13439|UMPS_M	16,04	16,7	15,7	16,5	16,4	16,4	17	16	16	15,2	17	17	16,2	15,6	16	16	16	15,6	16,364	16,1251	Umps	-0,2	16,2	-1,09	0,293	0,6059	-7
>sp|P61027|RAB10_	22,41	21,5	22,1	22,8	22,6	22,8	23	22	23	20,9	21	23	21,3	23,1	20	23	22,8	22,7	22,408	21,9099	Rab10	-0,5	22,2	-1,09	0,293	0,6066	-7
>sp|Q6P1F6|2ABA_M	20,01	20,7	20,5	21,9	21,8	22,6	20	19	19	20,9	21	20	21,3	21,6	22	21	21	21,1	20,683	21,1281	Ppp2r2a	0,44	20,9	1,081	0,295	0,609	-7
>sp|Q7TSE6|ST38L_M(	16,99	15,1	15,4	17	16,5	15,5	17	13	20	16,6	20	20	14,9	15,7	17	17	17,5	16,1	16,288	17,1954	Stk38l	0,91	16,7	1,081	0,295	0,609	-7
>sp|Q91VJ4|STK38_M	16,99	15,1	15,4	17	16,5	15,5	17	13	20	16,6	20	20	14,9	15,7	17	17	17,5	16,1	16,288	17,1954	Stk38	0,91	16,7	1,081	0,295	0,609	-7
>sp|Q8CI51|PDLI5_M	17,01	16,3	17	16,7	16,5	16,9	16	17	17	17,5	16	16	16,3	16,1	17	16	16,8	16,7	16,719	16,5462	Pdlim5	-0,2	16,6	-1,08	0,295	0,609	-7
>sp|Q80VD1|FA98B_	0	0	0	0	0	0	0	0	15	14	14	15	0	0	0	0	0	0	1,6587	4,75418	Fam98b	3,1	3,21	1,079	0,296	0,61	-7
>sp|Q9WUP7|UCHL5_M	15,79	15,5	15,3	16,6	16,5	16,1	16	16	16	16,1	17	16	15,7	16,1	17	17	16	15,6	15,991	16,1972	Uchl5	0,21	16,1	1,076	0,297	0,6124	-7
>sp|Q91WC3|ACSL6_M	14,48	15,1	15,8	15	15,6	15,9	15	15	15	15,5	16	16	16,4	16,4	16	14	14	15,8	15,258	15,621	Acsl6	0,36	15,4	1,076	0,298	0,6124	-7
>sp|Q9CR57|RL14_M	18,45	15,8	15,5	15,4	16,5	15,8	17	17	16	16,8	14	0	14,8	16,6	17	15	15,6	18,9	16,369	14,3692	Rpl14	-2	15,4	-1,08	0,298	0,6124	-7
>sp|Q8R322|GLE1_M	17,72	18,9	18,4	19,8	20	20,3	19	19	20	18,6	19	19	19,5	19,3	20	19	18,3	18,6	19,287	18,9471	Gle1	-0,3	19,1	-1,07	0,299	0,6137	-7
>sp|Q9D7X3|DUS3_M	19,88	20,8	19	19,8	21	20,2	21	21	21	20	20	21	20,2	20,5	20	20	20	20,9	20,451	20,1469	Dusp3	-0,3	20,3	-1,07	0,3	0,6159	-7
>sp|P84075|HPCA_M	16,21	16	16,7	16,9	16,4	16,1	17	18	17	18,1	19	17	16,1	16,1	16	16	17	17,1	16,593	16,9547	Hpca	0,36	16,8	1,07	0,3	0,6162	-7
>sp|Q8JZK9|HMCS1_I	19,11	19,5	19,8	20,2	18,8	19,9	21	20	20	19,7	20	20	20,9	20,6	20	20	20	19,9	19,811	20,0697	Hmgcs1	0,26	19,9	1,069	0,3	0,6162	-7
>sp|Q9Z2H7|GIPC2	22,11	19,5	20	20,5	20,3	21,3	22	22	22	21,8	20	20	21,6	21,9	22	21	21,6	21,6	20,966	21,3796	Gipc2	0,41	21,2	1,065	0,302	0,6195	-7
>sp|O99P21|MUTYH_	15,36	17	14,9	14,9	17,1	18	17	17	16	16,5	16	18	17,9	17	18	15	17,9	17,3	16,379	16,9257	Mutyh	0,55	16,7	1,063	0,303	0,621	-7
>sp|P33175|KIF5A_M	14,53	13,9	12,9	14,7	13,8	15,5	14	15	14	14,7	12	13	13,8	13,5	15	13	11,9	16,5	14,318	13,73	Kif5a	-0,6	14	-1,06	0,305	0,6238	-7
>sp|A2AX52|CO6A4_	20,95	21,2	18,3	19,4	19,5	19,2	18	19	19	18,1	19	19	18,8	19,7	19	18	19,1	19,1	19,392	18,9588	Col6a4	-0,4	19,2	-1,06	0,306	0,6257	-7
>sp|Q8C1A5|THOP1_	20,63	20,7	21,2	20	20,8	20,3	21	20	20	20	22	22	21,1	20,7	21	20	21,7	19,6	20,551	20,8466	Thop1	0,3	20,7	1,057	0,306	0,6257	-7
>sp|Q00PI9|HNRL2_M	16,82	17,7	17,5	17,5	17,5	17,1	17	18	17	17,6	19	17	17,7	18,1	17	17	16,9	17,4	17,373	17,6063	Hnrnpul2	0,23	17,5	1,056	0,306	0,626	-7
>sp|P97427|DPYL1_I	21,25	21,3	20,7	21,1	20,6	21	21	21	20	20,8	20	21	21	20,8	21	21	20,6	20,8	20,969	20,7895	Crmp1	-0,2	20,9	-1,06	0,307	0,6263	-7

>sp|P14432|HA1T_M	14,96	14,4	13,7	14,6	13,9	13,5	14	14	15	14,1	14	0	14,2	13,7	14	14	14,5	14,3	14,278	12,6208	H2-T3	-1,7	13,4	-1,05	0,307	0,6267	-7
>sp|Q6NXH9|K2C73_	21,72	21,9	22,1	21,5	21	20,9	21	21	21	20,8	21	20	21,8	21,2	22	23	23,3	22,4	21,25	21,6622	Krt73	0,41	21,5	1,052	0,308	0,6282	-7
>sp|P36536|SAR1A_	18,15	15,8	17,7	18,3	17,5	15	18	19	18	18,5	18	18	17,9	17,6	19	18	18,1	18,3	17,562	18,0407	Sar1a	0,48	17,8	1,049	0,309	0,6307	-7
>sp|Q9CYL5|GAPR1_I	21,55	17,4	18	19,5	16,2	15,8	17	16	18	15,1	18	17	16,5	18,2	16	17	17,2	16,5	17,631	16,8965	Glipr2	-0,7	17,3	-1,04	0,311	0,6341	-7
>sp|Q9Z110|P5CS_M	17,28	18	17,7	0	15,4	17,6	14	0	18	0	17	0	14,7	0	15	17	11,4	10,9	13,095	9.467289	Aldh18a1	-3,6	11,3	-1,04	0,312	0,6349	-7
>sp|Q9JHU9|INO1_M(	19,65	20,1	22,5	19,3	19,1	20	20	20	20	19,2	22	20	19,4	18,8	18	19	17,9	20,7	20,009	19,4637	Isyna1	-0,5	19,7	-1,04	0,312	0,6354	-7
>sp|Q91WQ3|SYYC_M	21,98	21,7	20,6	20,9	20,8	20,8	21	21	21	20,9	21	21	20,7	20,7	22	21	21,3	21,1	21,106	20,9127	Yars	-0,2	21	-1,04	0,313	0,6354	-7
>sp|Q8BH04|PCKGM	19,2	17,7	18,4	18,1	18,1	18	18	19	19	18,8	18	18	18,5	18,3	18	18	18	18,3	18,401	18,2004	Pck2	-0,2	18,3	-1,04	0,313	0,6354	-7
>sp|P51885|LUM_M(	23,13	22,9	22,7	23,5	23,3	23,2	23	23	23	23,2	23	23	23,1	23,7	24	23	23,6	23,4	23,21	23,3324	Lum	0,12	23,3	1,036	0,315	0,6402	-7
>sp|Q64669|NQO1_M	21,05	21,4	21,5	21	22,9	23	21	22	21	21,9	22	22	22,6	21,9	22	22	22	21,8	21,75	22,0219	Nqo1	0,27	21,9	1,035	0,316	0,6402	-7
>sp|O08599|STXB1_I	16,05	16	15,6	16,6	15,8	16,1	0	15	15	15,2	15	16	13,6	12,7	0	12	0	15,9	14,002	11,1593	Stxbp1	-2,8	12,6	-1,04	0,316	0,6402	-7
>sp|P47757|CAPZB_	23,83	23,8	22,7	24,5	23,6	25	23	25	24	24,1	24	24	23,8	24	24	22	22	23,9	23,833	23,4492	Capzb	-0,4	23,6	-1,03	0,317	0,6433	-7
>sp|Q9ES46|PARVB_I	0	15,4	15,2	0	0	15,7	0	16	15	16	17	17	0	13,1	0	16	15,8	15,8	8.56026	12,1826	Parvb	3,62	10,4	1,026	0,32	0,6479	-7
>sp|Q9WUR2|ECI2_M	19,66	19,9	20,8	19,3	19,1	17,3	18	21	21	18,2	18	23	17,6	17,6	17	19	17,6	20,5	19,616	18,8076	Eci2	-0,8	19,2	-1,02	0,321	0,6493	-7
>sp|Q9Z0N2|IF2H_MC	20,64	20,5	20,9	21,3	21,6	20,8	21	22	21	21,4	21	21	21,6	21,1	21	21	21,4	21,1	21,083	21,2344	Eif2s3y	0,15	21,2	1,023	0,321	0,6493	-7
>sp|Q9CPT3|NANP_M	21,17	19,6	18,7	18,8	18,3	17,6	18	19	19	19,1	19	19	18,9	19,4	20	19	19,5	19,4	18,974	19,3167	Nanp	0,34	19,1	1,023	0,321	0,6493	-7
>sp|P63330|PP2AA_	24,06	23,5	23,4	23,7	23,5	22,6	23	23	23	23,5	24	23	22,2	22,3	22	23	23,4	23,7	23,363	23,0809	Ppp2ca	-0,3	23,2	-1,02	0,321	0,6493	-7
>sp|Q9D8U8|SNX5_M	14,38	15,7	16,6	16,3	16,7	16,7	14	15	15	13,7	15	16	0	14,9	17	16	16,1	16,5	15,715	13,9088	Snx5	-1,8	14,8	-1,02	0,324	0,6545	-7
>sp|Q9CXA2|T3HPD_	18,81	17,6	18,8	19	19,2	19,4	19	19	19	18,8	18	18	19,3	19,1	19	19	18	18,9	18,882	18,6347	L3hypdh	-0,2	18,8	-1,02	0,325	0,6554	-7
>sp|Q99LI7|CSTF3_M(	16,87	16,8	21,3	21,2	21,5	21,2	22	21	21	19,4	16	20	20,3	19,9	20	20	19,8	20	20,364	19,5261	Cstf3	-0,8	19,9	-1,01	0,325	0,6554	-7
>sp|Q9CT10|RANB3_	18,74	18,7	17,4	18,8	18,4	18,8	19	18	18	17,9	19	19	19	14,5	20	19	13,9	19,1	18,491	17,7859	Ranbp3	-0,7	18,1	-1,01	0,325	0,6554	-7
>sp|Q9JIL4|NHRF3_M	0	17,3	17,4	16,4	17,2	17,4	16	17	17	17,4	17	17	17,4	16,7	18	16	17,1	17	15,103	17,015	Pdzk1	1,91	16,1	1,014	0,325	0,6554	-7
>sp|Q8BJW5|NOL11_	16,08	15,6	15,2	16,4	13,5	16,3	15	15	14	15,9	16	16	16	15,4	15	15	15,3	15,8	15,174	15,5353	Nol11	0,36	15,4	1,013	0,326	0,6554	-7
>sp|Q9CQ92|FIS1_MC	0	0	0	0	0	0	0	0	0	15,9	0	0	0	0	0	0	0	0	0	1,76803	Fis1	1,77	0,88	1,012	0,326	0,656	-7
>sp|P97431|IRF6_MC	0	0	0	0	15,1	0	0	0	0	0	0	0	0	0	0	0	0	0	1,6763	0	Irf6	-1,7	0,84	-1,01	0,326	0,656	-7
>sp|Q8R010|AIMP2_	0	0	0	0	0	0	0	14	0	0	0	0	0	0	0	0	0	0	1,5427	0	Aimp2	-1,5	0,77	-1,01	0,326	0,656	-7
>sp|Q9CQN1|TRAP1_	19,92	16,4	20,5	20,4	19,9	20,6	20	17	17	17,3	22	18	21,4	20,7	23	16	20,4	21,8	19,119	20,0788	Trap1	0,96	19,6	1,009	0,328	0,6578	-7
>sp|Q99MR0|ACL6B_	18,98	19,3	20,1	19,3	19,5	19	19	20	20	19,5	20	20	19,4	19,8	19	18	18,1	18,3	19,434	19,15	Actl6b	-0,3	19,3	-1,01	0,328	0,6578	-7
>sp|Q9JLT2|TREA_MO	18,7	18,9	16	19,4	18,1	16,6	17	17	16	16,8	18	17	16,5	16,3	17	18	17,5	16,7	17,486	17,0017	Treh	-0,5	17,2	-1	0,331	0,664	-7
>sp|Q9QX60|DGUOK_	20,13	17,5	18,7	16,7	17,9	17,3	19	20	19	20,4	21	19	17,1	16	16	17	0	20,4	18,498	16,3397	Dguok	-2,2	17,4	-1	0,332	0,6656	-7
>sp|Q6PIP5|NUDC1_I	18,28	15,4	15,4	0	16,4	16	14	14	15	15,9	15	14	16,2	15,9	15	16	16,2	15,7	13,848	15,62	Nudcd1	1,77	14,7	0,996	0,334	0,6683	-7
>sp|Q8BX80|ENASE_M	16,76	15,8	16,4	16,8	16,3	16,6	16	16	16	16,2	16	16	16,4	16,2	16	16	16,2	16	16,294	16,1517	Engase	-0,1	16,2	-1	0,334	0,6683	-7
>sp|Q9CXF4|TBC15_I	0	0	14,6	15,9	16	14	16	16	12	12,7	14	15	14,3	14	14	13	14,3	13,8	11,626	13,8426	Tbc1d15	2,22	12,7	0,995	0,334	0,6683	-7
>sp|P31254|UBA1Y_	19,22	20,3	20	22,6	22,6	19,5	20	20	20	20,3	19	20	20,4	19,8	19	22	19,5	19,4	20,451	19,9476	Uba1y	-0,5	20,2	-0,99	0,335	0,6683	-7
>sp|Q3TW96|UAP1L_	21,45	21,9	21,1	20,6	20,6	20,8	20	20	21	20,5	21	20	20,9	20,8	21	21	20,5	20,6	20,821	20,6111	Uap1l1	-0,2	20,7	-0,99	0,335	0,6683	-7
>sp|Q9CZU3|MTREX_I	18,8	18,7	18,3	19	18,6	18,4	19	18	18	17,6	18	18	18,7	18,5	18	19	18,4	17,6	18,404	18,1889	Mtrex	-0,2	18,3	-0,99	0,335	0,6683	-7
>sp|Q04519|ASM_M(	14,77	15,3	15	15	14,9	14,9	15	14	14	0	14	15	15,1	15,4	15	15	14,9	15,4	14,886	13,2498	Smpd1	-1,6	14,1	-0,99	0,336	0,6703	-7
>sp|Q9JI75|NQO2_M(	18,87	18,6	17,9	19,7	19,4	18	20	18	18	19,1	18	17	18,3	18,7	19	18	19,1	19,2	18,727	18,3947	Nqo2	-0,3	18,6	-0,99	0,336	0,671	-7
>sp|Q9Z1G3|VATC1_I	19,06	17,7	17,5	17,2	15,6	16,6	17	16	16	16	17	17	17	17,1	17	16	15,8	16,8	16,984	16,618	Atp6v1c1	-0,4	16,8	-0,99	0,337	0,6715	-7
>sp|Q7TNP2|2AAB_M	19,51	17,2	18,4	18,4	15,8	19	18	18	18	17,9	17	19	18,7	18,5	17	21	20,4	18,2	18,117	18,649	Ppp2r1b	0,53	18,4	0,989	0,337	0,6718	-7
>sp|Q05D44|IF2P_M(	16,22	16,9	16,1	16,5	16,3	16,6	17	16	17	16,3	15	17	16,8	16,4	17	17	15,9	16,5	16,531	16,3397	Eif5b	-0,2	16,4	-0,99	0,338	0,673	-7
>sp|P70404|IDHG1_I	17,22	18,1	20,5	17,1	19	20,9	19	19	19	20,1	20	20	17,8	21,2	19	19	17,8	18,7	18,693	19,2635	Idh3g	0,57	19	0,986	0,339	0,6736	-7
>sp|Q8K3H0|DP13A_	20,18	20,6	20,8	20,6	20,4	20,4	16	20	20	20,3	15	20	20	20,1	20	20	20,1	16,2	19,936	19,1253	Appl1	-0,8	19,5	-0,98	0,339	0,675	-7
>sp|P61971|NTF2_M	20,8	21	20,2	20,6	21,3	21,4	22	21	21	21,8	22	20	19,8	19,8	20	21	20,8	21,4	21,013	20,6887	Nutf2	-0,3	20,9	-0,98	0,34	0,6759	-7
>sp|P97471|SMAD4_	17,13	17,7	18,8	17,6	18,8	19,1	18	17	19	17,8	17	18	18,1	18,3	17	18	18	18	18,137	17,8742	Smad4	-0,3	18	-0,98	0,343	0,681	-7
>sp|Q9R190|MTA2_M	0	15,6	14,7	13,6	14,6	16,1	15	15	14	0	14	14	0	14,3	14	14	13,1	12,6	13,211	10,6769	Mta2	-2,5	11,9	-0,98	0,343	0,681	-7
>sp|Q8K386|RAB15_	22,15	21,2	21,7	22,5	22,1	22,5	22	22	22	20,6	20	23	21	22,8	18	22	22,5	22,4	22,067	21,5515	Rab15	-0,5	21,8	-0,98	0,343	0,681	-7
>sp|Q91W97|HKDC1	17,67	16,3	17	17,8	17,7	17,6	18	17	16	21,1	15	17	16,6	16,8	21	16	16,4	20,9	17,196	17,9886	Hkdc1	0,79	17,6	0,975	0,344	0,6818	-7

>sp|Q9DB27|MCTS1_	20,38	21,1	20,7	21,1	19,7	21,1	22	21	22	21,2	21	21	21,4	19,9	21	22	21,2	21,4	20,931	21,1847	Mcts1	0,25	21,1	0,974	0,344	0,6822	-7
>sp|Q9DBP5|KCY_MC	20,8	21,2	21,2	21,2	20,9	21	22	21	22	21,5	21	21	21,4	20,8	21	21	21,1	21,2	21,251	21,1049	Cmpk1	-0,1	21,2	-0,97	0,345	0,6827	-7
>sp|Q149F1|RUSD2_I	17,66	16,1	15,1	17,8	14,8	14,1	14	14	13	13,6	14	15	14,9	14,5	14	14	14	16,7	15,176	14,5607	Rpusd2	-0,6	14,9	-0,97	0,345	0,6827	-7
>sp|Q9JII6|AK1A1_M	24,3	24,3	24,4	25	25,3	25,1	25	25	25	24,8	25	25	25,6	25,2	25	25	24,7	25,4	24,809	24,9825	Akr1a1	0,17	24,9	0,971	0,346	0,6836	-7
>sp|Q9D1Q6|ERP44_	22,38	20,5	20,4	21,8	21,1	20,9	22	22	21	21,1	20	20	21,2	21	21	22	22,2	19,9	21,268	20,9215	Erp44	-0,3	21,1	-0,97	0,348	0,6878	-7
>sp|Q8K2Q2|GSTO2_I	21,64	21,5	0	24	24,4	21,9	22	23	18	23,7	23	23	23,9	21,9	22	17	22,1	22,2	19,638	22,1441	Gsto2	2,51	20,9	0,965	0,349	0,6883	-7
>sp|Q8BHG1|NRDC_M	19,69	20	19,7	19,7	19,4	20,1	20	20	21	20,5	20	20	20,1	19,6	20	20	20,1	20,1	19,93	20,0711	Nrdc	0,14	20	0,965	0,349	0,6883	-7
>sp|P01942|HBA_M(	28,41	28,8	27,1	28,4	26,9	26	28	28	28	27,4	26	28	27,4	27,5	27	28	27,7	27,4	27,752	27,4274	Hba	-0,3	27,6	-0,96	0,349	0,6886	-7
>sp|Q9R0H5|K2C71_	21,85	22	22,1	21,6	21,1	21	21	21	21	20,9	21	20	21,9	21,3	22	23	23,5	22,4	21,354	21,727	Krt71	0,37	21,5	0,961	0,35	0,6907	-7
>sp|Q9Z0N1|IF2G_MC	21,02	20,9	21,5	21,7	21,8	21,3	21	22	22	21,7	21	22	21,8	21,6	22	21	21,8	21,5	21,467	21,5855	Eif2s3x	0,12	21,5	0,961	0,351	0,6907	-7
>sp|O08528|HXK2_M	19,85	17,9	18,4	19	19	19,4	19	19	17	17,9	18	19	19,1	18,7	17	20	18,4	17,4	18,784	18,3798	Hk2	-0,4	18,6	-0,96	0,351	0,6912	-7
>sp|O35639|ANXA3_	18,05	19,5	19,6	19,7	20,3	20	20	20	20	19,5	20	20	20,1	20	20	20	19,7	19,6	19,645	19,8657	Anxa3	0,22	19,8	0,959	0,351	0,6912	-7
>sp|P08905|LYZ2_M(	18,28	19,8	20,3	17,2	19,5	20,3	20	20	20	20,1	20	21	20,1	19,9	20	19	19,9	19,3	19,539	19,9098	Lyz2	0,37	19,7	0,954	0,354	0,6964	-7
>sp|Q91WR5|AK1CL_	16,79	18,2	18,5	18,4	18	18,3	19	18	18	17,4	18	18	18	18	18	18	17,9	17,7	18,095	17,8899	Akr1c21	-0,2	18	-0,95	0,354	0,6967	-7
>sp|Q9ESY9|GILT_MOL	19,23	19,4	19	18,7	19,3	19,9	19	20	20	21,1	19	21	18,7	18,7	19	19	20,6	20,8	19,38	19,7746	Ifi30	0,39	19,6	0,953	0,355	0,6967	-7
>sp|Q62441|TLE4_M(	18,46	18,8	18,1	18,5	18,5	18,2	18	19	18	19,7	18	17	18,2	18,6	19	19	19,5	17,7	18,401	18,6629	Tle4	0,26	18,5	0,951	0,356	0,698	-7
>sp|Q9QZ08|NAGK_M	21,75	22,3	24,5	24,2	24,5	24,2	24	24	24	21,5	24	24	23,8	23,8	24	23	23,6	23,4	23,78	23,3852	Nagk	-0,4	23,6	-0,95	0,356	0,6982	-7
>sp|Q6PHN9|RAB35_	22,03	21,1	21,7	22,4	22,1	22,4	22	22	22	20,5	20	23	21	22,7	19	22	22,5	22,3	22	21,5512	Rab35	-0,4	21,8	-0,95	0,356	0,6982	-7
>sp|Q6PIC6|AT1A3_M	0	13,6	13,5	14	14,3	13,5	0	0	13	8,49	0	14	14,4	13,8	15	13	12,9	13,7	9.06104	11,6539	Atp1a3	2,59	10,4	0,948	0,357	0,6996	-7
>sp|Q8K3A0|HSC20_	17,24	17,3	20,8	17,1	17,4	18,1	17	0	16	17,7	21	18	0	0	0	18	18,2	17,3	15,634	12,2027	Hscb	-3,4	13,9	-0,95	0,358	0,7002	-7
>sp|Q62440|TLE1_M(	18,5	18,8	18,2	18,6	18,6	18,3	18	19	18	19,7	19	17	18,3	18,6	19	19	19,5	17,8	18,452	18,7139	Tle1	0,26	18,6	0,946	0,358	0,7002	-7
>sp|P62717|RL18A_	19,73	21,1	20,1	19,2	20,2	19,3	21	21	19	18,9	18	20	20	19,3	20	20	20,3	20,2	20,001	19,6647	Rpl18a	-0,3	19,8	-0,95	0,358	0,7002	-7
>sp|Q6PIE5|AT1A2_M	0	13,5	13,3	13,9	14,2	13,4	0	0	13	8,43	0	14	14,4	13,8	15	13	12,7	13,5	8.99619	11,5643	Atp1a2	2,57	10,3	0,945	0,358	0,7003	-7
>sp|P61759|PFD3_M	18,55	19,4	18,5	19,7	20,3	19	19	20	19	19,6	19	18	19	19,3	19	19	19,1	18,8	19,28	19,0319	Vbp1	-0,2	19,2	-0,94	0,359	0,7005	-7
>sp|Q9DCT2|NDUS3_I	17,91	18,1	17,5	13,9	15,2	16,5	14	18	18	16,1	18	17	18	18,2	16	16	15,8	17,8	16,498	17,121	Ndufs3	0,62	16,8	0,943	0,359	0,7012	-7
>sp|Q99J83|ATG5_M	17,26	16,4	17	16,9	15,7	16,5	17	17	17	16,4	16	17	16,5	16,3	16	17	17,1	16,1	16,689	16,4816	Atg5	-0,2	16,6	-0,94	0,36	0,7025	-7
>sp|P16054|KPCE_M	15,81	15,6	13,4	0	0	0	0	0	0	8,76	0	0	13,7	11,5	0	12	12,9	12,9	4,9878	7,99709	Prkce	3,01	6,49	0,94	0,361	0,7034	-7
>sp|Q8K2B3|SDHA_M	23,31	23,7	21,9	23,4	23,5	21	23	24	24	22,7	23	23	23,2	22,7	23	23	22,7	22,2	23,075	22,7642	Sdha	-0,3	22,9	-0,94	0,362	0,7049	-7
>sp|P11859|ANGT_M	15,59	15,6	15,3	15,9	15,4	15,9	16	16	15	16	17	17	16,1	14	16	16	15,5	15,9	15,691	16,0246	Agt	0,33	15,9	0,938	0,362	0,7049	-7
>sp|Q9CQW9|IFM3_M	0	0	20,2	0	0	16,8	0	17	16	17,9	17	17	0	17,7	19	0	0	18,1	7.81911	11,7922	Ifitm3	3,97	9,81	0,937	0,362	0,7053	-7
>sp|P17533|DFAR1_	16,02	16,4	23,5	23,4	22,2	22,3	24	23	23	20,7	23	23	21,3	21,7	23	23	23,2	23,2	21,49	22,4679	Defa-rs1	0,98	22	0,936	0,363	0,7057	-7
>sp|Q6IFZ9|K2C74_M	21,93	22,1	22,2	21,7	21,1	21	21	21	21	21	21	20	21,9	21,3	22	23	23,5	22,4	21,424	21,7868	Krt74	0,36	21,6	0,936	0,363	0,7057	-7
>sp|Q9EPC1|PARVA_	20,61	21,4	21,1	21,3	21,3	21,4	22	21	21	21,3	21	22	21,4	21,7	22	21	21,6	21,3	21,263	21,3863	Parva	0,12	21,3	0,935	0,363	0,7058	-7
>sp|Q78PG9|CCD25_	20,07	19,6	20,1	19,9	19,2	19,8	19	19	21	19,2	19	21	20,1	20,1	20	20	20	20,1	19,715	19,9597	Ccdc25	0,24	19,8	0,934	0,364	0,7061	-7
>sp|O88531|PPT1_M	20,37	20,4	18,9	18,3	19,7	20,1	18	18	18	18,3	18	19	18,6	18,6	19	19	18,5	20,7	19,168	18,7894	Ppt1	-0,4	19	-0,93	0,364	0,7061	-7
>sp|P97321|SEPR_M	19,82	20	19,6	15,9	19,3	20,9	20	17	19	15,8	23	23	18,4	18,1	18	23	22,9	18	19,101	20,1146	Fap	1,01	19,6	0,933	0,364	0,7065	-7
>sp|P14148|RL7_MC	16,92	20,6	19,7	17,2	17,3	16,9	17	17	18	17,5	18	19	18,6	17,9	18	18	17,4	21,2	17,783	18,3366	Rpl7	0,55	18,1	0,931	0,365	0,7078	-7
>sp|O88796|RPP30_	14,49	15,3	15,2	16,5	14,1	15,2	15	15	16	16,1	15	14	14,4	15,8	15	16	15,9	16,3	15,07	15,399	Rpp30	0,33	15,2	0,929	0,366	0,7093	-7
>sp|Q6NV83|SR140_	14,74	16,1	17,2	16,9	17,4	17,2	16	17	17	16,2	17	15	16,6	17	17	15	15	16,9	16,578	16,2017	U2surp	-0,4	16,4	-0,93	0,367	0,7101	-7
>sp|Q61532|MK06_I	17,37	17,1	14,6	16,3	15,7	16	17	16	16	15,1	16	16	17,4	17,1	17	17	16,5	16,6	16,093	16,4638	Mapk6	0,37	16,3	0,928	0,367	0,7101	-7
>sp|Q9CQR4|ACO13_	21,23	20,2	0	20,7	15,3	18,1	16	20	19	18	20	19	19	18,5	20	16	17,2	19,7	16,637	18,6783	Acot13	2,04	17,7	0,927	0,367	0,7104	-7
>sp|Q91VJ2|CAVN3_	19,51	19,5	17,9	19,4	19,3	17,6	19	19	20	18	18	20	18,9	19,3	19	18	18,8	17,7	18,962	18,6379	Cavin3	-0,3	18,8	-0,92	0,37	0,714	-7
>sp|Q99LE6|ABCF2_M	16,79	16,6	17,8	16,8	16,1	16,2	17	16	17	16,7	16	17	16,6	17,3	17	17	17,2	17	16,657	16,8602	Abcf2	0,2	16,8	0,922	0,37	0,714	-7
>sp|Q99LF4|RTCB_M(	20,39	20,9	20,5	20,3	21	20,6	20	21	21	20,4	20	21	20,5	20,7	21	20	20,2	20,1	20,583	20,4868	Rtcb	-0,1	20,5	-0,92	0,37	0,714	-7
>sp|Q61820|RANT_M	22,84	22	22,7	23,1	23,1	22,9	23	22	19	20,9	23	23	22,9	23,1	23	23	22,4	22,4	22,272	22,6975	Rasl2-9	0,43	22,5	0,921	0,371	0,7141	-7
>sp|P11930|NUD19_	18,38	16	15,3	15,5	0	15,7	14	16	16	16,3	16	16	14,7	15	17	16	16	15,4	14,083	15,7301	Nudt19	1,65	14,9	0,921	0,371	0,7141	-7
>sp|P07214|SPRC_M	17,54	17,4	15	16	16,1	16	16	16	16	15,6	0	15	16,3	16,8	17	16	16,3	16,6	16,145	14,4721	Sparc	-1,7	15,3	-0,92	0,371	0,7141	-7
>sp|P97823|LYPA1_I	22,72	25	24,2	22,6	26,3	24	27	24	24	23,9	24	23	23,3	24,4	24	24	24,3	24,5	24,413	23,9168	Lypla1	-0,5	24,2	-0,91	0,374	0,7198	-7

>sp|P58044|IDI1_MC	21,67	20,9	21,7	21	20,2	20,5	22	21	21	21,4	21	21	20,9	21	21	22	22,1	20,9	21,054	21,2627	Idi1	0,21	21,2	0,912	0,375	0,7212	-7
>sp|P06909|CFAH_M	14,9	14,3	15,4	16,1	15,4	15,4	15	14	15	8,98	13	12	15,9	15,9	16	15	15,6	15,5	15,049	14,2967	Cfh	-0,8	14,7	-0,91	0,375	0,7219	-7
>sp|Q91Y86|MK08_M	20,59	20,9	21,1	20,8	20,4	20,5	21	21	18	20,8	21	21	17,8	17,5	18	21	20,9	20,6	20,429	19,8768	Mapk8	-0,6	20,2	-0,91	0,376	0,722	-7
>sp|Q6P5G0|MK04_I	17,28	17	14,5	16,2	15,6	15,8	16	15	15	14,9	15	16	17,2	16,9	17	17	16,4	16,5	15,963	16,3276	Mapk4	0,36	16,1	0,91	0,376	0,722	-7
>sp|Q91X83|METK1_	18,76	18,9	18,8	18,5	18,6	19,3	18	19	19	19,5	19	19	19,1	19,3	17	19	17,4	17,3	18,813	18,5261	Mat1a	-0,3	18,7	-0,91	0,376	0,7228	-7
>sp|Q8K010|OPLA_M	21,07	19,8	19,9	20,5	19,6	19,2	20	21	20	21,7	20	20	19,7	20,1	21	21	20,4	20,1	20,142	20,3893	Oplah	0,25	20,3	0,908	0,377	0,723	-7
>sp|Q9WU65|GLPK2_	21,83	22	19,6	19,8	19,8	18,2	22	20	21	20,5	21	20	19,7	18	20	20	21	20	20,514	20,0293	Gk2	-0,5	20,3	-0,91	0,378	0,7238	-7
>sp|Q01065|PDE1B_	15,62	17,4	16,2	15,3	16,3	16,5	14	15	14	12,6	0	15	17,1	16	17	17	15,7	15,4	15,614	13,9587	Pde1b	-1,7	14,8	-0,91	0,378	0,7238	-7
>sp|Q9D0K2|SCOT1_I	21,41	21,8	21,7	21,8	21	21,3	21	21	22	21,7	22	22	21,6	21,7	22	21	21,3	21,4	21,421	21,5556	Oxct1	0,13	21,5	0,906	0,378	0,7244	-7
>sp|P62827|RAN_MO	23,24	23,4	23,7	23,3	24	23,9	24	22	23	23	24	24	24	24	24	23	23,4	22,7	23,36	23,5778	Ran	0,22	23,5	0,901	0,381	0,7285	-7
>sp|P62320|SMD3_M	19,26	18,8	19	18,3	18	17,9	18	19	17	17,6	19	19	19,1	18,9	19	18	17,9	18,1	18,319	18,6222	Snrpd3	0,3	18,5	0,9	0,381	0,7285	-7
>sp|Q9JM14|NT5C_M	22,17	21,4	22,1	22,2	22,5	22,1	22	23	23	22,8	23	23	22,2	22,1	22	22	22,1	22,3	22,215	22,3605	Nt5c	0,15	22,3	0,9	0,381	0,7285	-7
>sp|Q03734|SPA3M_	19,92	20	18,6	19,2	18,5	19,1	19	19	19	20	20	20	19,8	19,1	18	19	19	19,9	19,179	19,4023	Serpina3n	0,22	19,3	0,899	0,382	0,7285	-7
>sp|Q8BHZ0|FA49A_I	17,43	16,1	18,5	17,2	17,9	18,4	18	18	18	17,8	20	17	16	17,1	17	18	16,6	17,6	17,804	17,4221	Fam49a	-0,4	17,6	-0,9	0,382	0,7285	-7
>sp|Q61831|MK10_I	20,43	20,7	20,9	20,6	20,3	20,3	20	21	18	20,6	21	21	17,6	17,3	18	20	20,7	20,4	20,245	19,6969	Mapk10	-0,5	20	-0,9	0,382	0,7285	-7
>sp|Q64311|NTAN1_	16,33	15,6	14,2	16,8	16,6	15,3	17	0	16	16,7	15	17	14,5	16,3	17	15	13,4	16,9	14,147	15,7765	Ntan1	1,63	15	0,898	0,382	0,7285	-7
>sp|Q8K009|AL1L2_I	21,3	21,7	20,6	17,7	20,1	19,5	20	20	21	19,8	20	20	19,6	19,9	20	20	19,6	19,8	20,192	19,8448	Aldh1l2	-0,3	20	-0,9	0,382	0,7285	-7
>sp|P28352|APEX1_	20,28	20,3	20,1	19,7	20,8	19,7	20	20	21	20,8	20	21	20,7	21,1	20	19	20,3	20,4	20,299	20,4921	Apex1	0,19	20,4	0,895	0,384	0,7303	-7
>sp|O89079|COPE_M	22,17	21,3	21,3	21,2	21,5	21,2	22	23	22	22,7	23	21	21,1	21	21	21	20,9	21,5	21,723	21,4493	Cope	-0,3	21,6	-0,9	0,384	0,7303	-7
>sp|Q9WTU6|MK09_I	20,58	20,8	21	20,7	20,4	20,5	21	21	18	20,7	21	21	18,1	17,7	18	21	20,8	20,5	20,423	19,916	Mapk9	-0,5	20,2	-0,89	0,384	0,7308	-7
>sp|Q9R0M5|TPK1_M	21,56	18,5	19,5	21,1	20,8	20,7	22	21	20	20,7	21	20	20,9	18,2	20	20	19,6	20,7	20,535	20,1299	Tpk1	-0,4	20,3	-0,89	0,385	0,733	-7
>sp|P48758|CBR1_M	24,73	24,9	22,4	24,4	24,5	22,2	25	25	25	24,6	23	24	25,1	24,9	25	25	24,7	25	24,162	24,5382	Cbr1	0,38	24,4	0,889	0,387	0,7354	-7
>sp|P50431|GLYC_M	24,56	23,9	24,9	22,5	24,6	22,7	25	23	23	23,9	25	25	23,9	24,2	23	24	23,8	24	23,736	24,0787	Shmt1	0,34	23,9	0,889	0,387	0,7354	-7
>sp|Q61699|HS105_	22,04	21	20	20,6	21,5	20,9	22	20	20	20,6	20	21	20,6	20,7	21	21	20,7	20,8	20,945	20,7132	Hsph1	-0,2	20,8	-0,89	0,389	0,7381	-7
>sp|Q8K3W0|BABA2	18,54	18,4	18,7	15,7	18,1	17,6	19	17	19	18,6	19	19	17,3	18,5	18	18	17	18,7	17,906	18,2685	Babam2	0,36	18,1	0,884	0,39	0,7395	-7
>sp|Q9CQ26|STABP_I	19,07	19,4	18,7	17,9	18,8	18,8	19	20	20	19,9	20	19	19,2	18,2	19	18	18,1	18	19,104	18,7938	Stambp	-0,3	18,9	-0,88	0,39	0,7401	-7
>sp|Q91Y47|FA11_M	18,52	19,9	23,2	19,9	19	19,1	20	19	19	18,4	22	19	18,9	19,1	19	19	18,6	19,1	19,761	19,2494	F11	-0,5	19,5	-0,88	0,391	0,7401	-7
>sp|P46467|VPS4B_	16,62	16,9	15,9	16,9	16,8	17	16	16	16	15,8	16	17	17,5	16,2	18	15	15,8	15,1	16,526	16,211	Vps4b	-0,3	16,4	-0,88	0,392	0,7431	-7
>sp|P61211|ARL1_M	17,53	16,9	17,2	13,5	18,7	17,6	17	19	18	18,2	18	18	17,3	18	17	18	17,1	18	17,303	17,7645	Arl1	0,46	17,5	0,877	0,393	0,7446	-7
>sp|Q9D2M8|UB2V2	21,2	24,1	21,3	20,2	24	24,7	21	21	21	21,2	21	22	21,2	24,4	21	21	20,9	21,2	22,161	21,5967	Ube2v2	-0,6	21,9	-0,87	0,395	0,7462	-7
>sp|Q80WP8|GADL1_	17,23	16,9	16,4	15,4	14,8	0	16	15	15	15,1	16	13	16	16,6	17	16	14,8	16,4	13,945	15,5206	Gadl1	1,58	14,7	0,874	0,395	0,7462	-7
>sp|P55258|RAB8A_	22,49	21,6	22	22,7	22,4	22,7	23	22	23	20,8	21	23	21,4	23,1	20	23	22,7	22,6	22,325	21,9602	Rab8a	-0,4	22,1	-0,87	0,396	0,7473	-7
>sp|P63094|GNAS2_	18,1	18,1	17,2	18,8	19,3	18,8	19	18	17	15,8	18	19	19,2	19,1	19	19	19,7	19,6	18,317	18,7157	Gnas	0,4	18,5	0,872	0,396	0,7476	-7
>sp|Q01405|SC23A_	20,9	20,4	21,2	20,9	21,1	21,3	21	21	21	21,3	21	21	21,4	21,1	21	21	21	21,1	20,984	21,0931	Sec23a	0,11	21	0,871	0,396	0,7479	-7
>sp|Q8CGN5|PLIN1_M	0	0	18,1	0	0	12,4	0	17	18	0	14	0	15,4	13,3	14	11	12,7	12,9	7.33251	10,3916	Plin1	3,06	8,86	0,868	0,398	0,7507	-7
>sp|Q8BZ98|DYN3_M	15,69	15,8	15,5	15,1	14,9	15,6	15	16	15	17,5	15	17	13	16,4	13	16	17,6	18,6	15,402	15,9876	Dnm3	0,59	15,7	0,867	0,398	0,7509	-7
>sp|Q9DB77|QCR2_M	16,81	19,8	20,6	17,7	19,9	20,2	17	20	20	18,4	19	19	18,6	18,3	18	18	18,2	20,5	19,217	18,7273	Uqcrc2	-0,5	19	-0,87	0,399	0,7509	-7
>sp|P70288|HDAC2_	20,15	20,3	18,8	19	19	18,7	19	19	19	18,8	19	20	19,7	19,8	19	19	18,7	19,7	19,177	19,3864	Hdac2	0,21	19,3	0,865	0,399	0,752	-7
>sp|Q504N0|CBPA2_	18,72	17,6	17,2	16,8	17,4	18,6	19	18	18	18,2	18	18	16,7	16,7	17	18	18,2	17,6	17,907	17,61	Cpa2	-0,3	17,8	-0,86	0,401	0,7541	-7
>sp|Q9D8C4|IN35_M	18,42	18,2	18,4	18	17,5	17,3	15	17	16	15,5	17	16	16,2	18,1	19	16	16,6	18	17,385	16,9544	Ifi35	-0,4	17,2	-0,86	0,402	0,7552	-7
>sp|P61161|ARP2_M	23,68	23,8	24,1	23,4	23,5	24,5	24	23	24	24	24	24	24,3	24,3	23	24	23,6	23,7	23,801	23,9468	Actr2	0,15	23,9	0,859	0,403	0,7565	-7
>sp|Q4VBE8|WDR18_	14,41	16,3	16,3	16,3	15,6	16,4	16	17	17	15,2	16	17	15,7	15,3	16	16	15,7	15,6	16,119	15,8674	Wdr18	-0,3	16	-0,86	0,403	0,7565	-7
>sp|Q9D753|EXOS8_I	0	16,1	16,2	17,4	16	15,8	15	17	16	16,8	16	16	14,8	16,3	16	16	16,7	15,8	14,433	15,983	Exosc8	1,55	15,2	0,859	0,403	0,7565	-7
>sp|Q8K2Q7|BROX_M	0	17,7	15,1	16,8	15,5	16,1	15	17	17	15,7	17	16	15,7	15,9	16	16	16,1	15,7	14,436	15,9929	Brox	1,56	15,2	0,857	0,404	0,7578	-7
>sp|Q8C1B7|SEP11_I	25,16	21,5	20,8	20,7	21,1	20,7	21	21	21	20,8	20	21	21,2	20,8	21	21	21,1	21,7	21,419	20,9941	Sept11	-0,4	21,2	-0,85	0,405	0,7596	-7
>sp|P53810|PIPNA_I	21,04	20,8	19,3	19	18,6	18,5	19	19	19	19,7	19	19	19,5	19,6	20	20	19,7	19,8	19,376	19,6446	Pitpna	0,27	19,5	0,854	0,405	0,7596	-7
>sp|Q62384|ZPR1_M	16,06	0	14,5	13,7	16,7	16,7	16	15	15	15	15	15	14,6	14,7	14	14	16,7	17,5	13,682	15,1904	Zpr1	1,51	14,4	0,854	0,406	0,7596	-7
>sp|P62908|RS3_MO	20,43	22,2	22,6	21,4	22,6	22,9	22	22	22	22,2	22	22	22,8	22,5	23	21	22,2	21,9	21,949	22,2135	Rps3	0,26	22,1	0,851	0,407	0,7609	-7

>sp|P01864|GCAB_M	18,18	18,3	19	18,9	18,9	18,1	18	19	18	18,7	18	16	18,5	17,6	19	19	18,7	18,6	18,452	18,128	>sp|P018	-0,3	18,3	-0,85	0,407	0,7609	-7
>sp|Q8CHP8|PGP_M(	20,08	19,9	19,9	20,1	20,9	20,4	19	20	20	20	21	20	20,1	20,3	20	20	20,1	20,8	20,085	20,2548	Pgp	0,17	20,2	0,851	0,407	0,7609	-7
>sp|Q9Z1X4|ILF3_MO	19,37	17,9	20,8	19,7	18,5	20,1	18	19	19	19,4	20	20	19	19,5	20	19	18,9	19,6	19,175	19,4852	Ilf3	0,31	19,3	0,85	0,408	0,762	-7
>sp|Q9WVB2|TLE2_M	18,12	18,4	17,6	18	18	18,1	18	18	18	19,6	18	17	17,8	18,4	19	19	19,3	17,5	18,111	18,3807	Tle2	0,27	18,2	0,849	0,408	0,762	-7
>sp|P23953|EST1C_M	17,84	17,8	18	15,2	15,3	20,4	21	21	21	22	17	19	14,7	14	14	20	14,9	21,1	18,545	17,4472	Ces1c	-1,1	18	-0,85	0,408	0,7624	-7
>sp|Q8VE70|PDC10_	17,15	18,4	16,8	16,3	18,1	18,1	17	19	19	16,1	17	16	16,6	17,9	16	16	16,4	21,8	17,725	17,1354	Pdcd10	-0,6	17,4	-0,85	0,409	0,7624	-7
>sp|Q3UNA4|NXT2_M	18,36	18,4	17,5	18,3	18,2	18,5	18	18	17	17,7	17	18	18,6	17,9	19	19	18,7	18,8	18,028	18,2422	Nxt2	0,21	18,1	0,848	0,409	0,7624	-7
>sp|Q3THG9|AASD1_I	18,19	17,2	20,1	18	18,1	20,1	15	18	17	19	19	19	18,7	18,8	19	18	17,8	17,6	18,015	18,4522	Aarsd1	0,44	18,2	0,846	0,41	0,7632	-7
>sp|Q8VCT4|CES1D_M	17,96	18,1	18,2	16,2	15,2	20,3	21	21	21	21,9	18	19	16	13,9	14	20	15,4	21	18,678	17,6739	Ces1d	-1	18,2	-0,84	0,411	0,7663	-7
>sp|P62259|1433E_	23,72	25,1	24	25,6	24,6	24	24	24	23	23,4	24	24	23,8	23,3	25	24	24,4	23,6	24,232	23,992	Ywhae	-0,2	24,1	-0,84	0,413	0,7681	-7
>sp|Q02257|PLAK_M	21,67	21,5	21,6	21,4	21,1	21,3	21	21	22	21	21	21	21,3	21,4	21	22	22	22,1	21,345	21,5124	Jup	0,17	21,4	0,84	0,413	0,7684	-7
>sp|P59383|LRRN4_	15,75	16,5	16,9	14,9	15,7	15,7	15	12	16	17	19	16	15,4	17,6	15	14	15,3	15,5	15,424	16,0124	Lrrn4	0,59	15,7	0,837	0,414	0,7704	-7
>sp|Q9DBB5|IF4E3_M	19,21	17,3	15,9	17,7	17,6	17,6	17	17	17	17	16	17	17,9	16,9	17	18	17,2	17,2	17,389	17,1121	Eif4e3	-0,3	17,3	-0,84	0,415	0,7705	-7
>sp|P61028|RAB8B_	22,5	21,7	22	22,8	22,5	22,7	23	22	23	21,1	21	23	21,4	23,1	20	23	22,7	22,6	22,367	22,0392	Rab8b	-0,3	22,2	-0,83	0,417	0,7743	-7
>sp|Q9Z2D0|MTMR9_	15,14	16,2	14,4	15,6	15,3	14,4	15	16	16	13,9	17	15	15,5	14,6	16	14	14,2	15,4	15,329	15,0023	Mtmr9	-0,3	15,2	-0,83	0,418	0,7763	-7
>sp|Q9DBD0|ICA_MO	20,7	19,6	20	20,6	19,6	19,9	21	20	19	19	20	19	20,2	20,2	21	20	19,7	19,5	20,006	19,8015	Ica	-0,2	19,9	-0,83	0,419	0,7769	-7
>sp|Q9JHU2|PALMD_	14,85	17,6	16,5	18,1	0	16,2	17	16	16	15,8	14	17	15,9	16,7	16	17	17	17,1	14,628	16,1701	Palmd	1,54	15,4	0,824	0,422	0,7815	-7
>sp|Q9D1G1|RAB1B_	22,95	21,5	22	22,6	22,6	22,6	23	22	23	21,6	22	23	21,5	22,6	21	23	22,7	22,7	22,424	22,1975	Rab1b	-0,2	22,3	-0,82	0,422	0,7816	-7
>sp|Q9ERL9|GCYA3_M	19,81	16,6	17,1	17,3	15,3	14,2	17	17	17	16,1	19	17	15,9	16,9	18	17	16,7	17,6	16,713	17,2059	Gucy1a3	0,49	17	0,818	0,425	0,7869	-7
>sp|P05784|K1C18_	23,04	20,6	19,3	20,8	19,2	19,4	18	20	20	17,8	20	21	19,1	21,3	20	23	21,5	23,3	20,127	20,7104	Krt18	0,58	20,4	0,816	0,426	0,7891	-7
>sp|O35309|NMI_MC	19,79	20,4	20,4	20,7	19,9	20,6	21	21	20	20,8	20	20	20,9	20,2	20	21	18,7	20,2	20,408	20,1936	Nmi	-0,2	20,3	-0,81	0,429	0,793	-7
>sp|P31324|KAP3_M	20,44	19,6	20,6	19,3	18,9	19,1	20	19	19	19,4	19	20	20	19,4	20	19	19	18,9	19,575	19,364	Prkar2b	-0,2	19,5	-0,81	0,429	0,793	-7
>sp|Q5F2E7|NUFP2_M	17,64	18,6	14,7	19,1	13,9	13,1	19	18	18	16,3	14	0	18,7	12,6	19	19	18,7	18,7	16,98	15,2178	Nufip2	-1,8	16,1	-0,81	0,43	0,7941	-7
>sp|Q7TN29|SMAP2_	16,3	17,1	15,8	16,4	15,5	15,2	15	16	15	14,3	15	16	15,8	15,6	15	15	15,2	17,2	15,826	15,5404	Smap2	-0,3	15,7	-0,81	0,431	0,7951	-7
>sp|Q9EPB5|SERHL_M	18,91	17,7	18,6	19,2	18,3	18,2	18	18	18	18,8	19	18	18,3	18,7	18	18	19,8	18,4	18,368	18,5659	Serhl	0,2	18,5	0,807	0,431	0,7954	-7
>sp|Q8BHA3|DTD2_M	21,75	17,7	22,5	19,8	19,8	20,4	20	20	21	19,6	21	21	19,9	20,2	20	22	21,8	22,1	20,361	20,7985	Dtd2	0,44	20,6	0,803	0,434	0,7998	-7
>sp|Q9CQ62|DECR_M	21,61	21,6	24	21,3	24,2	24,3	21	20	20	21,1	21	24	21,4	21,2	22	21	21,4	21,6	22,098	21,6074	Decr1	-0,5	21,9	-0,8	0,435	0,801	-7
>sp|Q8C0L6|PAOX_M	20,1	20,2	22,5	20,5	22,1	20,2	20	20	20	18,2	20	19	20,6	21,1	21	20	20,5	21	20,594	20,2278	Paox	-0,4	20,4	-0,8	0,435	0,8011	-7
>sp|Q9EQG3|SCEL_MC	15,55	15	16,6	15,6	15	16	14	15	14	13,2	15	15	14,8	16,3	16	14	14,7	14,4	15,225	14,9046	Scel	-0,3	15,1	-0,8	0,435	0,8016	-7
>sp|Q9D8S3|ARFG3_I	18,09	18,1	16,8	18,9	16,7	17,1	19	18	18	17,1	19	17	17,5	18,3	19	19	18,8	18,4	17,815	18,1289	Arfgap3	0,31	18	0,798	0,436	0,8025	-7
>sp|Q8VCW2|K1C25	21,77	21,7	20,5	20,2	20	16,3	20	20	19	19,4	19	19	22,4	18,5	19	22	23	22,4	19,923	20,5573	Krt25	0,63	20,2	0,796	0,437	0,804	-7
>sp|Q8CGK7|GNAL_M	17,8	17,8	16,1	18,6	19,2	18,6	19	18	16	14,7	17	19	19,2	18,8	19	19	19,6	19,5	17,896	18,3869	Gnal	0,49	18,1	0,796	0,437	0,804	-7
>sp|P62748|HPCL1_	17,63	18,2	16,8	16,3	16,8	17,3	17	16	18	17,2	17	17	17,1	16,5	17	18	17,6	18,1	17,037	17,2703	Hpcal1	0,23	17,2	0,795	0,438	0,8045	-7
>sp|P80315|TCPD_M	21,76	21,9	19,7	19,5	19	19,1	19	19	20	21	20	21	21,2	20,3	21	19	19,1	19,6	19,945	20,3074	Cct4	0,36	20,1	0,795	0,438	0,8045	-7
>sp|P01639|KV5A7	18,73	18,7	0	18,4	17,8	18,8	18	17	17	17,4	0	0	17,6	17,7	18	17	17,6	16,5	16,075	13,5154	Gm5571	-2,6	14,8	-0,79	0,439	0,8047	-7
>sp|Q9QYG0|NDRG2_	18,69	18,6	18,1	18,7	17,6	18,9	18	18	18	18	18	18	19,1	18,9	19	19	18,2	18,5	18,399	18,5347	Ndrg2	0,14	18,5	0,792	0,44	0,8067	-7
>sp|P80318|TCPG_M	21,4	21,4	21	21,1	21,3	21,5	21	21	21	21,2	21	21	21,4	21,6	21	21	21,3	21,3	21,273	21,1866	Cct3	-0,1	21,2	-0,79	0,44	0,8068	-7
>sp|Q9D7G0|PRPS1_	23,05	22,1	22,8	22,1	22,3	22,8	22	23	23	22,8	21	22	22,9	20	23	23	22,6	22,7	22,484	22,2118	Prps1	-0,3	22,3	-0,79	0,441	0,8083	-7
>sp|P18872|GNAO_M	17,63	17,6	15,9	18,5	19	18,5	18	18	16	14,5	17	18	19	18,7	19	19	19,4	19,3	17,728	18,2115	Gnao1	0,48	18	0,784	0,444	0,8132	-7
>sp|Q9Z320|K1C27_	21,87	21,8	20,6	20,3	20,1	16,4	20	20	19	19,5	20	19	22,5	18,6	19	22	23,1	22,4	20,01	20,6357	Krt27	0,63	20,3	0,783	0,445	0,8139	-7
>sp|Q99K85|SERC_M	21,46	21	20,8	20,9	22,7	20,5	21	21	21	21,3	21	22	21,9	21,2	21	21	21	21,1	21,186	21,3608	Psat1	0,18	21,3	0,783	0,445	0,8139	-7
>sp|Q91XD6|VPS36	0	15,4	16,4	15,3	15	15,2	15	15	15	13	15	15	15,7	15,9	15	16	15,1	13,2	13,548	14,8819	Vps36	1,33	14,2	0,775	0,449	0,8195	-7
>sp|P27600|GNA12_	17,73	17,7	16	18,6	19,1	18,6	19	18	16	14,6	17	18	19,1	18,8	19	19	19,5	19,4	17,813	18,2921	Gna12	0,48	18,1	0,775	0,449	0,8195	-7
>sp|O35566|CD151_	17,61	18,4	20,5	17,8	18	18,4	17	17	16	18,4	18	17	16,3	17,8	18	17	17,5	17,5	17,97	17,6338	Cd151	-0,3	17,8	-0,78	0,449	0,8195	-7
>sp|Q8VCR7|ABHEB_	21,16	20,6	21	20,7	21,7	20,7	21	21	21	21	21	21	21,1	20,7	21	21	20,7	21,1	21,057	20,939	Abhd14b	-0,1	21	-0,78	0,449	0,8195	-7
>sp|Q6PDI6|MINY2_M	18,44	17,8	18,5	18	13,9	18,4	18	17	17	17,7	18	18	18,2	14,1	18	15	15,6	18,1	17,527	16,9717	Mindy2	-0,6	17,2	-0,77	0,449	0,8195	-7
>sp|Q68FL6|SYMC_MC	22,78	15,2	14,5	22,4	22,5	12,9	15	14	22	13,8	15	16	15	13,5	16	22	21,9	15,7	17,929	16,5497	Mars	-1,4	17,2	-0,77	0,45	0,8195	-7
>sp|Q9JKB1|UCHL3_I	21,36	20,1	20,7	20,5	20,2	20,6	20	21	21	21,8	21	20	20,4	20,7	20	20	20	20,2	20,645	20,4511	Uchl3	-0,2	20,5	-0,77	0,451	0,8212	-7

>sp|Q64726|ZA2G_M	14,69	17,4	17,9	15	17,8	18,1	18	18	16	16,9	16	16	17	17	18	17	14,4	16,6	16,969	16,5418	Azgp1	-0,4	16,8	-0,77	0,451	0,8212	-7
>sp|Q9QYC0|ADDA_M	15,68	17,4	19,6	18,5	18,9	19,2	18	19	20	17,6	20	20	20,2	19,7	20	18	17,6	17,6	18,446	18,8951	Add1	0,45	18,7	0,771	0,452	0,8217	-7
>sp|Q99LS3|SERB_MC	18,74	18,7	16,6	18,8	18,6	21,5	17	15	15	20,5	15	21	21,5	21,3	17	17	17	17,2	17,849	18,6551	Psph	0,81	18,3	0,769	0,453	0,8231	-7
>sp|Q9CQ21|MCTS2_	17,55	19	18,2	19,4	18,3	20,2	20	20	21	20,7	20	20	18,8	18,6	19	21	19,8	19	19,285	19,6285	Mcts2	0,34	19,5	0,768	0,454	0,8245	-7
>sp|Q62095|DDX3Y_	18,6	19,2	19,4	19,2	18,7	19,1	19	19	19	18,8	19	20	19,1	18,8	19	19	19	18,5	19,139	19,0247	Ddx3y	-0,1	19,1	-0,77	0,454	0,8245	-7
>sp|P27601|GNA13_	17,54	17,5	15,9	18,4	18,9	18,4	18	18	16	14,4	17	18	18,9	18,6	18	19	19,3	19,2	17,656	18,1286	Gna13	0,47	17,9	0,765	0,455	0,8257	-7
>sp|P22892|AP1G1_	18,86	19,3	21,7	22,3	19,1	22,1	19	20	19	22,7	22	23	19,7	19,9	20	19	19,6	19,6	20,088	20,6243	Ap1g1	0,54	20,4	0,763	0,456	0,8275	-7
>sp|Q91WU5|AS3MT_	23,02	22,1	25,1	22	23,1	24,5	23	21	23	23,2	21	24	23,9	21,5	25	22	21,7	21,1	22,996	22,5446	As3mt	-0,5	22,8	-0,76	0,457	0,8286	-7
>sp|Q505F5|LRC47_I	22,22	20,1	17,6	17,4	21,3	21,4	20	20	18	19,9	18	17	19,5	19,1	21	21	20,1	17,3	19,717	19,16	Lrrc47	-0,6	19,4	-0,76	0,458	0,8298	-7
>sp|Q9QXK3|COPG2_	16,91	16,7	14,1	15	15,1	14,6	16	15	13	14,4	17	15	14,9	16,1	16	15	15,2	15,5	15,064	15,4142	Copg2	0,35	15,2	0,759	0,458	0,8303	-7
>sp|P04117|FABP4_	19,76	17,7	18,4	19,6	20,3	19,4	19	17	17	18,8	18	18	20,7	20	20	20	17,6	19,9	18,752	19,1901	Fabp4	0,44	19	0,758	0,459	0,8314	-7
>sp|Q8BHJ9|SLU7_MC	16,97	17,1	16,1	0	15,9	15,6	16	15	15	15,4	13	16	16	16,3	16	16	15,8	16,7	14,312	15,6799	Slu7	1,37	15	0,754	0,461	0,8347	-7
>sp|Q62193|RFA2_M	16,98	18,9	18,8	18,1	18,3	18,6	19	19	19	18,4	19	18	18,7	18,6	19	18	18,5	18,4	18,418	18,5774	Rpa2	0,16	18,5	0,75	0,464	0,8384	-7
>sp|P35585|AP1M1	19,09	18,5	18,8	18,9	18,5	18,8	19	19	18	19	18	18	19,2	19,4	19	19	18,5	18,7	18,673	18,8346	Ap1m1	0,16	18,8	0,75	0,464	0,8384	-7
>sp|Q9DCT1|AKCL2_I	21,11	24	22,8	23,2	21,7	23,4	22	23	22	22,6	22	22	23,4	23,1	23	23	23,1	23,1	22,558	22,826	Akr1e2	0,27	22,7	0,749	0,464	0,8389	-7
>sp|Q99J39|DCMC_M	15,77	18,9	15,5	15,9	18,6	15,5	19	16	15	16,2	17	17	15,1	16,4	16	15	17,7	14,4	16,626	16,1518	Mlycd	-0,5	16,4	-0,75	0,466	0,8414	-7
>sp|O35685|NUDC_M	18,07	17,9	16	17,2	17,2	16,6	17	18	16	17	16	18	17,7	17,7	18	17	17,3	17,1	17,132	17,353	Nudc	0,22	17,2	0,745	0,467	0,8417	-7
>sp|Q9ERG2|STRN3_M	18,05	18	21,1	18,1	19,4	18,4	18	18	18	19,5	19	20	19,6	18,4	18	19	18	17,8	18,537	18,8484	Strn3	0,31	18,7	0,745	0,467	0,8417	-7
>sp|Q922H4|GMPPA_	22,4	21,7	23,2	23,2	21,3	21,2	21	22	22	21,9	23	23	22,3	22,4	22	23	22,4	21,5	22,081	22,2886	Gmppa	0,21	22,2	0,745	0,467	0,8417	-7
>sp|Q8R1B4|EIF3C_M	18,97	16,4	20,4	16,8	16,8	17	16	17	17	17,1	22	21	16,9	17,3	18	16	17,3	16,6	17,392	17,9641	Eif3c	0,57	17,7	0,736	0,472	0,8502	-7
>sp|P16406|AMPE_M	20,97	20,8	21,5	20,7	21,3	22	21	21	21	21,1	21	21	20,6	21,5	21	21	21,2	20,7	21,231	21,1122	Enpep	-0,1	21,2	-0,74	0,472	0,8502	-7
>sp|O89110|CASP8_	20,01	18,7	20,7	19,2	19	19,6	19	19	20	19,4	20	20	20,1	18,7	19	18	18,3	18,6	19,414	19,1507	Casp8	-0,3	19,3	-0,73	0,474	0,8524	-7
>sp|Q9DBT5|AMPD2_	17,27	16,8	16,4	17,8	18,3	17,9	18	16	16	16,8	15	18	17,1	17,7	18	16	17,2	16,4	17,233	16,9599	Ampd2	-0,3	17,1	-0,73	0,474	0,8525	-7
>sp|Q8CI75|DI3L2_M	18,55	18,6	17,9	18,7	18,3	17,5	18	18	18	18,3	19	18	17,7	18,7	19	20	18,2	17,5	18,198	18,3906	Dis3l2	0,19	18,3	0,732	0,474	0,8525	-7
>sp|P40936|INMT_M	19,84	20,3	20,4	22,6	21,6	21,7	22	21	22	21,7	20	21	22,3	21,6	22	19	20,4	21	21,318	20,978	Inmt	-0,3	21,1	-0,73	0,475	0,8528	-7
>sp|P26516|PSMD7_	18,07	18,7	17,5	17,9	16,4	17,5	18	18	18	18	18	18	18,4	18,1	19	18	18	17,5	17,841	18,0269	Psmd7	0,19	17,9	0,73	0,475	0,8536	-7
>sp|P16546|SPTN1_I	19,21	19,1	19	18,9	19	18,8	19	20	20	19,7	19	19	18,5	18,7	19	19	20,2	19,4	19,269	19,073	Sptan1	-0,2	19,2	-0,73	0,476	0,8543	-7
>sp|Q9DB05|SNAA_M	19,37	19,3	18,6	18,6	19,5	20	20	21	21	19,6	19	19	18,6	19,9	20	20	20	19,9	19,736	19,4743	Napa	-0,3	19,6	-0,73	0,477	0,8551	-7
>sp|Q9D1P4|CHRD1_	20,83	22,7	20,7	20,4	19,7	22,8	20	22	22	19,5	20	20	22,8	22,9	19	20	22,9	18,8	21,218	20,7207	Chordc1	-0,5	21	-0,73	0,478	0,856	-7
>sp|P10605|CATB_M	22,42	22,5	22,4	21,9	22,4	22,5	22	23	23	23,1	22	23	22,7	22,6	22	22	22	21,9	22,583	22,4304	Ctsb	-0,2	22,5	-0,73	0,478	0,8562	-7
>sp|Q8CHT0|AL4A1_I	15,55	16	15,7	0	15,9	14,5	15	16	16	14,8	16	16	15,2	13,7	15	15	15,6	13,8	13,837	15,1006	Aldh4a1	1,26	14,5	0,725	0,479	0,8568	-7
>sp|Q99LB7|SARDH_I	17,82	17,5	16,7	17,7	17,7	17,8	18	16	16	17,2	17	18	17,8	17,5	18	17	17,3	17,4	17,23	17,4084	Sardh	0,18	17,3	0,725	0,479	0,8568	-7
>sp|Q9EQ80|NIF3L_M	20,75	20,6	20,4	20,2	20	20,2	20	20	20	20,3	20	20	20,7	20,2	21	20	20,3	21,1	20,342	20,4531	Nif3l1	0,11	20,4	0,723	0,48	0,8582	-7
>sp|Q9D020|5NT3A_	19,31	18,6	20,1	19,2	20,5	20	21	21	20	20,5	19	21	20,8	20,3	20	20	20,2	20,1	19,969	20,2028	Nt5c3a	0,23	20,1	0,722	0,481	0,8582	-7
>sp|P16092|FGFR1_I	16,03	13,9	16,5	14,6	18,4	14,5	16	16	18	18	16	13	16,7	16,4	14	16	15,8	13,3	16,058	15,5185	Fgfr1	-0,5	15,8	-0,72	0,481	0,8582	-7
>sp|Q3TRM8|HXK3_M	19,13	17,9	20,8	20	19,9	20,7	20	20	19	18,7	17	19	20,1	20,1	20	21	19,6	18,4	19,683	19,3181	Hk3	-0,4	19,5	-0,72	0,481	0,8582	-7
>sp|Q9CQ19|MYL9_M	20,81	23,1	21,7	23,8	21,7	21,1	24	24	22	23,1	20	24	20,7	24,1	24	20	20,4	20,4	22,5	21,951	Myl9	-0,5	22,2	-0,72	0,482	0,8593	-7
>sp|Q9CZD3|GARS_M	21,23	20	19,7	20,3	21,2	20,9	20	20	20	19,9	20	20	20,6	20,3	24	20	20,6	20,4	20,399	20,7273	Gars	0,33	20,6	0,72	0,482	0,8593	-7
>sp|P30285|CDK4_M	17,33	15	17,9	15,9	19,8	16,1	17	17	20	19,3	17	15	17,9	17,7	16	17	17,1	14,9	17,393	16,8776	Cdk4	-0,5	17,1	-0,72	0,484	0,8607	-7
>sp|Q80YP0|CDK3_M	17,33	15	17,9	15,9	19,8	16,1	17	17	20	19,3	17	15	17,9	17,7	16	17	17,1	14,9	17,393	16,8776	Cdk3	-0,5	17,1	-0,72	0,484	0,8607	-7
>sp|Q64277|BST1_M	14,98	14,5	14,4	14,5	14,4	17,2	14	16	16	14,2	14	15	16,7	13,6	20	16	14,4	16,1	15,077	15,5918	Bst1	0,52	15,3	0,717	0,484	0,8607	-7
>sp|Q62264|THRSP_I	22,22	18,1	20,6	22,7	19,7	21,3	16	20	18	15,4	16	20	22	23,2	22	22	22,5	21,7	19,736	20,6011	Thrsp	0,87	20,2	0,716	0,484	0,8607	-7
>sp|P62137|PP1A_M	23,53	23,4	23,4	23,5	23,3	23,5	23	24	24	23,7	23	23	22,9	23,6	23	23	23,5	23,7	23,481	23,4105	Ppp1ca	-0,1	23,4	-0,72	0,484	0,8607	-7
>sp|Q9JM71|K1B27_	21	20,7	20,6	20,8	23,2	21,7	22	21	21	21,9	21	21	21,8	22	21	22	21,8	21,1	21,359	21,5621	Klk1b27	0,2	21,5	0,712	0,486	0,8644	-7
>sp|Q8BM72|HSP13_	18,93	18,1	18,2	18,1	18,1	19,1	17	18	18	17,9	18	18	18,1	18,4	18	19	20,1	17,9	18,236	18,4544	Hspa13	0,22	18,3	0,71	0,488	0,866	-7
>sp|Q61206|PA1B2_	20,02	19,5	19,1	18,9	18,6	18	20	20	20	21,8	21	19	18,3	17,7	18	21	21	20,6	19,275	19,6637	Pafah1b2	0,39	19,5	0,709	0,488	0,866	-7
>sp|Q61851|FGFR3_I	16,1	14	16,6	14,7	18,6	14,6	16	16	18	18	16	13	16,7	16,5	15	16	15,9	13,4	16,136	15,6079	Fgfr3	-0,5	15,9	-0,71	0,488	0,866	-7
>sp|Q8BYA0|TBCD_M	17,18	16,7	16	16,7	15,3	17	17	16	16	15	16	15	16,1	18,5	18	16	16,3	14,9	16,473	16,1126	Tbcd	-0,4	16,3	-0,71	0,489	0,8666	-7

>sp|P62878|RBX1_M	21,54	18,8	19,2	20	20,1	19,9	18	19	18	19,2	19	19	19,7	19,8	20	20	19,7	19,6	19,337	19,6197	Rbx1	0,28	19,5	0,707	0,489	0,8666	-7
>sp|Q04859|MAK_M	16,14	14	16,6	14,7	18,6	14,6	16	16	18	18,1	16	13	16,8	16,5	15	16	15,9	13,5	16,18	15,6579	Mak	-0,5	15,9	-0,71	0,489	0,8666	-7
>sp|Q9JM76|ARPC3_	23,54	22,1	21,7	23,1	22,8	22,1	23	22	23	22,5	22	22	22,3	22	23	23	22,4	22,7	22,589	22,4328	Arpc3	-0,2	22,5	-0,71	0,49	0,8666	-7
>sp|P15949|K1KB9_	20,31	21	21,2	20,8	20,1	20,8	20	20	20	19,7	21	21	20,7	20,5	21	19	20	20,1	20,443	20,2774	Klk1b9	-0,2	20,4	-0,71	0,49	0,8666	-7
>sp|Q3ULD5|MCCB_M	16,47	17,5	17,5	16	17,3	15,3	18	17	18	17,1	19	19	17	17,3	17	17	16,3	17,1	16,991	17,2641	Mccc2	0,27	17,1	0,705	0,491	0,8681	-7
>sp|Q9JMK0|B4GT5_	18,62	16,5	17	18,2	16,6	17,1	17	17	17	17,3	17	18	15,6	15,5	17	18	17,2	17,6	17,195	16,9328	B4galt5	-0,3	17,1	-0,7	0,491	0,8682	-7
>sp|Q9D0R2|SYTC_M(	23,42	22,4	23,2	23,4	22,2	22,2	23	23	24	23,1	23	22	23,4	23,4	23	23	22,4	23	22,9	23,0573	Tars	0,16	23	0,703	0,492	0,8694	-7
>sp|P49442|INPP_M	18,89	18,4	17,3	18,3	18,4	18,9	19	19	18	19,1	17	18	19	18,1	19	17	17,8	18,8	18,362	18,1535	Inpp1	-0,2	18,3	-0,7	0,493	0,8709	-7
>sp|P68254|1433T_	24,4	25,6	23,9	26,6	24,2	24,8	25	25	25	24,5	25	25	25,2	24,9	26	25	25,2	24,7	24,883	25,0892	Ywhaq	0,21	25	0,7	0,494	0,8709	-7
>sp|Q8K1R7|NEK9_M	17,4	17,7	15,7	15,6	14,2	17,5	15	15	18	17	18	18	18,1	15,9	15	18	15,9	14,6	16,324	16,7849	Nek9	0,46	16,6	0,7	0,494	0,8709	-7
>sp|P25444|RS2_MC	18,15	18,4	17,6	18,5	18,8	19	19	19	19	18,2	18	19	19,2	19,2	18	19	18,9	18,5	18,57	18,7145	Rps2	0,14	18,6	0,697	0,495	0,8734	-7
>sp|P97377|CDK2_M	17,05	14,8	17,6	15,7	19,5	15,7	17	17	19	19	17	14	17,6	17,4	15	17	16,8	14,7	17,123	16,6243	Cdk2	-0,5	16,9	-0,7	0,496	0,8741	-7
>sp|Q9R1T4|SEPT6_M	25,23	21,2	20	20	20,4	20,6	21	20	21	20,2	20	21	20,6	20	21	21	20,8	21,1	20,983	20,5995	Sept6	-0,4	20,8	-0,7	0,496	0,8741	-7
>sp|Q9ES64|USH1C_M	0	0	0	0	0	0	0	12	0	0	13	13	0	0	0	0	0	0	1,3	2,8869	Ush1c	1,59	2,09	0,695	0,497	0,8748	-7
>sp|Q9D6Y7|MSRA_M	21,48	21,8	19,5	20,7	20,7	21,2	21	20	20	20,5	21	21	20,4	20,5	21	20	20,2	20,5	20,621	20,4273	Msra	-0,2	20,5	-0,69	0,498	0,8759	-7
>sp|P11440|CDK1_M	17,16	14,9	17,6	15,8	19,6	15,8	17	17	19	19,1	17	15	17,8	17,5	15	17	16,9	14,8	17,208	16,7107	Cdk1	-0,5	17	-0,69	0,499	0,8761	-7
>sp|Q99J95|CDK9_M	17,16	14,9	17,6	15,8	19,6	15,8	17	17	19	19,1	17	15	17,8	17,5	15	17	16,9	14,8	17,208	16,7107	Cdk9	-0,5	17	-0,69	0,499	0,8761	-7
>sp|Q03142|FGFR4_I	16,23	14,1	16,7	14,8	18,7	14,8	16	16	19	18,2	16	13	16,9	16,6	15	16	16	13,7	16,276	15,7734	Fgfr4	-0,5	16	-0,69	0,499	0,8761	-7
>sp|Q9JKV2|ICK_MOI	16,2	14,1	16,7	14,8	18,6	14,7	16	16	18	18,1	16	13	16,8	16,6	15	16	16	13,6	16,224	15,7166	Ick	-0,5	16	-0,69	0,499	0,8761	-7
>sp|P49443|PPM1A	17,41	20,7	18	19,8	19,5	19,9	20	20	20	19,1	18	18	19,7	18,4	20	20	19,3	19,7	19,433	19,1482	Ppm1a	-0,3	19,3	-0,69	0,5	0,8765	-7
>sp|P51855|GSHB_M	20,84	22,1	18,2	21,9	21,7	21,6	21	22	22	21,8	18	20	20,7	20,3	20	22	21,9	22,1	21,229	20,8237	Gss	-0,4	21	-0,69	0,501	0,8781	-7
>sp|Q9D358|PPAC_M	21,37	21,8	21,6	21,6	21,6	22,9	22	22	22	21,5	21	22	22,4	22	22	21	21,6	21,4	21,824	21,6955	Acp1	-0,1	21,8	-0,68	0,505	0,8841	-7
>sp|P97494|GSH1_M	18,5	20,3	20,7	18,1	20,4	20,9	21	21	20	20,2	20	20	19,9	20	19	20	20,2	19,1	20,17	19,8953	Gclc	-0,3	20	-0,68	0,505	0,8845	-7
>sp|Q9CQW1|YKT6_M	20,08	20,6	19,7	18,9	19,6	20,1	20	21	21	20,3	21	20	19,1	20,1	20	20	20,2	19,1	20,077	19,9016	Ykt6	-0,2	20	-0,68	0,507	0,8872	-7
>sp|Q04735|CDK16_	16,59	14,4	17,2	15,3	19,2	15,4	17	17	19	18,6	17	14	17,3	17,1	15	17	16,4	14,3	16,717	16,2281	Cdk16	-0,5	16,5	-0,68	0,508	0,8889	-7
>sp|Q8K0D0|CDK17_	16,52	14,4	17,1	15,3	19,1	15,2	17	17	19	18,6	17	14	17,2	17	15	17	16,4	14,1	16,649	16,1584	Cdk17	-0,5	16,4	-0,67	0,509	0,8902	-7
>sp|P49615|CDK5_M	17,7	16	18,4	17,9	19,9	17	18	18	20	19,3	17	17	18,1	18	17	18	18	16,9	18,037	17,7101	Cdk5	-0,3	17,9	-0,67	0,51	0,8912	-7
>sp|P15327|PMGE_M	20,52	19,1	21	20,6	20,9	21,9	22	22	20	21,4	20	22	20,7	19,9	21	21	20	20,7	20,948	20,6741	Bpgm	-0,3	20,8	-0,67	0,511	0,8929	-7
>sp|Q9WTZ1|RBX2_M	21,09	18,3	19,6	18,6	18,9	19,5	18	20	19	17,3	21	21	20,2	20,4	20	18	18,3	20,8	19,271	19,6264	Rnf7	0,36	19,4	0,67	0,512	0,8936	-7
>sp|Q99LI8|HGS_MOU	16,37	18	18,2	16,5	17,7	17,7	18	16	17	16,4	17	17	17,8	18	17	18	17,8	17,7	17,302	17,4939	Hgs	0,19	17,4	0,67	0,512	0,8936	-7
>sp|Q9JHU3|CDK20_	16,96	14,8	17,5	15,6	19,5	15,6	17	17	19	19	17	14	17,6	17,4	15	17	16,8	14,6	17,044	16,5636	Cdk20	-0,5	16,8	-0,67	0,512	0,8936	-7
>sp|Q3U0B3|DHR11_	23,81	24,4	23,6	23,7	24,1	23,9	24	24	24	24	24	24	23,9	24,3	24	24	23,9	24,2	23,998	24,0773	Dhrs11	0,08	24	0,669	0,513	0,8936	-7
>sp|P17183|ENOG_M	23,18	23,3	23,1	22,9	23,8	22,2	24	24	24	23,8	24	23	23	22,9	23	24	23	22,6	23,347	23,1761	Eno2	-0,2	23,3	-0,67	0,513	0,8936	-7
>sp|P62192|PRS4_M	18,14	18,3	17,5	18,1	18	18,1	18	17	18	17,5	18	18	18,4	18,4	18	18	17,4	17,9	17,973	18,0849	Psmc1	0,11	18	0,666	0,515	0,8962	-7
>sp|P63213|GBG2_M	15,79	16	21,4	21,3	19	18,7	21	21	21	19,5	20	20	20	20,2	20	20	19,5	20,1	19,431	19,9232	Gng2	0,49	19,7	0,663	0,516	0,8986	-7
>sp|O35495|CDK14_	16,64	14,5	17,2	15,4	19,2	15,4	17	17	19	18,7	17	14	17,3	17,2	15	17	16,5	14,4	16,777	16,3006	Cdk14	-0,5	16,5	-0,66	0,517	0,899	-7
>sp|Q04899|CDK18_	16,64	14,5	17,2	15,4	19,2	15,4	17	17	19	18,7	17	14	17,3	17,2	15	17	16,5	14,4	16,777	16,3006	Cdk18	-0,5	16,5	-0,66	0,517	0,899	-7
>sp|P14234|FGR_MC	16,52	14,4	17,1	15,2	19,1	15,2	17	17	19	18,6	17	14	17,2	17	15	17	16,4	14,1	16,641	16,1584	Fgr	-0,5	16,4	-0,66	0,518	0,899	-7
>sp|P16277|BLK_MC	16,52	14,4	17,1	15,2	19,1	15,2	17	17	19	18,6	17	14	17,2	17	15	17	16,4	14,1	16,641	16,1584	Blk	-0,5	16,4	-0,66	0,518	0,899	-7
>sp|Q9QXE7|TBL1X_M	19,77	20,4	19,3	19,5	20,3	19,6	20	20	20	19,6	20	20	19,6	19,9	20	20	19,4	19,6	19,854	19,7494	Tbl1x	-0,1	19,8	-0,66	0,519	0,9004	-7
>sp|Q3V3A1|CDK15_	16,74	14,5	17,3	15,5	19,3	15,5	17	17	19	18,8	17	14	17,4	17,2	15	17	16,6	14,4	16,843	16,3678	Cdk15	-0,5	16,6	-0,66	0,519	0,9008	-7
>sp|Q8VDN2|AT1A1_	17,71	18	19,5	18,6	19,3	18,6	17	19	18	18,8	19	19	18,2	17,7	18	18	17,6	17,6	18,412	18,2269	Atp1a1	-0,2	18,3	-0,66	0,52	0,9011	-7
>sp|Q7TMW6|NARFL_	16,17	17,6	18,1	17,6	17,2	17,1	17	17	18	17,6	17	17	16,8	16,5	17	17	17,7	17,2	17,34	17,1971	Narfl	-0,1	17,3	-0,65	0,522	0,9043	-7
>sp|Q61191|HCFC1_	19,34	19,1	17,3	19,2	17,6	17,9	18	17	17	17,7	17	17	19,3	19	18	19	18,7	18,8	18,037	18,2965	Hcfc1	0,26	18,2	0,653	0,523	0,9055	-7
>sp|Q9D172|ES1_MO	21,68	21,3	23,4	22,5	23,2	22,6	23	23	22	22,1	22	22	22,2	22,4	22	22	22,8	23,4	22,492	22,305	D10Jhu8	-0,2	22,4	-0,65	0,523	0,9057	-7
>sp|Q9DAJ2|TEKT1_M	18,35	18	17,9	15,1	16,9	17,4	18	16	17	17,6	16	16	17,4	15,5	17	17	17,7	17,6	17,149	16,842	Tekt1	-0,3	17	-0,65	0,524	0,9067	-7
>sp|Q9WVJ2|PSD13_	22,3	22,7	21,6	21,3	21,4	21,6	21	21	21	21,4	22	22	21,6	21,9	20	21	21,5	21,6	21,571	21,4172	Psmd13	-0,2	21,5	-0,65	0,525	0,9074	-7
>sp|Q3UMC0|SPAT5_	14,02	21,6	21,3	21,6	15,6	15,3	22	16	15	8,6	13	15	20,3	20,2	14	20	20	20	17,944	16,782	Spata5	-1,2	17,4	-0,65	0,527	0,9102	-7

>sp|P70268|PKN1_M	17,4	16,7	17,1	16,2	21,1	20,1	20	20	16	16,2	20	20	16,7	14,1	17	19	16,5	19,4	18,351	17,7492	Pkn1	-0,6	18	-0,65	0,527	0,9102	-7
>sp|Q5SUV5|MYLK4_I	21,01	21,2	21,4	21,1	20,8	20,9	21	22	14	21,2	22	22	17,6	17,6	18	21	17,7	21	20,393	19,7758	Mylk4	-0,6	20,1	-0,64	0,529	0,913	-7
>sp|E9Q7P9|CDHR2_	20,7	20,5	16,9	20,5	17,4	17,6	18	18	17	18,1	18	18	18,2	18,2	18	19	18	18,3	18,529	18,183	Cdhr2	-0,3	18,4	-0,64	0,529	0,913	-7
>sp|P62313|LSM6_M	19,43	19,1	20,6	20,4	20,9	20,4	20	20	20	20,1	20	20	20,3	20,7	21	20	20	20,3	20,129	20,2576	Lsm6	0,13	20,2	0,642	0,53	0,913	-7
>sp|P63242|IF5A1_M	22,23	22,3	21,4	22	22,1	21,6	22	22	22	21,9	22	22	22,1	22,1	22	22	21,5	21,8	21,964	21,8692	Eif5a	-0,1	21,9	-0,64	0,53	0,9131	-7
>sp|Q810P2|OD3L1_	18,78	18,4	18,3	15,6	17,3	17,9	18	16	18	18	16	16	17,8	16	18	18	18,1	18	17,575	17,2778	Odf3l1	-0,3	17,4	-0,64	0,53	0,9131	-7
>sp|Q9D0B8|RIBC1_I	18,78	18,4	18,3	15,6	17,3	17,9	18	16	18	18	16	16	17,8	16	18	18	18,1	18	17,575	17,2778	Ribc1	-0,3	17,4	-0,64	0,53	0,9131	-7
>sp|P14685|PSMD3_	19,5	19,3	20	19	19,1	19,5	19	18	19	19,1	20	19	19	19	19	19	19,2	19,5	19,258	19,1488	Psmd3	-0,1	19,2	-0,64	0,531	0,9131	-7
>sp|Q8R0K2|TRI31_M	16,07	15,7	15,7	15,3	0	13,9	15	14	15	0	16	16	14,8	15	14	15	0	14	13,418	11,6596	Trim31	-1,8	12,5	-0,64	0,532	0,9156	-7
>sp|Q62422|OSTF1_M	20,27	20,5	18,6	20,6	19,9	19,3	19	20	17	21	18	18	21,3	19,4	19	20	20,6	20,6	19,503	19,8481	Ostf1	0,35	19,7	0,635	0,534	0,9182	-7
>sp|Q8R238|SDSL_MO	17,45	17,1	17,7	16,9	18	17,8	18	18	17	16,4	17	18	17,3	18	18	16	18	17,8	17,576	17,3744	Sdsl	-0,2	17,5	-0,63	0,535	0,9193	-7
>sp|O35490|BHMT1_	16,58	16,7	16,7	16,8	16,5	16,3	17	17	16	15,9	17	17	16,7	16,8	17	17	16,9	16,1	16,703	16,5962	Bhmt	-0,1	16,6	-0,63	0,536	0,921	-7
>sp|P21614|VTDB_M	17,65	19,7	18,4	18,3	18	18,6	18	22	21	20,3	19	19	18,1	18,7	19	18	18,2	18,2	19,081	18,747	Gc	-0,3	18,9	-0,63	0,537	0,9219	-7
>sp|Q9D646|KRT34_	16,51	0	20,3	20,1	20	19,8	17	20	20	18,1	19	18	18,3	18,5	18	18	18,9	18,9	17,059	18,4219	Krt34	1,36	17,7	0,629	0,538	0,9224	-7
>sp|Q921J2|RHEB_M	16,85	16,2	15,5	14,8	16,6	17,2	0	16	16	15,6	14	15	15	14,9	16	15	15,4	17,2	14,324	15,4554	Rheb	1,13	14,9	0,626	0,54	0,9252	-7
>sp|P01887|B2MG_M	16,47	16,8	17,6	18,7	17,7	16,3	19	19	17	17,2	18	18	17,7	18	16	19	19,2	18,7	17,63	17,9214	B2m	0,29	17,8	0,625	0,54	0,9257	-7
>sp|Q9D0M0|EXOS7_	18,25	18,1	18,6	19,1	18,3	19,4	19	19	19	19,2	20	19	19,2	19,4	17	19	18,9	19,9	18,762	18,9858	Exosc7	0,22	18,9	0,625	0,541	0,9257	-7
>sp|Q3UGC7|EI3JA_M	18,44	18,4	0	18	16,8	16,4	16	17	16	16,9	16	16	16,9	15,7	16	19	15,2	16	15,223	16,4302	Eif3j1	1,21	15,8	0,624	0,541	0,9257	-7
>sp|Q66JS6|EI3JB_MO	18,44	18,4	0	18	16,8	16,4	16	17	16	16,9	16	16	16,9	15,7	16	19	15,2	16	15,223	16,4302	Eif3j2	1,21	15,8	0,624	0,541	0,9257	-7
>sp|Q8VI36|PAXI_MO	18,54	17	17,4	16,7	16,7	17,7	16	18	19	17,8	18	17	18	18,2	18	18	17	17,6	17,473	17,6697	Pxn	0,2	17,6	0,623	0,542	0,9259	-7
>sp|Q64516|GLPK_M	22,86	22,7	22,2	21	22,2	21,5	22	22	23	22,4	22	22	21,9	21,4	21	22	22,4	22,7	22,267	22,0987	Gk	-0,2	22,2	-0,62	0,542	0,9259	-7
>sp|P21836|ACES_M	18,14	15,4	17,6	18,2	17,5	17,6	17	17	17	17	17	17	17,9	17,4	17	19	17,5	16,9	17,32	17,5254	Ache	0,21	17,4	0,622	0,543	0,9269	-7
>sp|D3Z4S3|PTRD1_M	17,23	22,7	22,9	23	23	23,1	22	22	23	19,7	19	22	23	23	21	22	22,4	21,6	22,059	21,5857	Ptrhd1	-0,5	21,8	-0,62	0,544	0,928	-7
>sp|Q8BGT1|FLRT3_M	16,32	18,4	16,7	17,1	16,6	20,2	16	18	19	17,2	17	18	16,4	17,1	16	18	18,1	18,2	17,637	17,3252	Flrt3	-0,3	17,5	-0,62	0,544	0,9285	-7
>sp|Q9WUU6|HNF4G_	17,5	16,8	16,8	17,6	17,7	16,8	17	18	18	14,7	17	17	17,2	17,6	18	18	17,6	18,2	17,443	17,2111	Hnf4g	-0,2	17,3	-0,62	0,545	0,9285	-7
>sp|P61939|THBG_M	0	15,6	18,5	17,9	17,8	18,5	18	18	18	17	18	18	18,4	15,1	19	15	18,1	15,5	15,919	17,1845	Serpina7	1,27	16,6	0,618	0,545	0,9285	-7
>sp|Q9JHC0|GPX2_M	23,35	23	23,1	23	23,3	23,3	24	24	24	23,6	23	23	23,6	23,3	23	23	23,3	23,5	23,431	23,3383	Gpx2	-0,1	23,4	-0,62	0,546	0,9293	-7
>sp|Q7M6Y3|PICAL_M	21,78	21,6	21,7	21,3	19,1	19,5	19	19	19	19,6	20	20	20,6	19,5	21	21	20,4	19,9	20,29	20,0172	Picalm	-0,3	20,2	-0,62	0,546	0,9294	-7
>sp|Q6Q473|CLA4A_	18,96	18,3	18,2	19,4	18,5	17,6	18	18	18	19,3	17	17	18,8	18,8	19	19	18,3	18,1	18,47	18,2818	Clca4a	-0,2	18,4	-0,61	0,547	0,9313	-7
>sp|P01819|HVM43	16,71	18,8	16,7	0	0	17,3	0	16	17	18,3	18	18	18,1	18,1	18	0	0	16,4	11,484	13,8477	>sp|P018	2,36	12,7	0,614	0,548	0,9314	-7
>sp|P56382|ATP5E_I	21,32	21,2	23,1	24,2	22,7	22,6	23	23	23	23,2	24	22	23,6	22,8	24	22	21,7	23,5	22,683	22,9481	Atp5e	0,27	22,8	0,613	0,548	0,9314	-7
>sp|Q00623|APOA1_	24,45	23,3	25	24,1	24,3	24,8	24	23	24	23,5	24	24	24	24,9	24	23	24,2	23,4	24,192	24,038	Apoa1	-0,2	24,1	-0,61	0,548	0,9314	-7
>sp|Q8BGQ7|SYAC_M	19,3	20,6	22,3	21,6	22,5	22,1	21	22	22	22,3	22	21	19,8	22,6	22	21	22,2	21,7	21,406	21,6867	Aars	0,28	21,5	0,612	0,549	0,9318	-7
>sp|Q9QYB1|CLIC4_M	20,36	21,1	21,1	20,8	21,3	21,1	21	21	21	21	21	21	21,5	21,3	21	21	20,9	21,1	21,02	21,0954	Clic4	0,08	21,1	0,611	0,549	0,9324	-7
>sp|P36993|PPM1B	17,21	20,7	17,7	19,7	19,2	19,7	20	20	19	19,2	18	18	19,6	18,1	20	20	19,2	19,9	19,276	18,9865	Ppm1b	-0,3	19,1	-0,61	0,551	0,9349	-7
>sp|O08749|DLDH_M	20,99	20,6	20,6	20,7	20,8	19	21	19	21	22,1	21	20	22,2	20,5	19	18	22,2	21,7	20,394	20,7529	Dld	0,36	20,6	0,608	0,552	0,9351	-7
>sp|Q3UM45|PP1R7	21,68	21,9	22,6	22,7	21,5	21,8	22	23	24	23,5	22	23	22,2	22,2	22	22	22,1	22,2	22,262	22,4357	Ppp1r7	0,17	22,3	0,606	0,553	0,9361	-7
>sp|Q91WM1|STRBP_	16,7	14,6	17,6	17,3	16,4	16,3	17	17	17	17,1	17	17	16,2	16,9	16	16	17	18,4	16,697	16,9202	Strbp	0,22	16,8	0,606	0,553	0,9361	-7
>sp|Q62348|TSN_MO	19,06	18,9	21,4	19,3	16,7	17,5	19	21	21	18,4	21	21	20,8	21	18	19	18,8	20,2	19,289	19,6837	Tsn	0,39	19,5	0,604	0,554	0,9382	-7
>sp|P01820|HVM44	17,39	19,4	17,2	0	0	17,9	0	17	18	18,9	18	19	18,6	18,7	18	0	0	17	11,9	14,3035	>sp|P018	2,4	13,1	0,603	0,555	0,9382	-7
>sp|P58321|UCHL4_	19,58	19,3	20,1	19,2	19,4	19,7	20	21	21	21,7	19	19	20	19,2	20	19	19,1	19,4	19,864	19,6522	Uchl4	-0,2	19,8	-0,6	0,555	0,9382	-7
>sp|P70663|SPRL1_I	15	0	0	0	15	0	13	0	0	0	12	0	0	0	0	0	14,7	0	4,8349	2,97341	Sparcl1	-1,9	3,9	-0,6	0,555	0,9384	-7
>sp|Q9Z1B7|MK13_M	20,79	21	21,3	20,8	20,6	20,7	21	21	17	21	21	21	18,1	17,9	18	21	21,1	20,8	20,49	20,0963	Mapk13	-0,4	20,3	-0,6	0,556	0,9384	-7
>sp|Q60866|PTER_M	0	0	16,3	15,6	0	16,1	16	0	15	0	0	0	14,4	14,9	15	0	0	14,6	8,7942	6,53781	Pter	-2,3	7,67	-0,6	0,556	0,9387	-7
>sp|O08788|DCTN1_	22,34	20,5	20,9	19,5	17,5	17,9	18	21	21	20,7	20	19	19,5	18,8	21	19	18,7	18,6	19,853	19,4514	Dctn1	-0,4	19,7	-0,6	0,558	0,9413	-7
>sp|Q920Q8|NS1BP_	17,43	17,5	16,5	16,6	16,2	16,9	16	16	0	15,1	16	16	16,4	16,4	16	17	16	14,9	14,841	15,9475	Ivns1abp	1,11	15,4	0,598	0,558	0,9416	-7
>sp|Q03404|TFF2_MO	22,19	22,4	22,5	21	21,8	22,9	23	23	22	22,5	21	23	22,5	22,6	22	23	21,8	21,8	22,364	22,204	Tff2	-0,2	22,3	-0,6	0,559	0,9425	-7
>sp|Q9D2V7|CORO7_	20,51	20,9	21,8	20	22,4	22,6	20	20	20	22	22	22	22,3	22,2	22	20	19,8	19,8	20,968	21,2784	Coro7	0,31	21,1	0,596	0,559	0,9425	-7

>sp|Q9EQ20|MMSA_M	20,44	20,7	23,8	20,4	19,9	19,3	20	20	20	20,6	21	20	20,4	20,7	21	21	21,3	21,2	20,53	20,7942	Aldh6a1	0,26	20,7	0,594	0,56	0,9435	-7
>sp|P10922|H10_M(	18,13	20,4	17,7	20,8	17,3	18,8	17	17	20	17	19	18	22,2	18,3	22	18	18,2	18,2	18,584	19,0555	H1f0	0,47	18,8	0,592	0,562	0,9452	-7
>sp|Q921I9|EXOS4_M	19,5	19,5	19,3	19,1	18	18,2	20	18	19	19,2	21	20	19,2	18,7	16	20	20,8	19,8	19,078	19,3946	Exosc4	0,32	19,2	0,589	0,564	0,9482	-7
>sp|O70274|TP4A2_	0	0	0	0	0	0	0	0	15	14,5	0	15	0	0	0	0	0	0	1,7021	3,31182	Ptp4a2	1,61	2,51	0,587	0,565	0,9494	-7
>sp|Q63739|TP4A1_	0	0	0	0	0	0	0	0	16	14,7	0	15	0	0	0	0	0	0	1,7252	3,35602	Ptp4a1	1,63	2,54	0,587	0,565	0,9494	-7
>sp|P41317|MBL2_M	17,94	20,3	18,7	19,7	20	19,6	20	20	20	19,8	19	20	19,5	19,2	19	19	19,5	19,9	19,648	19,4831	Mbl2	-0,2	19,6	-0,59	0,565	0,9494	-7
>sp|E9PVB3|CC175_	15,7	15,8	15,8	16	15,7	16,8	0	15	16	15,4	0	13	13,3	12,9	15	14	15,6	15,3	14,058	12,67	Ccdc175	-1,4	13,4	-0,59	0,566	0,9494	-7
>sp|Q9Z204|HNRPC_	16,06	18	17,6	17,8	17,8	16,3	20	18	20	18,2	22	18	17,3	17,7	17	18	18,3	18,7	17,961	18,3315	Hnrnpc	0,37	18,1	0,583	0,568	0,952	-7
>sp|Q8BHJ5|TBL1R_M	19,56	19,3	19,1	19,3	20	21,2	20	20	19	19,9	19	19	19,7	19,1	20	20	19,5	19,9	19,727	19,5814	Tbl1xr1	-0,1	19,7	-0,58	0,568	0,952	-7
>sp|P22907|HEM3_M	15,25	0	15,1	16,2	15	0	17	15	15	15,5	0	16	15,4	15,1	16	15	14,4	15,4	12,027	13,6736	Hmbs	1,65	12,9	0,583	0,568	0,952	-7
>sp|Q9DAR7|DCPS_M	22,72	20,9	20,7	20,9	22	21,1	20	22	22	22,3	22	22	20,7	21	21	21	22	21,3	21,3	21,4914	Dcps	0,19	21,4	0,58	0,57	0,9543	-7
>sp|Q923D2|BLVRB_	19,88	21,5	21,7	21,5	20,7	23,5	22	21	22	21,1	21	21	23,4	21,2	21	21	20,7	21,2	21,506	21,2626	Blvrb	-0,2	21,4	-0,58	0,57	0,9543	-7
>sp|P28665|MUG1_I	20,45	20,5	24,1	24	23,7	22,6	23	24	23	22,5	22	24	23,6	23	24	23	23,1	22,9	22,82	23,1039	Mug1	0,28	23	0,579	0,57	0,9545	-7
>sp|P61294|RAB6B_	20,71	17,4	20,3	20,8	20,7	21,3	21	16	21	20,4	20	20	20,9	20,7	18	21	20,6	20,4	19,825	20,234	Rab6b	0,41	20	0,578	0,571	0,9547	-7
>sp|Q9D733|GP2_M(	14,56	14,1	14,1	14,2	13,3	13,7	14	13	11	12,2	14	14	14,5	14,2	14	14	13,2	13	13,522	13,7669	Gp2	0,24	13,6	0,577	0,572	0,9556	-7
>sp|Q91WV7|SLC31_	16,65	15,5	15,9	19	18,6	19,5	19	19	19	19	16	17	18,4	19	19	19	18	19,8	18,04	18,4029	Slc3a1	0,36	18,2	0,576	0,572	0,9565	-7
>sp|P15105|GLNA_M	22,38	20,9	22	21,3	22	22	22	22	21	21,4	22	21	22,1	21,5	23	22	22,1	21,9	21,724	21,8549	Glul	0,13	21,8	0,575	0,573	0,9571	-7
>sp|Q8CCX5|KT222_	20,49	20,3	20,8	20,3	17,8	15,8	18	17	21	14,4	20	21	19,4	20	16	21	17	16,6	18,978	18,3995	Krt222	-0,6	18,7	-0,57	0,578	0,9643	-7
>sp|O09172|GSH0_M	19,03	18,9	15,2	18,6	18,7	15,9	19	19	17	18,9	17	17	18,2	16,3	16	19	18,6	16,8	17,938	17,5768	Gclm	-0,4	17,8	-0,57	0,578	0,9643	-7
>sp|P57722|PCBP3_	19,8	19,4	19,4	19,9	19,7	19,6	20	19	19	19,1	19	19	19,9	19,9	20	20	19,3	18,8	19,509	19,4049	Pcbp3	-0,1	19,5	-0,56	0,58	0,967	-7
>sp|Q99KP3|CRYL1_I	19,62	20,7	20,8	20,4	20,2	20,2	20	21	21	20,2	21	21	20,8	19,8	21	21	20,6	20,4	20,45	20,5507	Cryl1	0,1	20,5	0,562	0,581	0,9688	-7
>sp|P34022|RANG_M	19,25	17,8	17,9	19,6	19,2	19,6	20	18	0	18	18	18	18,1	20	18	15	20	16,4	16,761	17,9666	Ranbp1	1,21	17,4	0,562	0,582	0,9688	-7
>sp|P62821|RAB1A_	23,56	22	22,2	22,9	22,6	23,7	23	22	23	22,2	22	24	21,7	23,5	21	23	22,8	22,7	22,757	22,5774	Rab1A	-0,2	22,7	-0,56	0,582	0,9691	-7
>sp|Q80X95|RRAGA_	19,75	20,7	19,1	19,8	20	19,2	20	19	16	19,6	17	17	19,3	19,7	19	19	20,2	19,3	19,215	18,881	Rraga	-0,3	19	-0,56	0,582	0,9691	-7
>sp|Q9CS42|PRPS2_I	21,88	22,1	22,7	21,8	22,1	22,6	22	23	22	22,7	21	22	22,9	18,1	23	23	22,6	22,6	22,221	21,9327	Prps2	-0,3	22,1	-0,56	0,586	0,9737	-7
>sp|Q8VD62|CK068_	19,19	22,4	21,5	18,1	18,6	22,2	19	22	22	18,9	22	18	18,1	21,6	22	21	18,2	21,3	20,542	20,0797	Bles03	-0,5	20,3	-0,55	0,586	0,9745	-7
>sp|Q9CZM2|RL15_M	17,54	17,8	18,6	17,4	17,6	17,8	19	18	18	18,5	19	19	18,7	18,4	19	18	16	18,3	18,065	18,2646	Rpl15	0,2	18,2	0,554	0,587	0,9745	-7
>sp|Q9D5J6|SHPK_M	20,77	21,3	23,5	21	20,7	23,6	21	20	20	20	19	24	23,9	25	22	21	21,1	20,3	21,448	21,8879	Shpk	0,44	21,7	0,554	0,587	0,9745	-7
>sp|Q61171|PRDX2_	23,38	22,8	24,5	22,9	23,8	24,5	22	23	22	23,7	23	23	23,6	22,8	22	23	23,7	23,1	23,312	23,127	Prdx2	-0,2	23,2	-0,55	0,587	0,9745	-7
>sp|Q8BH69|SPS1_M	19,04	17,7	16,5	17,7	16	17,7	19	19	20	18,4	20	19	17,8	17,9	18	18	18,3	18,1	18,052	18,3162	Sephs1	0,26	18,2	0,553	0,588	0,9752	-7
>sp|P56387|DYLT3_M	17,99	19,1	21,7	22,3	21,8	21,9	22	22	22	22,5	22	22	21,8	21,8	22	23	22,3	17,8	21,249	21,6416	Dynlt3	0,39	21,4	0,552	0,588	0,9754	-7
>sp|Q05793|PGBM_I	18,85	18,9	19,2	18,8	18,8	18,6	20	19	19	19,3	19	19	18,6	19,1	20	19	19,2	18,7	19,008	19,0979	Hspg2	0,09	19,1	0,552	0,589	0,9754	-7
>sp|Q02013|AQP1_M	17,95	18	19	17,7	19,4	16,8	19	19	18	15,6	19	17	15,4	20,4	17	17	20,1	20	18,386	17,9915	Aqp1	-0,4	18,2	-0,55	0,589	0,9757	-7
>sp|Q62167|DDX3X_	18,86	19,4	19,5	19,4	19	19,4	20	19	20	19	20	20	19,4	19,1	19	19	19,2	18,8	19,317	19,2424	Ddx3x	-0,1	19,3	-0,55	0,589	0,9757	-7
>sp|P06344|HB2U_M	18,4	18	17,5	18,2	18,9	18,3	18	19	18	17,5	18	18	18,4	18,4	19	18	17,9	18,1	18,316	18,217	>sp|P063	-0,1	18,3	-0,55	0,59	0,9757	-7
>sp|Q91WG0|EST2C_I	21,66	22,9	22,5	22,2	22,8	21,5	22	22	22	22,6	22	22	22,2	22	22	23	22,4	22,8	22,278	22,3735	Ces2c	0,1	22,3	0,548	0,591	0,9771	-7
>sp|Q9JHW2|NIT2_M(	19,9	21,1	20	20,4	19,6	19,9	20	21	21	20,7	19	19	20	20,1	20	21	20,4	20,3	20,25	20,1304	Nit2	-0,1	20,2	-0,55	0,591	0,9772	-7
>sp|Q9CQC9|SAR1B_	18,54	17,5	18,4	18,7	18,1	17,6	19	19	19	18,7	18	18	18,4	18,4	19	18	18,6	18,7	18,385	18,5087	Sar1b	0,12	18,4	0,547	0,592	0,9778	-7
>sp|Q61553|FSCN1_I	19,99	23,1	21,1	22,6	22,9	23	23	23	23	22,5	20	21	22,9	22,9	23	22	22,7	22,8	22,467	22,1741	Fscn1	-0,3	22,3	-0,54	0,593	0,9797	-7
>sp|Q8VEH3|ARL8A_I	18,16	17,7	17,8	19,8	18,1	17,8	19	18	18	17,3	16	21	18,5	21,7	18	18	18	18,1	18,15	18,5117	Arl8a	0,36	18,3	0,544	0,594	0,9799	-7
>sp|P40237|CD82_M	15,51	16,2	18,7	16,7	16,2	14,7	16	17	20	18,7	18	17	15,8	16,4	16	16	16	18,6	16,645	16,989	Cd82	0,34	16,8	0,543	0,595	0,981	-7
>sp|P01680|KV4A1_	16,92	18,9	17,1	17,9	17,9	18,2	18	19	18	18,8	18	18	18,8	17,2	20	18	16,4	18,6	18,01	18,2281	>sp|P016	0,22	18,1	0,542	0,595	0,981	-7
>sp|Q921V5|MGAT2_	17,48	19,1	18,7	18,4	18,6	18,5	19	18	18	18,1	20	17	18	18,2	18	18	18,2	18,3	18,404	18,2752	Mgat2	-0,1	18,3	-0,54	0,597	0,9834	-7
>sp|Q91ZR1|RAB4B_	20,78	19,4	20,4	20,8	20,7	21,2	21	19	21	20,4	20	21	20,9	20,6	19	21	20,3	20,3	20,459	20,2774	Rab4b	-0,2	20,4	-0,54	0,597	0,9836	-7
>sp|Q9JI91|ACTN2_M	20,23	20,2	20	19,8	19,9	19,3	20	21	21	20,2	19	19	20,9	20,6	20	20	20,2	19,8	20,105	19,9369	Actn2	-0,2	20	-0,54	0,598	0,9836	-7
>sp|Q8VCR8|MYLK2_	20,08	20,4	20,6	20,2	19,9	20	20	21	13	20,3	21	21	16,8	16,7	17	20	16,8	20,1	19,423	18,8806	Mylk2	-0,5	19,2	-0,54	0,598	0,984	-7
>sp|P62751|RL23A_	0	16,3	16	16	16,7	16,9	17	0	16	15,7	0	16	16,4	16,5	15	15	17	16,8	12,731	14,3223	Rpl23a	1,59	13,5	0,535	0,6	0,9866	-7
>sp|Q61656|DDX5_M	21,08	22,7	21,5	21	21,2	21,1	20	21	24	23,3	23	23	20,4	20,5	20	21	22,8	22,8	21,563	21,8542	Ddx5	0,29	21,7	0,534	0,6	0,987	-7

>sp|Q3UE37|UBE2Z_M	20,73	21,1	21	21,1	20,8	20,5	20	21	21	21,1	21	21	20,6	20,6	21	21	20,8	21,9	20,788	20,8747	Ube2z	0,09	20,8	0,529	0,604	0,9916	-7
>sp|Q99KK7|DPP3_M	22,31	22,4	22,8	22,8	21,9	21,8	21	22	21	22	22	22	22,1	22,5	22	22	22,3	22,1	21,97	22,1049	Dpp3	0,14	22	0,529	0,604	0,9916	-7
>sp|O88643|PAK1_M	14,01	0	0	13,5	0	0	0	15	0	0	13	15	0	0	0	0	0	0	4,6739	3,05659	Pak1	-1,6	3,87	-0,53	0,604	0,9918	-7
>sp|P84089|ERH_MO	20,54	20,9	21	19,9	20,1	20,9	21	21	21	21	20	21	20,5	20,8	21	21	20,9	20,5	20,696	20,7914	Erh	0,1	20,7	0,527	0,605	0,9921	-7
>sp|Q9QZB7|ARP10_	17,06	18,5	18,1	18,2	18,3	17,5	18	16	17	16,6	17	17	17	17,4	18	18	18,4	17,7	17,668	17,4951	Actr10	-0,2	17,6	-0,53	0,605	0,9921	-7
>sp|Q61036|PAK3_M	13,98	0	0	13,4	0	0	0	14	0	0	13	15	0	0	0	0	0	0	4,6473	3,04324	Pak3	-1,6	3,85	-0,53	0,605	0,9921	-7
>sp|P68040|RACK1_	24,19	24,2	23,6	24	23,9	24	24	25	25	24,5	23	24	24,1	23,9	24	24	24,1	24	24,167	24,0793	Rack1	-0,1	24,1	-0,52	0,61	0,998	-7
>sp|Q61187|TS101_M	17,01	18,4	17,8	16,2	18,4	16,6	16	20	21	20,2	18	17	16,9	16,7	17	17	17,2	17,8	17,976	17,6336	Tsg101	-0,3	17,8	-0,52	0,61	0,998	-7
>sp|Q8BU30|SYIC_MO	19,55	19,5	19,3	17,3	17,7	19,2	18	21	20	18,2	20	20	18,5	19,3	19	19	19,4	19,1	19,042	19,2778	Iars	0,24	19,2	0,52	0,61	0,998	-7
>sp|P70335|ROCK1_	15,5	16,7	13,2	16,1	15,1	15,7	15	15	15	14,6	15	15	14,9	14,9	15	14	16	15,1	15,211	15,0273	Rock1	-0,2	15,1	-0,52	0,611	0,9986	-7
>sp|Q99JG3|ANX13_	18,13	16,6	16,8	16	16,9	15,2	17	20	20	21,6	21	18	16,1	17,2	17	17	17	15,9	17,426	17,8786	Anxa13	0,45	17,7	0,518	0,611	0,9991	-7
>sp|Q6PER3|MARE3_	16,46	16,4	0	0	17,4	15,6	17	0	16	15,2	17	0	0	0	0	15	16,8	17	10,957	8.939436	Mapre3	-2	9,95	-0,52	0,612	1	-7
>sp|Q91YP2|NEUL_MO	17,85	17,5	17,5	17,8	17,8	17,5	18	18	20	17,5	21	20	16,8	16,8	17	17	18,5	16,3	18,048	17,7573	Nln	-0,3	17,9	-0,52	0,613	1	-7
>sp|Q8BTY1|KAT1_MO	15,34	15,7	15,4	15	14,5	15	16	16	16	16,5	0	17	15,9	16,2	18	16	15	16,4	15,437	14,4991	Kyat1	-0,9	15	-0,52	0,613	1	-7
>sp|P40124|CAP1_M	24,71	24,8	24,2	24,2	23,7	24,2	24	25	25	24,4	24	24	24,5	25	25	25	24,1	23,9	24,312	24,4026	Cap1	0,09	24,4	0,515	0,614	1	-7
>sp|O70362|PHLD_M	16,4	17	16	17,3	0	15	17	16	16	14,2	15	15	15,7	15,8	16	15	15	15,4	14,404	15,3316	Gpld1	0,93	14,9	0,515	0,614	1	-7
>sp|P21550|ENOB_M	24,23	24,6	24,9	24,2	23,7	22,3	24	24	24	24,1	24	24	24,4	23,6	24	24	23,6	23,2	23,992	23,8508	Eno3	-0,1	23,9	-0,51	0,614	1	-7
>sp|Q9D0T1|NH2L1_M	17,69	17,7	18,4	17,6	17,9	18,3	18	18	18	17,8	18	18	18,4	18,2	18	18	17,6	18,1	17,958	18,0244	Snu13	0,07	18	0,51	0,617	1	-7
>sp|Q9R182|ANGL3_M	16,12	16,6	15	16,7	16,6	17	17	16	14	16,5	14	17	16	16,6	17	16	16,1	16,7	16,039	16,2363	Angptl3	0,2	16,1	0,51	0,617	1	-7
>sp|Q04750|TOP1_M	22,03	21,5	19,9	22,6	19,8	19,8	22	21	20	19	18	20	22,5	19,8	20	23	22,1	22,1	20,943	20,6134	Top1	-0,3	20,8	-0,51	0,619	1	-7
>sp|Q6IME9|K2C72_M	17,52	18,8	16,8	19,3	19,6	19,6	19	19	19	19,7	17	20	20,3	20,2	20	17	17,4	20,3	18,83	19,137	Krt72	0,31	19	0,506	0,62	1	-7
>sp|Q3UWA4|TRI40_M	21,4	21,5	16,7	21,5	15,8	15,4	22	21	21	19,9	17	17	20	16,8	20	21	20,3	20,7	19,634	19,0837	Trim40	-0,6	19,4	-0,51	0,62	1	-7
>sp|Q9WTL2|RAB25_M	16,37	20,5	17,5	17,8	17,5	17,7	17	17	17	17	18	18	17,9	17,2	18	18	18,5	18	17,67	17,8766	Rab25	0,21	17,8	0,505	0,62	1	-7
>sp|Q8R1M8|MPTX_M	18,09	15,6	18,7	19	18,8	17,6	18	19	18	18,5	18	16	19,6	19,2	16	19	18,6	15,4	18,063	17,7621	Mptx1	-0,3	17,9	-0,5	0,62	1	-7
>sp|P97355|SPSY_MO	19,53	19,7	18,5	16,3	16,6	17,7	18	17	17	16,9	18	18	18	18,1	19	18	18	18,1	17,803	18,0335	Sms	0,23	17,9	0,503	0,621	1	-7
>sp|Q9CZ28|SNF8_MO	21,44	18,4	18,3	18,1	17,5	17,8	18	18	18	18,4	19	17	18,5	17,6	18	19	17,9	18,3	18,345	18,1277	Snf8	-0,2	18,2	-0,5	0,622	1	-7
>sp|Q3THE2|ML12B_M	18,9	22,7	20,8	23,6	20,6	18,8	24	24	21	23	19	24	18,9	24	24	18	18,9	19,1	21,57	21,0052	Myl12b	-0,6	21,3	-0,5	0,623	1	-7
>sp|P62838|UB2D2_M	18,67	24,4	23,7	23,9	19,8	24,1	24	25	20	22,6	23	23	23,3	23,2	19	23	19	22,8	22,549	22,0731	Ube2d2	-0,5	22,3	-0,5	0,625	1	-7
>sp|Q9D3R6|KATL2_M	14,32	22,5	22,1	22,4	16,5	16,2	22	17	16	12,1	14	16	21,1	21	15	21	20,7	20,8	18,744	17,9199	Katnal2	-0,8	18,3	-0,5	0,626	1	-7
>sp|P17751|TPIS_MO	26,05	25,4	26,9	26,7	27,2	26,6	26	26	26	26,4	26	26	26,3	26,5	26	28	26,4	26,5	26,414	26,5246	Tpi1	0,11	26,5	0,497	0,626	1	-7
>sp|Q3TDX8|NB5R4_M	17,87	14,7	15,6	17,2	0	17,3	16	16	16	15,9	15	16	14,8	14,7	15	15	16,9	14,7	14,51	15,4144	Cyb5r4	0,9	15	0,492	0,629	1	-7
>sp|P15946|K1B11_M	19,94	19,8	20,7	20,1	19,9	20,1	19	20	20	20	20	20	20,1	20,3	19	20	20,1	20,3	20,048	19,9752	Klk1b11	-0,1	20	-0,49	0,631	1	-7
>sp|Q8K0G5|EIPR1_M	17,88	19	17	16,4	16,5	16,8	18	18	18	17,8	18	18	18	17,3	17	18	16,7	18	17,546	17,7136	Eipr1	0,17	17,6	0,49	0,631	1	-7
>sp|Q61233|PLSL_MO	21,19	20,7	21,1	20,4	21	20,7	19	20	21	20,5	21	20	20,3	20,5	20	20	20,8	21,4	20,607	20,481	Lcp1	-0,1	20,5	-0,49	0,634	1	-7
>sp|Q3UIZ8|MYLK3_M	19,85	20,1	20,3	20	19,6	19,7	20	20	13	20,1	21	21	16,6	16,5	17	20	16,6	20	19,163	18,6696	Mylk3	-0,5	18,9	-0,48	0,635	1	-7
>sp|Q3TTY5|K22E_MO	20,32	20,6	20	19,6	19,6	19,1	20	19	19	18,5	19	20	18,4	18,9	21	21	21,6	21,9	19,674	19,9189	Krt2	0,24	19,8	0,484	0,635	1	-7
>sp|Q9Z0Y1|DCTN3_M	18,82	17,8	18,4	18,9	18,4	17,3	18	18	17	17,6	19	17	17,7	18	18	18	18,5	18,4	18,133	18,0033	Dctn3	-0,1	18,1	-0,48	0,636	1	-7
>sp|Q6IFX3|K1C40_M	20,84	16,6	20,4	20,3	20,3	20	17	21	21	18,3	21	19	18,7	21,3	19	23	19,1	22,5	19,692	20,0736	Krt40	0,38	19,9	0,482	0,636	1	-7
>sp|Q8CIH5|PLCG2_M	13,96	15,5	16,5	15,4	13,7	13,7	15	14	15	14,2	17	15	14,5	14	14	14	13,9	14,5	14,769	14,5588	Plcg2	-0,2	14,7	-0,48	0,637	1	-7
>sp|P49817|CAV1_M	20,47	20,6	21,8	19,9	21,9	21,5	19	19	20	21	21	21	19,4	20,9	25	18	19,9	20,6	20,411	20,7497	Cav1	0,34	20,6	0,48	0,637	1	-7
>sp|P28653|PGS1_M	19,15	18,7	17,2	15,6	15,9	18,8	18	16	15	17,5	17	17	18,1	17,2	19	18	16,8	17	17,124	17,4066	Bgn	0,28	17,3	0,48	0,638	1	-7
>sp|Q9JJV2|PROF2_M	18,3	17,9	18,3	17,9	23,4	18,3	19	17	18	22	15	23	23	17,2	16	16	22,8	16,7	18,613	19,2279	Pfn2	0,61	18,9	0,48	0,638	1	-7
>sp|Q9EST4|PSMG2_M	15,02	18,2	17,5	15	14,9	17,1	17	17	15	16,8	17	16	17,4	14,7	16	17	16,6	17	16,238	16,4868	Psmg2	0,25	16,4	0,477	0,639	1	-7
>sp|P16332|MUTA_M	16,11	20,6	21,1	21,5	22,1	21,7	21	21	21	21	17	21	21,9	20,6	21	20	20,5	20,4	20,749	20,396	Mut	-0,4	20,6	-0,48	0,64	1	-7
>sp|O08573|LEG9_M	20,96	20,4	20,6	21	20,1	20,6	21	20	21	21	20	20	20,5	20,5	20	20	20,3	20,7	20,553	20,4791	Lgals9	-0,1	20,5	-0,47	0,642	1	-7
>sp|P61079|UB2D3_M	20,76	24,5	23,7	23,9	19,7	24,1	24	25	20	22,7	23	23	23,4	23,4	21	23	20,2	22,9	22,789	22,4195	Ube2d3	-0,4	22,6	-0,47	0,643	1	-7
>sp|P01750|HVM06	19,96	19,7	20,2	19,4	18,4	20,2	19	19	19	20,1	19	18	19,2	18,9	19	21	20,5	18,2	19,472	19,3087	>sp|P017	-0,2	19,4	-0,47	0,643	1	-7
>sp|P01751|HVM07	19,96	19,7	20,2	19,4	18,4	20,2	19	19	19	20,1	19	18	19,2	18,9	19	21	20,5	18,2	19,472	19,3087	Ighv1-72	-0,2	19,4	-0,47	0,643	1	-7

>sp|P03980|HVM48	19,96	19,7	20,2	19,4	18,4	20,2	19	19	19	20,1	19	18	19,2	18,9	19	21	20,5	18,2	19,472	19,3087	>sp|P039	-0,2	19,4	-0,47	0,643	1	-7
>sp|P06329|HVM50	19,96	19,7	20,2	19,4	18,4	20,2	19	19	19	20,1	19	18	19,2	18,9	19	21	20,5	18,2	19,472	19,3087	>sp|P063	-0,2	19,4	-0,47	0,643	1	-7
>sp|Q9JKM7|RAB37_	20,21	16,8	19,7	20,2	20,1	20,7	20	15	20	19,7	20	20	20,3	20,1	16	20	20,1	19,9	19,198	19,5619	Rab37	0,36	19,4	0,472	0,643	1	-7
>sp|O54782|MA2B2	15,97	15,3	17	16,1	16,4	14,5	17	15	15	15,8	15	15	16,6	16,4	16	16	16,9	16,2	15,911	16,0867	Man2b2	0,18	16	0,47	0,644	1	-7
>sp|P49962|SRP09_	18,38	18	18,5	18,5	20,2	19,3	19	19	19	19,5	18	21	18,7	18,8	19	19	18,9	18,4	18,858	19,0113	Srp9	0,15	18,9	0,47	0,645	1	-7
>sp|Q9CZH3|PSMG3_	21,21	20,5	19,5	20,2	20,8	19,7	20	20	21	20,8	20	21	20,2	20	20	22	21,2	19,9	20,348	20,4879	Psmg3	0,14	20,4	0,47	0,645	1	-7
>sp|P12849|KAP1_M	16	16,7	14,5	14,9	15,1	16,3	16	16	15	15,3	15	16	16,5	15,8	16	16	16,2	15,6	15,685	15,8374	Prkar1b	0,15	15,8	0,467	0,647	1	-7
>sp|Q80Z19|MUC2_M	20,8	20,8	21,3	20,6	20,4	20,5	21	21	21	20,4	21	21	20,8	20,8	21	21	20,7	20,8	20,753	20,8051	Muc2	0,05	20,8	0,466	0,647	1	-7
>sp|Q3TXS7|PSMD1_I	16,87	17,1	18,4	17,5	17,8	17,4	18	18	18	18,3	18	18	17,5	17,2	17	18	18,2	18,2	17,636	17,7396	Psmd1	0,1	17,7	0,466	0,648	1	-7
>sp|Q9ES30|C1QT3_M	18,23	18,2	20,7	19,9	20,7	20,6	16	20	17	20,1	21	19	20,7	20,4	20	20	17,6	16,9	19,171	19,5024	C1qtnf3	0,33	19,3	0,464	0,649	1	-7
>sp|Q3T9E4|TGTP2_M	15,91	16,1	18	15,7	15,5	14,9	16	15	15	14,1	17	17	16,9	17,4	17	14	14,1	16,6	15,786	16,0618	Tgtp2	0,28	15,9	0,463	0,649	1	-7
>sp|Q62293|TGTP1_I	15,91	16,1	18	15,7	15,5	14,9	16	15	15	14,1	17	17	16,9	17,4	17	14	14,1	16,6	15,786	16,0618	Tgtp1	0,28	15,9	0,463	0,649	1	-7
>sp|Q80UG5|SEPT9_M	20,08	20,1	18,7	19,7	19,6	17,6	20	19	20	18,9	17	19	19,9	19,9	20	19	19,5	19,2	19,394	19,2247	Sept9	-0,2	19,3	-0,46	0,649	1	-7
>sp|Q9CXY6|ILF2_MO	20,72	21,1	20,4	19,3	21,4	20,9	21	21	20	20,8	22	21	20,5	20,5	20	21	20,7	20,9	20,668	20,7849	Ilf2	0,12	20,7	0,462	0,65	1	-7
>sp|P20108|PRDX3_	20,06	19,9	18,8	17,8	18,9	18,9	16	20	20	20,4	20	19	18,4	17,9	19	19	18,7	19,6	18,876	19,1056	Prdx3	0,23	19	0,462	0,65	1	-7
>sp|Q8BWY3|ERF1_M	18,78	19,1	21,8	18,3	19,3	21,4	22	19	22	18,3	19	21	21	21	21	21	21,1	21,3	20,197	20,4786	Etf1	0,28	20,3	0,461	0,651	1	-7
>sp|P01749|HVM05	20,27	20,1	20,5	19,7	18,8	20,5	20	19	19	20,4	19	19	19,6	19,3	20	21	20,8	18,5	19,793	19,6327	Ighv1-61	-0,2	19,7	-0,46	0,651	1	-7
>sp|P01754|HVM10	20,27	20,1	20,5	19,7	18,8	20,5	20	19	19	20,4	19	19	19,6	19,3	20	21	20,8	18,5	19,793	19,6327	Ighv1-62-	-0,2	19,7	-0,46	0,651	1	-7
>sp|P06328|HVM49	20,27	20,1	20,5	19,7	18,8	20,5	20	19	19	20,4	19	19	19,6	19,3	20	21	20,8	18,5	19,793	19,6327	>sp|P063	-0,2	19,7	-0,46	0,651	1	-7
>sp|Q8VEE4|RFA1_M(	19,49	19,5	19	19,2	19,6	19	19	19	20	20,1	20	19	19,3	19,3	20	19	19,4	19,2	19,316	19,3771	Rpa1	0,06	19,3	0,46	0,652	1	-7
>sp|P70698|PYRG1_	19,57	19,9	19,5	21,4	21,4	21,2	19	18	21	20,7	20	20	18	21,4	18	21	18,1	21,1	20,13	19,8462	Ctps1	-0,3	20	-0,46	0,652	1	-7
>sp|Q5U4D9|THOC6_	15,22	15,7	17,8	14,4	14,8	18,1	16	15	18	17,6	15	16	15,2	17,9	16	15	17	17,2	16,031	16,3055	Thoc6	0,27	16,2	0,458	0,653	1	-7
>sp|Q9DA97|SEP14_I	17,83	18,1	18,5	18,2	18,8	18	18	19	19	19,6	0	19	19,6	19,6	19	19	19,8	20,1	18,356	17,3743	Sept14	-1	17,9	-0,46	0,655	1	-7
>sp|P35283|RAB12_	20,3	16,9	19,8	20,3	20,2	20,8	20	15	20	19,8	20	20	20,4	20,2	16	20	20,1	19,9	19,3	19,6485	Rab12	0,35	19,5	0,455	0,655	1	-7
>sp|Q922Q4|P5CR2_	14,94	19,9	18,8	18,7	19,7	18,4	19	19	19	20	20	18	17,5	17,3	17	18	18,9	19	18,671	18,399	Pycr2	-0,3	18,5	-0,45	0,655	1	-7
>sp|Q922W5|P5CR1	14,94	19,9	18,8	18,7	19,7	18,4	19	19	19	20	20	18	17,5	17,3	17	18	18,9	19	18,671	18,399	Pycr1	-0,3	18,5	-0,45	0,655	1	-7
>sp|Q9CQC6|BZW1_M	21,73	22	19,7	21,2	21,1	18,7	21	20	21	21	18	21	21	21,1	21	21	17,3	20,8	20,637	20,3616	Bzw1	-0,3	20,5	-0,45	0,657	1	-7
>sp|Q64176|EST1E_M	14,55	15	13,9	15	13,7	14,4	15	14	15	14,8	16	15	13,8	15	15	15	12,2	15,3	14,514	14,6923	Ces1e	0,18	14,6	0,451	0,658	1	-7
>sp|P63028|TCTP_M	22,33	21,5	22,9	21	22,1	22,1	21	21	22	21,7	22	22	21,3	21,2	21	22	21,3	22,4	21,782	21,6611	Tpt1	-0,1	21,7	-0,45	0,659	1	-7
>sp|P97464|EXT1_M	16,9	16,8	16,6	17,4	0	16,8	17	15	15	16,1	14	16	15,4	14,9	15	0	16,7	14,3	14,696	13,5737	Ext1	-1,1	14,1	-0,45	0,66	1	-7
>sp|Q9ER72|SYCC_M(	20,05	20,4	20,3	20,1	20	19,8	20	20	20	20,3	20	20	20,2	20,2	20	20	20,1	19,9	20,06	20,0995	Cars	0,04	20,1	0,447	0,661	1	-7
>sp|Q61166|MARE1_	18,85	19,4	19,3	19,6	19,7	20,5	20	19	19	19,5	20	20	18,9	19,8	20	19	19,4	19,9	19,514	19,6104	Mapre1	0,1	19,6	0,447	0,661	1	-7
>sp|Q8BFQ8|GALD1_I	16,57	16,2	16,8	0	16,8	14,7	15	18	17	19,5	17	20	0	14,7	0	14	14,7	18,4	14,562	13,1615	Gatd1	-1,4	13,9	-0,45	0,662	1	-7
>sp|Q99NB1|ACS2L_I	20,51	20	20,6	20,5	19,7	20,3	20	19	20	20,5	21	21	20,1	20	19	21	20,5	19,4	20,091	20,2026	Acss1	0,11	20,1	0,444	0,663	1	-7
>sp|P13707|GPDA_M	22,01	23,2	23,7	23,4	24,1	23,9	24	23	24	23,7	24	23	23,7	23,6	24	24	24	23,1	23,509	23,6105	Gpd1	0,1	23,6	0,443	0,663	1	-7
>sp|P11031|TCP4_M	18,68	17,7	19,5	19,5	19,1	19,3	20	19	20	19	20	20	19,9	18	19	20	19	18,6	19,142	19,2894	Sub1	0,15	19,2	0,443	0,664	1	-7
>sp|Q9D7X8|GGCT_M	0	16,6	17,8	0	17,1	17,5	18	18	18	17,4	18	18	17,3	16,8	0	14	17,6	17,1	13,725	15,1286	Ggct	1,4	14,4	0,439	0,666	1	-7
>sp|Q3TC72|FAHD2_I	18,39	16,6	18	18,9	16,2	17,8	18	17	18	18,4	18	18	16,8	17,1	18	18	17,2	18,2	17,666	17,8162	Fahd2	0,15	17,7	0,437	0,668	1	-7
>sp|Q8BFS6|CPPED_M	25,03	20	20,2	19,7	20	20,4	20	25	20	21,3	20	21	21,2	20,7	21	22	21,1	24,4	21,086	21,4424	Cpped1	0,36	21,3	0,435	0,669	1	-7
>sp|Q60604|ADSV_M	20,88	22	21,9	20,9	21,3	20,8	21	24	24	22,9	23	22	21,4	21,3	21	21	21,2	21,4	21,893	21,6885	Scin	-0,2	21,8	-0,43	0,669	1	-7
>sp|Q9QWK4|CD5L_M	15,46	15,7	15,8	15,4	14,9	15,4	15	15	14	14,6	17	14	14,7	15,9	15	14	14,2	14,7	15,126	14,9596	Cd5l	-0,2	15	-0,43	0,67	1	-7
>sp|Q923S9|RAB30_	20,5	17,1	20	20,5	20,4	21	21	15	20	20,1	20	20	20,6	20,4	17	20	20,3	20,1	19,518	19,8458	Rab30	0,33	19,7	0,434	0,67	1	-7
>sp|Q8CG50|RAB43_	20,32	16,2	19,9	20,3	20,2	20,9	20	15	20	19,9	20	20	20,4	20,2	16	20	20,2	20	19,271	19,6333	Rab43	0,36	19,5	0,432	0,671	1	-7
>sp|P08607|C4BPA_	18,3	19,1	16,8	18,5	18,4	18,5	18	18	16	18,7	15	17	18,5	18	18	18	18,5	18,8	18,071	17,8709	C4bpa	-0,2	18	-0,43	0,673	1	-7
>sp|P35762|CD81_M	18,01	17,5	17,9	17,2	19,8	18,5	21	18	18	18,4	18	18	16,8	18,6	17	17	19,6	19,6	18,431	18,2062	Cd81	-0,2	18,3	-0,43	0,673	1	-7
>sp|Q80V26|IMPA3_	15,57	15,4	18,3	18	17,7	17,8	14	18	18	16	18	17	15,3	17,6	18	17	15,1	15,2	16,937	16,6525	Impad1	-0,3	16,8	-0,43	0,674	1	-7
>sp|Q3UZZ4|OLFM	0	0	0	14,1	0	0	14	15	16	13,8	15	16	0	13,7	0	0	13,6	0	6,462	7,98276	Olfm4	1,52	7,22	0,427	0,675	1	-7
>sp|P49698|HNF4A_	17,67	17,1	17	17,9	18,5	17	18	19	19	17,2	18	18	17,5	17,9	18	18	18,1	18,3	17,795	17,9081	Hnf4a	0,11	17,9	0,427	0,675	1	-7

>sp|P39054|DYN2_M	16,87	17	16,9	16,7	16,4	16,9	16	17	18	17,9	17	17	15,4	17,1	15	17	18	18,8	16,852	17,0227	Dnm2	0,17	16,9	0,426	0,675	1	-7
>sp|Q8C0X8|SMKX_M	14,87	13,9	17	15,6	16	15,3	15	18	18	12,4	17	17	16,7	16,7	14	15	14,5	16,9	15,928	15,6226	>sp|Q8C0	-0,3	15,8	-0,43	0,676	1	-7
>sp|Q9CW03|SMC3_I	17,36	17,4	14	17	14,6	14	14	12	16	15,3	16	16	15,2	15,6	16	15	15,3	15,2	15,197	15,4622	Smc3	0,26	15,3	0,425	0,676	1	-7
>sp|O35963|RB33B_	20,42	16,2	20	20,5	20,3	21	20	15	20	20	20	20	20,5	20,3	16	20	20,3	20,1	19,381	19,7358	Rab33b	0,35	19,6	0,425	0,676	1	-7
>sp|Q62168|K1H2_M	20,58	20,5	16,4	17	16,7	16,2	16	20	19	14,1	20	17	16,9	20,8	17	22	16,8	22,2	18,028	18,506	Krt32	0,48	18,3	0,419	0,681	1	-7
>sp|Q9CQW2|ARL8B_	18,64	18,2	17,8	19,8	18,1	17,8	19	18	18	17,6	16	21	18,5	21,7	18	18	18,4	18,1	18,318	18,5905	Arl8b	0,27	18,5	0,419	0,681	1	-7
>sp|P42932|TCPQ_M	21,35	22,1	20,9	20,8	19,7	20,8	21	20	20	20,8	20	21	20,4	21	21	21	20,6	20,7	20,763	20,661	Cct8	-0,1	20,7	-0,42	0,681	1	-7
>sp|P29351|PTN6_M	19,71	20,2	18,3	20,4	16,2	20	20	19	18	19,3	14	20	19,7	19,8	19	19	19,3	18,9	19,126	18,8057	Ptpn6	-0,3	19	-0,42	0,681	1	-7
>sp|Q9CQM9|GLRX3_	19,59	18,8	17,7	19,5	19,2	16,5	17	18	18	18,3	18	17	20	18,2	17	19	19,7	17,2	18,18	18,3942	Glrx3	0,21	18,3	0,418	0,681	1	-7
>sp|P61082|UBC12_	19,54	20,2	21,6	21,1	21,3	19,6	20	22	22	19,8	18	21	21	21,3	20	22	19,9	21,4	20,701	20,4961	Ube2m	-0,2	20,6	-0,42	0,682	1	-7
>sp|Q9WV55|VAPA_I	20,38	21,8	21,8	20,3	20,4	20,2	20	21	20	21,3	22	21	20,2	19,8	20	20	20,8	20,5	20,711	20,5902	Vapa	-0,1	20,7	-0,42	0,683	1	-7
>sp|O35400|ST2B1_I	15,98	14,4	19,1	14,7	15	14,1	15	14	18	16,8	14	16	14,5	15	17	17	15,4	17,3	15,601	15,9135	Sult2b1	0,31	15,8	0,416	0,683	1	-7
>sp|P15532|NDKA_M	28,17	21,5	28,5	22,3	28,6	21,6	22	22	29	26,4	26	22	23,1	22,6	26	26	23	22	24,816	24,2679	Nme1	-0,5	24,5	-0,41	0,684	1	-7
>sp|P55050|FABPI_M	21,82	20,3	24,6	21,2	20,7	24,6	24	24	25	25,2	25	23	22	23,3	22	25	22,1	21,3	22,945	23,2786	Fabp2	0,33	23,1	0,415	0,684	1	-7
>sp|P47811|MK14_I	20,67	21	21,2	20,8	20,6	20,7	21	21	18	21,2	21	21	18,1	18,9	20	21	21,1	21	20,622	20,4202	Mapk14	-0,2	20,5	-0,41	0,685	1	-7
>sp|P32233|DRG1_M	20,33	16,5	20	15,8	20,3	20,9	21	20	20	20,8	21	17	20,4	20	20	21	21,7	16,1	19,44	19,7937	Drg1	0,35	19,6	0,413	0,685	1	-7
>sp|Q8BT60|CPNE3_I	17,69	17,2	17	16,7	17,1	17,9	18	17	18	16,2	17	17	17,2	16,8	18	19	16,6	17,3	17,279	17,1639	Cpne3	-0,1	17,2	-0,41	0,687	1	-7
>sp|Q8K0C5|ZG16_M	16,3	17,3	15,8	16,9	16,6	17,5	16	17	0	17,6	0	18	18,3	18,4	18	17	17,6	17,7	14,792	15,8926	Zg16	1,1	15,3	0,409	0,688	1	-7
>sp|Q8R016|BLMH_M	23,69	24,4	23,6	22,6	23,9	23,7	24	24	24	24,2	23	24	23,3	23,1	23	24	24,2	23,8	23,759	23,6642	Blmh	-0,1	23,7	-0,41	0,688	1	-7
>sp|Q9D379|HYEP_M	13,94	13,3	12,8	13,4	13,1	15,9	13	16	15	16,2	14	21	13,1	10,2	0	19	12,5	12,7	14,05	13,2258	Ephx1	-0,8	13,6	-0,41	0,688	1	-7
>sp|Q99J36|THUM1_	0	19,9	19,6	0	19,2	19,1	19	20	21	15,9	16	19	16,2	15,6	15	13	18,5	19,1	15,288	16,4763	Thumpd1	1,19	15,9	0,404	0,692	1	-7
>sp|O88342|WDR1_I	23,36	24,1	24	24	24,3	24,4	25	24	24	23,8	24	24	24,2	24,2	24	23	24,1	24,4	24,098	24,0195	Wdr1	-0,1	24,1	-0,4	0,692	1	-7
>sp|Q6ZWY6|U2D2B_	17,79	24,4	23,6	23,9	17,6	24,1	24	24	19	22,6	23	23	23,2	23,2	18	23	16,6	22,7	22,112	21,5927	Ube2d2b	-0,5	21,9	-0,4	0,692	1	-7
>sp|P01633|KV5A1_	15,71	21,3	18,4	17,2	17,2	18,2	21	20	20	17,5	20	19	19,9	20	20	19	17,7	19	18,855	19,1468	Igk-V19-1	0,29	19	0,4	0,694	1	-7
>sp|P10852|4F2_MO	14,73	16,6	16,8	15,1	17	16,9	15	18	18	17,3	17	17	15	15,5	15	17	16,7	16,5	16,418	16,2215	Slc3a2	-0,2	16,3	-0,4	0,695	1	-7
>sp|O88783|FA5_MO	19,6	19,4	19,5	19,9	20,1	19,7	20	23	23	19,2	20	19	18,7	19,7	20	23	19,6	22,7	20,493	20,1972	F5	-0,3	20,3	-0,4	0,695	1	-7
>sp|Q6PB44|PTN23_	14,76	16,4	16,3	16,1	15,9	17,2	16	17	17	16,1	15	16	14,8	16,9	17	17	17,1	16,8	16,216	16,3565	Ptpn23	0,14	16,3	0,399	0,695	1	-7
>sp|P41731|CD63_M	17,57	17,6	18,6	17,7	17,5	18,5	18	18	18	17,5	18	18	17,6	17,8	18	18	17,2	17,7	17,883	17,8086	Cd63	-0,1	17,8	-0,4	0,695	1	-7
>sp|Q9WTP6|KAD2_M	20,71	20,3	20,3	21,5	20,7	20,3	20	20	21	20,8	21	21	20,1	20,3	21	21	20,5	20,9	20,6	20,6718	Ak2	0,07	20,6	0,399	0,695	1	-7
>sp|P28666|MUG2_I	19,8	19,8	22,6	23	22,3	22,4	23	23	23	20,9	22	23	22,7	22,8	23	22	22,1	22,1	22,07	22,2584	Mug2	0,19	22,2	0,394	0,699	1	-7
>sp|Q03265|ATPA_M	20,91	20,6	23	24,8	24,6	20,8	25	21	21	22	22	22	22,1	21,6	24	22	22,1	21,7	22,503	22,2421	Atp5a1	-0,3	22,4	-0,39	0,699	1	-7
>sp|Q01339|APOH_M	20,74	20,7	17,8	20,6	20,5	19,3	17	17	17	20	17	16	19,5	20,3	20	19	19,8	16,6	18,985	18,6706	Apoh	-0,3	18,8	-0,39	0,7	1	-7
>sp|P35279|RAB6A_	21,55	18,3	21,2	20,9	21,4	21,8	21	20	21	20,8	21	21	21,3	20,9	19	21	20,7	20,5	20,773	20,6095	Rab6a	-0,2	20,7	-0,39	0,7	1	-7
>sp|P02469|LAMB1_	18,89	19	17,9	18,9	19	18,9	19	19	19	18,5	19	18	19,5	19,4	18	19	19,2	19,5	18,826	18,9123	Lamb1	0,09	18,9	0,392	0,7	1	-7
>sp|O35900|LSM2_M	20,82	22,8	23,9	19	23,6	23,5	20	24	21	22,6	22	20	22,4	22,8	23	20	21,1	22,8	22,089	21,8048	Lsm2	-0,3	21,9	-0,39	0,701	1	-7
>sp|Q8R527|RHOQ_M	0	0	14,8	15,4	14,9	15,1	15	0	14	11,9	14	14	14,7	14,8	15	0	0	15,4	9.95319	11,218	Rhoq	1,26	10,6	0,389	0,702	1	-7
>sp|Q76LS9|MINY1_M	19,1	18,7	19,2	18,8	16,8	19	19	18	18	18,7	19	19	19,1	18,1	19	17	17,3	18,9	18,584	18,4541	Mindy1	-0,1	18,5	-0,39	0,702	1	-7
>sp|Q504M8|RAB26_	20,65	16,5	20,3	20,7	20,5	21,2	21	16	21	20,3	20	20	20,7	20,6	16	21	20,5	20,3	19,64	19,9627	Rab26	0,32	19,8	0,388	0,703	1	-7
>sp|Q8BHC1|RB39B_	20,65	16,5	20,3	20,7	20,5	21,2	21	16	21	20,3	20	20	20,7	20,6	16	21	20,5	20,3	19,64	19,9627	Rab39b	0,32	19,8	0,388	0,703	1	-7
>sp|Q8BHD0|RB39A_	20,65	16,5	20,3	20,7	20,5	21,2	21	16	21	20,3	20	20	20,7	20,6	16	21	20,5	20,3	19,64	19,9627	Rab39a	0,32	19,8	0,388	0,703	1	-7
>sp|Q3UFF7|LYPL1_M	17,68	17,8	18,3	17,6	17,8	17,9	18	18	18	18,2	18	19	18,6	16,7	19	18	17,8	17,3	17,916	18,0138	Lyplal1	0,1	18	0,388	0,703	1	-7
>sp|O09131|GSTO1_I	24,42	24,8	24,5	25,3	25,5	25	25	25	25	24,7	25	25	25,3	25,1	25	25	24,5	24,9	24,921	24,8644	Gsto1	-0,1	24,9	-0,39	0,703	1	-7
>sp|Q8CGC7|SYEP_MO	22,38	22	20,4	22	21,8	21,4	21	22	21	21,6	21	22	21,4	20,7	21	22	22,3	21,8	21,639	21,5344	Eprs	-0,1	21,6	-0,38	0,708	1	-7
>sp|P15947|KLK1_M	21,3	21,3	21,9	21,6	21,5	21,6	21	22	22	21,4	21	21	21,2	21,1	22	21	22	21,8	21,507	21,462	Klk1	-0	21,5	-0,38	0,708	1	-7
>sp|Q9Z2Y8|PLPHP_M	17,74	18,5	18,1	18,4	18,2	19	18	19	19	18,8	19	18	19,1	18,5	19	18	18,3	18,7	18,457	18,5447	Plpbp	0,09	18,5	0,38	0,709	1	-7
>sp|O88520|SHOC2_	14,7	14,9	14,7	14,4	14	14,1	15	15	15	14,6	15	16	14,3	15,2	15	14	13,7	13,5	14,615	14,5084	Shoc2	-0,1	14,6	-0,38	0,711	1	-7
>sp|P29621|SPA3C_	19,66	19,9	18,2	19,1	18,1	18,9	19	17	18	18,6	19	19	19,5	18,8	18	19	18,6	19,1	18,671	18,7827	Serpina3c	0,11	18,7	0,376	0,712	1	-7
>sp|Q9CQA3|SDHB_M	23,13	21,5	21,5	21,1	21	23,7	22	22	23	22,8	23	21	21,8	22	22	22	22,1	21,6	22,094	21,9659	Sdhb	-0,1	22	-0,38	0,712	1	-7

>sp|Q8CIE6|COPA_M(	21,6	21,7	20,2	20,9	20,9	20,6	21	21	21	21,2	21	21	20,8	21	21	21	21,1	20,8	20,899	20,9596	Copa	0,06	20,9	0,375	0,713	1	-7
>sp|Q9CQ80|VPS25_	19,36	19,8	23,7	19,1	24,1	23,9	19	24	18	22	18	19	22,7	22,5	23	22	22,2	22,3	21,203	21,5696	Vps25	0,37	21,4	0,373	0,714	1	-7
>sp|Q03249|GALT_M	17,27	15,2	14,8	19,1	0	15,8	16	15	0	14,9	15	15	15,3	0	16	16	15,5	15,9	12,535	13,6204	Galt	1,09	13,1	0,372	0,715	1	-7
>sp|Q8QZY1|EIF3L_MC	23,02	22,9	22,3	22,3	22,4	22,7	23	22	22	22,4	22	22	22,7	23,2	22	22	22,7	23	22,471	22,5375	Eif3l	0,07	22,5	0,371	0,715	1	-7
>sp|Q9DCC4|P5CR3_	21,78	21,6	21,8	22,2	22,3	22,2	22	22	22	21,6	22	22	21,9	22,5	23	22	21,9	22	22,035	22,0889	Pycr3	0,05	22,1	0,371	0,716	1	-7
>sp|Q921I1|TRFE_MO	20,3	20,5	21,2	21	20,8	21	21	21	20	20,4	21	21	21	20,5	21	20	20,6	20,5	20,758	20,7071	Tf	-0,1	20,7	-0,37	0,716	1	-7
>sp|P08775|RPB1_M	18,33	17,1	18,3	18,6	17	17,4	18	17	18	17,2	17	17	18,3	18,6	18	18	17	16,9	17,715	17,5997	Polr2a	-0,1	17,7	-0,37	0,717	1	-7
>sp|Q60967|PAPS1_	20,66	20,9	21,9	22,3	20	22	20	20	20	22,8	23	23	19,6	23,4	20	20	19,9	19,3	20,981	21,211	Papss1	0,23	21,1	0,366	0,719	1	-7
>sp|Q8K274|KT3K_M	17,51	17,4	16,2	17,4	17,4	16,1	17	17	18	16,2	17	17	16,7	16,5	17	17	17,8	17,1	17,037	16,9459	Fn3krp	-0,1	17	-0,36	0,721	1	-7
>sp|Q921M3|SF3B3_	19,41	19,9	18,9	20,1	18,9	18,8	19	19	19	19	19	19	19,9	19,6	20	20	19,7	18,7	19,267	19,3556	Sf3b3	0,09	19,3	0,363	0,721	1	-7
>sp|Q8K4Z3|NNRE_M	17,66	19,6	19,3	18	19,2	18,6	19	19	19	19,8	19	18	18,8	19,1	18	19	18,8	18,4	18,81	18,7012	Naxe	-0,1	18,8	-0,36	0,721	1	-7
>sp|P47955|RLA1_M	15,99	14,5	13,7	13,6	13,7	0	0	19	18	19,4	0	0	21,7	20,9	21	0	0	12,3	12,064	10,5603	Rplp1	-1,5	11,3	-0,36	0,721	1	-7
>sp|Q8CHW4|EI2BE_M	14,67	14,5	13,7	14,7	14,2	13,3	14	14	14	15,2	0	16	15,1	15,2	15	16	14,5	15,3	14,184	13,5742	Eif2b5	-0,6	13,9	-0,36	0,722	1	-7
>sp|Q8CEC6|PPWD1_	18,63	18,8	0	0	0	0	18	18	18	9,02	15	0	0	13,7	0	20	0	19,8	10,067	8.528594	Ppwd1	-1,5	9,3	-0,36	0,723	1	-7
>sp|O54962|BAF_MC	22,15	22,4	19,9	23,6	23,6	22,8	23	23	22	23,3	22	22	22,8	22,9	22	23	23,1	23,2	22,549	22,7017	Banf1	0,15	22,6	0,361	0,723	1	-7
>sp|Q9CWU9|NUP37_	20,72	21,9	21,5	21,6	22	21,5	22	20	22	21,5	21	21	21,7	20,8	22	22	21,9	22,1	21,419	21,5246	Nup37	0,11	21,5	0,359	0,724	1	-7
>sp|Q80X76|SPA3F_I	19,6	19,8	18,2	19	18	18,8	18	17	18	18,6	19	19	19,4	18,7	18	19	18,5	19	18,613	18,7181	Serpina3f	0,11	18,7	0,356	0,726	1	-7
>sp|Q99P31|HPBP1_	20,03	18,6	20	19,7	17,2	20,1	19	19	19	20,2	20	20	16,5	20,3	16	19	19,3	18,4	19,14	18,9228	Hspbp1	-0,2	19	-0,36	0,727	1	-7
>sp|Q99M74|KRT82_	19,36	20,1	17,3	18,2	18,6	16,7	19	17	17	18,1	17	17	17,8	18,3	19	20	18,6	18,1	18,129	18,3124	Krt82	0,18	18,2	0,354	0,728	1	-7
>sp|Q62Q88|KDM1A_	17,51	17,5	18,7	17,1	16	17,1	17	17	19	17,3	17	17	18,2	17,7	18	17	17,4	17,5	17,425	17,5277	Kdm1a	0,1	17,5	0,351	0,73	1	-7
>sp|Q9D312|K1C20_	20,77	21,7	21,3	21,2	21,1	19,9	21	20	21	19,7	21	21	20,9	21,1	21	22	20,4	20,4	20,857	20,7673	Krt20	-0,1	20,8	-0,35	0,73	1	-7
>sp|Q80X41|VRK1_M	18,61	18,8	18	19,2	19,3	17,5	19	19	19	19	19	18	18,3	17,4	19	19	19,2	19	18,693	18,589	Vrk1	-0,1	18,6	-0,35	0,731	1	-7
>sp|P0C872|JMJD7_	16,23	16,2	18,3	15,9	14,3	16,9	15	15	19	16,5	21	18	16	16,2	18	12	17,5	16,4	16,385	16,7237	Jmjd7	0,34	16,6	0,349	0,731	1	-7
>sp|Q922V4|PLRG1_	17,46	17,9	16,4	17,5	17,3	14,1	18	18	18	19,7	19	17	17,5	16,7	16	17	17,5	16,7	17,203	17,3963	Plrg1	0,19	17,3	0,348	0,732	1	-7
>sp|P67984|RL22_M	20,36	21	20,1	19,9	20,6	21,2	21	21	21	19,9	21	21	20,4	20,8	21	21	20,9	20,8	20,706	20,7783	Rpl22	0,07	20,7	0,348	0,732	1	-7
>sp|Q8VCM7|FIBG_M	20,24	20,9	21,1	21,3	21,2	21,3	21	21	21	21,1	21	21	21,3	20,8	22	21	21,5	21,2	21,122	21,1762	Fgg	0,05	21,1	0,347	0,733	1	-7
>sp|Q921F4|HNRLL_M	14,8	15,1	13,1	16,4	14,7	15,7	17	16	16	16,5	15	14	16,3	15,5	15	16	15,9	15,8	15,424	15,5797	Hnrnpll	0,16	15,5	0,347	0,733	1	-7
>sp|P14434|HA2B_M	18,49	18,2	18,5	18	18	18,5	17	19	19	18,4	19	17	17,7	19,8	19	18	18,1	18,2	18,309	18,4038	H2-Aa	0,09	18,4	0,346	0,734	1	-7
>sp|P70265|F262_M	14,04	13,8	13,8	13,5	13	12,7	14	13	12	13,3	12	13	13,6	13,3	13	12	13,3	14	13,229	13,1332	Pfkfb2	-0,1	13,2	-0,34	0,735	1	-7
>sp|Q91WU0|CES1F_I	22,65	22,7	16,6	23,8	23,6	16,7	23	19	18	20,2	20	20	20,3	20,6	18	22	19,8	20,4	20,582	20,2215	Ces1f	-0,4	20,4	-0,34	0,736	1	-7
>sp|P56371|RAB4A_	20,42	16,8	20	20,5	20,4	21	20	15	20	20	20	20	20,5	20,3	16	20	20,3	20,1	19,48	19,7547	Rab4a	0,27	19,6	0,341	0,737	1	-7
>sp|Q9Z0Z4|HEPH_M(	20,68	19,7	20,4	19,7	19,5	19,7	20	20	20	19,5	20	21	19,3	21,2	19	19	21,5	19,7	19,937	20,0497	Heph	0,11	20	0,339	0,739	1	-7
>sp|P99029|PRDX5_	22,52	23,2	23,3	22,6	24,4	23,7	24	24	24	24,5	24	24	22,5	23,6	23	23	23,4	22,2	23,462	23,3579	Prdx5	-0,1	23,4	-0,34	0,74	1	-7
>sp|Q9CYA6|ZCHC8_I	17,92	20,7	21,4	17,5	17,5	17,5	17	16	16	9,61	22	22	18,8	22,3	20	18	17,7	17,4	18,078	18,5402	Zcchc8	0,46	18,3	0,33	0,745	1	-7
>sp|Q922E4|PCY2_M	18,27	23,3	20,9	20,4	19,4	19,9	23	22	22	20,1	20	20	20	20,9	20	23	20,3	22,7	21,061	20,8389	Pcyt2	-0,2	21	-0,33	0,746	1	-7
>sp|Q61151|2A5E_M	16,54	19,9	19,5	19,5	19,6	19,6	20	17	19	18,8	17	19	19,5	19,4	20	19	17,8	18,7	19,019	18,862	Ppp2r5e	-0,2	18,9	-0,33	0,746	1	-7
>sp|P24549|AL1A1_	25,01	25	25,2	25,6	25,6	25,7	26	26	26	25,3	25	25	25,7	25,6	26	25	25,5	25,6	25,485	25,5222	Aldh1a1	0,04	25,5	0,326	0,748	1	-7
>sp|Q00898|A1AT5_	24	23,9	23,3	21,6	21,2	24,1	24	24	24	24,1	23	22	23,2	22,7	24	23	24,2	22,2	23,358	23,2097	Serpina1e	-0,1	23,3	-0,33	0,749	1	-7
>sp|Q921W4|QORL1_	18,15	18,3	19,1	19	18,6	18,8	20	21	20	18,6	19	19	18,7	18,9	19	20	20,1	18,9	19,19	19,0794	Cryzl1	-0,1	19,1	-0,33	0,749	1	-7
>sp|Q8CG72|ARHL2_	17,61	22,2	22	21,9	22	21,9	22	17	16	19	21	21	21,3	20,8	21	21	20,7	20,4	20,378	20,656	Adprhl2	0,28	20,5	0,325	0,749	1	-7
>sp|Q9DC61|MPPA_I	21,64	22,3	21,5	21,9	22,1	22,5	22	22	22	21,4	21	20	23,1	23	23	22	22,1	19,9	21,933	21,7994	Pmpca	-0,1	21,9	-0,32	0,752	1	-7
>sp|Q3UW53|NIBAN_	21,24	20,4	19,9	20	20,3	19,8	21	20	20	20	20	20	20,4	20,4	20	20	19,9	20,2	20,337	20,2721	Fam129a	-0,1	20,3	-0,32	0,754	1	-7
>sp|Q9R0Q6|ARC1A_	19,29	19,6	19,4	19,2	19	20,3	19	20	20	19,5	20	19	21	19	19	19	19	21,1	19,577	19,6814	Arpc1a	0,1	19,6	0,319	0,754	1	-7
>sp|Q6P8X1|SNX6_M	18,99	18,8	17,9	18,9	17,3	17,4	18	18	17	18,1	18	17	18,7	17,8	18	19	18,2	16,7	18,044	17,9454	Snx6	-0,1	18	-0,31	0,757	1	-7
>sp|Q9D9C6|CC182_	17,32	16,9	18,7	17,2	18,5	16,8	17	19	18	17,5	16	18	17,7	18,3	19	18	17,4	18	17,701	17,8262	Ccdc182	0,13	17,8	0,314	0,758	1	-7
>sp|Q07076|ANXA7_	18,47	19,1	21,6	18,2	17,8	17,7	18	19	19	18,3	22	22	18	17,5	18	19	18,7	17,6	18,738	18,9669	Anxa7	0,23	18,9	0,313	0,758	1	-7
>sp|P09405|NUCL_M	18,08	17,8	18	18	17,5	16,5	18	18	18	18,1	18	18	17,3	17,2	17	18	18,1	18,1	17,743	17,8114	Ncl	0,07	17,8	0,313	0,758	1	-7
>sp|P40142|TKT_MO	25,2	25	25,7	25,7	25,6	25,8	26	26	26	25	26	25	25,6	25,4	25	26	25,8	25,8	25,559	25,5193	Tkt	-0	25,5	-0,31	0,759	1	-7

>sp|Q497I4|KRT35_M	20,49	16,3	16,4	16,5	16,3	15,6	16	19	19	8,48	20	17	16,6	20,7	17	22	17,3	22,1	17,364	17,8344	Krt35	0,47	17,6	0,312	0,759	1	-7
>sp|A6X935|ITIH4_M	22,64	22,4	22	22,2	22,9	22,2	22	22	21	21,6	23	23	23,1	22,9	23	18	22,7	21,8	22,218	22,0426	Itih4	-0,2	22,1	-0,31	0,761	1	-7
>sp|Q9QZE5|COPG1_I	23,61	23,5	23,5	20,2	23	19,1	22	22	19	23,3	23	20	23,5	23,6	24	23	19	19,1	21,781	22,0759	Copg1	0,3	21,9	0,308	0,762	1	-7
>sp|P60867|RS20_M	23	20,7	20,5	20,6	20,7	21,2	20	20	21	20,6	21	21	20,5	20,2	21	20	21,2	21	20,847	20,7515	Rps20	-0,1	20,8	-0,31	0,762	1	-7
>sp|P29341|PABP1_	21,72	20,5	20,7	20,3	20,6	21	20	20	21	20,3	21	21	20,7	20,8	21	21	20,8	20,7	20,652	20,7025	Pabpc1	0,05	20,7	0,307	0,763	1	-7
>sp|P53994|RAB2A_	20,51	20,4	20,2	20,1	19,6	20,5	20	21	21	20,7	20	20	20,5	20,3	20	21	20,5	20,3	20,374	20,4211	Rab2a	0,05	20,4	0,307	0,763	1	-7
>sp|P59108|CPNE2_	16,96	14,9	15,9	15,5	16,2	15,7	17	16	17	15,5	16	16	15,6	15,7	18	18	15,6	16,5	16,168	16,2984	Cpne2	0,13	16,2	0,305	0,764	1	-7
>sp|O88939|ZBT7A_I	16,48	17,5	14	13,9	18	14,2	16	16	16	16,3	15	16	14,3	14,5	16	18	18,4	16,9	15,903	16,1099	Zbtb7a	0,21	16	0,305	0,764	1	-7
>sp|P97346|NXN_M(	14,3	13,7	13,5	14,1	13,2	14,7	13	11	12	8,31	12	12	16,8	11,9	17	12	10,9	15,3	13,266	12,9511	Nxn	-0,3	13,1	-0,3	0,765	1	-7
>sp|Q8R164|BPHL_M	19,76	21	24,2	19	18,9	19,4	20	23	24	23,1	24	23	19,2	23,4	19	19	19,1	21,6	21,01	21,3105	Bphl	0,3	21,2	0,304	0,765	1	-7
>sp|P45591|COF2_M	23,08	23,1	25	22,8	23,2	23,2	23	24	25	22,7	24	23	23,5	24,3	24	23	24,5	23,1	23,517	23,6176	Cfl2	0,1	23,6	0,304	0,765	1	-7
>sp|P82198|BGH3_M	21,68	22	23	22	23	22,6	23	22	23	22,2	22	22	22,9	23,4	23	22	22,3	22,5	22,441	22,5124	Tgfbi	0,07	22,5	0,303	0,766	1	-7
>sp|Q8CG03|PDE5A_	19,27	19,2	19,1	18,5	19,2	19	19	19	19	18,7	19	19	19	19,2	19	19	18,4	19	19,029	18,9913	Pde5a	-0	19	-0,3	0,767	1	-7
>sp|Q8BYM8|SYCM_M(	14,58	15,2	16,5	14,8	17	17,1	16	16	17	15	14	15	16,9	16,2	19	15	16	15,9	16,033	15,8676	Cars2	-0,2	16	-0,3	0,768	1	-7
>sp|Q99NB9|SF3B1_I	14,6	13,8	16,8	14,6	14,8	14,1	18	15	16	15,3	17	17	15,3	14,5	15	15	14,7	14,5	15,18	15,3367	Sf3b1	0,16	15,3	0,3	0,768	1	-7
>sp|Q7TMB8|CYFP1_I	18,79	18,3	18,4	18,1	18,1	18	17	18	17	18,9	18	18	18,4	17,3	18	18	17,9	17,5	18,046	17,9734	Cyfip1	-0,1	18	-0,3	0,77	1	-7
>sp|B1AQ75|KRT36_	20,42	20,4	16,9	17,1	16,7	16,4	16	19	19	13,6	20	17	16,9	20,7	17	22	17,3	22	18,099	18,4257	Krt36	0,33	18,3	0,297	0,77	1	-7
>sp|Q8CGA0|PPM1F_	16,76	18	18	16,7	17,8	18,1	18	18	18	17,5	18	18	17,9	17,6	17	17	17,6	17,7	17,72	17,6581	Ppm1f	-0,1	17,7	-0,29	0,772	1	-7
>sp|P63073|IF4E_MC	20,22	21,8	22,2	20,9	20,6	21,2	21	21	21	21,1	21	20	20,9	20,7	21	21	21,6	20,6	21,039	20,9631	Eif4e	-0,1	21	-0,29	0,773	1	-7
>sp|Q61646|HPT_MC	16,1	16,3	14,3	23,9	15,7	24	24	16	16	22,4	23	15	16,5	16,7	23	14	15,3	15,2	18,373	17,8311	Hp	-0,5	18,1	-0,29	0,774	1	-7
>sp|P62849|RS24_M	18,35	16	14,8	15	15,7	15,7	16	17	0	18,5	18	0	16,5	16,1	0	15	16,8	18,1	14,203	13,3057	Rps24	-0,9	13,8	-0,29	0,775	1	-7
>sp|Q9D518|F227B_	18,82	0	18,8	18,6	17,6	19,1	18	17	17	17,3	18	18	14,5	18,7	0	17	17,8	16,9	16,168	15,3591	Fam227b	-0,8	15,8	-0,29	0,776	1	-7
>sp|Q80YX1|TENA_M(	18,11	18,2	18	18,3	17,8	18,2	18	17	18	17,7	20	20	17,8	18,1	18	17	17,8	17,1	17,982	18,075	Tnc	0,09	18	0,287	0,778	1	-7
>sp|Q9CQ65|MTAP_M	20,9	21,3	25,7	24,7	24,8	21,1	22	25	22	23,7	21	24	24,2	20,1	24	24	24	23,9	22,973	23,2102	Mtap	0,24	23,1	0,283	0,781	1	-7
>sp|Q62418|DBNL_M	0	0	0	16	15,2	0	15	0	0	0	12	0	0	0	0	0	14,2	12,2	5,1854	4,24932	Dbnl	-0,9	4,72	-0,28	0,782	1	-7
>sp|Q9Z1Q9|SYVC_M(	22,37	21,7	21,5	21,7	21,7	21,6	22	22	22	21,7	21	22	21,6	21,8	22	22	21,6	21,8	21,736	21,7087	Vars	-0	21,7	-0,28	0,782	1	-7
>sp|Q8VE47|UBA5_M	16,36	16,1	16,9	16,9	16,6	15,1	16	16	16	14,5	16	17	16,8	17,1	17	16	16,8	15,9	16,285	16,3785	Uba5	0,09	16,3	0,28	0,783	1	-7
>sp|Q9D826|SOX_MC	17,34	17,3	17	20,6	20,8	21,6	21	18	17	17,9	18	18	19,4	20,6	20	21	17,2	17,1	18,989	18,7669	Pipox	-0,2	18,9	-0,28	0,783	1	-7
>sp|Q9ESB3|HRG_MO	19,59	19,9	19,4	19,6	19,4	19,1	20	19	19	19,3	19	19	20,6	19,1	20	19	19,4	19,7	19,507	19,554	Hrg	0,05	19,5	0,278	0,784	1	-7
>sp|O70624|MYOC_M	14,88	15,7	15,2	15,2	15,4	15,6	15	14	15	14,3	15	16	15,5	15,2	15	15	14,9	15,2	15,16	15,1031	Myoc	-0,1	15,1	-0,28	0,785	1	-7
>sp|Q1RLL3|CPNE9_M	16,63	14,7	15,7	15,2	15,9	15,4	17	16	17	15,1	16	15	15,4	15,4	17	18	15,3	16,2	15,892	16,0097	Cpne9	0,12	16	0,277	0,785	1	-7
>sp|Q8JZW4|CPNE5_I	16,63	14,7	15,7	15,2	15,9	15,4	17	16	17	15,1	16	15	15,4	15,4	17	18	15,3	16,2	15,892	16,0097	Cpne5	0,12	16	0,277	0,785	1	-7
>sp|P46471|PRS7_M	19,03	19,4	20,3	19,1	19,5	19	19	21	21	19,1	19	20	20,8	20,4	20	19	19	19,5	19,703	19,6058	Psmc2	-0,1	19,7	-0,28	0,785	1	-7
>sp|O35098|DPYL4_I	19,69	19,9	18,8	19,9	18,5	19	19	19	18	18,2	19	19	18,6	19,3	19	20	19	19,2	19,121	19,0387	Dpysl4	-0,1	19,1	-0,28	0,786	1	-7
>sp|Q61107|GBP4_M	0	0	16,3	16,6	16,4	16,6	17	16	16	14,6	0	15	15,8	15,9	16	15	14,9	15,3	12,819	13,6274	Gbp4	0,81	13,2	0,276	0,786	1	-7
>sp|Q5U5V2|HYKK_M	17,53	17,2	17,1	17,3	17,3	16,5	17	17	17	15,8	17	17	17,1	17,7	17	17	16,4	17,6	17,111	17,0501	Hykk	-0,1	17,1	-0,27	0,787	1	-7
>sp|Q91W10|S39A8_	24,6	24,5	17,6	24,6	14,8	24,7	19	19	19	16,8	16	17	25	17	25	25	25	17,1	20,912	20,3915	Slc39a8	-0,5	20,7	-0,27	0,788	1	-7
>sp|Q9CYR6|AGM1_M	23,45	23,3	21,8	21,9	22,1	21,9	23	22	23	21,3	21	21	21,7	21,2	24	24	24,3	24,2	22,512	22,6681	Pgm3	0,16	22,6	0,273	0,788	1	-7
>sp|Q9D7B6|ACAD8_	18,33	18,1	18,8	19,2	19	18,9	19	19	18	18,9	19	19	18,8	18,2	19	18	18,4	18,4	18,65	18,6987	Acad8	0,05	18,7	0,271	0,79	1	-7
>sp|Q8JZR0|ACSL5_M	15,38	15	14,9	14,2	16,1	16,1	16	16	15	14,7	20	14	14,9	15,3	14	14	14,5	15,6	15,436	15,2679	Acsl5	-0,2	15,4	-0,27	0,79	1	-7
>sp|O88543|CSN3_M	19,16	18,8	18,8	18,1	18,3	18,5	18	19	21	20,2	19	19	18,7	19	18	18	18,9	18,5	18,869	18,9527	Cops3	0,08	18,9	0,269	0,791	1	-7
>sp|Q99KV1|DJB11_	15,04	14,5	14,1	16,7	13,3	14,1	16	19	20	19,6	18	15	15	14,9	14	15	14,8	14,1	15,812	15,5497	Dnajb11	-0,3	15,7	-0,27	0,792	1	-7
>sp|Q9DC53|CPNE8_	16,59	14,6	15,6	15,1	15,8	15,4	17	16	17	15,1	16	15	15,3	15,4	17	18	15,2	16,2	15,835	15,9481	Cpne8	0,11	15,9	0,267	0,793	1	-7
>sp|Q9Z140|CPNE6_I	16,59	14,6	15,6	15,1	15,8	15,4	17	16	17	15,1	16	15	15,3	15,4	17	18	15,2	16,2	15,835	15,9481	Cpne6	0,11	15,9	0,267	0,793	1	-7
>sp|Q0VE82|CPNE7_I	16,7	14,8	15,7	15,2	16	15,5	17	16	17	15,2	16	15	15,4	15,5	17	18	15,4	16,2	15,96	16,0723	Cpne7	0,11	16	0,265	0,794	1	-7
>sp|Q8BLR2|CPNE4_I	16,7	14,8	15,7	15,2	16	15,5	17	16	17	15,2	16	15	15,4	15,5	17	18	15,4	16,2	15,96	16,0723	Cpne4	0,11	16	0,265	0,794	1	-7
>sp|Q9JLI8|SART3_M(	16,49	16,4	15,6	16,3	18,7	19,4	19	19	16	14,7	18	18	17,5	17,6	17	17	17,4	17,3	17,411	17,2472	Sart3	-0,2	17,3	-0,26	0,795	1	-7
>sp|P16110|LEG3_M	24,34	24,3	23,7	23,8	25,1	25	25	23	23	22,6	23	25	24,7	24,5	24	24	24,1	24,3	24,096	23,9957	Lgals3	-0,1	24	-0,26	0,795	1	-7

>sp|P59113|FERM1_	16,18	15,8	14,9	14,1	17,3	16,7	16	16	16	14	18	18	15,5	15	14	14	15	17,2	15,814	15,6467	Fermt1	-0,2	15,7	-0,26	0,795	1	-7
>sp|Q99MN9|PCCB_I	23,39	21,6	21,5	22,6	20,7	20,8	22	21	22	22,1	22	23	21,9	23,2	23	20	21,6	19,3	21,723	21,8575	Pccb	0,13	21,8	0,263	0,796	1	-7
>sp|Q9JMA2|TGT_MO	19,47	19,1	20,9	19,3	19,6	19,9	20	20	21	18,9	19	20	20,1	20,1	20	20	19,7	19,5	19,794	19,729	Qtrt1	-0,1	19,8	-0,26	0,796	1	-7
>sp|P63328|PP2BA_	20,34	20,1	19,6	20,7	20,6	20,2	20	20	21	19,8	21	20	20,3	20,3	21	20	20,8	20,3	20,367	20,4137	Ppp3ca	0,05	20,4	0,262	0,796	1	-7
>sp|O55142|RL35A_	21,94	21,1	22	24,2	22,2	21,7	21	21	22	21,4	22	22	22,4	22,2	23	22	21,5	21,3	21,944	21,8554	Rpl35a	-0,1	21,9	-0,26	0,797	1	-7
>sp|Q9R099|TBL2_M	16,52	18,2	19	18	17,9	17,9	17	18	17	19,1	16	20	17,6	16,1	17	18	18	17,5	17,734	17,609	Tbl2	-0,1	17,7	-0,26	0,797	1	-7
>sp|Q3V0K9|PLSI_MC	23,66	23,1	23	22,8	23,2	23,1	23	23	23	22,8	23	23	23,5	22,9	23	23	23,2	23,3	23,002	22,9666	Pls1	-0	23	-0,26	0,8	1	-7
>sp|Q6A4J8|UBP7_M	17,99	18,2	17,5	18,4	17,1	17,7	18	16	17	17,5	17	17	18	17,5	18	17	18,8	17,5	17,61	17,6781	Usp7	0,07	17,6	0,255	0,802	1	-7
>sp|P05202|AATM_M	21,1	21,1	20,1	20	19,9	23,8	20	20	24	20,8	22	21	20,8	23,1	21	21	21,3	20,7	21,061	21,214	Got2	0,15	21,1	0,255	0,802	1	-7
>sp|P17156|HSP72_	24,57	24,8	25	24,8	24,8	25,7	25	25	25	25	25	25	24,8	25	25	25	25,4	25,4	25,055	25,0902	Hspa2	0,04	25,1	0,253	0,803	1	-7
>sp|P23492|PNPH_M	23,36	23	22,1	23	22,6	22,5	23	23	23	23,3	22	22	23,3	23,3	23	23	23,5	23,1	22,935	22,9935	Pnp	0,06	23	0,253	0,804	1	-7
>sp|P46935|NEDD4_	19,42	17,7	18,5	18,9	18,5	18,5	19	19	19	18,7	18	19	19,6	19,6	17	19	19,3	19	18,816	18,895	Nedd4	0,08	18,9	0,253	0,804	1	-7
>sp|Q8K0E8|FIBB_MC	21,36	21	21,1	21,3	21,5	21,4	21	21	21	21,1	23	20	21	20,8	22	21	20,8	20,5	21,149	21,0854	Fgb	-0,1	21,1	-0,25	0,804	1	-7
>sp|P16294|FA9_MC	19,92	0	0	0	0	0	0	0	0	0	0	0	0	0	0	0	0	13,9	2,2134	1,54269	F9	-0,7	1,88	-0,25	0,805	1	-7
>sp|P97798|NEO1_M	16,15	15,4	15,3	16	15,4	14,3	16	16	14	15,3	15	15	16,3	15,4	16	15	14,7	15	15,298	15,2228	Neo1	-0,1	15,3	-0,25	0,805	1	-7
>sp|O35381|AN32A_	22,47	21,8	23,6	21,7	21,4	20,9	21	21	21	22,5	22	23	22,9	22,5	23	20	20,3	20,6	21,741	21,8524	Anp32a	0,11	21,8	0,251	0,805	1	-7
>sp|Q60994|ADIPO_I	18,86	19,3	19,7	19,6	19,4	20,1	20	19	19	18,9	19	19	19,8	19,9	19	19	20,1	20	19,505	19,454	Adipoq	-0,1	19,5	-0,25	0,805	1	-7
>sp|Q99LB2|DHRS4_I	19,59	19,7	17,7	17	19,1	19,5	19	18	18	18,4	19	19	18,6	19,3	19	18	18,3	19,3	18,663	18,7526	Dhrs4	0,09	18,7	0,249	0,806	1	-7
>sp|Q9WV91|FPRP_M	15,12	15,9	16,5	15,8	15,7	15,2	16	14	15	15,5	16	16	15,5	15,6	15	15	15,5	15,3	15,506	15,5647	Ptgfrn	0,06	15,5	0,249	0,807	1	-7
>sp|Q9WTP7|KAD3_M	19,01	20,5	20,1	20,2	20,1	20,3	20	20	21	20,1	20	20	20,4	20	21	20	20,4	19,9	20,195	20,2442	Ak3	0,05	20,2	0,249	0,807	1	-7
>sp|Q6ZWU9|RS27_M	19,61	20,1	20,1	18,7	18,9	19,1	19	20	20	19,8	19	20	19,3	19,5	20	19	18,9	19,4	19,438	19,487	Rps27	0,05	19,5	0,247	0,808	1	-7
>sp|Q6ZWY3|RS27L_M	19,61	20,1	20,1	18,7	18,9	19,1	19	20	20	19,8	19	20	19,3	19,5	20	19	18,9	19,4	19,438	19,487	Rps27l	0,05	19,5	0,247	0,808	1	-7
>sp|Q9DCM2|GSTK1_	19,29	19,3	19,6	19,6	15	19	19	19	16	19,9	20	20	19	19	19	17	18,8	14,3	18,387	18,5906	Gstk1	0,2	18,5	0,245	0,81	1	-7
>sp|Q8R3P0|ACY2_M	16,66	17,7	17,9	17,4	17,3	17,3	18	18	18	17,3	17	18	16,2	18,1	18	17	17,9	17,8	17,493	17,5546	Aspa	0,06	17,5	0,244	0,81	1	-7
>sp|P62835|RAP1A_	21,99	22,1	21	22,2	21,8	22,2	22	22	21	21,2	23	22	22,6	22,5	22	21	20,7	22,1	21,741	21,8148	Rap1a	0,07	21,8	0,243	0,811	1	-7
>sp|P18760|COF1_M	24,47	24,1	24,1	24,4	24,2	24,3	24	25	24	24,2	24	24	24,7	23,9	24	24	24,7	24,2	24,328	24,2943	Cfl1	-0	24,3	-0,24	0,811	1	-7
>sp|Q99L13|3HIDH_M	19,2	19,9	20,4	18,1	19,1	18,7	20	20	20	19,5	20	20	18,9	19,8	19	20	19	20	19,359	19,4243	Hibadh	0,07	19,4	0,241	0,813	1	-7
>sp|Q9WVP1|AP1M2	20,35	20,5	20,1	20,6	20,3	20	20	20	19	20,2	20	20	20	20,4	20	20	19,9	20,1	20,145	20,1781	Ap1m2	0,03	20,2	0,24	0,813	1	-7
>sp|P45700|MA1A1	20,63	20,7	19,3	19,4	19,3	18,9	19	18	20	19,4	19	19	17,7	18	18	21	21,7	18,9	19,391	19,2545	Man1a1	-0,1	19,3	-0,24	0,814	1	-7
>sp|Q8BTZ7|GMPPB_	21,87	22,2	22,5	22,3	23,8	23,5	23	23	23	22,7	23	23	22,4	22,8	23	22	22,7	22,9	22,788	22,7323	Gmppb	-0,1	22,8	-0,24	0,814	1	-7
>sp|P39039|MBL1_M	17,21	18,3	21,8	17,5	17,6	16,7	18	18	15	17,4	23	17	16,4	17	17	16	17,6	17,3	17,821	17,6175	Mbl1	-0,2	17,7	-0,24	0,815	1	-7
>sp|Q3TMX7|QSOX2_	15,85	16,4	15,3	18,8	17,2	15	19	19	18	14,4	14	16	14,6	15,6	15	21	20,8	20,5	17,16	16,9023	Qsox2	-0,3	17	-0,24	0,815	1	-7
>sp|P61965|WDR5_I	21,99	17,8	17,6	18,3	17,7	18,1	18	18	19	18,5	20	19	17,1	18,5	18	19	18,1	17,9	18,575	18,45	Wdr5	-0,1	18,5	-0,24	0,815	1	-7
>sp|Q99K30|ES8L2_M	14,81	14,8	13,6	15,8	15,2	15,7	16	14	14	15,2	15	15	15,5	15	15	15	13,4	14,8	14,796	14,8781	Eps8l2	0,08	14,8	0,237	0,815	1	-7
>sp|P46660|AINX_M	0	17,2	17	17,3	17,4	18,1	18	18	17	15,3	16	16	16,1	16,1	16	16	16,3	15,8	15,53	15,9856	Ina	0,46	15,8	0,237	0,816	1	-7
>sp|Q8QZZ7|TPRKB_M	15,31	13,5	13,1	0	0	0	0	18	18	18,6	16	16	18,4	0	0	0	0	0	8,6606	7,69308	Tprkb	-1	8,18	-0,24	0,816	1	-7
>sp|Q64437|ADH7_M	20,29	20,2	16,2	21,4	21	15,8	21	20	20	19,3	20	20	20,8	16,2	17	22	22,2	16,9	19,629	19,3899	Adh7	-0,2	19,5	-0,23	0,817	1	-7
>sp|O88685|PRS6A_	20,21	19,4	18,8	19,9	20,8	20,1	20	19	19	18,4	21	18	20,5	20,6	20	20	19,7	20,5	19,709	19,8007	Psmc3	0,09	19,8	0,233	0,819	1	-7
>sp|Q99K51|PLST_MC	21,8	21,7	21,8	20,8	21,3	21,5	21	22	22	21,2	22	21	20,9	21,1	21	21	21,5	22,3	21,447	21,4033	Pls3	-0	21,4	-0,23	0,82	1	-7
>sp|Q99JI6|RAP1B_M	22,35	22,4	21,6	22,4	22,1	22,3	22	22	22	21,9	23	22	22,9	22,6	23	21	20,7	22,1	22,096	22,0371	Rap1b	-0,1	22,1	-0,23	0,82	1	-7
>sp|O08795|GLU2B_	15,73	15,9	0	16,4	15,8	16,2	16	16	16	14,8	0	15	15,6	15,8	16	15	15,1	15,6	14,244	13,6783	Prkcsh	-0,6	14	-0,23	0,82	1	-7
>sp|P70694|DHB5_M	18,09	19,1	19,9	19,9	19,9	20	20	20	20	19,9	18	20	19,9	19,9	20	20	19,6	19,4	19,677	19,613	Akr1c6	-0,1	19,6	-0,23	0,82	1	-7
>sp|P54823|DDX6_M	18,17	18	16,3	16,7	17,3	17,8	18	18	17	17,2	18	17	17	18,5	19	18	16,8	17,3	17,505	17,5804	Ddx6	0,08	17,5	0,228	0,822	1	-7
>sp|Q9CQV8|1433B_	24,64	26,4	23,5	25,8	24	24,3	25	25	25	24,4	25	25	25,1	24,7	25	25	25	24,4	24,825	24,8971	Ywhab	0,07	24,9	0,228	0,823	1	-7
>sp|Q8K0Y2|KT33A_I	16,91	14,9	20,2	20	20	19,8	17	20	20	18,1	19	18	18,5	18,8	19	18	19	19	18,689	18,5389	Krt33a	-0,2	18,6	-0,23	0,823	1	-7
>sp|P08226|APOE_M	20,77	21	19,9	19,5	20,6	20,8	21	20	20	19,9	21	21	20,1	20,9	21	20	20,4	19,4	20,309	20,371	Apoe	0,06	20,3	0,227	0,823	1	-7
>sp|P80317|TCPZ_M	20,94	20,8	20,1	20,7	20,9	21,3	19	21	19	20,6	21	21	19,9	19,9	20	20	20,8	20,6	20,478	20,4115	Cct6a	-0,1	20,4	-0,23	0,823	1	-7
>sp|Q61554|FBN1_M	19,02	18,5	20,4	18,2	18,4	19,3	18	20	20	18,1	20	20	19,2	20,4	19	18	18,7	18,3	19,068	19,1536	Fbn1	0,09	19,1	0,227	0,824	1	-7

>sp|P47962|RL5_MC	20,99	20,9	18,5	20,6	19,6	19,7	21	19	20	18,5	24	20	19,3	19,3	20	21	19,8	19,2	20,001	20,1419	Rpl5	0,14	20,1	0,225	0,825	1	-7
>sp|Q6X893|CTL1_M	16,13	0	0	16,5	15,4	15,8	16	15	14	0	14	0	14,2	12,4	14	16	15,7	16,4	12,15	11,4459	Slc44a1	-0,7	11,8	-0,22	0,826	1	-7
>sp|Q6P8J7|KCRS_M	23,77	21,6	21,7	21,5	21,9	23,5	23	22	22	23,2	23	22	21,8	19,5	22	24	21,3	22	22,23	22,1157	Ckmt2	-0,1	22,2	-0,22	0,827	1	-7
>sp|Q9CR39|WIPI3_M	17,36	16,5	20,8	17,4	17,4	17,1	18	18	17	15,5	20	20	17,1	17,1	17	17	16,1	16,7	17,682	17,5292	Wdr45b	-0,2	17,6	-0,22	0,827	1	-7
>sp|Q8BIP0|SYDM_M(	15,7	16,4	16,7	14,3	16,8	15,1	15	16	16	16,4	16	16	15,1	14,8	17	16	15,5	16,1	15,814	15,8952	Dars2	0,08	15,9	0,22	0,829	1	-7
>sp|Q99JX3|GORS2_I	13,88	15,1	17,7	0	0	0	0	0	0	17,8	18	18	0	0	0	0	0	0	5,189	6,05423	Gorasp2	0,87	5,62	0,219	0,829	1	-7
>sp|Q91X51|GORS1_	13,91	15,2	17,8	0	0	0	0	0	0	17,9	18	18	0	0	0	0	0	0	5,2182	6,08538	Gorasp1	0,87	5,65	0,218	0,83	1	-7
>sp|Q9WUI1|MK11_M	20,88	21,1	21,4	21	20,7	20,8	21	21	14	21,1	22	22	17,6	17,5	18	21	21,2	20,9	20,295	20,092	Mapk11	-0,2	20,2	-0,22	0,832	1	-7
>sp|Q9WV54|ASAH1_	18,32	18,3	19,2	19,6	21,7	22,1	19	13	14	17,8	18	18	18,1	18,5	19	19	18,5	17,4	18,405	18,1918	Asah1	-0,2	18,3	-0,22	0,832	1	-7
>sp|P11983|TCPA_M	22,58	22,6	19,7	20,6	19,6	20,7	20	19	19	19,9	21	21	21,2	20	21	20	20,4	19,2	20,469	20,3687	Tcp1	-0,1	20,4	-0,21	0,835	1	-7
>sp|Q3THK7|GUAA_M	19,01	20,5	20,4	20,3	18,8	20,5	20	20	20	20,1	19	20	19,8	20,3	19	20	19,7	20,1	19,923	19,8714	Gmps	-0,1	19,9	-0,21	0,838	1	-7
>sp|P70124|SPB5_M	16,31	15,9	15,8	16,2	16	16,2	16	17	17	17	17	17	15,8	15,9	17	15	16,5	15,8	16,274	16,3325	Serpinb5	0,06	16,3	0,207	0,839	1	-7
>sp|Q8CHH9|SEPT8_M	25,08	20,2	19,2	19,6	19,8	19,5	19	19	20	20	18	20	20,3	20,3	21	20	20,3	20,5	20,201	20,0633	Sept8	-0,1	20,1	-0,21	0,839	1	-7
>sp|Q3U3R4|LMF1_M	0	17,3	17	18,5	18,1	17,2	17	17	18	16,3	0	17	17,8	16,9	17	17	16,7	16,4	15,566	15,0153	Lmf1	-0,6	15,3	-0,21	0,84	1	-7
>sp|O08911|MK12_I	20,61	20,9	21,1	20,8	20,5	20,6	21	21	14	20,9	21	21	17,4	17,3	18	21	21	20,7	20,052	19,857	Mapk12	-0,2	20	-0,21	0,84	1	-7
>sp|Q5FWK3|RHG01_	17,98	19,5	19,2	19,5	18,6	18,3	18	20	20	20,8	19	18	19,9	18,6	20	18	18,4	17,9	18,928	19,0157	Arhgap1	0,09	19	0,205	0,84	1	-7
>sp|Q9D964|GATM_M	16,27	17,3	18,6	18	18,5	17,9	19	19	17	17,3	18	18	17,7	17,5	18	19	17,8	18,3	17,887	17,9515	Gatm	0,06	17,9	0,204	0,841	1	-7
>sp|P13595|NCAM1	16,26	16,3	15,4	17,2	14,8	16,1	19	18	17	15,1	17	17	16	16,5	17	17	17	16,8	16,665	16,5697	Ncam1	-0,1	16,6	-0,2	0,841	1	-7
>sp|Q9QZE7|TSNAX_M	17,8	20	16,7	18,1	17,9	20,4	17	20	17	20,2	18	16	18	18,1	18	18	20	18,7	18,393	18,269	Tsnax	-0,1	18,3	-0,2	0,842	1	-7
>sp|P63323|RS12_M	21,59	20,5	19,5	19,3	19,5	20,1	22	20	20	19,8	21	21	20,5	20,7	20	20	20,2	20,3	20,284	20,35	Rps12	0,07	20,3	0,201	0,843	1	-7
>sp|Q8BTF8|RALYL_M	14,92	17,9	17,2	17,9	16,6	15,9	21	17	20	16,4	22	18	16,9	17,5	17	17	17,3	15,6	17,588	17,4151	Ralyl	-0,2	17,5	-0,2	0,843	1	-7
>sp|P62334|PRS10_	18,88	18,7	18,7	18,9	17,9	19	19	20	19	20,1	20	18	18,5	18,2	19	18	18,1	18,4	18,854	18,7855	Psmc6	-0,1	18,8	-0,2	0,844	1	-7
>sp|Q91VD9|NDUS1_	21,03	20,6	20,1	20,6	18,6	21,2	21	21	20	20,9	19	21	20,4	20,4	20	21	20,5	20,6	20,363	20,4251	Ndufs1	0,06	20,4	0,196	0,847	1	-7
>sp|O70310|NMT1_M	20,5	20,6	19,4	17,3	18,2	18,9	20	20	20	19,3	20	19	19,3	19,2	19	20	18,8	19,8	19,378	19,4557	Nmt1	0,08	19,4	0,196	0,847	1	-7
>sp|Q641P0|ARP3B_	20,97	21,3	22,1	20,3	22,6	20,5	21	22	22	20,9	21	21	20,7	22,2	20	22	22,2	22,2	21,483	21,4072	Actr3b	-0,1	21,4	-0,2	0,847	1	-7
>sp|P48722|HS74L_I	20,33	20,9	22,4	20,5	20,7	21	21	21	21	20,8	22	22	20	19,9	20	22	21,6	21,6	20,986	21,053	Hspa4l	0,07	21	0,194	0,848	1	-7
>sp|P63011|RAB3A_	20,69	18,8	20,5	20,7	20,6	21,1	21	18	21	20,3	21	20	20,8	20,7	19	21	20,5	20,3	20,252	20,3277	Rab3a	0,08	20,3	0,194	0,848	1	-7
>sp|Q9CZT8|RAB3B_I	20,69	18,8	20,5	20,7	20,6	21,1	21	18	21	20,3	21	20	20,8	20,7	19	21	20,5	20,3	20,252	20,3277	Rab3b	0,08	20,3	0,194	0,848	1	-7
>sp|O70591|PFD2_M	18,65	18,5	19	18,7	18,8	18,9	18	17	19	16,5	19	18	19,4	17	20	19	18,5	18,7	18,432	18,3501	Pfdn2	-0,1	18,4	-0,19	0,851	1	-7
>sp|P51410|RL9_MC	20,81	20,9	21,8	20,9	20,8	18,1	21	21	21	18,7	22	22	18,8	22	22	20	20,5	19,3	20,686	20,5795	Rpl9	-0,1	20,6	-0,19	0,852	1	-7
>sp|Q499X9|SYMM_M	19,52	15,3	15,5	18,8	18,4	16	21	16	15	16,6	18	15	17,4	17,5	17	19	17,6	18,3	17,286	17,4289	Mars2	0,14	17,4	0,187	0,854	1	-7
>sp|Q08122|TLE3_MC	18,11	18,4	18,8	18,7	18,1	18,3	18	19	19	19,8	18	17	18,5	18,3	19	19	19,4	17,3	18,442	18,5019	Tle3	0,06	18,5	0,187	0,854	1	-7
>sp|O00897|A1AT4_	24,31	24,3	24	22,9	23,4	24,4	25	25	25	24,6	24	24	24,1	23,5	24	24	24,6	23,5	24,109	24,0656	Serpina1d	-0	24,1	-0,18	0,856	1	-7
>sp|Q9DBM2|ECHP_M	0	0	0	0	0	0	16	15	14	0	0	0	16	16,1	19	0	0	0	4,9609	5,65032	Ehhadh	0,69	5,31	0,185	0,856	1	-7
>sp|Q8BGW1|FTO_MC	15,56	14,7	13,8	13,2	15,1	12,9	15	13	0	14,8	0	15	13,8	16	16	15	14,6	12,1	12,598	13,0189	Fto	0,42	12,8	0,183	0,857	1	-7
>sp|Q9WVE8|PACN2_	21,51	20,1	19,5	19,5	21,4	19,6	19	20	20	20,2	20	20	20,2	20,3	21	19	19,1	20	19,963	19,8986	Pacsin2	-0,1	19,9	-0,18	0,858	1	-7
>sp|P62331|ARF6_M	16,43	24,6	19,3	15,2	16,5	16,7	15	18	18	17,7	18	18	17,4	18	18	18	18,3	17,9	17,733	17,9062	Arf6	0,17	17,8	0,181	0,859	1	-7
>sp|Q99PE9|ARL4D	16,43	24,6	19,3	15,2	16,5	16,7	15	18	18	17,7	18	18	17,4	18	18	18	18,3	17,9	17,733	17,9062	Arl4d	0,17	17,8	0,181	0,859	1	-7
>sp|P45376|ALDR_M	23,89	23,9	26	23,7	24,5	23,9	24	24	24	23,9	25	25	23,9	24,3	24	24	23,5	24,2	24,234	24,1819	Akr1b1	-0,1	24,2	-0,18	0,859	1	-7
>sp|P35123|UBP4_M	14,18	13,7	15,9	15,4	16,1	15,7	14	15	15	15,5	16	15	15	15,6	15	15	14,9	13,7	14,995	15,0604	Usp4	0,07	15	0,178	0,861	1	-7
>sp|Q9DCD0|6PGD_M	25,14	25	24,3	24,6	25,5	24,7	26	25	24	25,1	25	25	24,8	25	25	25	25	25,1	24,9	24,927	Pgd	0,03	24,9	0,178	0,861	1	-7
>sp|Q8BVE3|VATH_M	18,56	19,2	18,9	19,5	16,5	18,6	19	20	20	17,6	19	18	19,4	17,7	20	19	19,2	19,2	18,867	18,7928	Atp6v1h	-0,1	18,8	-0,18	0,861	1	-7
>sp|Q9CQV6|MLP3B_	18,18	17,3	19,2	17,3	18,3	18,8	17	17	17	16,8	17	19	19,1	17,8	19	17	17,1	17,6	17,814	17,8882	Map1lc3b	0,07	17,9	0,175	0,863	1	-7
>sp|Q9D8X1|CUTC_M	19,26	19,3	18,8	19,4	19	18,3	19	19	20	19,6	20	19	19,7	16,5	18	19	19,5	19,7	19,129	19,0637	Cutc	-0,1	19,1	-0,17	0,864	1	-7
>sp|P63017|HSP7C_	26,68	25,5	25,9	25,8	26	26,5	26	27	26	25,9	26	26	25,7	26	26	28	26,3	26	26,195	26,1556	Hspa8	-0	26,2	-0,17	0,865	1	-7
>sp|O88512|AP1G2_	19,29	19,9	20,8	19,7	19,4	19,9	20	21	20	22,2	18	22	21,2	18	22	18	17,7	21,6	19,92	20,0496	Ap1g2	0,13	20	0,173	0,865	1	-7
>sp|Q99KB8|GLO2_M	18,06	18,2	19,2	18,9	18,1	17,9	20	19	19	18	21	19	18,5	18,3	19	18	18,3	17,5	18,663	18,602	Hagh	-0,1	18,6	-0,17	0,866	1	-7
>sp|Q6P6M7|SPCS_M	19,09	18,8	19,2	16,7	16,6	16,9	16	17	17	16,7	21	21	17,4	17,4	17	13	12,1	19,4	17,419	17,2317	Sepsecs	-0,2	17,3	-0,17	0,866	1	-7

>sp|Q9Z1Z0|USO1_M(	18,97	18,5	19	20,4	20,5	18,9	21	21	21	20	20	20	19,7	19,6	20	20	19,7	19,8	19,8	19,8538	Uso1	0,05	19,8	0,171	0,866	1	-7
>sp|Q8BIJ6|SYIM_MOI	20,57	20	19,8	20,3	20,4	20	21	20	20	20,3	21	21	20,4	20,4	20	20	20,6	20,1	20,322	20,345	Iars2	0,02	20,3	0,168	0,868	1	-7
>sp|Q62470|ITA3_M(	16,62	15,2	17	16,2	15,4	16,7	16	17	15	15,5	17	17	16,7	15,3	16	16	15,6	16,3	16,148	16,2024	Itga3	0,05	16,2	0,168	0,868	1	-7
>sp|Q8R121|ZPI_MOI	18,63	20,5	17,8	17	17,2	18,3	18	18	18	17,4	19	17	19,4	19,2	20	17	17,9	17,3	18,181	18,2649	Serpina10	0,08	18,2	0,167	0,87	1	-7
>sp|Q3U5Q7|CMPK2	21,18	20,8	21	23	22,6	21	21	21	21	22,7	21	20	20,9	21,3	22	21	21,3	21,6	21,446	21,3857	Cmpk2	-0,1	21,4	-0,17	0,871	1	-7
>sp|Q8CI33|C19L1_M	17,85	17,5	16,9	16,1	17,3	17,6	16	17	19	17,1	17	17	17,1	17,3	17	17	18,9	16,8	17,286	17,2233	Cwf19l1	-0,1	17,3	-0,17	0,871	1	-7
>sp|P58710|GGLO_M	0	19,6	20	20,5	22,2	20	20	21	22	20	0	20	20,9	19,4	20	20	20	20	18,326	17,8024	Gulo	-0,5	18,1	-0,16	0,871	1	-7
>sp|Q9DAS9|GBG12_	0	22,7	22,9	18,6	22,9	17,9	18	23	23	23,4	22	23	0	19,8	19	18	18,7	19	18,699	18,147	Gng12	-0,6	18,4	-0,16	0,872	1	-7
>sp|Q3UJU9|RMD3_M	0	14,7	14,7	14,5	0	0	15	14	0	13,1	0	0	13,9	0	14	13	13,8	0	8,126	7,55638	Rmdn3	-0,6	7,84	-0,16	0,872	1	-7
>sp|Q99KK9|SYHM_M	15,64	16,1	15,8	15,9	16,3	16,4	14	16	13	17	16	16	14	14,2	14	16	16,1	16,3	15,463	15,5503	Hars2	0,09	15,5	0,164	0,872	1	-7
>sp|Q62188|DPYL3_I	21,51	21,7	21,5	21,8	21,7	21,6	22	21	21	21,4	22	22	21,6	21,8	22	21	21,2	21,6	21,582	21,567	Dpysl3	-0	21,6	-0,16	0,873	1	-7
>sp|Q9CW46|RAVR1_	19,7	19,5	16,1	19,7	16,5	16,4	20	20	19	17	17	18	17,3	17,1	21	20	20,5	20,3	18,5	18,6245	Raver1	0,12	18,6	0,16	0,875	1	-7
>sp|P62823|RAB3C_	21,14	19,5	20,6	20,9	20,7	21,2	21	18	21	20,4	21	21	20,9	20,7	19	21	20,5	20,3	20,39	20,4547	Rab3c	0,06	20,4	0,159	0,875	1	-7
>sp|Q9D5V5|CUL5_M	18,79	19,2	20,9	21,3	21,3	20,8	21	19	21	18,8	21	21	21,1	20,7	21	19	20,6	20,7	20,31	20,3841	Cul5	0,07	20,3	0,158	0,876	1	-7
>sp|Q99JF8|PSIP1_M	17,12	14,6	19	19,3	19,4	18	17	19	19	18,7	19	19	19	18,7	18	18	15,5	17,3	18,022	18,1218	Psip1	0,1	18,1	0,157	0,877	1	-7
>sp|Q99L04|DHRS1_I	14,68	15,7	16	16,1	15,7	16,2	0	16	14	13,3	15	0	15,5	15,1	16	15	15,7	14,9	13,83	13,453	Dhrs1	-0,4	13,6	-0,16	0,877	1	-7
>sp|P63325|RS10_M	15,08	14,8	20,4	16,4	15,2	16,4	0	0	0	16,2	16	17	0	16,4	0	0	16,1	11,5	10,917	10,324	Rps10	-0,6	10,6	-0,16	0,878	1	-7
>sp|O55029|COPB2_	21,16	22,1	21,2	22	21,8	21,6	22	21	21	21,4	21	21	22,2	21,4	21	22	22	21	21,583	21,5558	Copb2	-0	21,6	-0,16	0,878	1	-7
>sp|P59708|SF3B6_I	20,67	20,5	20,8	21,5	21,2	19,9	20	20	21	20,2	19	20	22	22,3	21	20	20,3	20	20,611	20,5524	Sf3b6	-0,1	20,6	-0,16	0,878	1	-7
>sp|P47856|GFPT1_I	19,05	19	20	19,5	19,3	19,3	20	20	20	19,7	19	19	19,5	19,5	20	20	19,5	19,5	19,539	19,5596	Gfpt1	0,02	19,5	0,153	0,88	1	-7
>sp|P01803|HVM34	16,45	16,7	16,3	19,4	14,5	14,8	16	18	17	18	16	17	19,6	15,3	14	19	16,6	15,1	16,592	16,712	>sp|P018	0,12	16,7	0,153	0,88	1	-7
>sp|Q8VC30|TKFC_M	20,7	21,1	23,7	21,1	21,1	20,7	22	21	24	21,6	20	23	20,7	22,5	23	21	21,1	21,4	21,651	21,5752	Tkfc	-0,1	21,6	-0,15	0,882	1	-7
>sp|Q9ERL7|GMFG_M	17,22	17	19,8	17,6	19	19,3	20	21	21	19,4	20	16	19,2	19,2	19	20	19,7	19,8	19,027	19,1215	Gmfg	0,09	19,1	0,15	0,882	1	-7
>sp|O70570|PIGR_M	20,39	20,9	21	21,5	21,6	21,9	21	21	21	19,9	20	20	21,9	20,5	22	22	21,6	22	21,165	21,1129	Pigr	-0,1	21,1	-0,15	0,883	1	-7
>sp|Q91WK2|EIF3H_M	19,3	19,9	19,8	17,4	16,8	18,3	18	18	17	18,1	19	19	17,7	18,9	19	17	16,8	17,3	18,236	18,1647	Eif3h	-0,1	18,2	-0,15	0,884	1	-7
>sp|P57746|VATD_M	18	17,5	0	16,9	18	15,6	0	16	17	17,2	0	0	18,3	17,6	19	16	17,4	17,3	13,214	13,7333	Atp6v1d	0,52	13,5	0,145	0,886	1	-7
>sp|Q8BX02|KANK2_	17,19	16,9	23,8	17,5	16,8	23,7	16	17	16	16,8	23	23	16,8	17,9	18	17	15,7	15,6	18,325	18,1294	Kank2	-0,2	18,2	-0,14	0,887	1	-7
>sp|Q6PD03|2A5A_M	15,26	16,4	15,7	16,6	16,2	16,3	16	16	16	16,3	16	16	16,5	16,5	16	16	15,6	16,3	16,12	16,1439	Ppp2r5a	0,02	16,1	0,143	0,888	1	-7
>sp|Q9CR16|PPID_M	20,45	21,2	23,2	21,8	23,4	20,4	22	23	21	20,8	23	22	20,9	22,1	22	22	21,7	21,7	21,785	21,7266	Ppid	-0,1	21,8	-0,14	0,889	1	-7
>sp|P53612|PGTB2_	17,97	18,4	20,7	21,2	21,1	17,8	21	17	18	17,9	18	20	19,6	19,7	20	20	19,9	19,9	19,221	19,3114	Rabggtb	0,09	19,3	0,14	0,89	1	-7
>sp|P35282|RAB21_	20	21	20,8	21,3	21,1	21,1	21	21	19	21,7	21	19	21,2	20,2	22	20	20,9	19,9	20,709	20,6553	Rab21	-0,1	20,7	-0,14	0,893	1	-7
>sp|Q9D0S9|HINT2_M	18,75	18,8	17,7	18,8	18,5	19,2	19	19	21	19,1	19	19	19,1	19	18	19	19,1	19,3	18,891	18,9308	Hint2	0,04	18,9	0,136	0,893	1	-7
>sp|Q8VHY0|CSPG4_I	16,1	16,3	18,4	18,9	18,7	16,7	18	17	18	17,5	17	18	17,6	17,9	18	18	18,1	17,7	17,673	17,6221	Cspg4	-0,1	17,6	-0,13	0,895	1	-7
>sp|Q62468|VILI_MO	23,12	23,1	22,9	23	22,9	22,9	23	23	23	24	23	22	22,8	22,6	23	23	24,2	22,5	23,008	23,0363	Vil1	0,03	23	0,134	0,895	1	-7
>sp|Q8BT51|COA4_M	15,21	18,8	15,3	18,6	18,8	19	17	16	21	17,6	19	16	19,8	15,5	20	16	16,1	20,1	17,66	17,7839	COA4	0,12	17,7	0,133	0,896	1	-7
>sp|Q6ZWX6|IF2A_M(	20,12	20,5	21,3	22,4	22,5	22,2	22	22	22	21,6	21	21	21,8	21,6	22	22	21,6	21,8	21,642	21,6029	Eif2s1	-0	21,6	-0,13	0,897	1	-7
>sp|Q9CPX6|ATG3_M	16,68	16,6	16,8	17,9	18,3	20,7	18	18	18	17,4	17	18	17,3	15,2	17	19	19,4	19	17,844	17,7628	Atg3	-0,1	17,8	-0,13	0,897	1	-7
>sp|Q9WVA3|BUB3_I	20,48	21,4	21,3	20,7	21,2	20,9	21	21	20	21,2	21	21	20,8	20,8	21	21	20,5	21,2	20,851	20,8759	Bub3	0,03	20,9	0,131	0,898	1	-7
>sp|Q8BP40|PPA6_M	15,18	14,6	16,2	14,5	15,4	16,2	15	15	13	12,9	15	15	15,3	15,4	16	15	14,9	15	14,95	14,8978	Acp6	-0,1	14,9	-0,13	0,898	1	-7
>sp|O55013|TPPC3_	18,27	19,4	19,2	18,8	19,2	18,2	19	19	19	18,8	20	19	19	18,8	19	18	19,3	18,5	18,9	18,9259	Trappc3	0,03	18,9	0,13	0,898	1	-7
>sp|P52825|CPT2_M	18,17	19,1	18,7	18,2	17,8	19,3	19	19	18	18,9	18	18	18,7	18,4	19	19	19,5	18,4	18,603	18,5722	Cpt2	-0	18,6	-0,13	0,9	1	-7
>sp|Q8BGE6|ATG4B_I	0	15,8	14,1	17,1	17,1	16,9	16	17	15	16,7	0	15	18,1	17,2	17	17	15,1	16,4	14,371	14,7001	Atg4b	0,33	14,5	0,127	0,9	1	-7
>sp|Q8VEJ4|NLE1_MC	15,94	16,3	15,8	16,9	17	17,1	17	17	17	16,6	15	16	16,6	17,4	17	16	17,4	17,2	16,631	16,5948	Nle1	-0	16,6	-0,13	0,9	1	-7
>sp|P58252|EF2_MO	24,49	24,5	25,6	25,2	24,2	25	24	24	26	24,9	24	25	25,3	24,2	25	24	25,2	25	24,828	24,796	Eef2	-0	24,8	-0,13	0,902	1	-7
>sp|P21278|GNA11_	19,12	20,3	20,8	20,4	20	19,5	20	20	20	20,1	20	20	19,6	20,1	20	20	19,8	19,8	20,057	20,0344	Gna11	-0	20	-0,12	0,904	1	-7
>sp|O35103|OMD_M	17,53	17,6	16,7	17	16,3	16,4	17	19	15	16,5	16	16	16,5	17,3	16	17	17,4	17,4	16,883	16,8336	Omd	-0	16,9	-0,12	0,904	1	-7
>sp|Q9D892|ITPA_M(	21,61	22,1	22,5	22,8	21,6	22,7	23	22	23	22,4	22	22	22,4	22,8	23	22	22,4	22,5	22,352	22,376	Itpa	0,02	22,4	0,123	0,904	1	-7
>sp|Q8C650|SEP10_I	24,92	19,7	19,4	18,7	18,8	19,4	20	20	22	20,1	19	22	20	20,3	20	20	20,3	20,2	20,289	20,2045	Sept10	-0,1	20,2	-0,12	0,905	1	-7

>sp|Q6DTY7|F264_M(	14,06	14	14	13,6	13,1	13	14	13	12	13,6	13	13	13,7	13,6	13	13	13,6	14,2	13,393	13,3613	Pfkfb4	-0	13,4	-0,12	0,907	1	-7
>sp|Q8VDJ3|VIGLN_M	15,53	13,7	15,7	14,4	14,3	16	15	15	15	15	15	16	14,6	15,2	16	13	15,2	15,2	14,965	15,0067	Hdlbp	0,04	15	0,117	0,908	1	-7
>sp|P35235|PTN11_	20,54	19,8	19,8	19,9	19,9	19,9	19	20	20	19	21	20	18,7	20,6	20	20	20,2	19,9	19,872	19,9002	Ptpn11	0,03	19,9	0,117	0,908	1	-7
>sp|Q9DAF3|DDI1_M(	17,67	17,6	18,2	17,8	17,7	17,5	18	17	17	17,8	18	18	18,5	18,6	19	15	18,5	15,5	17,644	17,59	Ddi1	-0,1	17,6	-0,12	0,909	1	-7
>sp|O70311|NMT2_M	0	0	0	0	0	0	0	16	16	18,6	17	0	0	0	0	0	0	0	3,5579	3,95933	Nmt2	0,4	3,76	0,115	0,91	1	-7
>sp|Q6NSR8|PEPL1_M	20,97	20,8	19,5	21,8	21,1	22,6	23	22	22	21,8	20	22	21,6	22,2	21	22	21,9	22	21,54	21,5834	Npepl1	0,04	21,6	0,113	0,911	1	-7
>sp|P30416|FKBP4_	21,43	22,4	22,2	24,9	25,2	21,9	25	22	25	23,5	24	24	21	24,3	24	24	24,2	21,7	23,353	23,4268	Fkbp4	0,07	23,4	0,11	0,914	1	-7
>sp|P97864|CASP7_	19,28	22,2	21,4	18,3	18,1	18,5	19	19	19	18,8	19	19	19	19,4	20	21	18,8	18,5	19,342	19,2821	Casp7	-0,1	19,3	-0,11	0,915	1	-7
>sp|P97927|LAMA4_	17,88	17,4	17,6	17,6	17,4	18,1	18	17	17	17,8	18	16	16,4	15,9	18	19	18,4	18,5	17,527	17,4897	Lama4	-0	17,5	-0,11	0,915	1	-7
>sp|Q9QXA5|LSM4_M	22,71	21,7	25,5	21,8	21	20,9	21	21	21	21,3	22	22	22	22,2	22	23	21,5	21,2	21,829	21,8847	Lsm4	0,06	21,9	0,107	0,916	1	-7
>sp|Q5I2A0|SPA3G_M	19,93	20,1	19	19,3	18,6	19,2	19	19	19	19,1	19	19	19,7	19,2	19	19	19	19,2	19,158	19,18	Serpina3g	0,02	19,2	0,107	0,916	1	-7
>sp|Q9JHK4|PGTA_M	19,48	19,7	19,8	21	21,1	22,2	20	21	21	21,4	20	20	20,9	20,1	20	21	20	21,6	20,567	20,6053	Rabggta	0,04	20,6	0,106	0,917	1	-7
>sp|Q9WTM5|RUVB2	15,67	15,2	16,3	16,2	14,9	15,3	15	17	17	17,1	17	17	15,2	15,7	15	16	15,8	15,1	15,938	15,9826	Ruvbl2	0,04	16	0,106	0,917	1	-7
>sp|Q62395|TFF3_M(	19,88	21,4	0	20,4	19,8	19,2	21	22	22	18	20	19	18,3	19,2	18	18	18,6	17,9	18,279	18,5152	Tff3	0,24	18,4	0,103	0,919	1	-7
>sp|P62855|RS26_M	18,42	17,7	14,6	15,5	19,3	19,1	18	16	17	16,5	19	17	15,6	15,2	15	19	19,6	18,5	17,415	17,3331	Rps26	-0,1	17,4	-0,1	0,919	1	-7
>sp|Q7M758|NALDL_	19,16	19,2	19,9	20,1	19	19,3	20	19	19	19,1	19	19	19,8	19,6	20	19	19,2	19,4	19,407	19,4227	Naaladl1	0,02	19,4	0,099	0,922	1	-7
>sp|P17710|HXK1_M	20,57	20,5	20,7	20,6	20,3	20,1	20	21	19	21,6	18	20	19,9	19,9	22	20	19,8	21,4	20,362	20,3227	Hk1	-0	20,3	-0,1	0,922	1	-7
>sp|Q922D8|C1TC_M	19,92	19,8	19,6	19,4	20,2	19,7	20	20	19	19,7	20	19	18,9	20	20	20	20	19,7	19,687	19,7021	Mthfd1	0,02	19,7	0,099	0,922	1	-7
>sp|Q8VE95|CH082_	15,28	0	14,9	14,1	17,1	0	16	16	15	16,7	17	15	0	14,7	0	17	16,8	14,8	12,107	12,4252	>sp|Q8VE	0,32	12,3	0,098	0,923	1	-7
>sp|Q8C1N8|DFA22_	21,74	23,7	22,6	23,2	21	21,7	23	23	23	22,7	24	23	24	20,9	23	22	22,5	21,9	22,567	22,6105	Defa22	0,04	22,6	0,097	0,924	1	-7
>sp|Q8C1P2|DFA21_	21,74	23,7	22,6	23,2	21	21,7	23	23	23	22,7	24	23	24	20,9	23	22	22,5	21,9	22,567	22,6105	Defa21	0,04	22,6	0,097	0,924	1	-7
>sp|Q8BFU3|RN214_	14,82	18,3	15,2	18,5	18,9	19,5	19	19	19	17,8	18	18	18,3	18,1	19	18	17,8	18,3	17,998	18,0529	Rnf214	0,06	18	0,095	0,925	1	-7
>sp|Q91VH6|MEMO1	21,69	21,8	21,9	21	20,7	20,3	21	20	21	21,5	21	21	21,4	20,8	21	21	21	20,6	20,971	20,9942	Memo1	0,02	21	0,094	0,926	1	-7
>sp|Q6PAK3|ANM8_I	21,22	19,8	18,6	19,1	20,3	19,8	20	19	19	19,8	19	19	20,5	18,6	19	20	19,4	19,9	19,559	19,5276	Prmt8	-0	19,5	-0,09	0,926	1	-7
>sp|Q9CZD4|CSN7A_I	18,04	19,1	18,2	17,9	17,7	17,9	18	18	18	16,9	18	19	18,3	18,9	18	19	17,6	17,9	18,129	18,1549	Cops7a	0,03	18,1	0,092	0,928	1	-7
>sp|P52430|PON1_M	19,84	18,6	18,6	20,1	19,8	18,4	20	24	20	20,5	20	20	19	19,5	19	21	20,5	19,7	19,815	19,8665	Pon1	0,05	19,8	0,09	0,929	1	-7
>sp|Q6PDY2|AEDO_M	0	15,9	15,9	15,5	15,7	0	15	16	15	14,8	0	0	16,3	16,9	16	15	16,2	15,9	12,116	12,4081	Ado	0,29	12,3	0,09	0,929	1	-7
>sp|Q02105|C1QC_M	18,46	21,9	0	22,1	22	15	22	21	22	14,9	17	22	16,2	16,2	15	22	21,4	18	18,273	18,0435	C1qc	-0,2	18,2	-0,09	0,93	1	-7
>sp|Q9JLF6|TGM1_M(	16,42	19,2	16,5	18,8	18,8	16,5	17	19	19	18,3	17	17	18,5	17,5	19	18	17,8	18,4	17,833	17,8766	Tgm1	0,04	17,9	0,089	0,93	1	-7
>sp|Q9CZ30|OLA1_M	21,17	22	21,6	21,6	21,7	21,9	22	22	21	21,3	21	21	22	22,4	22	22	21,8	21,3	21,708	21,7239	Ola1	0,02	21,7	0,087	0,932	1	-7
>sp|Q61235|SNTB2_I	19,2	19,9	20	19,3	20,4	19	19	20	21	19,3	21	21	20	19,6	19	20	19,4	19,5	19,861	19,8915	Sntb2	0,03	19,9	0,084	0,934	1	-7
>sp|P56380|AP4A_M	17,31	18,3	19,5	18,3	17,2	18	17	21	21	19,5	20	19	18,8	18,7	18	17	17,6	18,1	18,606	18,5587	Nudt2	-0	18,6	-0,08	0,936	1	-7
>sp|P56389|CDD_M(	22,09	22,3	22,6	22,3	22	22,4	22	23	23	22,8	23	23	21,7	22,4	22	22	22,9	22,4	22,523	22,5066	Cda	-0	22,5	-0,08	0,938	1	-7
>sp|O70562|SPR2K_	17,04	17	17,7	18,6	17,7	18,8	16	17	18	19,6	20	20	0	20,4	19	17	20,9	21,1	17,594	17,4196	Sprr2k	-0,2	17,5	-0,08	0,938	1	-7
>sp|Q61765|K1H1_M	21,51	21	20,5	20,8	20,2	20,1	18	21	21	19,4	21	19	19,7	21,2	19	22	19,3	22,3	20,348	20,3909	Krt31	0,04	20,4	0,078	0,939	1	-7
>sp|Q61897|KT33B_	21,51	21	20,5	20,8	20,2	20,1	18	21	21	19,4	21	19	19,7	21,2	19	22	19,3	22,3	20,348	20,3909	Krt33b	0,04	20,4	0,078	0,939	1	-7
>sp|P58389|PTPA_M	22,57	20,7	20,9	21,3	21	21,1	21	21	21	21,4	22	21	20,8	20,6	21	22	21,8	20,9	21,284	21,2628	Ptpa	-0	21,3	-0,08	0,94	1	-7
>sp|P27046|MA2A1	15,33	15,5	15,1	0	12,9	0	0	12	15	14,5	16	15	13,3	15,2	14	0	0	0	9,5193	9,7757	Man2a1	0,26	9,65	0,075	0,941	1	-7
>sp|P28474|ADHX_M	23,43	23,5	24,5	23,9	23,9	24	24	24	24	23,9	24	24	23,7	23,7	24	24	23,9	23,9	23,886	23,8751	Adh5	-0	23,9	-0,07	0,942	1	-7
>sp|O88456|CPNS1_	19,78	19,1	19,2	20	19,7	19,5	20	19	19	18,3	20	20	19	19	20	19	19,9	20	19,435	19,4152	Capns1	-0	19,4	-0,07	0,942	1	-7
>sp|Q8JZN5|ACAD9_I	24,51	20,9	21,4	24,4	24,6	24	24	25	24	24,3	22	22	25	22,4	25	25	24,4	24,6	23,696	23,7446	Acad9	0,05	23,7	0,072	0,943	1	-7
>sp|Q10738|MMP7_	18,47	20,5	18,8	21,1	18,5	21,1	21	21	19	20,7	20	21	22	21,1	18	18	17,5	20	19,812	19,7655	Mmp7	-0	19,8	-0,07	0,944	1	-7
>sp|Q8R0F8|FAHD1_I	19,98	19,7	22,7	22,4	22,8	19,9	20	21	23	21,1	21	21	21	22,8	21	21	21,2	20,8	21,229	21,2635	Fahd1	0,03	21,2	0,069	0,946	1	-7
>sp|O70554|SPR2B_	16,73	16,7	17,4	18,3	17,4	18,5	16	17	18	19,3	19	19	0	20,1	19	17	20,7	20,8	17,325	17,1834	Sprr2b	-0,1	17,3	-0,06	0,949	1	-7
>sp|O70558|SPR2G_	16,73	16,7	17,4	18,3	17,4	18,5	16	17	18	19,3	19	19	0	20,1	19	17	20,7	20,8	17,325	17,1834	Sprr2g	-0,1	17,3	-0,06	0,949	1	-7
>sp|P00493|HPRT_M	18,74	18,4	19,2	18,5	18,8	18,9	18	19	18	18,8	19	18	18,5	18,9	18	19	18,5	18,4	18,682	18,6916	Hprt1	0,01	18,7	0,064	0,95	1	-7
>sp|Q99KH8|STK24_I	19,51	17,9	17,4	17	17,5	18,2	17	17	17	17,1	18	18	17,5	18,3	18	17	17,3	17,7	17,682	17,7002	Stk24	0,02	17,7	0,061	0,952	1	-7
>sp|Q9QZN4|FBX6_M	16,67	17,6	16,9	17,3	17,2	17,2	17	0	17	16	14	17	18	17,4	19	17	0	16,9	15,124	14,9665	Fbxo6	-0,2	15	-0,06	0,954	1	-7

>sp|O88895|HDAC3_	19,29	19,2	14,9	16,2	15,3	15	15	14	16	16,2	15	17	17,1	17,4	18	15	15,4	15,8	16,158	16,2005	Hdac3	0,04	16,2	0,058	0,954	1	-7
>sp|O70555|SPR2D_	16,5	16,5	17,2	18,1	17,2	18,4	16	17	18	19,1	19	19	0	19,9	18	16	20,5	20,5	17,099	16,9747	Sprr2d	-0,1	17	-0,06	0,955	1	-7
>sp|P35276|RAB3D_	21,06	19,6	20,5	20,9	20,6	21,1	21	18	21	20,4	21	21	20,8	20,7	19	21	20,5	20,3	20,386	20,4051	Rab3d	0,02	20,4	0,058	0,955	1	-7
>sp|Q99LC2|CSTF1_M	19,71	19,6	24,6	20,1	19	19,3	19	20	24	20	24	24	19,4	19,2	19	19	19,4	19,4	20,563	20,5057	Cstf1	-0,1	20,5	-0,06	0,955	1	-7
>sp|Q80TY0|FNBP1_M	18,5	19,2	18,8	19,2	19,3	19,5	18	19	19	19,1	18	19	19,4	19,4	20	19	18,8	19,1	18,93	18,9438	Fnbp1	0,01	18,9	0,056	0,956	1	-7
>sp|Q923B1|DBR1_M	0	15,8	15,4	15,7	16	15	16	14	15	14,9	0	15	15,4	15,5	16	16	15,6	15,4	13,62	13,7523	Dbr1	0,13	13,7	0,055	0,957	1	-7
>sp|P03958|ADA_MO	17,6	17,3	16,6	15,4	16,6	17	16	17	16	15,6	16	17	17	17,3	17	17	17,1	16,1	16,66	16,6757	Ada	0,02	16,7	0,05	0,961	1	-7
>sp|Q61205|PA1B3_	19,79	17,1	18,3	17,3	18,1	18	18	19	17	18,2	19	18	17	17,5	16	19	19,3	19,4	18,05	18,0751	Pafah1b3	0,02	18,1	0,05	0,961	1	-7
>sp|P62869|ELOB_M	20,6	23,6	21,8	20,2	20,5	22,4	20	22	21	21,5	22	22	21,5	21,9	22	21	20,7	20,4	21,411	21,3898	Elob	-0	21,4	-0,05	0,961	1	-7
>sp|Q9D0B6|PBDC1_	18,67	19,5	19,5	19,5	18,5	19,4	19	21	21	19,5	21	20	18,9	18,9	21	19	18,6	18,8	19,532	19,511	Pbdc1	-0	19,5	-0,05	0,962	1	-7
>sp|Q99LG2|TNPO2_I	16,26	18,2	15,6	17,2	16,8	16	16	18	16	17,3	17	17	16,2	16,8	16	15	18	16,3	16,618	16,6375	Tnpo2	0,02	16,6	0,048	0,962	1	-7
>sp|O88487|DC1I2_I	18,3	16,2	18,5	18	20,4	20,5	18	19	20	19,6	16	18	20	20,3	18	18	20,2	18,8	18,744	18,7748	Dync1i2	0,03	18,8	0,048	0,962	1	-7
>sp|Q61147|CERU_M	19,45	17,9	20,1	17,6	18,4	20,3	18	18	19	19,8	19	19	18,2	18,5	18	18	18,5	19,7	18,788	18,8063	Cp	0,02	18,8	0,046	0,964	1	-7
>sp|Q9EP82|WDR4_M	17,32	17,3	17,6	17,3	16,9	16,8	17	18	18	17,8	17	17	16,9	17	17	18	16,7	17,7	17,303	17,2936	Wdr4	-0	17,3	-0,05	0,964	1	-7
>sp|Q922Q1|MARC2_	17,86	18,3	18	17,5	18,9	18,6	18	18	18	17,8	18	18	18,1	18,7	19	18	18,8	17,7	18,249	18,2403	Marc2	-0	18,2	-0,04	0,965	1	-7
>sp|P00920|CAH2_M	16,35	15,8	18,6	17,9	18,2	15,6	15	18	18	18,5	17	19	16,8	16,9	17	16	15,6	17,5	17,109	17,0848	Ca2	-0	17,1	-0,04	0,966	1	-7
>sp|Q61730|IL1AP_M	16,42	16,8	14,3	16,3	16,1	16,6	17	17	15	16	16	17	16,5	16,1	16	16	15,9	15,9	16,118	16,1037	Il1rap	-0	16,1	-0,04	0,968	1	-7
>sp|O70559|SPR2H_	16,22	16,2	16,9	17,8	16,9	18	16	16	17	18,7	19	19	0	19,6	18	16	20,2	20,2	16,75	16,6656	Sprr2h	-0,1	16,7	-0,04	0,969	1	-7
>sp|Q8BX94|OSBL2_I	0	0	0	15,7	12,9	0	0	0	0	0	18	0	0	0	0	12	0	0	3,1781	3,29506	Osbpl2	0,12	3,24	0,039	0,97	1	-7
>sp|Q62448|IF4G2_M	15,57	14,8	16,1	14,8	15,8	15,9	15	15	12	14,4	14	15	15,6	14,7	15	15	16,6	15,5	15,095	15,0795	Eif4g2	-0	15,1	-0,03	0,973	1	-7
>sp|Q62465|VAT1_M	19,61	19	19,8	19,3	19,8	19,8	22	20	20	19,7	20	19	18,8	19,6	20	19	19,9	23,1	19,855	19,8386	Vat1	-0	19,8	-0,03	0,973	1	-7
>sp|Q9Z2N8|ACL6A_I	21,18	21,4	21,2	21	21,5	21,3	22	22	22	22	22	21	21,3	21,3	22	21	21,1	21,2	21,438	21,4429	Actl6a	0	21,4	0,032	0,975	1	-7
>sp|P0C027|NUD10_	17,49	16,4	0	17,6	17,4	18	18	0	17	16,4	0	0	17,2	16,8	18	18	17,5	18	13,555	13,4407	Nudt10	-0,1	13,5	-0,03	0,975	1	-7
>sp|P0C028|NUD11_	17,49	16,4	0	17,6	17,4	18	18	0	17	16,4	0	0	17,2	16,8	18	18	17,5	18	13,555	13,4407	Nudt11	-0,1	13,5	-0,03	0,975	1	-7
>sp|P63087|PP1G_M	23,51	23,7	23,5	23,5	22,9	23,2	23	24	24	23,7	24	23	22,8	23,5	23	23	23,6	23,8	23,42	23,4241	Ppp1cc	0	23,4	0,029	0,977	1	-7
>sp|P63321|RALA_M	19,14	18,4	20,2	18,5	18	18,7	19	20	20	19,2	20	21	18,2	19,4	18	18	19,8	19,1	19,186	19,1742	Rala	-0	19,2	-0,03	0,977	1	-7
>sp|O08756|HCD2_M	15,92	18,3	16,7	15,3	15,5	15,2	15	17	17	13,7	15	16	17,9	17,3	21	15	15,1	15,8	16,301	16,3214	Hsd17b1	0,02	16,3	0,028	0,978	1	-7
>sp|P63037|DNJA1_	17,98	18,1	19,3	19,3	16,4	17,2	19	18	18	18,2	19	19	17,8	18,3	18	17	17,8	17,5	18,104	18,0941	Dnaja1	-0	18,1	-0,03	0,98	1	-7
>sp|P00329|ADH1_M	27,61	27,7	23,9	27	27	23,9	28	28	26	26,2	27	26	26,1	26,3	26	28	26,5	26,5	26,505	26,4934	Adh1	-0	26,5	-0,02	0,983	1	-7
>sp|Q922B2|SYDC_M	22,06	23,2	21	22,5	22,5	22,1	21	22	20	22,3	21	22	22,1	22,6	22	22	21,2	21,2	21,838	21,8456	Dars	0,01	21,8	0,022	0,983	1	-7
>sp|Q3TYL0|YH010_M	14,36	17,3	14	17,3	17,3	17,5	16	14	19	16,1	17	14	18,3	13,9	19	14	14,4	18,5	16,229	16,2097	>sp|Q3TYL	-0	16,2	-0,02	0,984	1	-7
>sp|P97496|SMRC1_	14,42	14,3	14,2	13,9	14	13,9	14	12	14	13,9	15	14	15,1	11,7	14	14	14	13,4	13,958	13,9659	Smarcc1	0,01	14	0,021	0,984	1	-7
>sp|Q8R0W0|EPIPL_M	16	16	14,7	16	15,8	15,4	16	15	16	15,8	16	16	15,5	15,7	15	15	15,9	15,7	15,598	15,5948	Eppk1	-0	15,6	-0,02	0,985	1	-7
>sp|Q8JZV7|NAGA_M	18,41	19	20,2	18,8	20	19,1	19	18	19	18,5	19	19	19,6	19,9	20	19	18,6	17,6	19,072	19,0779	Amdhd2	0,01	19,1	0,018	0,986	1	-7
>sp|P00755|K1KB1_	19,78	19,7	19,3	19,1	19,7	19,4	19	19	19	19,4	19	19	20	19,5	19	19	19,8	19,8	19,364	19,361	Klk1b1	-0	19,4	-0,02	0,986	1	-7
>sp|Q8BFQ4|WDR82_	22,01	19,5	20	20,1	19,9	19,3	20	20	20	19,7	20	20	20,1	20	21	20	19,5	19,6	19,983	19,9784	Wdr82	-0	20	-0,02	0,987	1	-7
>sp|Q61390|TCPW_M	19,53	19,2	19,4	16,7	15,8	20,3	16	20	16	19,2	20	19	16,2	18,8	16	18	19,8	15,5	18,094	18,1074	Cct6b	0,01	18,1	0,016	0,988	1	-7
>sp|P62270|RS18_M	20,72	20,7	20,8	19,8	20,5	20,3	20	20	20	19,6	21	20	20	20,4	21	20	20,3	20,6	20,328	20,3307	Rps18	0	20,3	0,014	0,989	1	-7
>sp|Q9DCS2|MTL26_I	17,64	16,8	19,7	17,3	17,3	18,1	18	17	22	18	22	18	17,7	17,8	18	17	17,4	17,5	18,138	18,1482	Mettl26	0,01	18,1	0,014	0,989	1	-7
>sp|P48678|LMNA_M	17,96	20,8	20,4	20,8	20	20,3	20	20	20	19,9	21	20	20,2	20,1	20	20	20,1	19,9	20,106	20,1021	Lmna	-0	20,1	-0,01	0,99	1	-7
>sp|P70303|PYRG2_	19,6	19,4	19,6	21,3	21,4	21,3	19	18	21	21,1	20	20	18,8	21,6	19	21	18,4	21,3	20,222	20,2271	Ctps2	0	20,2	0,008	0,993	1	-7
>sp|P97351|RS3A_M	19,91	21,7	19,7	19,5	21,8	21,7	20	22	19	20,4	20	21	20,4	21,2	20	20	20,9	21,2	20,591	20,5942	Rps3a	0	20,6	0,007	0,995	1	-7
>sp|Q64511|TOP2B_	17,5	20,6	20,8	20	19,7	19,9	20	20	21	20,1	22	21	19,8	19,3	19	20	19,8	19,5	20,035	20,0372	Top2b	0	20	0,006	0,995	1	-7
>sp|P02798|MT2_MO	16,34	0	0	0	0	0	0	0	17	15,8	0	0	0	0	0	0	17	0	3,6603	3,64806	Mt2	-0	3,65	-0	0,997	1	-7
>sp|Q921K8|TCAF2_I	14,08	13,7	16	13,7	14,7	14,9	14	14	12	11,5	13	14	14,8	15,2	15	14	14,1	14,4	14,066	14,0639	Tcaf2	-0	14,1	-0	0,997	1	-7
>sp|P61924|COPZ1_	23,79	20,4	24,3	23,7	23,6	24	24	24	24	24	25	24	18,9	23,7	24	24	24,1	24,2	23,467	23,4647	Copz1	-0	23,5	-0	0,998	1	-7
>sp|Q8CA72|GAN_MO	15,52	15,8	15,8	15,7	14,2	15,6	0	15	14	11,2	15	13	14,4	14,5	14	14	13,5	11,7	13,468	13,4724	Gan	0	13,5	0,002	0,998	1	-7
>sp|Q8VBV7|CSN8_M	19,13	19,5	19,4	20,3	22,7	22,7	23	22	20	22,1	22	22	19,5	19,4	20	20	22,1	22,2	20,98	20,9806	Cops8	0	21	6E-04	1	1	-7